

N88-25680

JPL Publication 88-9

Proceedings of the Mobile Satellite Conference

May 3-5, 1988

William Rafferty
Conference Technical Program Chairman

(NASA-CR-1829(4) PROCEEDINGS OF THE MOBILE
SATELLITE CONFERENCE (Jet Propulsion Lab.)
536 p CSCL 17B

N88-25680
--THRU--
N88-25758
Unclas
0146558

G3/32

May 1988



National Aeronautics and
Space Administration

Jet Propulsion Laboratory
California Institute of Technology
Pasadena, California

JPL Publication 88-9

Proceedings of the Mobile Satellite Conference

May 3-5, 1988

William Rafferty
Conference Technical Program Chairman

May 1988

NASA

National Aeronautics and
Space Administration

Jet Propulsion Laboratory
California Institute of Technology
Pasadena, California

This publication was prepared by the Jet Propulsion Laboratory, California Institute of Technology, under a contract with the National Aeronautics and Space Administration.

ABSTRACT

A satellite-based mobile communications system provides voice and data communications to mobile users over a vast geographic area. Currently, many emerging international Mobile Satellite Systems (MSSs), including the U.S., Canadian, Australian, European and INMARSAT systems, have been proposed to supply such mobile services for land, maritime and aeronautical applications. The technical and service characteristics of these, and other, international systems are presented within these proceedings and form an in-depth view of the current MSS status at the system and subsystem levels. Major emphasis is placed on developments, current and future, in the following critical MSS technology areas: vehicle antennas, networking, modulation and coding, speech compression, channel characterization, space segment technology and MSS experiments. Also, the mobile satellite communications needs of government agencies are addressed, as is the MSS potential to fulfill them.

Over 70 papers, covering 10 technical areas and the government agency MSS application, are published within these proceedings. The breadth and diversity of these papers are a clear indication of the maturity of MSS system concepts and the supporting technology.

Yesterday's Dream - Today's Reality

The idea of providing two-way voice and data communications to small, low-cost, remotely located mobile terminals has long been a dream of many inside and outside of government. In 1980, after a number of years of independent work, Canada's Department of Communications and NASA embarked on a joint effort to accelerate the introduction of a Mobile Satellite System (MSS) in North America. In 1982 and 1983, this effort received added momentum with NASA's petition for frequencies and the formation of the first MSS entrepreneurial companies. This initial business interest, aided by the allocation of operational frequencies and the development of key technologies, has since blossomed into widespread activity, as evidenced by the papers to be presented at this conference.

Over this time period we have also seen a dramatic shift in attitude from doubt and caution to innovation and action. For example, the 12 independent U.S. applicants that spoke at our last conference have now become eight and have formed the American Mobile Satellite Consortium (AMSC), with plans to implement and operate MSS in the United States. AMSC has been working closely with Telesat Canada to jointly provide an operational voice and data service in North America by the early 1990's. Also, Omninet, one of the early applicants, has plans to provide data service in the U.S. using existing K_u-band satellites.

In addition to these U.S. and Canadian initiatives, there is strong international interest in mobile satellite communications, as indicated by the conference papers from Australia, ESA, Inmarsat and AVSAT. The emergence of these domestic and international organizations, coupled with the technology developed and field-tested by NASA/JPL and others, creates new services and business opportunities that will benefit both the public and private sectors. To me, it is an excellent example of what can be accomplished when government and industry work together to pursue worthwhile goals.

I would like to thank Bill Weber, William Rafferty and their JPL staff for their excellent work and dedication in structuring this conference and carrying out the technology development goals of the NASA program. Also, many thanks to Lynn Polite and Laura Crary for their work as conference organizers.

George H. Knouse
Manager, Mobile Satellite Program
NASA Headquarters

PRECEDING PAGE BLANK NOT FILMED

LIST OF PRESENTATIONS FOR THE MOBILE SATELLITE CONFERENCE

OPENING REMARKS

1. R.J. Arnold, Director of Communications and Information
Systems Division, NASA *
2. W.J. Weber, Manager, NASA Technology Program, Jet Propulsion
Laboratory *

SESSION A. MOBILE SATELLITE SYSTEMS 1

SESSION CHAIR: G. Knouse, NASA Headquarters
SESSION ORGANIZER: W. Rafferty, Jet Propulsion Laboratory

1. "The AMSC Mobile Satellite System" 3
Representatives of the companies comprising the AMSC;
American Mobile Satellite Consortium
2. "NASA's Mobile Satellite Development Program" 11
W. Rafferty, K. Dessouky, and M. Sue; Jet Propulsion Laboratory
3. "Mobile Satellite Service for Canada" 23
D. Sward; Telesat Canada
4. "AUSSAT Mobile Satellite Services" 31
W. Nowland, M. Wagg, and D. Simpson; AUSSAT Pty Ltd
5. "A Satellite System for Land-Mobile Communications in Europe" . . . 37
P. Bartholome and R. Rogard; European Space Agency
6. "System Capacity and Economic Modeling Computer Tool for
Satellite Mobile Communications Systems" 43
R.A. Wiedeman, W. Doong, and A.G. McCracken; Ford Aerospace
Corporation
7. "Developing A Global Aeronautical Satellite System" 51
D.K. Dement; Aeronautical Radio, Inc.
8. "World-Wide Aeronautical Satellite Communications" 57
P. Wood and K. Smith; INMARSAT
9. "An Overview of the OmniTRACS - The First Operational Mobile
Ku-Band Satellite Communications" 63
A. Salmasi; Omninet Communications Services

* Presentation is not reprinted here.

SESSION B. REGULATORY ISSUES 69

SESSION CHAIR: J. Freibaum, NASA Headquarters
SESSION ORGANIZER: V. Gray, Jet Propulsion Laboratory

1. "International and Domestic Mobile Satellite Regulatory Proceedings: A Comparison of Outcomes and Discussion of Implications" 71(a)
J. Freibaum; NASA Headquarters
2. "Mobile Satellite Services: International Co-Ordination, Co-Operation and Competition" 71
O. Lundberg; INMARSAT
3. "International and Domestic Regulatory Issues Facing the Canadian MSAT System" 79
B. Azarbar, J.R. Langlois, and C.J. Frank; Telesat Canada
4. "Status of Domestic Proceedings Speaker" *
FCC

SESSION C. PROPAGATION 85

SESSION CHAIR: A. Neul, German Aerospace Research (DFVLR)
SESSION ORGANIZER: F. Davarian, Jet Propulsion Laboratory

1. "Propagation Effects by Roadside Trees Measured at UHF and L-Band for Mobile Satellite Systems" 87
J. Goldhirsh and W.J. Vogel; Johns Hopkins University
2. "Propagation Modeling for Land Mobile Satellite Systems" 95
R.M. Barts and W.L. Stutzman; Virginia Tech
3. "Attenuated Direct and Scattered Wave Propagation on Simulated Land Mobile Satellite Service Paths in the Presence of Trees" 101
R.L. Campbell and R. Estus; Michigan Technological University
4. "Mobile Satellite Propagation Measurements and Modeling: A Review of Results for Systems Engineers" 107
W.L. Stutzman et al.; Virginia Tech
5. "Propagation Measurements for an Australian Land Mobile-Satellite System" 119
A. Bundrock and R. Harvey; Telecom Research Laboratories, Australia
6. "Land Mobile Satellite Propagation Results" 125
D.C. Nicholas; Rockwell International Corporation
7. "Propagation Effects on Spread-Spectrum Mobile-Satellite Systems" 133
W.L. Flock and E.K. Smith; University of Colorado

* Presentation is not reprinted here.

8. "Multipath Measurements for Land Mobile Satellite Service Using Global Positioning System Signals" 139
 J.J. Lemmon; Institute for Telecommunication Sciences, National Telecommunications and Information Administration

SESSION D. MOBILE SATELLITE SYSTEMS TECHNOLOGY 145

SESSION CHAIR: W.C.Y. Lee, PacTel
 SESSION ORGANIZER: R.F. Emerson, Jet Propulsion Laboratory

1. "Development of a Mobile Satellite Communication Unit" 147
 R. Suzuki, T. Ikegami, N. Hamamoto, T. Taguchi, N. Endo, O. Yamamoto, and O. Ichiyoshi; NEC Corporation
2. "Development of the Network Architecture of the Canadian MSAT System" 155
 N.G. Davies, A. Shoamanesh, and V.C.M. Leung; Telesat Canada
3. "System Architecture for the Canadian Interim Mobile Satellite System" 163
 M. Shariatmadar, K. Gordon, B. Skerry, H. El-Damhougy, and D. Bossler; Telesat Canada
4. "Design, Development and Trials of an Airline Passenger Telephone System" 171
 J. Schoenenberger and R. McKinlay; Racal Avionics Limited
5. "Satellite Communications Experiment for the Ontario Air Ambulance Service" 177
 J.S. Butterworth; Communications Research Centre
6. "Land-Mobile Satellite Demonstration System" 183
 G.M. Gooch and D.C. Nicholas; Rockwell International Corporation
7. "MOBILESTAR Field Test Program" 189
 W. Rubow; Hughes Aircraft Company
8. "The JPL MSAT Mobile Laboratory and the Pilot Field Experiments" . . 195
 J.B. Berner and R.F. Emerson; Jet Propulsion Laboratory
9. "Technical Characteristics of the OmniTRACS - The First Operational Mobile Ku-Band Satellite Communications System" 203
 F.P. Antonio, K.S. Gilhousen, I.M. Jacobs, and L.A. Weaver Jr.; QUALCOMM, Inc.

SESSION E. VEHICLE ANTENNAS 209

SESSION CHAIR: P.E. Mayes, University of Illinois
 SESSION ORGANIZER: K. Woo, Jet Propulsion Laboratory

1. "An Adaptive Array Antenna for Mobile Satellite Communications" . . 211
 R. Milne; Communications Research Centre

2.	"MSAT Mobile Electronically Steered Phased Array Antenna Development"	217
	F. Schmidt; Ball Aerospace Systems Group	
3.	"MSAT-X Electronically Steered Phased Array Antenna System"	223
	H.H. Chung et al.; Teledyne Ryan Electronics	
4.	"MSAT-X Phased Array Antenna Adaptions to Airborne Applications"	229
	C. Sparks, H.H. Chung, and S.Y. Peng; Teledyne Ryan Electronics	
5.	"Adaptive Interference Techniques for Mobile Antennas"	235
	L.J. Griffiths and E. Satorius; University of Southern California	
6.	"The JPL Mechanically Steered Antenna"	241
	J.B. Berner and D.J. Bell; Jet Propulsion Laboratory	
7.	"Simple, Low-Profile, Circularly Polarized Arrays"	249
	P. Mayes, J. Drewniak, J. Bowen, and J. Gentle; University of Illinois	
8.	"Omni-Directional L-Band Antenna for Mobile Communications"	255
	C.S. Kim, N. Moldovan, and J. Kijesky; Prodelin Corporation	

SESSION F. MODULATION AND CODING I 261

SESSION CHAIR: G. Ungerboeck, IBM Zurich Research Laboratory

SESSION ORGANIZER: D. Divsalar, Jet Propulsion Laboratory

1.	"Trellis-Coded CPM for Satellite-Based Mobile Communications"	263
	F. Abrishamkar and E. Biglieri; Technology Group	
2.	"Interleaver Design for Trellis-Coded Differential 8-PSK Modulation With Non-Coherent Detection"	271
	F. Edbauer; German Aerospace Research (DFVLR)	
3.	"Codes for QPSK Modulation With Invariance Under 90° Rotation"	277
	G. Ungerboeck and S.S. Pietrobon; IBM Zurich Research Laboratory	
4.	"Trellis Coded MPSK Modulation Techniques for MSAT-X"	283
	D. Divsalar and M.K. Simon; Jet Propulsion Laboratory	
5.	"Modulation and Coding for Fast Fading Mobile Satellite Communication Channels"	291
	P.J. McLane et al.; Queen's University	
6.	"Performance of the ICAO Standard 'Core Service' Modulation and Coding Techniques"	297
	J. Lodge and M. Moher; Communications Research Centre	
7.	"Comparison of CDMA and FDMA for MOBILESTAR System"	303
	I.M. Jacobs et al.; Hughes Aircraft Company	

SESSION G. MODULATION AND CODING II 309

SESSION CHAIR: G. Ungerboeck, IBM Zurich Research
Laboratory

SESSION ORGANIZER: D. Divsalar, Jet Propulsion Laboratory

1. "An 8-DPSK TCM Modem for MSAT-X" 311
T.C. Jedrey, N.E. Lay, and W. Rafferty; Jet Propulsion Laboratory
2. "Development of a Coded 16-ARY CPFSK Coherent Demodulator" 317
K. Clarke, R. Davis, and J. Roesch; Harris Corporation
3. "Modem for the Land Mobile Satellite Channel" 323
S.J. Henely; Rockwell International Corporation
4. "Pilot-Aided Modulation for Narrow-Band Satellite
Communications" 329
G.J. Saulnier and W. Rafferty; Rensselaer Polytechnic Institute
5. "An Error Floor in Tone Calibrated Transmission" 337
J.K. Cavers; Simon Fraser University
6. "Extending the Impulse Response in Order To Reduce Errors Due
to Impulse Noise and Signal Fading" 345
J.A. Webb, A.J. Rolls, and H.R. Sirisena; University of
Canterbury, New Zealand
7. "ACSB - A Minimum Performance Assessment" 351
L.T. Jones and W.A. Kissick; Institute for Telecommunication
Sciences, National Telecommunications and Information
Administration
8. "A Study on the Co- and Adjacent Channel Protection
Requirements for Mobile Satellite ACSB Modulation" 359
J.T. Sydor; Communications Research Centre

SESSION H. NETWORKING 365

SESSION CHAIR: H. Tan, University of California,
Irvine

SESSION ORGANIZER: T.-Y. Yan, Jet Propulsion Laboratory

1. "A Framework for Implementing Data Services in Multi-Service
Mobile Satellite Systems" 367
M.O. Ali, V.C.M. Leung, and A.I. Spolsky; Microtel Pacific
Research Limited
2. "L-Band and SHF Multiple Access Schemes for the MSAT System" 373
M. Razi, A. Shoamanesh, and B. Azarbar; Telesat Canada
3. "Rearrangement Procedures in Regenerative Multibeam Mobile
Communications Satellites With Frequency Reuse" 381
G. Columbo, F. Settimo, and A. Vernucci; Centro Studi e
Laboratori Telecomunicazioni (CSELT)

4.	"Design Mobile Satellite System Architecture as an Integral Part of the Cellular Access Digital Network"	387
	E.S.K. Chien, J.A. Marinho, and J.E. Russell Sr.; AT&T Bell Laboratories	
5.	"An Access Alternative For Mobile Satellite Networks"	395
	W.W. Wu; INTELSAT	
6.	"An Operational Open-End File Transfer Protocol for Mobile Satellite Communications"	405
	C. Wang, U. Cheng, and T.-Y. Yan; Jet Propulsion Laboratory	
7.	"Integrated Voice/Data Protocols for Satellite Channels"	413
	C.-S. Wu and V.O.K. Li; University of Southern California	
8.	"Evaluation of CDMA System Capacity for Mobile Satellite System Applications"	423
	P.O. Smith and E.A. Geraniotis; Techno-Sciences, Inc.	
 <u>SESSION I. SPACECRAFT TECHNOLOGY</u>		429
	SESSION CHAIR: Y. Rahmat-Samii, Jet Propulsion Laboratory	
	SESSION ORGANIZER: Y. Rahmat-Samii, Jet Propulsion Laboratory	
1.	"Considerations for Spacecraft Design for M-SAT"	431
	K. Hing and H.J. Moody; Spar Aerospace Limited	
2.	"Antenna System for M-SAT Mission"	437
	I. Karlsson, Y. Patenaude, and L. Stipelman; Spar Aerospace Limited	
3.	"Antenna Technology for Advanced Mobile Communication Systems"	443
	E. Rammos, A. Roederer, and R. Rogard; European Space Agency	
4.	"Frequency Addressable Beams for Land Mobile Communications"	449
	J.D. Thompson and G.G. DuBellay; Hughes Aircraft Company	
5.	"Large Antenna Experiments Aboard the Space Shuttle-- Application of Nonuniform Sampling Techniques"	459
	Y. Rahmat-Samii; Jet Propulsion Laboratory	
6.	"15-Meter Antenna Performance Optimization Using an Interdisciplinary Approach"	465
	W.L. Grantham et al.; NASA Langley Research Center	
7.	"A Microstrip Array Feed for MSAT Spacecraft Reflector Antenna" . . .	471
	J. Huang; Jet Propulsion Laboratory	
8.	"Technologies for Antenna Shape and Vibration Control"	477
	E. Mettler, R. Scheid, and D. Eldred; Jet Propulsion Laboratory	

SESSION J. SPEECH COMPRESSION 483

SESSION CHAIR: N.S. Jayant, AT&T Bell Laboratories
SESSION ORGANIZER: T. Jedrey, Jet Propulsion Laboratory

1. "Speech Coding at 4800 BPS for Mobile Satellite Communications" . . . 485
A. Gersho et al.; University of California, Santa Barbara
2. "A 4.8 KBPS Code Excited Linear Predictive Coder" 491
T.E. Tremain, J.P. Campbell, Jr., and V.C. Welch; U.S.
Department of Defense
3. "Real-Time Speech Encoding Based on Code-Excited Linear
Prediction (CELP)" 497
W.P. LeBlanc and S.A. Mahmoud; Carleton University
4. "Sinusoidal Transform Coding From 2400 to 9600 BPS" 503
R.J. McAulay and T.F. Quatieri; MIT Lincoln Laboratory
5. "The Design and Performance of a Real-Time Self Excited Vocoder" . . . 509
R.C. Rose, T.P. Barnwell III, and S. McGrath; Georgia
Institute of Technology
6. "Robust Vector Quantization for Noisy Channels" 515
J.R.B. de Marca, N. Farvardin, N.S. Jayant, and Y. Shoham;
AT&T Bell Laboratories
7. "Development of an 8000 bps Voice Codec for AvSat" 521
J.F. Clark; Aeronautical Radio, Inc.
8. "Analysis and Improvement of the Vector Quantization in SELP" . . . 527
W.B. Kleijn, D.J. Kransinski, and R.H. Ketchum; AT&T Bell
Laboratories

SESSION K. GOVERNMENT AGENCY 533

SESSION CHAIR: G. Knouse, NASA Headquarters
SESSION ORGANIZER: V. Gray, Jet Propulsion Laboratory

1. "NASA Program Update and Demonstration Preview" *
- G. Knouse; NASA Headquarters
2. "Canadian Government Trials Program for the MSAT Service" *
- D. Buchanan; Government of Canada, Department of Communications
3. "Potential of Mobile Satellite To Support National Security
Emergency Preparedness Requirements" *
- G.G. Shibles; National Communications System

* Presentation is not reprinted here.

4. "System Requirements to Support Federal, State, and Local Users and Potential Communications Deficiencies for a San Bernardino County Earthquake Scenario" *
- G. Duke; Jet Propulsion Laboratory

5. "Mobile Satellite Communications in the Forest Service" 535
- J.R. Warren; U.S. Forest Service

6. "The Impact of Satellite Communications on Future Coast Guard Operations" *
- Lt. H. Creech and Lt. Cdr. C. Isherwood; U.S. Coast Guard

7. "Mobile Satellite Service in the United States" 539
- Representatives of the companies comprising the AMSC; American Mobile Satellite Consortium

* Presentation is not reprinted here.

SESSION A
MOBILE SATELLITE SYSTEMS

SESSION CHAIR: George Knouse, NASA Headquarters
SESSION ORGANIZER: William Rafferty, Jet Propulsion Laboratory

THE AMSC MOBILE SATELLITE SYSTEM

DR. CARSON E. AGNEW, Hughes Communications Mobile Satellite Services, Inc., United States; JAI BHAGAT, MCCA Space Technologies Corporation, United States; EDWIN A. HOPPER, McCaw Space Technologies, Inc., United States; JOHN D. KIESLING, Mobile Satellite Corporation, United States; MICHAEL L. EXNER, Skylink Corporation, United States; LAWRENCE MELILLO, North American Mobile Satellite, Inc., United States; GARY K. NOREEN, Transit Communications, Inc., United States; BILLY J. PARROTT, Satellite Mobile Telephone Co., United States.

TRANSIT COMMUNICATIONS, INC.
P.O. Box 90425
Pasadena, California 91109-0425
United States

ABSTRACT

The American Mobile Satellite Consortium (AMSC) is the designated provider of domestic land, maritime and aeronautical Mobile Satellite Service (MSS) in the United States. This paper describes the AMSC MSS system. AMSC will use three multiple-beam satellites to provide L band MSS coverage to the United States, Canada and Mexico. The AMSC MSS system will have several noteworthy features, including a priority assignment processor that will ensure preemptive access to emergency services, a flexible SCPC channel scheme that will support a wide diversity of services, enlarged system capacity through frequency and orbit reuse, and high effective satellite transmitted power. Each AMSC satellite will make use of 14 MHz (bi-directional) of L band spectrum. K_u band will be used for feeder links.

INTRODUCTION

The U.S. Federal Communications Commission (FCC) has mandated that Mobile Satellite Service (MSS) be provided in the United States by the American Mobile Satellite Consortium (AMSC). The eight companies that make up AMSC all filed MSS applications with the FCC on April 30, 1985 and have been determined by the FCC to be qualified MSS applicants.

AMSC filed a Joint Amendment of the original applications of its member companies on February 1, 1988. This paper is a synopsis of the technical portion of the AMSC Joint Amendment. AMSC and the services it will provide are described in a companion paper in this volume.

AMSC and Telesat Canada plan to jointly procure MSS spacecraft and provide mutual on-orbit backup. It is anticipated that the AMSC and Telesat spacecraft will be nearly identical and will occupy complementary orbital positions.

NASA has offered to launch the first AMSC spacecraft in exchange for initial system capacity for technology development and government demonstrations.

The system described here may be modified somewhat as a result of negotiations with Telesat and NASA or other changed circumstances.

PRECEDING PAGE BLANK NOT FILMED

SYSTEM DESIGN

The AMSC system consists of three basic elements: the space segment, user terminals, and hub stations (Figure 1). Four types of user are shown to illustrate some of the more common applications, namely, a land mobile user with an omnidirectional antenna, a land mobile user with a steered directional high gain antenna, an aeronautical mobile user, and a transportable user. Users can access the public switched telephone network through gateway stations or private networks through base stations.

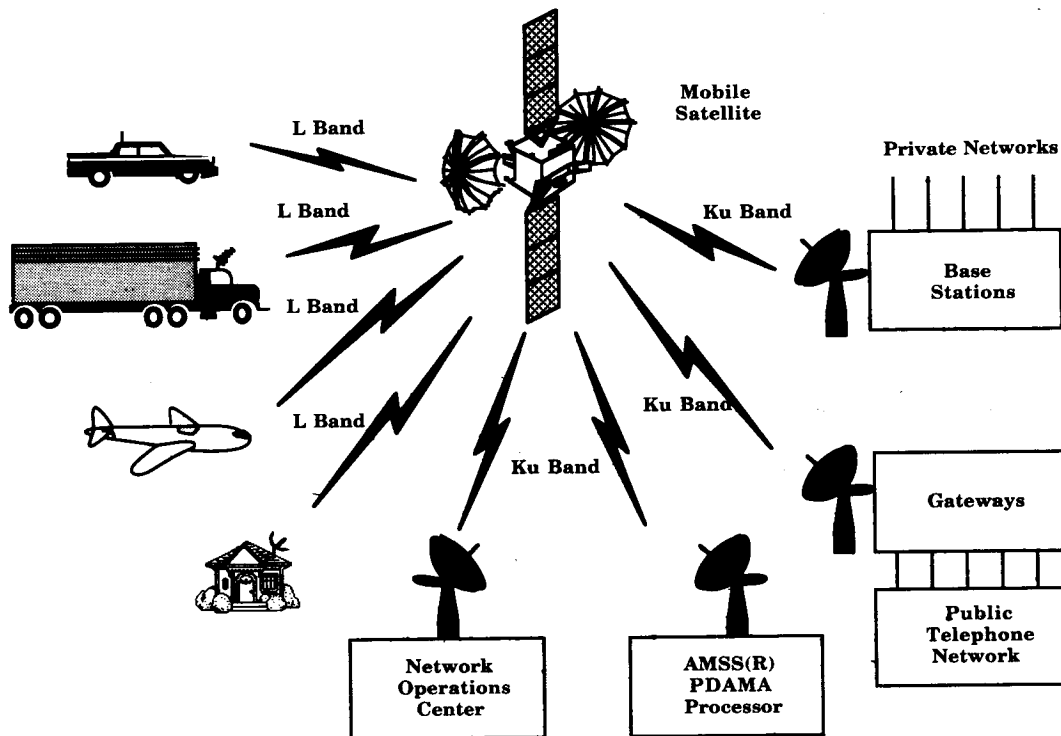


Figure 1. Network Configuration

The AMSC system uses L band frequencies for links between users and the satellite and K_u band for feeder links. All circuits are controlled by the Priority Demand Assignment Multiple Access (PDAMA) system and are routed to a K_u band gateway or base station.

All L band satellite circuits are connected to K_u band feeder link circuits in the satellite. L band-to-L band circuits require two satellite hops via a gateway or base station. There is no satellite path for direct single hop L band-to-L band circuits.

AMSC will construct and operate one K_u band Network Operations Center (NOC) for network monitoring and control. Satellite TT&C can be performed at this site or at another facility. AMSC will also operate two gateway stations for test and monitoring purposes. Operational gateway stations will be constructed and operated by common carriers purchasing space segment capacity from AMSC. Base stations will be used by private network operators.

As illustrated in Figure 1, the ground segment includes two primary classes of earth stations (user terminals and hub stations) and the Network Operations Center. These elements are described below.

User Terminals

Three classes of user terminals – mobile/omni, mobile/steered, and transportable – are required because users vary widely in average air time requirements, intended use, and their vehicle's characteristics. Communications between satellites and user terminals will be at L band.

Mobile/omni terminals will be the lowest cost terminals, but because of the low gain of omni antennas, a relatively high satellite EIRP is required for each channel. This results in high airtime charges. Mobile/omni land and maritime terminals will be able to use antennas with 3 to 6 dBi gain.

Mobile/steered terminal antennas must be actively pointed towards the satellite. This requires determining the position of the satellite relative to the vehicle, an antenna that is directional in azimuth, and a method for steering the antenna towards the satellite. These requirements result in a higher cost terminal, but also substantial reductions in airtime charges. Mobile/steered aeronautical, land and maritime terminals are expected to have antenna gains in the 10 to 14 dBi range.

When transportable terminals can be used, both terminal cost and airtime charges are minimized. Transportable antenna gain is expected to be in the range of 15 to 22 dBi.

All three user terminal classes will support voice and/or data service using ACSB or a variety of digital modulation formats. Terminal signalling and modulation standards will be developed in cooperation with manufacturers.

The PDAMA system will communicate with a micro-controller in each user terminal to dynamically allocate spectrum and network capacity to active terminals. Despite many functional differences, user terminals will share a common pool of 5 kHz channels for nearly all applications. All channels will be constructed of contiguous 2.5 kHz subchannel sets; every terminal will be capable of tuning to any center frequency in 2.5 kHz increments throughout the entire 14 MHz operating band.

All aeronautical terminals will have at least the "core" capability defined by ICAO, 1986. The core capability is a two-way 600 bps data link and is used for air traffic control. All aviation communications, including voice, will be digital.

The aircraft antenna is expected to be a phased array system including two high gain phased arrays looking abeam and mounted 45° from the horizon on each side of the aircraft, or a single high gain antenna mounted on the top of the fuselage or tail. In addition, a single low gain hemispherical antenna can be used with at least 0 dBi gain over 360° in azimuth, above 7° elevation for level flight. These antennas will be right hand circularly polarized with an axial ratio less than 6.0 dB.

Hub Stations

The AMSC network will consist of many semi-autonomous star networks. At the logical center of each star network will be a hub station. All user terminals will communicate through one or more hub stations. Hubs will be of two basic types: (1) gateway stations for interconnection of telephone and other traffic to the PSTN; and (2) base stations for termination of private networks at dispatch centers and monitoring and control sites. Like user terminals, all hub stations will be under the control of the NOC.

Hub stations will access the satellites through duplex K_u band feeder links. All hub stations will have frequency agile channel modems, each able to use any of the feeder link channels.

Gateways. Gateways will interconnect traffic with the public switched telephone network. They will typically have a capacity of 5 to 100 or more channels. AMSC expects that service providers will install gateways throughout the country. Traffic will be routed to a point of interconnection close to the final destination.

Base Stations. Hub stations used to terminate private network traffic are referred to as base stations. They are analogous functionally to base stations in the conventional private land mobile radio service. Private base stations differ in architecture from gateways only in that channels are not connected to the telephone network, except as required for private company communications. Instead, they will generally be interfaced with dispatch consoles or SCADA control stations. AMSC expects fleet operators to install a large number of K_u band base stations across the country.

Network Operations Center. The Network Operations Center (NOC) will communicate with all user terminals and hub stations through a K_u band RF subsystem consisting of frequency agile digital channel units. Precision time, referenced to the National Bureau of Standards, will be disseminated over the network control channels to synchronize the network and to provide a public service. In addition, MSS satellite ephemeris data and real-time information concerning the status of the Global Positioning System (GPS) satellites, Loran, and other navigation systems will be disseminated for use in integrated communications/surveillance networks.

PDAMA System

The Priority Demand Assignment Multiple Access (PDAMA) system controls access to the network. It monitors usage of channels and assigns channels to users. It coordinates assignment of channels in all beams on each satellite on a dynamic basis to minimize interbeam and intersystem interference. Channel assignments between user terminals and hub stations can be switched similar to the way in which cellular channels are dynamically allocated.

When a user originates a call, the user terminal communicates the call request to the PDAMA system on an L/ K_u band signaling circuit. The PDAMA system sets up the call using a K_u band common signalling circuit to the hub station serving the called party. After the called party answers, the PDAMA system sets up a duplex L/ K_u band circuit between the user terminal and the hub station. The PDAMA system monitors the call duration on a common signalling circuit using the K_u band link with the hub station.

When a call originates through a hub station, a similar sequence occurs. The station communicates the call request to the PDAMA system on a common K_u - K_u signalling circuit. The PDAMA system signals the user terminal on a K_u /L packet circuit. When the user terminal acknowledges, the PDAMA system assigns a duplex L/ K_u circuit to the call.

The entire 14 MHz allocation is available through each beam, maximizing the flexibility of the PDAMA system to dynamically respond to market variations between beams. While the same SCPC channel cannot ordinarily be reused in adjacent beams, frequencies can be reused in beams separated by at least one beam through the use of channel interleaving and interbeam isolation.

The central PDAMA processor will recognize different levels of message priority to ensure that air traffic control and other safety-of-life services receive certain access to network capacity whenever it is needed. Additional levels of priority will be used as needed in the various hub stations, according to the specific end use involved.

The PDAMA system will be implemented using a distributed control architecture, whereby specialized private networks, such as will be required for AMSS(R) networks, will have their own dedicated PDAMA processor and software. AMSC will establish interface standards that will enable private networks to operate nearly autonomously.

The central PDAMA processor and a gateway can be collocated with the TT&C equipment in the NOC, enabling common antennas for K_u band uplinks and downlinks.

Space Segment

The fully developed space segment will consist of three high performance satellites in geosynchronous orbit. The first satellite is anticipated to be launched in 1992.

To accommodate the market demand, it is anticipated that all satellites will employ 3-axis buses with 2500 watts prime payload power, weighing 1200 kg on orbit. The nominal launch mass, including apogee stage, is 2500 kg. Each satellite will have batteries sufficient for at least 25% service capability during eclipse.

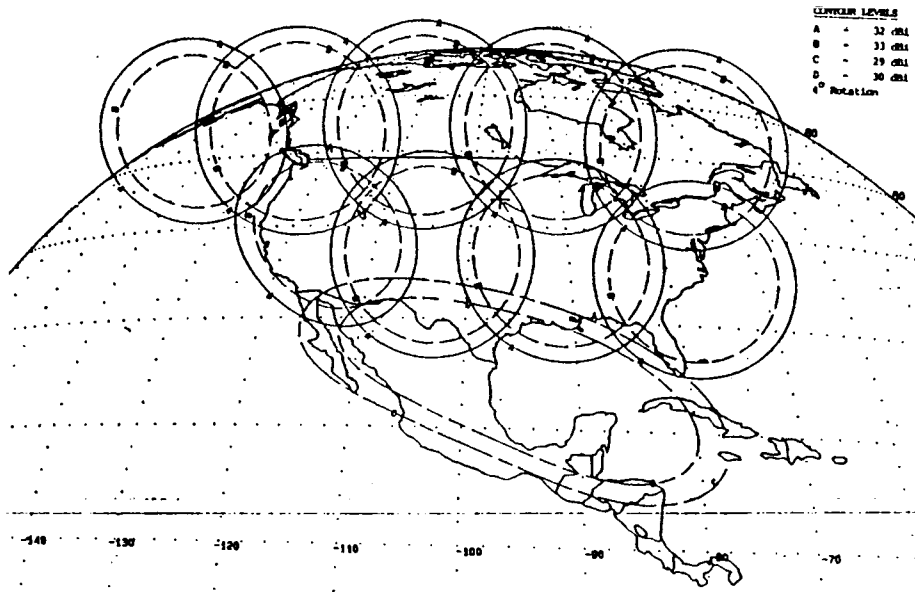


Figure 2. L Band Coverage, 101° W Orbit Location

A pair of 5.5 meter diameter unfurlable reflectors will each generate ten L band spot beams covering North America (see Figure 2). Separate transmit and receive antennas are used to minimize the effects of passive intermodulation (Hoerber, 1986). Maximum aggregate linearized L band Effective Isotropic Radiated Power (EIRP) of all beams is 60 dBW; L band G/T of each beam is 3 dB/K at edge-of-coverage.

AMSC has requested 75°, 101°, and 136° West Longitude orbital assignments. The Canadian MSAT satellite will be located near 106° W longitude. Frequencies at K_u band are 14.0 to 14.5 GHz (earth-to-space) and 11.7 to 12.2 GHz (space-to-earth); at L band, 1646.5-1660.5 MHz (earth-to-space) and 1545-1559 MHz (space-to-earth).

K_u band communications are subdivided into two groups: a K_u-K_u group and a K_u-L group. The K_u-K_u group is 10 MHz wide, including 5.0 MHz for initial operations and an additional 5.0 MHz for future expansion. The K_u-L group consists of 10 channels for use by the first spacecraft in each orbital slot, and 10 channels for an additional collocated spacecraft, if needed. Horizontal uplink polarization will be used by the U.S.; the opposite polarization will be used on the downlinks.

The AMSC satellites can be launched as a one-half payload on the Titan 3 or on another suitable launch vehicle.

NASA has offered to provide launch services to AMSC in exchange for mobile satellite capacity for MSAT-X activities. NASA includes a reservation for this launch in its current ELV manifest. NASA would use the mobile satellite capacity it would receive from AMSC for technology experiments and government demonstrations.

Table 1 shows a representative link budget for communications quality voice to an omnidirectional land mobile antenna.

Table 1. Example Link Budget for Omnidirectional Land Mobile Terminal

	<i>Hub-to-Mobile</i>		<i>Mobile-to-Hub</i>		
	<i>Uplink</i>	<i>Downlink</i>	<i>Uplink</i>	<i>Downlink</i>	
Frequency	14000	1549.5	1651.0	11700	MHz
Available RF Power (dBW)	10.0	28.1	3.0	13.0	dBW
Power Amplifier	10.0	640.0	2.0	20.0	Watts
Power Loss	-2.0	-1.8	-1.0	-1.0	dB
Transmit Antenna Gain	51.8	33.8	4.0	25.0	dB _i
EIRP	59.8	60.1	6.0	37.0	dBW
Capacity	1	2650	1	2650	Erlangs
Voice Duty Cycle	35	35	35	35	Percent
EIRP/Channel	64.4	30.4	10.6	7.3	dBW
Path Loss	-207.41	-188.29	-188.84	-205.85	dB
Polarization Loss	-0.5	-0.5	-0.5	-0.5	dB
Receive Antenna Gain	25.0	4.0	33.8	50.1	dB _i
Data Rate	4800	4800	4800	4800	bps
E_b	-155.4	-191.2	-181.8	-185.7	dBW/Hz
Receiver Temperature	480.0	190.0	900.0	385.0	°K
Antenna Noise	290.0	100.0	290.0	40.0	°K
Total Thermal Noise	28.9	24.6	30.8	26.3	dBK
G/T	-3.9	-20.6	3.0	23.8	dB/K
Thermal Noise Density, N_0	-199.7	-204.0	-197.8	-202.3	dBW/Hz
IM NPR	20.0	15.0		20.0	dB
E_b/N_0	44.4	12.8	16.1	16.6	dB
I_0 From Other Systems	-300.0	-250.0	-250.0	-250.0	dBW/Hz
E_b/IM Level	58.2	19.0		37.3	dB
Uplink E_b/N_0		39.3		16.1	dB
K_u Fade Margin	5.0			5.0	dB
Combined $E_b/(N_0+I_0)$	39.3	11.8	16.1	10.2	dB
$E_b/(N_0+I_0)$, Minimum		8.9	8.9	8.9	dB
M=Modem Implementation Loss		0.9	0.9	0.9	dB
$(E_b/(N_0+I_0))_{min} + M$		9.8	9.8	9.8	dB
Total Margin		2.0	6.3	0.4	dB

SERVICES

A variety of services will be offered to the users. Each service will be optimized for a particular set of user criteria. Examples of optimization criteria include: antenna cost, installation cost, usage charge, and voice quality. Similarly, aeronautical services will have their own specific requirements as defined by ARINC characteristics 741 and by ICAO/FANS. Several areas of technology are experiencing rapid development, such as

digital speech processing. By the time system implementation is complete, it is expected that 4.8 kbps digitally encoded voice or ACSB will be adequate for most applications.

Position location will be available through the AMSC system through the use of Loran-C receivers, integrated MSS/GPS receivers or satellite ranging.

With the addition of a GPS processing board and the use of differential transmissions sent through the AMSC system, an integrated MSS/GPS transceiver can estimate its position to within 5 m.

Satellite ranging techniques will enable location of mobiles within a fraction of a mile with only minimal modifications of the mobile transceiver once multiple satellites are in orbit (Anderson, 1979 and 1980).

ACKNOWLEDGEMENTS

Ken Renshaw and Tim Murphy of Hughes Aircraft Company, Dean Garth of Hughes Communications, and Roy E. Anderson of Mobile Satellite Corporation made significant contributions to this paper. Figure 2 was provided by Spar Aerospace.

REFERENCES

- Anderson, R.E., et. al., 1979. Land Mobile Communications and Position Fixing Using Satellites. IEEE Transactions on Vehicular Technology. VT-28, No. 3, pp. 153-170, August 1979.
- Anderson, R.E., et. al., 1980. Position Surveillance Using One Active Satellite and Time-of-Arrival of a Signal from an Independent Satellite. Navigation. Vol. 27, No. 4, pp. 305-317, Winter, 1980-1981.
- Hoerber, C. F., et. al. 1986. Passive Intermodulation Product Generation in High Power Communications Satellites. Paper 86-0657 in AIAA 11th Communications Satellite Conference, San Diego, March 11-20, 1986.
- ICAO 1986. International Civil Aviation Organization special Committee on Future Air Navigational Systems, Third Meeting, 3-21 Nov. 1986 Report.

NASA'S MOBILE SATELLITE DEVELOPMENT PROGRAM

DR. WILLIAM RAFFERTY, Jet Propulsion Laboratory, United States;
DR. KHALED DESSOUKY, Telos Aerospace Systems, United States;
MILES SUE, Jet Propulsion Laboratory, United States.

JET PROPULSION LABORATORY
California Institute of Technology
4800 Oak Grove Drive 238-420
Pasadena, California 91109
United States

ABSTRACT

A Mobile Satellite System (MSS) will provide data and voice communications over a vast geographical area to a large population of mobile users. This paper provides a technical overview of the extensive research and technology studies and developments performed under NASA's mobile satellite program (MSAT-X) in support of the introduction of a U.S. MSS. The paper emphasizes the critical technologies necessary to enable such a system: vehicle antennas, modulation and coding, speech coders, networking and propagation characterization. Also proposed is a first, and future, generation MSS architecture based upon realized ground segment equipment and advanced space segment studies.

1. INTRODUCTION

NASA's involvement in mobile satellite communications can be traced back to the late 1970's. Around that time, NASA initiated system feasibility studies culminating in land mobile field tests using trucks and the ATS-6 experimental satellite. The studies and tests demonstrated the practicality of such a satellite link and were subsequently followed by market studies which led to the petitioning of the FCC by NASA for a mobile satellite system (MSS) frequency allocation in the UHF band. The NASA petition, and its active advocacy of MSS, then generated much interest in the private sector which resulted in the filing for developmental MSS licenses, and the eventual formation of a U.S. MSS Consortium.

In 1983, the Jet Propulsion Laboratory was designated by NASA as the lead center for MSS studies and critical technology identification and development under the Mobile Satellite Experiment (MSAT-X) program. Through this program it is intended to develop and demonstrate advanced ground and space segment technology to accelerate the introduction of a first generation, commercial mobile satellite system. This would be

achievable by the timely transition of high-risk critical technologies to industry. To ensure the economic viability of MSS, the research has as a general goal the development of technology which will enable low cost equipment for end users.

Throughout the program, JPL has tried to maintain a balance between general MSS studies and certain focused areas of technology development. These technology areas evolved out of the early system studies and are considered crucial to the eventual success of MSS. Thus, MSAT-X has proceeded with a nucleus around which the MSS concept could be developed and demonstrated. The core technology areas, all of which emphasize efficient utilization of scarce resources (power, frequency spectrum and orbital slots) are:

- o vehicle antennas,
- o near-toll-quality digital speech,
- o modem design,
- o networking and multiple access techniques, and
- o mobile satellite channel characterization and modeling.

MSAT-X is a multi-faceted program: this paper, and the other MSAT-X papers presented in this conference, are only capable of presenting the major findings. In an effort to make the material readily accessible, this paper concentrates on a baseline system concept which is firmly rooted in realized hardware. This requires certain system architecture assumptions, which are outlined in the body of the paper.

The paper will identify the MSS elements and propagation environment; elaborate on the critical technology areas; touch on testing and validation; and present MSS configurations based principally on the ground segment technology and system studies performed to date.

2. MSS ELEMENTS AND ENVIRONMENT

MSS is a satellite based communication network that provides voice and data communications to mobile users over a vast geographical area. The relay satellites in geosynchronous orbit permit an extremely large coverage area. The type of service provided is particularly suited to low density or rural areas and augments the terrestrial systems which are economical in localized areas. The services envisioned for MSS include two-way voice, two-way interactive data communication, and one-way data as in dispatch operations, position determination or data base query.

The MSS network concept is depicted in Fig. 1. The Network Management Center (NMC) oversees the operation of the network and performs vital functions such as answering requests for channel assignment, setting up call routes, billing, etc. The gateways are terminals that provide interfaces between the MSS and other networks such as the Public Switched Telephone Networks (PSTN). The base stations are not necessarily connected to other networks and are normally centers for dispatch operations.

The two other key elements in MSS are the mobile terminal (MT) and the satellite(s). The mobile operates in a hostile environment where multipath from terrain exists together with shadowing from trees or obstacles. The MT is located within the mobile vehicle and comprises the radio, antenna, and user interface. This equipment is constrained to be low-cost and small in size to ensure a wide customer base and

economic viability of the resulting MSS. The spacecraft, on the other hand, is limited by the feasible technology and evolves in steps or generations. As new technology becomes available, new spacecraft will be used to support the expected growth in MSS.

3. TECHNOLOGIES DEVELOPED UNDER MSAT-X

Although the choice of technologies to be developed under MSAT-X emphasized those that would be applicable to more than one MSS architecture, a broad MSS conceptual design had to be formulated to create a cohesive framework for the development. A system concept evolved out of JPL and NASA/contractor studies performed in the early eighties [Naderi 1982; TRW 1983; G.E. 1983]. A system based on FDMA combined with spacecraft that utilize multibeam technology to effect frequency reuse was adopted. Although architectures based on CDMA or TDMA cannot be dismissed without thorough analysis, they have drawbacks in the MSS environment which made them unattractive [Dessouky and Sue 88].

In conjunction with the FDMA architecture, studies have shown that a basic 5 kHz channel bandwidth is optimum for MSAT-X. This choice matched the selection of 4800 bps near-toll-quality vocoded voice, and represented the challenging goal of achieving a 1 bps/Hz modulation/coding throughput on the multipath channel with small inexpensive mobile terminals-- a heretofore unrealized feat.

The development effort in all areas (vehicle antennas, modulation/coding, speech compression and networking) is aimed at realizing working hardware/software that can be demonstrated reliably in the field. In parallel, better characterization of the propagation channel and its effects has been pursued. In what follows the salient achievements in the four technology areas and propagation modeling are highlighted.

Vehicle Antennas

Early in the MSAT-X program low gain antennas (LGA's) were investigated [Naderi, et al. 1984]. LGA's can provide up to 5 dBi in gain. An example is the crossed-drooping dipole antenna which provides 3.3 to 4.8 dBi for the desired elevation angles between 20 and 60°, with the minimum being at 20°. Preliminary tests have shown that a MT receiver (receiver noise figure = 0.86 dB) equipped with such an antenna would have a G/T of about -20 dB/K. The advantages of LGA's are their very low cost and simplicity. Their disadvantages are: 1) low gain, which creates a power burden on the satellite and may lead to the need for high risk spacecraft development; 2) susceptibility to multipath from near the horizon; and 3) because of their wide beams, the inability to support orbit reuse which will likely be needed to support the capacity of a mature MSS (see Section 5).

Motivated by the need to support orbit reuse and increase the vehicle antenna gain, medium gain antennas (MGA's) were developed. Three types of arrays were considered: mechanically steered tilted linear array, conformal electronically steered phased array, and planar mechanically steered array. Because of the low profile of these antennas and the presence of the conducting ground plane (car top), the most difficult challenge for these antennas is attaining the desired minimum gain at low elevation (i.e., at 20°).

A breadboard for the mechanically steered linear array with its pointing system was developed in-house at JPL. Two contractors, Teledyne Ryan Electronics (TRE) and Ball Aerospace, have developed and delivered breadboards of the phased arrays antennas. Photographs of the two phased arrays mounted on vehicles are shown in Fig. 2. The two contractors' antennas meet the very demanding MSS requirements with varying success. The important characteristics of the MGA breadboards are summarized in Table 1; as can be seen, the TRE phased array currently exhibits better RF and physical characteristics. Consequently, it is the likely candidate for further refinement. A major area requiring improvement is the insertion loss. Reducing the internal loss contributes to increasing the G/T (receiver gain to effective noise temperature) through both raising G and reducing T. One of the main thrusts for the continuing work in the phased array area will be achieving a higher G/T. Improvements in G/T of more than 1 dB can be expected. Finally, as a middle ground between the lower cost of the linear array and the conformity of the phased array, a planar mechanical array is presently being developed by TRE. Again, higher gain and G/T are design goals.

Modulation/Coding

The spectrally efficient schemes of MSK and GMSK were first investigated for MSAT-X and a practical DGMSK modem was implemented for 2400 bps [Davarian, et al. 85]. With the shift to 4800 bps speech compression, attention was redirected towards combined modulation/coding schemes that, in addition to enhanced spectral efficiency offer improved power performance on the fading channel. After consideration of a number of coding and detection schemes, including pilot-aided modulation techniques, research revealed that for the MSAT-X environment at L-band rate $2/3$ 16-state trellis-coded differentially-detected 8PSK (TCM/D8PSK) with 100% root raised-cosine pulse shaping yields the best performance [Simon and Divsalar 87, Rafferty and Divsalar 88]. Interleaving is essential on fading (bursty) channels when trellis encoding is used. Only limited interleaving is possible because of a 60 ms delay constraint imposed for voice. Simulation was used to establish that under such a constraint the best block interleaving is 128 symbols (8PSK) with 16 symbols in depth by 8 in span with a buffer size of 32.

Fig. 3 together with Table 2 give comparisons of TCM/D8PSK with other schemes considered. No timing jitter or ISI are considered in these results. Yet, tests of the TCM/D8PSK modem developed at JPL on the hardware fading channel simulator have exhibited less than 1 dB deviation from theory. This has been a positive result that has lent confidence in TCM/D8PSK.

Speech Coding

It was realized early in the MSAT-X program that speech quality acceptable to the public could not be achieved at 2400 bps. The goal then became the attainment of near-toll quality (telephone) at 4800 bps with an inexpensive, compact speech coder through outside contract development.

Two research and development contracts were awarded: one to the University of California at Santa Barbara (UCSB) and the other to Georgia Institute of Technology (GIT). Both contractors have now developed speech coders based on the classical Linear Predictive Coding

(LPC) model for human speech. Each contractor has derived a new class of algorithms for modeling the excitation sequence to be used in conjunction with the LPC. Other notable contributions in this area have been in the reduction of algorithm complexity and LPC parameter quantization. Realization of the delivered coders has been based on general purpose DSP chips. For example, both contractors' coders require a 4 Mips processor which could readily be transferred into a low cost, custom chip set. Both speech coders have achieved good speaker identification and naturalness, intelligibility is "fair" and algorithm refinements are still on-going.

Networking

The objective in the networking area has been to develop a protocol that meets the unique needs of the MSS environment. A novel demand-assigned time-multiplexed FDMA scheme was developed at JPL to integrate voice and data services [Li and Yan 84], namely, the Integrated Adaptive Mobile Access Protocol (I-AMAP). Over the years since 1984 the protocol has been undergoing continuous refinement. At present it uses slotted ALOHA for connection requests and includes the appropriate error control techniques, such as request packet replication, acknowledgments, etc. [Wang and Yan 87].

The original intention was to test the algorithm through an operational network. It was soon discovered that the software development would be very costly [Signatron 85]. The development work was therefore limited to a controlled laboratory environment. The packet format for both the network level and link level has been specified [Wang and Yan 87] and has shown robust performance in the simulated environment.

Recently, a free-access, tree-type protocol has been developed for the connection-request procedure. It promises a stable useful throughput at least 30% above slotted ALOHA. This algorithm will also be tested and validated on the network test-bed simulator at JPL.

Propagation

Research efforts here have focused on obtaining more accurate propagation models for the MSS environment. A wide range of experiments have been performed to obtain vital channel characteristics including signal attenuation statistics, fading rate, depth and duration statistics, doppler spread, tree attenuation, and scattering from road-side objects. Two critical results have emerged. The first is implicit in the curves shown in Fig. 4 [Vogel and Goldhirsh 87, Bostian 87]. It indicates that although multipath can be significant and result in as much as 8 dB attenuation, foliage shadowing is the dominant cause of degradation, with at least 8 dB more attenuation than multipath alone. The second result [Vogel and Hong 87] indicates that multipath effects restrict the usable bandwidth to a few tens of kHz (for specified acceptable amplitude variations over the channel bandwidth). The two results are significant: the first reaffirms the premise that MSS will be a line-of-sight (LOS) system for voice links, and the second supports the choice of FDMA as opposed to CDMA or TDMA.

The data obtained from the propagation experiments and analysis are being continually incorporated into software simulations and the hardware channel simulator developed at JPL.

4. TECHNOLOGY VALIDATION

A major objective of the MSAT-X project has been the field testing of all critical mobile satellite equipment developed within the program. A sequence of Pilot Field Experiments (PiFEx) was introduced as means to evaluate MSAT-X equipment on an incremental basis. The use of such a testing strategy has been necessary because a true MSS satellite will not be available before the early 1990's.

An essential component in system demonstration is the presence of a MT framework capable of integrating and supporting the different equipment developed. Consequently, a considerable effort at JPL went into developing a MT architecture, subsystem interface definitions, and supporting hardware.

The architecture of the MT is shown in Fig. 5 [Cheetham 87]. The architecture is modular to accommodate continued subsystem evolution, and is centered around the terminal processor. The terminal processor serves as the master controller of the terminal. It implements the networking protocol, supervises the operation of the subsystems and their interfaces, and is capable of taking real-time decisions to ensure the integrity of the link.

Another key subsystem in the MT is the RF transceiver. A breadboard transceiver has been developed at JPL to meet the unique MSAT-X requirements [Parkyn 88]. The transceiver is capable of receiving two channels (one for data and one for the pilot reference signal), which are settable within the desired L-band frequency range. It also tracks doppler shifts in the received pilot and provides the necessary control signals for the antenna pointing subsystem.

To support the performance of the PiFEx experiments, JPL also developed a mobile terminal laboratory housed in a Propagation Measurement Van (PMV) [Emerson 87]. Creation of the mobile laboratory involved integrating the test equipment with the mobile terminal and/or its subsystems, plus the development of a Data Acquisition System (DAS) with its elaborate software. The PMV has been used extensively in the field experiments and will continue to be invaluable to the validation of MSS technology.

The early PiFEx experiments that have been conducted have, for example, demonstrated the viability of the vehicle antennas and their ability to acquire and track the transmitted reference pilot while the vehicle is moving. Present plans call for PiFEx experiments that will test the end-to-end link and all subsystem technologies developed and as yet not validated in the field.

5. MSS CONFIGURATION

Multibeam frequency reuse technology provides a means to maximize spectrum utility and is expected to be employed by MSS. The extent of frequency reuse is related to the size of the spacecraft antenna. Because of market and economic considerations, extensive frequency reuse is not expected until later generations. The following is a brief description of a possible system design for a first and second generation MSS.

5.1 First-Generation Satellite

Using a commercial high-power communications satellite bus, the first-generation MSS design would call for two 14-ft. (4.2 m) L-band multibeam antennas, one for transmit and the other receive. Separate transmit and receive antennas alleviate the potential problem of passive intermodulation generation. Four beams will be needed to cover CONUS and some coastal areas (Fig. 6). For the backhaul link, a 0.4-m ku-band antenna will generate a single beam covering CONUS. The satellite would have G/T values of 9.2 and 4.0 dB/K for the L- and Ku-bands, respectively. It would also have a 5000-lb GTO mass and 3 kW of spacecraft power. The number of channels and number of users that this satellite can support (and consequently the required spectrum) depend on several factors, viz., channel duty cycle, traffic mix, and service quality. For a service quality with 2% blocking probability and 3.2 sec. message delay, an assumed user traffic requirement of 1 90-sec. voice call or 1 4096-bit data message per hour per user, and assuming 40% of the traffic is attributable to voice, the satellite would support 1900 channels. These channels would be partitioned, according to the I-AMAP protocol, into 204 voice channels, 260 channels, and 1465 reservation channels. (The seemingly large number of reservation channels could be reduced if a longer delay can be tolerated.) This partitioning results in a total of 89,000 users being accommodated by one satellite, corresponding to approximately 50 users per channel.

A limited frequency reuse (by a factor of 4/3) can be achieved by the 4-beam system by re-using the same frequency in the two outer beams. Coupled with the bandwidth-efficient modulation that enables the transmission of 4.8 kbps in a 5-kHz channel, the system can potentially achieve 1.28 bps/hertz efficiency. Fig. 6 shows the satellite footprint. Table 3 briefly summarizes the link design, which is based on existing MSAT-X technologies, viz., medium gain antenna with 9.9 dBi gain at 20° elevation, low-noise amplifier with 0.86 dB noise figure, and a low-loss (0.6 dB) diplexer with 90 dB isolation.

5.2 Second-Generation Satellite

By employing a larger antenna, a second-generation satellite would achieve more extensive frequency reuse and provide higher capacity. Studies have indicated the feasibility of employing a 15-m mesh deployable on a high-power commercial satellite bus (Figs. 7 and 8, [FACC 85; RCA 85]. A 15-m system has been designed for generic MSS applications [Sue 87]. Such a satellite would generate about 30 spotbeams (Fig. 9), reuse the available spectrum 4 times, and would have a potential spectral efficiency of 4.1 bps/hertz. The satellite would weigh about 6200 lb at GTO, have 3.7 kW of spacecraft power, support about 12,000 channels, and serve hundreds of thousands of users.

6. CONCLUSION

NASA's MSAT-X is a research and technology development program aimed at establishing a sound technical basis for the introduction of a U.S. mobile satellite system. The studies performed and the technology developed and tested to date clearly demonstrate the feasibility of such a system. Moreover, by maintaining a firm grasp on the overall system requirements and applications, it has been possible to cast the

subsystem elements in a first, and a future, generation MSS configuration with a high degree of confidence. The on-going field tests play an essential role in the incremental testing of system concepts and technology and their refinement. In the absence of a true MSS satellite, MSAT-X has strived, with a large measure of success, to establish meaningful alternatives to validate the system concepts and recommendations which have evolved out of the program.

Near term MSAT-X activities include the continued validation and evaluation of developed technology and system concepts and their transfer to industry. In addition, an experimental government agency network configuration is under consideration which would make use of channel capacity on a U.S. MSS.

The viability of a commercial MSS is dependent on many technical, economical, and social factors. NASA, through its various mobile satellite programs, continues to be a strong advocate for MSS and satellite communications in general.

REFERENCES

- C. Bostian, "Propagation Studies Related to LMSS," Proceedings of NAPEX XI (JPL Internal Document D-4647), Jet Propulsion Laboratory, Pasadena, California, August 31, 1987.
- C. Cheetham, "The Terminal Processor: The heart of the Mobile Terminal," MSAT-X Quarterly Report No. 12, October 1987.
- F. Davarian, et al., "DMSK: A Practical 2400-bps Receiver for the Mobile Satellite Service," Msat-X Report, JPL Publication 85-51, June 15, 1985.
- K. Dessouky and M. K. Sue, "MSAT-X: A Technical Introduction and Status Report," JPL Publication, to be published in Spring 1988.
- R. F. Emerson, "Pilot Field Experiments," Proceedings of NAPEX XI (JPL Internal Document D-4647), Jet Propulsion Laboratory, Pasadena, California, August 31, 1987.
- V. Li and T-Y. Yan, "An Integrated Voice and Data Multiple-Access Scheme for a Land-Mobile Satellite System," IEEE Proceedings, Vol. 72., No. 11, November 1984.
- F. Naderi, Editor, "Land Mobile Satellite Service (LMSS): A Conceptual System Design and Identification of the Critical Technologies," Part II, Technical Report, JPL Publication 82-19, Feb. 15, 1982.
- F. Naderi, et al., "NASA's Mobile Satellite Communications Program; Ground and Space Segment Technologies," Proc. 35th Annual International Astronautics Federation Congress, Lausanne, Switzerland, October 1984.
- J. Parkyn, "L-Band Receiver for MSAT-X," MSAT-X Quarterly No. 13, (Special Issue on PiFEX Tower-1 Experiments), January 1988.
- M. K. Simon and D. Divsalar, "The Performance of Trellis Coded Multilevel DPSK on a Fading Mobile Satellite Channel," JPL Publication 87-8, June 1, 1987.
- W. Rafferty and D. Divsalar, "Modulation and Coding with Doppler Estimation for Land Mobile Satellite Channels," To be presented at IEEE International Conference on Communications, June 1988.
- M. K. Sue, "A High-Capacity Aeronautical Mobile Satellite System," Proceedings of the 37th IEEE Vehicular Technology Conference, June 1987.

- W. Vogel and J. Goldhirsh, "Multipath Measurements at L-Band and UHF in Mountainous Terrain for Land-Mobile Satellite System," Proceedings of NAPEX XI (JPL Internal Document D-4647), Jet Propulsion Laboratory, Pasadena, California, August 31, 1987.
- W. Vogel and U. S. Hong, "Measurement and Modeling of Land Mobile Satellite Propagation at UHF and L-band," Proceedings of NAPEX XI (JPL Internal Document D-4647), Jet Propulsion Laboratory, Pasadena, California, August 31, 1987.
- C. Wang and T-Y. Yan, "A Simulator for the MSAT-X Request Channel," JPL MSAT-X Quarterly, No. 12, October 1987.
- C. C. Wang and T-Y. Yan, "Performance Analysis of An Optimal File Transfer Protocol for Integrated Mobile Satellite Services," Globcom, Nov. 1987, Tokyo, Japan.
- FACC, 1985. "Spacecraft Configuration Study for the Second Generation Mobile Satellite System," Final Report Prepared By Ford Aerospace and Communications Corporation Under Contract to JPL, January 1985.
- GE, 1983. "Mobile Radio Alternative Systems Study- Vol. 3: Satellite/Terrestrial (Hybrid) Systems Concepts," GE Technical Report, Prepared for NASA Lewis Research Center, June 1983.
- RCA, 1985. "Spacecraft (Mobile Satellite) Configuration Design Study," Final Report Prepared By RCA Astro Electronics Under Contract to JPL, June 1985.
- Signatron, 1985. "MSAT-X Networking System Study Final Report- Vol. 1: A Feasibility Assessment of I-AMAP," JPL Publication 9950-1198, 8 June 1985.
- TRW, 1983. "Mobile Communications Satellite Systems," Vol. 2, TRW Tech. Report, Prepared for NASA Lewis Research Center, April 11 1983.

Table 1. Salient Characteristics of Medium Gain Antenna Breadboards
 *: Averaging gains over 8 azimuth beam positions.
 #: Height of mechanical linear array to be reduced to 4.5"

	JPL Mech. Tilted Linear Array	TRE Phased Array	Ball Aerospace Phased Array
	-----	-----	-----
Average* Recv. Gain (1545 MHz) dBi			
20° elev.	10.0	9.9	8.2
40° elev.	11.5	11.3	11.6
60° elev.	10.0	12.8	11.5
Av.* Transmit Gain (1660 MHz) dBi			
20° elev.	10.0	7.8	8.1
40° elev.	12.0	10.1	11.4
60° elev.	10.0	12.2	12.4
Av.* Recv. Sys. G/T at 20° (Rcvr NF=.86) dB/k	-15.2	-15.4	-16.7
Acquisition Time sec.	15	< 10	< 10
Track. Interf. to data			
AM dB (p-p)	negligible	1.5	1.5
PM deg (p-p max)	negligible	15	37
Size (ht. " x diam.)	9.0# x 20.0	0.7 x 20.7	1.3 x 24.0
Est. Manfctng. Cost	\$600	\$1848	\$1610

Table 2. Comparison of the performances of TCM/D8PSK, DQPSK and DGMSK under typical MSS link conditions. (No ISI or timing jitter.)

	EB/NO (@ 1E-3) (K=10; 40 Hz doppler spread)	Relative BW (main lobe, also 99.9% BW)
DQPSK	12.2	1
DGMSK BT=.5	13	1.6
TCM/D8PSK (R=2/3; 16-state 128 8PSK Symbol Interleaving)	9.5	1

Table 3. Link Budget for First-Generation MSS (Assuming TCM/D8PSK at 1E-3 BER)

	FORWARD LINK		RETURN LINK	
	GRND-SAT	SAT-USER	USER-SAT	SAT-GRND
XTMR POWER, WATTS	1.0	0.8	1.6	0.1
ANTENNA GAIN, DBI	49.6	33.7	7.8	31.2
EIRP, DBW	47.6	31.1	8.5	19.7
PATH LOSS, DB	-206.9	-188.3	-188.9	-205.8
RECEIVE G/T, DB/K	4.0	-15.4	9.2	21.0
RECEIVE C/No, DB/HZ	66.3	51.9	53.2	56.7
OVERALL C/No, DB/HZ	--	51.1	--	51.1
REQUIRED C/No, DB/HZ	--	47.8	--	47.8
REQUIRED EB/No, DB	--	11.0	--	11.0
MARGIN, DB	--	3.3	--	3.3

ORIGINAL PAGE IS
OF POOR QUALITY

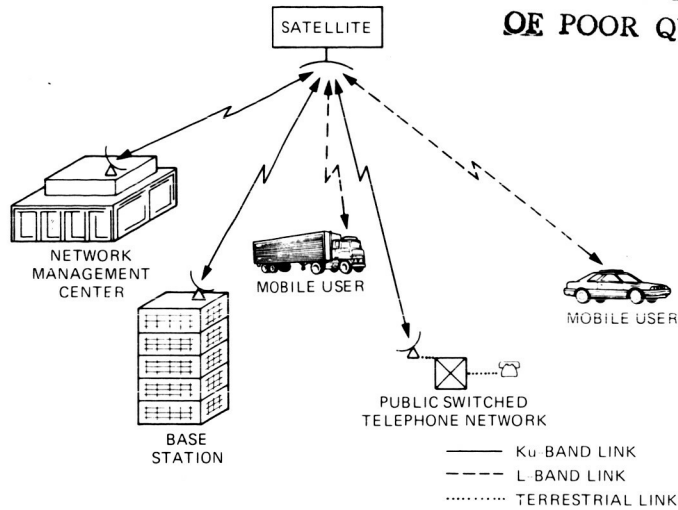


Fig. 1. Mobile Satellite Network Concept



BALL DESIGN



TELEDYNE DESIGN

Fig. 2. MSAT-X Phased Array Antennas Mounted on Vehicles

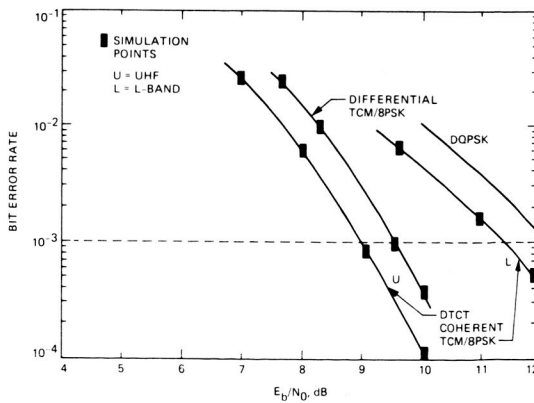


Fig. 3. Comparison of TCM/D8PSK With Coherent TCM/8PSK (Using DTCT With Noisy Pilot) and DQPSK at UHF and L-Band

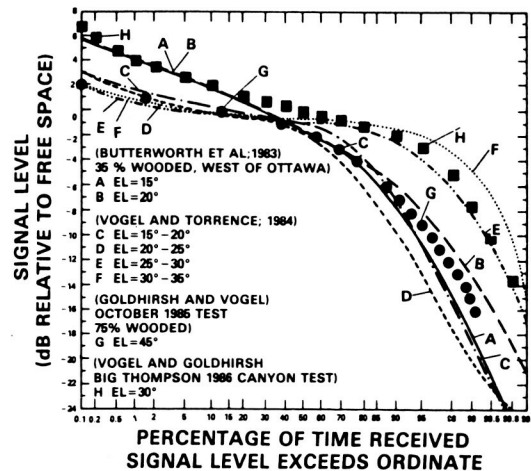


Fig. 4. Cumulative Signal Level Distribution for Various Geographical Locations and Elevation Angles. (See [Bostian, 87] for References Cited.)

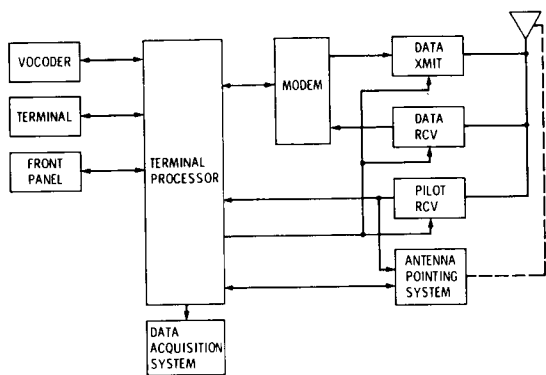


Fig. 5. Mobile Terminal Block Diagram

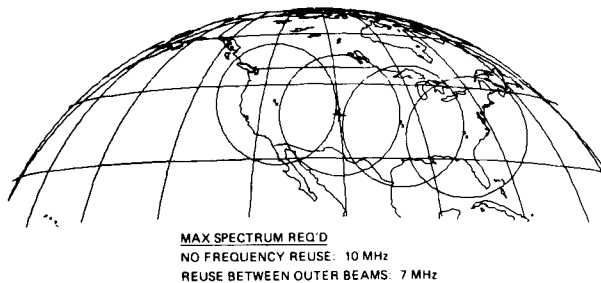


Fig. 6. A First Generation Satellite Beam Layout (Courtesy of Dr. Vahraz Jamnejad)

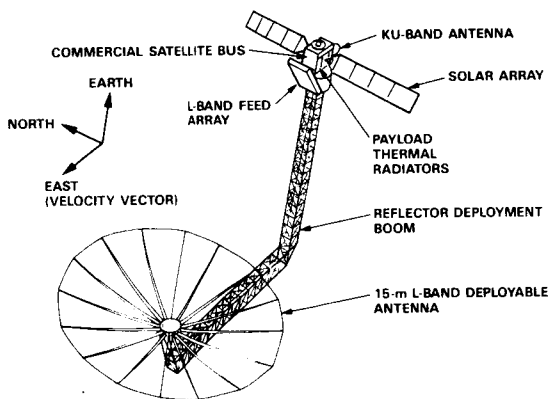


Fig. 7. On-Orbit Spacecraft Configuration (Second Generation) (FACC Design)

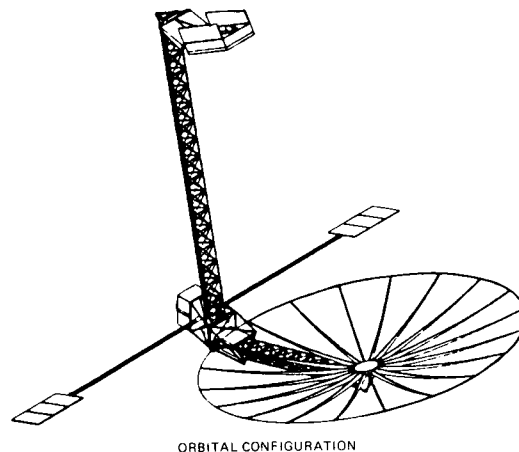


Fig. 8. On-Orbit Spacecraft Configuration (Second Generation) (RCA Astro-Electronics Design)

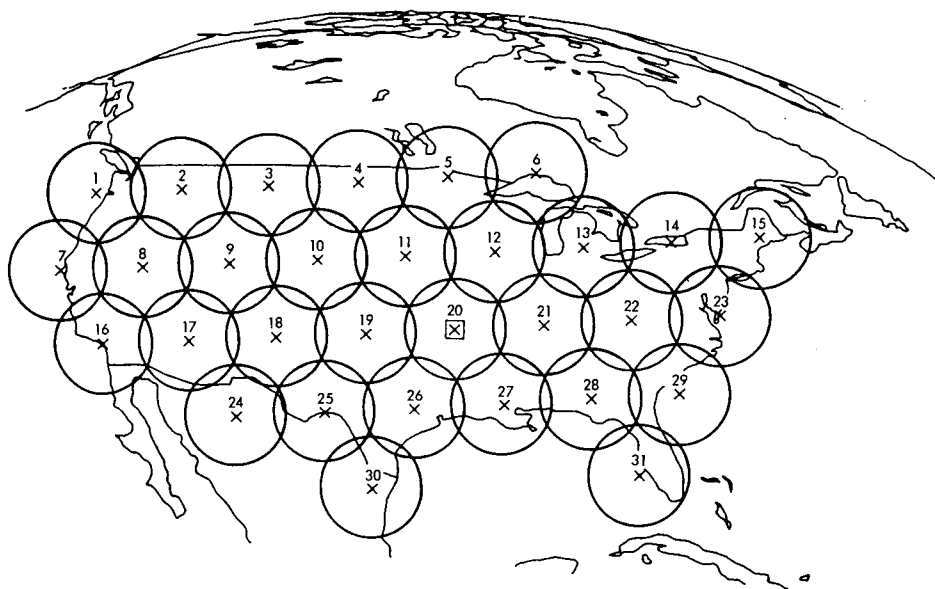


Fig. 9. A Second Generation Satellite Beam Layout

MOBILE SATELLITE SERVICE FOR CANADA

DAVID SWARD, Satellite Services Planning and Development, Telesat Canada

TELESAT CANADA
333 River Road
Vanier, Ontario
K1L 8B9
Canada

ABSTRACT

Canada has a market in search of a technology. The communications needs of industry, governments, and individuals have forced the development of unique technological solutions to overcome geographical and environmental barriers. A mobile satellite system is a key element in extending voice and data telecommunications to all Canadians. In order to realize this goal, the Federal Government and Telesat Canada have developed the MSAT system and made substantive commitments towards its implementation. This paper describes the MSAT system and a special program designed to provide interim mobile satellite services (IMSS) during the construction phase of MSAT.

INTRODUCTION

Pressures on business for improved productivity as well as growing demands for public safety services have resulted in a requirement for improved mobile communications with respect to coverage, reliability, and capacity. To date, the communications industry has responded to this need through the deployment of many separate terrestrially-based mobile communications networks. These networks, for economic reasons, are largely concentrated in and around urban centers and along major transportation corridors. Mobile communications satellites offer the opportunity to cost-effectively extend mobile services into rural and remote areas, thus paralleling the initial mission of fixed satellites in the early and mid-1970's.

Mobile communications satellites are not new from a technological standpoint. In addition to the international maritime mobile satellite system operated by INMARSAT, there have been numerous military and experimental mobile satellites launched since the early 1970's. The increasing importance and expanding market demand for extended mobile communications however has now developed to the point in North America that domestic mobile satellite systems can be seriously contemplated and supported on a stand-alone commercial basis.

With the introduction of the Canadian domestic mobile satellite service (MSAT) in the early 1990's, Canadians will enjoy the benefits of a truly ubiquitous mobile communications service encompassing land marine and aeronautical applications. Such benefits could also be extended to the countries that may never be able to justify their own dedicated system through the use of existing international mobile satellite authorities. Through effective co-operation between both international and domestic operators the benefits offered by mobile satellites can be expanded to all with interest in exploiting this technology.

SYSTEM DESCRIPTION

The current MSAT system concept consists of two satellites, one Canadian and one American, scheduled for launch in early 1992. The satellites are to be located in geostationary orbit at a nominal longitude of between 106° and 113° West. Each satellite will have the capability to provide back-up services to the other in case of satellite malfunction, as well as provide services to mobile users who move from one country to another. Figure 1 shows a typical Canada/U.S. co-operative system configuration.

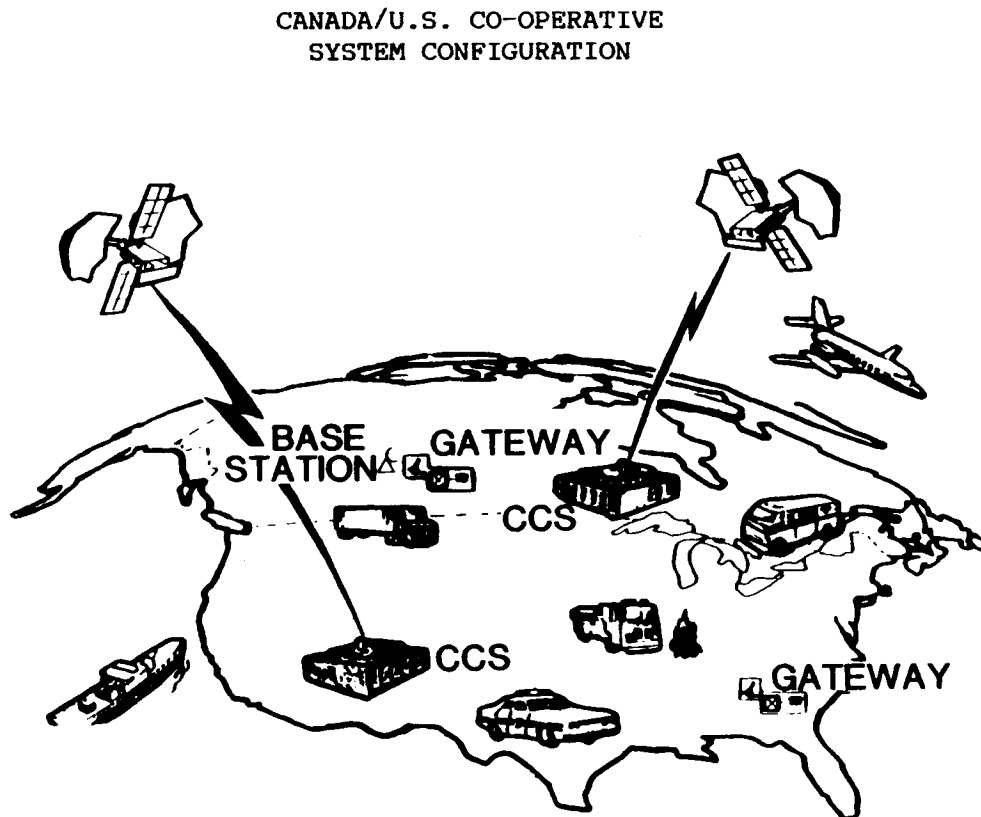


Figure 1 - Mobile Satellite Systems Serving Canada and the U.S.

At the recent World Administrative Radio Conference (WARC '87), 4 + 4 MHz in the bands 1555 - 1559 MHz (downlink) and 1656.5 - 1660.5 MHz (uplink) were allocated to land mobile satellite service (LMSS) on a primary, exclusive basis (except for 0.5 MHz from 1660 - 1660.5 that is shared with Radio Astronomy). Another 3 + 3 MHz in the bands 1530 - 1533 MHz and 1631.5 - 1634.5 MHz were allocated to LMSS on a co-primary basis. In addition, the frequency bands 1533 - 1544 MHz (downlink) and 1634.5 - 1645.5 (uplink) were allocated for low rate data LMSS on a secondary basis. The band 1626.5 - 1631.5 was also allocated for uplinking of low rate data in the LMSS on a secondary basis.

The current MSAT system is designed to operate primarily in the L-Band-to-SHF mode. All communications in the MSAT system will be linked through SHF Ku-band earth stations to user facilities. In other words, the communication between the satellite and fixed stations will use SHF Ku-band frequencies while the satellite-to-mobile communication will use the L-Band frequencies. This use of the SHF frequencies and SHF earth stations to provide such connections to user facilities economizes on the use of scarce L-Band frequencies and satellite power. The mobile-to-mobile terminal communications will be provided on a double-hop basis through the Network Control Center. Studies indicate that there is a limited requirement for such communications.

The base stations will provide interfaces for private mobile circuit switched services, such as voice dispatch systems. The gateway stations will provide direct connection to the PSTN (public switched telephone network) for mobile telephone service. The data hub stations will provide mobile packet switched data services with interconnections to terrestrial private and public data networks for applications such as vehicle locations and digital messaging to mobiles. These fixed stations will operate in the SHF frequency band. Although the specific SHF frequencies have not been formally specified, the current candidate bands include 14/12 GHz and 13/11 GHz frequencies. A diagrammatic representation of the system configuration is given in Figure 2.

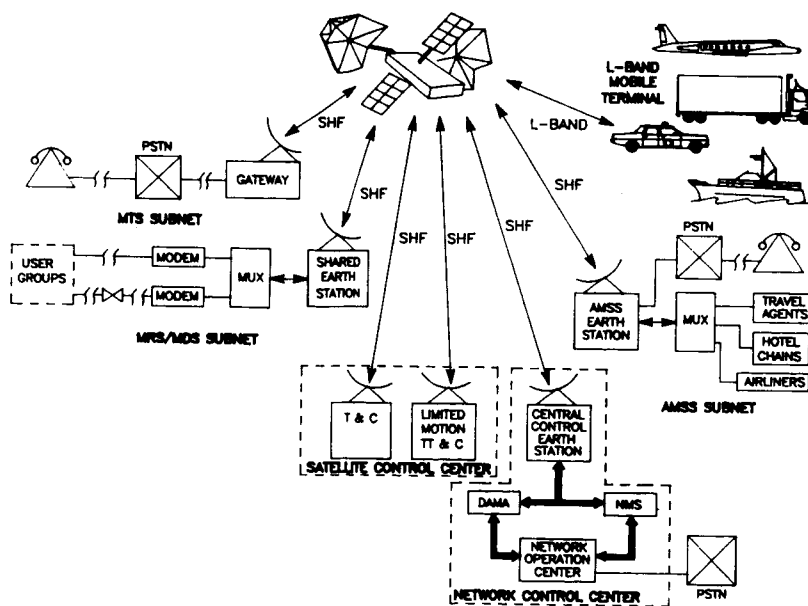


Figure 2 - MSAT System Configuration

In the present baseline design of the MSAT system, each satellite will have two large (a minimum of 5m in diameter) L-Band deployable parabolic reflectors which will generate nine beams covering Canada and the United States. Two additional beams may be incorporated to provide a capability for MSS within Mexico. Figure 3 shows the 9-beam coverage. Note that the design of the beams allows each satellite to service both Canada and the U.S. in the event that system restoration is required because of failure of either satellite.

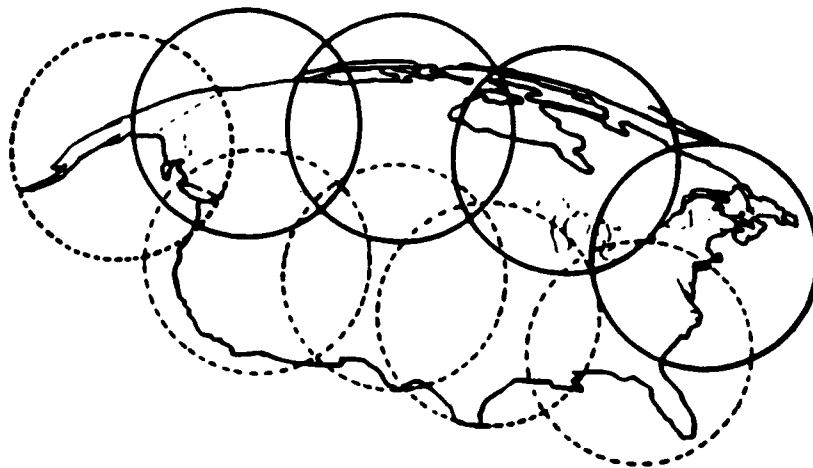


Figure 3 - 9-Beam L-Band Coverage of Canada and the U.S.

Because of the limited availability of spectrum in the L-Band, communication via MSAT will be established using 5 KHz channels as compared to the wider 30 KHz channels typically used in terrestrial systems. The satellite channels will be allocated to individual users on a demand assignment basis using a trunking concept, thus allowing the system to provide service to a large number of light-duty users. The demand assignment system (DAMA) and the network management system (NMS), will administer the communications capacity of the MSAT system and record airtime usage for billing purposes.

The speech modulation/coding techniques employed in the MSAT systems are constrained by the 5 KHz channel bandwidth. Two candidate modulation schemes currently under consideration and development are Amplitude Companded Single Sideband (an analog technique) and Differential Minimum Shift Keying with Pitch-Excited Linear Predictive Coding (LPC), (a digital technique).

The ground terminals which will constitute the ground segment of the first generation MSAT system fall into the following categories:

- (i) full and half-duplex mobile radio terminals;
- (ii) portable, transportable terminals;
- (iii) mobile data terminals;
- (iv) SHF base stations;
- (v) SHF gateway stations and finally;
- (vi) Network Control Stations (NCS) which will include the Network Management System (NMS) and the DAMA Control System (DCS).

The NCS base stations and gateway stations are fixed facilities and will employ highly conventional SHF parabolic antennas. The mobile units, and to a somewhat lesser extent, transportable terminals will employ relatively wide beam antennas with low gain in the 4 dBi to 12 dBi range.

SERVICE DESCRIPTION

MSAT will be used primarily in rural and remote regions where its wide-area coverage and extended range features are of greatest benefit. The MSAT system will provide a wide variety of telecommunication services such as voice, message and data communication to land vehicles, ships or aircraft. Some of the applications can be found in the following market sectors:

- trucking
- forestry
- coastal and inland shipping
- national paging
- remote monitoring and control of utilities
- mineral exploration
- law enforcement
- light aircraft communications
- environmental sensing
- emergency relief

Services offered initially on MSAT include mobile radio, mobile data, wide-area paging, supervisory control and data collection. A position location service will also be offered as a value-added feature. An analysis of the markets for MSAT services has indicated that 120,000 MSAT mobile units will be in operation by the turn of the century. 30% of these will be used for mobile radio applications and 70% for mobile data service. Recent studies of the demand for digital messaging/data services indicate that such data services may reduce demand for voice services in the future. For many applications, data transmission to text display terminals is equally effective as voice communications and offers additional benefits in terms of improved transmission efficiency, privacy, and cost.

Typical User Costs

An analysis of the MSAT system and market factors indicates that user costs would be as given in Table 1.

Table 1

Estimated MSAT User Costs excluding Terminal Equipment

Access Charges (per month/terminal)	\$50
Transmission Charges	
- Voice	\$1.50/minute
- Data	\$0.25 to \$ 0.75 per one-way message (32 to 128 characters)

Institutional Arrangements

In order to capitalize on the MSAT opportunity, Telesat has established a subsidiary organization called Telesat Mobile Incorporated (TMI). This subsidiary will furnish the necessary marketing, sales and service functions to provide mobile satellite services. The following diagram depicts the associated institutional arrangements.

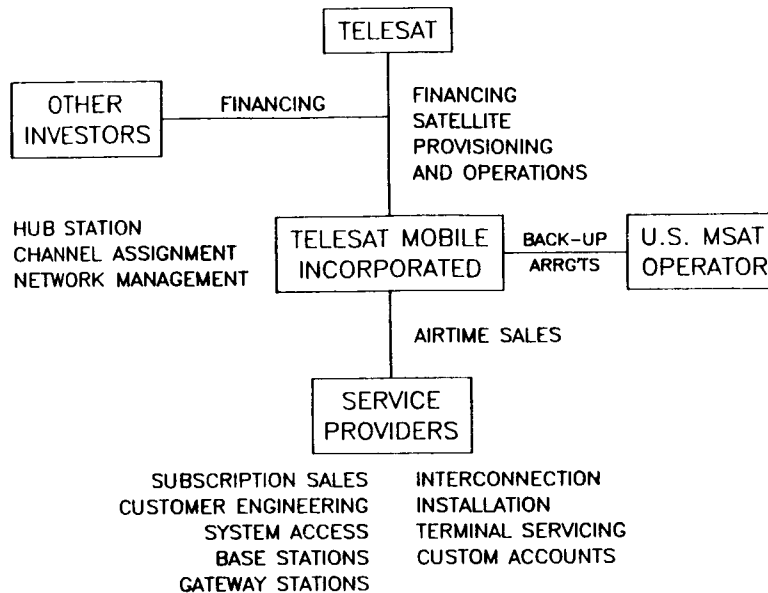


Figure 4 - The Corporate Structure for MSAT Services

Telesat will be the major shareholder of its subsidiary, Telesat Mobile Inc., with the remaining equity being held by other investors. TMI will own and operate the central control station and a network of base and gateway stations. It will contract with Telesat for the engineering expertise required for procuring and launching the satellite, as well as its technical operation in orbit. TMI will also be responsible for making a provision for back-up service with the U.S. mobile satellite operator.

TMI will engage in sales to end-users, private system operators, and independent value-added service providers. The service providers could include radio common carriers, telephone companies and large private mobile radio operations. All three groups operate terrestrial mobile communications systems today and MSAT would be a logical extension of this business. In addition, MSAT lends itself to the emergence of new entrepreneurial groups of service providers as only a small investment in base station equipment is required to provide MSAT services. Through business arrangements with both, traditional and new service providers, TMI will establish and manage a national distribution network for sales and customer service. For certain MSAT services and in areas where satisfactory agreements cannot be obtained with service providers, TMI may undertake to deal with end-users directly.

INTERIM MOBILE SATELLITE SERVICES

Although considerable momentum and commitment is building towards an eventual MSAT program, there remains a significant period of time, i.e. four to five years before MSAT will be in service. Today, amongst various industry and government sectors, there exists an immediate need for the types of services that only mobile satellite technology can deliver.

To meet this need, Telesat, in co-operation with Federal and Provincial Governments, and specific user groups, is developing a small portfolio of mobile satellite services using interim facilities.

Specifically, Telesat is working on two initial service offerings. The first is a trial of voice communications services to the Ontario Air Ambulance service. This program is sponsored by the Ontario Provincial Government with technical support from the Research Center of the Department of Communications. The objective is to provide two-way voice communications between hospitals and paramedics aboard air ambulances. This service is currently being tested over the INMARSAT MARECS satellite. Upon successful completion of trials, additional aircraft will be equipped and Telesat will endeavour to arrange for ongoing commercial service.

The second service offering under development is a data collection and two-way messaging service designed to meet the needs of the transportation industry. This service will allow fleet dispatchers to have continuous updates of location information from each vehicle in the fleet as well as the flexibility of transmitting and receiving 16 to 40 character messages. This program has several participants including the Ontario Ministry of Transportation and Communications, Federal Department of Communications, and representatives from the trucking industry.

It is planned to test this system over the INMARSAT MARECS satellite during the summer and fall of 1988 followed with commercial service in late 1989. Initially, the system will have a capacity of up to 6,000 vehicles. However, if additional INMARSAT capacity is available then, it will be possible to expand this service until such time as MSAT is available. Figure 3 depicts the operation of the proposed service to the transportation industry. Telesat has registered the name FLEET*STARTM to be used for this initial offering.

CONCLUSIONS

The Canadian MSAT system is a major component in a larger plan to provide mobile satellite services to all of North America. To achieve this, MSAT will be implemented in conjunction with a similar U.S. system in order to provide back-up and reduce development costs. MSAT will offer a full range of mobile telecommunications services including radio dispatch, digital messaging and data transfer.

In order to develop MSAT markets and technology prior to the launch of the dedicated system in 1992, Telesat plans to offer a limited portfolio of mobile satellite services using leased L-Band facilities. IMSS services will include two-way digital messaging, vehicle location, and voice services to high-need segments of market.

Telesat, through its MSAT and IMSS activities is preparing to enter the next domain of commercial satellite communications - mobile satellite services.

AUSSAT MOBILE SATELLITE SERVICES

DR WAYNE NOWLAND, Manager Space Division, AUSSAT Pty Ltd, Australia;
DR MICHAEL WAGG, Manager Mobile Services, AUSSAT Pty Ltd, Australia;
DANIEL SIMPSON, Business Development Manager Mobile Services, AUSSAT
Pty Ltd, Australia

AUSSAT Pty Ltd
GPO Box 1512
SYDNEY NSW 2001
AUSTRALIA

ABSTRACT

Australia will be introducing a domestic mobile satellite communications service early in 1992 using L Band capacity on AUSSAT's second generation satellites. The mobile satellite services are targeted at rural and remote area users throughout Australia. The prime services to be provided are mobile voice and data for land, maritime and aeronautical applications.

This paper provides an overview of AUSSAT's planned mobile satellite system and describes the development program which is being undertaken to achieve the 1992 service date. Both business and technical aspects of the development program are addressed.

INTRODUCTION

In July 1988, AUSSAT Pty Ltd, Australia's satellite communications operator, will be contracting for the supply of two high capacity communications satellite that will form part of its second generation system. These new satellites, termed AUSSAT B1 and B2, will replace two of the A-series 'birds' currently in orbit that are due to be retired from service around December 1992 and June 1993.

The AUSSAT-B satellites will be substantially larger and more powerful than the current series, each carrying 15 high power Ku Band transponders for telecommunications and broadcasting service both in Australia and New Zealand. Additionally, each will carry a high power L Band communications payload for the provision of domestic land, air and coastal marine mobile applications, making Australia one of the first nations in the world to implement its own commercial domestic mobile satellite system.

AUSSAT AND ITS FIRST GENERATION SYSTEM

AUSSAT Pty Ltd is a commercial company established by the Australian Government to own and operate Australia's domestic satellite system. AUSSAT currently employs around 250 staff, the majority located at the head office in the Sydney CBD and the TT&C facilities and network control centre in the Sydney suburb of Belrose with the remaining staff in earth stations in each of the capital cities.

The first generation AUSSAT system comprises three Hughes built HS 376 communications satellites operating at Ku Band. Each satellite has fifteen transponders operating to a range of national and spot beams covering Australia with the third satellite also providing coverage of the South West Pacific region. The AUSSAT ground segment comprises AUSSAT owned Major City Earth Stations (MCES) in each of the capital cities as well as a range of customer owned earth stations which provide fixed telecommunications and broadcasting services throughout Australia.

AUSSAT SECOND GENERATION

With the first of AUSSAT's current satellites due to run out of fuel in December 1992, planning is now well advanced for the second generation satellites (AUSSAT-B). The AUSSAT-B system has been designed to cater for the continuation of the existing services but with capacity for growth in the key market areas of television and radio, corporate voice and data, and offshore. As well a new market sector will be catered for, namely mobile services.

The mobile satellite market represents a major new business opportunity for AUSSAT on the next generation system, with prospective applications including two-way mobile voice and messaging services for land, aeronautical and maritime applications as well as remote low speed data collection for telemetry monitoring applications. The procurement timetable for the AUSSAT-B satellites, Table 1, will enable the introduction of the mobile satellite service during 1992.

Tender Evaluation	Dec 1987 - April 1988
Government Approval to Execute Contract	May - June 1988
Contract	July 1988
Likely Launch Dates	Mid 1991 - Mid 1992
Latest in service Date	4th Quarter 1992

Table 1. AUSSAT-B Procurement Timetable

AUSSAT MOBILE SATELLITE SYSTEM

The AUSSAT mobile system will comprise an L band package on-board each of the AUSSAT-B satellites and ground component of L Band mobile terminals, Ku Band base stations and a Ku Band control and monitoring centre (see Figure 1). L Band will be utilised for the mobile terminal to satellite communication links and Ku Band for the control and base stations to satellite links. No provision has been made in the system design for direct single hop L Band to L Band links in order to avoid unauthorised and uncontrolled access to the system. Hence all mobile to mobile communications will be with a double satellite hop via an intermediate base station. All access to the system will be under the control of a demand assignment network operated by AUSSAT.

The mobile satellite system has been designed to cater predominantly for those users of mobile communications who operate in the rural

and remote areas of the country outside the existing terrestrial communications infrastructure. The indicative services being catered for are mobile voice, both telephony and radio, mobile data including messaging, paging and position fixing as well as a range of fixed or transportable applications which become economically attractive when using an L Band satellite system. These include remote data collection, 'briefcase' communications, low cost rural telephony for applications such as School of the Air and transportable communications for short duration base camps such as in mining exploration or search and rescue.

AUSSAT MOBILE SATELLITE SYSTEM CONCEPT

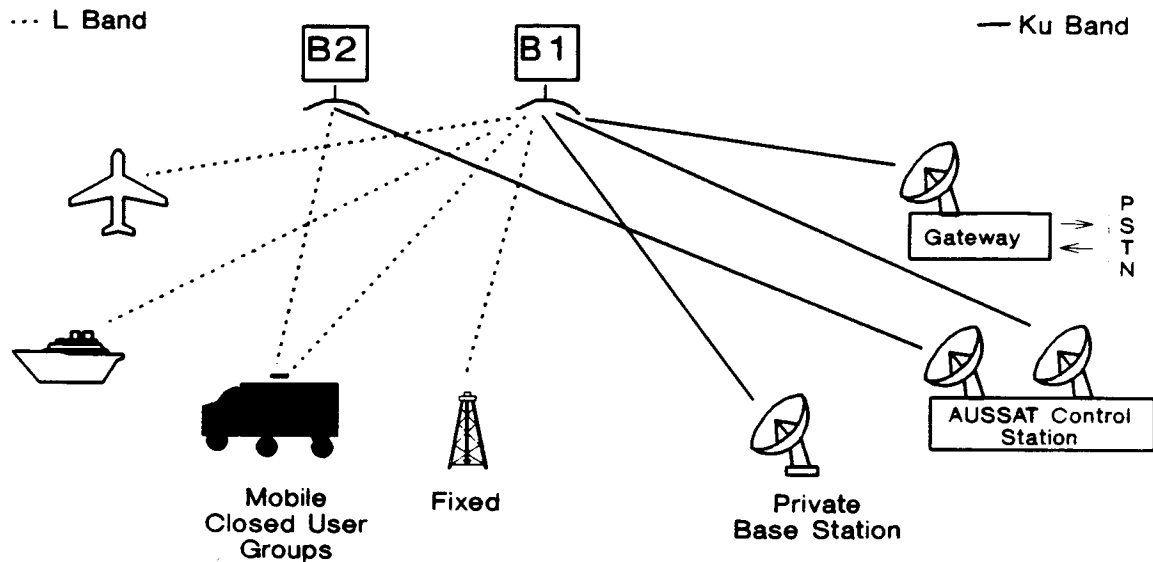


Figure 1. Mobile Satellite Configuration

MOBILE DEVELOPMENT PROGRAM

AUSSAT is undertaking an integrated business and technical development program for the mobile satellite services with the key aim of establishing a commercially viable mobile satellite service by early 1992.

Market Development

The market development program is being conducted in four phases:

- Phase I Strengths, Weaknesses, Opportunities & Threats
- Phase II Service and Segmentation
- Phase III Planning and Awareness
- Phase IV Specific Market Targetting

The first phase was carried out during the middle of 1986 at which stage the potential for mobile satellite services was proposed to the existing AUSSAT customer base as part of the planning for the overall

second generation system. This interactive process enabled a set of generic products and services to be postulated for the Australian marketplace which could later be analysed on their own merits in terms of commercial viability and attractiveness to AUSSAT. The culmination of this initial customer contact and supporting research and analysis was the decision by AUSSAT to undertake a formal investigation of the potential for Mobile Satellite Services as a future AUSSAT business.

The second phase which commenced in late 1986, consisted of a market study; model development and data analysis; revenue and growth projections; and competitive and sensitivity analyses. The market study was multi-faceted being aimed at assessing the market reaction to the features and benefits of the proposed new services as well as establishing estimates for the level of traffic and the total market demand for each of the service types. The market sectors targeted consisted of:

- the transport sector (road, rail, sea & air)
- the exploration sector
- the Government and emergency services sector.

The projected demand derived from this phase of the market research estimated in the order of 20,000 terminals within the first five years of service with around 50,000 in the eight to ten year period. The output of the second phase was a detailed business case which formed the basis of a decision by the Company during the second quarter of 1987 to include the L Band package in the second generation satellite design.

The third phase included a detailed market awareness program conducted by AUSSAT which provided the potential user organisations with sufficient detail to allow them to incorporate the mobile satellite products within their own planning cycles and to enable them to address the possibility of using these products and services. At this stage, AUSSAT also sought detailed information from the potential users in order to earmark those organisations who would be suitable for follow-on contact with AUSSAT either as a part of the customer consultancy program of phase IV or those who were potential business or joint venture partners with AUSSAT.

The fourth phase, which is currently in progress, has started with application consultancies involving a number of specific potential users. The aim of this work is to extract product and functional requirement information from the marketplace to feed back into the technical development program. In addition we are seeking commercial detail which will allow detailed viability analyses to be performed on specific products and services. Each service will be required to be self-sufficient in a business sense and in conducting the applications consultancies AUSSAT will ensure that the likes of tariff levels, functionality and user friendliness of the services will be in accordance with the market place demands. Another output from this phase will be a number of specific customer business cases which will be fed back into each of the organisations to provide a framework for them to proceed with the business planning and analysis of the mobile satellite services within their own organisations. These business cases will be developed by AUSSAT for the users from the users' perspective.

Business Development

As well as the market development activities AUSSAT is undertaking to establish a number of relationships with key organisations in the mobile satellite area. These include co-operation with potential joint service providers and joint ventures with organisations who can bring to AUSSAT guaranteed markets or other valuable assets such as market credibility, distribution channels and service capability in the provision of mobile satellite services to the marketplace. AUSSAT is also pursuing a strategy which includes establishing relationships and with other major organisations in the Australian telecommunications environment in order to insulate AUSSAT's projected market from erosion by competitors and competing products and services.

Technical Development

The key aim of the technical development program is to provide the technical infrastructure to enable the introduction of AUSSAT's mobile satellite service by early 1992. This includes outfitting the hub monitoring and control station, providing connection to public and private terrestrial networks and ensuring that the L Band terminals are available to the marketplace at acceptable costs. A supporting aim is to ensure that the AUSSAT Mobile Satellite System is as compatible as possible with other systems to be implemented throughout the world.

The major milestones of the program are summarised in Table 2.

July 1988	- Release of Draft Terminal & Network Control Specifications
July 1989	- Release of RFT for Hub Network Control Station
	- Release of RFT for 500 - 1,000 L Band Terminals
	- Release of Terminal & Base Station Specifications
January 1990	- Award Contract for Hub and Terminal Supply
January 1992	- Service Commencement Date

Table 2. Major Development Milestones

Experimental Program

The launch and deployment of the Japanese experimental satellite ETS-V has given AUSSAT a unique opportunity to undertake a practical experimental program to support the development of the mobile satellite services. The ETS-V satellite, which operates at L Band, has a beam that is centred near New Guinea which provides around 32-35 dBW of usable EIRP across Australia. AUSSAT earlier this year established an agreement with the Radio Research Laboratories, RRL, of Japan's Ministry for Posts & Telecommunications for the use of ETS-V within Australia.

AUSSAT is outfitting a hub station and a van both with communications, test and monitoring equipment to enable a range of tests to be undertaken. These include a series of propagation studies to evaluate the effects of multipath and fading within the Australian environment and a range of terminal prototype equipment tests. A number of parties have already committed equipment to the test program to enable the review of items such as antenna performance, voice encoding capability and digital and analog modems. AUSSAT is actively encouraging equipment and system providers to join in the test program using ETS-V.

Industry Liaison

Early in October 1987 AUSSAT released a worldwide call for registration of interest to all parties who may wish to participate in the development of the ground segment equipment for AUSSAT's Mobile Satellite Service. The aim of this exercise was to establish a mailing list of all interested parties, currently around 150 organisations, to whom AUSSAT would provide regular updates of the system technical progress. As well AUSSAT has distributed the list of all parties and their areas of interest in an attempt to encourage relationships and possible joint ventures in the development of the terminal products. This mechanism has been used previously by AUSSAT and is seen as an ideal means for the transfer of technology and ideas between parties aiming to achieve a common goal.

AUSSAT conducted during March 1988 a briefing for industry at which the Mobile Development Program was outlined in detail. As well a number of Australian Government representatives provided detail of the support and incentives provided to organisations wishing to manufacture and develop products for the Australian market.

CONCLUSIONS

The introduction of mobile satellite services to the Australian marketplace is an exciting new business venture for AUSSAT, Australia's national satellite operator, and is being implemented through a carefully co-ordinated business and technical development program. The potential system users have been consulted extensively in the development of the system features in order to ensure that the final mobile service offering meets the demands and requirements of the marketplace. The technical development activities have focused on close liaison with the equipment suppliers in both the testing and conceptual areas in order to ensure that the available equipment meets the needs of both AUSSAT and its customers.

A SATELLITE SYSTEM FOR LAND-MOBILE COMMUNICATIONS IN EUROPE

P. BARTHOLOME AND R. ROGARD
European Space Agency, Communications Satellite Department

EUROPEAN SPACE AGENCY
Postbox 299
2200 AG Noordwijk
The Netherlands

ABSTRACT

There exists a great unsatisfied demand for land mobile communications in Europe, particularly in sectors of the business activity such as the road transport industry which covers the entire European continent. This demand could best be satisfied by means of satellite-based private networks providing voice and data communications in a hub configuration. The potential market is estimated to encompass several hundred thousand road vehicles and the transmission capacity required would be several thousand channels. ESA is currently demonstrating the potential of satellite communications for this type of application, using a system called PRODAT. System studies are being performed with the aim of defining the architecture of a regional satellite system for Europe.

INTRODUCTION

Mobile communications is a fast growing market in Europe as it is in North America. Several countries are equipping themselves with cellular networks or are planning to do so in the near future. Most of these systems unfortunately have different characteristics which make them incompatible. Under pressure from the Commission of the European Communities, fourteen governments have recently agreed to adopt the same standard for the next generation of cellular system, the so-called "pan-European" system, that will eventually cover the entire continent. The principal milestones for its implementation are the coverage of major cities and airport areas by 1993 and the main roads connecting these cities by 1995. Thereafter, the network will continue to expand at a rate which is not specified and which will depend on circumstances prevailing in each country. Given the magnitude of the investments required for the infrastructure of this project (estimated at \$ 3200 million over the first five years), it can be expected that the coverage in terms of percentage of the total geographical area will still fall short of 100% by the year 2000. In fact, it is likely that the least populated areas of Europe will remain uncovered for a very long time.

Although the future pan-European cellular system no doubt raises very bright prospects and will be welcomed by millions of users (present estimates are 15 million subscribers by 2000), it will not be the universal panacea. In the framework of its prospective studies of new

satellite applications, ESA has identified certain categories of users whose specific needs are too urgent to wait for the new system and moreover would not be satisfied very well by it even if it existed. The purpose of the present paper is to outline the nature of these requirements and to give an overview of the ESA's current and planned activities to meet them.

RESULTS OF MARKET SURVEYS

Private Network Applications

For several years, ESA has been exploring new markets for mobile services by satellite in Europe. Several surveys have been completed and others are still going on. The sector that appears to have the largest and most urgent needs is the road transport industry. There are in Europe several thousand transport companies that might be interested in mobile communications by satellite, for the following reasons : they operate fleets of vehicles of significant size (more than 50) hence they have high operating costs which they try to reduce; and their activities are international i.e. their field of operation includes the whole of Western Europe, and sometimes extends to peripheral areas such as Eastern Europe, the Middle East and North Africa.

These companies fall into three categories :

(i) International haulage companies

This category includes a total of 5000 companies with more than 50 vehicles, 600 of them having more than 100 vehicles. The market survey shows that 2300 of these companies would respond positively to an offer of satellite services.

(ii) Companies that carry their own goods on an international scale

In this category, 300 companies operating more than 100 vehicles were identified as potential subscribers.

(iii) Freight forwarders

This category includes 250 very large companies, including 30 giants that operate thousands of vehicles each. 140 of them were identified as potential subscribers.

In addition to the above categories, the survey identified some 90 companies that would be interested, located in countries outside the coverage of the future pan-European cellular systems (Turkey, North Africa) .

The reasons for the interest of these organisations in satellite-based services are two-fold. On the one hand, they require access to these services everywhere in Europe and not only in those areas that the cellular system will cover; on the other hand, they need these services urgently and, if possible, not later than 1992, which is the year when all internal barriers to trade end services will be removed in the European Community. As far as types of service are concerned, they express the following requirements in order of decreasing priority : voice, message and data transmission, telex and facsimile, radio-location. A clear preference is also expressed for access to these services in the form of closed private networks rather than by

way of connection to a public network. Private networks certainly offer greater flexibility and the costs are more easily controlled.

The results of the survey are summarised in the table below :

	Number of companies interested	Number of vehicles (thousands)	Number of satellite channels
International haulage companies	2300	260	2600
Companies that carry their own goods	300	45	450
Freight forwarders	140	85	850
Companies in peripheral countries	90	10	100
Total	2800	400	4000

The above values correspond to the average of a range which goes from 2500 to 7000 channels depending on the assumed penetration of the service.

As mentioned earlier, surveys are also conducted in other sectors of activity such as inland waterway transport, railways, and environment control by government agencies. None of these sectors seems to have the same massive requirements as the road transport industry although, taken together, they might amount to a substantial market.

Public Network Applications

To many potential users in the categories described above, the pan-European cellular network would not be an attractive proposition because of its insufficient coverage and the fact that it would not offer the same flexibility and cost control possibilities as a private mobile radio (PMR) service by satellite. There is however a significant fraction of that population (5%) that would be interested in having access to both the cellular and a satellite-based PMR service.

The integration of a satellite system with the terrestrial cellular system also has a number of advantages, the most obvious one being that it would offer quasi-complete European coverage right from the outset, therefore adding another attractive feature to a system already designed to meet the needs of the international traveller.

In the case of a satellite used as part of the public network, the problem for the system designer is of a quite different nature. The services to be provided by satellite must be of the same quality as those of the associated terrestrial network. Furthermore, space and terrestrial links have to be interfaced in such a way that the complete network is perfectly transparent, to the point that users remain unaware of the type of channel used at a particular time to relay their communications. There are also problems of a less technical nature such as charging, harmonisation of tariffs and, last but not least, finding an adequate amount of frequency spectrum. Assuming that all these problems can be resolved in due time, it seems likely that in the long term a sizeable market will develop for public mobile communications by satellite, as a complement to the terrestrial cellular service.

OUTLINE OF ESA PROGRAMMES

ESA's activities in mobile communications by satellite are aimed at offering the following services, listed in order of increasing sophistication :

- (a) unidirectional wide-area paging
- (b) bidirectional low-rate data transmission for the following applications :
 - message delivery and telex communications
 - data collection
 - packet-voice message transmission
 - radio-location
- (c) voice/medium-rate data transmission for private network applications
- (d) voice/data transmission for public network applications in an integrated space/terrestrial system

The PRODAT System

The PRODAT system is a two-way data transmission system that has been developed to test the first two layers of the services mentioned above and to evaluate user reactions under operational conditions. In its design, emphasis has been placed on achieving the best performance at the lowest cost with terminals small enough to be installed easily on land vehicles, small boats and light aircraft [1].

An extensive campaign of propagation measurements, carried out at the outset of the programme, showed clearly that the land mobile environment presents a much tougher challenge to the system designer than either the maritime or the aeronautical. Indeed in the land-mobile case, shadowing by buildings, bridges, trees and all kinds of obstructions causes deep fades in the radio link or even interrupts it completely. A self-adaptive scheme has therefore been developed to take maximum advantage of the favourable time periods without being disturbed by momentary signal interruptions.

The services provided by the PRODAT system are :

- (a) Sending of messages from fixed user to mobile user and vice-versa, and from mobile to mobile users
- (b) Sending of messages to multiple mobile users (broadcast)
- (c) Request/reply function
- (d) Periodic polling of mobiles
- (e) Paging.

These services are implemented through the combined operation of the mobile satellite network and the terrestrial access networks, i.e. the telex and Packet-Switched Public Data networks. The interaction between these takes place in a store-and-forward mode in the Network Management Centre, which acts as the hub of the mobile network. This centre is located at ESA's Villafranca station in Spain, which controls the MARECS satellite over the Atlantic Ocean.

The forward link characteristics are as follows :

- Multiplexing mode : TDM
- Signalling rate : 1500 baud
- Data rate per channel : 47 bit/s
- Total number of channels : 23

The data rate on the return link can be set to around 200 bit/s using a signalling rate of 300 baud.

The preliminary system tests have been completed successfully. Although the system thresholds have not yet been accurately determined, results show qualitatively that the challenging design objectives of the mobile link have been met, thanks to the technical options selected. Messages can be exchanged in a heavily perturbed propagation environment in minimum time and with no errors.

The field trials that are currently in progress involve ten prototype mobile terminals installed on trucks of transport companies in France, the Netherlands and the Fed. Rep. of Germany. At a later stage, the scope of the trials will be extended to include the transmission of voice messages, digitally encoded at 800 bit/s and radio-location by coupling a navigation receiver to the PRODAT terminal.

The European Mobile Services (EMS) System

For the next step forward in the provision of land mobile services in Europe, ESA is developing a concept aimed mainly at offering voice/data channels in the form of private networks for users such as the road transport industry. This concept, called "EMS" could form the basis of an operational regional system.

The purpose of EMS is to provide, in the first instance, the following mobile services in Europe :

- Low-data-rate services for mobile terminals of the PRODAT type (G/T = -24 dBK^{-1})
- Business services (voice/data) for mobile terminals of a more advanced type (G/T = -12 dBK^{-1})

The EMS system is based on the use of a satellite payload dedicated primarily to the Land Mobile Satellite Service in Europe. This payload would be of a modest size (75 kg, 200 W), i.e. similar to the SMS payload belonging to EUTELSAT. The overall characteristics of the system are described below.

An orbital position will be selected between 10 and 20° East to provide a mobile service with the highest elevation angle in Europe. The coverage of EMS is a single elliptical beam illuminating Europe. The gain at edge of coverage is 26 dB minimum, and the EIRP at 1.5 GHz is at least 43 dBW. The transmission capacity available is :

- 10 TDM carriers (24 dBW each) for PRODAT-type terminals
- 500 business channels (19 dBW each with voice activation) for enhanced terminals

The polarisation is LHCP (axial ratio $\leq 1.5 \text{ dB}$).

The frequency bands used in the satellite-to-mobile direction are as follows :

1530 to 1533 MHz	: business services
1540 to 1544 MHz	: low-data-rate services
1555 to 1559 MHz	: business services

Frequencies in the up and down directions are paired with a fixed difference of 101.5 MHz.

Feeder links operate in the same 14/12 GHz bands as SMS and IBS.

Business services are intended to meet the specific requirements of enterprises and organisations which need a Private Mobile Radio (PMR) service at European scale. They would therefore be provided in the framework of closed networks in much the same way as is done by EUTELSAT with SMS. The fixed stations would operate at 14/12 GHz and would be small enough to be installed at the user's premises.

As far as the data services are concerned, the network is composed of sub-networks, each of which is roughly equivalent to the PRODAT demonstration network described above. Each participating country operates its own sub-network(s) through its earth station(s) (hub stations), where gateways to the corresponding national networks are installed. The feeder links to the satellite are at 14/12 GHz. The various sub-networks share a common satellite transponder, which provides the required geographical coverage for all mobiles.

FURTHER DEVELOPMENTS

To achieve the remaining objectives and to provide full quality telephony services by satellite as well as interconnectivity with the terrestrial public network, further advances are necessary both in satellite and in mobile terminal technology.

As far as space technology is concerned, the efforts currently concentrate on two key items, namely high-gain multibeam antennas and onboard processing. A companion paper reports on the latest achievements in multibeam antennas [2]. Work has started on onboard processing and on terminals more advanced than those used in PRODAT.

One remaining problem is the allocation of more frequency spectrum to the Land Mobile Satellite Service (LMSS), since the EMS system described previously would occupy all the spectrum available at 1.5/1.6 GHz in Europe.

In the long term, the problems encountered in trying to share frequencies between the LMSS and other radio services may be alleviated by the introduction of a new generation of satellites that would be placed in highly inclined and eccentric orbits of the Molnyia (12 hour) or Tundra (24 hour) type. Such satellites would spend a significant fraction of their orbital period in a region of space near the zenith of Europe and would provide quasi-vertical up and down links. This would have the advantage of minimising the shadowing problems that cannot be avoided with geostationary satellites. It would also facilitate the sharing of already used frequency bands.

CONCLUSIONS

The needs for Europe-wide land mobile services are already manifesting themselves. There are plans to deploy a new pan-European radio cellular network, but its implementation will take many years. In the short term a satellite system would go a long way towards meeting the most urgent needs. In the longer terms, having a satellite integrated into the cellular network would have many advantages.

REFERENCES

- [1] Rogard R., Jongejans A. and Bartholomé P.
Mobile Communications by Satellite in Europe - Overview of ESA Activities. IAF-87-476. October 1987
- [2] Rammos E., Roederer A. and Rogard R.
Antenna Technology for Advanced Mobile Communication Systems. This Conference.

**SYSTEM CAPACITY AND ECONOMIC MODELING COMPUTER TOOL
FOR SATELLITE MOBILE COMMUNICATIONS SYSTEMS**

ROBERT A. WIEDEMAN, Manager Commercial Programs; WEN DOONG, Engineer; & ALBERT G. McCracken, Financial Analyst; Ford Aerospace Corporation, Space Systems Division, Palo Alto, California, USA.

FORD AEROSPACE CORPORATION, Space Systems Division Palo Alto, California 94303, United States

ABSTRACT

This paper describes a unique computer modeling tool that combines an engineering tool with a financial analysis program. The resulting combination yields a flexible economic model that can predict the cost effectiveness of various mobile systems. This model was developed by Ford Aerospace in an effort to help the world mobile community in making key decisions on the design and implementation of a Mobile Satellite Communications System. Cost modeling is necessary in order to ascertain if a given system with a finite satellite resource is capable of supporting itself financially and to determine what services can be supported. Personal computer techniques using Lotus 123 are used for the model in order to provide as universal an application as possible such that the model can be used and modified to fit many situations and conditions. The output of the engineering portion of the model consists of a channel capacity analysis, link calculations for several qualities of service using up to 16 types of earth terminal configurations. The outputs of the financial model are a revenue analysis, an income statement, and a cost model validation section. The paper will describe the Ford Aerospace model and how it is used.

INTRODUCTION

Mobile Communications in the world community is important for thin routes where it is not economical to serve the desired coverage area with conventional terrestrial or satellite systems. These mobile satellite communications systems use low cost earth stations called transceivers which cost as low as \$2000 to \$4000 which in turn allows a large user base. These systems are used for mobile radio, mobile telephone, data services and position location. Emergency services and disaster communications round out the list of important services that are available with a mobile satellite system. Most industry analysts now predict a large pent up demand for these services. However, the market is unproven since no comparable service exists in most cases. Thus, many potential service providers are considering a pilot system for developing the service techniques and proving the market before stepping forth with an expensive dedicated system. One method for initiation of a pilot system is to place a low cost mobile satellite communications package on a host satellite that has another primary mission. Several such systems are under consideration now.

Systems are being introduced that use many types of user transceivers. These transceivers differ in performance, ranging from terminals with omni-directional antennas that are capable of only low speed data transmission, to units with directional hi-gain antennas coupled with voice codecs and data transmitters. A description of the various services and the antenna designs is beyond the scope of this paper; however, the services in Figure 1 show that there are a wide range of service needs and technical requirements. These ranges are used to model the number of channels and technical parameters that make for a cost effective system.

Cost modeling is necessary in order to ascertain if a given system with a finite satellite resource is capable of supporting itself financially and to determine what services can be supported. This paper describes a unique computer modeling tool that combines an engineering tool with a financial analysis program. The resulting technique yields a flexible economic model that can predict the cost effectiveness of various mobile satellite communications systems with differing technical parameters.

DEDICATED SATELLITE vs. PACKAGE ON A HOST SATELLITE

A mobile satellite system package carried on a host satellite makes sense where there is no previous history of the service market. Dedicated satellite systems would cost \$160 to \$300 million launched, whereas a pilot system as a package on a host satellite could be as low as \$15 to \$30 million. Of course the system capacity is reduced as well. The mass and power required for a mobile package added to a host satellite is on the order of 70 to 80 kg and typically consumes 400 to 1000 watts DC depending on how much power is available for the mobile payload. While multiple transponders with frequency reuse could be used, the usual pilot system is a single transponder with a single beam covering the country or area of interest. The

addition of multiple transponders complicates the system from the start. The question then arises as to the economic feasibility of the usage of such a system and how many channels and users can be supported.

BASIC PRINCIPLES OF MOBILE PILOT SYSTEM DESIGN

These pilot systems generally are downlink limited and the tradeoffs for channel capacity involve satellite DC power consumed and the management of the available power. The important parameters in the system are: The dedication of what portion of the satellite's power to the mobile system. The satellite Antenna gain, generally related to the size of the antenna to be used on the satellite. The earth station transceiver antenna gain (omni vs directional designs). Service reception characteristics related to toll quality vs. commercial quality, which are manifested in signal to noise ratios. Finally, channelization, the basic commodity that is being resourced in the system. For this analysis a 5 KHz Amplitude Companded Single Sideband (ACSB) channel is assumed for the basic quantity of resource. System tradeoffs are performed using this model. The engineering model relate these basic principles and determine the link parameters and indicate which are the most important.

CONNECTION BETWEEN DESIGN AND ECONOMICS

Generally, the revenue that can be derived from the mobile satellite system is channel dependent and the ultimate revenue is tied to the satellite design and the mix of antennas and service quality desired on the ground. For small systems the design is limited by the downlink to the mobile user and the power in any downlink channel in such a linear system is regulated by the uplink power applied. The method used by the model to determine channel capacity is to hold the downlink margin, carrier to noise ratio, and satellite system parameters constant and vary the percentage of satellite power assigned to individual carriers that correspond to several earth station configurations and users. The resulting output of the engineering model can predict the total number of carriers that can be supported in each category of service. A financial model takes the output of the engineering model and calculates the revenue potential of the system described by the engineering model.

MODELING TECHNIQUES

A personal computer technique was chosen to model the mobile satellite system in order to provide as universal an application as possible such that the model can be used and modified to fit many situations and conditions. Lotus 123 was chosen as the programming language since it lends itself to the financial prediction output desired and it is generally available world wide in any office situation. A simplified flow diagram of the model is shown in Figure 2. The total model was split into two sections (in order to keep the PC requirements to a minimum) that can be run independent of each other.

The model requires an IBM XT, AT, PS-2 or compatible computer and Lotus 1-2-3 Release 2.0 or higher. The model is user friendly and custom menu driven. The user must only have a rudimentary understanding of the IBM Personal Computers and Lotus 1-2-3 operations.

The models are comprised of many easy to use custom menus. Each menu consists of numerous parameters that allow user inputs such as satellite parameters, transceiver parameters, system margins, data rates etc. The link calculation formulas and calculated results are protected so they cannot be erased accidentally. In the view and print menus, the user can either view the selected service parameters on-line or obtain hard copies. Calculation and Return menus provide the means of recalculating the model according to the new inputs or returning to the previous menu. The financial model is likewise simple to use, as in the engineering model, customized menus are used for input, modification of databases and output functions. A user manual is available for both models.

ENGINEERING MODEL

The engineering model comprises of a set of link analyses tailored to the mobile satellite service. The analyses are based upon various user input parameters, such as satellite antenna size, transponder DC power, carrier frequency, ground antenna gain, digital data rate, and end-to-end C/No. All inputs are variable and are made by responding to the computer generated prompts on display menus.

The Model can analyze multiple service quality scenarios simultaneously to calculate the transponder channel capacities. For example, both toll quality and commercial quality links can be analyzed independently. The output of the model consists of a channel capacity analysis, link calculations for two qualities of service and eight types of earth terminal configurations for each service quality. The purpose of the output is to display the channel capacity of a specific satellite configuration from the perspective of a satellite system operator.

ENGINEERING PRINCIPLES AND ASSUMPTIONS

The satellite transponder is assumed to be occupied with many narrow bandwidth SCPC carriers. They are spaced uniformly across the band on 5 KHz centers. The carriers are either Amplitude Companded Single Sideband voice (ACSB) or GMSK digital traffic. GMSK has a band width equal or less than the ACSB voice channels. It is assumed that at any given time, only a fraction of the total channel capacity (in terms of number of channels) is transmitting. That is, a VOX activity factor of 4 db (also variable) is used in the link calculations.

The engineering model is developed based upon the following link calculations: First the transponder Effective Isotropic Radiated Power (EIRP) is calculated based upon transponder RF power, antenna gain and output losses. Next, the clear sky Carrier to Noise Ratio (C/No) is obtained based upon the required end-

to-end C/No (service quality can be expressed in terms of end-to-end C/No), Carrier to interference ratio (C/Io), loss margins, and uplink C/No. After the C/No is calculated a beam center EIRP is obtained. The Beam center EIRP per carrier is based upon ground antenna gain, system temperature, free space loss, an activity factor (VOX) and Boltzman's constant. Finally, the transponder capacity can be calculated in terms of number of channels from the known transponder EIRP and beam center EIRP.

FINANCIAL MODEL

The Financial Model uses the output cases from the engineering model to convert numbers of channels to air time revenue. The program generates air time revenue based upon several user defined parameters. The major variables that determine the revenue formulas are price per minute, demand over the life of the program and average daily utilization. The outputs of the model are a revenue analysis, an income statement, and a cost model validation section.

MODEL INPUTS & OUTPUTS

The input to the model are price, program demand, daily utilization, capital cost, cost of capital, and tax calculations. For preliminary system design analysis the program is loaded with united states market and tax parameters with a 14% cost of capital, however, the model is easily modified for other countries or situations. The output reports are hard copy detailed revenue statement for each service and an income statement for the project.

FINANCIAL PRINCIPLES AND ASSUMPTIONS

The method of charging the user for the use of the satellite resource is to obtain the cost of the users' portion of the satellite resource. Since the portion of the satellite resource used is relative to the downlink power used in order to meet a certain service quality, all users can be related in price to a standard (such as a user with an Omni-directional antenna transceiver, requiring voice service with toll quality). The cost of other services then are determined in some proportion to the standard. All services are capable of being varied in cost. Furthermore, certain users may want to use higher data rates and/or different modulation techniques than the standard 5 Khz ACSB modulation of the standard. The model can handle these variations and the model user has complete control to vary the use of the channels. Surcharges for multiple contiguous channel usage are allowed.

The model is completely flexible in determining the usage of the transponder. For example, Figure 3 shows that the rate of customer loading can be controlled for each quality of service. Daily transponder usage modeling is available for both weekday and weekend/holiday periods. Easy modification of the curves allow the model user to see the effect of time zones and system user demographics. The model also allows the user to input system start up costs (such as satellite costs, master

earth station(s), Demand Assignment Multiple Access controllers, office space and anything else the user wants to include. Depreciation, tax data, and the time value of money over the life of the program is included.

Present value formulas for uneven cash flows that are dependent on system usage are calculated on an annual basis and summed to achieve a Net Present Value (NPV) for the project. Internal Rate of Return (IRR) is also calculated.

FINANCIAL MODEL RESULTS

After a financial analysis of a case is calculated the results are displayed graphically using the present value of the cash flows of the project. The graph displayed shows the time adjusted sunk cost and break-even analysis for the project. Figure 4 is a simplified sample graph that would be displayed on the screen. The financial analysis is then checked against the average capacity of the basic system. A validation section is provided as a tool by which to check the average number of users the system can support. The parameters of the average user for each category of service can be varied and used to calculate the number of users the system can support on an average business or weekend day and the cost to these typical users per month. A balance between market mix and financial return can be displayed for a total system analysis for each engineering case.

CONCLUSION

This model can be used to predict the financial viability of simple, low cost mobile communications systems. The resulting calculations can be plotted against each other to show which systems are capable of sustaining themselves. An example of this process is shown in figure 5. In this simple example the model was run with various DC power levels on the satellite. The number of channels supported is then plotted against the DC power and the limits imposed by bandwidth availability, DC power availability, and link performance are established by model output. Financial viability can then be shown as the systems that fall within the surrounding "box". Shown in this simple example, System 1 with Hi-Gain antennas is financially viable while System 2 with Omni antennas would not be, even though a certain number of channels could be supported technically.

SERVICES	Gain Quality	MOBILE ANTENNA TYPE					
		OMNI		HI-GAIN		PORTABLE	
		Toll	Comcl	Toll	Comcl	Toll	Comcl
Land Mobile Telephone		■		■			
Land Mobile Radio/Paging			■		■		
Air Mobile Telephone		■		■			
Air Mobile Radio			■		■		
Position Location Services							■
Public Safety/Medical			■		■		
Public Utilities							■
Resource Extraction							■
Rural Telephone						■	
Interactive Data							■
Construction/Agriculture			■		■		■
Coastal Marine		■		■			
Rail		■		■			
Government Agencies		■		■			

OMNI = 5 - 7 dbi
 HI-GAIN = 10 - 15 dbi
 PORTABLE = 20 - 22 dbi

Toll Quality = 47 DB-Hz
 Commercial = 43 DB-Hz

Figure 1. Definition of Service Categories

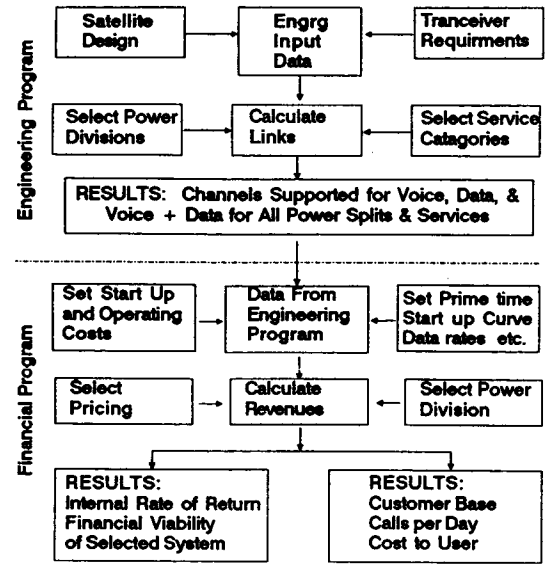


Figure 2. Model Flow Diagram

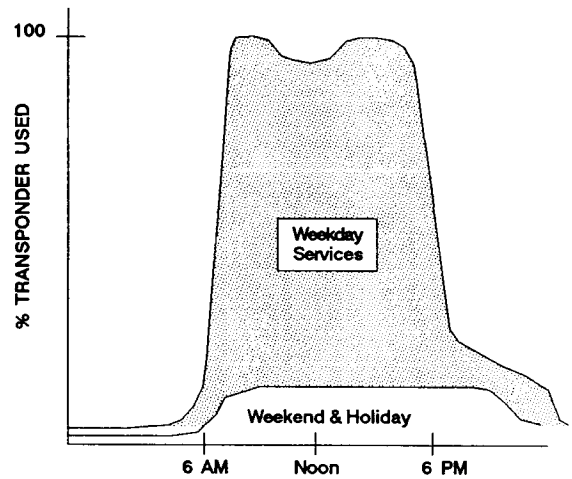
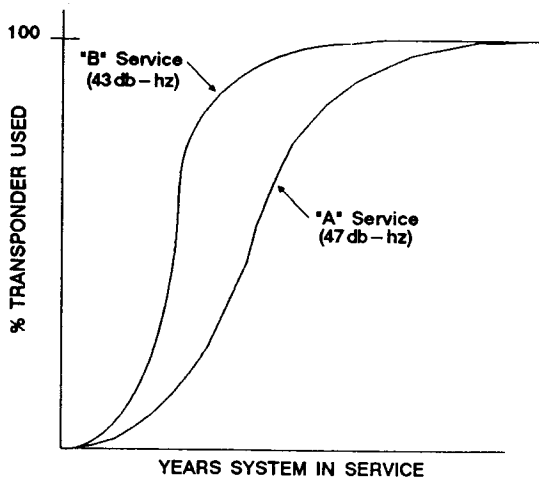


Figure 3. Transponder Usage Variables

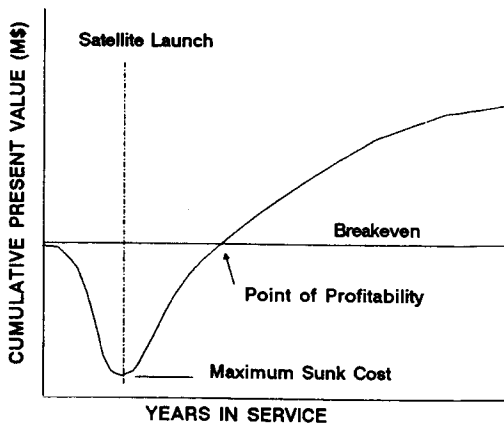


Figure 4. Example Cash Flow Analysis

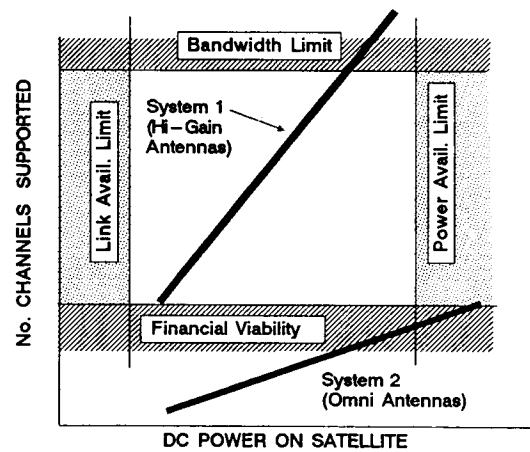


Figure 5. Example Tradeoff

DEVELOPING A GLOBAL AERONAUTICAL SATELLITE SYSTEM

DONALD K. DEMENT, AvSat Program, Aeronautical Radio, Inc., United States

AERONAUTICAL RADIO, INC.
2551 Riva Road
Annapolis, Maryland 21401
United States

ABSTRACT

Airlines have long recognized the crucial role of reliable communications to better secure a safe and profitable service. Arinc, an airline industry-owned and operated company in the United States, has taken steps toward establishing a global aeronautical satellite communications system. Plans call for initiation of a thin-route data operation in 1989, upgrading to establish voice communications via shared spot-beam transponders carried on other satellites, and finally deploying a worldwide network using dedicated satellites by 1994.

BACKGROUND

The concept of aeronautical communications via satellite began in the 1960s with NASA's VHF experiments, and at L-band during the mid-1970s in experiments using the ATS-6 satellite. AEROSAT, designed to cover Atlantic routes, was planned in the mid-1970s as a joint project among the U.S. FAA and NASA, Canada, and the European Space Agency, but for several reasons it was not pursued. Recently, interest has strongly revived. By 1987, voice and facsimile tests were being conducted over both the Pacific and Atlantic, and manufacturers and users are formulating a specification for avionics suitable for universal use.

TECHNOLOGY READINESS

Principal supporting technologies have matured and now can readily support initiation of commercial aeronautical satellite service. First, very thin conformal phased-array antennas with an electronically steerable beam now can be made for aircraft, having sufficient minimum gain to support very substantial communications capacity. Even mechanically-steered reflector antennas under a radome have already been put into service, and smaller ones are being considered for larger commercial aircraft. Implementation of a small, low-gain, hemispherical-coverage aircraft antenna for low-rate data service to a global satellite beam is practical. It may be used by an operator desiring a modest cost single antenna, and as a backup to a high-gain antenna.

The microchip processor will provide for in-flight compatibility with several possible signal characteristics from different service providers, without physical change-out. Digital voice is maturing, as codecs in the 9.6 and 8 kb/s area now are producing near-toll quality voice and are being evaluated. An accommodation to ISO rates (2000n) such as 8 kb/s is important for transparent ground terminal operations of the future.

USER MARKETS

Aircraft operators appear to have a unique opportunity for operational enhancements and cost reductions by using satellite communications. Savings in fuel costs from improved routing and bad weather avoidance are now being quantified as very significant. Also very important to costs may be near-real-time monitoring of engine performance.

Air traffic control is likely to benefit strongly from over-ocean position reports, timely weather knowledge, more rapid response to altitude clearance requests, and a corresponding increase in flying safety. Rapid reporting of accurate aircraft position could permit separation reductions that are predicted to bring major time and fuel savings because of improved routing.

Passengers will enjoy new services and improved efficiencies, principally via voice communications through any public switched network in the world. Until recently, voice service between aircraft and ground has been the province of crew communications. High-quality, distance-insensitive voice circuits worldwide through satellite earth stations will revolutionize the air-travel experience.

New passenger data services such as continuously available national and international news and other reports; inter-computer communications; and traveler support, such as reticketing, car rental, and special services, will further enhance the air travel environment.

The operational savings provided through reduced flight time, rapid clearances, reduced fuel reserves, improved weather information, and other benefits will offset satellite costs for data systems and crew voice services. Combining crew and passenger communications within a common avionics suite and system signal structure can provide for cost-effective delivery of both.

SPECTRUM AVAILABILITY

Recently, developers of aeronautical and land-mobile satellite systems have clashed because of direction of regulatory bodies that would require accommodation of both services in the same band. The 1987 WARC reduced the aeronautical satellite spectrum from 28 to 20 MHz (now 1545-1555 MHz down, 1646.5-1656.5 MHz up), but retained the exclusivity of this allocation and authorized countries to permit aeronautical communications in the remaining 4 MHz with land-mobile space stations. This WARC also clarified the rules that permit passenger communications in this band.

The Federal Communications Commission (FCC) is working to reconcile its domestic rulings for the U.S. -- which tend to unify AMSS and LMSS --

to the outcome of the international WARC, which retains these services' partitions.

Aeronautical mobile feeder links to and from the satellite and earth stations are being sought to operate at a portion of the C-band separate from domestic satellite uses. This will permit a global plan for aeronautical satellite orbital locations and coverage which is optimized for air traffic routes without conflict with other satellites.

SYSTEM DEFINITION ACTIVITIES

Characteristics of aircraft transceivers for satellite communications are being developed by system suppliers and manufacturers together with airline engineers in the Airline Electronic Engineering Committee (AEEC). Avionics form and fit are nearly complete, and functional specs are under development. Throughout, they follow closely the ISO standards, utilizing the "layer" concept to enable transparency to future global networks with a universality of protocols both in the RF (satellite) regime and within the system processors.

REQUIREMENTS AND CONSTRAINTS

In addition to requirements for maximum coverage, a global aeronautical system must assure the highest reliability because it often carries safety-related traffic.

Satellite links at low aircraft elevation angles must contend with four simultaneous impacts: fading; decreased G/T from off-boresight scanning, reflections, and potential blockage; power and sensitivity loss at the satellite antenna edge-of-coverage; and maximum satellite-aircraft range. Link fading that requires significant power margins in the land and maritime cases is less severe for aircraft at altitudes of tens of thousands of feet, amounting to about one dB for most cases. All these link impairments improve rapidly and largely disappear at aircraft elevation angles above 20-30 degrees.

Satellite RF link design choices have been made in the direction of robustness and spectrum efficiency while minimizing control complexity in the earth stations and avionics. The need for high reliability at lowest cost has led to use of the simplest technologies in both the aircraft and the satellite transponder, and to the use of all-digital techniques in network control and earth stations. These concepts are not in conflict when a TDMA (time division multiple access) system architecture is specified.

The satellite power assigned to any one user generally is a compromise among many factors. Class C operation of high-power RF amplifiers (HPAs) provides for efficient use of raw power -- an advantage both for the aircraft: small size, modest cooling, with multi-channel capability for six channels of high-quality voice plus wideband data to and from each aircraft; and for the satellites, making possible cost-efficient HPAs while maximizing capacity for the high EIRP required.

In combination with Class C HPAs, a TDMA operations architecture is ideal to realize these efficiencies because it (1) employs a single, wideband, multi-channel carrier and (2) avoids intermodulation distortion and interference, while conserving spectrum. It also promises

orderly growth to a large future network of thousands of channels using known controller designs.

SYSTEM DESIGN CONSIDERATIONS

A viable mobile satellite system requires a careful balance in sizing, because the satellite per-channel power output and system capacity, -- and therefore user cost -- depend strongly on the mobile unit's G/T.* System noise temperature is generally set at an irreducible minimum, so the mobile's receive antenna gain is the basic determinant of the required satellite EIRP.** But the need for maximum gain conflicts with a tolerance for only the smallest mobile antennas.

Similarly, because of limited spectrum allocations, the needed frequency reuse depends on each mobile unit's discrimination among same-frequency satellites. Therefore, the mobile units' beamwidth and sidelobe levels will determine overall system capacity. Yet obtaining narrow, clean patterns from small antennas mounted on indeterminate conducting surfaces is not a predictable task, and compromises must be made. Through AEEC activities aircraft operators have agreed on a steerable transmit/receive antenna system with minimum gain of 12 dBiC.

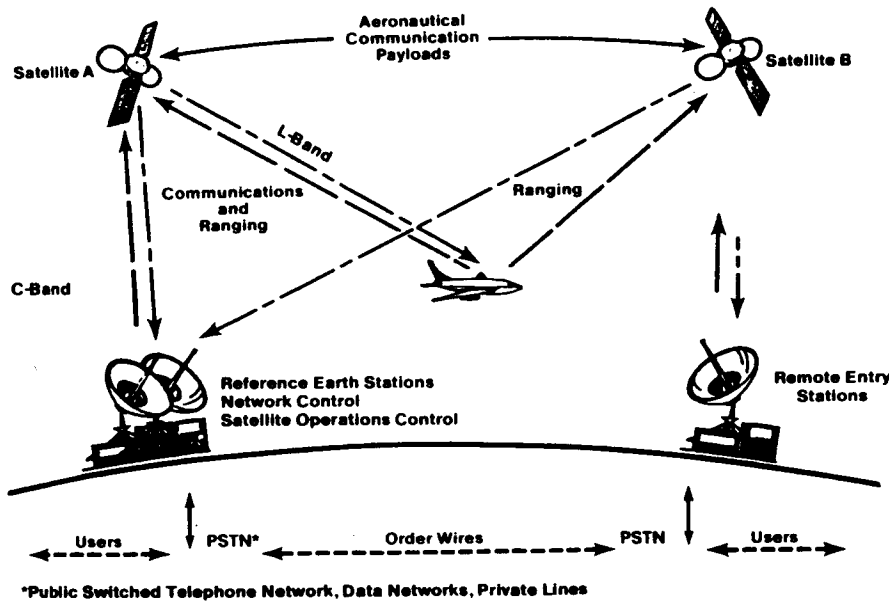


Fig. 1. Basic AvSat System

On the receive side, the achievable G/T for the mobile unit (using $T_{sys} = 320K$) is about -13 dB/K . For the satellite L-band transmission ("outbound"), the desired multi-channel data rate in a 25 dBiC spot beam has been set -- based primarily on available satellite HPA size -- at 320 kb/s. This carrier makes available 32 voice channels at 8 kb/s each, plus some considerable data capability (synchronous and slotted Aloha).

The aircraft transmission ("inbound") plan for spot-beam satellites uses a hybrid FDMA/TDMA approach called Multi-Carrier TDMA. In this sys-

* Gain-over-Temperature, a measure of receive sensitivity.

** Effective Isotropic Radiated Power.

tem, each aircraft transmits in a TDMA mode at 64 kb/s -- a fraction (1/5) of the incoming data rate (320 kb/s) -- which constrains the output power requirement while meeting multi-channel needs of six voice channels plus data. These rates are based on achievable satellite G/T of about -4 dB/K and an aircraft HPA limit of 40-50 RF watts.

In MC/TDMA, the satellite L/C transponder operates linearly in FDMA, each RF carrier containing bursts from up to six voice and several data channels from one or more aircraft. As a result, the TDMA "burst time plan" actually becomes a burst time-frequency plan. This scheme also reduces the number of earth station receivers by a factor of six, and has been successfully implemented in other applications. Detailed avionics MC/TDMA specification preparations are now well under way.

DEVELOPING A GLOBAL SYSTEM

Phase One: A Test Program

ETS-V, Japan's first three-axis stabilized satellite, was launched to 150 East in August 1987. It carries an L-band 20-watt solid-state HPA and a 1.5-meter reflector antenna, producing dual 10.5-degree spots with approximately 36 dBw maximum EIRP. Voice and data tests are now under way. Preliminary plans have been discussed among the Japanese JCAB, the FAA, and Arinc which would permit test of aeronautical satellite transmissions primarily for position reports.

INMARSAT test programs are also under way. Data transmissions to and from aircraft were tested in late 1985, and voice tests now are being conducted with Japan Air Lines over a Pacific route. Further tests are planned by several countries during 1988.

Phase Two: Initial Data Operations

The operation of aeronautical mobile satellite service is expected to begin as soon as sufficient avionics are mounted to comprise a significant user population. INMARSAT's second-generation satellites will operate within the aeronautical band, and are expected to provide for a new service, titled "International ACARS." This service will extend over oceans and remote areas an air-ground packet data service called ACARS, now operated by Arinc. The messages will interface with the ACARS network through INMARSAT satellite terminals equipped to provide the service.

Phase Three: Shared-Satellite Transponders for Voice and Data

The development of significant multi-channel aeronautical satellite services with full connectivity to all ground stations in view awaits the launch of higher-EIRP transponders. One concept is to provide to a "host" FSS (fixed-satellite service) satellite having a mutually desirable orbital location a set of transponders for aeronautical use. Such host satellites have been identified, preliminary business and technical arrangements have been discussed, and satellite manufacturers have cooperated in conceptual designs. Necessary IFRB actions have been completed by the host operator for the Pacific Ocean coverage area and are under way for other areas.

Using one or more Class C HPAs per spot beam operating at a 30-40 watt level, and a spot size of about seven degrees, the EIRP of 39 dBw at edge of coverage will provide adequate E_b/N_0 for a data rate of 320 kb/s. This data rate will enable at least thirty-two 8 kb/s voice channels, plus high-rate synchronous and asynchronous user data channels, and TDMA system overhead data.

Phase Four: Dedicated Aeronautical Satellites

System design requirements that (1) minimize the number of satellites while providing for maximum frequency reuse and position-location coverage and (2) minimize transitions between satellites during an aircraft flight segment result in a six geosynchronous-satellite constellation. Frequency reuse also is enhanced by the use of an interlaced inter-satellite frequency plan for the complete worldwide system. Orbital locations near to four of Arinc's selections were submitted by the FCC and Advance Published (AP) by the IFRB on November 17, 1987. The remaining two locations to serve the U.S. are to be coordinated with the FCC based on spectrum allocation developments.

An important system design requirement is to permit expansion to a large global system of thousands of channels with minimal or no disruption to aircraft over decades of operation. This requirement has driven a plan that permits similar transponders to be added on both host and dedicated satellites, raising the data rate and EIRP by means of smaller spot beams while operating within the same basic architecture.

Satellite technology of today completely supports these near-future needs. Using less than two watts of satellite conditioned power per voice channel, today's larger satellites could enable 2,000 voice channels. Antenna sizes to fit within launch vehicle shrouds without unfurling are adequate even at L-band for the needed EIRP and G/T.

A five-fold increase in the system data rate (from 320 kb/s to 1.544 Mb/s) would need less than a five-meter satellite antenna and could use the same satellite HPA. The additional spot beams would provide the system operator with more flexibility to fit power density to changing user traffic areas. For this upgrade, the necessary changes to avionics are in the filters, modems, and parts of the processors, all of which need only to be reprogrammed.

By upgrading with integral multiples of data rates, expansion of the system retains use of the avionics and the Phase Three shared-satellite transponders, permitting orderly transitions to dedicated satellites and utilizing all resources to their full lifetimes. Spectrum coordination and planning for all the world's aeronautical band users is a major requirement for integration.

CONCLUSION

Satellites for aeronautical communications are not only needed today, but have become essential because there is no alternative for remote-area voice and data so vital to efficient and safe aircraft operation. Supporting technology and radio spectrum allocations are ready, and a phased development plan for implementation is now under way. Shared and dedicated satellites for aeronautical communications are certain to play a large part in providing satisfactory service in the near future.

WORLD-WIDE AERONAUTICAL SATELLITE COMMUNICATIONS

Peter Wood, Manager-Aeronautical Department, INMARSAT
Keith Smith, Project Leader-Aeronautical Department, INMARSAT

INMARSAT
40 Melton Street
London, NW1 2EQ
England.

ABSTRACT

Faced with the resurgence of interest in aeronautical satellite communications, and with the encouragement of aviation organizations and its Signatories, INMARSAT decided to expand the spectrum covered by its new generation of satellites, INMARSAT-2, to include 1 MHz (subsequently increased to 3 MHz) of the spectrum designated for aeronautical use. It began a design study which led to the specifications for the system that is now being implemented. Subsequently INMARSAT has awarded contracts for the design of avionics and high gain antennas to a number of manufacturers, while several of the Signatories that provide ground equipment for communicating with the INMARSAT satellites are modifying their earth stations to work with the avionic equipment. As a result of these activities, a world-wide aeronautical satellite system supporting both voice and data will become operational in 1989.

SERVICE REQUIREMENTS.

There are four generic applications that will benefit from the use of satellite communications:

- **air traffic services**
communications for air traffic control purposes, including automatically relaying the position of an aircraft as determined by the on-board navigation equipment to the air traffic control center (automatic dependent surveillance)
- **airline operational control**
communications which involve the regularity and efficiency of flights, such as between an aircraft and its operating airline giving its estimated time of arrival.
- **airline administrative communications**
non-safety related communications which affect the administration of an airline. An example would be passenger connecting flight arrangements.
- **passenger correspondence**
communications to and from a passenger in flight. These would normally relate to telephone services, but could include telex and facsimile.

To meet the needs of these services, three basic forms of communication are required:

- a low data rate service (600 bit/sec). This has been defined by ICAO's FANS committee as the "core" system.
- a medium data rate service (up to 12.6 kb/s), and
- a voice service, with a quality equivalent to that of a good telephone service ("toll" quality).
At a later date, other services (such as a lower quality voice channel) may be necessary.

SYSTEM ELEMENTS

The major elements of the aeronautical satellite system comprise:

- (a) the Space Segment, in particular the satellite communications transponders, and the associated frequency bands assigned for use by the aeronautical satellite system. Figure 1 shows the provisions of INMARSAT-2 satellites compared with the outcome of Mobile-WARC-87;
- (b) Aircraft Earth Stations (AES) which interface in the aircraft with ACARS/AIRCOM and other data equipment, and with crew and passenger voice equipment, and with the space segment at L-band;
- (c) Aeronautical Ground Earth Stations (GES)* which interface with the space segment at C- and L-bands, and with terrestrial voice and data networks;
- (d) Network Coordination Stations (NCS), which interface with the GESs for the purpose of allocating satellite capacity.

INMARSAT's present space segment comprises nine satellites, three in each ocean region. One satellite in each region is classified as the "operational" satellite, the other two as spares. The three operational satellites provide effectively global coverage and INMARSAT reconfigures the satellite disposition from time to time to match traffic demand. These first generation satellites will be augmented from late 1989 by at least 3 2nd generation satellites (INMARSAT-2) which like the first generation, each offer "global beam" coverage. Figure 2 shows the coverage at 0 and 5 degree elevation angles. Plans are well under way for the introduction of spot-beam INMARSAT satellites in the 1991/93 timeframe.

The major L-band parameters of the first and second generation INMARSAT satellites are (at edge of coverage):

Satellite/ Package	EIRP (dBW)	G/T (dB/K)	
Marecs	34.5	-11.2	} 1st Generation
MCS	33.0	-13.0	
Marisat	27.0	-17.0	
INMARSAT-2	39.0	-12.5	

SYSTEM DESIGN CONSIDERATIONS

The system design uses a hybrid FDMA/TDMA/TDM approach. Data and signalling use a TDM/TDMA packet-transmission technique, while digital voice circuits use single channel per carrier (SCPC) transmission in order to take advantage of the characteristics of speech to minimize satellite resource demands. The factors that were considered included:

- The need to provide a global capability from the start of service.
- Spectral efficiency
- Power conservation

Many system designs were considered, but the reasons for choice of an SCPC approach to voice transmission appear from the analysis summarised in Table 1.

* Ground Earth stations are generally owned and operated by Signatories -- organizations nominated by their countries to invest in, and work with, INMARSAT. The Signatories are the organizations actually responsible for the provision of aeronautical satellite communication services.

Table 1 is based upon the SCPC design selected by INMARSAT, and a specific alternative TDMA approach that has been considered by the aeronautical industry. Both of these have been considered by the Airlines Electronic Engineering Committee (AEEC). It is apparent that, whether operating with global or spot beam satellites, or with high gain or low gain antennas, an SCPC system offers more capacity.

Contributory factors are:

- the transmitted power from the satellite is proportional to the number of channels being handled; for a TDMA system the power is constant, irrespective of the number of channels in use at one time,
- the transmitted power can be adjusted on each channel to deal with variations in path length, propagation conditions, and variations in antenna gain. This allows reduction of system margins and consequent power savings. In a TDMA system, the power has to be at a constant worst-case level.
- it is possible to use voice activation on voice circuits, using no power until someone is actually speaking.
- use of SCPC avoids the need to 'bundle' traffic into groups of circuits of preassigned size. Such bundling not only restricts system flexibility, but incurs significant efficiency penalties arising from the statistical nature of voice traffic.

Nevertheless, the present choice of SCPC does not preclude the future development of a more suitable TDMA design following the widespread introduction of spot beam satellites.

SYSTEM CONFIGURATION

The INMARSAT aeronautical system is configured around two types of transmission channel, data and voice, and two R.F. amplifier/antenna combinations on the aircraft, low-gain (0 dBi) and high gain (12 dBi). Aircraft Earth Stations (AES) are classified according to their equipment configurations and capabilities, as follows:

- Class 1: Low gain antenna only, data services only;
- Class 2: High gain antenna only, voice services only;
- Class 3: High gain antenna only, voice and data services;

In the initial configuration, transmissions over the data channel will be at either 600 or 1200 bits/second (selected by the ground earth station). As rate 1/2 forward error correction (FEC) coding is used to reduce the bit error rate, the effective information data rates are 300 and 600 bits/second respectively.

Voice signals are digitized at a 9.6 kbits/s rate, and are combined with signalling data, resulting in an information data rate of 10.5 kbits/s. Again, FEC encoding is used to reduce the bit error rate, giving a data transmission rate of 21 kbits/s over the voice channel.

The specific service capabilities of an AES will vary according to its class and the number of channel units installed. Examples of typical installations would be:

- (a) one data channel only. This would support data services only, to a single GES;
- (b) one data channel, plus two voice channels. This would support data and voice services simultaneously, with the voice and data able to use different GESs; and
- (c) two data channels, plus six voice channels. The data services could be to two different GESs. The voice services could use several GESs.

SYSTEM DESIGN SUMMARY

Modulation and Coding

Up to an RF transmission rate of 2400 bit/s, binary modulation is used with root 40% raised cosine filtering, and above that a quadrature technique is used with root 60% raised cosine filtering.

Both are "offset" techniques which minimize RF amplitude variations after filtering, and thereby permit close spacing of the RF channels. For the quadrature technique, initial channel spacings of about 0.83 of the bit rate are achieved.

FEC coding is provided, with rates of 1/2, 3/4 and 1 (no coding). Constraint-length seven convolutional coding is used, and interleaving is applied to randomize the bursty errors arising from the multipath L-band channel, which has a fade rate of about 30 Hz and above, with C/M of 10 dB and above. A common interleaver structure is applied at all bit rates, although the block size is varied to maintain a constant depth (randomizing power) to match the bit rate. When FEC-coded channels are used for voice transmission, the maximum interleaving delay is kept to between 30 and 40 mS, which slightly reduces the effectiveness of interleaving. It is also possible to operate without FEC.

Transmission Format (Data Link Layer)

Given the nature of the multipath fading channel, it is vital to design the transmission format to ensure the maximum resistance to burst errors. This implies a need for consistent link-level error detection performance, and the availability of error recovery procedures.

This has been handled at link layer by formatting all data, whether signalling, control, or user-data, into standard packets of pre-defined length, each protected by a common CCITT cyclic redundancy (CRC) code to ensure consistent packet-error detection. The format and length of these "Signal Units" (SUs) has been the subject of considerable study, representing a trade-off between efficiency (link-layer overheads, compatibility with signals and other message lengths) and error performance in the RF channel. The system user may request that packets are delivered to the application without error checking (Direct Link Service) or after ARQ (Reliable Link Service). The standard SU is 96 bits, of which 16 are Cyclic Redundancy Check (CRC) for error detection. Where included, aircraft addresses are 3 octets in length, and ground station addresses are one octet.

Data Applications (Network Layer)

The system provides full support for a network layer consistent with the ISO layered architecture for connectionless, connection-oriented, and special (e.g., polling) services.

Transmission Channel Characteristics

To accommodate the range of services, four basic RF transmission channels have been defined with different satellite access techniques. The four channel types are:

P-Channel:

Packet mode Time Division Multiplex (TDM) channel, used in the forward direction (ground-to-air) to carry signalling and user data. The transmission is continuous from each earth station in the satellite network.

R-Channel:

Random access (slotted Aloha) channel, used in the return direction (aircraft-to-ground) to carry some signalling and user data (short messages), specifically the initial signals of a transaction, typically request signals.

T-Channel:

Reservation Time Division Multiple Access (TDMA) channel, used in the return direction only. The receiving earth station reserves time slots for transmissions requested by aircraft earth stations, according to message length. The sending aircraft earth station transmits the messages in the reserved time slots according to priority.

C-Channel:

Bi-directional circuit-mode channel. The use of the channel is controlled by assignment and release signalling at the start and end of each call. A C-channel has a BER after FEC decoding of better than 10^{-3} (whereas the P, R and T channels have better than 10^{-5}) which is suitable for voice communications. Each C-channel may carry one or more voice channels, but to support more than two voice channels, more than one RF carrier is needed. A C-channel also carries a multiplexed low-rate data channel (about 200 bit/s) for signalling or user data.

TABLE 1

TDMA/FDMA COMPARISON: NUMBER OF AIR TO GROUND VOICE CHANNELS PER AIRCRAFT AS A FUNCTION OF HPA POWER

AIRCRAFT ANTENNA GAIN (SAT. ELEVN.)	12 dBIC (> 20°)		12 dBIC (> 5°)		0 dBIC (> 20°)	
SPACECRAFT ANTENNA GAIN (EOC)	'Global' (17 dBIC)		Spot (25 dBIC)		Spot (25 dBIC)	
HPA POWER*	FDMA	TDMA	FDMA	TDMA	FDMA	TDMA
40 W (AEEC)	4	0	14	6	2	0
30 W	3	0	10	6	1	0
20 W	2	0	7	6**	1	0
12 W	1	0	4	0	0	0
6 W	0	0	2	0	0	0
3 W	0	0	1	0	0	0

* Linear HPA needed for FDMA, ~~except~~ nonlinear (Class-C) may be used for single-carrier cases

** Marginal

TDMA/FDMA COMPARISON: NUMBER OF GROUND TO AIR VOICE CHANNELS PER SATELLITE SPOT BEAM

Aircraft Antenna Gain	12 dB		0 dB	
Satellite Beam EIRP (dBW, eoc)	Number of voice channels		Number of voice channels	
	FDMA	TDMA	FDMA***	TDMA
36	100	-	4	0
39**	200	30	9	0
42	400	30+30*	20	0

* Requires 2 transponders

*** Reduced voice activation advantage

** AvSat nominal (approx.)

System Designs: TDMA: as per ARINC Quick Check 39 (AvSat System Technical Description - 8.0 kbit/s voice)

FDMA: as per INMARSAT System Definition Manual - 9.6 kbit/s voice

eoc: edge of coverage = 5° elevation

FIGURE 1 - L-BAND FREQUENCY ALLOCATION

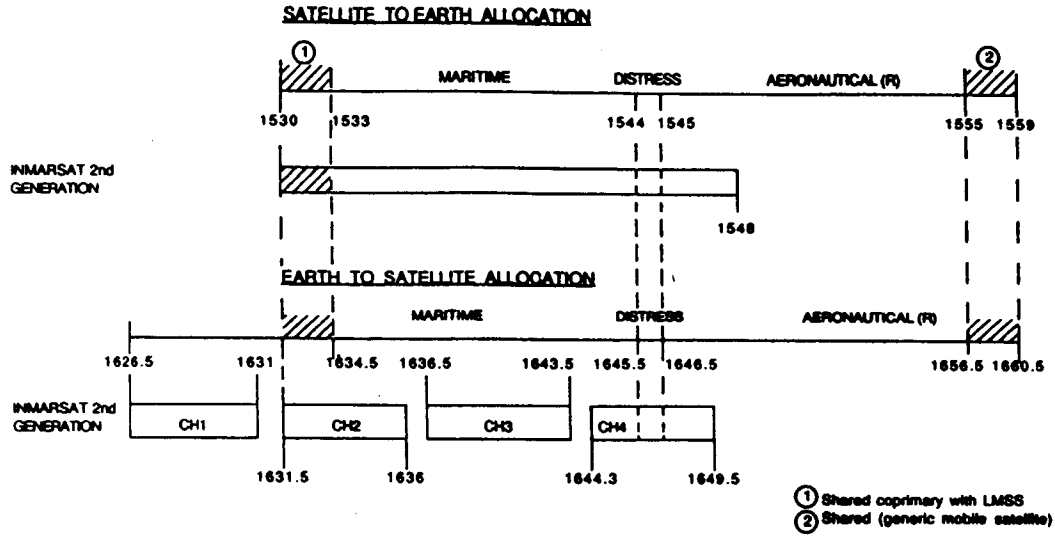
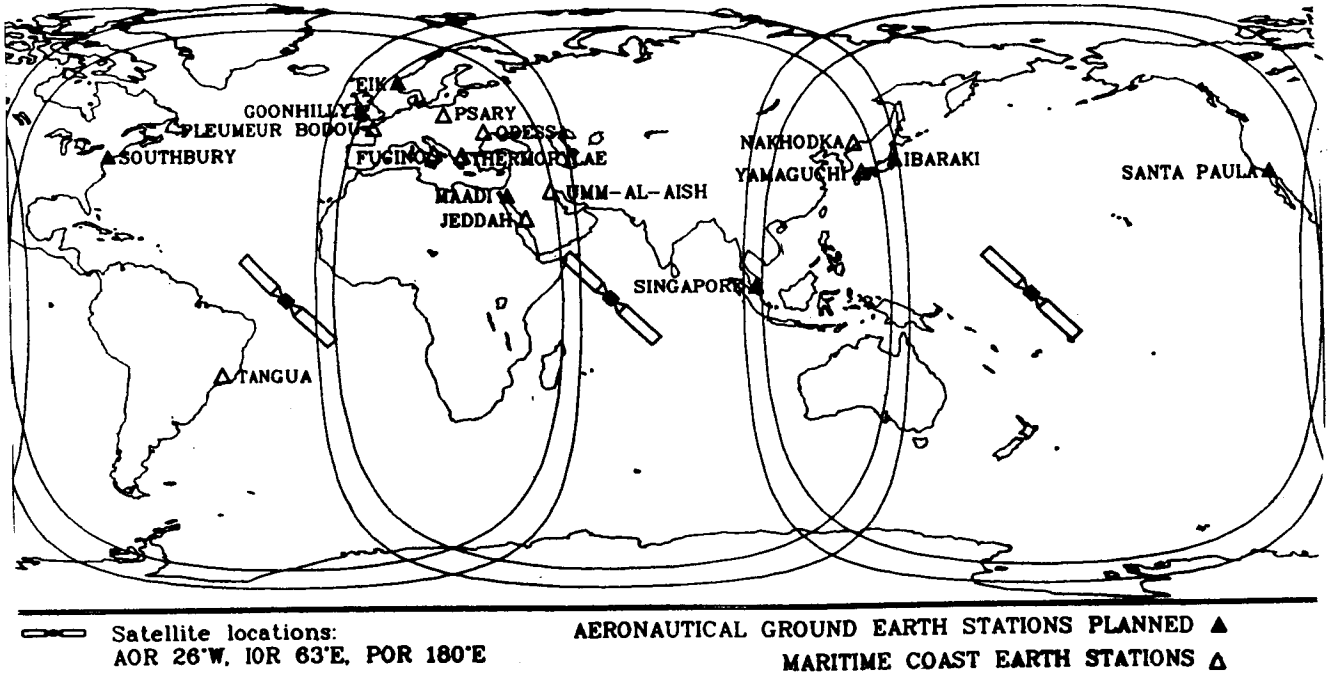


FIGURE 2 - INMARSAT GLOBAL COVERAGE



**AN OVERVIEW OF THE OMNITRACS - THE FIRST OPERATIONAL
MOBILE KU-BAND SATELLITE COMMUNICATIONS****ALLEN SALMASI, President****OMNINET COMMUNICATIONS SERVICES
3416 South La Cienega Boulevard
Los Angeles, California 90016-4496
United States****ABSTRACT**

The service features of the OmniTRACS system developed by Omninnet Communications Services of Los Angeles, California, are described. This system is the first operational mobile Ku-band Satellite Communications System that provides two-way messaging and position determination and reporting services to mobile users on a nationwide basis. The system uses existing Ku-band satellites under a secondary international allocation for mobile satellite services.

INTRODUCTION

Omninet Corporation was formed in 1984 to provide a nationwide mobile communications service. Omninnet has applied dramatic innovations to proven technologies creating a two-way messaging system for mobile and fixed applications.

The founder and president of Omninnet, Allen Salmasi, has been actively involved for over a decade in developing and refining the initial NASA concept for mobile satellite systems. He conceived the OmniTRACS product which has enabled Omninnet to develop a two-way mobile communications system employing in-orbit Ku-band satellites, with full operations commencing second quarter 1988.

The Federal Communications Commission (FCC) recently concluded there is an "outstanding need" for satellite-based position reporting and alphanumeric messaging. Because of such a demand for satellite-based mobile communications, the FCC over the past two years has given birth to two uniquely different services called the Mobile Satellite Service (MSS) and Radiodetermination Satellite Service (RDSS). Omninnet is one of the two companies currently holding the RDSS license and the general authorization to proceed with the launch of its RDSS services, granted by the FCC in March, 1987.

Working with Qualcomm, Inc. of San Diego, Omninnet is the first company to develop technology using existing Ku-band satellite capacity for mobile applications, eliminating the expense, risk and delays associated with satellite launches. Omninnet and Qualcomm have been working closely to develop the OmniTRACS product for over two years. Omninnet has contracted Qualcomm to design, implement and manufacture the OmniTRACS mobile and transportable VSAT's and the associated Network Management Facility exclusively for Omninnet. Representatives from a variety of industries have expressed a need for improved communications with mobile fleets. Companies involved in public safety, transportation, public utilities and others have a need to send and receive information to vehicles enroute. As vehicles travel across the country into rural areas, they move out of range of

conventional land-based communication systems. Omninet's satellite communication system - OmniTRACS - eliminates the range problems inherent with land-based systems, creating a true nationwide network.

The OmniTRACS system began operational tests in January, 1988, in which an OmniTRACS mobile terminal was driven from Coast to Coast in constant communication with a Network Management Facility located in San Diego, California. Operation was very successful in all kinds of environments from wide open Western freeways to the concrete canyons of New York City.

Ku-band satellite communications are common-place in the commercial market and, in fact, the fixed VSAT (Very Small Aperture Terminals) network applications is one of the major growing markets for the Ku-band satellite communications. Telephony, television and private data networks are already extensive users of Ku-band satellites, plus Ku-band components are mass produced, making terminal costs relatively inexpensive. This provides for very reasonably priced communications and VSAT equipment. Other potential mobile satellite service providers must rely on tentative satellite launches years into the future at a cost of hundreds of millions of dollars or on securing frequency spectrum not yet sufficiently available for such use. Omninet is utilizing existing hardware and facilities, both on the ground and in space, with an innovative system design that takes advantage of novel signal processing techniques to deliver the mobile and transportable VSAT network services.

SYSTEM DESCRIPTION

OmniTRACS is a unique satellite-based communication system enabling users to manage mobile resources efficiently and economically.

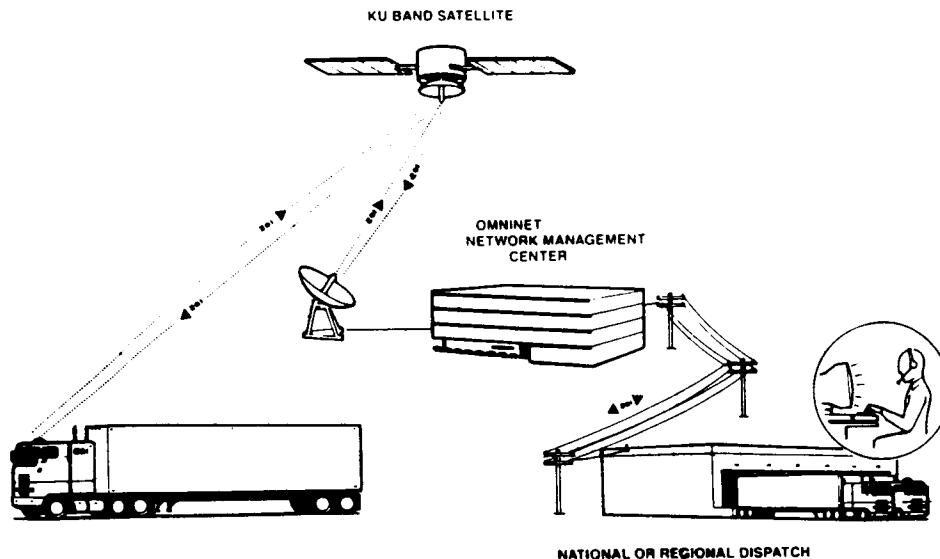


Fig. 1. OmniTRACS Service Network Concept

The OmniTRACS VSAT network has three major components:

1. A Network Management Facility (NMF) which controls and monitors the OmniTRACS network. The NMF, located in Los Angeles, California with back-up facilities in San Diego, California, consists of a computer facility, message switching and processing equipment, and a satellite earth station to transmit and receive customer messages.
2. Two Ku-band transponders aboard GTE Spacenet's GSTAR I satellite located at 103° west longitude.
3. Two-way data-communication and position-reporting mobile and transportable OmniTRACS VSAT's.

The OmniTRACS mobile and transportable VSAT network features two-way data messaging, position reporting, fleet broadcasting, call accounting and message confirmation. The service provides users with an unprecedented range of features in a variety of cost-effective packages. A complete technical description of this system is presented in this conference in a paper by the technical staff of Qualcomm, Incorporated, "Technical Characteristics of the OmniTRACS - The First Operational Mobile Ku-band Satellite Communications System."

OmniTRACS features

Nationwide Covers the continental United States, including metropolitan and rural areas, so long as a direct line-of-sight to the satellite from the mobile antenna is available. No other commercial system is offering similar coverage in North America.

Existing satellites Uses fully protected Ku-band transponders on existing geostationary satellites which have been operational for many years. There is no risk of satellite hardware failure in-orbit and no dependence on future launches.

Two-way Allows dispatcher or driver to initiate or respond to preformatted or free-form messages. Emergency, group and fleet-wide messages are also available. Most importantly, it provides a positive acknowledgement of each message sent, ensuring the sender of a successful transmission.

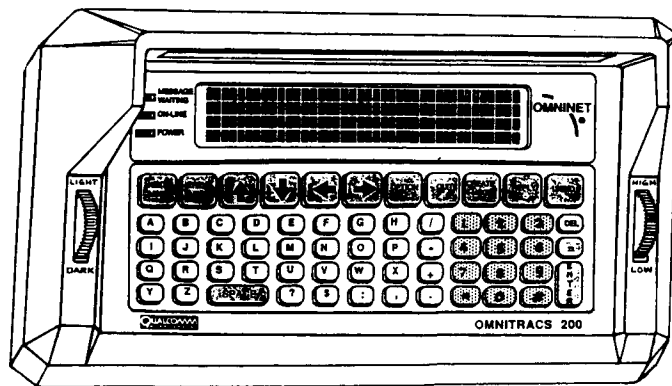


Fig. 2. The OmniTRACS Terminal Display Unit

Data Communication Dispatchers use computer terminals for message creation and response. Unlike traditional voice systems, messages are received by computer in a fraction of the time it takes for dictation of the same information, and can be stored for convenient viewing or later recall.

Demand for data communication systems has increased as the needs of mobile users have expanded and changed. The desire for greater speed and accuracy in mobile communications, the need to access information stored in computer databases, improvements desired in response time from the field, system security and privacy, and the need for preformatted and storable messages are some of the advantages that the OmniTRACS data communication system provides.

Position Reporting Satellite-aided Loran-C position information is available to the dispatcher after a message is sent to a mobile unit. It may also be provided on a scheduled basis or on demand.

By using the Ku-band satellite as a slave Loran-C station, the satellite-aided Loran-C provides highly accurate position information. This information is beneficial in vehicle management, such as ad-hoc dispatching, scheduling of shipments, vehicle arrival time management, accident location, recovery in the event of hijacking, and many other emergency and non-emergency situations.

Service Encompasses a range of equipment lease and purchase options, and a commitment to service at every level of customer involvement from training through customized system support.

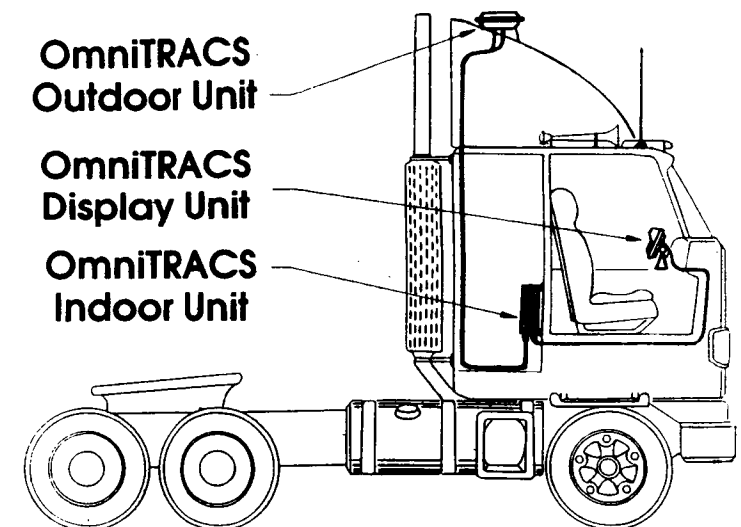


Fig. 3. A Typical OmniTRACS Terminal Installation

Other features of the OmniTRACS service include:

Compact User-Friendly Terminals
End-to-End Turnkey Network Service
Network Monitoring and Diagnostics
Individually Addressable Terminals
Highly Reliable Data Delivery
Easy Maintenance

Federal Data Encryption Standard
Multiple Message Memory
Quick Installation
Minimal Power Requirements
Unattended Service

APPLICATIONS AND BENEFITS

There are numerous applications for the OmniTRACS mobile satellite communication system. Any organization or a company with a fleet of mobile vehicles will derive notable benefits from the system.

To date, twenty potential user markets have been identified. The market for Omninet's services includes trucking and other commercial transportation services; utilities and public sector users including public safety, emergency and Federal Government agencies; construction and resource-extraction companies; agriculture and forest resource companies; regional and charter bus lines; railroads and marine vessels; consumer and small business mobile users as well as stationary and transportable users desiring their own private low-volume data networks.

Omninet has executed contracts with eighteen transportation companies for over 25,000 units to be installed over a period of two years. Omninet's marketing and sales personnel are working with major transportation companies. Omninet projects that the companies it is working with have the potential for utilizing over 100,000 units. This represents roughly one percent of the total addressable market for satellite-based mobile communications.

Transportation

The transportation industry has an increasingly acute need for mobile communications on a nationwide basis. Companies involved in public transit, trucking, railroads, marine transport, and aviation require communication with and tracking of their mobile fleets. Trucking operations are subject to frequent changes in routing and scheduling. Trucks are more vulnerable than other types of transportation to mechanical failure, accidents, local traffic delays and adverse road conditions, increasing the need for mobile communications. The transportation industry currently has no communications and position reporting services on a nationwide basis. The OmniTRACS system provides a cost-effective answer to the needs of the transportation industry. Three key factors make the system cost effective: Use of the currently operational in-orbit Ku-band satellites, the mode of the communication (data) and the unlimited range of the system.

Because the OmniTRACS system uses data messages to communicate information, the cost per message is significantly less than voice transmissions. The time spent sending and receiving messages is decreased, thus saving money at both the driver and dispatch levels. In addition, the unlimited transmission range of the system allows for messages to be sent enroute, which eliminates unnecessary stops.

Of particular interest to the transportation industry is the ability of the OmniTRACS system to track vehicles, specifically those carrying hazardous materials, weapons or petroleum. The cargo's value, coupled with the risks involved, requires constant surveillance of the truck, train or aircraft. The OmniTRACS system provides position reporting of vehicles on demand or at predetermined intervals.

Vehicle Location

The sheer number of government and private industry vehicles traveling across the country make it difficult to monitor the location of each vehicle at a specific time. The OmniTRACS position reporting system allows a dispatcher to locate any vehicle at any time with the desired level of accuracy. This feature is beneficial for day-to-day monitoring of a fleet, as well as locating a vehicle that has been stolen or involved in an accident. Recovery of valuable merchandise and equipment is possible by using the OmniTRACS system.

Public Safety

Fire, police and emergency medical organizations using the OmniTRACS system improve their ability to respond and communicate during emergency situations. In emergency situations, when lives may be at stake, it is imperative that the communication system be reliable and accurate. The OmniTRACS data transmission system provides the reliability and accuracy demanded by the public safety industry. Users eliminate the risk of missing vital information by sending and receiving messages in data form. In addition, all messages can be stored for later recall.

The system is not meant to replace voice communications, but rather to enhance the current systems and provide accurate relay of information anywhere in the country. In the event of earthquake, flood or other major disaster, the OmniTRACS satellite system will remain operational, while land-based communication systems may become inoperable. The system could be the key to keeping information flowing from the location of the disaster.

Public Utilities

The need for communication with vehicles servicing public utilities such as water, power, and telephone is apparent in major metropolitan areas as well as small rural towns. The ability to convey information via satellite from field to base and vice versa allows for efficient servicing of the public even in the most remote areas of the country.

In addition to using the OmniTRACS system for mobile applications in the public utility sector, fixed applications are also appropriate. For example, by placing transportable VSAT terminals at strategic locations along a river or aqueduct, water flow information can be transmitted quickly and accurately, without the need for human interaction. The flexibility of the OmniTRACS system from mobile to transportable applications make it a valuable tool for public utility companies across the country.

SESSION B
REGULATORY ISSUES

SESSION CHAIR: Jerry Freibaum, NASA Headquarters
SESSION ORGANIZER: Valerie Gray, Jet Propulsion Laboratory

INTERNATIONAL AND DOMESTIC MOBILE SATELLITE
REGULATORY PROCEEDINGS: A COMPARISON OF
OUTCOMES AND DISCUSSION OF IMPLICATIONS

JERRY FREIBAUM, Telecommunications Consultant
(formerly NASA)

6535 Elgin Lane
Bethesda, MD 20817
United States

ABSTRACT

We are at the threshold of advancing one of the most important developments in Communications -- a satellite service offering land, aeronautical and maritime mobile communications. This milestone has been reached as a result of 25 years of studies, experiments and technology development and more than ten years of public proceedings. Worldwide primary allocations are in hand, a single U.S. consortium has been formed and licensing appears imminent. However, several serious barriers still remain.

The 1987 World Administrative Radio Conference (WARC) on Mobile Communications fell short of meeting U.S. Mobile Satellite Service allocation needs. The International allocations are different than the proposed domestic allocations creating potential coordination problems. Challenges to the FCC's proposed Rulemaking and anticipated licensing may continue to delay the culmination of this process.

INTRODUCTION

How will differences between international and domestic allocations be reconciled and what protection can U.S. systems expect from foreign systems operating in accordance with the international tables?

Where do we go from here with respect to licensing, competition, tariffs, network control and transborder operations?

What is the nature and impact of domestic opposition to FCC proposals?

What are the implications of a planned WARC in 1992 which would address many of the issues left unresolved in the 1987 WARC?

A similar change was proposed for the portion of the band currently allocated to the Maritime Mobile Satellite Service (1530-1544 MHz and 1626.5-1645.5 MHz) with appropriate priority provisions for marine safety.

Specific frequency proposals and support for a Land Mobile Satellite Service were also presented by Canada, Japan, Australia, India, Mexico, European Space Agency (ESA) and INMARSAT.

The U.S. also made it clear that a minimum of 10 MHz up and 10 MHz down was needed by LMSS to ensure economic viability. The outcome of the WARC fell short of these needs and consequently the U.S. and Canada took reservations on the WARC's LMSS provisions.

The specific WARC spectrum allocations for the LMSS worldwide are:

- Primary, exclusive 4 MHz down (1555-1559) and 3.5 MHz up (1656.5-1660.0 MHz) in currently allocated AMSS(R) band.
- Co-equal primary .5 MHz up (1660.0-1660.5 MHz) shared with radio astronomy.
- Co-equal primary 3 MHz down (1530-1533 MHz) and 3 MHz up (1631.5-1634.5 MHz) shared with Maritime Mobile Satellite Service (MMSS).
- Secondary 11 MHz down (1533-1544 MHz) and 16 MHz up (1626.5-1631.5 and 1634.5-1645.5 MHz) in current MMSS band and limited to non-speech low bit rate data.
- Public correspondence by satellite (aircraft to ground mobile telephone) is also authorized in the 1545-1555 MHz and 1646.5-1656.5 MHz bands with some constraints.
- In the bands 1555-1559 and 1656.5-1660.5 MHz, Administrations may also authorize aircraft earth stations and ship earth stations to communicate with space stations in the Land Mobile Satellite Service.

Efforts were made by Canada and the United States to introduce a country footnote for LMSS for 6 MHz on a secondary basis adjacent to the newly proposed 4 MHz LMSS primary allocation. The 6 MHz would be used within national boundaries. However, this was defeated in the Plenary session.

Considering that very few of the almost 100 countries attending supported the U.S. proposals at the beginning of the conference the amount of spectrum allocated to LMSS on a worldwide primary basis should be looked upon as a tremendous achievement. The door appeared to be left open for additional allocations in a proposed 1992 WARC. At that time those opposed to the U.S. proposals such as ICAO, Inmarsat, European CEPT countries and ARINC, will be in better positions to deal competitively with the MSS and the environment should be more conducive to cooperation.

These and other questions are the subject of this and other papers to be presented and discussed at this Mobile Satellite Conference.

We are dealing with the painful, costly, and time consuming process of change. The combination of vested interests, politics, regulation, fear of change and spectrum managers represent a formidable barrier to change. To illustrate: cellular mobile took 13 years to break through this barrier; Direct Broadcast Satellite, 15 years; Aeronautical Mobile Satellite, 20 years; Aircraft collision avoidance systems, 30 years; automatic altitude reporting, 25 years; and, the subject of this conference, Mobile Satellite Service, 12 years.

The barriers to change are not always readily apparent. For example, in preparation for the 1977 WARC on Broadcast Satellites, position papers written by NASA and the Department of Commerce/ITS to facilitate the implementation of small ground terminals were blocked within the FCC. An FCC document stated that it was not in the U.S. interest to facilitate the proliferation of small ground terminals. A direct confrontation of that policy by NASA's Administrator, Robert Frosch and others resulted in modifying the policy.

Policies and regulations to accommodate a Mobile Satellite Service also had to be changed. This process was initiated by NASA in 1975 as part of U.S. preparations for the 1979 WARC. NASA proposed allocations in the 800 MHz or 1500/1600 MHz (L) bands.

An 800 MHz proposal ultimately was included in U.S. positions after 8 public Notices of Inquiry. Allocations, almost worldwide, for domestic LMSS in the 800 MHz band were approved in the 1979 WARC. Subsequent inaction on the part of the FCC and other barriers were put in place causing NASA to petition the FCC for a Rulemaking on frequency allocations for a Mobile Satellite Service in the 800 MHz and 1500/1600 MHz bands.

REMAINING PROBLEMS

Allocations

For purposes of clarity and time we will go right to the "L" band allocation issue, bypassing the 800 MHz controversy

Figure I compares prior "L" band allocations with the FCC's proposed Rulemaking, the U.S. position at the WARC and the outcome of the WARC.

The U.S. proposed that the 14 MHz up and 14 MHz down, originally allocated to the Aeronautical Mobile Satellite Service (1545-1559 MHz) and (1646.5-1660.5 MHz) be reallocated to a generic Mobile Satellite Service (Aeronautical, Land and Maritime), with priority and pre-emptive access provisions for aviation safety.

Coordination & Interoperability

The cross hatched segments in Figure 2 conceptually illustrate potential coordination problem areas resulting from overlapping service areas and differences in international and domestic allocations.

Coordination and technical, operational and institutional interoperability agreements between systems will be difficult, at best, to resolve. However, they must and can be solved with cooperation on the part of all parties.

In reality much of the U.S. and Canada lie within potential areas of conflict since the patterns of Inmarsat and the Soviet Union's Volna overlay these countries. Coordination with the Soviet Union should not be too difficult since they are not competing for U.S. markets. Volna also uses very little spectrum.

Let's also presume that conflicts with Inmarsat can be worked out in the spirit of cooperation and self interest. The question of protection to U.S. entities is then raised with respect to other service providers that may enter the market 3-5 years later operating in accordance with the new international tables in the same service areas.

What protection, if any, would the U.S. "Reservation" provide in this case?

Here is where the importance of the proposed 1992 conference becomes quite evident.

U.S. Domestic Proceedings

The American Mobile Satellite Consortium (AMSC) has applied for 14 MHz (1545-1559 and 1646.5-1660.5 MHz) and 3 orbital positions. The legality of allocating spectrum for Land Mobile Satellite Service in L band has been challenged by ARINC in recent filings.

Another question is the extent of flexibility and protection available to the AMSC and the FCC as a result of the "Reservation" taken by the U.S. at the 1987 WARC.

Some contend that the "Reservation" may offer psychological comfort but no protection. Others argue that the Reservation may allow some flexibility and, somewhat, questionable protection consistent with existing treaties and in particular with certain provisions of the 1982 Nairobi Convention.

The question of who provides public correspondence (air to ground mobile telephone) is also the subject of debate within the current proceedings.

Perhaps, additional information on the status of these proceedings can be provided by the FCC.

Standards

Extensive joint effort by the Land, Aeronautical and Maritime interests is needed.

Feeder Links

To be addressed in the 1988 Space WARC.

Summary

We are on the threshold of implementing a new multibillion dollar industry which can enhance economic development, dramatically improve disaster assessment and relief operations, improve rural health care and solve many safety and security concerns of the transportation industry (Air, Land and Marine).

Further delays in resolving conflicts between the vested interests will be extremely costly to users, providers and equipment manufacturers.

I urge you all to move quickly and decisively.

Let's use the 1992 conference to document and legalize what we must and can do now, namely:

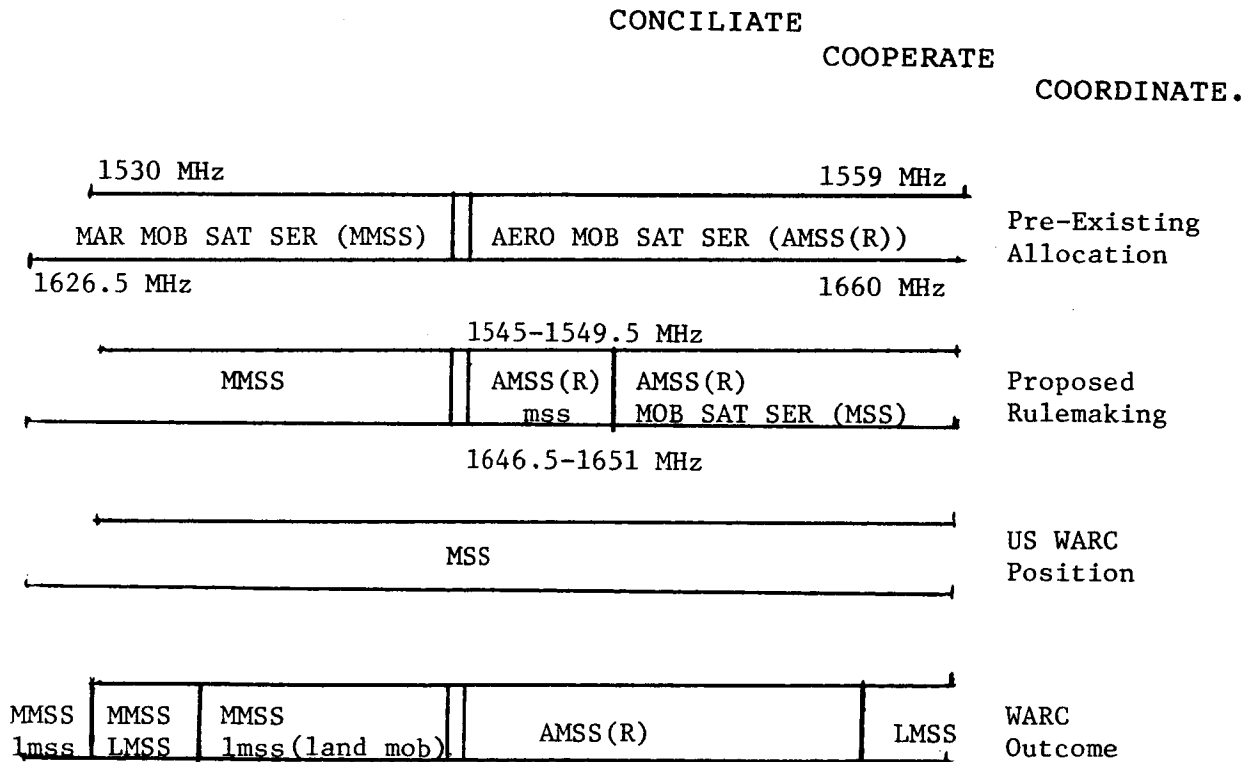


Fig. 1 Comparison of "L" Band Proposals

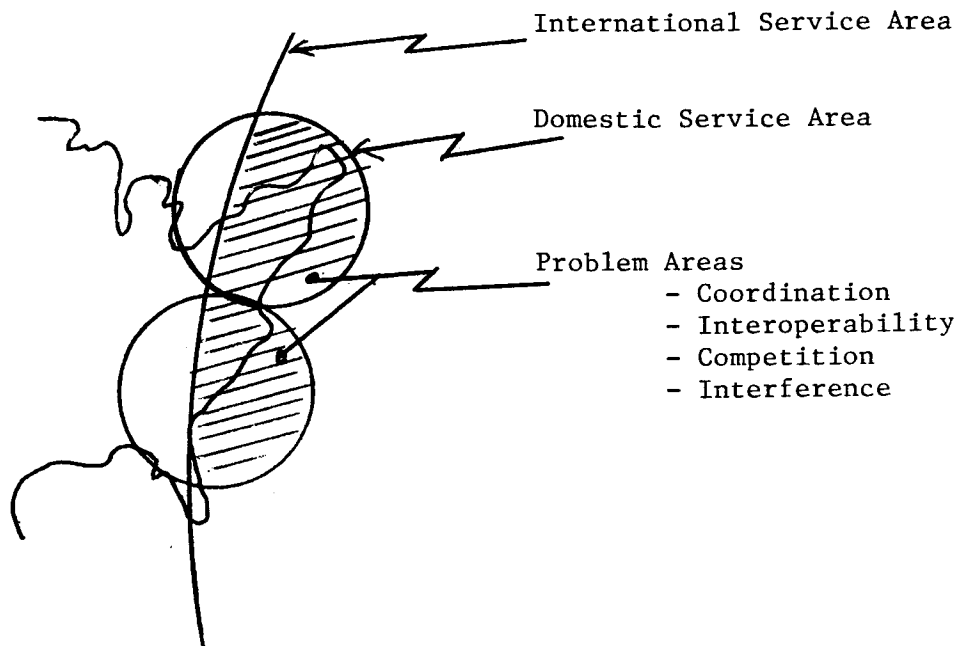


Fig. 2. Overlapping Service Areas

REFERENCES

- NASA. 11/24/82 Petition for Rulemaking to Establish a Mobile Satellite Service and to Allocate Frequencies (Filed with the FCC November 29, 1982)
- The Federal Communications Commission 7/24/86. General Docket #84-1234, a Report and Order allocating spectrum to the Mobile Satellite Service
- ITU. Geneva, 1987 Final Acts of the World Administrative Radio Conference for the Mobile Services (MOB-87)
- USA. MOB 9/18/87 Document 156-E Mobile-Satellite Service Implementation and Institutional Considerations (WARC 87 Information Paper)
- USA. MOB 9/7/87 Document 79-E Economic and Operational Advantages to Users And Providers of Satellite Systems in the Mobile-Satellite (WARC 87 Information Paper)
- American Mobile Satellite Consortium. 2/1/88 (Joint Amendment Filed with the FCC)

**MOBILE SATELLITE SERVICES:
INTERNATIONAL CO-ORDINATION, CO-OPERATION AND COMPETITION**

OLOF LUNDBERG, Director General, INMARSAT

INMARSAT
40 Melton Street
London, NW1 2EQ
England

INTRODUCTION

My remarks on international co-ordination, co-operation and competition in the mobile satellite services are based on the following assumptions:

First, there will be more than one civil mobile satellite system in the 1990s.

Second, competition between these separate mobile satellite systems is inevitable. No system should, however, enjoy monopoly protection or subsidies.

Third, since the available L-band spectrum is in short supply and given the peculiar technical characteristics of the mobile satellite services, coordination and cooperation are desirable and necessary.

COORDINATION

The IFRB has so far been notified of L-band networks planned by Australia, Canada, France, INMARSAT, Japan, Papua-New Guinea, the US and the USSR. Additional L-band networks are likely to be notified.¹

INMARSAT has so far sought only the lower 3 MHz of the aeronautical mobile satellite service band, but it may well seek to cover the full 14 MHz of the aeronautical and land mobile satellite bands (i.e., 1545-1559 MHz and 1646.5-1660.5 MHz) in its third generation satellites.

INMARSAT's assessments indicate the potential for unacceptable levels of interference between the networks already notified. Consequently, we have begun or will soon begin coordination with these networks. (We also need to coordinate our feeder links with several other fixed satellite service networks.)

Coordination of L-band networks is necessary because, as the FCC put it, "existing and incipient technology does not allow discrimination between two or more MSS systems operating on the same frequencies".² Others have recognized that "intersatellite interference has become a serious concern"³ and that "it would be extremely difficult to obtain adequate isolation ... even at orbital separations of 30 degrees or more."⁴ Unless operational arrangements can be worked out, it appears to me that the only solution is to share the available spectrum.⁵

It would be easier to co-ordinate the various L-band networks and to share the limited spectrum available if significant frequency reuse could be achieved. In reality, the degree of frequency reuse appears minimal at this stage. The American Mobile Satellite Consortium (AMSC)

in its 1 February 1988 filing to the FCC envisages a frequency reuse factor of only 1.5.

Clearly, more L-band spectrum is needed. WARC-MOB-87 recommended that another WARC be convened not later than 1992 to provide more spectrum for the mobile satellite services.⁶ It also invited the CCIR to study as a matter of urgency the spectrum requirements and inter-system and intra-system sharing aspects of the mobile-satellite systems.

For its part, WARC-ORB-88 was asked to consider the particular characteristics of the mobile satellite services when dealing with procedures for coordination and notification⁷ and to take note of the concerns expressed with respect to feeder links for the mobile satellite services in the L-band.⁸

WARC-ORB-88 takes place for six weeks starting in August 1988. The first session of the WARC-ORB held in 1985 adopted a report containing the planning principles and methods recommended for use by the second session, as well as inter-service sharing considerations and recommendations regarding feeder links.

The second session will revise or establish new regulatory provisions for implementation of a dual planning approach for the fixed-satellite service. Regulatory provisions will also be adopted to meet improved planning and co-ordination requirements for other services in order to meet the needs of all ITU members.

INMARSAT provided a contribution to the Joint Interim Working Party (JIWP) of the CCIR which met in December to prepare a Technical Report to WARC-ORB-88. The INMARSAT contribution, which forms part of the Technical Report, addresses the unique aspects of mobile-satellite systems and the technical incompatibility of feeder links in a mobile satellite environment with the concept and requirements of allotment planning.

The Technical Report also recommends changes in the criteria used to determine whether there is a need to coordinate.

INMARSAT supports the view that the unique aspects of multi-administration networks should be considered in the development of future intersystem coordination procedures.

Those planning or operating networks requiring co-ordination must show good faith in trying to resolve the technical difficulties. If they cannot successfully coordinate, the IFRB will try to facilitate an agreement between the parties.

COOPERATION

Cooperation between mobile satellite systems can take many forms. For example, INMARSAT has frequently granted free use of its system for tests and demonstrations by other organizations, some of whom are potential competitors.

Today, however, I would like to focus on cooperation in setting standards for mobile earth stations. The benefits of common standards are well known. Users can roam anywhere and still use the same equipment. Manufacturers benefit from the economies of scale inherent in mass production, which means users buy equipment of lower cost than would be the case if manufacturers are producing smaller volumes to meet several different standards. The need to drive down the cost of equipment is especially important when there are doubts about the size of the market and how quickly it can be penetrated. When considering

standards, we should remember the saying "United we stand, divided we fall."

Happily, I note from its filing that the AMSC is "committed to ensuring that the system will be interoperable with other satellites in a worldwide network to serve aviation"⁹ and that, like INMARSAT, it plans to adopt the system architecture defined by ICAO for AMSS(R) services.

In addition to ICAO and the AEEC which are setting global standards for aeronautical satellite communications, the CCIR and CCITT play important roles in setting world-wide standards.

The Plenary Assembly of each committee draws up a list of technical "Questions", which are entrusted to a number of Study Groups, composed of experts from different countries. The Study Groups draft and revise Recommendations which are submitted to the next Plenary Assembly for ratification. CCIR and CCITT Recommendations have an important influence on telecommunication administrations and companies, manufacturers and designers of equipment throughout the world.

Although the activities of the CCIR and CCITT are nominally quite distinct, the one concerned with radio, the other with telephony, telegraphy and data communications, it is worth noting that both are studying various aspects of mobile as well as fixed communications. It is no coincidence that both the mobile and fixed networks are developing independently towards a scheme of universal personal telecommunications.

INMARSAT has been an active participant in several CCIR and CCITT Study Groups concerned with mobile communications or whose work affects the setting of mobile standards. The main CCIR Study Group of interest to us is Study Group 8, which has two Interim Working Parties, 8/7 and 8/13, dealing directly with mobile satellite issues.

IWP 8/7, which met last in Tokyo in May 1987, has been considering the technical and operating characteristics of the maritime mobile satellite service. It has also discussed aeronautical satellite communications issues and if it continues after the Study Group 8 Interim Meeting (20 Apr to 6 May 1988), its terms of reference could be broadened to include aeronautical and perhaps also land mobile satellite services.

At its last meeting, IWP 8/7 revised Report 509 on modulation and coding techniques for mobile satellite communications services. It also drafted a new Question on the impact of ISDN and public data networks on the technical characteristics of the future Mobile-Satellite Systems.

IWP 8/13 is studying the requirements for Future Public Land Mobile Telecommunication Systems (FPLMTS), draft recommendations on which are to be presented to the Interim CCIR meeting which concludes on 6 May. The FPLMTS would provide a system architecture which would allow anyone to communicate wherever in the world they may be. The FPLMTS would accommodate a variety of mobile terminals, from pocket-sized to vehicle-mounted. A primary objective is "to allow the co-existence with, and interconnection with, mobile systems which use direct satellite links".

The IWP noted that mobile users operating over wide areas could benefit by having direct access to both mobile satellite and terrestrial systems. According to the IWP 8/13, this could most readily be achieved by the use of adjacent satellite and terrestrial mobile frequency bands. In this regard, remember that WARC-MOB-87 recommended

that the next competent WARC should consider designating a suitable band or bands for future public land mobile telecommunication systems.¹⁰

The IWP also said that given the prospect of more than one mobile satellite system, it is desirable that technical and/or functional compatibility of mobile earth stations be a goal of the FPLMTS, so that mobile users are able to roam regionally and/or world-wide with the same piece of equipment.¹¹

Like the CCIR, the CCITT has several important Study Groups dealing with mobile matters, especially in regard to how mobile systems interwork with the fixed networks.

The current four-year CCITT Study Period is coming to an end. The IXth CCITT Plenary Assembly which is being held in Melbourne in November 1988 is expected to reorganize its Study Groups and to approve many new questions on mobile communications.

INMARSAT has been participating in those CCITT Study Groups dealing with matters of importance or interest to us.

Several CCITT Study Groups (SG I on telegraphy, SG II on telephony and SG VII on data) have been drafting recommendations for numbering plans that would treat mobile satellite services in a consistent way and that would in particular describe how new INMARSAT mobile services are accessed via the fixed terrestrial networks. They are also developing standardized selection procedures for mobile subscribers to access the telephone, telex and data services. Specialized operational procedures for the interworking between the telex service and the Standard C services have also been drafted by Study Group I, as telex is currently the only mandatory Standard C service.

Study Group XI is producing texts for the network signalling architecture required for the interfacing of digital mobile systems. It has prepared several Recommendations so that the INMARSAT user can access the fixed networks in a standardized way no matter where in the world he goes.

The aviation industry is in the process of adopting the network layer of the CCITT X.25 interface standard as a means of transferring data between the mobile satellite network and existing avionics. Since this standard is already in widespread use, it will enable the aircraft to communicate no matter where in the world it is flying.

Study Group XVIII is carrying out long range studies of digital networks, including the possible services which digital mobile systems may provide in conjunction with the PSTN/ISDN. (Other Study Groups, such as I, II, III, VII and XI, are also studying the implications of ISDN evolution and paving the way for the transition.) It is also concerned with digital codec standardization. While INMARSAT, NASA, the Canadian Department of Communications and others are considering voice transmission methods which are very economical of power and bandwidth - e.g., 4.8 kbit/s digital or amplitude companded single side band (ACSSB) -- such methods have not been adopted yet by the CCITT. Study Group XVIII has cleared 32 kbit/s and is now working on 16 kbit/s codecs. It has only recently begun considering voice coding algorithms at bit rates below 16 kbit/s (for the aeronautical satellite service), but it does at least recognize the need for new recommendations on transmission planning to cover the growing numbers of mobile users who will want to interconnect with the PSTN.

From the considerable amount of work being devoted in CCIR and CCITT Study Groups, it is apparent that an objective of growing

importance is the development of common mobile standards which can be used anywhere in the world and which can be functionally integrated with the fixed networks.

This objective is shared by the aviation and maritime communities. It seems increasingly likely that the FDMA SCPC protocol supported by INMARSAT and other mobile satellite applicants in the US and Canada will prevail both in the AEEC and ICAO.

Standard-C

I would now like to mention the status of the two main standards being developed by INMARSAT for use in the land mobile environment. The first is Standard C, which we developed for low speed data communications for use on the smallest of fishing boats, yachts and even liferaft. Standard C could be regarded as a general purpose digital link, for either two-way messaging or as a one-way outbound or one-way inbound link, which means it could be used for point-to-multipoint broadcasting (enhanced group call), polling and monitoring, can be provided as a subset of Standard C.

The International Maritime Organization's subcommittee on radiocommunications has adopted INMARSAT's Standard-C for its global maritime distress and safety system which comes into being from 1991. It has also adopted our enhanced group call system for promulgation of maritime safety information.

Standard C has stimulated considerable interest for land mobile applications because of its low cost and small size. Standard C is being used in a series of technical and pre-operational trials planned by 13 European telecom administrations to start later in 1988 following establishment of a test coast earth station or gateway station in mid-1988.

We have had numerous discussions with Telesat, DOC and others in Canada and it would seem that there are minimal differences between Standard C and the Canadian MSAT equivalent and that there is a recognition of the benefits of a common standard. It is my hope that others planning domestic or regional mobile satellite systems could also support Standard C as a world-wide standard for low speed data communications.

CCITT Study Group I is at present finalizing three Recommendations related to the Standard C system. These relate to the Standard C telex numbering plan, the selection procedures and the interworking procedures to be used between the telex network and the Standard C system.

The standard effectively has the support of INMARSAT Signatories from 53 member countries. A preoperational trial service which can support up to 1,000 terminals in the Atlantic ocean region will start in the third quarter of 1988 and a full world-wide commercial service should start in mid-1989.

Standard-M standard setting

We have also begun work on establishing a second land mobile standard, that is, for voice. In January 1988, we wrote to Signatories, manufacturers, potential users and others suggesting the establishment of a group of interested parties, whose purpose would be to define an internationally acceptable standard for a low cost land mobile

satellite telephony service, which we call Standard M.

A common land mobile satellite standard would allow mobile subscribers to communicate anywhere, no matter where they are, and through any mobile satellite system. A common standard would allow manufacturers to address much larger markets and to spread development costs over larger production quantities. Achieving economies of scale is critical to the mobile satellite market which is likely to be considered to be a high risk venture for some years to come.

We envisage Standard M as having an antenna gain in the range of 10-15 dBi (with a G/T of the order of -13 dBK). It could be either a digital (4.8 kbit/s) or ACSSB standard, but it would be specified for production at the lowest possible cost. These and other issues are planned for discussion at the first meeting scheduled to take place in London on 28-29 March 1989. Participation in this and subsequent meetings is open to all interested parties, including competitors.

COMPETITION

While the potential for significant and productive cooperation exists between the mobile satellite competitors, so does the prospect of competition.

Domestic MSS monopolies have been assumed for Canada and US. For example, the FCC said three years ago that it did "not foresee the development of a competitive market in the near term".¹² If domestic systems compete with INMARSAT, however, it does seem to me that INMARSAT should be allowed to compete with the domestic systems, particularly those with regional aspirations. I did note in a US contribution to last year's Mobile WARC a line that said, "Domestic markets can be served by international systems, regional systems or by domestic systems, depending on the circumstances."¹³

The FCC and other domestic regulatory agencies should come out with clear policy statements as to whether they will allow inter-system competition. In doing so, they should note that INMARSAT has not sought nor has it been given a monopoly in the provision of aeronautical or land mobile satellite services. On paper, INMARSAT has a maritime monopoly, but in practice, many fixed satellite services among others have not let that paper protection stand in their way, nor have we tried to enforce it.

It has been said that competition between INMARSAT and the domestic MSS is not on, because INMARSAT is a foreign controlled communications provider and under US law, no more than 20 per cent of a common carrier can be under foreign control. This argument, however, disregards the fact that it is not INMARSAT which provides service to the end user; it is the US Signatory, i.e., Comsat. Hence, the question of foreign ownership would appear to be a red herring.

MSS and MSAT should not fear competition. It will stimulate the size of the market, drive down the cost of equipment and improve service. Competition will be good for us all. Not all of that competition will be inter-system in nature; the inter-modal competition, that is, from cellular radio and other such terrestrial technologies, will be severe. Bob Maher, president of the US Cellular Telephone Industry Association (CTIA), recently predicted that 80-85 per cent of the land area of the US will be served by cellular radio within three years. If 85 per cent of the long haul trucker's route is covered by cellular radio, how likely is he to buy a mobile earth station?

The answer to that question may come from a lease of capacity by INMARSAT to Teleglobe Canada for Telesat Canada's interim MSAT service.

In leasing capacity to a potential competitor, INMARSAT has promoted inter-system competition even though we have many concerns about leases, especially of the non-preemptible kind. Such leases effectively remove capacity from the "pool" available to the international community on a demand-assigned basis and thus strike at the heart of the concept of an international co-operative for mobile services.

Competition could be further promoted if governments ended their subsidies. Among such subsidies, I count research and development paid for by taxpayers, free launches and guaranteed government use of services. Competition can be further thwarted if one potential competitor seeks to use the standards-setting process as a means of delaying the introduction of service by others.

Another drawback we see to effective competition is the risk of a conflict of interest. This particularly touches the INMARSAT Parties, who may, for example, delay ratification of amendments to the INMARSAT Convention because they are also supporting a domestic competitor.

Another major risk is that Parties will not support INMARSAT's access to spectrum if a domestic system operator wants the same spectrum. Neither Canada nor the US has supported INMARSAT's having access (non-exclusive access, I hasten to add) to even 3 MHz of the AMSS bands, even though they are seeking the full 14 MHz of the AMSS and LMSS bands for their own domestic use.

Another potential policy minefield relates to the use of mobile communications as a substitute for fixed services. I noted that the US said in its 18 September 1987 contribution to the Mobile WARC that "the applications for which mobile-satellite service systems will be employed are mobile in nature... the mobile satellite service will not substitute for fixed satellite services."¹⁴ Yet the day before, the FCC said "if there is a demand for fixed services that can be provided on a mobile satellite system, there is no reason why they should be excluded."¹⁵

AN OPEN DOOR POLICY

I would like to summarize my message, as follows: We believe in the benefits of competition and we have supported competition by granting free use of our system to potential competitors for tests and demonstrations and by leasing them capacity, even though leases are regarded by many as inimical to the interests of an international co-operative for mobile satellite services.

While competition is important and beneficial, so is co-operation. Cooperation will be vital to solve the formidable co-ordination difficulties which lie before us. Cooperation in developing common mobile standards will serve the interests of users, manufacturers and facilities providers. Many of those attending this conference sponsored by JPL hold the keys to cooperation, especially in designing mobile equipment allowing the user to roam anywhere. I urge you to open doors, not to close them.

REFERENCES

1. Following the amendments to the Radio Regulations made by the WARC-MOB-87, which come into force in October 1989, INMARSAT plans to register with the IFRB for the provision of aeronautical public correspondence in the 1545-1548 MHz and 1646.5-1649.5 MHz bands; of a land mobile satellite service, limited to non-speech low bit rate data transmissions in the maritime mobile satellite bands; and of a telephony land mobile satellite service in the 1530-1533 MHz and 1631.5-1634.5 MHz bands.
2. p. 24, MSS NPRM, released January 1985.
3. p. 6, MSAT-X Quarterly, July 1987. Article by Dr. John Huang, Jet Propulsion Laboratory, NASA.
4. p. 60, MSSLP filing to the FCC, 4 Sept 1987.
5. The 4 Sept 1987 MSSLP filing proposed (see p. A-8) that the Canadian spacecraft utilize 6.75 MHz while the US spacecraft use the remaining 6.75 MHz.
6. RESOLUTION COM4/14 of the MOB-WARC-87 Final Acts.
7. Ibid.
8. RECOMMENDATION COM4/A of the Final Acts.
9. p. 22 of 1 Feb 88 AMSC filing to the FCC.
10. RECOMMENDATION COM4/G of the Final Acts.
11. WARC-MOB-87 Resolution 44 also urges administrations to encourage the development and manufacture of compatible user equipment in the mobile satellite service.
12. p. 24 of MSS NPRM released January 1985.
13. p. 2, Document 156-E, USA Information Paper "Mobile Satellite Service Implementation and Institutional Considerations" to Committee 4 of WARC-MOB-87.
14. p. 2, Ibid.
15. p. 13, Memorandum Opinion and Order, adopted 17 Sept 1987; see also Second Report and Order, Gen. Docket 84-1234, at para 34.

INTERNATIONAL AND DOMESTIC REGULATORY ISSUES FACING THE CANADIAN MSAT SYSTEM

BAHMAN AZARBAR, Communications Systems Engineering, Telesat Canada;
JACQUES R. LANGLOIS, Regulatory Matters and Corporate Policy, Telesat
Canada; CHRISTOPHER J. FRANK, Satellite Services Planning and
Development, Telesat Canada.

TELESAT CANADA
333 River Road
Vanier, Ontario
K1L 8B9
Canada

ABSTRACT

This paper addresses international and domestic regulatory issues which affect the implementation of a mobile satellite system (MSAT) over North America. It deals with WARC-MOB-87, MSAT frequency co-ordination, frequency sharing and key Canadian domestic issues.

INTRODUCTION

Introduction of MSAT service is the next logical progression in satellite communications in Canada and the U.S. The first part of this paper deals specifically with issues related to frequency/orbit co-ordination of MSAT within the context of the prevailing international Radio Regulations. It reviews briefly the results of the 1987 World Administrative Radio Conference on Mobile Service and its foreseen effects on the MSAT frequency co-ordination environment. Possible approaches to frequency sharing between the existing and planned systems will also be examined. The second part addresses the domestic regulatory issues surrounding the development of a commercial MSAT service in Canada.

WARC-MOB-87

The 1987 World Administrative Radio Conference on Mobile Services (WARC-MOB-87), as part of its agenda dealing with the contentious issue of spectrum re-allocation, finally recognized the need and made specific provision for land mobile satellite service (LMSS) in the 1.5 - 1.6 GHz range. Under the new provisions, the full complement of satellite based mobile services now can be provided in this part of the spectrum, subject to successful co-ordination under the international Radio Regulations. The conference, however, chose to preserve the distinction between various types of services. For a multi-beam mobile satellite system such as MSAT, this means that the provision of a full complement of services within each beam now requires multiplexing distinct segments of the corresponding spectrum allocated to each class of service. Furthermore, the allocations to LMSS now come in three categories - Exclusive (LMSSE), Co-primary (LMSSC) with, and Secondary (lmss) to maritime mobile satellite service (MMSS), depending on location in the band in question.

While the decision of the conference obviously entails changes to the technical design of the MSAT associated hardware, it is the international co-ordination aspect of the new provisions which will be dealt with in the following sections.

MSAT CO-ORDINATION ENVIRONMENT

In order to gauge broadly the co-ordination environment for the Canadian MSAT system, Figure 1 was prepared to represent graphically the population and distribution of existing and planned mobile systems in this band, as identified through the ITU publications. The systems within the arc $23^{\circ}\text{E} - 150^{\circ}\text{E}$ are not depicted, as they are not likely to affect the Canadian MSAT. The service classification under which these systems have been filed with the ITU as well as the dates of Advance Publication Information (API) and start of the co-ordination phase are identified in Table 1.

A more detailed consideration of the entries in Table 1 in terms of their relative orbital positions, the expected in-service dates, operational life and the intended service area reveals that the systems subject to detailed co-ordination with the Canadian MSAT are likely to be reducible to a shorter list as presented in Figure 2. In this figure, the exact downlink frequencies as identified in the ITU publications are also shown to indicate the extent of spectrum overlap which may require detailed frequency co-ordination. It is to be noted, however that some of these systems are expected to change in the process of realignment with the outcome of WARC-MOB-87. These changes, along with new entries which may emerge in the coming years, will no doubt impact the co-ordination picture just described.

A POSSIBLE APPROACH TO FREQUENCY SHARING

In this section, by way of a simple example, some technical principles and guidelines which have the potential to facilitate the co-ordination process are discussed in a qualitative fashion. To better understand the concept, the following notes are in order. The MSAT related co-ordination activities can be divided into two broad categories: 1) co-ordination with existing systems or their replacements, and 2) co-ordination with planned systems. These two groups could conceivably each be divided into global systems and national or regional systems. National or regional systems are quite likely to utilize spot-beams to conserve satellite power over the intended service area, a fact that greatly enhances their frequency re-use capability and facilitates the frequency co-ordination process. The global systems on the other hand, have been traditionally characterized by large beams with little or no re-use capability. Frequency co-ordination of the spot-beam based systems amongst themselves is expected to be relatively simple to achieve. Indeed the models developed for the North American MSAT systems to date are indicative of the feasibility and efficiency with which such beam topologies could be implemented. The basic concept has been shown to be easily extendable to South America and other ITU regions [Ref. 1]. Co-ordination with the global systems, however will require special measures.

Before searching for a solution, we should first understand the nature of the problem. The primary mode of interference between a spot-beam system and a global one is uplink interference into the former case and downlink interference into the latter one simply caused by the large inhomogeneity in the associate coverage gains. This observation suggests that if the intended service areas are to a large extent mutually exclusive, then sharp roll-off characteristics of the spot-beams will quickly localize and limit the interference to the overlap boundaries of the two systems. Once the potential incompatibilities become localized, then detailed frequency co-ordination becomes a feasible task. This can be achieved in two principal ways. Either the mobiles belonging to the global system and roaming in the areas close to the overlap region will not be assigned common frequencies with those utilized in the boundary spot-beams, or alternatively, these spot-beams will use a set of frequencies not used by the global beam.

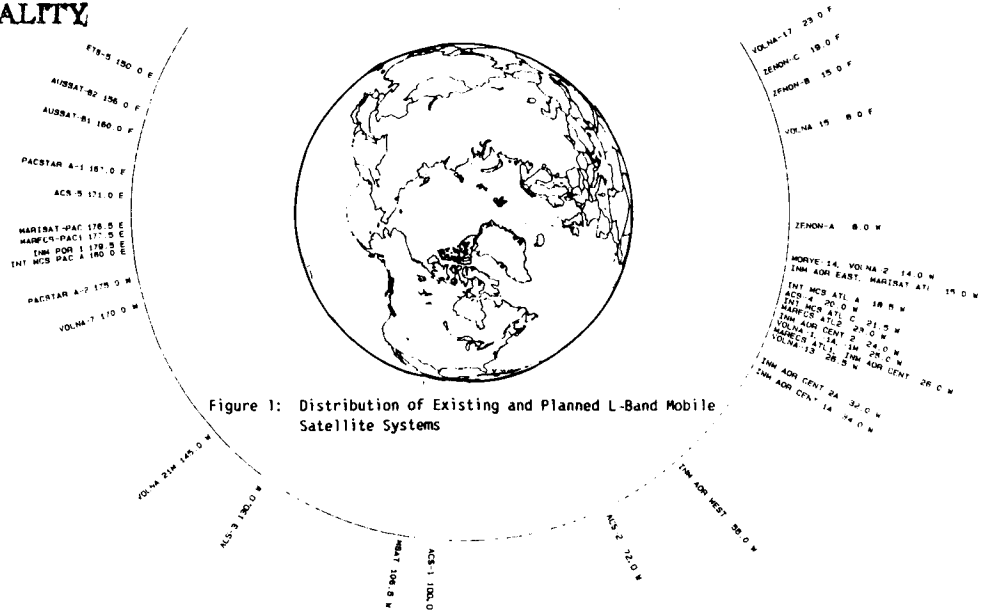
A PLAUSIBLE SCENARIO

A simplistic example of the application of such a sharing concept is depicted in Figure 3. Sub-bands from LMSSE allocation are used to construct the coastal beams for a hypothetical North American system and the frequency is reused wherever feasible within the intended coverage area. Noting the fact that WARC-87 resolutions require that the LMSSE allocation only be used for national or regional coverage, it is necessary to utilize spot-beam technology for controlling emissions over adjacent service areas. The entire frequency band used in this fashion could therefore be reused several times within the remainder of the Region II outside of North America. The spectrum for central beams could come from the LMSSC allocation to complete the coverage of the land mass in North America. The separation of the central spot-beams from coastal areas would make it feasible for the global maritime systems, which share this band on a co-primary basis with LMSS, to fully utilize it over their primary service areas. Similarly, AMSS(R) and lmss allocations could be used over North America. However in this case, the coastal beams need to be subjected to detailed frequency co-ordination with global systems over the interface areas. The fact that AMSS(R) is not currently utilized could facilitate significantly the process of frequency planning between the emerging systems.

REGULATORY DEVELOPMENTS IN CANADA

Satellite services and associated tariffs charged by Telesat are regulated by the Canadian Radio-television and Telecommunications Commission (CRTC). Rapid changes in the field of telecommunications technology and service development have prompted the CRTC to re-examine its approach to regulation. Spurred by increased competition created by the introduction of new products and services, the CRTC has strived to find ways and means to ensure a "level playing field" for facilities-based service providers and non-facilities-based service providers where competition exists. In order to satisfy the pressures of the marketplace and its statutory responsibilities, the CRTC has used a process called "forebearance" which exempts certain companies or their respective services from the requirement to file tariffs.

ORIGINAL PAGE IS
OF POOR QUALITY



LMSS MMSS	MMSS, lms	AMSS(R)	LMSS

1530 33 44 45 55 1559 MHZ
Figure 2: Systems Most Affecting Coordination of a North American MSAT System

ORBIT POSITION	SATELLITE	SERVICE CLASS	DATE API	COORD
150.0E	JAP ETS-5	A M	85	86
156.0E	AUSAT B2	A	87	
160.0E	AUSAT B1	A	87	
167.0E	PNG PACSTAR A-1	A	86	
171.0E	USA ACS-5	A	87	
176.5E	INMARSAT MARISAT	A M	73	76
177.5E	INMARSAT MARECS	A	79	80
180.5W	INMARSAT POR-1	A M	86	
180.0W	INTELSAT MCS PAC A	A M	81	82
175.0W	PNG PACSTAR A-2	A	86	
170.0W	USSR VOLNA-7	A	77	78
145.0W	USSR VOLNA-21M	A M	85	
130.0W	USA ACS-3	A	86	87
106.5W	MSAT	A	86	87
100.0W	USA ACS-1	A	86	87
72.0 W	USA ACS-2,	A	86	87
55.0 W	INMARSAT WEST	A M	86	
34.0 W	INMARSAT CENT 1A	A M	87	
32.0 W	INMARSAT CENT 2A	A M	87	
26.5 W	USSR VOLNA-13	A	85	87
26.0 W	INMARSAT CENT	A M	84	86
26.0 W	INMARSAT MARECS ATL1	M	79	80
25.0 W	USSR VOLNA-1	A	77	78
25.0 W	USSR VOLNA-1M	M	85	
W	USSR VOLNA-1A	A	86	
24.0 W	INMARSAT CENT 2	A M	86	
23.0 W	INMARSAT MARECS ATL2	M	79	80
21.5 W	INTELSAT MCS ATL C	M	80	81
20.0 W	USA ACS-4	A	87	
18.5 W	INTELSAT MCS ATL A	M	79	79
15.0 W	INMARSAT EAST	A M	84	86
W	INMARSAT MARISAT ATL	M	73	77
14.0 W	USSR MORE-14	M	85	
14.0 W	USSR VOLNA-2	A	77	78
8.0 W	FRA ZENON-A	A	87	
8.0 E	USSR VOLNA-15	A	85	87
15.0 E	FRA ZENON-B	A	87	
19.0 E	FRA ZENON-C	A	87	
23.0 E	USSR VOLNA-17	A	85	87

Table 1: Coordination Status of Existing and Planned L-Band Mobile Satellite Systems

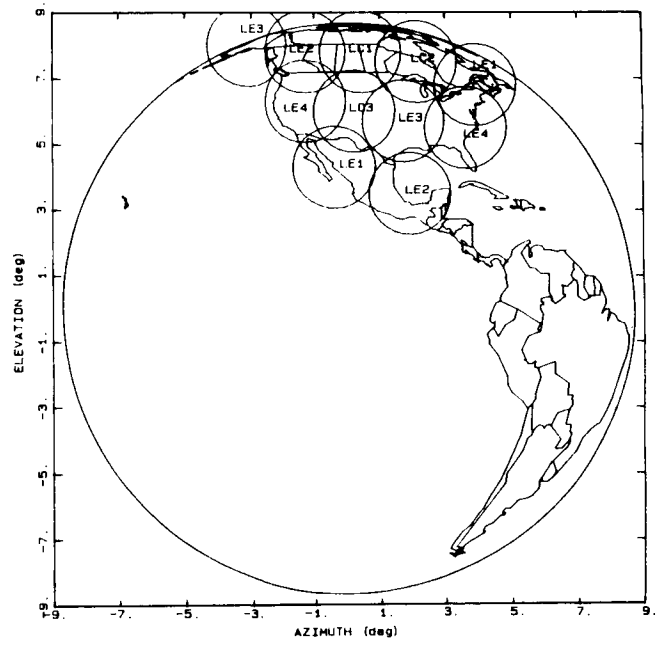


Figure 3: AMERICA AS SEEN FROM 106.5 DEGREES WEST 82

REGULATORY APPROACH TO MSAT

New mobile services, such as cellular telephone, have been foreborne from regulation because of effective competition and public interest arguments. It seems appropriate that a similar regulatory approach be applied to an analogous service such as MSAT.

There are four main arguments in support of this approach:

(a) Effective Competition from Other Mobile Satellite Services

Other satellite services are being offered as an alternative to MSAT. Several U.S. companies are currently in business or are expected to launch mobile satellite services in the near future. These include two-way messaging, voice and radio determination service. One U.S.-based company is attempting to offer mobile and radio-determination satellite services to Canadian users through a subsidiary established in Canada. Plans are also under way to develop a public switched aeronautical voice and data service for major airlines. INMARSAT wants to expand its business to include land mobile services. From the aforementioned, it is evident that effective competition will exist in the mobile satellite market.

(b) Terrestrial mobile Radio Competition

MSAT will compete with cellular telephone and other terrestrial-based service providers. Mobile voice and paging services are provided in most urban areas. In areas where mobile services are firmly established, satellite-based mobile services will need to be priced competitively in order to capture a share of the maturing mobile market. In more remote areas, appropriate pricing will be required to attract users to the satellite-based service.

(c) Attraction of Investment Capital for A High Risk Venture

The construction and deployment of mobile satellites is capital-intensive involving considerable financial and technical risk. The possibility of either launch or in-orbit failure is a serious consideration in any satellite venture. In addition, MSAT is a new service that has no established customer base.

(d) The Public Interest

It generally is recognized that there is a basic social and economic need to extend cost-effective voice and data communications to remote and thinly populated areas of Canada. MSAT will play an important commercial role increasing the demand for fast and reliable communications for users operating on land, sea or air. This will stimulate growth in the telecommunications equipment business, increase the productivity of Canadian manufacturing and business and create new employment opportunities. The Federal Government has strongly endorsed the implementation of a domestic MSAT service and has committed substantial funds to this end.

CANADA-U.S. MSS TREATY

The question of a formal bilateral arrangement between Canada and the U.S. to govern MSAT service is under discussion by the two respective governments. There is ample precedent for such an agreement beginning with the 1952 convention re: radio operation by pilot's license holders to the 1982 Exchange of Letters, re: FSS transborder satellite usage.

It is likely that an agreement, if one transpires, will address such issues as transborder satellite usage, provision of coverage in the other country (for service to that country's subscribers), base and gateway ownership and the question of licensing (will MSAT equipment operators require license, especially in the context of operation in the other country?).

The two governments, in conjunction with MSAT operators on both sides of the border, will have to determine if such an agreement is warranted. It may be possible, for instance, to develop a business agreement that could handle the key financial, technical and reciprocity issues. Whether or not the political process would be satisfied by such a business driven agreement is another question. What is clear is that such negotiations should not impede progress towards the co-operative development of MSAT in Canada and the U.S.

CONCLUSIONS

A certain amount of pragmatism was necessary on both sides of the 49th parallel in order to achieve a suitable bilateral arrangement which is conducive to the development and implementation of a North American MSAT system. It is important that such an attitude be adopted during international frequency sharing negotiations and by domestic regulators. The concept of regulatory forbearance is important to ensure sufficient regulatory flexibility so that MSAT enters the next decade on a sound technical and financial footing.

REFERENCES

"Information Paper - Frequency Re-use Considerations in Sharing Common Frequency Allocations by Various Mobile Satellite Services", WARC-MOB-87, International Telecommunications Union, Geneva; September-October 1987, Document No. 56, Canada.

SESSION C
PROPAGATION

SESSION CHAIR: Andreas Neul, German Aerospace Research (DFVLR)
SESSION ORGANIZER: Faramaz Davarian, Jet Propulsion Laboratory

PROPAGATION EFFECTS BY ROADSIDE TREES MEASURED AT UHF AND L-BAND FOR
MOBILE SATELLITE SYSTEMS

JULIUS GOLDBIRSH, Applied Physics Laboratory, Johns Hopkins University,
United States: WOLFHARD J. VOGEL, Electrical Engineering Research
Laboratory, University of Texas at Austin, United States.

APPLIED PHYSICS LABORATORY
Johns Hopkins Road
Laurel, MD 20707
USA

ABSTRACT

During June 1987, The Applied Physics Laboratory of the Johns Hopkins University and the Electrical Engineering Research Laboratory of the University of Texas at Austin performed the fifth in a series of cooperative propagation field tests related to planned Mobile Satellite Systems (MSS). These tests were performed in Central Maryland and involved a helicopter and mobile van as the source and receiving platforms, respectively. Whereas, the previous measurements in Central Maryland were performed only at UHF (870 MHz), the June 1987 tests were implemented at both UHF (870 MHz) and L band (1.5 GHz) during a period in which the trees were in full blossom and contained maximum moisture. Cumulative fade distributions were determined from the data for various fixed elevation angles, side of the road driving, and road types for both worst and best case path geometries and for overall average road conditions.

INTRODUCTION

The results described here add to the existing data base of propagation measurements at L Band (1.5 GHz) [see references]. They are considered particularly useful in that systematic propagation effects are derived from repeated and controlled runs pertaining to different path elevation angles, road types, and path geometries defining "shadowing" and "multipath" modes. In addition, simultaneous L Band and UHF measurements were performed for the purpose of establishing scaling factors applicable to previous UHF (870 MHz) measurements [Vogel and Goldhirsh, 1986; Goldhirsh and Vogel, 1987]. Since the source platform was a helicopter and the receiver was located on a mobile van, control of the propagation path geometry enabled systematic determination of fade distributions for various road types, fixed elevation angles, and propagation path aspects.

EXPERIMENTAL ASPECTS

Transmitter Platform

The source platform was a Bell Jet Ranger Helicopter carrying two antenna systems. The UHF antenna (870 MHz) consisted of a microstrip configuration, and the L Band antenna (1.5 GHz) was a helix. Both radiated right hand circular polarizations with beamwidths nominally 60° . The two antennas were located on a steerable mount below the aircraft with the pointing controlled by an observer inside the helicopter. Also located on the steerable mount was a video camera. The experimenter within the aircraft observed the scene viewed by the camera as it appeared on a TV screen. In this manner, the geometrical pointing axis of the antennas was nearly coincident with the direction to the van location. The pilot maintained a height of nominally 300 m above the van employing a barometer/altimeter system. For each run, the depression angle relative to the horizontal (elevation angle at the van) was maintained fixed employing an angle gauge with a digital readout of angle which also appeared on the TV screen. With the height and depression angle kept nominally constant through pilot maneuvering of the aircraft, the range to the van was also maintained fixed at nominally 600 m, 430 m, and 350 m corresponding to the respective elevation angles of 30° , 45° , and 60° .

Receiver System

The receiving antennas were mounted on the van roof and consisted of crossed drooping dipoles which have relatively flat elevation pattern function values with nominal half beamwidths within the interval 75° to 15° . Below 15° the gain function drops off rapidly and any multipath arriving via scatter from objects near or below the horizontal is diminished by the pattern by at least 10 dB or more. The receiver systems inside the van were connected through data acquisition electronics to an IBM PC compatible computer. The received data were sampled at a rate of 1 KHz and stored on sequential records containing 1024 samples. In addition to recording the UHF and L Band received signal levels, the vehicle speed and receiver gain settings were also recorded once per second.

Road Features

Replicating the roads of previous tests, measurements were made along three stretches of roads in Central Maryland. These were: (1) Route 295 north and south between Routes 175 and 450, a distance of 25 km (2) Route 108 southwest and northeast between Routes 32 and 97, a distance of 15 km, and (3) Route 32 north and south between Routes 108 and 70, a distance of 15 km. Route 295 is a popular four lane highway (connecting Baltimore and Washington DC). This road contains pairs of lanes carrying traffic in opposite directions with trees located along

75% of the extreme sides and along 35% of the center median. Route 108 is a relatively narrow two lane rural road containing approximately 55% roadside trees along the stretch examined. Route 32 is also a two lane rural road with more sparsely placed trees displaced further away from the sides and containing approximately 30% trees.

Attenuation resulting from roadside tree shadowing was obtained for the geometry in which the helicopter traveled along a trajectory parallel to that of the van such that the propagation path was normal to the line of roadside trees. Such a configuration is considered "worst case" for corresponding satellite paths as they give maximum attenuation. The dB attenuation levels were computed by comparing the shadowed and unshadowed signal levels corresponding to a fixed elevation angle run. The unshadowed signal levels were sampled at stretches of road containing no roadside trees such as at interchanges.

Eight cumulative fade distributions were generated for each fixed elevation angle run corresponding to 30° , 45° , and 60° . These eight runs correspond to the following pairs of cases: (1) right lane driving north and south on Route 295, (2) left lane driving north and south on Route 295 (3) driving northwest and southeast on Route 108, and (4) driving north and south on Route 32.

CUMULATIVE FADE DISTRIBUTIONS DUE TO SHADOWING GEOMETRIES

UHF and L Band Fades

Of the three roads sampled, Route 295 gave the highest fades and for this reason we emphasize the results for this road. In Figures 1 - 3 are given cumulative fade distributions at both UHF and L Band for the case in which the path elevation angles were 30° , 45° , and 60° , respectively. For this cases, the van traveled south in the right lane of Route 295 where the propagation path is to the right as depicted in the indicated cartoons. The ordinate represents the percentage of the distance exceeded such that the fade is greater than the abscissa value. Since in most instances the speed was maintained relatively fixed, the ordinates for these distributions and others shown here may also be considered to represent "the percentage of time" the fade is greater than the abscissa value. The negative values of fade depths in the abscissas represent signal enhancement caused by multipath constructive interference.

Dependence of Fade Distributions on Elevation Angles

In Figure 4 are shown the cumulative fade distributions at L Band for Route 295 south (right hand side driving) for the three elevation angles considered. We note a significant dependence on elevation angle; the smaller the angle, the larger the fade for any given percentage. This strong dependence on elevation angle is explained with reference to the cartoon in Figure 4 for which a reduction in path length through the foliage occurs as the elevation angle increases.

Comparison of Fade Distributions for Different Road Types

In Figure 5 is depicted an example set of distributions in which the L Band fade distributions (path elevation angle of 45°) for Routes

295 south (right lane driving and helicopter on the right side), 108 southwest (helicopter on the left) and 32 south (helicopter on the left). These results demonstrate that different types of roads and path orientations may result in both similar and dissimilar type distributions.

Right Side Versus Left Side Driving

In a previous effort [Goldhirsh and Vogel, 1987], right side of road versus left side of road driving was found to have a marked effect on the corresponding UHF fade distributions. This was consistently found to be the case for L Band. In Figure 6 is given a pair of fade distributions for 60° path elevation, respectively, derived for right and left side driving runs as characterized by the indicated cartoon. We note significant fade reductions for left lane driving relative to the right lane case. This is understood through an examination of the cartoons which depict a smaller propagation path through the tree canopies when the vehicle is located at greater distances from it. We have also noted a strong angle dependence (not shown here) in which significantly larger fade differences (right side versus left side) are noted at the higher elevation angles relative to those for the smaller [Goldhirsh and Vogel, 1988].

Best Fit Distributions

In Figures 7 (a), (b) and (c) are plotted the combined distributions derived from the eight shadowing runs (previously described) corresponding to each elevation angle. The three sets of points in each figure represent the median (center set of points), the 10 and 90 percentile cases (upper and lower sets of points). Also plotted for each set of points is the corresponding "least square" logarithmic fit, where the fade depth F in (dB) and the percentage P are considered to be the dependent and independent variables, respectively. The equations defining the least squares fits are given in the above mentioned figures. These curves were generated from the distribution of 90 second distributions (file size). The 10 and 90 percentiles indicate the variability of the statistics for the average road traveled for a 90 second sampling. Ninety seconds fortuitously may represent the nominal time of a single mobile telephone call.

FADE DISTRIBUTIONS DUE TO MULTIPATH

Fade distributions for multipath geometries in mountainous and canyon terrain were previously measured by Vogel and Goldhirsh [1988]. To insure that the phenomenon examined was caused by fading due to multipath in this previous effort, the helicopter followed the van maintaining unobstructed line of sight propagation paths. In a similar fashion, the multipath shadowing effects caused by roadside trees were also measured in Central MD during the June 1987 period. In Figure 8 are shown fade distributions at UHF and L Band for the above described multipath geometry for Route 295 south (right hand side driving) at the respective angles of 30° , 45° , and 60° . The corresponding cartoon in the figure depicts the helicopter following the van at the fixed

elevation angle. We have noted (not shown) that the L Band fades slightly and consistently exceed those at UHF by 1 to 2 dB in this percent range.

Except at the 15° path elevation angle, no angle dependence exists in the distribution characteristics. The dominant multipath most likely arises from scatter from the tops of nearby tree canopies and poles. For direct ray propagation paths at the higher elevation angles (30° and above), the dominant contributions of the direct and multiply scattered rays arise from incident energy at the higher antenna gain function values [Vogel and Hong, 1988]. Negligible contributions should arise due to scattering from nearby vehicles and from reflections from the ground since the corresponding ray paths are incident at the antenna at angles near the horizontal where the gain function is at least 10 dB down. At 15° , enhanced fades are noted to occur consistent with the above interpretation. That is, the significant multipath energy is incident at the higher gain function levels and combines with the direct ray path energy incident at the antenna at a consistently reduced gain value.

In comparing the distributions corresponding to multipath from roadside tree (Figure 8) relative to those obtained for mountainous and canyon terrain (not shown here) [Vogel and Goldhirsh, 1988; Goldhirsh and Vogel, 1988], the distributions are not significantly different. In fact, the multipath tree distributions may even exceed those for mountainous terrain. In comparing the distributions for shadowing and multipath, dramatic differences do arise. For example, we note 20 dB and 10 dB fades at the 1% and 10% levels, respectively, for the shadowing case at 45° elevation (Figure 2) as compared to 6 dB and 3 dB for the multipath roadside tree case (Figure 8).

CONCLUSIONS

We may conclude the following from the above described distributions. Unless otherwise specified, these characteristics pertain to L Band:

(1) Worst case fades due to shadowing occur at the smaller elevation angles (e.g., 30 degrees) (Figure 4).

(2) The best fit ratio of L Band to UHF fades (scaling factor) is in the range of 1.3 to 1.4 and is independent of exceedance percentage over the interval of 1% to 30%. These ratios are relatively insensitive to elevation angle [Goldhirsh and Vogel, 1988].

(3) Changing the lane of the road may lead to a considerable fade difference which is path angle dependent (Figure 6).

(4) Cumulative fade distributions follow with good approximations "logarithmic" least square fits in the exceedance interval between 20% and 1% (Figures 7 (a), (b), (c)). These best fit distributions correspond to the median, 10 and 90 percentile cases, and the corresponding equations are defined for the various elevation angles. These best fit curves correspond to the condition where the fade and exceedance percentage are the dependent and independent variable, respectively.

(5) Attenuation caused by shadowing of roadside trees considerably exceeds that due to multipath (Figures 1 and 8).

(6) The extent of fading due to multipath is dependent on the

receiving antenna pattern. The results are consistent with the fact that multipath is likely to arise from scattering from nearby tops of trees and poles.

(7) Attenuation caused by multipath from roadside trees was found to be comparable and in many cases slightly larger (e.g., 1 to 2 dB) than those obtained in canyon terrain [Vogel and Goldhirsh, 1988]. This may be attributed to the fact that roadside trees are nearby, tall and therefore give rise to more appropriate scattering geometries for the given antenna pattern (as described in the above paragraph). The canopy tops of the trees may also represent more of an isotropic scatterer than nearby faceted canyon walls.

ACKNOWLEDGEMENTS

The authors are grateful to J. R. Rowland for his ingenuity in outfitting the helicopter transmitter platform and to G. W. Torrence for his assistance in the development of the receiver data acquisition system. Many thanks are also extended to A. J. Walker, Steve Babin, and Jack Miller for assisting the experiment. This work was supported by NASA Headquarters Communications Division under Contract #N00039-87-C-5301 for APL and by the Jet Propulsion Laboratory for the University of Texas under Contract #JPL956520.

REFERENCES

- Bell, T. S. 1988. Technology '88 - Communications. IEEE Spectrum. January, pp 41-43.
- Butterworth, J. S. 1984. Propagation measurements for land mobile satellite systems at 1542 MHz. Communications Research Center Technical Report. Ottawa, Canada, Tech. Note No. 723, August.
- Goldhirsh J. and W. J. Vogel 1987. Roadside tree attenuation measurements at UHF for land-mobile satellite systems. IEEE Trans. Antennas & Propagat. Vol AP-35, pp 589-596.
- Goldhirsh, J and W. J. Vogel 1988. Attenuation statistics due to shadowing and multipath from roadside trees at UHF and L Band for mobile satellite systems. Applied Physics Laboratory Johns Hopkins University Technical Report. JHU/APL, SLR88U 004, February.
- Jongejans A, A. Dissanayake, N. Hart, H. Haugli, C. Loisy, and R. Rogard 1986. PROSAT - Phase 1 report, European Space Agency Technical Report. ESA STR-216, May 1986 (European Space Agency, 8-10 rue Mario-Nikis, 75738 Paris Cedex 15, France.
- Vogel, W. J. and J. Goldhirsh 1986. Tree attenuation At 869 MHz derived from remotely piloted aircraft measurements. IEEE Trans. Antennas & Propagat. Vol AP-34, pp 1460-1464
- Vogel, W. J. and J. Goldhirsh 1988. Fade measurements at L band and UHF in mountainous terrain for land mobile satellite systems. IEEE Trans. Antennas & Propagat. Vol AP-36, Jan.
- Vogel, W. J. and Ui-Seok Hong 1988. Measurement and modeling of land mobile satellite propagation at UHF and L Band. IEEE Trans. Antennas & Propagat. Vol AP-36, May.

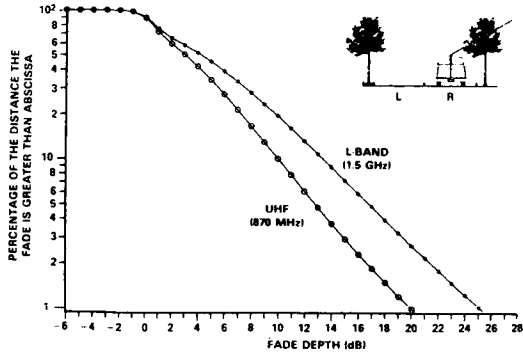


Fig. 1 Cumulative distributions for Route 295 South (RHS) 30° elevation for L-band and UHF - June 1987

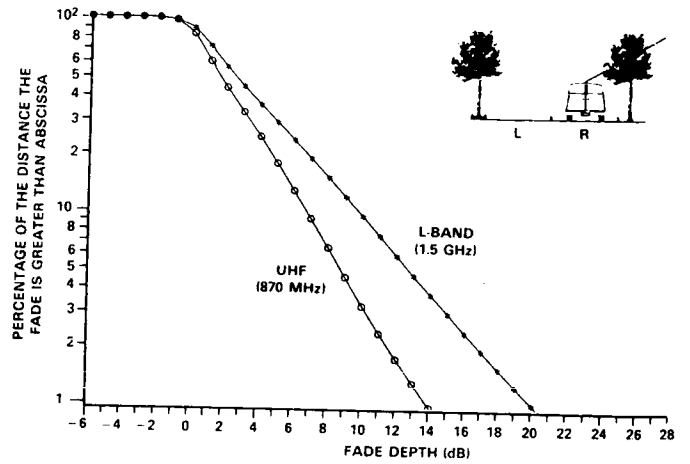


Fig. 2 Cumulative distributions for Route 295 South (RHS) 45° elevation for L-band and UHF - June 1987

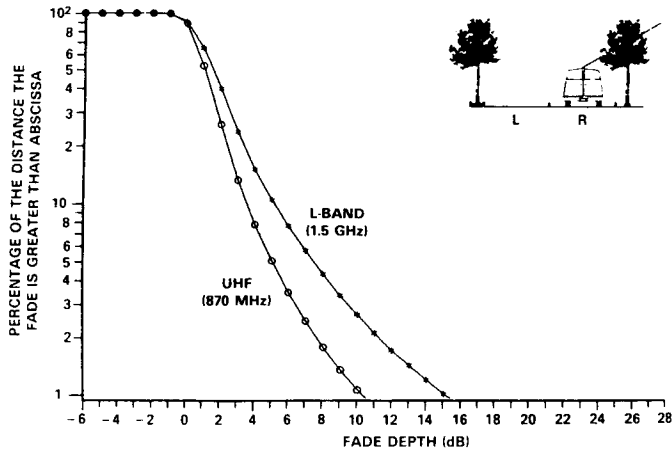


Fig. 3 Cumulative distributions for Route 295 South (RHS) 60° elevation for L-band and UHF - June 1987

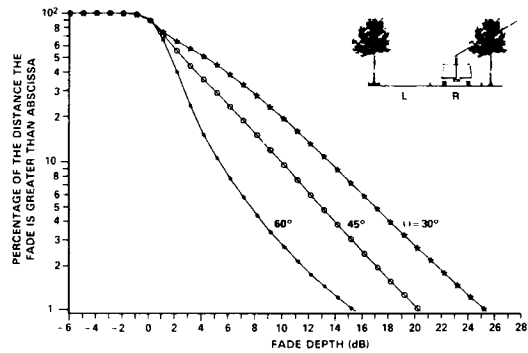


Fig. 4 Cumulative distributions for Route 295 South (RHS) comparison for different elevation angles at L-band

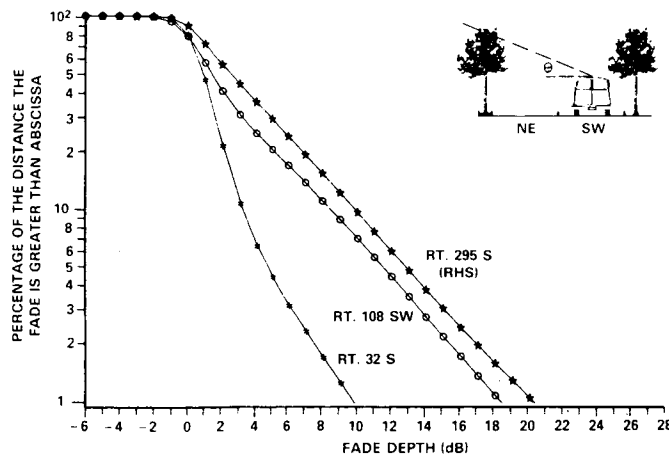


Fig. 5 Comparison of cumulative fade distributions for various roads at an elevation angle of 45° for L-band

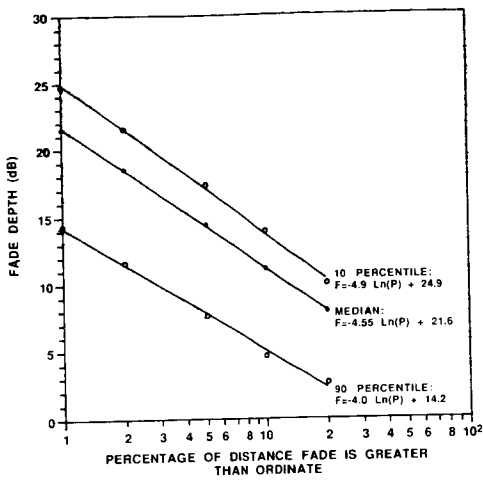


Fig. 7-a Best fit cumulative median fade distribution with 10 and 90 percentile bounds (elevation angle = 30°)

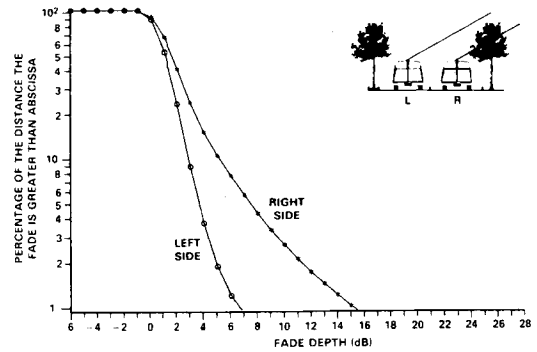


Fig. 6 Cumulative distributions for Route 295 South for right and left side of road driving L-band at 60°

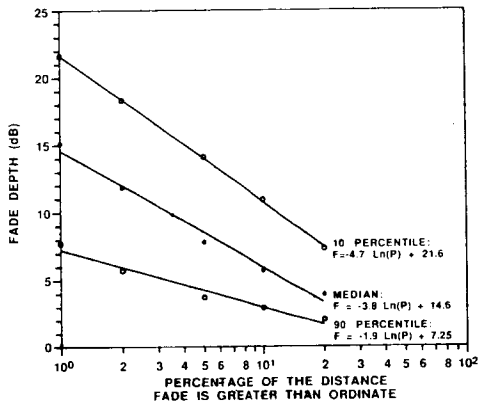


Fig. 7-b Best fit cumulative median fade distribution with 10 and 90 percentile bounds (elevation angle = 45°)

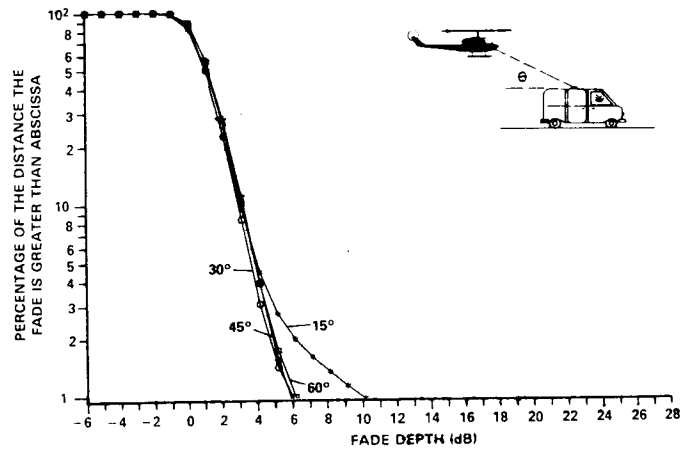


Fig. 8 Comparison of cumulative fade distributions due to multipath at various elevation angles at L-band Route 295 South (RHS)

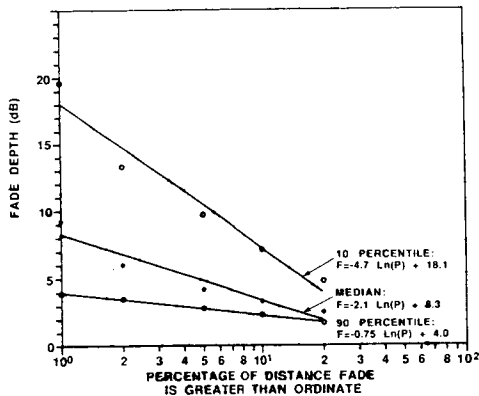


Fig. 7-c Best fit cumulative median fade distribution with 10 and 90 percentile bounds (elevation angle = 60°)

PROPAGATION MODELING FOR LAND MOBILE SATELLITE SYSTEMS

R. MICHAEL BARTS and DR. WARREN L. STUTZMAN

Virginia Tech
Bradley Department of Electrical Engineering
Satellite Communications Group
627 Whittemore Hall
Blacksburg, VA 24061

ABSTRACT

A simplified empirical model for predicting primary fade statistics for a vegetatively shadowed mobile satellite signal is presented, and predictions based on the model are presented using propagation parameter values from experimental data. Results from the empirical model are used to drive a propagation simulator to produce the secondary fade statistics of average fade duration.

INTRODUCTION

The reliability of Mobile Satellite Systems (MSS) is of major concern due to the unique problems that arise from propagation induced fading. Satellite-mobile links, operating with low signal margins, will encounter path outages due to obstruction by highway overpasses and vegetative shadowing. Whereas terrestrial land mobile systems are often able to exploit relatively strong multipath signals, MSS will be power limited and dependent on the line of sight signal component. This paper details efforts to model MSS signals and to predict fade distributions and fade durations using a combination of analytical modeling and simulation.

PROPAGATION THEORY

The MSS signal is divided into two propagation categories: unshadowed and vegetatively shadowed due mainly to trees. Each is treated separately and then the results are combined to form a complete model.

The unshadowed signal consists of an unobstructed line of sight (LOS) component and a multipath path component due to scattering from the surrounding

terrain. The LOS component is assumed to have a constant amplitude and phase; thus, phase variations due to changes in path length are ignored. The multipath component has been shown to have a Rayleigh amplitude distribution [1]. The sum of a constant signal and a Rayleigh distributed signal is Rice distributed. The Rician signal is specified by the parameter K , defined as the ratio of the average multipath power to the average LOS power, usually expressed in dB.

The shadowed signal consists of a vegetatively shadowed LOS component and a terrain induced multipath component. As in the unshadowed case, the multipath component is modeled as a Rayleigh distributed signal described by the parameter \bar{K} , defined as the ratio of the average multipath power to average direct path power. The shadowed LOS component fade is modeled as a lognormally distributed signal and is specified by its mean, μ , and standard deviation, σ . We model the shadowed direct component as being the sum of an unshadowed LOS component and a lognormally distributed scattered signal, the sum of which is still lognormally distributed. This slight deviation from the traditional representation permits more insight into the physics of the fading process.

A model for a mixed shadowed/unshadowed mobile path is obtained by combining the distributions described above weighted by the fraction of shadowing encountered along the route, P . The total distribution for a mixed shadowed/unshadowed mobile path is expressed as [2]

$$G(F) = G_u(F) * (1-P) + G_s(F) * P \quad (1)$$

where $G_u(F)$ is the fade distribution for an unshadowed signal, $G_s(F)$ is the fade distribution for a shadowed signal, and P is the fraction of vegetative shadowing along the mobile path.

A SIMPLE EMPIRICAL MODEL FOR FADE DISTRIBUTIONS

The statistical model for fade durations described in the previous section can be evaluated analytically if the parameter values K , \bar{K} , μ , σ , and P are known. But this requires the numerical evaluation of several integrals. A computer model to evaluate these fade distributions has been developed [2]; while valuable for validation, it is cumbersome for general use. So, a simple empirical model has been developed [3], which is

described next.

For an unshadowed signal, the probability that a fade will be less than F dB is

$$G_u(F) = 1 - e^{-(F-U1)/U2} \quad (2)$$

where

$$U1 = 0.01*K^2 - 0.378*K + 53.98$$

$$U2 = 331.35*K^{-2.29}$$

$$K = \text{avg. multipath power/avg. LOS power [dB]}$$

For a vegetatively shadowed signal, the probability that a fade will be less than F dB is

$$G_s(F) = 1 - [(F + 50)/V1]^{V2} \quad (3)$$

where

$$V1 = 0.275*b_0 + 0.723* \mu + 0.336* \sigma + 56.987$$

$$V2 = 0.006*b_0 - 0.008* \mu + 0.013* \sigma + 0.121$$

$$b_0 = \bar{K} - 3 \text{ [dB]}$$

$$= \text{avg. multipath power/ avg. direct power [dB]}$$

$$\mu = \text{mean of lognormal signal [dB]}$$

$$\sigma = \text{standard deviation of lognormal signal [dB]}$$

This simple model was developed from experimentally derived fade durations and the analytical computer model mentioned above.

We have compiled a data base of experiments including fade statistics reported in the open literature and raw data supplied by Vogel [4]. This MSS data base is used for model and simulator development, testing, and verification at Virginia Tech. Since it is difficult to measure the propagation model parameter values accurately, they were determined by a best fit of the analytical model to experimental data. The empirical model of (2) and (3) was developed from the analytical model. It provides good agreement to experimental data as illustrated in Fig. 1. The empirical model was developed for the typical propagation parameter value ranges given in Table 1.

THE PROPAGATION SIMULATOR AND SIMULATOR RESULTS

A software simulator has been developed by Schmier [4] to simulate MSS signals and predict primary and secondary fade statistics. This simulator is unique

because instead of generating the simulated signal from statistical functions, it is generated using databases, derived from experimental data supplied by Vogel, with known statistical properties. By processing Vogel's experimental data, databases for each signal component having the proper statistical properties can be created. These databases are scaled to have the proper statistical distribution and recombined to form a composite signal. The output of the simulator simulates a time sequence signal that can be used to produce secondary statistics of average fade duration and of level crossing rate. The simulator output is normalized to produce samples every 0.1 wavelength traveled in order to remove the effect of vehicle speed from the simulation.

The databases are generated by first separating the experimental data into shadowed and unshadowed data points using a 2 dB below LOS criterion. Then the running mean of the data is calculated using a 20 wavelength sliding window. For the shadowed data, this running mean has been found to be lognormally distributed. Subtracting the running mean from the shadowed data on a point by point basis, generates a database which has been found to be Rayleigh distributed.

In Schmier's original simulator, there were separate scattered multipath databases for shadowed and unshadowed signal; the difference being in the phase of the Rayleigh signals. The unshadowed Rayleigh database had a uniform phase distribution while the shadowed Rayleigh database had a phase distribution centered around 0 and 180 degrees. This difference in phases caused a disagreement between the simulator and the analytical model. According to theory, the phase of a Rayleigh signal is uniformly distributed between 0 and 360 degrees. Our modification to Schmier's original simulator consisted of regenerating the shadowed Rayleigh database with a uniform phase. The modified simulator now generates fade distributions that agree with the analytical model. Figure 2 shows a comparison of fade distributions predicted by the analytical model and the modified simulator showing good agreement.

A measure of the fade duration secondary statistic is the average fade duration (AFD) defined for a fade level F as

$$AFD(F) = \frac{D(S < F)}{N(F)} \quad (4)$$

where

$D(S < F)$ = total duration of data with signal levels less than F (wavelengths)
 $N(F)$ = total number of fade events below F

AFD is expressed in wavelengths since the simulator output is sampled in wavelengths. Figure 3 shows a comparison between the AFD predicted by the modified simulator and that measured from a one minute record of experimental data measured by Vogel.

A possible method of reducing fade effects is the use of two receive antennas on a mobile in a diversity configuration. The propagation simulator (with a 0.1 wavelength resolution) has been used in a preliminary study of diversity improvement. Our study indicates it is possible to obtain useful diversity gain with as small as 1 wavelength separation. At the 99 percentile, our simulation shows a diversity gain of 2 dB for 1 wavelength separation and a diversity gain of 3.5 dB for 5 wavelengths separation. There seems to be little improvement beyond 5 wavelengths.

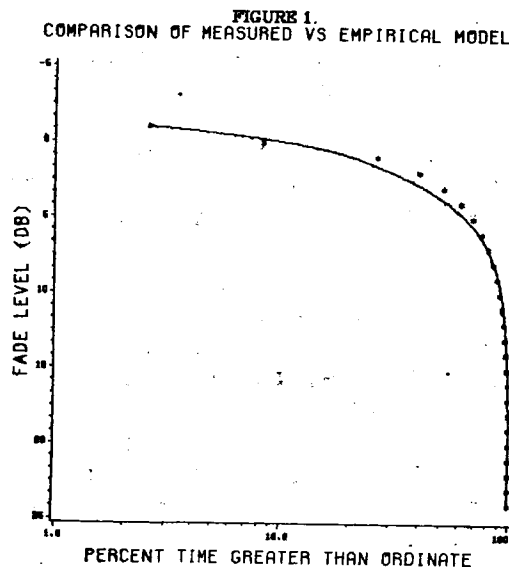


Table 1. Typical values for propagation parameters

-13 dB < K < -22 dB
 -12 dB < \bar{K} < -18 dB
 -1 dB < μ < -10 dB
 0.5 dB < σ < 3.5 dB

FIGURE 2.
 COMPARISON OF SIMULATOR VS ANALYTICAL MODEL

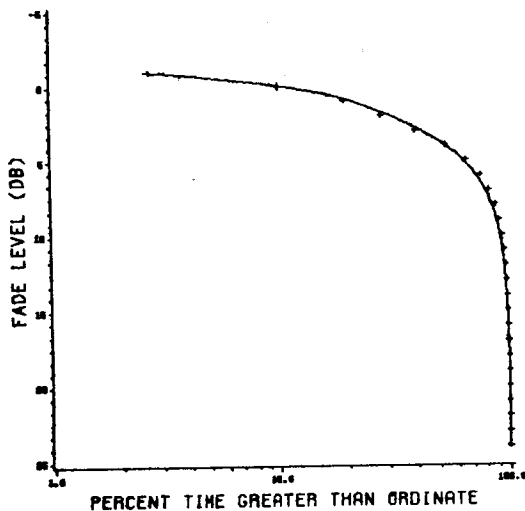
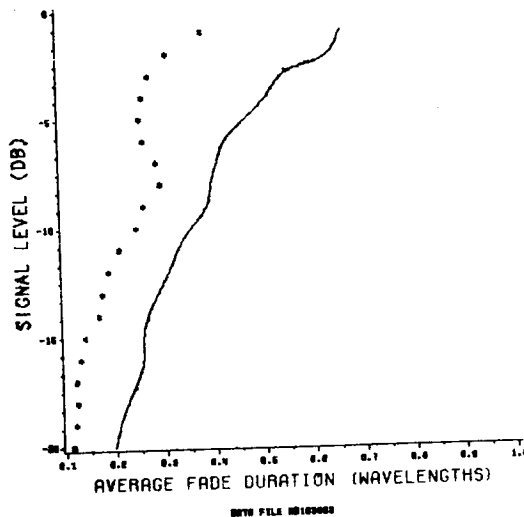


FIGURE 3.
 SIMULATED VS MEASURED AVERAGE FADE DURATION



REFERENCES

1. C. Loo, "A statistical model for a land mobile satellite link," **Proceedings of the 1984 IEEE International Communications Conference**, pp. 588-594, 1984.
2. W. T. Smith and W. L. Stutzman, "Statistical Modeling for Land Mobile Satellite Communications," Report submitted to NASA/JPL under NASA Contract 956512, August 1986.
3. R. M. Barts, W. L. Stutzman, W. T. Smith, R. S. Schmier, and C. W. Bostian, "Land mobile satellite propagation modeling," **Proceedings of the 1987 IEEE Antennas and Propagation Society International Symposium**, vol. I, pp. 20 - 23, 1987.
4. R. G. Schmier and C. W. Bostian, "Fade Durations in Satellite-Path Mobile Radio Propagation," Report submitted to NASA/JPL under NASA Contract 956512, December 1986.

**ATTENUATED DIRECT AND SCATTERED WAVE PROPAGATION ON SIMULATED LAND MOBILE
SATELLITE SERVICE PATHS IN THE PRESENCE OF TREES**

RICHARD L. CAMPBELL, Assistant Professor, Electrical Engineering Department,
Michigan Technological University, United States; ROBERT ESTUS, Electrical
Engineering Department, Michigan Technological University, United States.

MICHIGAN TECHNOLOGICAL UNIVERSITY
Electrical Engineering Department
Houghton, MI 49931
United States

ABSTRACT

Measurements have been made of direct path with no trees, attenuated direct, and tree scattered signal levels at 1.3 GHz. Signals were received in two small groves of mixed hardwood trees. In the groves studied, average total signal levels were about 13 dB below adjacent no-trees locations, with attenuated direct signal levels about 14.6 dB below the no-trees case and scattered signals about 17.3 dB below the no-trees case. A simple model for LMSS propagation in groves of trees is proposed. The model assumes a constant scattered signal contribution at 17 dB below no-trees levels added to an attenuated direct signal which varies, depending on the number and density of trees in the direct path. When total signal levels are strong, the attenuated direct signal dominates. When total signal levels are more than 15 dB below no-trees levels, the scattered signals dominate.

I. INTRODUCTION

Signals may arrive at a mobile receiver in the Land Mobile Satellite Service (LMSS) via several paths. Figure 1 shows a combination of absorption by one tree and scattering from another. In a grove of trees, the scattered signals may be received from many trees at once. This paper presents measurements of the levels of direct, attenuated direct, and scattered signals at 1.3 GHz on simulated LMSS paths.

II. COHERENT AND INCOHERENT INTENSITY

The direct, or coherent signal is characterized by deterministic amplitude, phase, and arrival angle. The complex envelope of the coherent field at the receiver is:

$$U_c = A_c e^{j\phi_c}$$

where A_c and ϕ_c are constants determined from the distance in wavelengths between the satellite and mobile receiver and any attenuation on the direct path.

The incoherent signal includes contributions from all the scatterers in the vicinity of the receiver. The incoherent signal is characterized by random amplitude, random phase, and a distribution of arrival angles. The complex envelope of the incoherent field is:

$$U_I = \sum_{i=1}^N A_i e^{j\phi_i}$$

where N is the number of scatterers and A_i and ϕ_i are determined by the relative positions of the satellite, scatterer and receiver and the scattering function $\hat{f}(o, i)$. [1]

The total signal is the sum of the direct and all the scattered signals. The complex envelope of the total field is U_T . The total intensity is:

$$I_T = \langle U_T U_T^* \rangle$$

where the brackets $\langle \rangle$ indicate ensemble average and the asterisk denotes the complex conjugate. The coherent intensity is:

$$I_c = |\langle U_T \rangle|^2$$

The incoherent intensity is the total intensity minus the coherent intensity [2].

$$I_i = \langle U_T U_T^* \rangle - |\langle U_T \rangle|^2$$

The measurement technique employed here uses the fact that the

direct wave arrival angle is deterministic and the arrival angles of the scattered waves are distributed. The distribution of arrival angles of the total field at the receiver is called the "Angular Spectrum" and is related to the previous definitions of coherent and incoherent intensity by a Fourier Transform [3].

III. MEASUREMENT OF THE ANGULAR SPECTRUM

If the signal transmitted from the satellite is at constant frequency f_0 and the receiver is moving at velocity V_0 , the signal will be received at the Doppler shifted frequency:

$$f = \frac{V_0}{\lambda_0} \cos \alpha + f_0$$

where λ_0 is the transmitted wavelength and α is the angle between the vehicle velocity V_0 and the signal arrival angle. If the vehicle moves in a straight line, the direct signal will be received at constant frequency:

$$f_c = \frac{V_0}{\lambda_0} \cos \alpha_c + f_0$$

Similarly, the i th scattered wave will be received at:

$$f_i = \frac{V_0}{\lambda_0} \cos \alpha_i + f_0$$

Scatterers close to the receiver will have the largest contributions, since the scattered waves are spherical and the intensity falls off as $1/R^2$, where R is the distance from the scatterer to the receiver.

IV. EXPERIMENTAL APPARATUS

The transmitter and receiver must be highly frequency and amplitude stable, such that the relative drift is much less than the expected Doppler shifts in the direct and scattered signals. The required stability is obtained by deriving the transmitter and receiver local oscillator signals from a pair of proportional oven controlled 5 MHz crystal oscillators. Measured drift is on the order of 0.2 Hz per hour.

The receiver is described in [4]. The receiver intermediate frequency (IF) output at 0.3 to 3.0 kHz is recorded on analog tape and then played into a Fourier Analyzer for processing. Two Fourier analyzers are used, an HP3582A for diagnostics and field data analysis and an HP5451C for final data reduction. The receiver has two identical channels, which allows two orthogonal polarizations to be received at once. The output of each antenna is downconverted from 1.3 GHz to 700 Hz, where the two outputs are recorded on the right and left channels of a stereo cassette recorder. After processing, the two

angular spectra are added to obtain an approximately isotropic horizontally polarized receive antenna pattern.

V. MEASUREMENTS

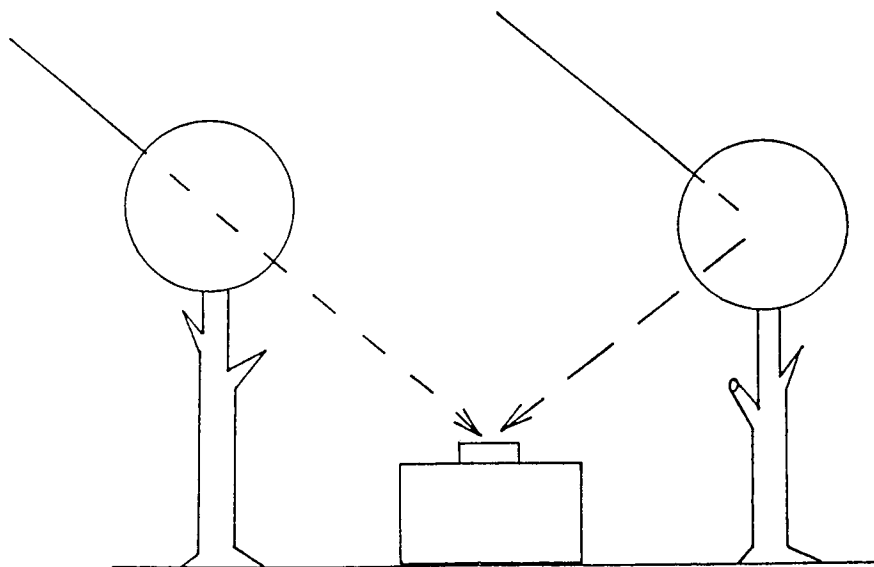
Two small groves of trees were chosen for this study. Vogel and Goldhirsch [5] have found that the total received signal power is commonly between 10 and 20 dB lower when trees are present. The two groves in this study have average total signal levels 12 and 14 dB less than the adjacent areas with no trees. There is a clear line of sight path between the transmitter and receiver, and the peak amplitude represents the total intensity when no trees are present. A top view drawing of Grove #1 is shown in Figure 2. The elevation angle to the transmitter is 7° . The arrival angle α_c varies from 110° relative to v_o at the west end of the path to 124° at the east end. The variation in α_c causes some broadening of the coherent peak in the Angular spectrum. Figure 3 is the sum of the two spectra from the orthogonal horizontally polarized dipoles. Since the power pattern of one dipole is roughly $\sin^2 \alpha$ and the power pattern of the other dipole is roughly $\cos^2 \alpha$, the power pattern of the sum is approximately 1_o (isotropic). The coherent component is clearly visible between $\alpha=110^\circ$ and $\alpha=124^\circ$. The coherent intensity is approximately the total intensity in the spectrum between $\alpha=110^\circ$ and $\alpha=124^\circ$. The coherent intensity in Figure 3 is approximately 15.7 dB below the total intensity in the no-trees case. The incoherent intensity is the total intensity in the whole angular spectrum minus the coherent intensity. The total intensity is approximately 14.0 dB below the no-trees case. The incoherent intensity is approximately 18.4 dB below the no-trees case. Thus, for grove number one, with total received signal power 14 dB below the no-trees case, .3 of the received signal is due to scattering and .7 is due to the attenuated direct path.

VI. CONCLUSIONS

When a Land Mobile Satellite Service receiver is located in a grove of trees illuminated from above by a satellite transmitter, each tree becomes a source of scattered signals. It appears that the total scattered signal power is on the order of 17 dB below the unattenuated direct signal power. When there are no trees in the direct path, as in figure 3, the total signal power will be dominated by the direct signal. When attenuation in the direct path increases to more than 13 dB, however, as will be the case when several large trees are in the direct path, the scattered signals become significant. In the balloon studies by Vogel and Goldhirsch, average fades commonly exceed 13 dB but seldom exceed 20 dB. The deep average fades exhibit fast fading characteristic of multipath. These observations are consistent with the measurements of the relative levels of unattenuated total signal power, attenuated direct signal power, and scattered signal power reported here.

REFERENCES

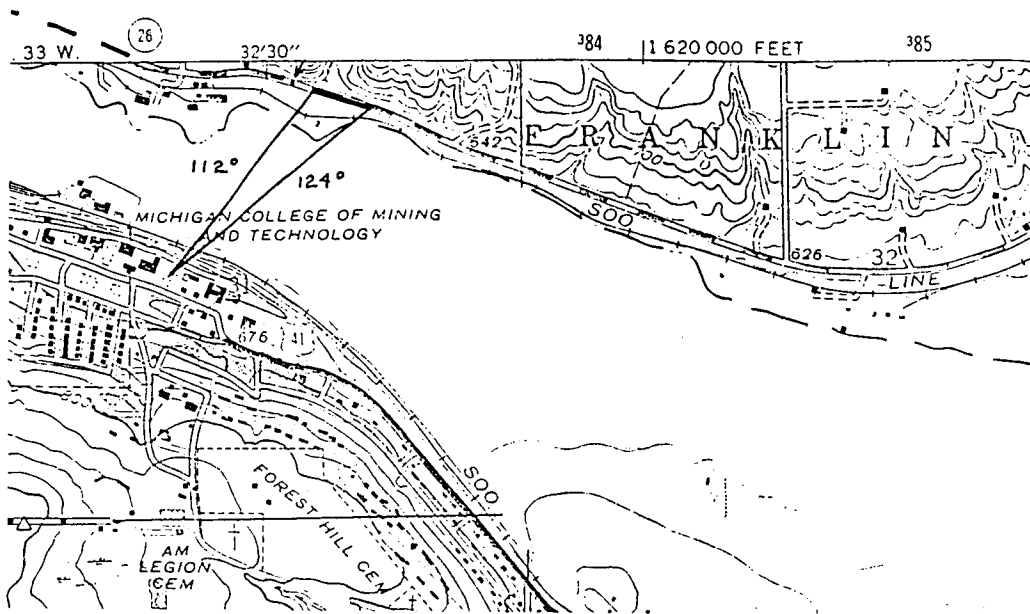
- Ishimaru, Akira, Wave Propagation and Scattering in Random Media, vol. 1, Academic Press, New York, 1978, p. 10.
- Ishimaru, Akira, Ibid.; p. 116.
- Ishimaru, Akira, Ibid.; p. 87.
- Campbell, Richard L., "Experimental Studies of VHF and UHF Propagation in an Urban Residential Medium Using High Resolution RF Spectrum Analysis," Ph.D. Dissertation, University of Washington, 1984, University Microfilms International No. 8501034, Ann Arbor, 1985.
- Goldhirsh, J. and W.J. Vogel [1987a] Roadside tree attenuation measurements at UHF for land mobile-satellite systems. IEEE Trans. Ant. & Propag., Vol. AP-35, No. 5, 589-596; May, 1987.



Direct Path with Absorption and Scattering

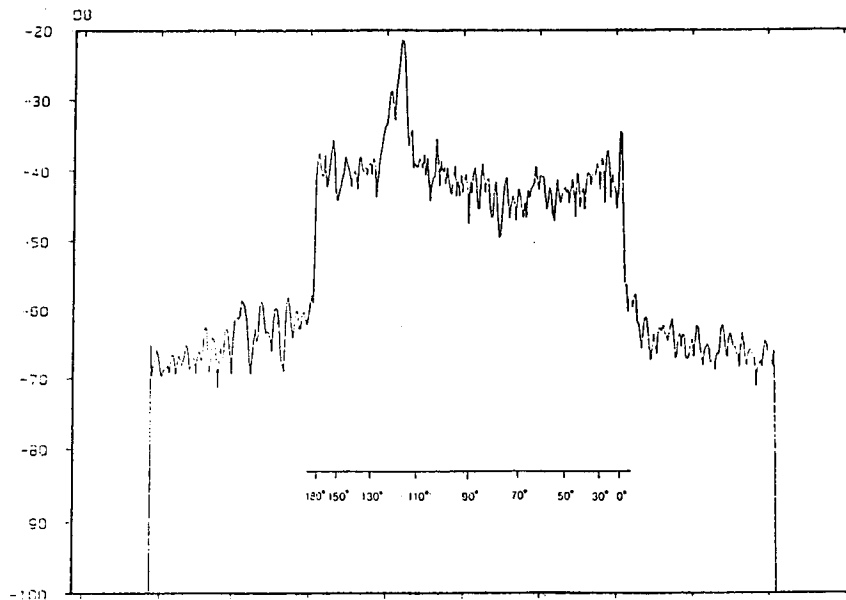
FIGURE 1

ORIGINAL PAGE IS
OF POOR QUALITY



Grove Number One Location

FIGURE 2



Grove Number One Angular Spectrum

FIGURE 3

**MOBILE SATELLITE PROPAGATION MEASUREMENTS AND MODELING:
A REVIEW OF RESULTS FOR SYSTEMS ENGINEERS**

Editor:

W. L. Stutzman Virginia Tech

Contributors:

R. M. Barts	Virginia Tech
C. W. Bostian	Virginia Tech
J. S. Butterworth	CRC, Canada
R. Campbell	Michigan Tech
J. Goldhirsh	Applied Physics Lab./JHU
W. L. Stutzman	Virginia Tech
W. J. Vogel	U. of Texas

VIRGINIA TECH

Satellite Communications Group
Bradley Department of Electrical Engineering
627 Whittemore Hall
Blacksburg, VA 24061

ABSTRACT

This overview of Mobile Satellite System (MSS) propagation measurements and modeling is intended as a summary of current results. While such research is on going, the simple models presented here should be useful to system engineers. A complete summary of MSS propagation experiments with literature references is also included.

INTRODUCTION

This paper is a collective effort by a group of researchers in the U. S. and Canada in the area of Land Mobile Satellite propagation. It concerns the propagation effects of the natural environment as encountered under highway conditions at UHF and L-Band frequencies. It presents results, experimental and theoretical, that are applicable to future operational Mobile Satellite Systems (MSS). Our understanding of MSS propagation is by no means complete. Much needs to be done both in measurement and in theory. This review is essentially a summary of the current state of knowledge.

This paper emphasizes results, not the details of how experiments were performed or the theoretical background of the models developed. A comprehensive list of MSS related propagation experiments is presented (see Table 1); literature references for these experiments as well as for key theory and modeling works are given.

CHARACTERISTICS OF MSS PROPAGATION EFFECTS

MSS communications system design presents new problems. Mobile terminals do not have the fixed-terminal advantage of placing antennas with a clear line of sight view to the satellite. Instead, a mobile with a roof mounted antenna will encounter several propagation effects that will influence the system margin, reliability, and modulation format selection. These may be classified as follows:

- (a) Tree shadowing of the direct wave
- (b) Blockage from natural terrain and structures like overpasses
- (c) Multipath scattering from terrain, and from simple scatterers like utility poles

Specular reflection is not significant above 15 degrees elevation with circularly polarized antennas [5] and therefore, we have not listed it as a propagation problem. Blockage from structures such as overpasses have been noted by Vogel during his balloon experiments [9]. They are obviously serious short term blockage problems but are not statistically significant. This paper does not include structure blockage effects, but concentrates on vegetative blockage and multipath scattering.

MSS PROPAGATION RESEARCH LITERATURE

Overview

The MSS propagation problem is attacked on three fronts: experimental, basic EM theory, and modeling. The most important of these is the establishment of an experimental data base. Satellite, helicopter, balloon, remotely piloted aircraft and tower platforms have been used, and most results appear to be applicable to satellite-to-earth mobile systems. This data base serves

two purposes. First, it may be used for system planning if data of the proper frequency, elevation angle, etc. are available or can be scaled. Second, experimental data are used in verifying theoretical models and to drive software simulators.

Complete analytical solutions from electromagnetic theory are not available due to the complexity of the propagation environment, but partial analytical and empirical statistical models of MSS propagation have been developed [14, 20, 21, 22]. These offer considerable insight into the physics of slant path propagation.

The mobile aspect of MSS propagation complicates the problem. Theoretical models do not provide complete information on the variation of the parameters in terms of highway and system constraints. Simple empirical models can be developed to give fade statistics for simple relationships with the highway and system parameters as inputs.

Experiments

Mobile satellite propagation experiments have been conducted since 1978. Table 1 presents a chronology of slant path propagation experiments in the UHF and L-bands. Most of the experiments produced fade depth and duration statistics for various mobile travel conditions. Some results from these are given in following sections.

Some experiments also collected phase data. The peak-to-peak variations of the phase, P , as a function of peak-to-peak signal level fluctuations in dB, L , can be expressed by [14]

$$P = C * L \quad [\text{degrees}] \quad (1)$$

where

C = 6.0	analytical value for unshadowed multipath
7.6	90th percentile) measured, includes
3.9	median } shadowing for fades up
2.1	10th percentile) to about 15 dB

The signal arriving at an MSS receiver has two components: a direct path component which can experience shadowing, and a diffuse component that is the sum of signals reflected from nearby objects. Campbell has performed experiments focusing on characterization of the diffuse component, which is quantified by the power level relative to the unattenuated direct signal power, b_0 , and the spatial distribution of arrival angles for the diffuse power. The measurements were made at 1300 MHz at

several elevation angles near 10 degrees along a section of a hardwood tree lined road in upper Michigan. The average total diffuse signal power is $17 \text{ dB} \pm 1 \text{ dB}$ below the unattenuated direct path signal. The diffuse signal has a rather even angular distribution, except for trees within about 100 m of the receiver which have significant contributions. The diffuse component is relatively unaffected by instantaneous blockage of the direct component; therefore, during deep fading the diffuse component will dominate.

FADE DISTRIBUTIONS

Form Of The Fade Distribution

Both experimental observations and basic theory indicate that the fade statistics measured over a large distance, become Rician at low fade levels, because of the dominant multipath effects. For high fade levels a number of experiments indicate that they become lognormal when vegetative shadowing dominates. Thus, MSS fading is modeled by a Rician distribution, described by the multipath-to-carrier ratio K , to predict fading when there is no blockage of the signal. When tree blockage is present, the fading is modeled by the sum of a lognormal distribution, described by the mean, μ , and standard deviation, σ , and a Rayleigh distribution, described by b_0 , the average scattered power in the multipath component. Bradley and Stutzman [18] showed how these distributions can be combined for an arbitrary percentage of shadowing along the travel route; apparently Lutz et al. [11] found this independently.

Experimental Results

Representative experimental results are plotted in Fig. 1. Shown are cumulative fade distributions over typically tens of km of road distance [18]. The distributions depend strongly on the elevation angle when shadowing by roadside trees dominates. A four-lane divided freeway lined with trees (Fig. 1a) can produce larger fades than a two-lane road lined with utility poles and trees (Fig. 1b). In comparison, a road with a wider cleared easement, even though tree lined (RT. 32), will have smaller probabilities. Measurements obtained at UHF on a road for various growing seasons (Leafless, March 1986; Fall Foliage, October 1985; Full Blossom,

June 1986) show only a small increase in attenuation due to leaves (Fig. 1c).

To scale UHF data to L-Band, the relationship

$$F_L = (1.35 \pm 0.1) * F_U \quad (3)$$

can be used where F_L and F_U are the L-Band and UHF fades in dB, respectively [18]. A comparison of distributions obtained in differing geographic areas (Fig. 1d) emphasizes the dependence of the distribution on the dominating environmental parameters, from heavy tree shadowing (Curve A) to pure multipath (Curve G).

Simple Model

A simple model for predicting the probability that the fades will be less than a certain amount F is given by [23]

$$G(F) = [1 - e^{-(F-U1)/U2}] (1-P) + [1 - \{(F + 50)/V1\}^{V2}] P \quad (2)$$

where

F = fade level with respect to LOS in dB
 P = fraction of time vegetative shadowing occurs along travel route

$U1, U2, V1, V2$ = fit coefficients

$$U1 = 0.01 * K^2 - .378 * K + 53.98$$

$$U2 = 331.25 * K^{-2.29}$$

$$V1 = 0.275 * b_0 + 0.723 * \mu + 0.336 * \sigma + 56.987$$

$$V2 = 0.006 * b_0 - 0.008 * \mu + 0.013 * \sigma + 0.121$$

where

K = average multipath-to-unshadowed carrier ratio for unshadowed path

b_0 = average multipath-to-carrier ratio for shadowed path

μ = mean of lognormal signal

σ = standard deviation of lognormal signal

This simple model is valid for typical ranges of the propagation parameters. Typical values for each of the parameters are as follows:

$$\begin{aligned}
-13 \text{ dB} < K < -22 \text{ dB} \\
-12 \text{ dB} < b_0 < -18 \text{ dB} \\
-1 \text{ dB} < \mu < -10 \text{ dB} \\
0.5 \text{ dB} < \sigma < 3.5 \text{ dB}
\end{aligned}$$

Behavior Of Statistical Parameters With Time

Cumulative fade distributions give information about the average link performance for a large number of transmissions for particular environmental conditions. A typical telephone call has a shorter duration (about 90 seconds) and therefore covers a shorter distance than the one on which Fig. 1 is based. When cumulative fade distributions are determined for successive 90 second intervals, they will vary, depending upon the short term variation of the shadowing parameter statistics. At percentage levels of main interest, from 1% to 20%, the 10th, 50th and 90th percentiles of the 90 second fade levels have been calculated and are given in Fig. 2 for elevation angles of 30, 45 and 60 degrees. The curve labeled **median** represents the median cumulative fade distribution and the upper and lower curves give the bounds into which 80% of the measured distributions fall. The curves can be fit by the relationship:

$$F(n,P) = A(n) * \ln(P) + B(n) \quad (4)$$

where

$$\begin{aligned}
F(n,P) &= \text{Fade at } n\text{th percentile for } P \text{ percent of} \\
&\quad \text{time fade is exceeded} \\
A(n), B(n) &= \text{fit coefficients}
\end{aligned}$$

Hence, these experimental results indicate that over the limited percentage interval a simple logarithmic relationship holds.

FADE DURATIONS

Measured fade durations for a 5 dB threshold are given in Fig. 3. The curves correspond to the combined results of repeated runs along several roads at the indicated elevation angles, both under predominantly shadowing or under multipath conditions. Two sets of statistics are provided, "fade durations": the duration the signal is below the threshold and "nonfade durations": the duration the signal is greater than the

threshold. The duration is expressed as spatial variable in wavelengths (0.2m) to gain independence from the vehicle speed. The durations are seen to systematically depend upon the elevation angle for the shadowing data. The lower the elevation, the longer the fades and the shorter the nonfades. Multipath durations are independent of the elevation angle, having very short fades and long nonfades.

The distribution of fade durations cannot in general be predicted analytically. Schmier and Bostian have reported a software simulator [24] which they claim will accurately predict the fade duration statistics of a signal whose cumulative fade distribution is known. The simulator operation is based on scaling values from a universal data set. Its predictions of the total number of fades exceeding specified thresholds agree well with experiment, but unpublished work by Barts indicates that it may not predict average fade durations well. Barts' work indicates that Schmier and Bostian's simulator works correctly, but its universal data set may have been incorrectly derived. Each side can make an effective case for the correctness of its results, and at the time this paper was written the issue was still unsettled.

Table 1

Summary of Slant Path UHF/L-Band
Propagation Experiments

Entry No.	Investigators	Date	Source	Freq (MHz)	Comments
1	Hess[1,2]	3/78	ATS-6	860	
2	Anderson[3,4]	78	ATS-6	1550	
3	Butterworth[5]	4-11/81	Tower	840	Static tests
4	" [5]	82	Tethered Balloon		
5	" [5]	9/82	Helicopter	870	
6	" [6]	6/83	Helicopter	870	
7	" [7]	11/82	MARECS A	1542	
8	" [6]	6/83	MARECS A	1542	
9	Vogel[8]	10/83 1/84	Balloon	869	
10	Vogel[9]	11/84	Balloon	869 1501	
11	Bultitude[10]	85	Tower	800 900	Spread spectrum measurements
12	Lutz, et. al.[11]	1/21-28/84 2/25-3/8/84 6/27-7/1/84	MARECS	1560	Measurements made in Europe
13	Vogel/Goldhirsh[12]	6/85	RPV	870	
14	Goldhirsh/Vogel[13]	10/85	Helicopter	870	
15	Vogel/Hong[14]	3/86 7/86	Balloon	870 1502	
16	Vogel/Goldhirsh[15]	8/86	Helicopter	870 1502	
17	PiFex[16,17]	3/87	Tower	870	No propagation data avail.
18	Goldhirsh/Vogel[18]	6/87	Helicopter	870 1502	
19	Vogel/Goldhirsh[19]	12/87	MARECS A	1541	21° elevation angle

CUMULATIVE DISTRIBUTIONS FOR ROUTE 295 SOUTH (RHS)
COMPARISON FOR DIFFERENT ELEVATION ANGLES AT L-BAND

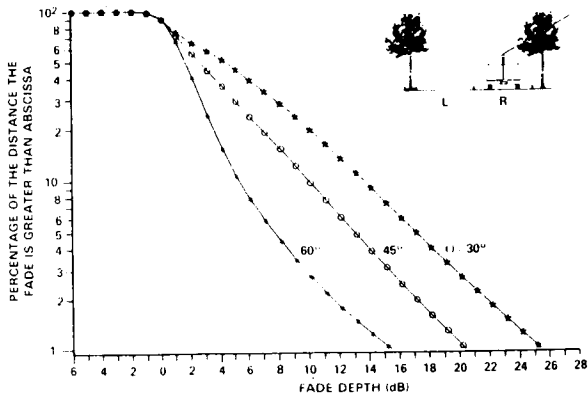


Figure 1a.

COMPARISON OF CUMULATIVE FADE DISTRIBUTIONS
FOR VARIOUS ROADS AT AN ELEVATION ANGLE OF
45° FOR L-BAND

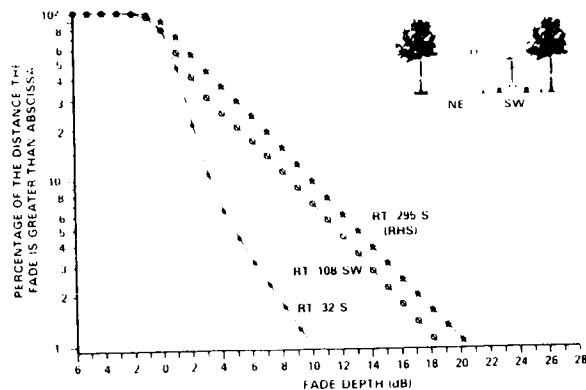


Figure 1b.

CUMULATIVE FADE DISTRIBUTIONS FOR
VARIOUS SEASONS
ROUTE 295 SOUTH (RHS) - UHF AT 45°

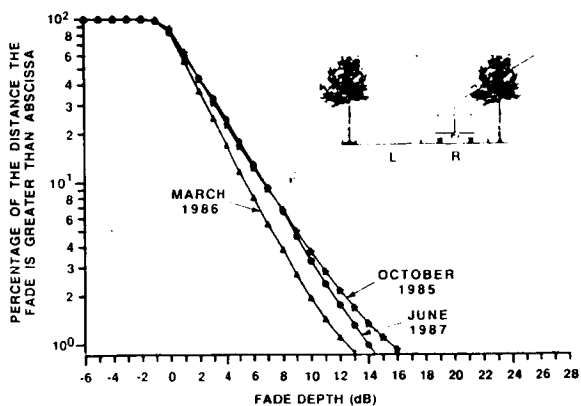


Figure 1c.

COMPARISON OF L BAND FADE DISTRIBUTIONS
FOR VARIOUS MSS INVESTIGATIONS

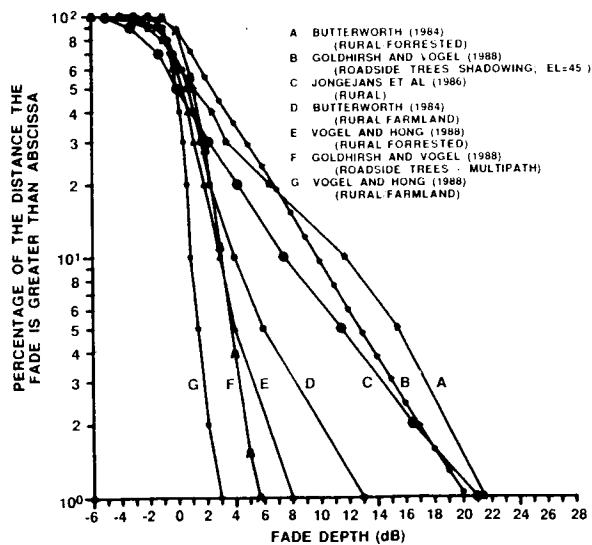


Figure 1d.

BEST FIT CUMULATIVE MEDIAN FADE DISTRIBUTION
WITH 10 AND 90 PERCENTILE BOUNDS
(ELEVATION ANGLE = 30°)

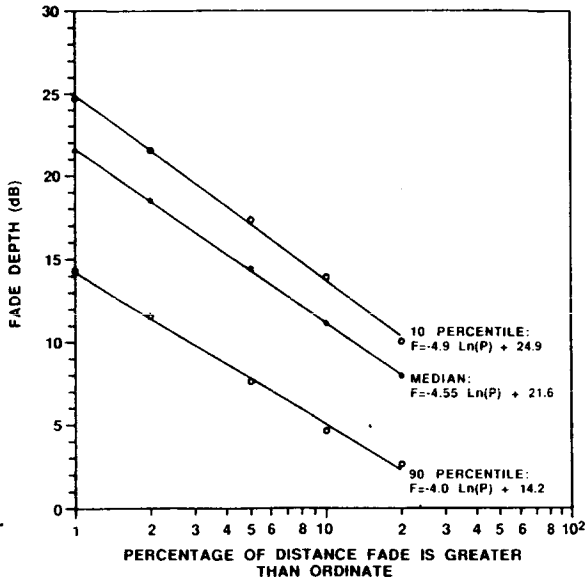


Figure 2a.

BEST FIT CUMULATIVE MEDIAN FADE DISTRIBUTION
WITH 10 AND 90 PERCENTILE BOUNDS
ELEVATION ANGLE = 45°

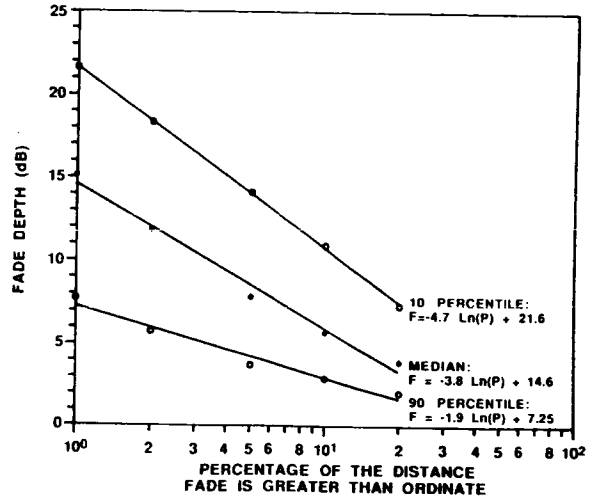


Figure 2b.

BEST FIT CUMULATIVE MEDIAN FADE DISTRIBUTION
WITH 10 AND 90 PERCENTILE BOUNDS
ELEVATION ANGLE = 60°

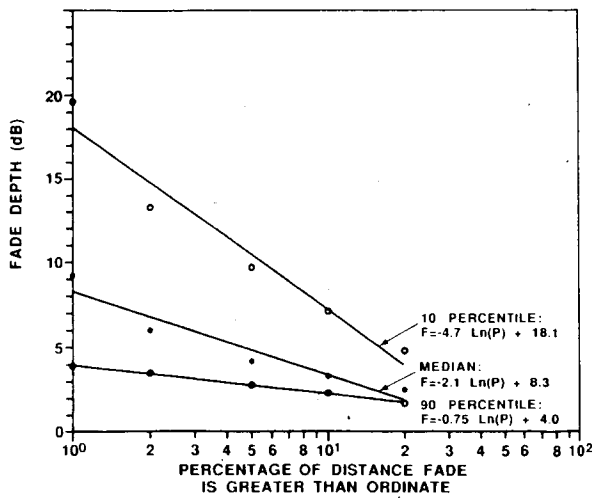


Figure 2c.

Fade/Nonfade Durations at L Band
5 dB Fade Threshold

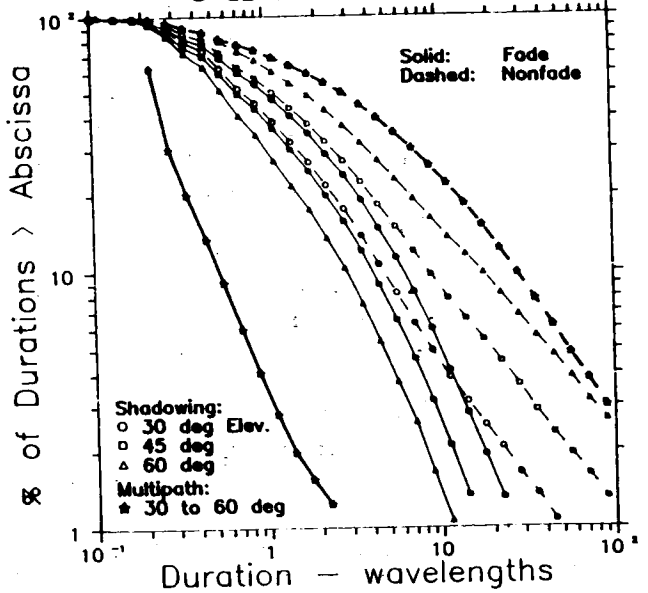


Figure 3.

REFERENCES

1. G. C. Hess, "Land Mobile Satellite Path Loss Measurements," Third Year ATS-6 Experiment Final Report, Motorola Inc., Schaumburg, IL, Sept. 6, 1978.
2. G. C. Hess, "Land mobile satellite excess path loss measurements," IEEE Trans. on Vehicular Technology, vol. VT-29, pp. 290-297, May 1980.
3. R. E. Anderson, R. L. Frey, and J. R. Lewis, "Satellite-Aided Mobile Communications Limited Operational Test in the Trucking Industry," Final Report for NASA Contract NAS5-24365 (N81-20338), June 1979.
4. R. E. Anderson, R. L. Frey, J. R. Lewis, and R. T. Milton, "Satellite-aided mobile communications: Experiments, applications, and prospects," IEEE Trans. on Vehicular Technology, vol. VT-30, no. 2, pp. 54-61, May 1981.
5. J. S. Butterworth, "Propagation Measurements for Land-Mobile Satellite Services in the 800 MHz Band," Communications Research Centre Technical Note No. 724, Department of Communications, Canada, Aug. 1984.
6. J. S. Butterworth, "Propagation data for land-mobile satellite systems," Proceedings of NAPEX VIII, Vancouver, B.C., Canada, Aug. 1985.
7. J. S. Butterworth, "Propagation Measurements for Land Mobile Satellite Systems at 1542 MHz," Communications Research Centre Technical Note No. 723, Department of Communications, Canada, Aug 1984.
8. W. J. Vogel and G. W. Torrence, "Measurement Results From A Balloon Experiment Simulating Land Mobile Satellite Transmissions," MSAT-X Report No. 101, NASA-JPL, Pasadena, CA, April 1984.
9. W. J. Vogel, "Land Mobile Satellite Transmission Measurements at 869 MHz," MSAT-X Report No. 106, NASA-JPL, Pasadena, CA, April 12, 1985.
10. R. J. C. Bultitude, "Measured characteristics of 800/900 MHz fading radio channels with high angle propagation through moderately dense foliage," IEEE Journal on Selected Areas in Communications, vol. SAC-5, No. 2, Feb. 1987.
11. E. Lutz, W. Papke, and E. Plochinger, "Land mobile satellite communications - channel modeling, modulation and error control," Proceedings of 7th International Conference on Digital Satellite Communications, Munich, Germany, May 1986.
12. W. J. Vogel, and J. Goldhirsh, "Tree attenuation at

- 869 Mhz derived from remotely piloted aircraft measurements," IEEE Trans. on Antennas and Propagation, vol. AP-34, No. 12, Dec. 1986.
13. J. Goldhirsh, and W. J. Vogel, "Roadside tree attenuation measurements at UHF for land mobile satellite systems," IEEE Trans. on Antennas and Propagation, vol. AP-35, No. 5, May 1987.
 14. W. J. Vogel, and U. Hong, "Measurement and modeling of land mobile satellite propagation at UHF and L-Band," IEEE Trans. on Ant. and Prop., vol. AP-36, May 1988.
 15. W. J. Vogel, and J. Goldhirsh, "Fade measurements at L-Band and UHF in mountainous terrain for land mobile satellite systems," IEEE Transactions on Antennas and Propagation, vol. AP-36, Jan 1988.
 16. J. B. Berner, "PiFEx Tower 1 Results," Proceedings of NAPEX XI, NASA-JPL, Pasadena, CA, Aug. 31, 1987.
 17. Special Issue on PiFEx Tower 1 Experiments, MSAT-X Quarterly, JPL, No. 13, Jan. 1988.
 18. J. Goldhirsh and W. J. Vogel, "Attenuation Statistics Due to Shadowing and Multipath from Roadside Trees at UHF and L-Band for Mobile Satellite Systems," Johns Hopkins University/APL Report No. S1R-88-U004, Feb. 1988.
 19. W.J. Vogel and J. Goldhirsh, "A Comparison of Mobile Satellite Fade Statistics Obtained with a Helicopter and a Geosynchronous Satellite," manuscript in preparation.
 20. W. S. Bradley, and W. L. Stutzman, "Propagation Modeling for Land Mobile Satellite Communications," Technical Report submitted to JPL under NASA Contract 956512, August 1985.
 21. W. T. Smith, and W. L. Stutzman, "Statistical Modeling for Land Mobile Satellite Communications," Technical Report submitted to JPL under NASA Contract 956512, August 1986.
 22. C. H. Loo, "A statistical model for the land mobile satellite link," Proceedings of the IEEE International Communications Conference, pp. 588-594, 1984.
 23. R. M. Barts, W. L. Stutzman, W. T. Smith, R. S. Schmier, and C. W. Bostian, "Land mobile satellite propagation modeling," Proceedings of 1987 IEEE Antennas and Propagation Society International Symposium, Blacksburg, VA, June 1987.
 24. R. G. Schmier and C. W. Bostian, "Fade durations in satellite path mobile radio propagation," IEEE Transactions on Vehicular Technology, Nov. 1987.

PROPAGATION MEASUREMENTS FOR AN AUSTRALIAN LAND MOBILE-SATELLITE SYSTEM

ANTHONY BUNDRICK, Telecom Research Laboratories, Australia; ROBERT HARVEY, Telecom Research Laboratories, Australia.

TELECOM RESEARCH LABORATORIES
P.O. Box 249
Clayton
Vic., 3168
AUSTRALIA.

ABSTRACT

The Australian domestic satellite service provider Aussat Pty. Ltd. is planning to introduce Land Mobile-Satellite Services (LMSS) at L-band in 1991/92. This will be a new service for Australia and many technical details need resolution. Although it is known that attenuation due to roadside trees is significant it is not well quantified. This paper describes measurements of attenuation statistics using a helicopter and an instrumented van. Results are given for two different tree densities, for elevation angles of 30, 45, and 60 degrees and for frequencies of 893, 1550, and 2660 MHz. These results show that at 1550 MHz and 45 degrees elevation angle, attenuation values of 5.0 and 8.6 dB were exceeded 10% of the time for roadside tree densities of 35% and 85% respectively. Comparisons with other results based on measurements made in the Northern Hemisphere are made and show general agreement. The implication of the measured values on system design are discussed, and it is shown that, for Australia, an adaptive margin allocation scheme would require an average margin of approximately 5 dB.

INTRODUCTION

Domestic satellite communications in Australia are provided by 3 Ku-band satellites operated by Aussat Pty. Ltd., which is a company owned by the Australian federal government and Telecom Australia, the nation's telecommunications company. In 1991/92 Aussat will launch two new second generation satellites to replace those currently in service. Each of these satellites will include one L-band transponder (as well as a Ku-band communications payload) designed to provide a Land Mobile-Satellite Service (LMSS) for the Australian continent.

A LMSS will be a new service for Australia and the Telecom Research Laboratories is studying the various technical issues involved with such a system. The effects of propagation on the path between the mobile terminal and the satellite are a major concern and while there are a number of effects ranging from ionospheric scintillation to multipath, attenuation by roadside vegetation can be most significant (Vogel and Smith, 1985). For economic reasons satellite systems are designed with the minimum propagation margin consistent with desired performance objectives. The attenuation due to roadside vegetation must be properly quantified, and a number of measurements of attenuation statistics have been made in the northern hemisphere over

the past few years (Butterworth, 1984; Vogel and Smith, 1985; and Goldhirsh and Vogel, 1987).

Telecom has also measured attenuation statistics for parts of Australia because the data available from these previous measurements was not directly applicable. Australia has its own unique flora with non-deciduous eucalyptus and acacia trees predominant alongside roads. Further, the frequency and elevation angle ranges of interest differed from those measured elsewhere. In any event, the data base for attenuation statistics is currently narrow and further measurements will contribute to the broadening of this base.

MEASUREMENT CONFIGURATION

The Australian continent covers just over 30 degrees of latitude and elevation angles to the Aussat satellites vary from approximately 30 to nearly 70 degrees with most of the continent over 45 degrees. The tree type varies from dense tropical rainforest to sparse stunted growth in areas of low rainfall. There are also vast treeless plains such as the Nullarbor plain (*L. nullus*, not any, *arbor*, tree) which has an area of over 16 million ha. When the measurement programme was planned, there was uncertainty on the appropriate frequency bands for LMSS and data were required at various frequencies to cover possible eventualities. Data were therefore desired on the effects of elevation angle, frequency and tree type on the attenuation statistics.

A helicopter was chosen as the platform for the transmitters used in the measurements. The elevation angle could be readily varied by using the helicopter and also measurements could be made at chosen locations. Measurements were made at three frequencies, 893, 1550, and 2660 MHz which were transmitted continuously from the helicopter through drooping dipole antennas. The minimum spacing between antennas and to the edge of the groundplane on which they were mounted was two wavelengths and the resulting groundplane was approximately 1.2 by 2.0 meters. This was mounted between the skids of a Bell Jet Ranger and lowered in flight to just below the level of the skids, to avoid spurious results due to scatter from parts of the helicopter.

A van fitted with three receivers measured signal strengths as it was driven along selected roads with the helicopter flying parallel at constant relative height and elevation angle. The output level from each receiver was digitised at a 1.5 kHz rate under control of an IBM PC-AT compatible computer, and the results of a run were stored on a magnetic tape cartridge. Distance travelled was also recorded at the same time.

In October 1987 WARC-MOB allocated frequencies to the LMSS in the previous Aeronautical Mobile-Satellite Service (Route), AMSS(R), at 1545 to 1559 MHz and Australia will use these bands for LMSS. It was decided to continue the attenuation measurements at the three frequencies because the data obtained at 893 MHz will provide a point of comparison with equivalent North American data and 2660 MHz could be a possible future band for LMSS in Region 3.

RESULTS

This paper reports on data obtained on a typical double lane road close to the Telecom Research Laboratories in Melbourne, Australia. Messmate (stringybark) eucalyptus trees approximately 15 metres high lined the road with varying densities. Attenuation measurements were made on two different sections of road where the incidence of trees was 35% and 85%. All measurements were made with the helicopter

on the same of the road as the van. The raw data, scaled to decibels, was analysed by first searching for periods when there was clear line-of-sight between the helicopter and the van. These periods were recognised by the small peak-to-peak variation in signal strength and crosschecks were made that the results from the three frequencies coincided. These periods were used to adjust the data by removing the frequency independent helicopter - van distance variation, giving data scaled in decibels relative to line - of - sight.

Figure 1 shows the effect of elevation angle on the statistics for 35% tree density measured at 1550 MHz. The data are shown with a gaussian probability scale on the vertical axis and attenuation in positive decibels on the horizontal. Negative values of attenuation indicate signal strengths above line-of-sight due to multipath effects. With this scaling, straight line plots represent a log normal distribution for signal strength. From the data in Fig. 1 we note that at the 10% probability level the attenuation values are 5.7, 5.0, and 4.2 dB for 30, 45 and 60 degrees respectively. Figure 2 contains equivalent data for 85% tree density and the equivalent values for the 10% level are 10.8, 8.6, and 6.9 dB. Thus increasing elevation angle significantly reduces attenuation for equivalent percentage levels.

The distributions plotted in Figs. 3 and 4 show the increasing attenuation as the frequency increases. The axes and presentation in these Figures is identical to that in Figures 1 and 2 and data for 45 degrees elevation angle is shown. We note that at the 10% probability level the attenuations are 4.2, 5.0, and 7.8 dB for 897, 1550, and 2660 MHz respectively for 35% tree density and the corresponding attenuations for the 85% case are 6.6, 8.6, and 10.8 dB.

COMPARISON WITH OTHER DATA

There are obvious difficulties in making comparisons with other data which has most often been collected with somewhat different parameters and one purpose of these measurements is to assess the applicability of other data to Australia. Figure 5 compares cumulative distributions reported by Goldhirsh and Vogel (1987) obtained at 870 MHz using a helicopter in a very similar manner to that reported here. The data is for 45 degrees elevation angle and the percentage values categorising tree density is equivalent to that used here. The results for the distributions derived from the more densely wooded sections of road are in good agreement: at the 10% level, 6.9 dB vs 6.5 dB for Goldhirsh and Vogel. The agreement for 35% tree density is not as good: 4.5 dB reported here vs 2.7 dB at the 10% level.

Figure 6 compares results reported by the European Space Agency's PROSAT programme (Jongejans et al, 1986). These results are based on measurements made using the INMARSAT satellite in the frequency band 1530- 1545 MHz and are for rural areas in Belgium. The elevation angle is over 25 degrees but no information on tree density is given except for a photograph indicating it would be between 35% and 85%. If this visual assessment is correct there is general agreement between the two distributions with an attenuation value of 7.5 dB from the European data compared to 10.8 and 5.7 dB measured in Australia for the 85% and 35% cases respectively at the 10% probability level.

The attenuation statistics reported here are therefore generally consistent with other data with some evidence that Australian conditions produce higher attenuation values.

COMMENTS

Given the above data, a prime question is how these results should be treated in a system design. It is clearly uneconomic to provide a 10.8 dB margin to all mobile receivers so that a required performance objective will be achieved, for example, 90% of the time in areas with 85% tree density and an elevation angle of 30 degrees to the satellite. One possible alternative could be to determine an average margin based on relative areas of different vegetation regions for given elevation angles. To illustrate this point, consider the data shown in Table 1 which is based on data estimating the natural vegetation coverage for Australia without the effects of settlement. This data is used on the basis that current roadside vegetation may closely resemble the original undisturbed environment. Contained in Table 1 are the margins at the 10% level based on the measurements reported here. Given the broad nature of these areas and the wide variation in coverage densities the margins used may not be appropriate but are included here to illustrate the principle. The margins are most probably conservative because it is estimated that the major part of the areas considered contain tree heights and densities less than that for which the margins have been measured. This would require further study. From these figures an average margin of 5.4 dB is required, a much reduced value.

Table 1. Relative areas (%) of different vegetation types^a and associated propagation margins (dB) for Australia

Tree Type	Elevation angle (degrees)					
	30-45		45-60		>60	
	%	Margin	%	Margin	%	Margin
1. Forest ^b Trees >10m cover 10-70%	4.6	10.8	14.7	8.6	3.4	6.9
2. Scrub ^c Trees and woody shrubs 1-10m cover 10-70%	19.7	5.7	12.2	5.0	1.5	4.2
3. Grasses ^d <1m	14.0	1.0	28.0	1.0	1.9	1.0

^aRussell and Coupe (1984)

^bAssumed to correspond to the 85% case

^cAssumed to correspond to the 35% case

^dA nominal margin is assumed

This average margin implies that the actual margin is adaptively allocated as required and the technical detail involved with such a scheme would need to be carefully studied. A more refined approach would use customer densities as the weighting function in the averaging process, rather than relative geographic area, but this approach is beyond the scope of this paper.

This type of argument provides information on where to focus future work: in Australia's case more attenuation statistics and geographic detail are required for the tree type areas 1 and 2 outlined in Table 1.

ACKNOWLEDGEMENT

The efforts of Dan Cerchi and his team in the development of the instrumentation and assistance in the data analysis are gratefully acknowledged. The permission of the Director, Research, of Telecom Research Laboratories to present this paper is acknowledged.

REFERENCES

- Vogel, W. and Smith, E. 1985. Propagation considerations in Land Mobile Satellite transmission. MSAT-X Report no. 105 (Pasadena, California: The Jet Propulsion Laboratory)
- Butterworth, J. 1984. Propagation measurements for Land Mobile Satellite Services in the 800 MHz band. Communications Research Centre Tech Note 724 (Ottawa, Canada)
- Butterworth, J. 1984. Propagation measurements for Land Mobile Satellite Services at 1542 MHz. Communications Research Centre Tech Note 723 (Ottawa, Canada)
- Goldhirsh, J. and Vogel, W. 1987. Roadside tree attenuation measurements at UHF for Land Mobile Satellite Systems. IEEE Transactions on Antennas and Propagation. Vol. AP-35, No. 5.
- Jongejans, A. et al 1986. PROSAT Phase 1 Report. ESA STR-216, (Noordwijk, The Netherlands: European Space Research and Technology Centre), p. 57.
- Russell, E. and Coupe, S. 1984. Natural Vegetation 1:20 000 000 map (Australia) The Macquarie Illustrated World Atlas. (Australia, Macquarie Library Pty. Ltd.), p. 148.

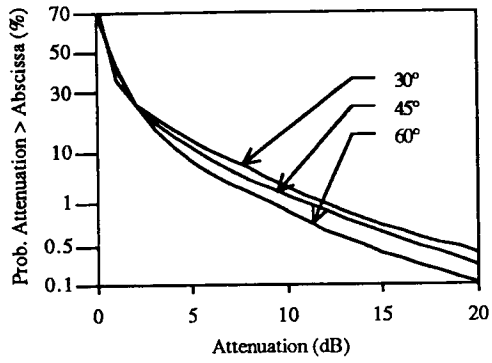


Fig. 1. Attenuation distributions for various elevation angles, 35% tree density and at 1550 MHz

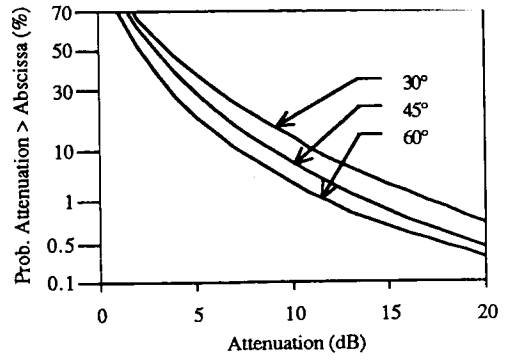


Fig. 2. Attenuation distributions for various elevation angles, 85% tree density and at 1550 MHz

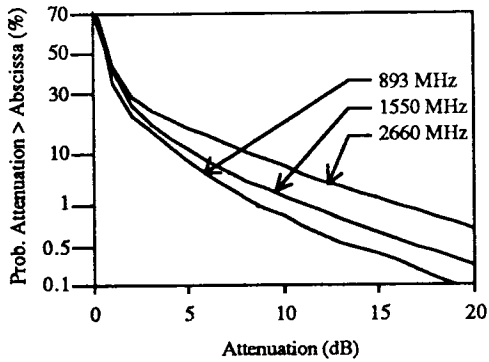


Fig. 3. Attenuation distributions for various frequencies, 35% tree density and at 45° elevation

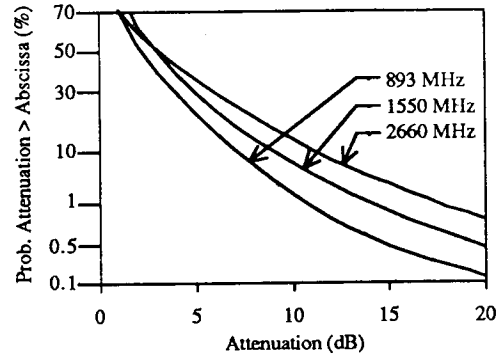


Fig. 4. Attenuation distributions for various frequencies, 85% tree density and at 45° elevation

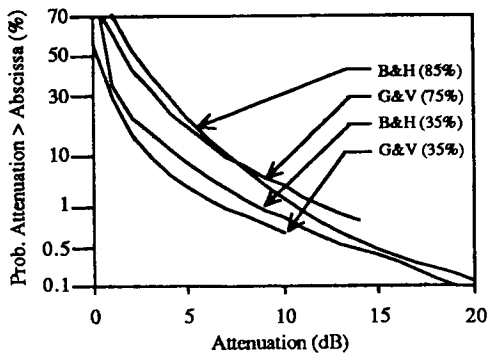


Fig. 5. Comparison between attenuation distributions measured by Bundrock & Harvey and Goldhirsch & Vogel for 45° elevation angle, at UHF frequencies and various tree densities.

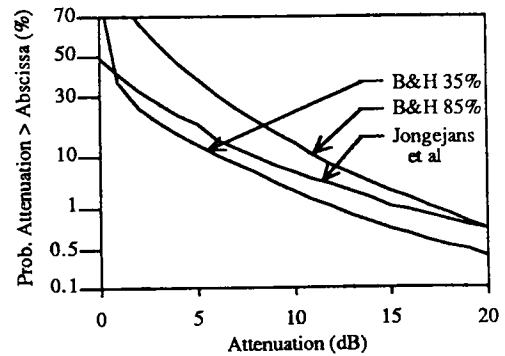


Fig. 6. Comparison between attenuation distributions measured by Bundrock & Harvey and Jongejans et al for 30° elevation angle, at L-band and various tree densities.

LAND MOBILE SATELLITE PROPAGATION RESULTS

DAVID C. NICHOLAS, Ph.D., P.E., United States

ROCKWELL INTERNATIONAL CORPORATION
Avionics Group
CedarRapids, Iowa 52498

ABSTRACT

During the Fall of 1987, Rockwell International in cooperation with COMSAT General and INMARSAT performed a land-mobile satellite demonstration using the MARECS B2 satellite at 26 degrees W. During this demonstration a van equipped with a satellite transceiver, a 1.8-inch monopole antenna, a demonstration computer system, and both LORAN-C and GPS navigators was driven over 2,000 miles in the Northeastern and Midwestern United States. Elevation angles to the satellite were 7 to 22 degrees. A narrow-band 200 b/s full-duplex data channel was demonstrated in a half-duplex protocol in which the van responded to an interrogation from the base station computer at Southbury, Connecticut through the satellite every two or three seconds. Results were summarized along with position approximately every two minutes. Messages ranged from 40 to 67 bits with continuous fill transmitted between messages on the base-to-mobile link. Burst transmissions of similar size preceded by 88-bit preambles were used on the mobile-to-base link. The overall success rate on 42,974 transactions during a trip from Cedar Rapids, Iowa, to Washington, DC, and back was 92.4 percent on the satellite-to-mobile link and 75.4 percent on the mobile-to-satellite link, for a combined poll-response success rate of 69.6 percent.

INTRODUCTION

During September, October, and November 1987 a two-way data communications experiment was conducted between an instrumented van and a simulated dispatch station. The dispatch station was connected by dial-up telephone link to a base station computer located at COMSAT General's Maritime Services Coast Earth Station at Southbury, Connecticut. A two-way 200 b/s full-duplex radio link was then established through the INMARSAT MARECS B2 satellite located at 26 degrees West longitude to a mobile van. A half-duplex protocol simulated a future lower-cost, half-duplex mobile unit.

The route of the experiment is depicted in Figure 1, which also shows elevation angles to the satellite. The general purpose, system configuration, and overall results of the experiment are discussed in [1]. The modem is discussed in [2]. Overall propagation performance results and preliminary detailed results are discussed below.

SYSTEM DESCRIPTION

For purposes of the propagation experiments the forward link of the system may be characterized as transmitting a continuous 200 b/s data signal through the satellite. The satellite broadcasts this signal to the coverage area at the experimental frequency of 1541.3 MHz along with the other traffic in the system. The minimum power at the satellite corre-

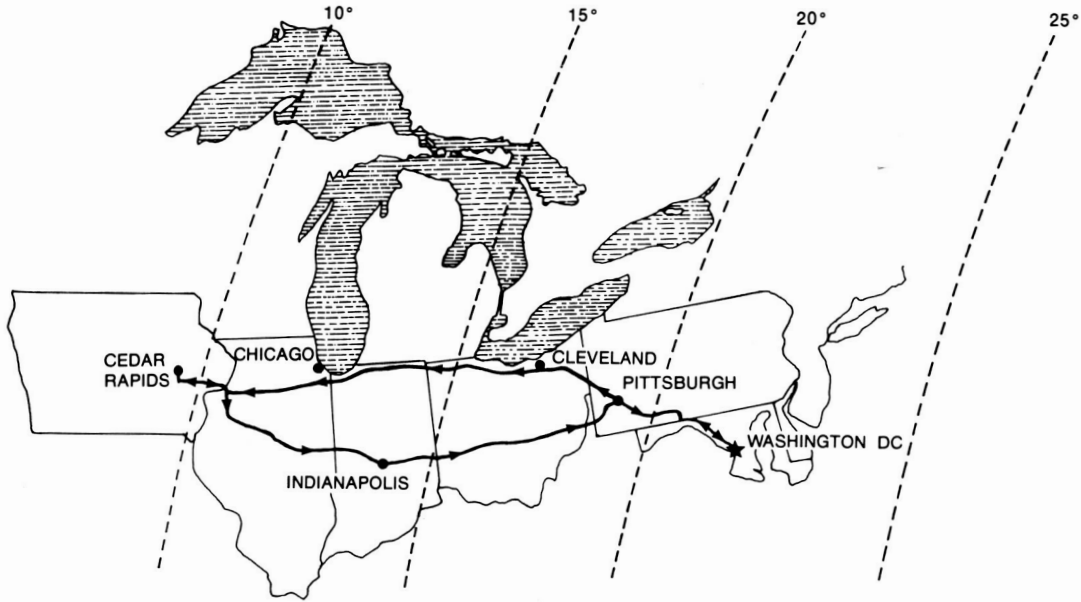


Fig. 1. Map of demonstration route

sponds to 24 dBW EIRP which is the power normally assigned to four "standard-A" channels. A standard-A channel is normally used with a three-foot steerable parabolic antenna on a ship to provide FM voice service in a 50-kHz channel.

For the eastbound trip, the mobile unit utilized a 1.8-inch monopole antenna over a 12-inch square ground plane. Due to a mechanical failure, a Dorne-Margolan Model DMC146-2-1 GPS antenna was pressed into service for the return trip. These were mounted on a passenger van type vehicle and are shown in Figures 2 and 3. It is probable that the monopole antenna pattern is uniform in azimuth, and has a fairly broad peak in elevation beam width with 3-dB points around 10 to 50 degrees elevation angle. It provides a peak gain of perhaps 4 dB for vertically polarized signals but theoretically incurs a 3-dB penalty for the circularly polarized INMAR-SAT signal. See [3] for example.

Hence, the transmit and receive power budgets shown in Table 1 reflect a 0-dB gain antenna for the vehicle.

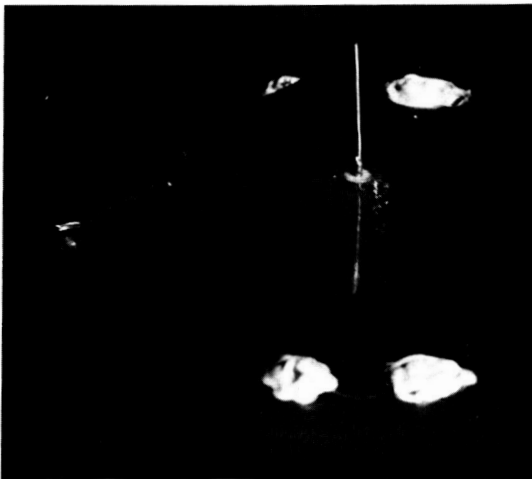


Fig. 2. Monopole antenna

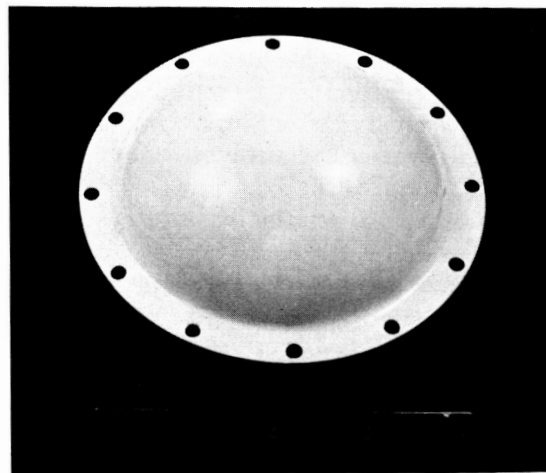


Fig. 3. Crossed curved dipole antenna

Table 1. Power budgets

FORWARD LINK

CES to Satellite

6.42 GHz, El. Angle 22.7°, d = 31.130 km
 CES EIRP 64 dBw
 Path loss = 200.9 dB
 Absorption loss = 0.4 dB
 Satellite G/T = -15 dB/K
 Mean uplink C/N₀ = 76.3 dB
 Mean sat C/I₀ = 58.4 dB

Satellite to Mobile

1.54 GHz, El. Angle 10°, d = 42,440 km
 Satellite mean EIRP = 24 dBw
 Path loss = 188.8 dB
 Absorption loss = 0.4 dB
 Mobile G/T = -27 dB/K
 Mean downlink C/N₀ = 36.4 dB
 Interference loss = 0.5 dB
 Total RSS random loss = 1.5 dB
 Overall C/N₀ = 34.4 dB
 C/N (200 Hz) = 11.4 dB

RETURN LINK

Mobile to Satellite

1.64 GHz, El. Angle 10°, d = 42.440 km
 Mobile EIRP = 14.7 dBw
 Path loss = 189.3 dB
 Absorption loss = 0.4 dB
 Sat G/T = -11 dB/K
 C/N₀ = 40.9 dB
 Sat C/I₀ = 49.7 dB
 T_{pdr} gain = 150.9 dB

Satellite to CES

4.2 GHz, El. Angle 22.7°, d = 41,130 km
 Sat EIRP = -25.8 dBw
 Path loss = 197.19 dB
 Absorption loss = 0.5 dB
 CES G/T = 32 dB/K
 Mean downlink C/N₀ = 37.11 dB
 Mean downlink C/N₀ + I₀ = 35.4 dB
 Interference loss = 0.5 dB
 Total random RSS loss = 1.35 dB
 Overall C/N₀ = 33.55 dB
 200 Hz = 23 dB
 C/N (200 Hz) = 12.2 dB

Several circularly polarized antennas were procured, tested, and resulted in poorer performance than the monopole antennas in prior laboratory tests. These tests included the antenna actually used on the return trip. It is theorized that this may be due to the loss of the horizontal component of the received wave due to low elevation angles, poorer matching, or losses in these larger, more complex antennas.

The return trip antenna has maximum gain at the zenith and is characterized as having at least -2 dBic gain at all angles above 5 degrees for the GPS frequencies. It is a circularly polarized crossed dipole with the arms curved to fit the interior of a 4-inch hemispherical radome.

The power budgets reflect a higher carrier to noise ratio for the return link than for the forward link, yet the forward link was more reliable. This may be due to extra actual forward link power, to the superior performance of the modem on the continuous forward link signal, or to slightly greater interference and noise problems on the return link.

A companion paper [2], discusses the modem in detail. Unshaped (square) 180-degree differential phase shift modulation is used. The modem is designed to rapidly acquire the 200 b/s signal in an initial acquisition bandwidth of about 2000 Hz. Thus, in acquisition, the signal-to-noise ratio is about 10 dB worse than during tracking. As explained in the companion paper, the modem produces a bit error rate of 10⁻³ at a signal to noise ratio of about 8 dB. For the burst transmission on the return link a preamble of 88 bits was most often used. The modem requires a minimum preamble of about 40 bits, but results improve with preamble length, especially with high noise.

For purpose of the propagation experiments, the base station interrogates the mobile unit with a packet of meaningful data 42 to 67 bits long imbedded in a continuous 200 b/s signal which is mostly filler. This normally occurs every three seconds. The mobile unit then responds with a burst of data at 1642.8 GHz consisting of an 88-bit preamble followed by a similar variable length packet of 42 to 67 bits.

successful responses resulting in a retransmit (R) are shown in Figure 4 as a string of 49 characters in the base station statistics. These message totals are composed of five message types 0, 1, 5, 6, and 7 ranging in length from 42 to 67 bits.

October 8, 1987, is considered in detail. This is a route segment from Indianapolis to Pittsburgh. There were 7847 interrogations and 4715 successful responses for an overall success rate of 60.1 percent. In terms of individual link performance, 7137 interrogations were received by the mobile, so that overall forward link performance was 91.0 percent and reverse link performance was 66.2%.

At a higher level of detail Figure 5 shows the overall round trip success rate for the 153 reports covering the Indianapolis to Pittsburgh portion of the trip on October 8, 1987, from 1:15 PM to 7:15 PM EDT. Most would be two-minute reports. Note that the success rate varies from 100 percent to near zero. A linear regression superimposed on the data shows that the overall success rate was about 85 percent near Indianapolis decreasing during the day to 55 percent near Pittsburgh reflecting a change in the terrain. A 10-point moving average is also shown.

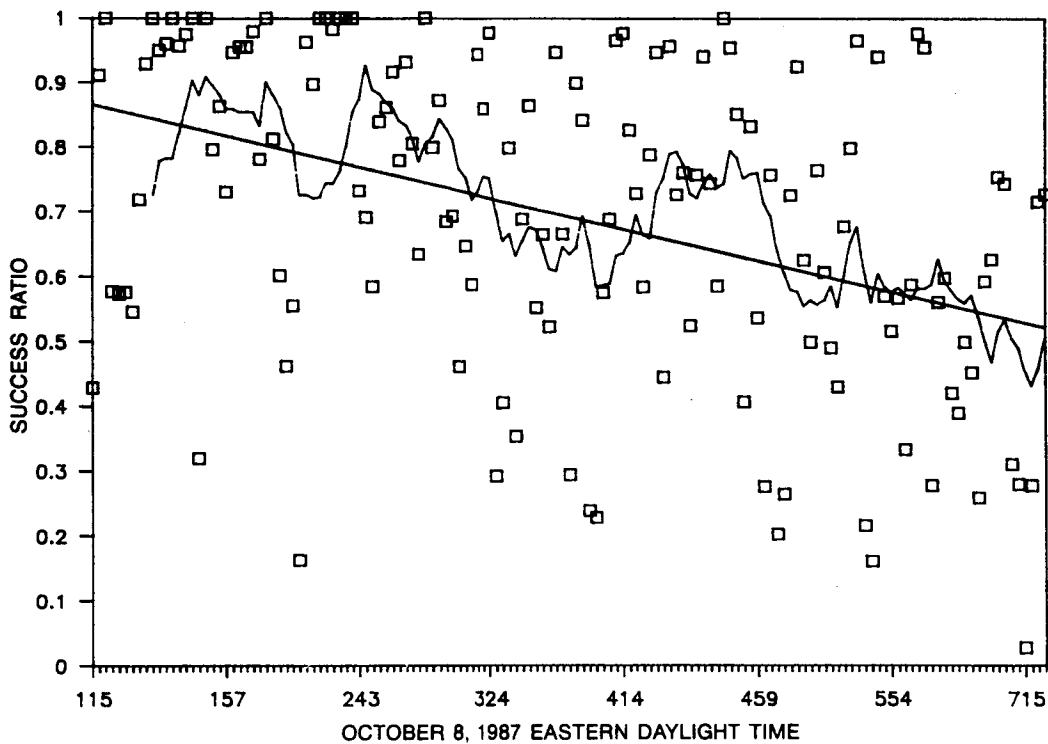


Fig. 5. Indianapolis to Pittsburgh results

At a finer level of detail yet Table 2 presents a fourth order Markov model for the success of a transaction given the history of the previous four transactions. Reduced order models are also shown.

We see that propagation failures are clustered — so are buildings and trees.

Finally, Figure 6 shows the overall round trip on October 7, 8, and 9, 1987, eastbound and October 26, 27 and 28, 1987, westbound. The antenna change occurred between the East and West legs. The probability of a round trip success for the 42,974 transactions covered by 853 two-minute reports is shown as a 10 point moving average (about 20 minutes) and also as a linear regression. Figure 7 separates the forward (upper curve) and return link individual success probabilities in the form of 30 point (about one hour) moving averages for the same data.

Table 2. Conditional probabilities of success — percent

Order	4	3	2	1
	SSSS 89.18	SSS 88.49	SS 86.10	S 82.69
	SSSR 66.23	SSR 62.12	SR 55.27	R 28.89
	SSRS 78.68	SRS 75.34	RS 66.42	
	SSRR 38.92	SRR 35.18	RR 18.18	
	SRSS 75.60	RSS 71.27		
	SRSR 55.45	RSR 41.70		
	SRRS 59.06	RRS 55.40		
	SRRR 23.50	RRR 14.40		
	RSSS 83.20			
	RSSR 51.95			
	RSRS 65.49			
	RSRR 30.38			
	RRSS 64.00			
	RRSR 32.30			
	RRRS 53.42			
	RRRR 12.87			

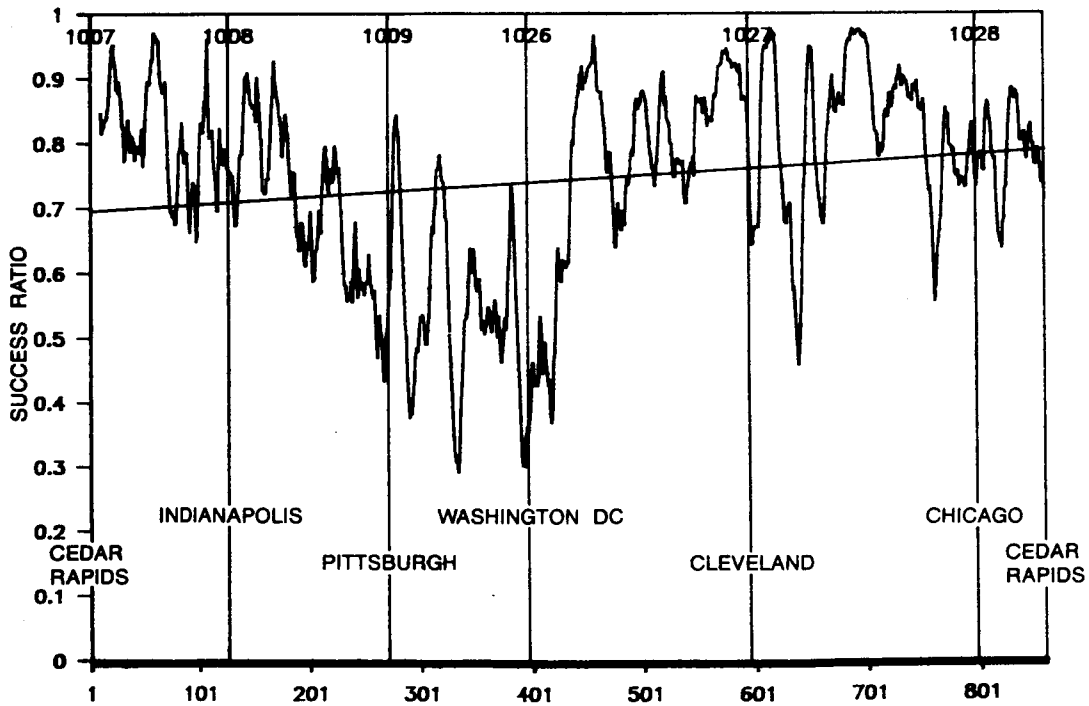


Fig. 6. Two-way success ratio - two minute intervals - 10 point moving average

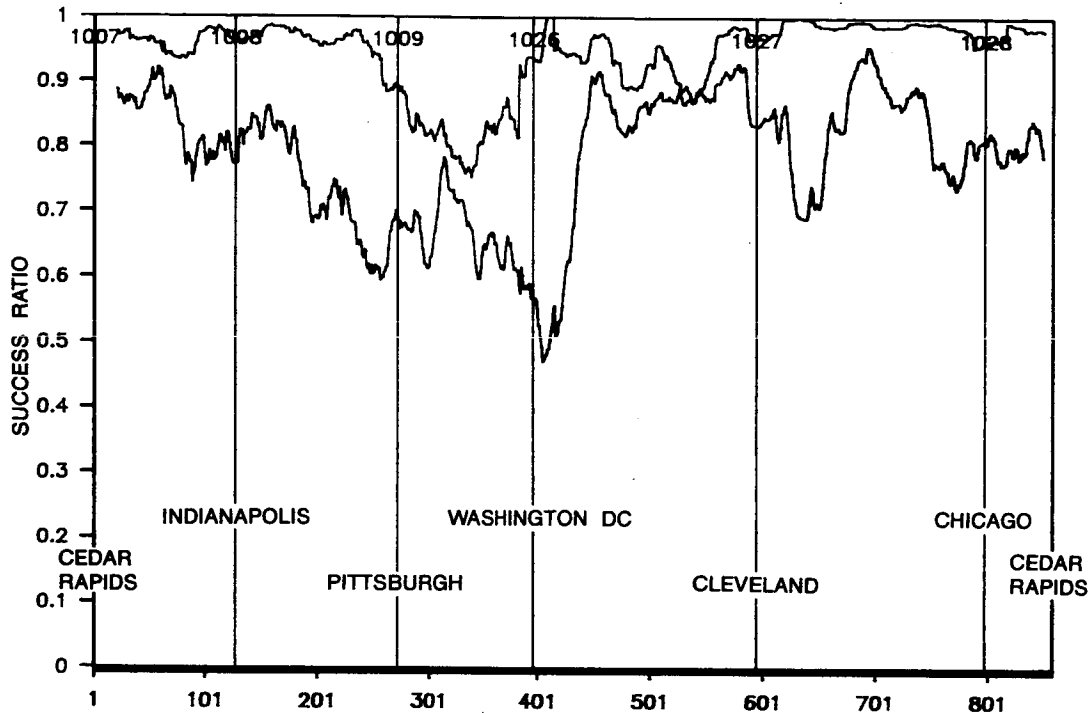


Fig. 7. Forward (upper) and return (lower) link success ratios - 30 point average

OBSERVATIONS

While all the data have not been digested, some observations are in order. First, the system worked remarkably well for the margins indicated. Second, when the system worked poorly, the experimenters could almost always identify terrain or other obstacles causing blockage. Third, the forward link seems relatively more reliable than the return link, and occasional return link problems occurred which have not been entirely explained.

ACKNOWLEDGEMENTS

This project was a joint undertaking of Rockwell International, COMSAT General, and INMARSAT. At Rockwell about 15 people were involved over about a year, including S. D. Smith and D. W. Sutherland who reduced the data for this paper.

REFERENCES

1. Gooch, G. M. and Nicholas, D. C., "Land Mobile Satellite Demonstration System." NASA, JPL Mobile Satellite Conference, Pasadena, CA, May, 1988.
2. Henely, S. J. "Modem for the Land Mobile Satellite Channel." NASA, JPL Mobile Satellite Conference, Pasadena, CA, May, 1988.
3. Johnson, R. C. and Jasick, H. Antenna Engineering Handbook, Second Edition. McGraw-Hill Book Company, New York, 1984, p. 4-31.

PROPAGATION EFFECTS ON SPREAD-SPECTRUM MOBILE-SATELLITE SYSTEMS

DR. WARREN L. FLOCK, Department of Electrical and Computer Engineering,
University of Colorado, United States; DR. ERNEST K. SMITH, Department of
Electrical and Computer Engineering, University of Colorado, United States.

UNIVERSITY OF COLORADO
Campus Box 425
Boulder, Colorado 80309
United States

ABSTRACT

In contrast to the situation at L band, wide bandwidths of 500 MHz or more have been allocated for mobile-satellite service at frequencies between 20 and 50 GHz. These broad bandwidths are well suited for the use of spread spectrum. Certain system considerations about the use of such high frequencies for mobile-satellite service are mentioned first, and attention is then given to propagation effects on high-frequency broad-band systems. Attenuation due to rain is a constraint at 20 to 50 MHz but would not be a serious problem if outages occurring for one to three percent of the time, depending on location, are considered to be acceptable. Procedures are available for estimating rain attenuation for percentages of time from 0.001 to 1. Clear-air absorption becomes a significant factor above 40 GHz but should not exceed 2 dB at a 10 deg elevation angle and frequencies below 40 GHz. Spread spectrum provides a form of frequency diversity that helps to minimize the effects of multipath. An experimental program would be needed to determine the performance of spread-spectrum systems in the presence of diffuse scatter and shadowing by trees.

1. INTRODUCTION

The World Administrative Radio Conference for Mobile Services of October 1987 (WARC-MOB-87) allocated 3 MHz and 4 MHz bands for both downlink and uplink voice service by land mobile-satellite systems at frequencies between 1530 and 1660.5 MHz. The 3 MHz bands are shared with maritime mobile-satellite service, and the 4 MHz bands are unshared except for 0.5 MHz shared with radio astronomy. Also there are allocations for non-speech low-bit-rate data. These allocations represent a step forward but are small compared to the 500 MHz and wider bands allocated for mobile-satellite service between 20 and 50 GHz. Table 1 lists allocations for mobile-satellite service within, or close to, the 20 to 50 GHz range. The desirable 19.7 to 20.2 GHz and 29.5 to 30.0 GHz ranges are available for mobile-satellite use on only a secondary basis, it is true, and the equally appealing 20.2 to 21.2 GHz and 30.0 to 31.0 bands are allocated for governmental use in the United States. The potential of these broad-band allocations for commercial service is nevertheless worthy of attention. Spread-spectrum systems have a low susceptibility to interference and tend to not cause significant interference. Indeed spread spectrum is characterized by what is referred to as a low probability of intercept (Proakis, 1983). Spread spectrum could well be used for mobile service in the 19.7 to 20.2 and 29.5 to 30 GHz bands without interfering with fixed service that has the primary allocation for these bands.

Table 1. Allocations for Mobile Satellite Service, 20 to 50 GHz

<u>Frequency (GHz)</u>	<u>Service</u>	<u>Allocation</u>
19.7-20.2	Downlink (Sec.)	Non-government in U.S.
20.2-21.2	Downlink (Primary)	Government in U.S.
29.5-30.0	Uplink (Sec.)	Non-government in U.S.
30.0-31.0	Uplink (Primary)	Government in U.S.
39.5-40.5	Downlink (Primary)	Gov. & Non-gov. in U.S.
43.5-45.5	Uplink (Primary)	Government in U.S.
45.4-47.0	Uplink (Primary)	Gov. & Non-gov. in U.S.
50.4-51.4	Uplink (Sec.)	Gov. & Non-gov. in U.S.

2. SYSTEM CONSIDERATIONS

This paper is devoted to the role of propagation in a possible high-frequency (20 GHz or higher) mobile-satellite system. Certain other aspects of such a system are discussed briefly in this section. We do not present definitive treatments of these other topics but believe that they should be mentioned to provide a suitable background.

Antennas are crucial elements of mobile-satellite systems. It is desirable to employ phased-array antennas on land vehicles used for land mobile-satellite systems, in order to keep the antennas pointed at the satellite as the vehicles turn and tilt. But phased-array antennas tend to be costly--at L band and probably equally or more so above 20 GHz. In considering possible systems operating above 20 GHz, one approach could be to use a first-generation L Band system as a reference and assume that the antenna gains above 20 GHz should be the same as at L Band. Analysis shows, however, that keeping antenna gain constant with frequency puts the higher frequencies at a power disadvantage. That is, the ratio of received to transmitted power, P_R/P_T , decreases with frequency when constant gain, G_{RGT} , is maintained (Fig. 1). Another possible approach, maintaining antenna areas, A_{RAT} , constant with frequency, gives a power advantage to the higher frequencies (Fig. 2). But a satellite antenna as large above 20 GHz as the antennas planned for L band would present major practical problems and tend to be very costly. The satellite antenna and power problems could be solved by keeping the satellite antenna gain constant and the land-vehicle antenna area constant with frequency. In this case there is no advantage from the power viewpoint of either high or low frequencies. But the cost of maintaining the vehicle phased-array antenna area constant with frequency may still present a problem, and it may be necessary to move from constant area of the vehicle antenna towards constant gain. By such a procedure, a suitable tradeoff may be found between antenna costs and power considerations.

A favorable point is that, if constant gain for the satellite antenna is maintained as a function of frequency, the satellite antenna will tend to be relatively small and lightweight above 20 GHz. It may then be feasible to increase the power transmitted from the satellite to compensate for the power handicap otherwise encountered at high frequencies when constant gain is maintained.

The spread-spectrum technique could be applied to a single 4 MHz bandwidth, such as that allocated for land mobile-satellite use at L band. Analysis in such a case would indicate that a certain number, A , of signals could be carried simultaneously. Utilizing the wide bandwidths above 20 GHz, the same number A could also be carried in a 4 MHz bandwidth, or perhaps a somewhat wider bandwidth such as 5 MHz would be used. In addition some number, B , of 4 or 5 MHz channels could be employed. Then the total number of signals that could be carried would be A times B . Spread spectrum has

been of interest in military circles for a considerable period of time (Sass, 1983). In recent years commercial non-military applications have been increasing (Parker, 1984). A number of papers have attempted to define the role of spread spectrum and to determine the number of simultaneous signals that can be accommodated in spread-spectrum channels characterized by certain parameters (Yue, 1983). The advance program for this Mobile Satellite Conference of May 3-5, 1988 lists two papers on these topics. Continuing attention needs to be given to these matters. One general conclusion is that spread spectrum is most suitable for thin-route applications, and land mobile-satellite service falls into this category.

3. PROPAGATION CONSIDERATIONS

The logic of using 30-20 GHz frequencies for satellite service, as planned for the ACTS program for example, is well established by now and it does not seem necessary to further justify it. The situation is somewhat different for fixed and mobile-satellite service, however, and propagation problems become more severe very far above 30 GHz. Power control (increasing transmitted powers as needed) and forward error correction are measures planned to mitigate signal degradation due to rain for ACTS. Power control could also be used in mobile-satellite service, and a spread-spectrum system may be able to employ forward error correction or measures having much the same effect. It seems only realistic to expect that land mobile-satellite service, however, will not be able to achieve the low outage percentage (0.01) commonly expected for fixed service. For land mobile-satellite service it may be quite reasonable to accept outage percentages of 1 to 3, depending on location. If such outage percentages are accepted, rain would not present a serious problem for land mobile-satellite service even without employing sophisticated techniques to combat attenuation due to rain.

Procedures are available for estimating attenuation due to rain exceeded for percentages of time from 0.001 to 1. The CCIR procedure is described in CCIR Report 564 (CCIR, 1986a). Even though interest may lie in a percentage other than 0.01, attenuation A for a percentage of 0.01 is calculated first by using

$$A = \alpha_p L \Gamma_p \text{ dB} \quad (1)$$

where α_p is an empirically derived attenuation constant in dB/km, L is path length through rain in km, and Γ_p is a path reduction factor that takes account of the fact that intense rain tends to be localized and can not be expected to occur with the same high intensity along the entire length of the path. The path length L can be determined from $H = L/\sin \theta$ for values of θ above 10 deg where θ is elevation angle and H is the height of the 0 deg C isotherm, taken in the CCIR 1986 model to be given in km by

$$H = 4.0 - 0.075 (\phi - 36^\circ) \quad \phi \geq 36^\circ \quad (2)$$

with H equal to 4.0 km for latitude $\phi < 36^\circ$. The path reduction factor Γ_p is given by

$$\Gamma_p = 1/(1 + 0.045 D) \quad (3)$$

where D is the horizontal projection of H . Attenuation exceeded for a percentage p other than 0.01 is computed from the value $A_{0.01}$ for 0.01 percent by use of

$$A_p = A_{0.01} (0.12) p^{-(0.546 + 0.043 \log p)} \text{ dB} \quad (4)$$

It develops that the attenuation exceeded for a percentage of time of one is 0.12 of that exceeded for a percentage of 0.01. The constant α_p is determined by using the relation

$$\alpha_p = aR^b \quad \text{dB/km} \quad (5)$$

where information for determining a and b are given in CCIR Report 721 (CCIR, 1986b). Values of rain rate R in mm/h exceeded for a percentage of time of 0.01 can be estimated from worldwide plots provided in CCIR, 1986c and reproduced by Flock (1988).

An alternative procedure that was presented in earlier versions of the CCIR model involved using tables giving rain rates R exceeded for various percentages of time and calculating attenuation directly using these rain rates. The values of rain rate obtained by this procedure for a percentage of 0.01 and for a percentage of 1 are given in Table 2. The table demonstrates how very much smaller the rain rates exceeded for a percentage of time of 1 are than the rain rates exceeded for a percentage of time of 0.01.

It should be kept in mind that attenuation is accompanied by an increase in noise and that the degradation in signal-to-noise ratio due to rain, clouds, or atmospheric gases is due to both attenuation and the accompanying increase in noise.

Clouds become a significant factor for frequencies of about 20 GHz and higher. For example, for the rather extreme case of clouds 4 km in thickness containing 1 g/m^3 of water, an attenuation of 3.9 dB and an increase in noise temperature of about 160 K are encountered at 30 GHz (Slobin, 1982). Clouds occur for a larger percentage of time than intense rain and tend to be relatively more important when emphasis is given to effects occurring for one percent of the time or more instead of 0.01 percent.

Table 2. Rain Rates (mm/h) Exceeded for 0.01 and 1 Percent of the Time for Regions A to P of CCIR Model

<u>Region</u>	<u>Rate, 0.01</u>	<u>Rate, 1</u>	<u>Region</u>	<u>Rate, 0.01</u>	<u>Rate, 1</u>
A	8	< 0.5	H	32	2
B	12	1	J	35	8
C	15	2	K	42	2
D	19	3	L	60	2
E	22	1	M	63	4
F	28	2	N	95	5
G	30	3	P	145	12

Clear air absorption becomes a factor above about 40 GHz as shown in Fig. 3 (Smith, 1982). Attenuation due to the clear air should not exceed 2 dB, however, for an elevation angle of 10 deg and frequencies below 40 GHz.

The broad bandwidths employed in spread-spectrum systems tend to minimize the effects of multipath, a common source of signal degradation in land mobile-satellite systems. Multipath effects can be expected when driving on broad interstate highways, etc. A number of experimental studies, however, have tended to emphasize the importance of shadowing by trees instead of multipath effects (Vogel and Smith, 1985; Goldhirsh and Vogel, 1986). It appears that additional experimental efforts are needed to determine the performance of spread-spectrum systems in the presence of diffuse scatter and shadowing by trees.

4. CONCLUSION

The broad bandwidths allocated for the mobile-satellite service at frequencies above 20 GHz suggest that serious consideration should be given to the exploitation of these frequencies by the use of spread spectrum, for commercial as well as governmental applications.

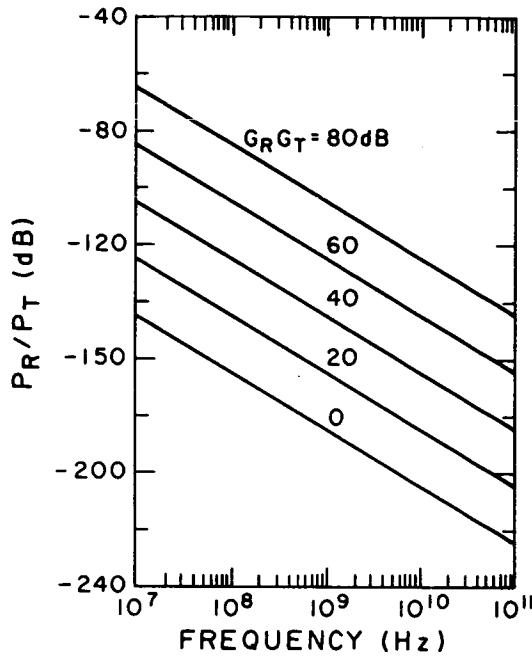


Fig. 1. P_R/P_T as a function of frequency and $G_R G_T$

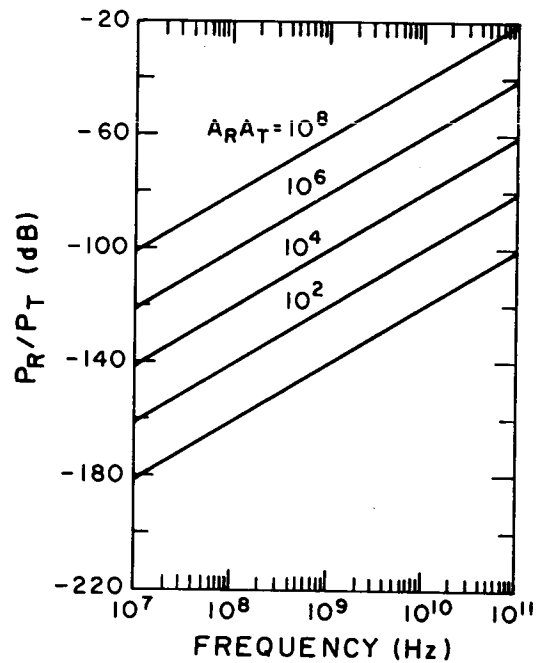


Fig. 2. P_R/P_T as a function of frequency and $A_R A_T$

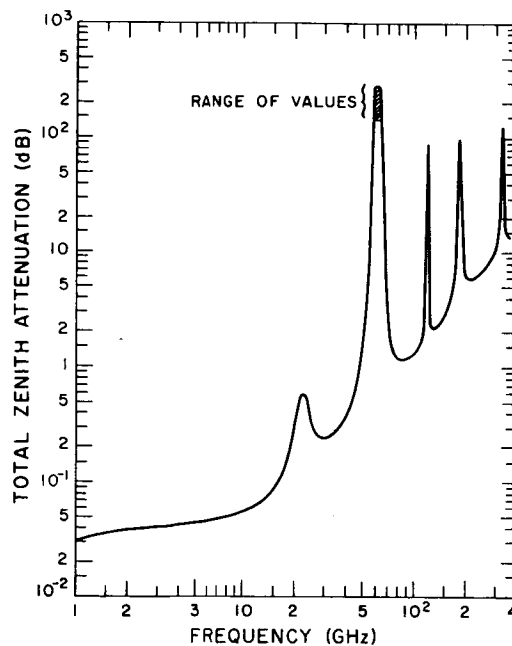


Fig. 3. Vertical one-way attenuation through atmosphere for a water vapor content of 7.5 g/m^3 at the surface

REFERENCES

- CCIR 1986a. Propagation data and prediction methods required for earth-space telecommunication systems, Report 564-3. Volume V, Propagation in Non-ionized Media, Recommendations and Reports of the CCIR, 1986 (Geneva: Int. Telecomm. Union).
- CCIR 1986b. Attenuation by hydrometers, in particular precipitation, and other atmospheric particles, Report 721-2. Volume V, Propagation in Non-ionized Media, Recommendations and Reports of the CCIR, 1986 (Geneva: Int. Telecomm. Union).
- CCIR 1986c. Radiometeorological data, Report 563-3. Volume V, Propagation in Non-ionized Media, Recommendations and Reports of the CCIR, 1986 (Geneva: Int. Telecomm. Union).
- Flock, W.L. 1988. Propagation Effects on Satellite Systems at Frequencies Below 10 GHz, NASA Reference Publication 1108(02). (Washington, DC: National Aeronautics and Space Administration).
- Goldhirsh, J. and W.J. Vogel 1987. Roadside tree attenuation measurements at UHF for landmobile satellite systems. IEEE Trans. Antennas Propagat. AP-35: pp. 589-596, May.
- Parker, E. B. 1984. Micro earth stations as personal computer accessories. Proc. IEEE. 72: pp. 1526-1531, Nov.
- Proakis, J.G. 1983. Digital Communications. (New York: McGraw-Hill).
- Sass, P.F. 1983. Propagation measurements for UHF spread spectrum mobile communications. IEEE Trans. Veh. Technol. VT-32: pp. 168-176, May.
- Slobin, S.D. 1982. Microwave noise temperature and attenuation of clouds. Radio Science. 17: pp. 1443-1454, Nov. -Dec.
- Smith, E.K. 1982. Centimeter and millimeter wave attenuation due to atmospheric oxygen and water vapor. Radio Science. 17: pp. 1455-1464, Nov.-Dec.
- Vogel, W.J. and E.K. Smith 1985. Propagation Considerations in Land Mobile Satellite Transmission, MSAT-X Report No. 105. (Pasadena: Jet Propulsion Laboratory).
- Yue, O. 1983. Spread spectrum mobile radio, 1977-1982. IEEE Trans. Veh. Technol. VT-32: pp. 98-105, Feb.

**MULTIPATH MEASUREMENTS FOR LAND MOBILE SATELLITE SERVICE USING
GLOBAL POSITIONING SYSTEM SIGNALS**

JOHN J. LEMMON, Institute for Telecommunication Sciences, National Telecommunications and Information Administration, U.S. Department of Commerce, United States

U.S. DEPARTMENT OF COMMERCE

National Telecommunications and Information Administration
Institute for Telecommunication Sciences
325 Broadway
Boulder, Colorado 80303
United States

ABSTRACT

A proposed multipath measurement system for the land mobile satellite radio channel using the Global Positioning System (GPS) is presented. The measurement technique and equipment used to make multipath measurements on communications links are briefly described. Then the system configuration and performance specifications of the proposed measurement system are discussed.

INTRODUCTION

For many years the Institute for Telecommunication Sciences (ITS) has been active in the area of multipath measurements over radio transmission channels. Using channel probes developed at ITS, such measurements have been made over line-of-sight microwave, troposcatter, and land mobile communication links, and are discussed in Linfield et al. (1976), Hubbard (1983), Hubbard et al. (1978), Hufford et al. (1982), and Lemmon (1987). Briefly, the channel probe transmitter develops a signal that is biphase modulated by a pseudonoise (PN) binary code; the probe receiver performs a cross-correlation between the received signal and a locally generated signal that is modulated by the same PN code developed by a "slow clock." Thus, the local PN code is allowed to slip very slowly in time with respect to the received PN code, thereby enabling one to measure the impulse response (and hence, the multipath) of the radio channel as a function of time delay.

As part of the National Aeronautics and Space Administration's Mobile Satellite Communications Program, ITS has been funded to perform multipath measurements in the land mobile satellite radio channel using signals from the Global Positioning System (GPS) satellites and a GPS receiver modified to develop the necessary time-multiplexed correlator signal. The feasibility of such an experiment and various measurement strategies have been discussed by Lemmon and Hubbard (1985). The objective is to measure the impulse response function of the radio channel using a multipath measurement system (MMS) installed in a mobile van. The data so obtained will provide an initial assessment of

multipath propagation in the land mobile satellite channel and will be valuable in planning mobile satellite services.

GPS APPROACH TO MULTIPATH MEASUREMENTS

The GPS signal consists of two components, Link 1 (L1) and Link 2 (L2), at center frequencies of 1575.42 MHz and 1227.6 MHz, respectively. Each of these two signals (L1 and L2) is phase modulated by two binary signals: a 10.23 MHz clock rate precision P signal, and/or a 1.023 MHz course/acquisition C/A signal. Each of these two signals (P and C/A) has been formed by a P code or a C/A code which is modulo-2 added to a 50 bps data stream D, to form P+D and C/A+D, respectively.

The P code for each satellite is a pseudonoise (PN) binary sequence with a clock rate of 10.23 Mbps and a period of exactly 1 week. The C/A code is a Gold code with 1023 bits and a clock rate of 1.023 Mbps. The C/A code therefore has a period of exactly 1 ms. The 50 bps data stream D is also a binary sequence that contains navigational information (time, satellite position, etc.) as well as the current P code epoch time.

In its normal mode of operation, a GPS receiver acquires and tracks a GPS signal using the C/A signal and obtains a navigational fix upon extracting the data from four or more satellites. With knowledge of the P code epoch time, the P signal can be acquired and a more precise fix can be obtained. The signals are acquired and tracked by performing a cross-correlation between the received signal and a locally generated signal modulated with the same PN code as the received signal. Once the correlation peak of the PN sequence has been located and locked onto (i.e., zero relative time delay and Doppler between the received and locally generated PN codes), the data can be recovered by modulo-2 subtraction of the PN sequence from the received signal.

In order to perform multipath measurements with a GPS receiver, the locally generated PN code must be allowed to slip in time relative to the received PN code. However, due to variations in time delay and Doppler in the propagation channel, the tracking loops in the receiver cannot be disturbed if one is to maintain control over the time delay (and Doppler) between the two PN codes used to make an impulse response measurement. Thus, a dual-channel receiver is required. The first channel will operate in the normal GPS mode to acquire and lock onto the signal and recover the 50 bps data stream. The second channel will be used to make the impulse response measurements by shifting the local PN code relative to that of the received signal, which is being tracked by the first channel. The proposed measurement system is shown schematically in Figure 1.

ITS intends to award a subcontract for the development of a GPS multipath measurement system. The measurement system shall be a GPS receiver capable of tracking the GPS L1 P-code signal and extracting multipath signal information. In order to be eligible for acceptance, the MMS shall conform to the system configuration and performance specifications below.

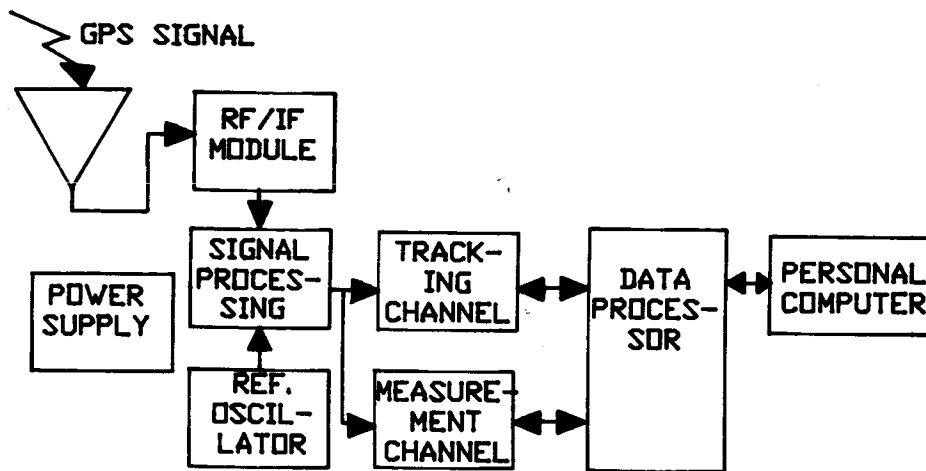


Figure 1. Multipath measurement system.

MMS CONFIGURATION

The MMS shall be comprised of the following functions:

1. Antenna. The antenna shall be omnidirectional that multipath signals are not discriminated against.
2. RF/IF Module. The RF/IF sections of the receiver shall provide the necessary low-noise amplification and conversions to IF necessary for further signal processing.
3. Signal Processing. Signal processing shall be required to convert IF signals to information required for dual channel processing.
4. Reference Oscillator. A reference oscillator shall be provided with the receiver from which all required local oscillators and clocking shall be derived.
5. Tracking Channel. The tracking channel shall be capable of acquiring and tracking one GPS L1 signal at a time and providing pseudorange, pseudorange rate, and AGC information necessary to aid the measurement of multipath signals in the measurement channel. The GPS navigation data shall also be provided.
6. Measurement Channel. The measurement channel shall be capable of measuring post-correlation signals delayed from that of the signal tracked in the tracking channel. Simultaneous measurements at 15 delays, one-half P-chip (50 ns) apart, shall be provided. An

incrementing capability shall also be provided so that finer resolution delays can be measured.

7. Data Processor. A data processor shall be provided to control the two channels, to coordinate their activities, to collect the measurement data, and to provide that data and other pertinent data to the personal computer.
8. Personal Computer. The personal computer will be provided by ITS. However, any interfacing board required for communications to the receiver shall be provided by the contractor.
9. Power Supply and Chassis. The power supply shall convert 115 VAC-60 cycle power to voltage required by the MMS functions, with the exception of the personal computer. The MMS, except the personal computer, shall be packaged in a chassis appropriate for installation in a van.

PERFORMANCE SPECIFICATIONS

Input Signal Levels

The input GPS L1 signal level will be the nominal GPS P-code signal power level of -133 dBm. The C/A signal may be used for acquisition and will have a nominal power level of -130 dBm. The MMS shall track these signals in relatively extreme multipath environments.

Output Signal-to-Noise Ratio

The signal-to-noise density ratio (for zero relative delay between the local and received PN codes) at the correlator outputs will have a nominal value of 37 dB-Hz. Thus, the signal-to-noise ratio in a 50 Hz bandwidth (corresponding to a 20 ms integration time) will have a nominal value of 20 dB.

Tracking Accuracy

The tracking accuracy of the tracking channel with the signal levels specified above shall be as follows:

1. Pseudorange error ≤ 0.075 P-chips, one sigma
2. Pseudorange rate error ≤ 0.03 P-chips/second, one sigma

These accuracies shall be applicable to independent measurements taken at 1-second intervals. In a multipath environment, the pseudorange is allowed to deviate from the "true" pseudorange at rates consistent with that environment, but the one sigma accuracy about that deviation shall apply.

GPS Navigation Data and Bit Error Rate

The MMS shall decode the GPS navigation data with a bit error rate less than 1×10^{-5} . Bit errors shall be detected. The GPS navigation data shall be provided for possible modulation of the multipath measurement data.

Interchannel Bias

The pseudorange bias between channels shall be less than 0.1 P-chips.

Measurement Channel Performance

Measurement channel capabilities. The measurement channel is not required to track the GPS signal. Instead, using data provided via the data processor from the tracking channel (pseudorange, pseudorange rate, and AGC level), the measurement channel shall be capable of positioning its code generator relative to the code state tracked in the tracking channel in order to measure the received multipath signals that arrive after the signal tracked in the tracking channel. The measurement channel shall measure 15 code states simultaneously, positioned one-half P-chip apart. It shall also have the capability to "slew" the code state in increments so that finer resolution measurements can be accomplished. Pseudorange measurements shall be made to verify code state positions.

The following data for each of the code states shall be provided at a 50 Hz rate:

1. I integrated over the 20 ms data bit
2. Q integrated over the 20 ms data bit
3. $\sum_1^{20} (I^2 + Q^2)$ for I's and Q's integrated over 1 ms

where I and Q are the in-phase and quadrature phase baseband components, respectively. A gain control capability shall be provided to allow adjustment of the I and Q levels relative to the tracking channel AGC level.

Measurement channel accuracy. Each of the three quantities specified above shall be a 16-bit number for a total of 90 bytes every 20 ms (4.5 Kbaud).

Data Processor Performance

The data processor shall control the MMS receiver to acquire an assigned GPS signal, to track that signal, to aid the multipath measurement channel with measurements from the tracking channel, to control the measurement channel code phase position, and to collect the GPS navigation data and the measurement data specified above. It shall buffer that data in appropriate data blocks and provide that data to the personal computer for processing.

Testing

The capabilities of the MMS shall be verified by testing with a simulated multipath environment (sum of two GPS signals with the same PN code, variably delayed with respect to one another). Failure to meet the performance specifications above will be cause for rejection of the equipment.

DATA ANALYSIS

The MMS will be installed in a mobile van and multipath measurements will be made in a variety of urban, suburban, rural, and mountain environments in the Denver/Boulder area. The data will be analyzed for relative multipath power and phase, delay spread, and the time rates-of-change of these quantities in various source/receiver geometries and environments. In addition, the signal-to-noise ratio can be computed by measuring $(I^2 + Q^2)$ over two different bandwidths. For example, let $(I^2 + Q^2) = P_N$ for I's and Q's integrated over 20 ms and $(I^2 + Q^2) = P_W$ for I's and Q's integrated over 1 ms. Then P_N is the total power (signal plus noise) in a 50 Hz bandwidth and P_W is the total power in a 1 kHz bandwidth. Let N denote the noise power in a 50 Hz bandwidth and let S denote the signal power. Then it follows that

$$S + N = P_N$$

and

$$S + 20N = P_W$$

which imply that the signal-to-noise ratio in a 50 Hz bandwidth is

$$\frac{S}{N} = \frac{20 P_N - P_W}{P_W - P_N}$$

REFERENCES

- Hubbard, R.W. 1983. Digital microwave transmission tests at the Pacific Missile Test Center, Pt. Mugu, California. NTIA Report 83-126, (NTIS Order No. PB83-251454).
- Hubbard, R.W.; Linfield, R.F.; and Hartman, W.J. 1978. Measuring characteristics of microwave mobile channels. NTIA Report 78-5, (NTIS Order No. PB283944/AS).
- Hufford, G.A.; Hubbard, R.W.; Pratt, L.E.; Adams, J.E.; and Paulson, S.J. 1982. Wideband propagation measurements in the presence of forests. Research and Development Technical Report, CECOM 82-CS029-F, U.S. Army Commun. Electronics Command, Fort Monmouth, NJ.
- Lemmon, J.J. 1987. Propagation and performance measurements over a digital troposcatter communications link. NATO/AGARD Conf., Proc. No. 419, Scattering and Propagation in Random Media, Rome, Italy, Paper No. 30.
- Lemmon, J.J. and Hubbard, R.W. 1985. Multipath measurements for the land mobile satellite radio channel. MSAT-X Report No. 126, Jet Propulsion Laboratory, Pasadena, CA.
- Linfield, R.F.; Hubbard, R.W.; and Pratt, L.E. 1976. Transmission channel characterization by impulse response measurements. OT Report 76-96, (NTIS Order No. PB258577).

SESSION D
MOBILE SATELLITE SYSTEMS TECHNOLOGY

SESSION CHAIR: William C.Y. Lee, PacTel
SESSION ORGANIZER: Richard F. Emerson, Jet Propulsion Laboratory

DEVELOPMENT OF A MOBILE SATELLITE COMMUNICATION UNIT

MR. RYUTARO SUZUKI, Communications Research Laboratory (CRL), MPT, Japan; MR. TETSUSHI IKEGAMI, CRL, MPT, Japan; MR. NAOKAZU HAMAMOTO, CRL, MPT, Japan; MR. TETSU TAGUCHI, NEC Corporation, Japan; DR. NOBUHIRO ENDO, NEC Corp, Japan; MR. OSAMU YAMAMOTO, NEC Corp, Japan; MR. OSAMU ICHIYOSHI, NEC Corp, Japan.

COMMUNICATIONS RESEARCH LABORATORY (CRL)
4-2-1 NUKUI-KITA-MACHI
KOGANEI-SHI
TOKYO
184 JAPAN

NEC Corporation
Microwave and Satellite Communications Div.
4035, IKEBE-CHO, MIDORI-KU
YOKOHAMA, 226 JAPAN

ABSTRACT

This paper describes a compact (210(W) x 280(H) x 330(D) mm) mobile terminal capable of transmitting voice and data through L-band mobile satellites. The Voice Codec can convert an analog voice to/from digital codes at rate of 9.6, 8 and 4.8 kb/s by an MPC algorithm.

The terminal functions with a single 12 V power supplied by a vehicle battery. The equipment can operate at any L-band frequency allocated for mobile uses in a full duplex mode and will be soon put into a field test via Japan's ETS-V satellite.

1. Introduction

The WARC Mobile 87 has opened a wide path for land mobile satellite communications using L-band frequencies. It is highly expected that satellite systems will take major roles for mobile communications because of their extremely wide coverages^[1]. Field data on L-band radio propagation have been accumulated^[2] making the mobile satellite services highly realistic. Developments projects for such equipments or systems are going on in various organizations^[3,4,5,6,7].

2. Basic Design Philosophy

Demands for mobile satellite communications are versatile^[6,7,8] and the transmission paths characteristics are often under frequent changes.

Considering above factors, the mobile satellite communication equipments must possess multi-functional capabilities. Such highly adaptive equipments can be most easily implemented by application of DSP (Digital Signal Processing) techniques^[8].

ORIGINAL PAGE IS
OF POOR QUALITY

3. Basic Design Parameters

3.1 Link Budget and Basic Design

Table 3-1 shows link calculations for communications through Japan's ETS-V satellite^[6] between the Base Earth Station (BES) located at KASHIMA and Mobile Earth Stations (MES) on board automobiles moving around central area of Japan. The calculation is made for the data rate of 9.6 KBPS and for two types of antennas, i.e. omnidirectional (4 dBi gain) and directional (12 dBi gain). The structure and front view of the mobile equipment is each shown in Fig. 3-1 and Photo 3-1.

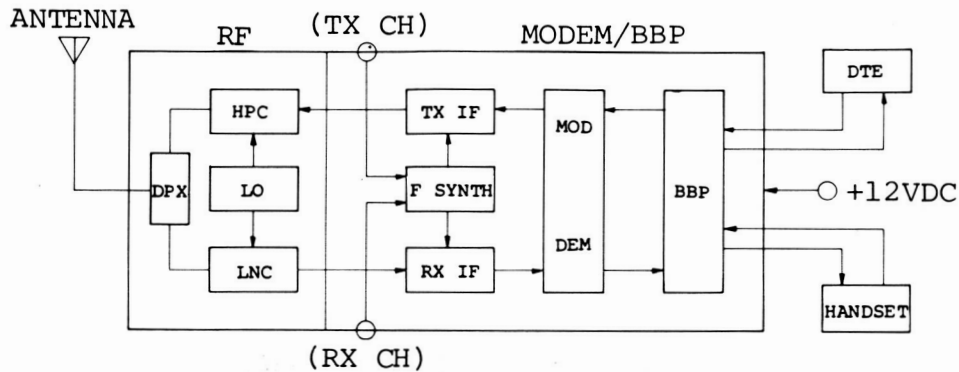


Fig. 3-1 Structure of the Mobile Equipment

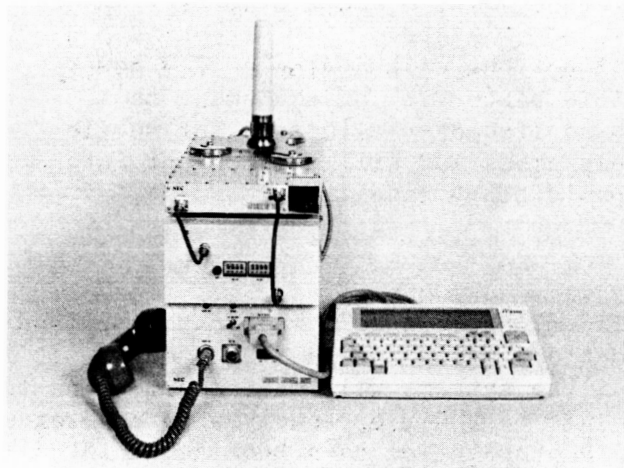


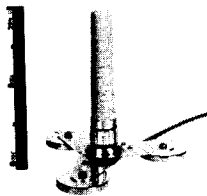
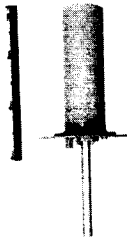
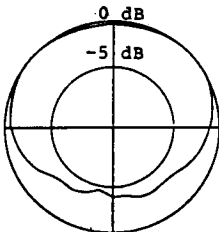
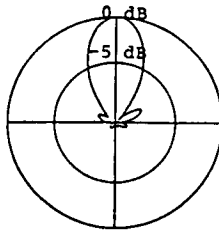
Photo 3-1 External View of
the Mobile Equipment

3.2 ANTENNA

Two types of antennas are provided for land mobile satellite communications. One is a 3 dBic omni-directional quadrifilar helix type antenna. It can be attached on the vehicle roof easily with magnets and operates without tracking function. Another is a 12 dBic helical antenna for portable communications. It can be mounted on a tri-pod and manually steered for the satellite easily.

Table 3-1 Link Budget

DATA RATE		9600 BPS		DATA RATE		9600 BPS	
Mobile earth station		Kashima		Mobile earth station		Car	
Feeder link earth station		Kashima	Kashima	Mobile earth station		Car	Car
TX power	dBW	14.0	14.0	MES nominal TX power	dBW	14.7	14.7
Feeder loss	dB	3.5	3.5	Feeder loss	dB	2.0	2.0
Antenna gain	dB	54.7	54.7	Antenna gain	dB	4.0	12.0
FES nominal EIRP	dBW	65.2	65.2	Tracking loss	dB	0.0	0.0
Path losses (Kashima-SAT)				Radome loss	dB	0.0	0.0
Frequency	GHz	5.96	5.96	MES nominal EIRP	dWB	16.7	24.7
FES elevation angle	degree	47.0	47.0	Path losses			
Range	Km	37289.0	37289.0	(Land mobile-SAT)			
Free space path loss	dB	199.4	199.4	Frequency	GHz	1.64	1.64
Atmospheric absorption loss	dB	0.2	0.2	MES elevation angle	degree		
47.1							
Satellite RX				Range	Km	37302.7	30302.7
Antenna gain (Kashima)	dB	21.5	21.5	Free space path loss	dB	188.2	188.2
Feeder loss	dB	3.2	3.2	Atmospheric absorption loss	dB	0.1	0.1
Satellite RX Power	dBW	-116.1	-116.1	Satellite RX	dB	23.0	23.0
System noise temperature	K	440.0	440.0	Feeder loss	dB	3.1	3.1
Satellite No.	dBW/Hz	-202.2	-202.2	Satellite RX Power	dBW	-151.7	-143.7
Satellite G/T	dBK	-8.1	-8.1	System noise temperature	K	386.0	386.0
Up-link C/No	dBHz	86.1	86.1	Satellite No.	dBW/Hz	-202.7	-202.7
Satellite TX				Satellite G/T	dBK	-6.0	-6.0
Transponder gain	dB	127.7	127.7	Up-link C/No.	dBHz	51.1	59.1
(+0dB mode)				Satellite TX			
Satellite TX power	dBW	11.6	11.6	Transponder gain	dB	132.7	132.7
Total TX power	dWB	11.6	11.6	Satellite TX power	dBW	-19.0	-11.0
(MAX 11.6 dBW)				Total TX power	dBW	-19.0	-11.0
Feeder loss	dB	3.9	3.9	Feeder loss	dB	3.0	3.0
Antenna gain	dB	23.0	23.0	Antenna gain (Kashima)	dB	19.9	19.9
Satellite nominal EIRP	dBW	30.7	30.7	Satellite nominal EIRP	dBW	-2.1	5.9
Path losses				Path losses (SAT-Kashima)			
(SAT-Land mobile)				Frequency	GHz	5.23	5.23
Frequency	GHz	1.54	1.54	FES elevation angle	degree	47.0	47.0
MES elevation angle	degree	47.1	47.1	Range	Km	37289.0	37289.0
Range	Km	37302.7	37302.7	Free space path loss	dB		
Free space path loss	dB	187.6	187.6	Atmospheric absorption loss	dB		
Atmospheric absorption loss	dB	0.1	0.1	47.1			
37289.0				Mobile earth station			
Mobile earth station				Radome loss	dB	0.0	0.0
Radome loss	dB	0.0	0.0	Tracking loss	dB	0.0	0.0
Tracking loss	dB	0.0	0.0	Antenna gain	dB	4.0	12.0
Antenna gain	dB	2.0	2.0	Feeder loss	dB	2.0	2.0
Feeder loss	dB	-155.0	-147.0	MES RX power	dBW	478.6	478.6
MES RX power	dBW	478.6	478.6	System noise temperature	K	-201.8	-201.8
System noise temperature	K	-201.8	-201.8	MES No.	dBW/Hz	-24.8	-24.8
MES No.	dBW/Hz	-24.8	-24.8	MES G/T	dBK	46.8	46.8
MES G/T	dBK	46.8	46.8	Down-link C/No.	dBHz	46.8	46.8
Down-link C/No.	dBHz	46.8	46.8	Satellite link C/No.	dBHz	42.0	42.0
Satellite link C/No.	dBHz	42.0	42.0	Required C/No.	dBHz	4.8	4.8
Required C/No.	dBHz	4.8	4.8	Margin	dB	12.8	12.8
Margin	dB	12.8	12.8				

	Omni-directional	Directional
Outside View		
Gain	3 dBic	12 dBic
Polarization	LHCP	LHCP
Axial Ratio	Less than 2 dB	Less than 2 dB
Tracking	Unnecessary	Manual
Radiation Pattern (1625 MHz)		

3.3 RF Unit

Design concepts

i) Compactness

- . The size 213.5(W) x 312(D) x 40(H) mm, and the weight 3kg.
- . A heatsink with a fan keeps the temperature rise within 30°C in a continuous operation.
- . Compact duplexer (108(W) x 12.5(D) x 20(H) mm) by dielectric resonator technique.

ii) High performance and flexibility for many experimental uses

- . The high saturated transmit power and extended linearity achieved with power GaAs FETs (NE345L) usable for carriers of many modulation types.
- . The low noise GaAs FET (25K569) for the preamplifier stage of the receiver improves the noise figure.
- . Low phase noise synthesized local oscillators phase locked to a stable reference enable low rate communications.

Table 3.3 Major RF unit performance

HPC

- | | |
|------------------------------------|-----------------|
| a) Input frequency | 70 MHz band |
| b) Input level | 0 dBm |
| c) Output frequency | 1626 - 1661 MHz |
| d) Output power
(at DUP output) | 20W saturation |

LNC

- | | |
|---------------------|-----------------|
| a) Input frequency | 1530 - 1559 MHz |
| b) Output frequency | 70 MHz band |

- | | |
|---|-----------------------------------|
| c) Gain | 80 dB nominal |
| d) Noise figure typical
(at DUP input) | 2 dB at 25°C |
| DUP Loss transmit side 1.3 dB; | receive side 1.4 dB |
| Power requirements | +12 - +15 V DC, 10A (when HPA on) |

High power converter

The transmit BPFs including DUP attenuate more than 100 dB in the 1530 - 1551 MHz receive band to secure 60 dB D/U against local and negligible thermal noise leakages into receive amplifiers from HPC output. HPC output power linearity is shown in Figure 3-3-1.

Low noise converter

LNC gain and noise figure response is shown in Figure 3-3-2.

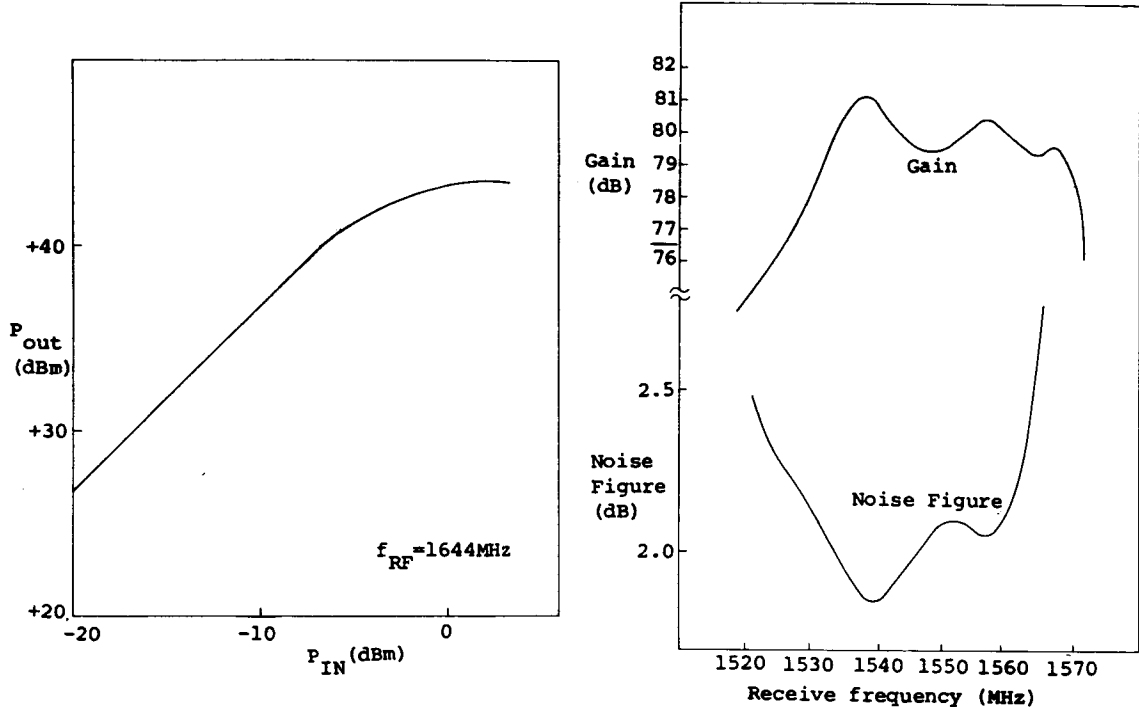


Fig. 3-3-1 HPC Output Power Linearity

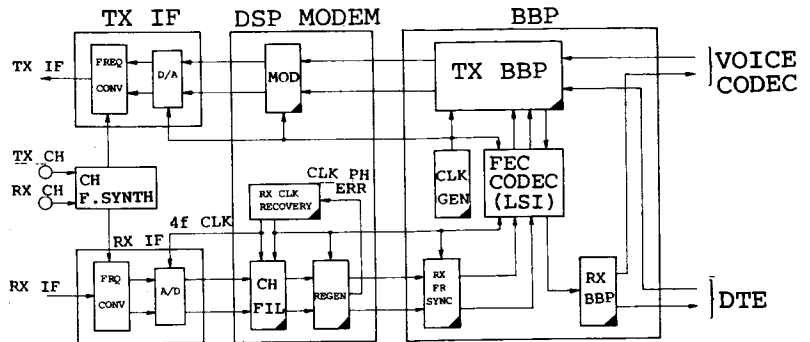
Fig. 3-3-2 LNC GAIN & NF Response

3.4 MODEM/BBP

Extensive uses of Digital Signal Processing (DSP) have realized a compact, rate variable MODEM/BBP as depicted in Fig. 3-4. The major design parameters are given in Table 3-4. For the demodulation of receive signals, a coherent detection was adopted because of its good BER performances in such poor C/N conditions as 5 dB E/No. A simple calculation shows that with the local phase noise specified for INMARSAT STANDARD-C system^[7], a coherent detection still gives a better BER performance than differential detections in poor C/N conditions for data rates above 4800 BPS.

Table 3-4 MODEM/BBP Parameters

MOD	Modulation Type	QPSK
	Transmit clock Frequency (Hz)	9900 Hz for 9600 BPS DATA 8300 Hz for 8000 BPS DATA 5100 Hz for 4800 BPS DATA
	TX FILTER Type	Root NYQUIST
	TX IF FREQ (MHz)	70 + 15 (5 KHz step)
DEM	TX IF Level	0 - -10 dBm/75
	RX IF FREQ (MHz)	70 + 15 MHz (5 KHz step)
	RX IF Level	-50 dBm/Ch
BBP	RX FILTER Type	Root NYQUIST
	Detection	Coherent Detection
	Method of Word Synchronization	By Frame Synch.
	FEC	R=1/2 Convolutional Coding, Constraint Length; 4 bits, 3 bit soft decision, Viterbi Decoding, Coding Gain 3.5 dB at BER 10 ⁻⁴



Note; Symbol  stands for a DSP (μPD77P20 by NEC)

Fig. 3-4 Structure of MODEM/BBP

3.5 VOICE CODEC

A 4.8 to 16 Kb/s high quality voice codec is implemented on NEC's single chip advanced floating point digital signal processor (ASP) UPD77230[9]. The codec is a multi-pulse excited linear predictive coder (MPELPC) based on a pulse search method which integrates the conventional cross correlation method [10] and the spectrum peak emphasis (SPE) method [11]. By adopting the SPE method, the segmental signal to noise ratio (SNR_{SEG})[12] has been improved by approximately 2.2 dB to 2.8 dB for bit rates below 7.2 Kb/s. The total coding delay is only 45 msec. This new codec can achieve speech coding at any rate between 16 and 4.8 Kb/s. Details of the codec specifications are shown in Table 3-5.

The codec is mounted on a single board as shown in Photo 3-5 and the structure illustrated in Fig. 3-5-1. The codec consists of a single ASP for digital signal processing, a single chip μ-LAW PCM codec for analogue interface, clock and timing circuits, and a digital line interface. The dimension of the board is 125 mm by 145 mm.

Fig. 3-5-2 shows the two SNR_{SEG} scores tested for eighteen short English sentences spoken by three American males and twelve short Japanese sentences spoken by two female and one male Japanese.

Table 3-5 Codec Specifications

NO	ITEM	SPECIFICATION
1	Sampling	8kHz (16K/9.6K/8K) 6.4kHz (7.2K/4.8K)
2	Quantization	8bits (255)
3	Frame Period	20 msec
4	LPC Analysis	Auto correlation method
5	LPC Order	12th (16K/9.6K/8K) 9th (7.2K/4.8K)

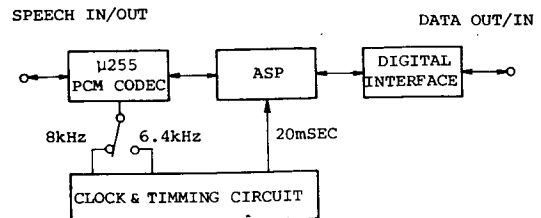
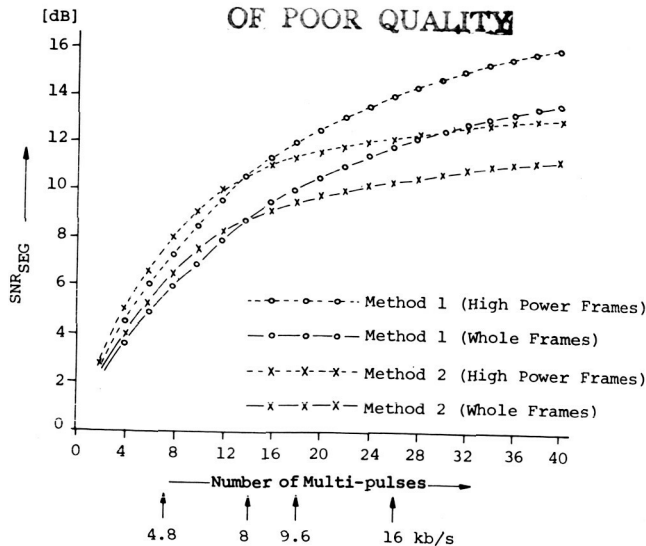


Fig. 3-5-1 The Block Diagram of Coder Hardware

ORIGINAL PAGE IS
OF POOR QUALITY



Method 1: Crosscorrelation Method [22]

Method 2: SPE Method [23]

Fig. 3-5-2 Results of SNR_{SEG}

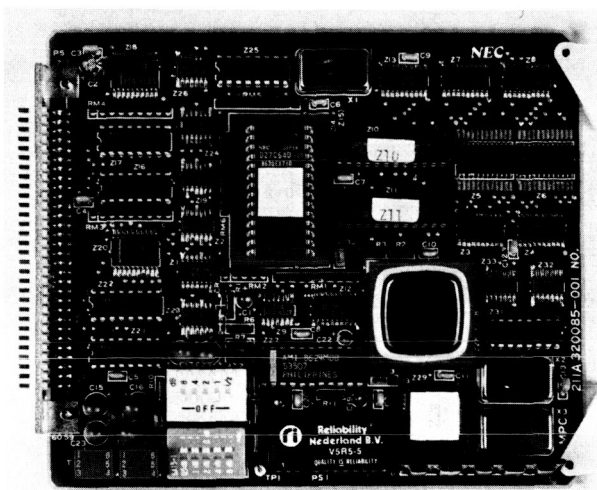


Photo 3-5 View of the New Codec Board

Conclusion

A compact multifunctional mobile terminal has been developed for field tests with Japan's ETS-V satellite.

REFERENCES

- [1] Bullock, C. 1986. The inviolable market? Mobile communications need satellites. In SPACE MARKETS Winter/No. 4 Quarterly.
- [2] R.W. Huck, J.S. Butterworth and E.E. MATT, 1983. "Propagation Measurements for Land Mobile Satellite Services" IEEE VTC
- [3] T. Ikegami, R. Suzuki, Y. Hase, S. Ohmori and K. Kosaka, 1987 "Land Mobile Communication Experiments with ETS-V satellite" IEEE VTC
- [4] T. SAKAI, H. KOMAGATA, N. TERADA, and E. HAGIWARA, 1987. "Compact Mobile Terminals for Multi-Beam Mobile Satellite Communication Systems" IEEE GLOBECOM, TOKYO
- [5] Y. YASUDA, M. OHASHI, F. SUGAYA, H. OKINAKA, Y. HIRATA, 1987. "Field Experiment on Digital Maritime Satellite Communication Systems" IEEE GLOBECOM TOKYO
- [6] S. MIURA, M. WAKAO, N. FUTAGAWA, 1985. "L-BAND Transponder of ETS-V for Experimental Mobile Satellite System" IEEE ICC
- [7] INMARSAT STANDARD-C Specification
- [8] J.H. LODGE, D. BOUDREAU, 1986. "The Implementation and Performance of Narrowband Modulation Techniques for Mobile Satellite Applications" IEEE ICC
- [9] T. Nishitani, 1986. "Advanced Single-Chip Signal Processor", Proc. ICASSP '86, Apr. 1986
- [10] T. Araseki, 1983. "Multi-Pulse Excited Speech Coder Based on Maximum Crosscorrelation Search Algorithm", GLOBECOM 83, Dec. 1983.
- [11] T. Taguchi, 1987. "Implementation of a 4.8 - 16 Kbps Multi-Pulse Codec on a Single Chip DSP Based on Spectrum Peak Emphasis", 30th Midwest Symposium on Circuits & Systems
- [12] T. Watanabe, 1982. "Comparison of Performance of Voiceband Coders by Several Speech Quality Measures", Trans. of the committee on Speech Research, The Acoustical Society of Japan. Vov. 29, '82

DEVELOPMENT OF THE NETWORK ARCHITECTURE OF THE CANADIAN MSAT SYSTEM

N. GEORGE DAVIES, MSAT Project, Telesat Canada; ALIREZA SHOAMANESH, Telesat Canada; VICTOR C.M LEUNG, Chinese University of Hong Kong, (formerly with Microtel Pacific Research, Canada).

TELESAT CANADA
333 River Road
Ottawa, Ontario
K1L 8B9
Canada

ABSTRACT

This paper provides a description of the present concept for the Canadian Mobile Satellite (MSAT) System and the development of the network architecture which will accommodate the planned family of three categories of service; namely, a Mobile Radio Service (MRS), a Mobile Telephone Service (MTS), and a Mobile Data Service (MDS).

The MSAT satellite will have cross-strapped L-band and Ku-band transponders to provide communications services between L-band mobile terminals and fixed base stations supporting dispatcher-type MRS, gateway stations supporting MTS interconnections to the public telephone network, data hub stations supporting the MDS, and the network control centre. This paper briefly discusses the currently perceived centralized architecture with demand assignment multiple access for the circuit switched MRS, MTS and permanently assigned channels for the packet switched MDS.

INTRODUCTION

The technology to provide commercial mobile satellite communications services, and the market need in North America, have been explored for more than ten years. The lack of frequency spectrum to accommodate land mobile satellite communications, which has been a major impediment to the implementation of the service, was finally overcome at WARC 87. Bands of frequencies between 1530 and 1559 MHz and between 1626.5 and 1660.5 MHz were allocated, respectively, for space-to-earth and earth-to-space links for the land mobile satellite service (LMSS) on a primary, shared primary and secondary basis.

While the allocation is not generous, analyses show that the frequency re-use that can be provided with multi-beam satellites can accommodate the anticipated market demand, at least for the first

generation systems. Operational experience and advances in technology are expected to increase the capacity of the present allocation and to provide evidence to support the allocation of additional spectrum to meet the requirements.

Telesat Canada anticipates that very soon the design of satellites, to be launched in the early 1990s, will be determined. Procurement action for the space segment should begin in late 1988. Shortly thereafter, the design of the basic MSAT communications systems will be frozen in order that procurement of the ground segment may proceed. While much of the work in the past has focussed on technological development, this must now be integrated into the design for an operational system.

MSAT COMMUNICATIONS SERVICES

The Canadian MSAT system will provide services to L-band mobile terminals under three main service categories, namely:

- Mobile Radio Service (MRS)
- Mobile Telephone Service (MTS)
- Mobile Data Service (MDS)

Mobile Radio Service (MRS)

The MRS will provide two-way voice and optional voice-band data communications between a base station and user terminals belonging to the same private network. This service is primarily targeted to meet customers' needs for voice dispatch operations. The MRS will be a circuit switched service and subscribers will be charged for the air time used. The service will be provided through privately owned or shared base stations.

Mobile Telephone Service (MTS)

The MTS is intended to provide an extension of the public switched telephone service (PSTN) mainly to mobile terminals, but also to some portable and fixed terminals. The service will be provided through a number of gateway stations interconnected with the PSTN. The service will operate on a circuit-switched basis and subscribers will be charged for air time.

Mobile Data Service (MDS)

The packet-switched MDS will provide data communication capabilities between mobile terminals and a subscriber's office through an MDS data hub station. Subscribers will be charged for each packet of data transmitted. Most of the MDS applications will be supported through a Data Hub owned by Telesat Canada, located at the Network Control Centre (NCC), and interconnected with user headquarters and dispatch centres by means of a Ku-Band VSAT network or via public packet data networks. If it is required, there will be more data hubs located in other locations. These data hubs can be connected to the NCC through the SHF link or by terrestrial means.

Some applications, such as an Aeronautical Mobile Data service, will require facilities which are compatible with international standards and therefore require their own unique capability. The special purpose data hub could be located at the NCC or at the location of the service provider.

The MDS will be capable of bearer and value-added data communications, including:

- Interactive Digital Messaging
- Vehicle Dispatch/Location
- Paging
- Data Acquisition and Control
- Data Collection
- Data Broadcast
- Bulk Data Transfer (Data/Image/Text)

POTENTIAL MARKET FOR MSAT SERVICES

The potential market, or need, for MSAT services in Canada is presently (1986) estimated at 660,000 mobile units, growing to close to a million units by the year 2000. Ninety-two percent of the market is for land mobile, 5% for marine and 3% for aeronautical services.

The demand for MSAT voice services is anticipated to grow to 80,000 mobile units some 10 years after the introduction of MSAT service. It is estimated that 75% of MSAT voice terminals will be used to provide an MRS and 25% to provide an MTS. It is expected that 70% of this demand will be generated by six major industry sectors: transportation, minerals, services, forestry, government and construction.

The demand for MDS has not yet been investigated as thoroughly as that for MRS and MTS but it is expected to exceed that for the MRS and MTS terminals.

MSAT SYSTEM DESCRIPTION

The communications payload of the geostationary MSAT satellites will be cross-strapped L-Band and Ku-band transponders. These transponders will provide communications paths between mobile terminals, which will operate at L-band in portions of the 1.5 GHz and 1.6 GHz frequency bands (as will be coordinated by Telesat Canada) and fixed Ku-band (14/12 GHz or 13/11 GHz) earth stations. SHF - SHF communications between the network control centre and the other SHF stations in the system will also be supported.

Telesat Canada plans to cooperate with the U.S. MSS Consortium to implement the first generation system with one Canadian and one American satellite, each of which will have the capability to provide back-up services to the other country, as well as to provide services to mobile users who move from one country to the other.

In the present baseline design of the Canadian system [1], each satellite will have two large (a minimum of 5 m in diameter) L-Band deployable parabolic reflectors which will generate nine 2.7° beams

covering Canada and the United States. Another pair of beams may cover Mexico.

One or more transponders may transmit into each beam, probably in specific sub-bands of the L-band allocations, as coordinated for each beam. There will be re-use of frequencies in beams that are separated by at least two beamwidths.

The nominal channel spacing will be 5 kHz for both voice and data signals. Some services may require a multiple or one half of a basic channel. Initial planning is to have paired L-band downlink (forward) and uplink (reverse) 5 kHz channels. However, the number of reverse channels may not be so severely limited as the forward channels. Within an overall bandwidth limit, it may be possible to associate more than one return channel with an L-band downlink channel and thereby improve the message handling capability of channels, particularly for the MDS and perhaps for the signalling channels.

The SHF transponder will operate with an antenna that provides coverage of North America. As there are far fewer design constraints on the SHF links, there is considerable flexibility in the implementation of the back-haul links to the base, gateway and the NCC.

Demand assignment multiple access (DAMA) techniques will be employed to provide MRS and MTS voice subscribers with access to a satellite channel. Over 60,000 voice terminals in Canada can be served by the Canadian satellite in the first generation system.

The capacity of the satellite system, expressed as the number of mobile subscribers that can be offered service, is determined through the application of statistical utilization factors (e.g. a 40% activity factor for a voice conversation) and estimate of the traffic generated by an average subscriber. Studies have indicated that the average MRS voice subscriber will use a channel for approximately 150 minutes/month (the average busy hour traffic is 0.0106 erlang). The tolerable probability of all channels being busy, the probability of a call blockage, has been assumed to be 15 percent. Under these conditions, for the initial system, an average of approximately 95 voice users can share each 5 kHz channel.

Packet switching techniques will be used to provide data transmission services. It is anticipated that 2,000 - 5,000, perhaps somewhat more, MDS subscribers can be accommodated within a 5 kHz channel. The number of subscribers that can be accommodated will depend upon the particular user application and implementation of the packet switched links. The MDS will likely use permanently assigned multiple access (PAMA) channels with the capability to augment capacity for certain data applications with DAMA channels.

The allocation of PAMA channels for the MDS will reduce the capacity available for the MRS and MTS services. At any one time, there will be an optimum balance between the capacities allocated for the respective services (optimization based on maximizing revenue, service capacity, or other criteria).

The signalling to communicate the DAMA control functions and to provide for requests to access the network will be implemented through specific DAMA signalling channels within each satellite antenna beam. Mobile terminals will use L-band DAMA access signalling channels to request capacity and to receive instructions on the channels to be used for communications. Correspondingly, SHF DAMA signalling channels will be used to communicate DAMA control functions to the base, gateway and possibly the data hub stations.

The use of the SHF bands and North American coverage for back-haul to the NCC, base, gateway and data hub earth stations economizes on the use of scarce L-Band frequencies, and provides for economical assignment of channel capacity from one location (rather than from within each beam). In addition, it allows access by a mobile terminal in any beam to any designated base, gateway or data hub station in the system, permits monitoring and control of L-Band access to the system and allows precise control of the signal levels transmitted via the L-Band transponders to the mobile terminals.

Studies have indicated that there is a very limited requirement for mobile-to-mobile communications. Such communications will be double-hopped through the Network Control Centre.

MSAT NETWORK ARCHITECTURE

Figure 1 illustrates the concept for the MSAT network architecture. The network is controlled from one Central Control Station (CCS) which embodies the coordinated functions of a Network Control Centre (NCC) to manage the communications network, and a Spacecraft Control Centre (SCC) to manage the satellite.

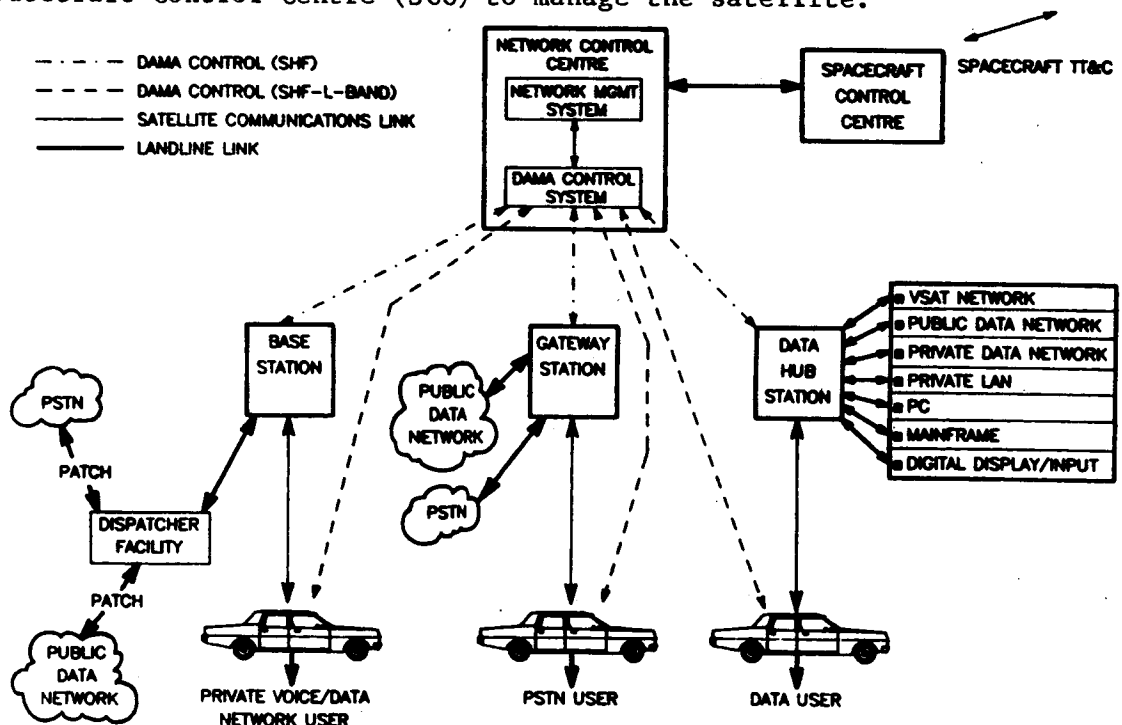


Figure 1: MSAT Network Architecture and Interconnections

The NCC maintains control of the communications network through DAMA signalling channels which use SHF - SHF links to interconnect the NCC with the SHF base, gateway and data hub stations and SHF - L-band links to interconnect the NCC with the mobile terminals. The signalling controls the allocation of L-band - SHF communications links between the mobile terminals and designated base, gateway and data hub stations.

The NCC incorporates a Network Management System (NMS) and a DAMA Control System (DCS). The major functions of these two systems in the management of all aspects of the communications network are as follows:

Network Management System

■ Network Operation

- Initialization and re-initialization of the network
- Generation of call routing algorithms
- Maintenance of a database of logged-on subscribers
- Optimum transponder partitioning
- Management of resources to meet service priority objectives

■ Network Monitoring and Maintenance

- Monitor power levels of transponder access
- Gather alarms, monitor and control activation of redundant network elements
- Report on network status and performance
- Run network diagnostic tests

■ Network Administration

- Collect call records
- Compile traffic, network performance and maintenance history statistics
- Control security of subscriber access
- Generate billing records

DAMA Control System

■ Call Processing (Call Handling)

- Respond to call requests, assign resources and set up the call, if possible, or otherwise signal calling party and take down call
- Inform subscribers of the status of the network
- Generate alarms for unusual conditions

■ Call Administration

- Manage orderly subscriber log-on and log-off
- Establish and maintain DAMA assignment and request channels in each beam of the system
- Respond to individual terminal status reporting
- Record call data
- Generate polls of network elements
- Command changes to mobile terminal transmit power under control of NMS
- Monitor emergency channels

The other elements of the network architecture are:

- L-Band mobile and transportable terminals
- SHF Base Stations which support the MRS
- SHF Gateway Stations which support the MTS
- SHF Data Hub Stations which support the MDS, which have been discussed earlier, and
- the signalling channels

The protocols and access techniques that will be used on the signalling channels are a critical aspect of the network architecture. A number of protocols have been explored [2]. Considerable simulation and testing will be required to confirm the performance and ensure that all the problems have been addressed and overcome. The performance of the whole MSAT system will depend upon the performance of these signalling channels.

SUMMARY

Telesat Canada anticipates cooperating closely with the U.S. MSS Consortium to develop a common system concept and architecture in order to reap the benefits of providing a "standard" service throughout North America. This approach will result in large scale production of lower cost units built to a common functional specification. Action during the next year will determine whether the system will be a common coordinated design, perhaps along the lines described in this report, or be a more fragmented collection of services.

More investigative, analytical, simulation, and experimental work must be done to improve the understanding of the user requirements and to optimize the technical approaches and the system design.

Very little of the hardware or software necessary for the implementation of a mobile satellite system exists as a manufactured product at this time. For this reason, the design, specification and procurement of the first generation MSAT system to serve over 100,000 mobiles in Canada and over three times that number in the United States will challenge the technical and management capabilities of the Canadian and U.S. organizations.

REFERENCES

- [1] Bertenyi, E., and Wachira, M. 1987. Telesat Canada's Mobile Satellite System, 38th Congress of the International Astronautical Federation, Brighton, U.K.
- [2] Razi, M., Shoamanesh, A., and Azarbar, B. 1988. L-Band and SHF Multiple Access Schemes for the MSAT System, NASA JPL Mobile Satellite Conference, Pasadena, U.S.A.

SYSTEM ARCHITECTURE FOR THE CANADIAN INTERIM MOBILE SATELLITE SYSTEM

M. SHARIATMADAR, K. GORDON, B. SKERRY, H. EL-DAMHOUGY, D. BOSSLER
Telesat Canada, Canada

TELESAT CANADA
333 River Road
Ottawa, Ontario, Canada
K1L 8B9

ABSTRACT

This paper reviews the system architecture for the Canadian Interim Mobile Satellite Service (IMSS) which is planned for commencement of commercial service in late 1989. It also discusses the results of an associated field trial program which has been carried out to determine the limits of coverage and the preliminary performance characteristics of the system.

1.0 INTRODUCTION

In Canada, there is considerable momentum and commitment building towards a Mobile Satellite System (MSAT) implementation program; however there still remains a significant period of time before MSAT becomes a service reality. Since an immediate need exists amongst various industries for the types of services that are best delivered by mobile satellite technology, Telesat Canada is cooperating with specific user groups to develop a portfolio of mobile satellite services whose initial implementation will use the Inmarsat MARECS-B satellite and could last until the launch of a dedicated MSAT.

To this end, Telesat issued a Request for Proposal in July, 1987 which called for a complete hub messaging facility and an initial consignment of fifteen mobile data terminals which were intended to prove the IMSS concept prior to making available for procurement additional volume quantities of mobile terminals to offer commercial service in 1989. This service would permit fleet dispatchers to have regular updates of location and vehicle status information as well as the flexibility of transmitting and receiving general messages. This paper describes the IMSS system concept and architecture, and outlines the anticipated range of services and applications, systems design parameters, and projected system capacity. It also discusses the results of a pre-implementation field trial program which involved monitoring the reception of data transmission from the Inmarsat satellite in Eastern Canada during the fall of 1987.

2.0 SYSTEM CONCEPT

The IMSS uses a star network configuration to provide low-rate data satellite communication services to the mobile user community as

illustrated in Figure 1. The initial coverage of this system is in Eastern Canada from 30° to 15° elevation angle as shown in Figure 2. The frequency of operation covers the entire WARC-87 allocation, i.e., 1626.5-1660.5 MHz for transmit and 1530-1559 MHz for receive with 5 kHz channel spacing.

In a configuration of over 4,000 mobile terminals, six 5 kHz satellite channels over the INMARSAT MARECS-B satellite are shared by the mobile terminals in the IMSS network. One of these channels, the outbound, is used by the hub to send network control information, signalling messages, and traffic information to all mobile terminals. Of the remaining five inbound channels, three channels are used to send position reports, one channel for two-way messaging and request, and one for text transfer.

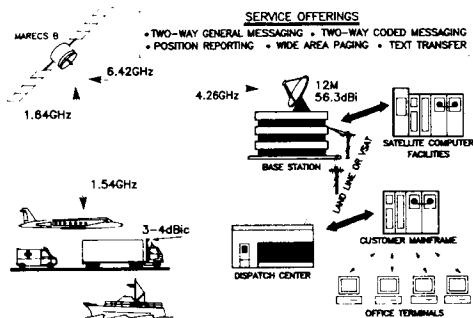


Figure 1: IMSS Service Illustration

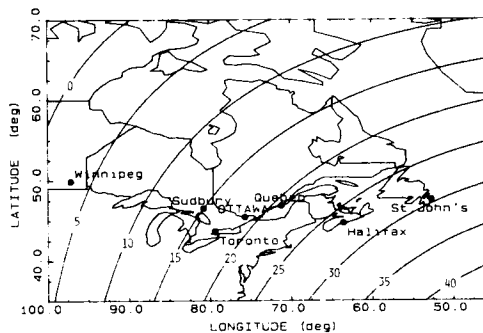


Figure 2: Canadian Coverage by MARECS-B

3.0 SERVICES

Three distinct services are planned for IMSS network which are explained in terms of the type of information, length of messages and traffic capacity objectives.

Vehicle location is the primary service planned for the system and is characterized by 7-character messages, representing vehicle position in terms of longitude and latitude to the second of degree plus a coded message, sent at periodic intervals of 15 minutes or multiples, from a population of over 4,000 mobile terminals. Vehicle position information is determined via the Loran-C receiver which is integrated with the mobile terminal. A mobile terminal failing to report its position on the scheduled slot or those whose transmission is lost due to fading conditions will repeat its transmission on a contention basis after being polled by the hub. This channel has a capacity of about 4000 position reports per hour.

Two-way general messaging is characterized by the transfer of messages of variable length with an average length of 32 bytes and maximum of up to 128 bytes, either from the hub to a particular mobile terminal or from a mobile terminal to the hub. In the mobile-to-hub direction, the messages are transmitted on the request/messaging channel on a reservation basis, where the first packet of each message is handled with a random access mechanism over the available unreserved capacity of that channel. Subsequent packets, each containing 10 bytes of information, are sent over reserved slots on

the same channel. An estimated 330 messages per hour with the average length of 32 characters can be accommodated on one channel.

Text transfer is characterized by transfer of relatively long messages in the order of 4,000 characters long. This service will be offered on a demand assignment basis by allocation of a dedicated inbound channel carrying consecutive 127 byte packets. This channel has a capacity of about 32.9 characters/second.

4.0 SYSTEM DESIGN PARAMETERS

Communication Modes: The key system parameters are summarized in Table 1 below. Eight communication modes are used in the system to provide high system throughput and efficient channel assignment. For example: (i) the inbound multi-packet modes provide the concatenation of several fixed length packets into a single message transmission by combining random and reserved slots in the request/messaging channel; (ii) the inbound scheduled mode is a low overhead method to send short messages from mobile terminals to the hub at periodic intervals and is used for the vehicle location service. Recovery from errors is performed by the inbound polling mode where a new polling command from the hub is sent to the mobiles after the expiration of a time out period.

SYSTEM PARAMETER	Values & Applications
Modulation	BPSK
Symbol Rate	1200 & 600 bps
Interleaving	(64 R X 162 C)
FEC Encoding	Rate 1/2 Viterbi, K=7
Multiplexing	TDM, TDMA, S&R-ALOHA
Communication Modes:	
1-Inbound Unsolicited	Log on/off & Request
2-Inbound Scheduled	Position Reports
3-Inbound Polling	Lost Position Reports
4-Inbound Multipacket	Two-Way Messaging
5-Inbound Demand Asg.	Text Transfer
6-Outbound Broadcast	Network Control
7-Outbound Unsolicited	Two Way Messaging
8-Outbound Demand Asg.	Text Transfer

		OUTBOUND (1200 bps)	INBOUND (600 bps)
Earth Station EIRP	(dBW)	60.8	16.0
Path & Absorb. Loss	(dB)	200.7	189.0
Satellite G/T	(dB/K)	-15.0	-10.6
Uplink C/NO	(dB-Hz)	73.7	45.0
Satellite C/I0 (Inter-Mod)	(dB-Hz)	55.8	53.7
Satellite EIRP	(dBW)	21.6	-21.8
Path & Absorb. Loss	(dB)	188.4	197.1
Earth Station G/T	(dB/K)	-22	32.0
Downlink C/NO	(dB-Hz)	39.8	41.7
Norm. Unfaded C/NO+10	(dB-Hz)	39.7	39.8
Interference Loss (Adj. Sat.)	(dB)	0.5	0.5
Overall C/NO+10	(dB-Hz)	39.2	39.3
Overall Eb/NO+10	(dB)	11.4	14.5
Min. Unfaded Eb/NO+10	(dB)	4.6	5.5
Modem Implement. Loss	(dB)	1.0	1.0
Fade Margin	(dB)	5.8	8.0

Table 1: IMSS System Parameters

Table 2: IMSS Link Budget

Link Budget: With an omni-directional antenna adopted for the mobile terminal and having a minimum effective G/T of -22 dB/K, the link budget, Table 2, provides 5.8 and 8.0 dB margins for the outbound and inbound links, respectively, over the Eb/No needed for a 10^{-5} BER considered as the threshold requirement. The lower operation margin adopted for the outbound link is justified by the use of interleaving in this link and is supported by the field trial results to give adequate performance in non shadowed areas. In the inbound links where the relatively short burst transmission makes the use of interleaving ineffective, the higher operation margin of 8.0 dB has been adopted.

Frame Structure: Currently, several frame formats and packet structure options are being considered, of which a potential candidate is shown in Figure 3. The outbound TDM frame contains 639 information bytes which are used for network control, signalling and traffic information from the hub to the mobile terminals. Network control information broadcast by the hub to all mobile terminals is positioned within the first 48 information bytes following the frame synchronization words. The remaining 591 information bytes are available for fixed and variable length outbound packets. The frames for the inbound request/messaging and reporting channels have a period of 8.64 seconds which is divided into 14 slots, each capable of 10 bytes of information.

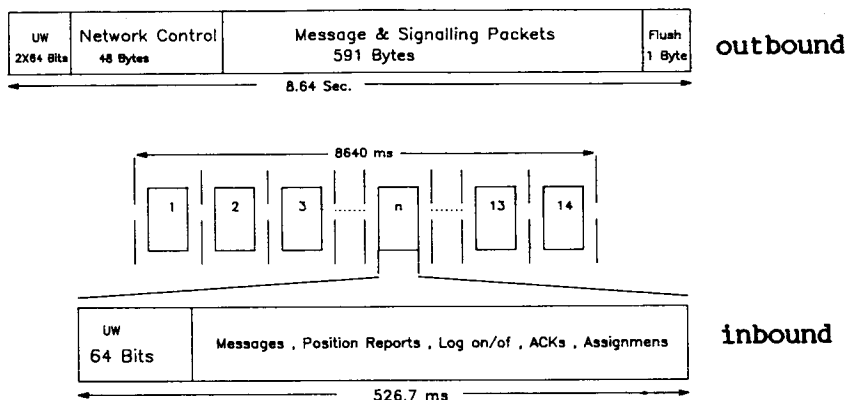


Figure 3: Frame and Packet Structure

5.0 SYSTEM CAPACITY

The estimate of system capacity for the IMSS network is shown in Table 3. Because of the nature of frame and packet structure, the capacities are expressed in terms of: (a) reports/second for the position reporting channel; (b) 10-byte packets/second for the messaging and request channel; and (c) bytes/second for the text transfer channel.

The position reporting channel has an available capacity of 1.62 reports/second which is split into 1.11 reports/second for the TDMA scheduled reports and .51 report/second for the retried reports. Based on this arrangement, the usable capacity of the system, reflected by the reserved capacity, is 4000 position reports per hour per channel.

Similarly, the request/messaging channel has a total capacity of 1.62 ten-byte packets/second but its usable capacity is .45 ten-byte packet/second, of which: (i) 0.09 packet/second is used for the first packet of the message and transmitted on a random access basis, and includes 20% random access and 90% ARQ efficiencies; (ii) 0.2 packet/second is the reserved capacity for subsequent packets of the message and includes only the ARQ efficiency; (iii) the remaining .16 packet/second is used for signalling purposes as part of other functions. These combinations will allow 330 messages with an average length of 32 characters plus 576 ten-byte signalling packets per hour. Should the average message length change, for example, from 32 to 96 characters, one can still accommodate the 330 messages per hour. However, the signalling capacity for other functions will drop

to 144 packets per hour. Requirements exceeding the above limits would have to be accommodated by adding more channels to the network.

The text transfer channel is basically a demand assigned channel and can accommodate about 32.9 characters/second.

Inbound									Outbound (Bytes/Sec.)
Request/Messaging (Ten-Byte Packets/Sec.)						Position Reports/Sec.		Text Transfer (Bytes/Sec.)	
Reserved		Unreserved				Reserved (Reports)	Unreserved (Retried)	Assigned	
Request		Signalling							
32 Char. Message	96 Char. Message	32 Char. Message	96 Char. Message	32 Char. Message	96 Char. Message				
0.202	0.789	0.0916	0.0916	0.16	0.04	1.11	0.51	32.95	61.5

Table 3: System Capacity

6.0 FIELD TRIALS

Operating Conditions: To monitor the reception of data transmissions from the Inmarsat MAREC-B satellite in an actual land mobile operating environment, a prototype omni-directional mobile satellite antenna and receiver were procured and fitted into a van along with associated monitoring equipment. Signal reception was recorded as the van was driven along typical commercial routes from Quebec City (20°) to Winnipeg (3°). A personal computer was used to capture system performance data on a frame-by-frame basis directly to disk while a printer displayed any messages received.

Data transmission was from the Inmarsat Enhanced Group Call (EGC) channel which uses coherent BPSK modulation transmitted at 1200 BPS with rate 1/2 convolutional coding and constraint length 7. The frame length is 8.46 seconds long and starts with two packets of 40 and 14 bytes which are used to check channel performance and provide information on the frame, respectively. The rest of the frame capacity is left for messages, when no messages are sent, binary zeroes are transmitted instead.

The link budget for the field trials is similar to Table 2 with the following changes. There is an average gain in the satellite EIRP of 1.5 dB because the satellite was not operating at full capacity between 10 a.m. to 4 p.m. Eastern Canada time when daily field trials were being conducted. Also, there is no interference loss due to adjacent satellites and the antenna G/T was higher by 1 dB due to half duplex mode of operation. These changes result in an overall fade margin of 8.9 dB.

Route Characterization: Figure 4 shows a sample of Frame Success Rate (FSR) from Quebec City to Sudbury in two hour intervals and as such characterizes the typical commercial routes within the coverage limits of the IMSS. The FSR is either 0% or 100% for each frame received. Given the scale of the graph, one frame in error appears as a downward 'spike'. An outage, that is, no frame received, is indicated by the FSR 'disappearing' over the graph and 'reappearing' once reception has resumed. The number to the right of each two hour interval is its average FSR. The results indicate that reception is

very good until Sudbury with 15° elevation. Beyond that (not shown for the sake of brevity), system performance degrades due to the lower elevation angles and the very hilly terrain encountered just past Sudbury until the prairies are reached. The FSR is 94% (98% excluding outages) for greater than 15° elevation angles and 75% (97% excluding outages) for the entire field trials. For greater than 15° elevation, the ratio of the number of frames that were not received, due to outages, to the number received incorrectly was 2.7. For the entire area tested, this ratio was increased to 8. In general, outages were caused by complete blockage of the signal such as by a hill or building. A few more dB in fade margin would probably not improve reception in these areas. After blockage of the signal, it is likely that the receiver loses synchronization with the carrier. This can make the outage time longer than the blockage time. Thus, the length of time the receiver takes to reacquire synchronization is critical.

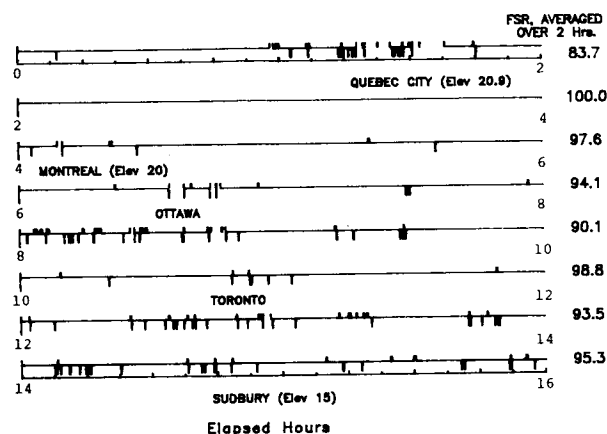


Figure 4: Propagation Measurements in Terms of Frame Success

Multipath Fading: The effects of multipath fading were studied in areas with no shadowing. Figure 5 shows a sample of the relative fade depth for a half-hour period approaching Winnipeg and Quebec City. The fade depth is relative to the fade needed to produce an error in a frame and is not identical to the fade margin because the fade margin is referenced to a BER of 10^{-5} . Both the prairies and Quebec City fades are drawn to the same scale with the right vertical axis showing the number of renormalizations. This is the actual parameter measured within the decoder and is related to the fade depth in a non-linear fashion. Clearly, multipath was more pronounced at the lower elevation angle and the threshold for producing errors was exceeded a few times. Near Quebec City at 20° elevation, multipath is still present but the overall majority is within 3 dB of the error threshold.

Fade Margin Sensitivity: Given the importance of fade margin in system capacity and performance, the sensitivity of the system to a reduction in fade margin was investigated for elevation angles greater than 15°. Knowing the relative fade depth for every frame, we can simulate a reduction in fade margin (say by X dB) by assuming that any frame with a fade depth of X dB or more would have been received in error. Thus, the total FSR can be calculated for that reduction in fade margin. This is shown graphically in Figure 6.

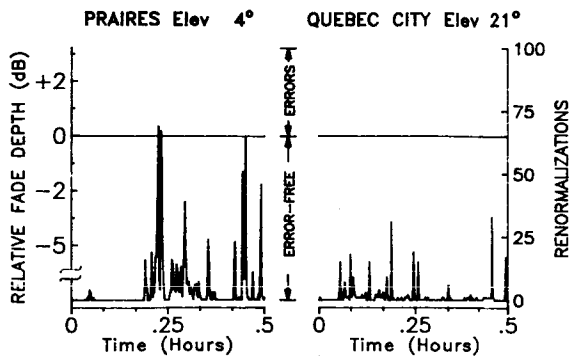


Figure 5: Effects of Multipath Fading Near Winnipeg and Quebec

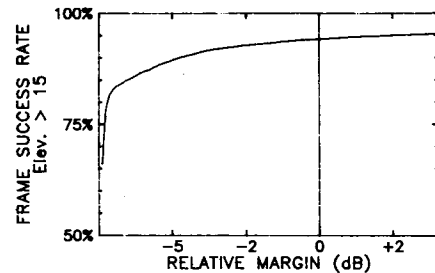


Figure 6: Frame Success Rate Vs. Margin Reduction

This assumes that, when the fade margin is reduced, the fade depth will remain the same. While this is true for shadowing, it is hard to predict for multipath fading because the depth of fade is related to the power of the signal (the exact relationship is dependent on the carrier to multipath ratio as well as the absolute level of the carrier). The worst case scenario is assumed that the fade depth remains the same regardless of a reduction in transmitted power (i.e. fade margin).

Keeping these limitations in mind, the graph shows that a reduction of 3.5 dB will reduce the overall FSR by 3%. This enables us to adopt, for the interim, a fade margin of 5.4 dB for the outbound channel subject to the second phase field trial results in the spring of 1988.

7.0 CONCLUSIONS

The interim mobile satellite services are viewed as an important and integral part of the Canadian mobile satellite program and serve a real purpose in achieving an eventual domestic MSAT system. Telesat is currently in the process of securing both space segment and ground segment facilities to meet the requirement of these services.

8.0 ACKNOWLEDGEMENT

The authors wish to acknowledge the contributions of their colleagues both at Telesat Canada and at the Canadian Department of Communications for development of the IMSS services.

DESIGN, DEVELOPMENT AND TRIALS OF AN AIRLINE PASSENGER TELEPHONE SYSTEM

DR. JIM SCHOENENBERGER, Racal Avionics Ltd., United Kingdom;
ROGER MCKINLAY, Racal Avionics Ltd., United Kingdom.

RACAL AVIONICS LIMITED
88 Bushey Road
London SW20 0JW
UNITED KINGDOM

ABSTRACT

The paper describes the design, development and trials of a satellite telephone system for airline passengers. The requirements for ground and space infrastructure are discussed and the aeronautical system is described. Design criteria for the antennas and avionic boxes are given and system operation and technical flight trial requirements are discussed, together with test methodology and development towards fully commercial trials. Finally, an indication of development requirements to achieve the desired aims of airline users is given.

INTRODUCTION

The world airline market is now being presented with the reality of providing passengers with advanced communications via satellite. These communications will include voice (telephone) and data (telex, telefax and personal data) services.

Racal Avionics have embarked on a programme of fulfilling all the communications needs of airline passengers in a series of phased developments including data only, voice only and data plus voice services [1]. The purpose of this paper is to detail the design, development and trials of a voice only passenger telephone system for airline use.

Trials are to take place on a Racal-owned British Aerospace Jetstream and also on two Boeing 747-200s belonging to British Airways.

GROUND AND SPACE INFRASTRUCTURE

Various aeronautical satellite communication systems have been proposed over the last few years [2,3], but all of the communication channel infrastructure, including satellite and ground segments, must be present before service can start. For the purposes of these trials, INMARSAT-operated satellites are to be used. The British Telecom International (BTI) Ground Earth Station (GES) at Goonhilly in south-west England has already commissioned an antenna and RF system dedicated to the INMARSAT aeronautical service. The GES also contains the ground modems and interfaces to a fixed 64kbps digital link to BTI's International Switching Centre (ISC) in London. In a manner analogous to current practice in placing credit card calls via an international operator, the ISC staff will make the final call interconnect into the international telephone networks.

This operator service will be replaced by a fully automatic world-wide

service upon commissioning of the Automatic Control and Signalling Equipment at Goonhilly in mid-1989[4].

AERONAUTICAL SYSTEM DESCRIPTION

The satellite link requirements for the INMARSAT aeronautical system are well defined [5], and are summarised here for the voice service in Table 1, together with other pertinent system parameters.

The Racal trials programme was instigated before the 12dBic antenna gain figure became standard, making use of 10dBic gain, limited coverage, antennas for the first trials. Although not fulfilling the final system requirements, these antennas present a reasonable compromise in terms of performance and installation simplicity.

Also under development is a full coverage, 12dBic gain antenna, designed specifically for aeronautical satellite communications. This antenna will be used during the trials on British Airways Boeing 747s.

AIRBORNE TERMINAL DESIGN AND DEVELOPMENT

Antennas

Two antenna types are to be used during the trials. Both are of the blade form containing electronically-steerable microstrip phased arrays.

10dBic Gain Antenna. This antenna was designed specifically for sideways satellite viewing, being suited to British Airways route structures between Europe and the eastern seaboard of the USA.

The antenna consists of two vertical back-to-back phased arrays in the same radome, each of 3 x 3 elements, the resulting beam being steerable to three azimuth positions at fixed elevation. Array coverage is portrayed in Fig.1. Coverage is a minimum of 10dBic gain over azimuth angles 50° to 130° (relative to forward) and 20° to 50° in elevation. The antenna is narrow band, requiring separate transmit and receive units to be provided.

Mechanical performance constraints are to provide adequate sideload and stress properties whilst minimising drag. Drag has been maintained at under 5N at Mach 0.84 at 10,700m altitude.

Full lightning and static protection is, of course, also provided. Each antenna has an associated Beam Steering Unit (BSU) which provides suitably-phased RF signals for beam pointing.

12dBic Gain Antenna. In order to provide coverage of the super-hemisphere, this antenna is built on the same principle as the 10dBic unit, but with an additional horizontal "top hat" section mounted within the radome. Since the antenna has little aperture available fore and aft, coverage at 12dBic gain cannot be maintained in these directions. Fill-in radiators at a lower gain level are, however, provisioned for. Dual band (transmit and receive) operation is also accommodated.

The phased arrays comprise 16 elements for the vertical sections, and 14 elements for the upward-looking horizontal section. 3 bit digital PIN-diode phase shifters are used with each array element to provide continuous coverage as shown in Fig.2.

The antenna has associated with it a Beam Steering Unit (BSU) to convert relative angle pointing information into phase shifter settings. The BSU also contains BITE and closed-loop steering control circuits.

Free airflow drag of this antenna is 125N at Mach 0.84 at 10,700m.

RF Subsystem

Of primary importance to terminal performance is station EIRP and G/T. These parameters are influenced by the antenna, the output power of the High Power Amplifier (HPA), the noise figure of the Low Noise Amplifier (LNA) and any losses incurred in RF plumbing and diplexing.

The availability of cooling air and suitably stressed mounting positions affects the installation of the HPA, often implying a Main Equipment Centre (MEC) location and a long cable run to the antenna. Long cable runs cannot be achieved without high cable losses, resulting in the remote mounting of the HPA units. For the British Airways trial, HPAs will be mounted on specially-provided racks at STA1650 within 7m of the antenna.

The power output capability of the HPAs is 70W, operating in class C. This capability exceeds the requirement stated in Table 1, primarily to accommodate the lower gain of the 10dBic gain antenna. When used with the higher gain antenna, the HPA output is de-rated by its in-built power level control circuit.

The transmit-receive diplexing function is achieved either by transmit-receive antenna isolation combined with pre-LNA bandpass filtering (in the case of the dual antenna installation) or by a dedicated, diplexer/LNA device (in the case of the dual band 12dBic gain antenna). In either case, state-of-the-art technology is used to minimise noise figure and filter insertion loss, which, combined with the short antenna to LNA cable runs, ensure that the -13dB/K G/T requirement is met. Achieved diplexer/LNA performance is 0.8dB diplexer filter loss and 1.0dB LNA noise figure at +70°C.

Digital Subsystem.

The digital subsystem provides the digital modem functions required by the aeronautical system as well as avionics control and monitoring.

Upconversion and downconversion are performed in a separate LRU - the Radio Frequency Unit (RFU). VHF synthesisers based on proprietary LSI devices are used to provide 100MHz and 200MHz local oscillators for up/down-conversion, frequency selectable in 1Hz steps to counteract the effects of Doppler shift due to aircraft motion. A prime requirement in the up/down-conversion process is spectral purity, particularly phase noise. This is especially relevant on aircraft where vibration effects completely dominate oscillator performance. Fig.3 illustrates the phase noise specification and results obtained from a high quality crystal reference oscillator installed on shock mounts and vibrated to standard specification [6]. Fig.4 illustrates the resulting performance from a 200MHz synthesiser, measured at 1200MHz using a x6 multiplier.

The digital modem and control functions are housed in a dedicated LRU - the Satellite Data Unit (SDU). A block diagram of the SDU is shown in Fig.5. Quadrature detection is performed in the Analogue Module, the Demodulator Module performing symbol timing recovery and AGC/AFC control. The Frame Sync Module performs unique word detection and de-interleaving. Error correction is performed in the FEC Module, (containing an LSI Viterbi Decoder) as well as de-scrambling and data/voice demultiplexing. The System Interface Module and Data Interface Module provide interfaces with other LRUs in the system (for control and BITE) and other avionic systems.

The modules described above also perform the inverse of the functions given for the transmit chain. The modulation scheme employed in both forward and reverse directions is A-QPSK as specified by ICAO's Future Air

Navigation Systems committee and the AEEC[7].

Voice Coding.

Many algorithms exist for encoding and decoding voice. The Inmarsat SDM [5] calls for a coding rate of 9.6kbps, in order to provide commercially acceptable call charges by maintaining a low channel bandwidth without compromising quality.

Both RELP and APC type algorithms have been considered in these trials, RELP being chosen as a suitable codec was available. Since the final choice of algorithm for airline use must be universal and approved by users and service providers alike, a compromise approach has been used in the design, the voice coding elements being housed in a separate LRU, the Voice Management Unit (VMU).

For the trials, both hardwired telephone type handsets (with noise reducing microphones) and cordless telephones as manufactured by GTE Airfone Inc. will be used.

TECHNICAL TRIALS

The technical trials are to be performed on the Rcal Jetstream aircraft. The trials will make use of two 10dBic antennas (1 off each transmit and receive), a BSU for each antenna, and an HPA, LNA, RFU, SDU and VMU as shown in Fig.6. Additional peripheral equipment will be a Control and Display Unit (CDU), a seven channel tape recorder (Rcal Store 7), a Compaq 286 PC with 14Mbyte hard disk for data logging and a headset/microphone.

The primary objectives of these trials fall into the following areas:

- Verification of antenna performance (coverage and discrimination)
- Compatibility (environment, electrical, mechanical and acoustic)
- System tests (technical specifications and continuous and sampled)
- Speech coding evaluation (evaluations of alternative algorithms)
- Propagation tests (line of sight, multipath and airframe effects)
- Limited user evaluation (subjective conversation tests).

The technical trials will take place over pre-planned flight profiles in different geographical locations. Trials are planned on variable headings relative to the Atlantic Ocean Region satellite over land and water and at optimum and extreme instances of satellite elevation. Test flight routes encompassing Norway, Portugal, the Atlantic Ocean, the North Sea and continental Europe will provide the test conditions listed above. In all, some 4 weeks of test flying will be involved.

COMMERCIAL TRIALS

The commercial trials will take place on two British Airways owned Boeing 747-200 aircraft starting during the summer of 1988. Each aircraft will support two simultaneous telephone channels, the user interface being 4 cordless handsets, manufactured by GTE Airfone Inc.

The first of the two 747 aircraft will utilise the 10dBic limited coverage antennas; two transmit (one per RF channel) and one receive.

The second aircraft will be fitted with the single, transmit/receive 12dBic antenna with full coverage.

The 747 trials will start with a two-week commissioning period during which technical performance will be verified. Commercial trials will then start, during which passengers will be charged (via credit card) for all

telephone calls.

These trials will be used to demonstrate the commercial viability of such a system as well as continuing to provide data on antenna performance and the subjective quality of the communications link.

FUTURE DEVELOPMENTS

The world airlines expect to fit production equipment from about 1990, as the automatic GESs come on line. This requires the avionic boxes to become compatible with the internationally-recognised form, fit and function specification being generated by the Airlines Electronic Engineering Committee [7].

Further development to satisfy the requirements of Automatic Dependent Surveillance (ADS), currently under definition by ICAO's Future Air Navigation Systems committee, will also be required for the mid 1990s.

The modular approach used, both in terms of LRUs and the component modules, enables a simple upgrade approach to be a realistic and cost-effective solution for the airlines future satellite communication needs.

ACKNOWLEDGEMENTS

The authors wish to acknowledge the directors of Racal Avionics for permission to publish this work.

The authors would like to thank their many colleagues, throughout the Racal Group, British Airways, British Telecom International, Inmarsat, SNEC and GTE Airfone for their technical assistance and the British National Space Centre for funding assistance.

REFERENCES

1. Diederich, P. 1987. Satellite Avionics - serving the market. Proc. RAEs Int.Conf. "Satellite Services for Aviation", June 1987.
2. Smith, G.K, Branch, P. 1987. Inmarsat Plans for Early Introduction of Aeronautical Satellite Communications. Proc. ICC 87.
3. Dement, D.K. 1987. AvSat: An Aeronautical Terminal for Satellite Communications. Proc. ICC 87.
4. Stone, D. 1987. Aeronautical Satellite Services - Opportunities for Airlines. PROC. RAEs International Conference "Satellite Services for Aviation", June 1987.
5. Inmarsat Aeronautical System Definition Manual, 1987.
6. Eurocae specification ED14B, or RTCA specification DO160B.
7. ARINC Characteristic 741. 1988. Aeronautical Radio Inc.

Table 1.

Antenna Gain (min)	12dBic	Transmit Frequency	1626.5 - 1660.5MHz
Antenna Coverage, Az	0 to 360°	Receive Frequency	1530 - 1559MHz
, El	-20° to +90°	Transmission Rate	21000 bps
HPA	40W	Voice Coding Rate	9600 bps
Transmit RF Losses	2.5dB	Coding Scheme	1/2 Rate Convolutional + Interleaver
EIRP for MARECS	25.5dBW	Access Scheme	SCPC
" for INMARSAT-2	22.5dBW	Modulation Scheme	A-QPSK
G/T	-13dB/K		

ORIGINAL PAGE IS
OF POOR QUALITY

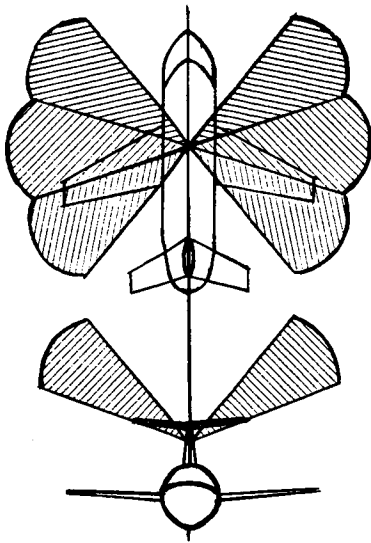


Fig. 1. 20dB Antenna Coverage

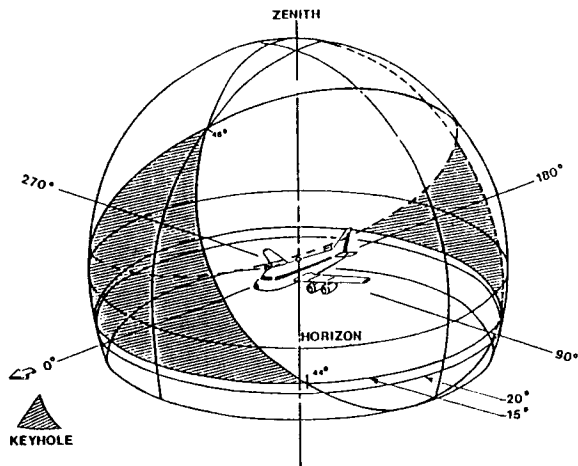


Fig. 2. 12dB Antenna Coverage

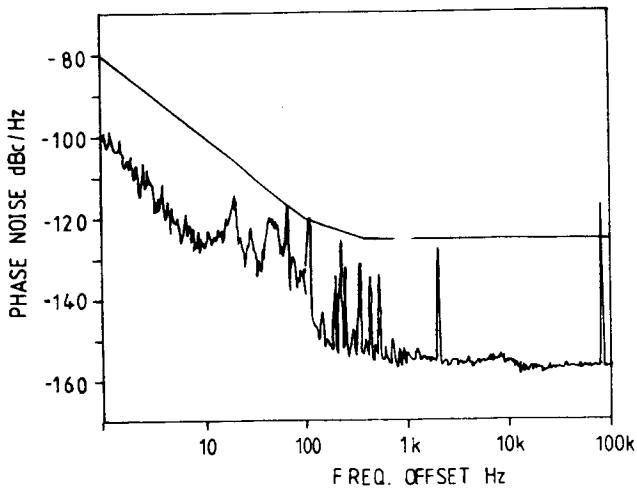


Fig. 3. Reference Oscillator Phase Noise Plot

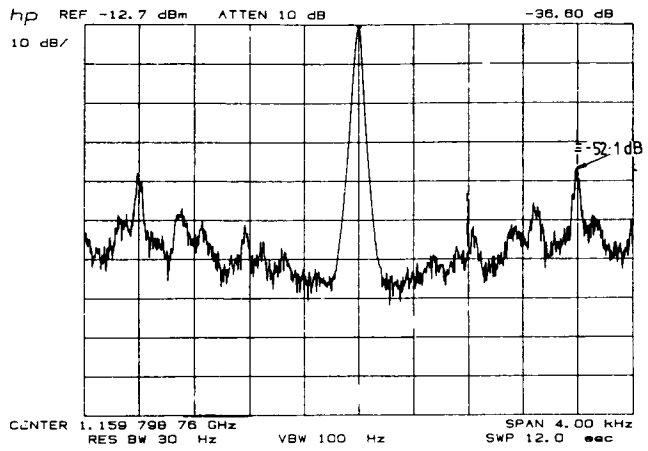


Fig. 4. Phase Noise of 200MHz Synthesiser (x6)

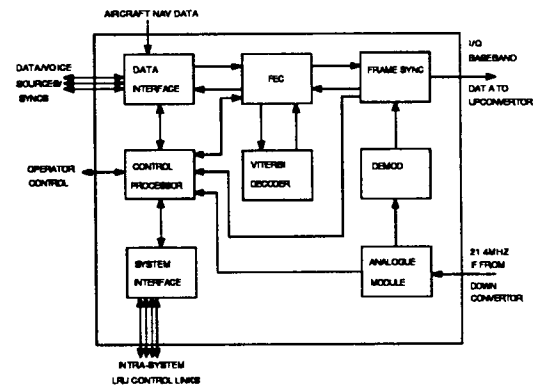


Fig. 5. SDU Block Diagram

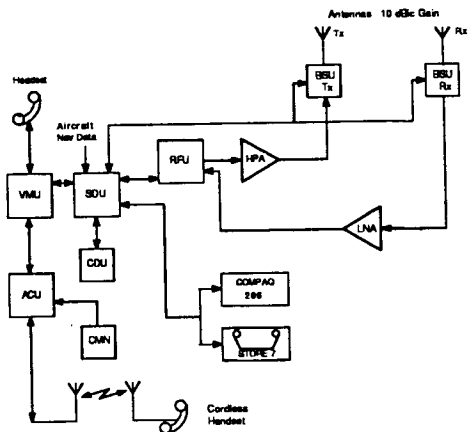


Fig. 6. Technical Trials Configuration

SATELLITE COMMUNICATIONS EXPERIMENT
FOR THE ONTARIO AIR AMBULANCE SERVICE

JOHN S. BUTTERWORTH, Mobile Satellite Program, Communications Canada

COMMUNICATIONS CANADA, Communications Research Centre,
P.O. Box 11490, Station H,
Nepean, Ontario, CANADA
K2H 8S2

ABSTRACT

Since 1976, the Government of the Province of Ontario, Canada, has operated an aircraft ambulance service for the benefit of remote communities. To support a decision to upgrade the air ambulance attendants to paramedic status, the Ministry of Health solicited the cooperation of Communications Canada/ Communications Research Centre to conduct a satellite communications experiment. The objectives of the experiment were to develop a reliable voice communications system between the paramedics and the doctors in certain larger medical centres.

The experiment used INMARSAT's Atlantic Ocean Region satellite which provides coverage to the western border of Ontario. Forward downlink power from the satellite is in great demand, so two highly power-efficient modulation schemes were chosen for evaluation during the experiment. These were amplitude-companded single-sideband (ACSSB) and linear-predictive coding in conjunction with DMSK modulation. Although both systems have been tested over the satellite, flight tests to date have concentrated on ACSSB. Good performance with a signal-to-noise ratio of about 10 dB has been demonstrated from many parts of the province with the elevation angle to the satellite ranging from five to twenty degrees and with the aircraft both in-flight and on the runway.

The experiment is presently in the service evaluation phase. It will evolve into a limited pre-operational service later in 1988.

INTRODUCTION

Since 1976 the Government of the Province of Ontario, Canada, has operated an aircraft ambulance service from northern Ontario communities to larger medical centres in the southern parts of the province. The air ambulances have been staffed by attendants trained to initiate and

maintain basic life support procedures only. A 1986 report, prepared by the Air Ambulance Section of the Ministry of Health, assessed the air ambulance program and recommended that the aircraft be staffed by paramedics who could provide more extensive life support services than the ambulance attendants. Subsequently, training of paramedics has commenced and they are expected to enter service in April 1988.

The radio links currently used by the air attendants must also be upgraded for paramedic use. Patients being evacuated from remote locations frequently require attention before take-off and the first thirty or forty minutes on the airstrip can be critical. Radio coverage for this situation and frequently when the aircraft is flying north of 50°N is not available with the present VHF system. After evaluation of a number of alternatives, Ontario Government officials came to the conclusion that INMARSAT's satellite facilities showed the greatest promise for fulfilling the service requirements. A cooperative experimental program was established with Communications Canada/Communications Research Centre, Teleglobe Inc. (Canada's INMARSAT signatory) and INMARSAT. The objectives of the program were to develop the necessary technology, to establish suitable institutional arrangements, to perform technical flight trials and to provide a service evaluation opportunity for the users.

In this paper we describe the technical considerations in the design of the experiment, the special equipment developed and qualified, the conduct of the flight trials, the evaluation of the results and the plans for transition to an operational service.

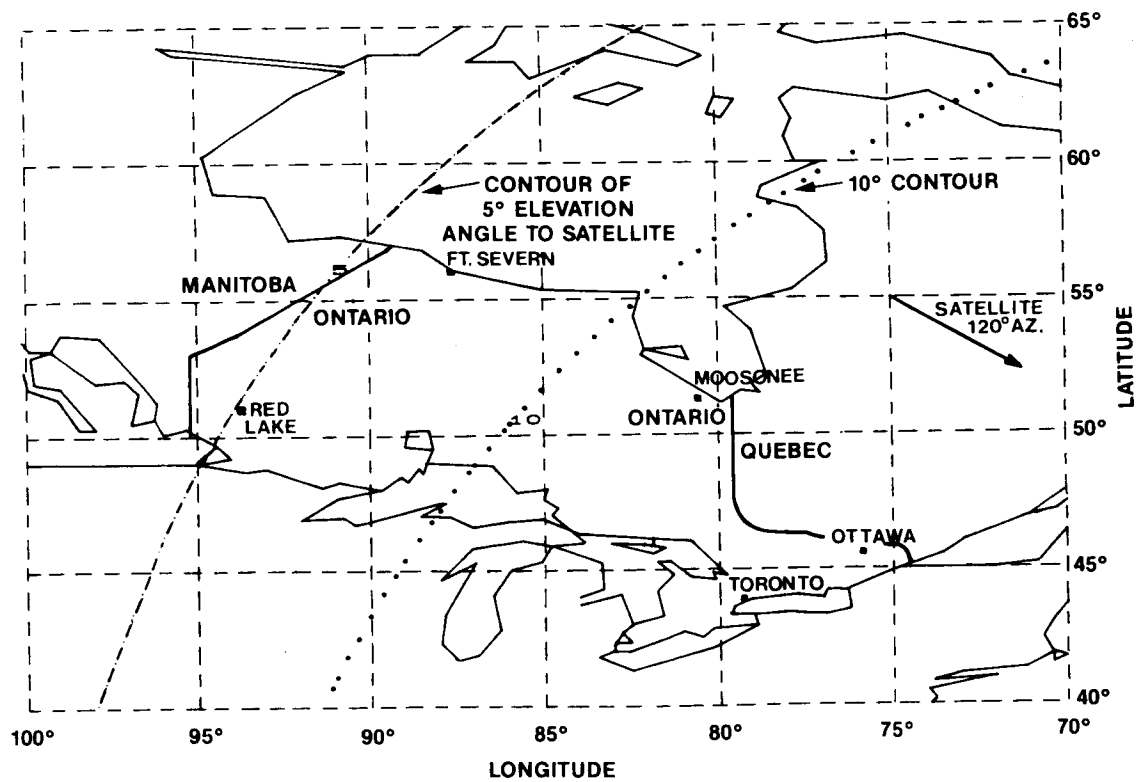


Fig. 1: Coverage of the INMARSAT AOR satellite over Ontario

GENERAL CONSIDERATIONS

Northern Ontario is at the edge of the coverage area of the Atlantic Ocean Region (AOR) satellite at 26° W. longitude. Fig 1 shows that much of the proposed service area lies between the contours of five and ten degrees elevation angle to the satellite. When using a 10 to 12 dB gain aircraft antenna at such low angles, discrimination against multipath signals scattered from the ground is not possible. The consequent direct signal-to-multipath ratio (C/M) is 8-10 dB with less than 100 Hz Doppler spreading of the multipath [Neul, 1987].

The maximum economic forward-link EIRP available from the satellite is judged to be 21 dBW. With this downlink power and a typical aircraft terminal G/T of -15 dB/K, only 45 dB-Hz unfaded received signal-to-noise power density ratio is available. This is 7 to 8 dB too low for the frequency modulation system used for INMARSAT ship terminals and so more efficient voice coding and modulation techniques must be used, at some sacrifice in terms of received signal quality.

Two schemes are being evaluated during the experimental program. These are amplitude-companded single sideband (ACSSB) and 2400 b/s linear predictive coding (LPC) coupled with DMSK modulation [Lodge, 1986]. Both these schemes operate well at 45 dB-Hz with a C/M of 8 dB. Ministry of Health officials currently favour ACSSB because of the good speaker recognizability and intelligibility down to 36-37 dB-Hz. A drawback is the requirement for a more expensive linear power amplifier for the aircraft transmitter in place of the standard Class C amplifier. A seven-module transistor amplifier providing 50 watts average output, 140 watts peak power and better than 20 dB C/IM was developed for the program.

LINK BUDGETS

Although the target of the linear power amplifier development program was to produce an amplifier with sufficient power to communicate using the standard marine band frequencies, permission was sought from INMARSAT to use the Search-and-Rescue (SAR) channel during the experiment period as a precaution. The SAR channel has 15 dB extra gain and so requires only a quarter of the transmit power from the mobile compared with the marine band.

Table 1 shows the link budgets. For the ACSSB system, signal levels given are long-term average values. Peak envelope power (1% of the time) is 3dB above these levels.

Table 1. Link Budgets

Uplink	To Aircraft	Return
Frequency	6423.9	1644.4
Transmit Power (Watts)	6.0	9.5
Feed Loss (dB)	1.0	3.8
Transmit Gain (dB)	54.2	12.3
EIRP (dBW)	61.0	18.3
Path Loss (dB)	200.6	189.0
Polarization Loss etc. (dB)	1.0	1.0
Satellite G/T (dB/K)	-13.0	-11.0
Uplink C/N ₀ (dB-Hz)	75.0	45.9
Downlink		
Frequency (MHz)	1541.4	4200.4
Satellite EIRP (dBW)	21.0	-8.0
Path Loss (dB)	188.4	196.9
Polarization Loss etc. (dB)	1.0	1.0
Earth Station G/T (dB/K)	-15.0	31.0
Downlink C/N ₀ (dB-Hz)	45.2	53.6
Overall C/N ₀ (dB-Hz)	45.2	45.2

THE AIRCRAFT EQUIPMENT

Disposition

The air ambulance used for the experiment was a twin-turbofan Cessna Citation 1. Normally a small five-passenger executive jet, this aircraft was equipped with two stretcher positions, two attendant seats and a selection of medical equipment. The electronics equipment for this experiment was located under the floor of the nose baggage compartment and so was exposed to the full range of environmental conditions. The diplexer, LNA and antenna selection switch were mounted under the cabin floor, between the control cables. The control panel and headset were located near the starboard attendant seat, while the antennas were mounted inside the front port and starboard cabin windows.

Antennas

We chose window-mounted antennas in order to commence the experiment in a relatively short time. An electronically-steered external antenna will eventually be required for the follow-on operational phase, but will require extra time and funds. The type of antenna used consisted of a three-element vertical phased array of square microstrip patch elements, providing thirty degrees elevation beamwidth, sixty degrees azimuth beamwidth and 10% bandwidth. Transmit peak gain was 12.3 dB RHCP, receive gain 11.6 dBic and the beam was squinted by 17.5 degrees so that when mounted in the cabin window, the beam was aimed at an elevation angle of 7.5 degrees.

EXPERIMENT PROCEDURES AND RESULTS

Ground-Based Tests

The experimental program started with performance verification of the prototype equipment while ground-based. The aircraft equipment was installed in a mobile laboratory which was parked near the 9 metre (C-band) base station installation located at the Communications Research Centre. Full-duplex tests of both the LPC/DMSK and ACSSB equipment were run over the INMARSAT satellite. Recordings of received voice signal quality were made at different transmit power levels and measurements of received C/N_0 were made to confirm the link budgets.

Flight Tests

The first flight test was held on the 24th November 1987 and consisted of a short flight in the Ottawa area to verify equipment operation using ACSSB modulation. The second flight was run from Ottawa to Moosonee on James Bay (fig. 1). The elevation angle to the satellite decreased from 20° at Ottawa to 12.8° at Moosonee. The ACSSB communications quality during the flight and while on the airstrip at Moosonee was at the expected level of about 45 dB-Hz C/N_0 . During flight, communications were maintained over a 90° range of aircraft headings, centred on 030° (starboard antenna) or 210° (port antenna). The satellite azimuth was 120° . Communications quality at the extremes of this range was reduced to 37 dB-Hz, which was fully intelligible though somewhat "gravelly". Note that this is a signal-to-noise ratio of only 2dB.

The third test flight ran from Ottawa to Moosonee, then to Fort Severn on Hudson Bay, to Red Lake near the western border of Ontario and then back to Ottawa (fig. 1). At Red Lake, the elevation angle to the satellite was only five degrees. Communications at Red Lake, both while in the air and on the airstrip were at the 45 dB-Hz level while the aircraft was on a suitable heading. No problems were observed attributable to the low elevation angle.

The final test flight of 1987 concentrated on routing of communications to and from the aircraft, through the base station in Ottawa and via an auto-ringdown telephone link to the Central Air Ambulance Communications Centre ("Medcom") in Toronto. Off and on-hook signalling from the aircraft were performed using the # and * DTMF tones which passed satisfactorily through the ACSSB equipment. A tone decoder at the base station then activated the telephone line to Medcom and alerted the dispatcher. Satisfactory results were obtained with the experimenter on the aircraft talking to the Medcom dispatcher and, when patched through Medcom, to other centres and even to a cellular mobile.

TRANSITION TO OPERATIONS

The experiment is currently in the service evaluation phase. The air ambulance attendants, dispatchers and doctors will have two evenings per week for about a two month period in which to use the satellite communications system in a non-operational role. Human factors specialists, under contract to the Ontario Government, will help in

orientation of the users to the new radio system and will assess their reactions to it. Their recommendations will be useful in integrating the new system into the Medcom network with the minimum disruption.

On May 1st, 1988, the satellite communications system is scheduled to enter limited pre-operational service. A tariff is being negotiated by Teleglobe, based on a minimum usage of 200 minutes per month.

The present base station will be used as an interim operational base station until Teleglobe can take over this role with a station of their own. The mobile transmit frequency will be changed to 1642.9 MHz which is in the lower-gain marine band rather than the SAR channel. Because of the lower gain, the aircraft terminal transmit power will need to be increased to about thirty watts from the ten watts previously used.

CONCLUSIONS

The air ambulance experiment has shown that existing satellite facilities can be used to provide voice links to general aviation aircraft. Communications were reliable to five degrees elevation angle with no performance degradation, airborne or on the airstrip. Several improvements remain to be implemented for the operational service. The first in priority is to replace the window-mounted antennas with an externally-mounted electronically-steerable antenna. Others concern details such as an improved method for transmission of signalling and supervisory information and to take into account any recommendations resulting from the human factors study.

ACKNOWLEDGEMENTS

We wish to thank our colleagues at Teleglobe Inc., and at INMARSAT for their help in making this experimental program successful. We also thank our colleagues in various ministries of the Ontario Government for involving us in this useful and interesting applications program.

REFERENCES

- Lodge, J.H. and Boudreau, D. 1986. The implementation and performance of narrowband modulation techniques for mobile satellite applications. IEEE International Conference on Communications, paper no. 44.6.
- Neul, A. et. al. 1987. Aeronautical channel characterization based on measurement flights. IEEE Global Telecommunications Conference, paper no. 42.3.

LAND-MOBILE SATELLITE DEMONSTRATION SYSTEM

GUY M. GOOCH, Ph.D.
DAVID C. NICHOLAS, Ph.D., P.E.

ROCKWELL INTERNATIONAL CORPORATION
Cedar Rapids, Iowa 52498

ABSTRACT

A land-mobile satellite demonstration system is described. The system was developed by Rockwell International with the cooperation of COMSAT Maritime Services and the International Maritime Satellite Organization (INMARSAT) and utilizes the INMARSAT MARECS B2 satellite at 26 degrees W. The system provides data transmission using a poll-response protocol with error detection and retransmission at a 200-b/s rate. For most tests, a 1.8-inch monopole antenna was used, along with a satellite EIRP normally used for four voice channels. A 30-watt mobile transmitter was used.

Key system objectives were to:

- Investigate propagation effects at low elevation angles to the satellite using a simple nondirective antenna
- Develop and demonstrate a MODEM which would accommodate system frequency errors and doppler shifts which total six times the data rate, short preambles, and the need for rapid bit as well as carrier synchronization.

The paper gives a brief summary of the results and describes the overall system consisting of three elements in addition to the satellite, namely the mobile unit, the base station, and the office terminal and map display. Throughput statistics from one trip are summarized.

INTRODUCTION

In October 1987, Rockwell International initiated a land mobile test and demonstration program.

Figure 1 illustrates the three elements developed for the test program:

1. A satellite transceiver equipped van which by December 1987 had been driven several thousand miles during testing including a trip from Iowa to Washington, DC, and back on two different routes. The van is equipped with both GPS and LORAN-C navigators which report position through the satellite system every two minutes in addition to user text messages.
2. A base station installed at COMSAT's facilities at Southbury, Connecticut.
3. A trucking company dispatcher's terminal consisting of a data terminal and electronic map display. The dispatching unit is portable and may be connected to the base station at Southbury, Connecticut, by dial-up telephone line.

Table 1 summarizes the system specification.

The dispatch terminal, base station, and mobile unit each include a COMPAQ II computer. In addition, the base station and mobile unit computers each house TMS32020 computer-based signal processors which provide the RF modem function.

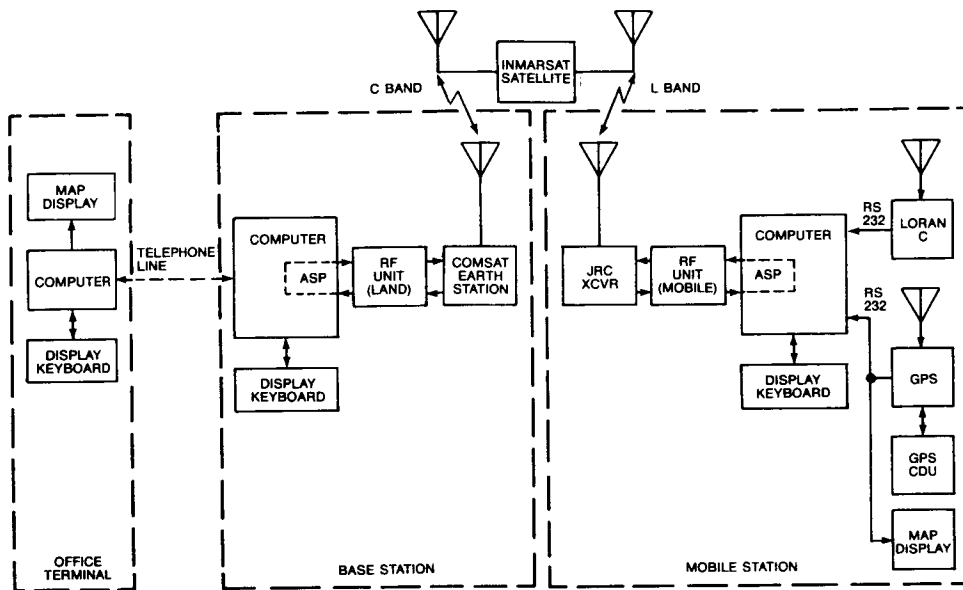


Fig. 1. Block diagram of demonstration

Table 1. System specification

System protocol	Poll response, half duplex
System data rate.....	200 b/s
Modulation.....	DPSK
Message block lengths.....	See figure 2
Error control	Cyclic redundancy check (CRC) with automatic repeat request (ARQ)
Return link	Burst mode
Mobile transmitter power.....	30 watts
Mobile transmit frequency.....	1642.8 MHz
Mobile antenna	Omnidirectional $\lambda/4$ Monopole
Forward link	Continuous with fill between blocks
Mobile receive G/T	-27 dB/k
Mobile receive frequency.....	1541.3 MHz
Mobile position sensor.....	GPS and LORAN C

A principal technical uncertainty resolved by these experiments was satellite-to-mobile propagation reliability at low power and low satellite elevations, to a mobile unit using an inexpensive omnidirectional antenna. A simple 1.8-inch (quarter-wave length) vertical antenna over a ground plane proved to be the best because of the low elevation angles (9°) in the Cedar Rapids, Iowa, region.

During more than 100 hours of testing, polling messages were sent to the mobile unit every 2 or 3 seconds requesting a mobile unit response. Statistics were automatically recorded on the

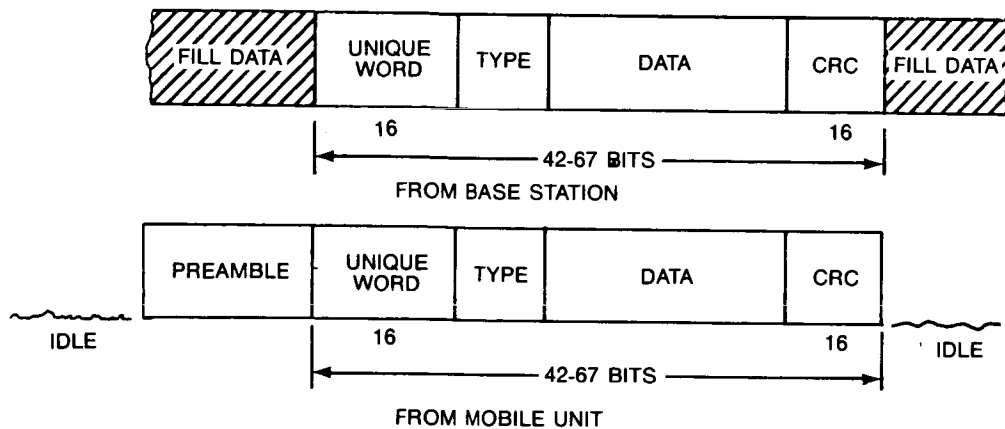


Fig. 2. Message formats

number of successful polls and responses at the mobile unit and at the base station, and were summarized every two minutes. As expected the principal propagation problem was related to blockage and not multipath fading. Detailed results are reported in Reference [1].

A major achievement of this program was the development of an RF modem which could quickly detect a 200-b/s phase-modulated signal burst with an E_b/N_o of 7.5 dB when the carrier uncertainty due to oscillator errors and satellite and mobile unit doppler shifts is plus or minus 600 Hz. Thus, the signal-to-noise ratio in the initial 1200-Hz detection bandwidth is -0.28 dB. This modem included a coarse frequency determining algorithm for the wide bandwidth low S/N initial detection, a frequency locked loop differential demodulator, and a unique symbol timing algorithm for bit-timing detection. In addition, it was necessary to develop a real-time multitasking operating system for the TMS32020 in order to implement these functions in one processor. A detailed discussion of this modem is provided in Reference [2].

Subsystem Descriptions

Dispatch Terminal: This unit communicates with the mobile unit through a dial-up 1200-b/s full-duplex data circuit to the base station and through the base station to the mobile unit via the satellite link at 200 b/s. It consists of a computer and map display and simulates, for one truck, the features which would be available to a dispatcher or other controller of a multi-truck fleet.

The position of each truck is displayed both as a numerical latitude and longitude and also visually on a map display. The display has several map scales ranging from 1/3 of the world, down to a few city blocks.

The dispatch terminal may request position updates from the mobile units at 2-minute to 8-hour intervals. Immediate position updates may be requested as well. Preformatted (canned) message and free text message capability is also provided.

Mobile Terminal: This unit consisted of:

1. components of a Japan Radio Corp. JUE 35A/B INMARSAT Standard-A shipboard terminal which included the LNA, Diplexer, PA, Main Unit, and Keyboard/Display. The JRC keyboard display was used to place the terminal in a test state that allowed fixed tuning for receive and transmit; therefore, did not require interaction with INMARST's link protocols.
2. An omnidirectional quarter wave monopole antenna.
3. A Rockwell NAVCORE®1 GPS receiver.
4. A LORAN-C receiver and antenna.
5. A COMPAQ II Personal Computer, containing the TMS32020 board that served as the digitally implemented modem. The PC also was used as the mobile terminal keyboard and display.
6. Internally developed hardware to interface the PC/Modem with the JRC main unit. Figure 3 is a photograph of the mobile terminal display showing an extensive library of preformatted text messages which can be selected with a few key strokes. This mode of operation is more suitable for a driver than free text entry, although this was also provided.

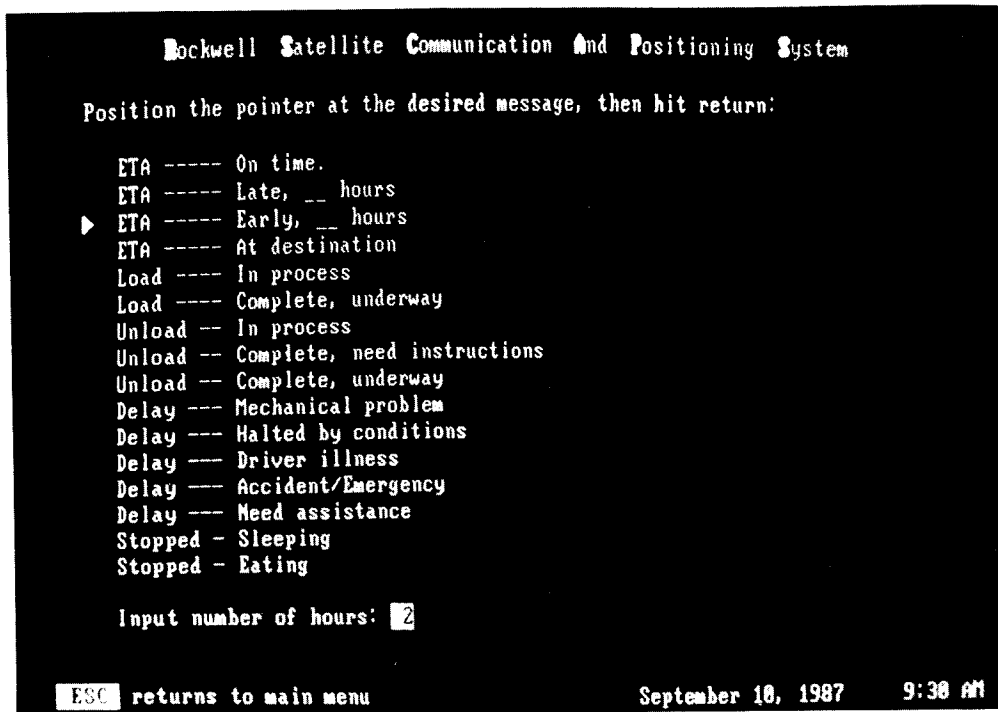


Fig. 3. Photograph of mobile terminal display

Base Station: The operation of the base station, while invisible to the user, is central to the system architecture in that it controls all satellite link functions. For experimental and test purposes, both the mobile unit and the dispatcher can send and receive text messages from the base station screen and keyboard; however, in normal operation the base station is unattended.

The base station consists of a COMPAQ II computer and its internally housed TMS32020 signal processor serving as the RF modem along with an 8-inch rack-mounted unit containing the transmit and receive oven crystal standards, several IF stages and a PSK modulator.

The base station computer contains an internally mounted autoanswer wire-line modem for communication with the dispatch terminal and a hard disk for statistics and software storage. Experimental statistics are extracted at the end of a test drive via the modem line to the dispatch location.

PROPAGATION TEST RESULTS

A major purpose of this project was to take extensive system performance data. System performance is primarily a function of the link between satellite and mobile terminal with signal variations due to blockage by buildings, trees, and terrain and due to multipath fading.

The principal means for quantizing the performance of the system is to monitor the success of the routine short message transactions which take place every three seconds in an idle system and as often as every two seconds when multiple segment messages are passed. The success of the transaction at the base station is determined by correct reception of the response message as indicated by a correct 16-bit cyclic redundancy check (CRC) code. These data are summarized every two minutes coincident with completion of a position report. Both the LORAN-C and the GPS positions are also recorded, Figure 4, shows a GPS position report at 41° 41' 45" N Latitude, 92° 18' 90" W Longitude. The LORAN-C report shows a discrepancy with GPS of about 2200 feet. This is within the normal error range for LORAN-C.

The message throughput statistics contain the number of messages transmitted, error-free messages received, and the number of retransmits listed by message type. Also shown is the number of messages received from the mobile unit. These statistics are updated at the base

Table 2. Summary of 1-hr 25-min run

Mobile unit			Loran-C pos	GPS pos	Base station	
Time intv	Transmitted	Revd			Transmitted	Revd
1:56 - 2:14 P	424	424	Lat 41 42' 00 N Long 92 34' 07 W	41 42' 46" N 92 34' 25" W	430	355
2:14 - 2:30 P	361	370	Lat 41 41' 34" N Long 92 52' 32" W	41 41' 12" N 92 52' 57" W	384	311
2:30 - 2:46 P	367	367	Lat 41 33' 34" N Long 92 56' 31" W	41 33' 19" N 92 56' 23" W	385	318
2:46 - 3:02 P	313	323	Lat 41 24' 16" N Long 92 54' 54" W	41 24' 00" N 92 55' 06 W	396	236
3:02 - 3:21 P	260	261	Lat 41 23' 49" N Long 92 56' 04" W	41 23' 34" N 92 56' 12" W	425	157
Total	1725	1745			2020	1377
Message throughput					Base to mobile unit	
Mobile unit to base - 1377/1725 = 0.798					1745/2020 = 0.864	

CONCLUSIONS

These tests have demonstrated the feasibility and usefulness of an LMSS. Of significance was the ability to provide a usable communication link at low elevation angles and minimal link margins.

REFERENCES

1. Nicholas, D. C., "Land Mobile Satellite Propagation Results" Proceedings of the Mobile Satellite Conference, Pasadena, CA, May 3-5, 1988.
2. Henely, S. J. et. al., "Modem for Land Mobile Satellite Channel" Proceedings of the Mobile Satellite Conference, Pasadena, CA, May 3-5, 1988.

MOBILESTAR FIELD TEST PROGRAM

WAYNE RUBOW, MOBILESTAR Program, Hughes Communications, Inc., United States.

Hughes Aircraft Company
P.O. Box 92919
Los Angeles, California 90009
United States

ABSTRACT

Systems currently under consideration for use in the Mobile Satellite System include Code Division Multiple Access (CDMA) and Frequency Division Multiple Access (FDMA) schemes. The choice between them is difficult because each approach has inherent advantages and disadvantages. The dissimilarity between the two approaches makes a direct comparison difficult and further complicates the choice. Initial studies have raised several questions which must be answered before an intelligent choice can be made.

Hughes Communications has performed various field tests in order to gain practical experience and a broader understanding of mobile communications. The field test program was divided into two main phases. The first phase consisted of CW propagation tests to develop firsthand experience of propagation phenomena. From this information, estimates of the feasibility and accuracy of power control were possible. The next phase tested the idea of power control. Equipment representative of that expected to be used in an actual mobile satellite communication system was assembled and tested under a variety of environments.

TEST PROGRAM DESCRIPTION

A significant problem in communications between mobile platforms and satellites is multipath. As the mobile unit moves, reflected signals add destructively to the desired signals causing fading of signal strength. At the frequency of interest (L-band) this fading occurs frequently and results in deep nulls in the received signal power. To insure a reliable communications link despite such signal fading it may be necessary to apply a significant power margin. Satellite power is directly related to the cost, and a significant power margin could also adversely affect the maximum system capacity. Digital signaling techniques such as coding and interleaving can offer some resistance to the effects of multipath. In addition, CDMA has inherent multipath resistance qualities.

In all cases, (FDMA digital, FDMA ACSSB, or CDMA) a particularly important issue is that of power control. There are two types of fading that are of concern. "Fast fading", the result of multipath, can cause fading at rates between 100 to 300 times per second. This type of fading is uncorrelated over the frequency band spanning the receive and transmit frequencies. Because of the long satellite to earth propagation delay it is not feasible to control the effects of this type of fading through power control. Some coding and interleaving schemes are being evaluated as possible solutions to this problem.

Another type of fading is that which results from shadowing. This "slow fading" affects the average power and may be controlled to some extent by power control. This type of fading is critical to the CDMA access schemes. In a CDMA system the capacity of the system is limited by the E_b/I_0 (the ratio of the user's energy per bit to the co-channel user's energy). In the forward link (from the satellite to the mobile receiver) the fading due to shadowing is not critical because all of the signals from the satellite follow the same path and hence fade together. In this case the E_b/I_0 does not change and the system capacity is unaffected. On the return link however, (from the mobile unit to the satellite) each user's signal follows a different path. At any given time some of the users may be experiencing fading due to shadowing. Hence the E_b (energy per bit) produced by those users as seen by the satellite is reduced. In this case the E_b/I_0 for those users decreases. To combat this problem some margin must be given to E_b/I_0 to ensure that the users experiencing fading due to shadowing still have sufficient E_b/I_0 to communicate. This margin will directly reduce the capacity of the system (which of course reduces revenue).

The return link margin can be reduced if the mobile unit can provide uplink power control. Conceptually, the mobile unit radio would monitor the downlink (forward) power. When it detected a slow decrease in the average power due to shadowing it would increase the uplink (return) transmitter power to compensate. The test program evaluated the effectiveness of providing this power control.

In the FDMA system, satellite capacity is limited by the bandwidth and total forward link power. Forward link power control is desired to compensate for the variation in each mobile unit's signal requirements. The satellite antenna has a N-S variation over the coverage area of about 3 dB. The antenna gain vs. the direction of a mobile unit in Maine will be 3 dB less than the gain in the direction of a user in Kansas. Furthermore, the Maine mobile unit's antenna gain will be perhaps 2 dB less than its peak gain due to the low elevation angle to the satellite. The Kansas mobile user will have the peak antenna gain at its satellite elevation. The Maine user may require 5 dB more satellite power than the Kansas user.

The mobile users power requirements will also vary with terrain. In hilly terrain more power may be required to compensate for partial shadowing. It is therefore desirable for the satellite power on the forward link to be varied; however, because of the long delay in the two way satellite propagation, the forward link power would be corrected only a few times a minute.

Regardless of which access scheme is chosen, some field testing was necessary. Modems representative of those to be used in the proposed system were built and field tested in a variety of typical mobile environments.

CW Propagation Tests

Lake Elsinore, CA, was chosen as the test site for the propagation tests because it provided typical mobile environments, both shadowing and doppler/multipath, and provided the highest available elevation angle in Southern California. The shadowing run that was selected was perpendicular to the hilltop transmitter site and provided approximately one-half mile of groupings of trees, which provided blockage, intermixed with areas of clear line of sight. The doppler/multipath run that was selected provided approximately one mile of clear line of sight with roadside trees, buildings, and other vehicles which provided sources of multipath interference. The elevation angle for the shadowing runs was approximately 15° , and the elevation angle for the doppler/multipath runs varied from 8° to 15° .

Since the performance of the FDMA and CDMA schemes being considered is dependent on controlling the effects of slow fading, data on the fading characteristics were collected. The objective of the propagation tests was to characterize the power correlation properties between the expected uplink and downlink frequencies in order to determine the

accuracy achievable in uplink power control (in the case of CDMA) or downlink power control (in the case of FDMA), and to develop firsthand experience of propagation phenomena.

Typical propagation phenomena results of both shadowing and doppler/multipath environments are given in Figures 1 and 2, respectively. Analysis of these plots indicate that trees reduce signal power approximately 7 dB to 15 dB, depending on the type of tree, size of tree, number and density of branches. Some trees produced as much as 20 dB of blockage. Analysis of the doppler/multipath environment in Figure 2 indicates that multipath effects create approximately 3 dB signal variations. Simulation results tend to indicate that since these variations are uncorrelated between the uplink and downlink frequencies, power control of the multipath disturbances is not feasible.

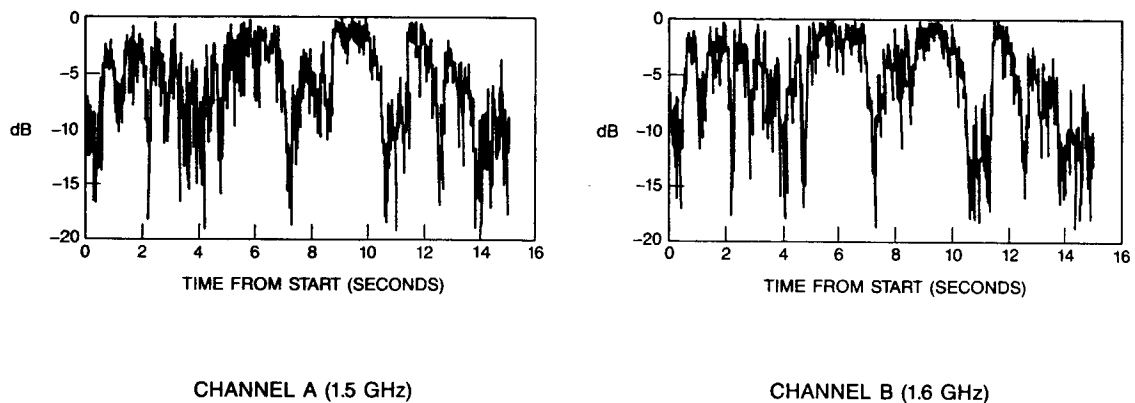


Figure 1. Typical Propagation Phenomena: Shadowing Environment

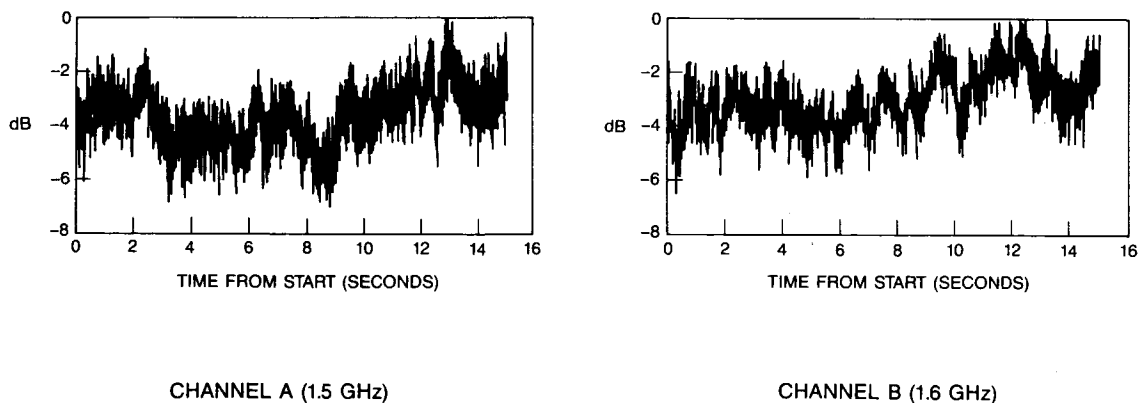


Figure 2. Typical Propagation Phenomena: Doppler/Multipath Environment

In addition to performing test runs using the omni-directional droopy dipole antenna on the mobile vehicle, the directional helical antenna was also tested. Figure 3 shows the antenna comparisons with the mobile vehicle traversing the same run. Analysis of the propagation data in Figure 3 showing the antenna comparison indicates that the multipath contributions are much lower using a directional mobile vehicle antenna, while the shadowing losses are approximately the same.

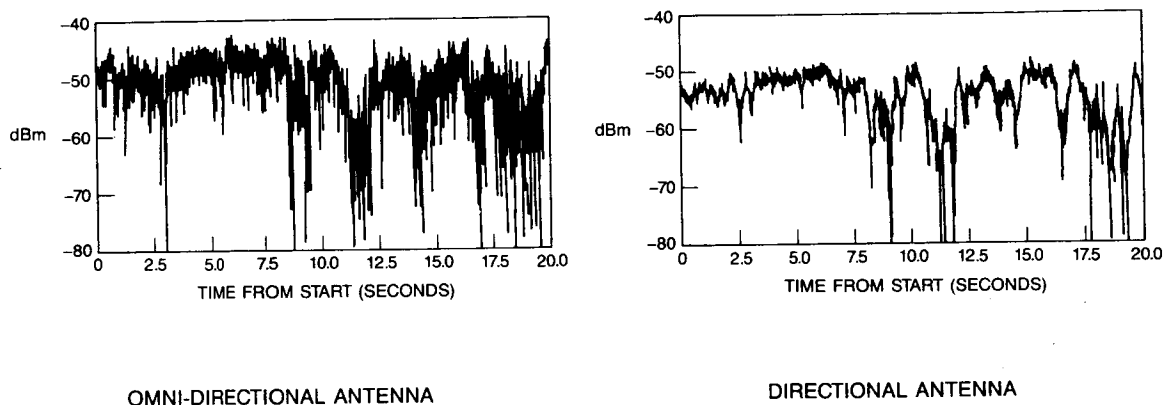


Figure 3. Antenna Performance Comparison

CDMA/FDMA Equipment Tests

The CDMA/FDMA equipment tests were a joint field test program which included participation by Hughes Communications, Inc. and the Canadian Department of Communications. The purpose of the equipment tests was to demonstrate the performance of three systems (FDMA digital, FDMA ACSSB, and CDMA) in actual mobile environments and to compare voice processing techniques in these environments. The performance of power control in the CDMA equipment was also tested. Demonstration of the performance of some of the above systems using both omni-directional and directional antennas was also desired.

The product of these tests was a video tape showing the automobile as it drove in both multipath and shadowing environments with a sound track of the transmitted speech. This video allowed a subjective comparison of the modulation techniques in field situations.

Since the system performance parameter (voice quality), which was used to compare one system to another, is somewhat subjective, appropriate steps were taken to insure that each system was initially calibrated to predetermined specifications. All of the testing used the same live speaker talking directly into telephone instruments in the automobile (as opposed to using a pre-recorded audio tape as the source).

The Canadian Department of Communications supplied the FDMA modems, both digital and ACSSB, along with a 2.4 kbps LPC-357 vocoder. The Canadian DoC also provided a directional antenna. Qualcomm, Inc., supplied the CDMA modems along with a 9.6 kbps RELP vocoder developed by M/A-COM and a 4.8 kbps vocoder developed by

Entropic, Inc.

Test runs at Lake Elsinore, CA, were selected which were representative of mobile system communication environments. These were the same test runs over which the propagation testing was performed. Table 1 describes the system/antenna combinations tested, along with the C/N_0 each system was initially calibrated for. The C/N_0 for the tests were as specified by the manufacturers. ACSSB was operated at the recommended 51 dB-Hz. The FDMA digital system was operated with a margin of about 8 dB above a 10^{-3} BER. The CDMA system was operated with a margin of 2 dB above a 10^{-3} BER.

Table 1. CDMA/FDMA Equipment Test List

<u>System</u>	<u>Data Rate</u>	<u>Vehicle Antenna</u>	<u>C/No</u>
CDMA	4.8 kbps	Omni-directional	41.5 dB-Hz
CDMA	4.8 kbps	Omni-directional	43.5 dB-Hz
CDMA	9.6 kbps	Omni-directional	41.5 dB-Hz
CDMA	9.6 kbps	Omni-directional	43.5 dB-Hz
FDMA ACSSB	N/A	Omni-directional	51.0 dB-Hz
FDMA ACSSB	N/A	Directional	51.0 dB-Hz
FDMA ACSSB	N/A	Omni-directional	48.0 dB-Hz
FDMA ACSSB	N/A	Directional	48.0 dB-Hz
FDMA digital	2.4 kbps	Omni-directional	48.0 dB-Hz

There were limitations to the test results. The 4.8 kbps and 9.6 kbps vocoders used with the CDMA modems were designed for operation in telephone systems under relatively constant signal strength and low bit error rate conditions. Some of the signal fading which occurred in the shadowing runs exceeded the bit error rate operating range of these modems. When such a fade was encountered, the vocoders produced annoying "bleeps". The low elevation angles used during the testing intensified the shadowing and multipath effects.

CDMA/FDMA Equipment Test Conclusions. The end result of these tests was a VHS format video tape. Each system had pros and cons, and, since the results were subjective, opinion varied from individual to individual. Advocates of FDMA ACSSB and advocates of CDMA both believe that the tests proved superiority of their techniques. Although the results were subjective, some generally agreed upon conclusions can be stated.

- The FDMA ACSSB system proved to be very robust in severe shadowing environments. Large signal changes due to shadowing caused a loss of voice quality but maintained a degree of intelligibility.
- In general, the subjective voice quality of ACSSB was generally considered to be less than that of the 4.8 kbps and 9.6 kbps digital voice.
- The CDMA system was able to operate effectively at 2 dB above a 10^{-3} BER, and was also able to operate effectively with 9.5 dB less C/N_0 than ACSSB.
- Above 30 mph, isolated trees did not cause appreciable voice degradation in either system.
- Shadowing by trees is generally much larger than a commercial operator would be willing to provide margin for.
- The voice quality of the FDMA ACSSB system with the omni-directional antenna was surprisingly better than when the directional antenna was used. Later analytical work

has indicated that there is a different propagation phenomena between using omni-directional and directional mobile vehicle antennas; however, no explanation of this anomaly is available at this time.

C-Band CDMA Equipment Tests

The equipment tests done at Lake Elsinore were tests using expected mobile communication environments; however, the hilltop transmission location merely represented the satellite. In order to get experience using an actual satellite, testing was performed using Galaxy II, a synchronous satellite located at 74° W. This provided an elevation angle of approximately 30°. This also provided the opportunity to assess the extent of shadowing on the Los Angeles freeway system.

Transmit equipment was located at the Fillmore, CA, earth station. Galaxy II, transponder 1, was used for the satellite link. The test vehicle was driven around the Fillmore area on freeways and rural streets for four hours. Interference from both other satellites and terrestrial microwave systems was rejected by the spread spectrum processing. The Qualcomm modems along with the Entropic 4.8 kbps vocoders were used for the tests. A 6 dB gain horn was used as the receive antenna. Simplex operation was established; voice transmission was from the Fillmore location to the mobile vehicle.

C-Band CDMA Equipment Test Conclusions. The performance of the CDMA modem with a C-Band link was very similar to that experienced at L-Band. If there was no shadowing, the speech was uninterrupted. The received voice transmission was the only test data recorded. Like the results of the CDMA/FDMA Equipment Tests, these results were also subjective. However, some generally agreed upon conclusions can be stated.

- Because there is very little shadowing on the LA freeway system, the system performance was near perfect, with full outages occurring only under overpasses.
- The system performance on the rural streets was similar to that experienced at Lake Elsinore for the shadowing runs. The system was able to operate effectively at 2 dB above a 10^{-3} BER during line of sight conditions.

Hughes Communications extends their appreciation to John Lodge and Rob Milne of the Canadian Department of Communications for their participation in the CDMA/FDMA equipment test phase of these field tests.

THE JPL MSAT MOBILE LABORATORY AND THE PILOT FIELD EXPERIMENTS

JEFF B. BERNER, Mobile Satellite Program, Jet Propulsion Laboratory, California Institute of Technology, United States; RICHARD F. EMERSON, System Subtask Manager, Mobile Satellite Program, Jet Propulsion Laboratory, California Institute of Technology, United States.

CALIFORNIA INSTITUTE OF TECHNOLOGY
JET PROPULSION LABORATORY
4800 Oak Grove Drive 161-228
Pasadena, California 91109
United States

ABSTRACT

JPL has developed a Mobile Laboratory/Propagation Measurement Van (PMV) to support the field experiments of the Mobile Satellite Experiment (MSAT-X) Project. This van was specially designed to provide flexibility, self-sufficiency, and data acquisition to allow for both the measurement of equipment performance and the measurement of the mobile environment. This paper will describe the design philosophy and implementation of the PMV. It will then discuss the special aspects of the PMV that are unique to Pilot Field Experiments (PiFEx). And finally, it will provide an overall description of the three experiments in which the PMV has been used.

INTRODUCTION

The Mobile Laboratory/Propagation Measurement Van (PMV) was developed to support field experiments for the Mobile Satellite Experiment (MSAT-X) Project. Since these experiments involve both a measurement of the environment and a measurement of the performance of equipment specifically designed for MSAT-X, special emphasis was placed upon flexibility, self-sufficiency and data acquisition. Following a brief description of the PMV, these three aspects will be addressed in more detail. In addition a brief description of the PiFEx tests that have been conducted will be given. Finally, future plans will be outlined.

PROPAGATION MEASUREMENT VAN

The PMV is composed of two elements-- the vehicle, itself, and the support trailer (Figure 1). These elements combine to provide the following functions: Power; Storage; Transportation; Equipment Mounting; Environmental Control; Support Test Equipment; Signal and Power Distribution; and Position Location, Speed and Time.

The vehicle portion of the PMV is a minimally modified "stretch" 1-ton Ford van with a payload capacity of 4200 pounds. The cargo volume of 300 cubic feet is sufficient for two pairs of 4 foot equipment racks. There is enough room between the racks for two people to work comfortably; unfortunately there is not enough room for two seats.

Two aspects of the van's environment are subjected to some control: temperature and shock and vibration. Heat exchangers for the standard truck air conditioner compressor are provided in the cab area and in the payload area. The capacity of the compressor is approximately 2.5 tons, which has proved sufficient even on days with above 90° F ambient temperatures. Air circulation is provided by 48 sixty CFM fans mounted in the equipment racks and heating is supplied by the standard truck heater. Shock and vibration are controlled to some degree by mounting the equipment in heavy racks which are, themselves, shock mounted to the van (Figure 2).

Laboratory instruments were included for the measurement of frequency, time interval, power, voltage, current, spectra and waveform. In addition, the van's position is measured by LORAN C, speed is determined by an interface to the van's transmission, and time is supplied by a WWV receiver. Signal and power distribution is through cable raceways built into the side of the van. This approach enhances the flexibility of the van without compromising safety.

The support trailer provides storage of spares, tools, and the equipment for the fixed station and transponder. It also provides mounting for the motor generator which supplies the 110 volt A/C. The capacity of the generator is 6500 W.

Design for Flexibility

The use of standard RETMA racks with slides allows for the flexible placement of the equipment within the van. Eleven spare RF cables and two spare cable raceways were included to allow a modest amount of expansion. Nearly 100% excess A/C power capacity was provided by the use of a 6.5 kW generator. (Future experiments are expected to use a significant portion of this capacity.)

Design for Self-Sufficiency

Spares were provided for all special equipment (MSAT-X) to the board level and, where appropriate, to the component level. Test equipment, tools, jigs and fixtures needed for repair and calibration with a wide selection of test cables and adapters were included. Emergency equipment including tire chains, trouble lamp, and battery charger were provided.

Data Acquisition

Data acquisition was provided for in three areas: Digital, analog, and visual.

Digital Data Acquisition is accomplished by an augmented industrialized IBM PC/AT (Figure 3). Four channels of simultaneous-sample-and-hold A to D converters were installed to collect the inphase and quadrature outputs of the two receivers-- MSAT-X and Reference. Further, eight channels of multiplexed A to D converters were provided to capture assorted slower data. Digital signals were captured with a 96 channel digital I/O card. The digital signals come from several of the units such as the antenna controller, transceiver, speedometer and, in the future, the terminal processor. RS-232C and IEEE 488 interfaces are also provided to interface with the LORAN C Receiver and laboratory instruments. The data are stored on a dual drive 20 MByte Bernoulli box; a removable cartridge disk. Data Acquisition software provides continuous sampling and recording of data with a modest amount of data displayed in real time. Calibration and verification software can be run in non-real time to validate the data acquisition process.

Analog recording was accomplished by using a 7 channel FM-FM data recorder capable of 10 kHz bandwidth. One of the channels is used for calibration and compensation which improves the fidelity of the recording.

Visual data was captured both on video tape and 35mm still camera.

EXPERIMENTS

The PMV has been thus far used on three major experiments: Tower-1 (T-1), Satellite-1a (S-1a), and Tower-2 (T-2). A brief description of each follows.

Tower-1

The Tower-1 experiments were conducted in Erie CO at the NOAA Wave Propagation Laboratory (WPL) Facility (Figure 4). This facility has a 1000 foot tower capable of supporting several hundred pounds of equipment at any height from ground level to 1000 feet. A translator and omni antenna were mounted on the tower carriage to simulate the spacecraft. These were illuminated from a fixed station housed in one of the WPL shelters. The van with test equipment, units under test, and data acquisition equipment was placed around the base of the tower so that the tracking antenna was illuminated at various angles from 15 to 60 degrees. Antenna pattern, antenna acquisition and modem performance tests were performed with the van stationary. In addition to verifying the system operation (fixed site, translator and mobile site equipments), the information gathered during these tests provides a basis for the comparison of results during the mobile tests and data to assist in subsystem optimization.

Antenna tracking and modem performance tests were also conducted with the van in motion. Several tests were conducted along the north-south road to the east of the tower. This path provided the greatest elevation angle of all those available at the site.

To conduct the mobile antenna tracking tests, the signal level was set and the antenna was acquired with the van stationary at one of the corners. Data acquisition was started and the van accelerated to 30 MPH. The 30 MPH speed was maintained for the 1 mile path to the other corner where the van was turned and driven back. A complete 2.5 minute data block was captured in this way. (For T-1, the DAS only had the capability to record data in 2.5 minute increments.) Tests were made at signal levels which represent the minimum, maximum and nominal values for the expected system.

A similar procedure was followed for the modem tests with the parameter being the signal-to-noise ratio of the modulated signal. The data were recorded on the analog tape recorder. The duration of the test was determined by the recording time per tape cartridge, about 6 minutes.

Satellite-1a

The S-1a experiments were conducted in Santa Barbara, CA, using the INMARSAT MARISAT satellite. This satellite provided an unmodulated L-band carrier from a beacon transmitter which the JPL developed mechanical antenna could track. Both the elevation angle and the received signal strength were well below the MSAT equipment's design values, but the experiment was still a success. Only the ability to track a satellite was tested in this experiment; no modem test could be done. The experiment consisted of acquiring the beacon while the PMV was mobile and tracking the satellite while driving over roads that provided a variety of conditions. For this experiment, the DAS was able to take data continuously, instead of in 2.5 minute slices. Over 500 MBytes of data were collected.

Tower-2

The T-2 experiments were again conducted in Erie, CO at the WPL Facility. This time, the main emphasis was to test the Teledyne-Ryan Electronics phased array antenna. The same set of tests conducted at T-1 (except for the modem tests) was accomplished with the phased array. For continuity, the mechanical antenna was also tested again at this time.

This experiment demonstrated the flexibility of the PMV. The PMV had to accommodate the pointing and control electronics for two different antennas, while allowing for the ability to switch from one antenna to the other with minimal effort and time. Also, a new addition to the DAS allowed the operators to observe assorted pointing information in real time. Previously, this data could only be observed after the test.

CONCLUSIONS

The complement of equipment was found to be appropriate for the experiments conducted during the three experiments. This will be reviewed prior to each subsequent experiment to assure success in the field. The data acquisition system was placed in the racks assuming

two people would be required to conduct the experiments. The experience has shown that the experiments can be conducted with only one operator. Therefore, the DAS should be moved to provide easier access.

Approximately 750 MBytes of digital data, 280 minutes of analog data, and several hours of video tape have been collected during the three experiments. Preliminary analysis of the antenna data has led to improvements in the design of the mechanical antenna and the modem data has been used in the development of the final version of the modem. The data collected from S-1a is being used by the MSAT system team to determine fade rates and fade durations that may be encountered. Due to the sheer mass of data that exists, complete evaluation of the data will not be completed for some time.

FUTURE PLANS

These tests were the first of several field tests to be done with the PMV and MSAT-X equipment. Tower-3 tests are planned for Summer of 1988 and will be used to conduct the first field end-to-end test of the MSAT system. Real-time modem tests will be conducted and initial verification of the Network ARQ protocol will be done.

Later this summer, the PMV will conduct the second satellite test (S-1b). This will take place in Hawaii, again using an INMARSAT satellite. Both of the antennae that have previously been tested and the second phased array antenna (Ball Aerospace) will be used in the experiment. Hawaii was selected because it will provide an elevation angle of 50° to the satellite. While the configuration only supports one way operation, this is adequate to continue performance measurements of the antennae and to conduct realistic propagation experiments with the L-Band satellite to mobile ground link.

ACKNOWLEDGMENTS

We appreciate the fine support that the staff at WPL provided, particularly the help of John Gaynor, Dave Gregg and Norbert (Ski) Szczepczynski. We also appreciate the PMV design assistance given by Dr. W. Vogel of the University of Texas. His experience with a similar vehicle so freely shared helped us avoid many a pitfall. Finally, a special word of appreciation for the dedication of the JPL MSAT-X team who accompanied us to the field: Walt Mushagian, Norman Lay, William Rafferty, Jim Parkyn and Vahraz Jamnejad.

ORIGINAL PAGE IS
OF POOR QUALITY

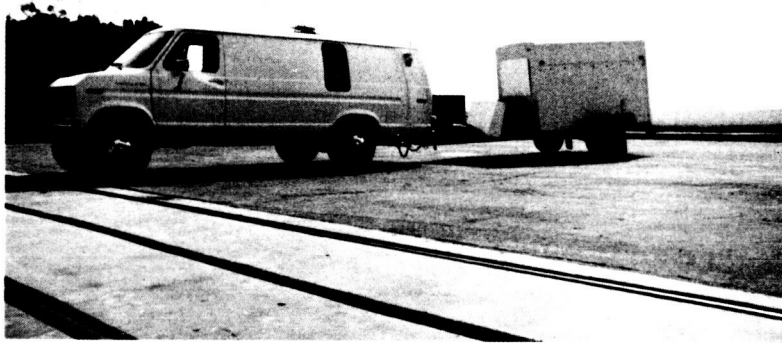


Figure 1: The Van and Trailer

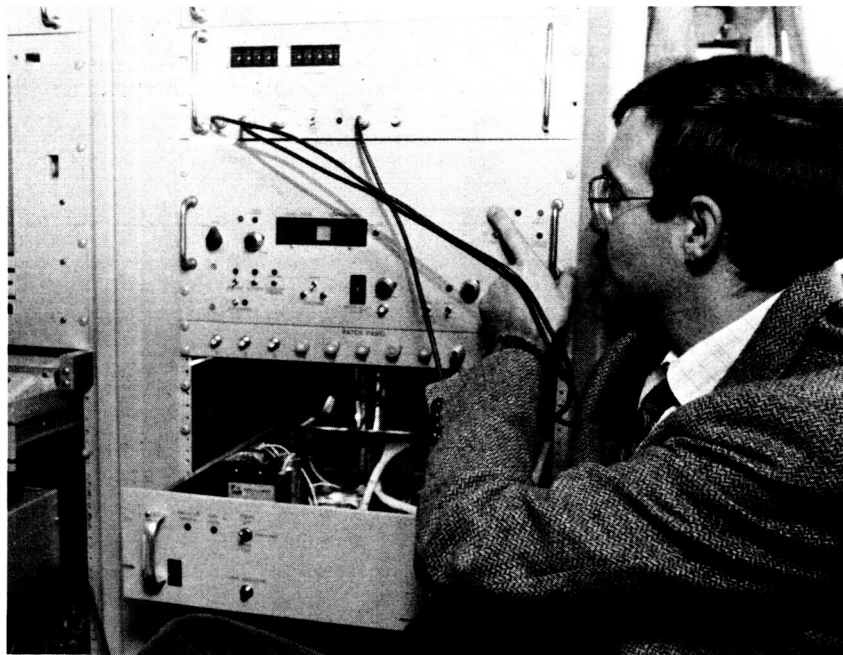


Figure 2: The Interior of the Van

ORIGINAL PAGE IS
OF POOR QUALITY

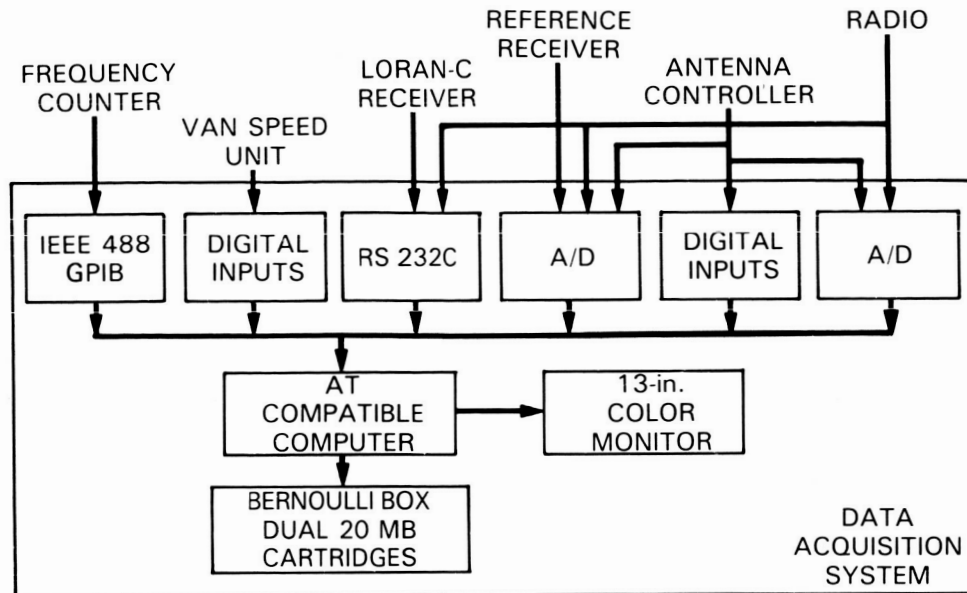


Figure 3: DAS Block Diagram

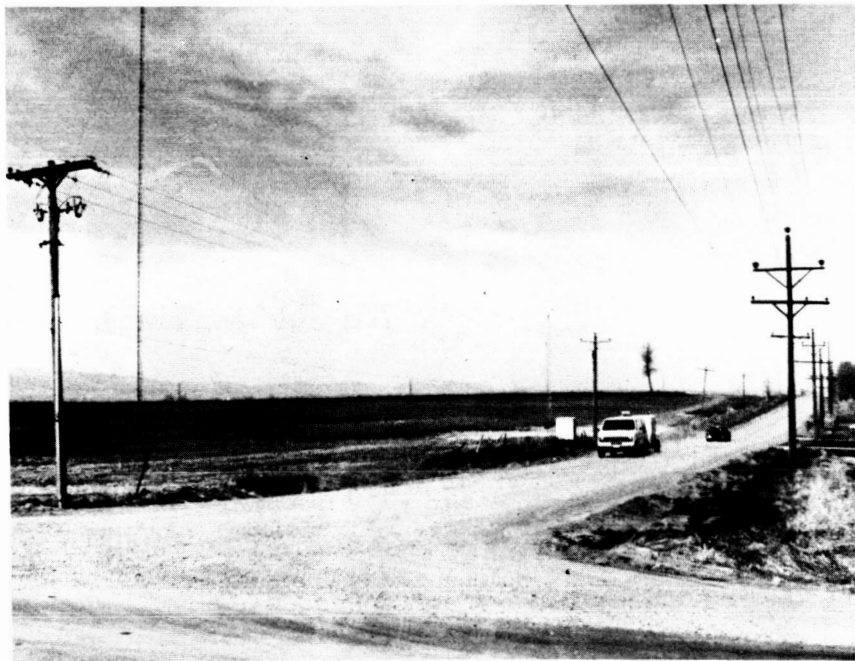


Figure 4: Tower and Van in Erie

TECHNICAL CHARACTERISTICS OF THE OMNITRACS - THE FIRST OPERATIONAL MOBILE KU-BAND SATELLITE COMMUNICATIONS SYSTEM

FRANKLIN P. ANTONIO; KLEIN S. GILHOUSEN; IRWIN M. JACOBS; LINDSAY A. WEAVER, Jr., all of QUALCOMM, Inc., United States.

**QUALCOMM, Incorporated
10555 Sorrento Valley Road
San Diego, California 92121
United States**

ABSTRACT

The technical characteristics of the OmniTRACS system are described. This system is the first operational mobile Ku-Band satellite communications system and provides two-way message and position determination service to Mobile Terminals using existing Ku-Band satellites. Interference to and from the system is minimized by the use of spread spectrum techniques, together with low power, low data rate transmissions.

INTRODUCTION

The OmniTRACS Network (developed for Omninet Corporation, Los Angeles, CA) provides Mobile users with a cost-effective, two-way message and position location service using existing Ku-Band satellites. An optional position-determination device integrated into the Mobile terminal allows the position to be transmitted automatically to the Hub. A variety of preformatted and free-form text messages of up to 2000 characters are supported. An optional printer will permit transcription of messages to hardcopy.

Figure 1 shows the basic OmniTRACS system. All message traffic passes through a central Hub or Network Management Facility (NMF). The NMF contains a 7.6 meter earth station including satellite modems for communication with the Mobile terminals via the satellite, a Network Management Computer for message management and tracking, and telephone modems for connection with customer operation centers.

Because transmission from a mobile platform at Ku-Band falls under a secondary allocation, the units must not interfere with fixed services but at the same time must tolerate interference from those services. This calls for a design approach akin to an LPI anti-jam system. Accordingly, a judicious combination of frequency hopping and direct sequence spread spectrum waveforms are utilized, together with low power, low data rate transmissions.

The OmniTRACS system began operational tests in January, 1988 in which a Mobile terminal was driven from coast to coast in constant communication with a Hub terminal located in San Diego, California. Operation was very successful in all kinds of environments from wide open Western freeways to the concrete canyons of New York City. The program is now entering production.

SYSTEM DESCRIPTION

The system uses two transponders in a single Ku-Band Satellite. One transponder is used for a moderate rate (5 kbs) continuous data stream from the Hub to all the Mobile

Terminals (system users can also be transportable or fixed) in the system. Messages are addressed to individual Mobile terminals or to groups of Mobile terminals on this channel. To aid in frequency co-ordination, two forward link modulations are provided. In one, frequency-hop spread-spectrum techniques are used to spread the power density over a wide bandwidth. These techniques reduce the downlink power density to acceptable levels and provide processing gain that the Mobile Terminals use to reject the signals from adjacent satellites. The other modulation for the forward link uses a triangle wave FM dispersal waveform similar to that used by satellite television signals, resulting in interference properties similar to television signals.

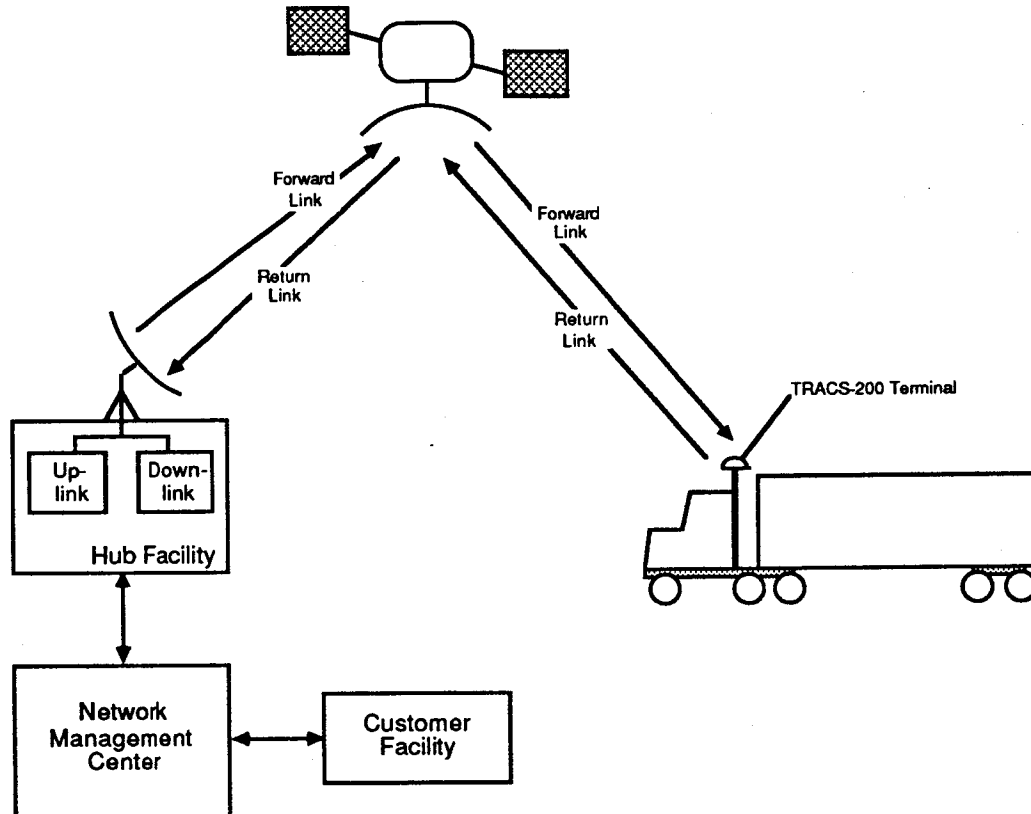


Figure 1: OmniTRACS System Block Diagram

A second transponder on the same satellite is used by the return link. Each Mobile terminal has a low transmit power level (+19 dBW EIRP). This power level allows data rates on the return link ranging from 22 to 132 bps, depending on available link margin for each individual terminal. The antenna pattern of the mobile terminal is rather broad (~6° beamwidth along the orbital arc) and therefore the potential exists—even at such low power levels—to cause interference to users in adjacent satellites. To mitigate this interference, several techniques are used:

1. Direct-sequence spread-spectrum techniques are used to spread the instantaneous power spectral density of each mobile uplink over a bandwidth of 1.0 megahertz.
2. Frequency hopping and FDM techniques are used to ensure that the power spectral density produced by the combination of all active Mobile Terminals is uniformly spread over a bandwidth of 48 megahertz.
3. The transmissions of the mobile terminals are very carefully controlled. A mobile terminal will not transmit unless commanded to do so, either as a direct request

(acknowledgement, report, etc.) or as a response to a carefully defined—and limited—group poll. This polling technique controls the number and frequency location of mobile transmitters at all times so that the level of interference can be tightly regulated. Furthermore, reception of the command implies that the antenna is correctly oriented for transmission.

As a result of the above techniques, interference to other satellite services by a network consisting of tens of thousands of Mobile terminals is less than that caused by conventional VSAT terminals.

MOBILE TERMINAL DESCRIPTION

Figure 2 shows a functional block diagram of the mobile terminal. A microprocessor implements all of the signal processing, acquisition and demodulation functions. The antenna has an asymmetric pattern ($\sim 40^\circ$ 3 dB beamwidth in elevation and $\sim 6^\circ$ beamwidth in azimuth). It is steerable in azimuth only. A low-noise amplifier and conventional down-conversion chain provide a signal to the microprocessor for acquisition, tracking and demodulation. During transmission, an up-conversion and spreading chain provide signal in the 14-14.5 GHz band to the 1.0 Watt power amplifier. This signal is transmitted via the steerable antenna that has a maximum gain of +19 dBi for a total transmit power of +19 dBW.

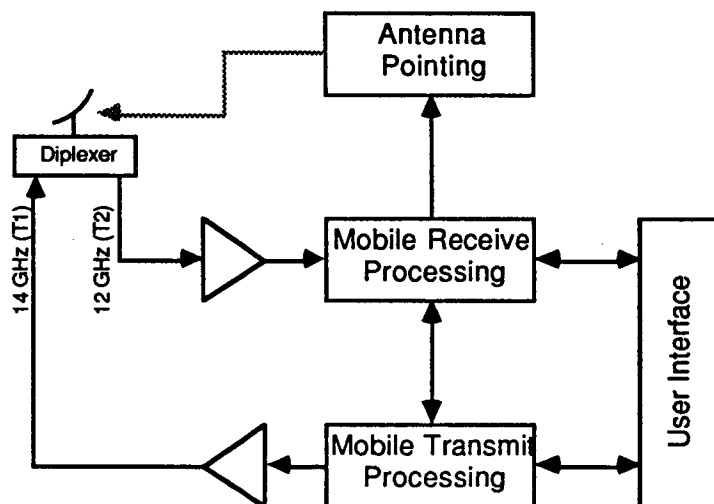


Figure 2: Mobile Terminal Block Diagram

Whenever the Mobile unit is not in receive synchronization, it executes a receive acquisition algorithm until data from the satellite can be demodulated. At this point, the antenna is pointed towards the satellite and messages can be received from the Hub. When commanded by the Hub, the Mobile may start transmission of a message. The terminal is half-duplex, and transmissions are done at a 50% duty cycle to allow for continued antenna tracking of the received downlink signal. If at any time during a transmission the receive signal is lost, the terminal ceases transmission to prevent interference from being generated.

DESCRIPTION OF RETURN LINK MODULATING SIGNAL

Binary data at 44.1 bits per second is rate 1/3 convolutionally encoded to produce code symbols at a rate of 132.3 symbols per second. These code symbols are used four at a time to drive a 16-ary FSK modulator at a rate of 33.1 FSK baud. A 50% transmit duty cycle produces an FSK symbol period of 15.1 ms. The tones out of the FSK modulator

are direct-sequence spread at a rate of 1.0 Megachip per second for an instantaneous bandwidth of 1.0 MHz. This 1.0 MHz bandwidth signal is then frequency hopped over a 48 MHz bandwidth. To maximize system capacity in areas with good satellite G/T and to provide adequate margin in areas with poor G/T, 0.5x and 3.0x data rates of 22.0 and 132.3 bps are also provided. These are implemented by FSK symbol repetition and a three times FSK symbol rate respectively.

RETURN LINK POWER DENSITY

The OmniTRACS Terminals meet the VSAT Inbound Guidelines for transmit power density along the equatorial arc. Figure 3 shows the Mobile Terminal antenna pattern in azimuth keeping elevation at maximum gain. This figure assumes a nominal boresight gain of 19 dBi. The sidelobes of this antenna are asymmetric and non-uniform, but stay below -12.0 dB relative to boresight gain.

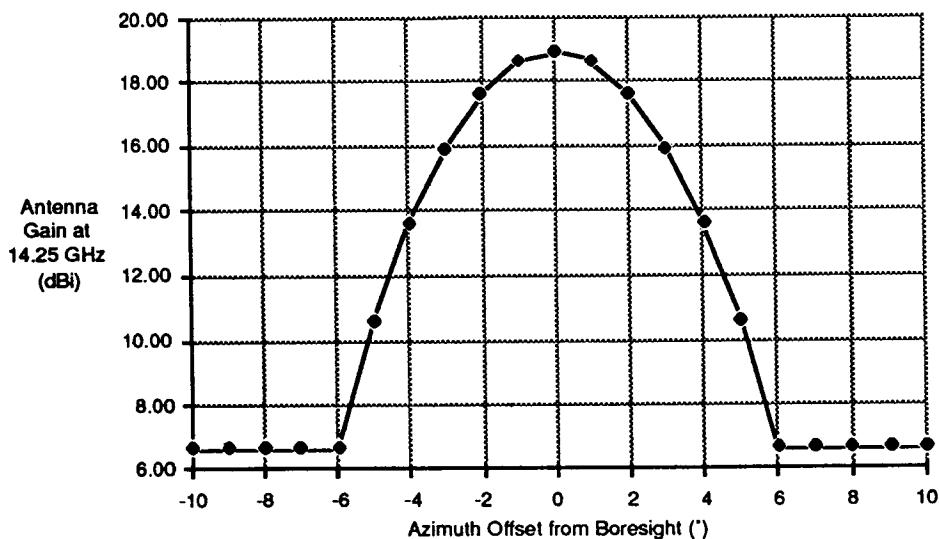


Figure 3: OmniTRACS Transmit Antenna Gain (Azimuth Cut)

Table 1 shows the maximum transmit power density link budget for the OmniTRACS System Return Link with 250 units transmitting simultaneously. Table 1 combined with the OmniTRACS transmit antenna pattern of figure 3 produces the EIRP power density shown in figure 4. Also shown in figure 4 is the guideline from footnote 35 of the April 9, 1986 Declaratory Order.

Table 1: OmniTRACS System Return Link Power Density		
Max. Tx Power	1.26 Watt	1.0 dBW
Max. Tx Antenna Gain		19.0 dBi
Occupied BW	48,000,000 Hz	-76.8 dB/Hz
FCC Reference BW	4,000 Hz	36.0 dB-Hz/4kHz
Number of Uplinks	250	24.0 dB
Tx Duty Cycle	50%	-3.0 dB
System EIRP Density		0.2 dBW/4kHz

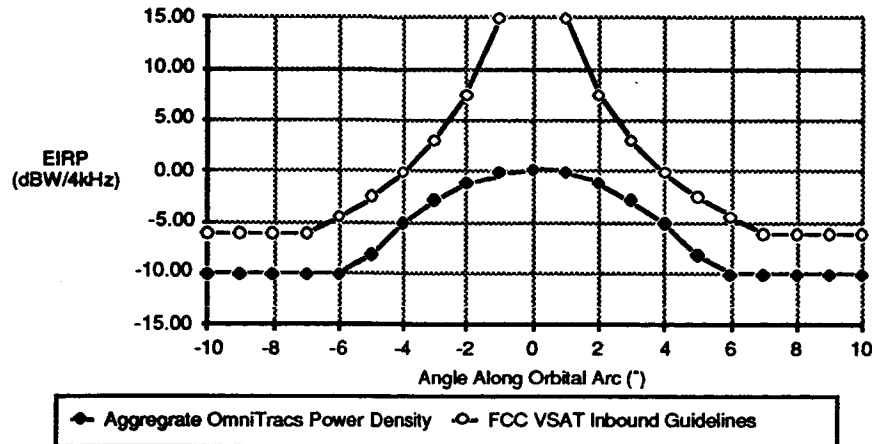


Figure 4: OmniTRACS Return Link Power Density Compared to FCC VSAT Inbound Guideline

DESCRIPTION OF FORWARD LINK MODULATING SIGNAL

Binary data at 4,960.3 bits per second is rate 1/2 block encoded to produce code symbols at a rate of 9,920.6 symbols per second. These code symbols are used to drive a BPSK modulator at a rate of 9,920.6 PSK baud. In mode A, this signal is frequency hopped to a new center frequency every 5.04 ms to occupy a total bandwidth of 24 MHz.

Mode B uses a triangle wave dispersal waveform instead of frequency hopping, resulting in similar co-ordination properties to video signals. The Mode B power density calculations are shown below in table 2.

Satellite Transmit EIRP		44.0 dBW
Occupied Bandwidth	2,000,000 Hz	-63.0 dB/Hz
Reference FCC Bandwidth	4,000 Hz	36.0 dB-Hz/4kHz
Transmit Power Density		17.0 dBW/4kHz

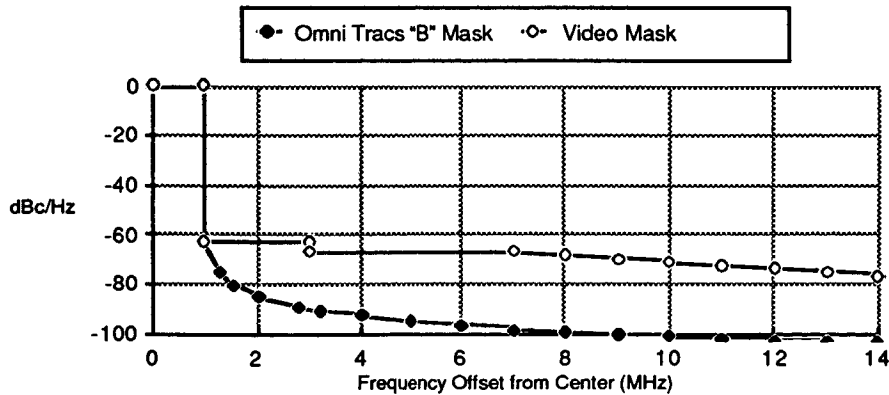


Figure 5: Suggested Coordination Mask for OmniTRACS Mode B Forward Link Compared with Video Coordination Mask

Coordination for Mode B will be easier than coordination of a video signal. The frequency band in the range of ± 1.0 MHz about the center of the dispersal waveform will contain relatively high instantaneous power densities, but the frequency bands outside of this ± 1.0 MHz range will drop off rapidly—even faster than video signals. Figure 5 shows the coordination mask that should be used with the OmniTRACS Mode B Forward Link Signal compared with the coordination mask suggested by the FCC Advisory Committee on 2° Orbital Spacing for video signals.

DESCRIPTION OF MOBILE TERMINAL HARDWARE

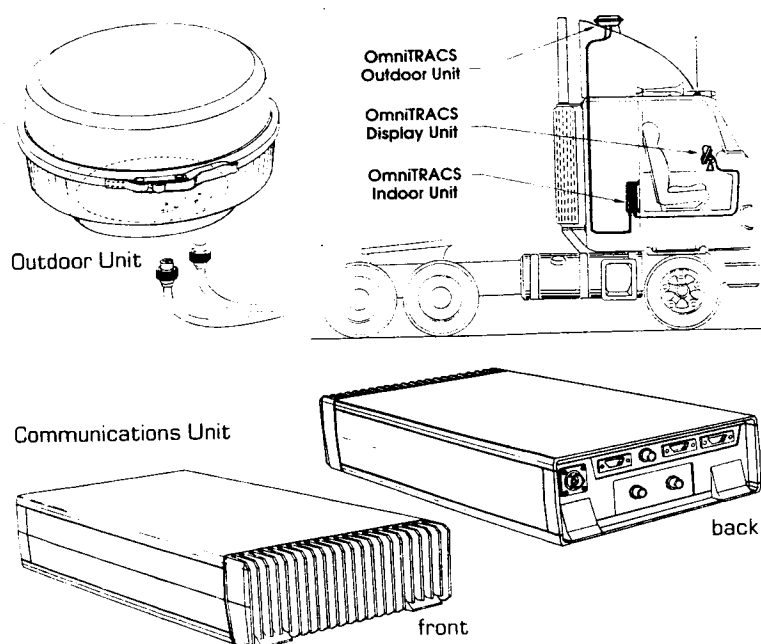
The OmniTRACS Mobile Terminal, shown below in Figure 6, consists of three units: the Outdoor Unit, the Communication Unit and the Display Unit. The OmniTRACS terminal can operate in a temperature range between -30° and 70°C .

The Outdoor Unit contains the antenna assembly and front-end electronics. The outdoor unit (including antenna) is approximately 10" in diameter, 6" high and weighs approximately 9 lbs. The Outdoor Unit can be mounted on a vehicle roof or a mast (for a truck cab).

The Communication Unit contains an analog section, digital electronics and the LORAN receiver which are contained on four circuit card assemblies. The approximate dimensions of the Communication Unit are 4"x8"x9" and it can be mounted anywhere in the vehicle since it does not require operator access.

The Display Unit consists of a 40 character by four line display and an ABCD or QWERTY keyboard. The display unit also provides several function keys for pre-programmed user functions. The display contains indicators for message waiting, satellite synchronization and power indication. The display unit also provides a maintenance mode for in-field troubleshooting and Mobile unit initialization. The display unit is 6"x10"x1" and can be located on the dashboard or any other convenient location.

Figure 6: Mobile Terminal Hardware



SESSION E
VEHICLE ANTENNAS

SESSION CHAIR: Paul E. Mayes, University of Illinois
SESSION ORGANIZER: Kenneth Woo, Jet Propulsion Laboratory

AN ADAPTIVE ARRAY ANTENNA FOR MOBILE SATELLITE COMMUNICATIONS

ROBERT MILNE, Mobile Satellite Project, Communications Canada, Canada.

Communications Canada
 Communications Research Centre
 3701 Carling Avenue
 P.O. Box 11490, Station "H"
 Ottawa, Ontario CANADA
 K2H 8S2

ABSTRACT

The adaptive array antenna is linearly polarized and consists essentially of a driven $\lambda/4$ monopole surrounded by an array of parasitic elements all mounted on a ground plane of finite size. The parasitic elements are connected to ground via pin diodes. By applying suitable biasing voltages, the desired parasitic elements can be activated and made highly reflective. The directivity and pointing of the antenna beam can be controlled in both the azimuth and elevation planes using high speed digital switching techniques. The design concept, combined with micro-processor technology, provides a powerful mechanism for optimizing the radiation patterns of the antenna under a wide range of operating conditions. The antenna RF losses are negligible and the maximum gain is close to the theoretical value determined by the effective aperture size. The antenna is compact, has a low profile, is inexpensive to manufacture and can handle high transmitter power.

DESCRIPTION

An antenna consisting of 5 rings of parasitic elements is shown in Fig. 1. It has an angular coverage of 360° in azimuth and between 15° and 60° in elevation. The antenna gain varies between 9 and 11 dBic in the receive band of 1530 - 1560 MHz and between 6 and 10.5 dBic in the transmit band of 1630 - 1660 MHz. The power handling capability is 100 watts. The antenna array, including radome, is less than 2 inches in height and 20 inches in diameter. The parasitic element, shown in Fig. 2, is a composite structure which acts as both radiator and RF choke and incorporates a pin diode and RF by-pass capacitor. The theory of operation is described using the co-ordinate system of Fig. 3. Ignoring the effects of mutual coupling between elements and the finite size of the ground plane, the total radiated field of the array is given by:

$$E(\theta, \phi) = A(\theta, \phi) + KG(\theta, \phi) \sum_{i=1}^N \sum_{j=1}^{M(i)} F_{ij}(r_i, \phi_{ij}, \theta, \phi)$$

$A(\theta, \phi)$ is the radiated field of the driven element, K is the complex scattering coefficient of the parasitic element, $G(\theta, \phi)$ is the radiated field of the parasitic element, $F_{ij}(r_i, \phi_{ij}, \theta, \phi)$ is the complex function relating the amplitude and phases of the driven and parasitic radiated fields. N is the number of rings of parasitic elements, $M(i)$ is the number of elements in the i ring.

By activating the required number of parasitic elements at the appropriate r_i , ϕ_{ij} co-ordinates, the directivity and pointing of the antenna beam can be controlled in both the azimuth and elevation planes.

GAIN

The antenna gain is a function of the array diameter, the number and directivity of the parasitic elements, the frequency of operation, ground plane size and the required angular coverage. Antenna arrays of 3, 4 and 5 rings have been designed, built and tested. The measured gains over the specified angular coverage of 15 - 60° in elevation and 360° in azimuth with the arrays mounted on a 36 inch diameter ground plane are as follows:

No. of Rings:	3	4	5
Rx Gain (dBic)	7.5 - 9.5	8.5 - 10.0	9.0 - 11.0
Tx Gain (dBic)	6.0 - 9.5	6.0 - 10.0	6.0 - 10.5

The measured received gain of a 5 ring array versus elevation angle is shown in Table 1.

RADIATION PATTERNS

To provide coverage between 15° and 60° in elevation 3 beams are required. A maximum of 32 beams are required to provide 360° coverage in azimuth. Typical azimuth and elevation patterns are shown in Figures 4-8. The patterns have been optimized to maximize received gain and inter-satellite isolation and minimize the effects of multipath on communications and tracking performance.

RETURN LOSS

The return loss of the antenna is a function of both frequency and the array switching configuration. The return loss versus frequency for the 3 basic elevation switching configurations is shown in Figure 9. The maximum return loss for all beam positions is less than -12 dB (VSWR < 1.7) in both the receive and transmit frequency bands.

RF LOSS/NOISE TEMPERATURE

The RF loss of the antenna is less than 0.1 dB which contributes about 7° K to the systems noise temperature. Noise temperatures of less than 85° K have been measured at the output of the antenna, mounted on a vehicle in a typical operational environment, with the beam pointing at 25° elevation. The noise temperature contribution should be significantly lower at higher elevation angles. The resulting systems G/T will be 1.5 to 2.0 dB higher than conventional phased array designs with higher RF loss but the same net gain.

VEHICLE INTERFACE/EFFECTIVE GROUND PLANE SIZE

The vehicle structure will affect the gain, polarization and radiation patterns of any antenna mounted on it. This is particularly true of an antenna designed for low elevation coverage. Measurements have been conducted using a 5 ring array to determine the effects of ground

plane sizes ranging from 4 feet x 5 feet to 10 feet x 5 feet for both flat and curved surfaces, with curvatures of 6°/foot. The effect of extending or curving the ground plane is to tilt the "low" beam towards the horizon, thereby increasing the gain at low elevation angles. A gain of 8 dBic can be achieved at 5° elevation with the array mounted on a 5 feet x 5 feet ground plane.

INTER-SATELLITE ISOLATION

The isolation achievable is a function of antenna directivity, satellite location and the latitude and longitude of the vehicle. Isolation measurements have been carried out using a 5 ring array in an anechoic chamber. The results are shown in Table 2 for various satellite separations and vehicle locations in the U.S. and Canada. Full duplex operation is assumed and that the land vehicle uses the satellite with the higher elevation angle. A $\pm 5^\circ$ pointing error results in a spread of isolation values. Higher values of isolation can be achieved in some cases at the expense of some loss in antenna gain.

Multipath effects will, however, determine the upper limit of isolation achievable. With the antenna beam pointing at one satellite, signals will be scattered by objects in the beam in the direction of the other satellite. The magnitude of the signals will depend on the proximity and reflecting properties of the scatterers, the relative satellite elevation and azimuth angles, and the directivity of the land vehicle antenna.

CONTROLLER DESIGN

The controller is required to accurately point the antenna beam at the satellite under all dynamic conditions of the host vehicle if the advantages of a directive antenna are to be realized. In the acquisition mode the beam is sequentially stepped through 360° and the beam with the strongest signal selected. The satellite is subsequently tracked by periodically switching the beam on either side of the previous satellite position and selecting the beam with the strongest signal. Successful field trials were conducted in an INMARSAT operational satellite system. The selected circuit time constants were based on a C/N ratio of 50 dB-Hz, a receiver output bandwidth of 1000 Hz and a S/N ratio at the input of the controller of 20 dB. After frequency locking it required less than 20 ms to re-acquire the satellite. The tracking sampling interval was less than 5 ms. The tracking sampling rate could be varied manually from 0.25 Hz to 4 Hz to match vehicle angular velocity.

COST

The predicted cost of the antenna and controller is less than \$1000 (Can.) in quantities of 10,000/year. The low cost is due to the elegant simplicity of design. The parasitic element has a minimum number of parts and lends itself to mass production techniques. Its electrical characteristics are highly repeatable and simple to measure, thereby reducing testing and assembly cost. The antenna ground plane provides a well defined interface between the RF and digital switching components and eliminates the need for expensive microstrip.

ORIGINAL PAGE IS
OF POOR QUALITY

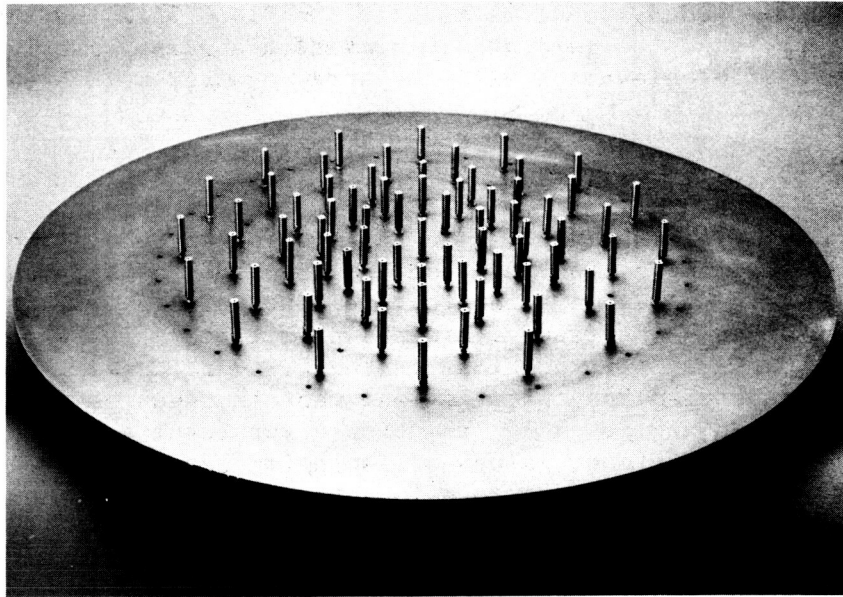


FIG. 1 ADAPTIVE ARRAY ANTENNA

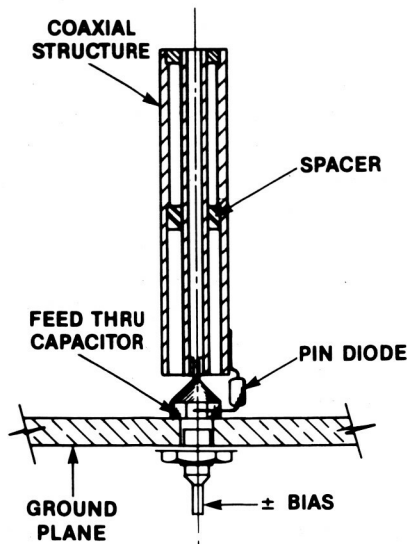


FIG. 2 PARASITIC ELEMENT

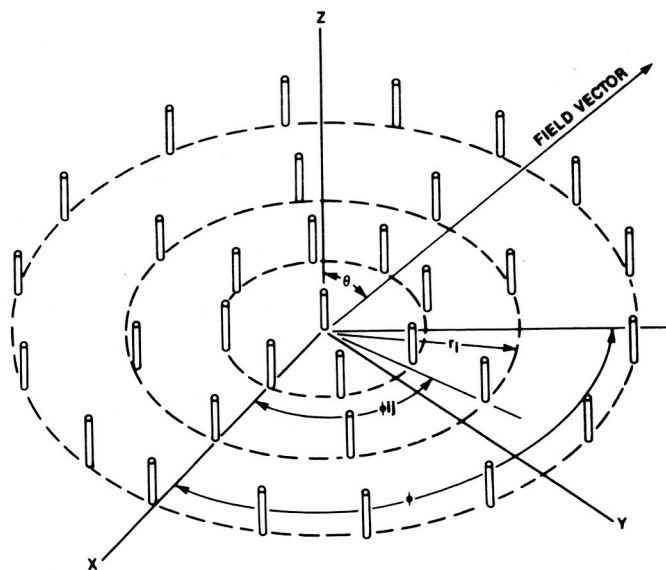


FIG. 3 CO-ORDINATE SYSTEM

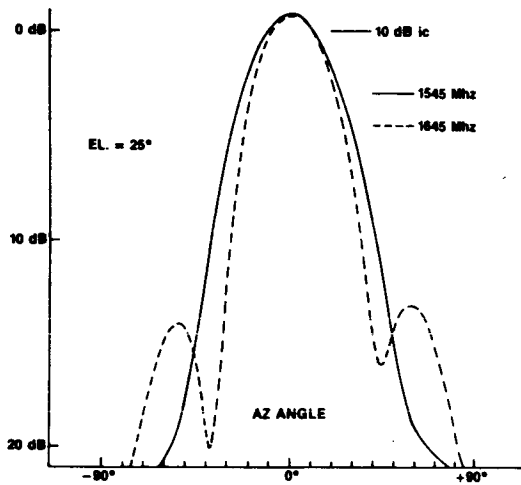


FIG. 4 AZ. PATTERN - LOW BEAM

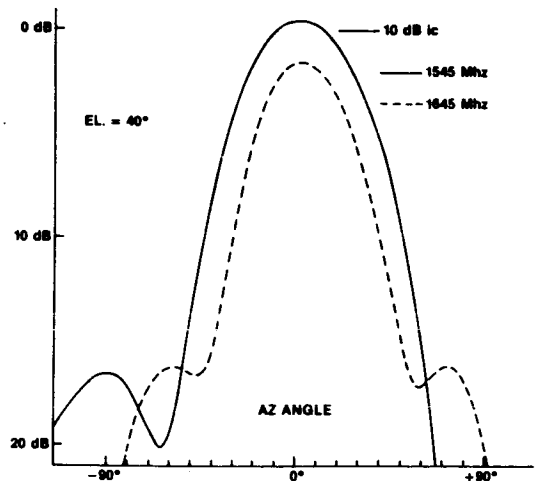


FIG. 5 AZ. PATTERN - INTERMEDIATE BEAM

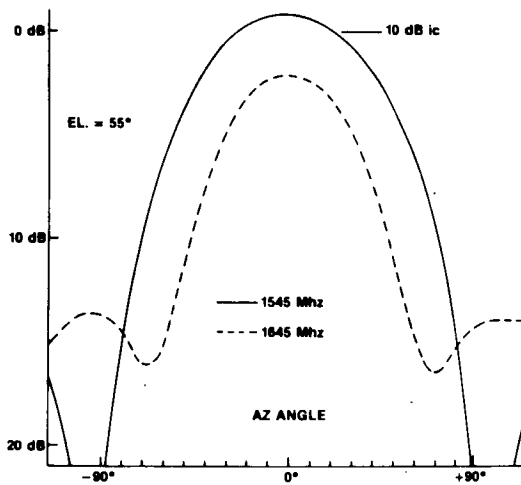


FIG. 6 AZ. PATTERN - HIGH BEAM

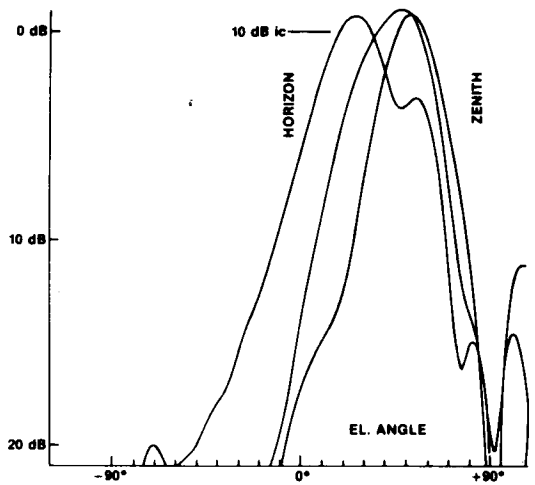


FIG. 7 EL. PATTERNS - 1545Mhz.

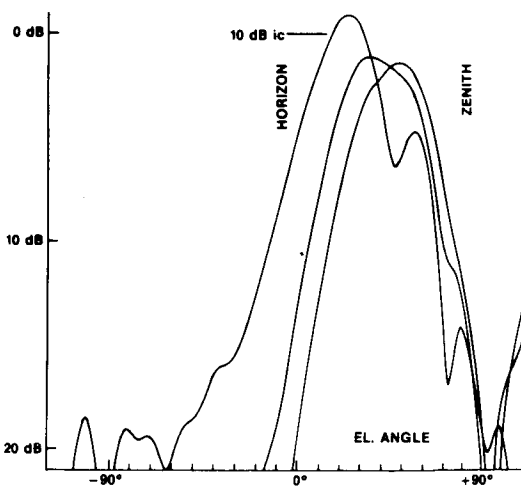


FIG. 8 EL. PATTERNS - 1645Mhz.

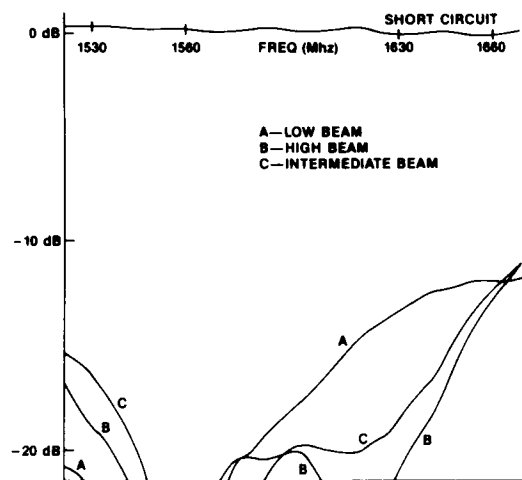


FIG. 9 RETURN LOSS VERSUS FREQUENCY

ORIGINAL PAGE IS
OF POOR QUALITY

ELEVATION ANGLE	LOW BEAM	INTERMEDIATE BEAM	HIGH BEAM
0	4.0	-2.6	-9.0
5	6.0	0.0	-6.8
10	7.5	1.8	-4.6
15	9.0	3.9	-2.0
20	10.0	5.7	0.2
25	10.4	7.3	2.7
30	10.4	8.5	4.9
35	9.6	9.6	6.9
40	8.1	10.0	8.4
45	5.8	10.1	9.7
50	4.3	9.9	10.4
55	4.5	8.6	10.4
60	4.6	6.7	9.6
65	3.2	3.7	7.7
70	-0.6	-0.6	5.2

TABLE 1 Measured Rx Antenna Gain (dbic)

Satellite Location	80, 115 (West)		80, 120 (West)		80, 125 (West)		80, 130 (West)	
	Rx	Tx	Rx	Tx	Rx	Tx	Rx	Tx
Ottawa	9-13	13-20	12-17	18-22	15-20	21-22	18-21	20-23
St. Johns	8-13	9-16	11-16	12-19	15-19	16-19	18-22	20-19
Vancouver	8-13	10-17	11-15	15-16	14-17	15-17	17-19	14-16
Winnipeg	10-15	14-16	13-17	13-15	15-18	13-14	17-19	13-15
Whitehorse	10-14	11-18	12-16	15-20	15-19	19-20	17-19	19-20
Frobisher	10-14	14-19	13-17	16-20	16-20	18-19	19-22	18-20
Inuvik	10-14	11-18	13-17	15-19	14-19	18-19	17-20	18-19
Honolulu	13-14	11-13	14-15	12-15	14-15	13-17	14-16	13-18
Miami	7-10	15-30	11-15	20-27	13-18	24-25	16-20	28-30
New Orleans	8-12	18-25	11-15	24-37	16-22	20-27	19-26	21-24
Los Angeles	10-15	13-18	14-18	17-18	18-20	18-19	20-21	18-21
Salt Lake City	9-15	15-20	13-18	19-20	16-20	19-20	19-22	19-22
Chicago	9-14	15-19	13-18	19-20	16-19	19-20	18-19	19-20
Boston	9-13	11-20	12-16	16-23	15-19	20-22	17-21	21-25
Anchorage	12-16	12-18	13-18	15-19	16-20	18-19	19-22	18-19

TABLE 2 ISOLATION (db) AS A FUNCTION OF SATELLITE LOCATION

**MSAT MOBILE ELECTRONICALLY STEERED PHASED ARRAY ANTENNA
DEVELOPMENT**

FRED SCHMIDT, MSAT Program Manager, Ball Aerospace Systems Group,
United States

BALL AEROSPACE SYSTEMS GROUP
10 Longs Peak Drive
Broomfield, Colorado 80020
United States

ABSTRACT

The MSAT-X breadboard antenna design demonstrates the feasibility of utilizing a phased array in a mobile satellite application. An electronically steerable phased array capable of tracking geosynchronous satellites from anywhere in the Continental United States has been developed. The design is reviewed, along with test data. Cost analyses are presented which indicate that this design (when optimized for volume production) can be produced at a cost of \$1620 per antenna.

INTRODUCTION

Ball Aerospace Systems Division developed a breadboard electronically steered phased array antenna for use in the MSAT-X mobile telephone communications system. The antenna transmit and receive bands are 1646.5-1660.5 MHz and 1545.0-1559.0 MHz, respectively. The antenna gain requirement is 10 dBic (RHCP) in the direction of the satellite throughout the coverage region (0-360 degrees in azimuth, 20-60 degrees in elevation). The ultimate goal of the program effort is to develop an antenna which meets the specs in addition to being manufacturable, reliable, and economical, in order to meet the needs of the MSAT end user.

DESIGN

The mounting configuration for the MSAT-X system is shown in Figure 1. The phased array is mounted on the car roof and the pointing system electronics are mounted in the trunk, along with the transceiver. The system block diagram is shown in Figure 2. The beam steering computer consists of a single-board PC clone and associated interface circuitry. This will be replaced with an 8086-based microprocessor system or single-chip micro-controller in later versions. The beam steering computer performs all antenna acquisition and tracking functions. For acquisition, the antenna scans a pattern of 48 beam positions, (every 15 degrees in azimuth, for two different elevations). Multipath and fading effects are minimized by taking a series of

FIGURE 1 MSAT-X ANTENNA SYSTEM

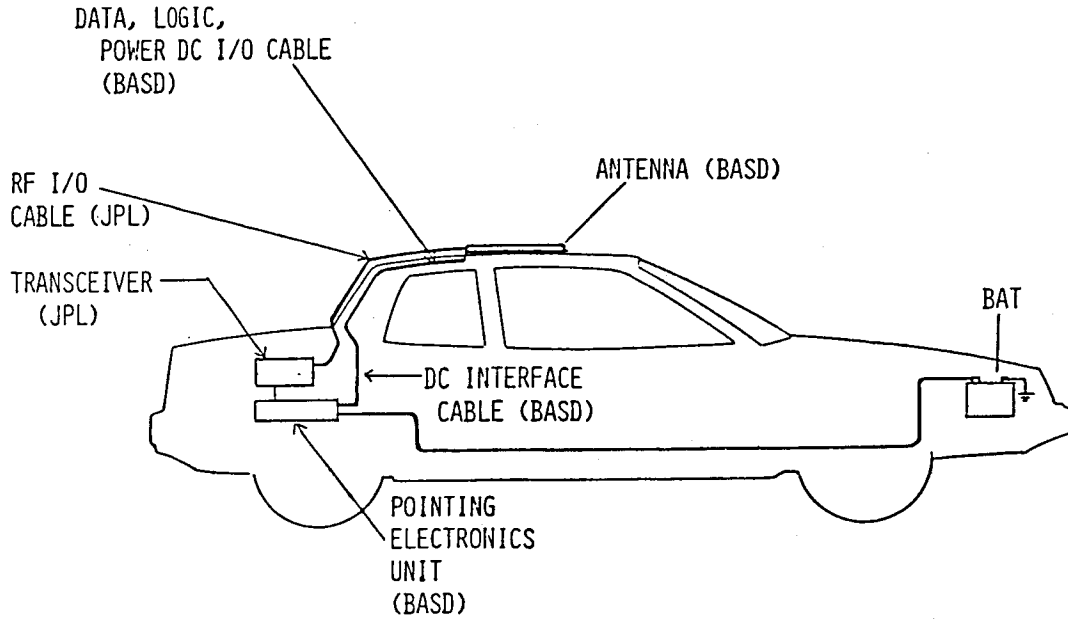
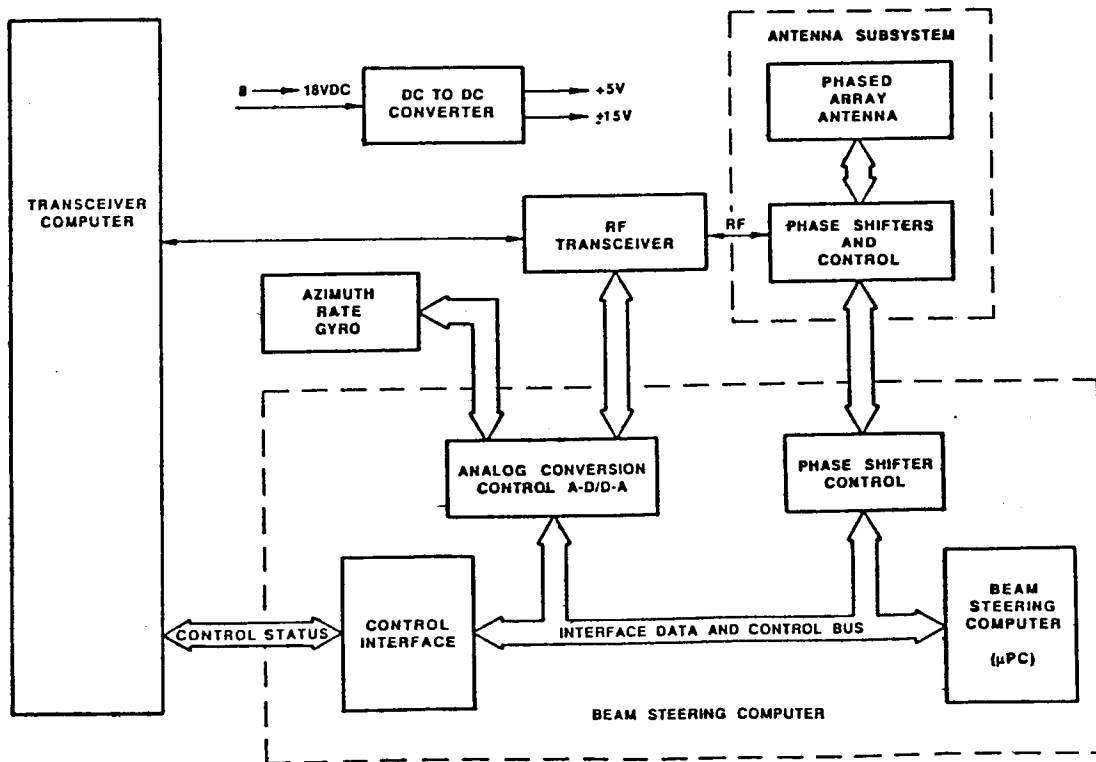


FIGURE 2 MSAT SYSTEM FUNCTIONAL BLOCK DIAGRAM



scans over a two-second acquisition period and averaging the results. In order to keep vehicle motion from distorting the scan data, the scan pattern is taken in reference to an inertially-fixed coordinate system, established using the azimuth rate sensor. Tracking is accomplished using a combination of closed-loop and open-loop control. The primary tracking mode is closed-loop tracking. In this mode, the beam is dithered about the satellite position in a diamond-shaped sequential lobing pattern at a rate significantly higher than the required pointing update rate. This allows a number of dither measurements (about 100) to be averaged in computing the satellite position. By dithering at a rate significantly higher than the maximum multipath rate, the tracking error due to multipath is virtually eliminated. Open loop tracking is conducted using information from the angular rate gyro. This is quite useful for maintaining pointing during short signal outages (10 seconds or less). It can also be used during normal tracking to reduce the amount of time the beam is dithered, thereby reducing tracking loss.

The antenna is an array of 19 capacitively fed stacked patches. The assembly is illustrated in Figure 3. The elements are arranged in a triangular lattice as shown. The 19-way power divider and 18 phase shifters (the center element does not use a phase shifter) are located on the lowest microstrip board. The power dividers are microstrip Wilkinson dividers. Three-bit distributed-element phase shifters are used. The 180 and 90 degree bits are reflection bits, and the 45 degree bit is a loaded line bit. Reflection and loaded line bits are chosen to minimize the diode count (switched line bits use twice as many diodes). The phase shifter outputs are passed through to the driver element board. This layer holds the lower elements of the stacked patches and the quadrature hybrids used to achieve circular polarization. The element and hybrid are illustrated in Figure 4. Capacitively fed stacked patches are used because they meet the 7% bandwidth requirement and are relatively inexpensive to manufacture. The upper patch element is mounted on a layer of PTFE which is separated from the driver element board by a dielectric spacer. The patch sizes, spacer thickness, and driven element board thickness are adjusted to yield optimum VSWR and pattern behavior for the element. The array is covered with a thin radome which provides environmental protection.

An analysis has been conducted to determine the cost of manufacturing the antennas in quantities of 10,000 per year. The cost figure for this production rate is \$1620 per unit. This figure is of medium confidence (+/- 25%). Using some optimistic assumptions, this figure could drop to \$1000 - \$1300. The changes made in these lower cost figures could result in performance degradation of 1 or 2 dB.

FIGURE 3 ANTENNA SANDWICH

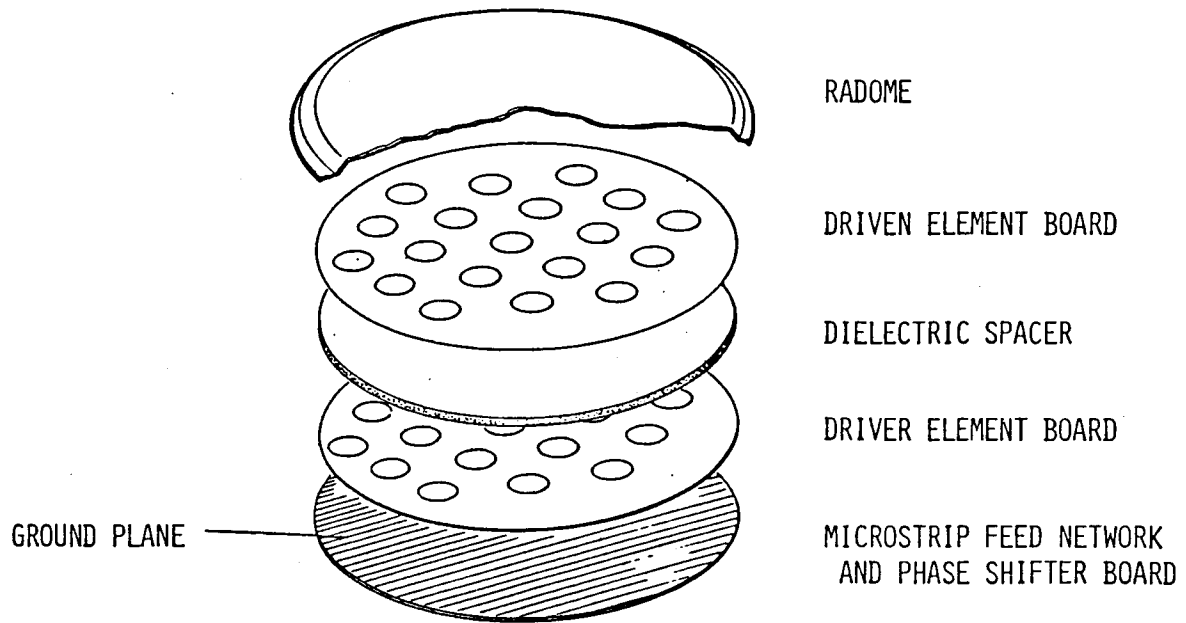
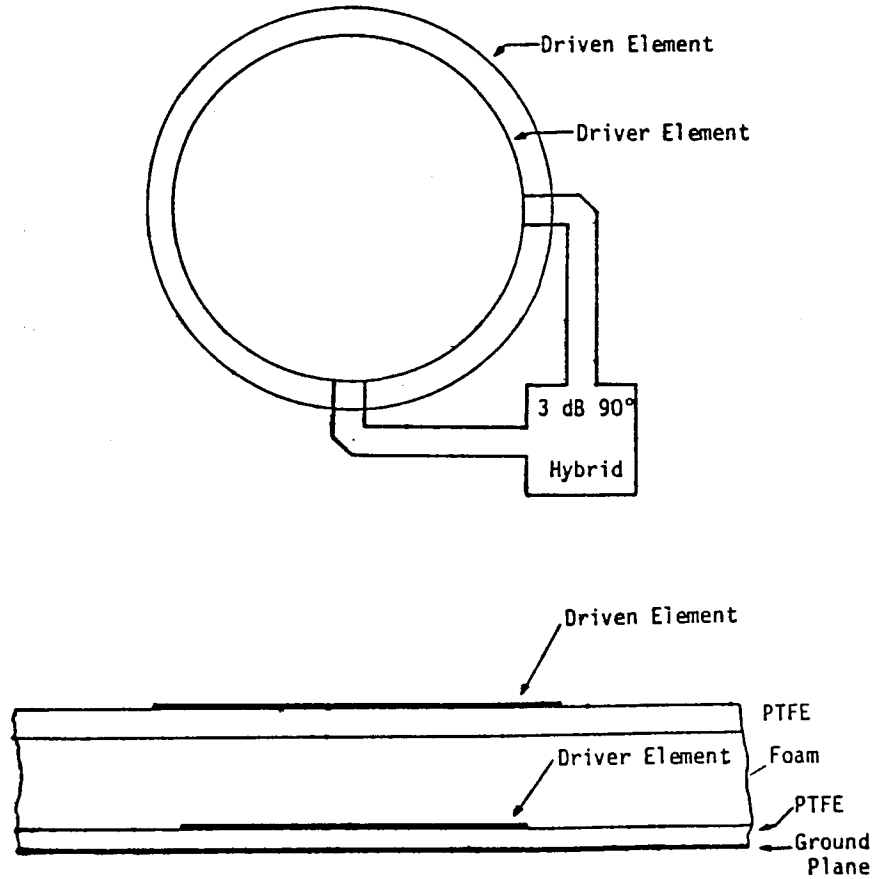


FIGURE 4 ELEMENT DESIGN



The assembled breadboard antenna and pointing system are shown in Figure 5. The RF portion of the antenna is similar to what would be used in an actual production antenna. The pointing system is a development unit and is not representative of the end product.

MECHANICAL/ENVIRONMENTAL CONSIDERATIONS

The antenna is packaged to meet the specific requirements of the mobile vehicle environment. The unit is quite strong. It has shown the ability to support the weight of an adult, in addition to resisting heavy blows and scraping from a ice scraper. The unit has very good sealing against external moisture. Furthermore, the use of hermetically sealed diodes insures that any moisture which can enter the unit will not result in degradation in performance. The unit is designed to be easily serviced. As shown in Figure 6, the antenna opens to provide access to all of the cables and phase shifter components. The Ball Aerospace breadboard MSAT antenna is representative of the technology which will meet MSAT environmental requirements as well as electrical.

RESULTS

Static testing has been conducted wherein the antenna is scanned throughout the coverage region. Gain measurements for the antenna range from 13.4 dB at 60 degrees elevation to 8-9 dB (depending on azimuth angle) at 20 degrees elevation. It is noted that these gain figures are also valid to 1530 MHz, which allows the antenna to function throughout the WARC LMSS frequency bands. Dynamic system testing was conducted with JPL's receiver. The acquisition routine works very well down to 40 dB Hz C/No. The tracking routine functions very well to 35 dB Hz for a stationary platform and 40 dB Hz for a platform rotation speed of 45 degrees per second. The system also shows very good immunity to fading. 5 dB fading at a rate of 400 Hz has a minimal effect on acquisition or tracking functions.

CONCLUSION

The MSAT-X breadboard antenna development has been quite succesful in demonstrating the feasibility of using an electronically steered antenna in the mobile MSAT application. While the antenna does not meet the gain spec, it does deomonstrate the required functions for the system, including pointing the beam, acquiring the satellite and tracking it during open and closed loop tracking conditions. BASG has been working with JPL to identify the areas where improvement is required to improve the antenna performance. We believe performance improvement of 1 dB or more could be obtained using the techniques identified.

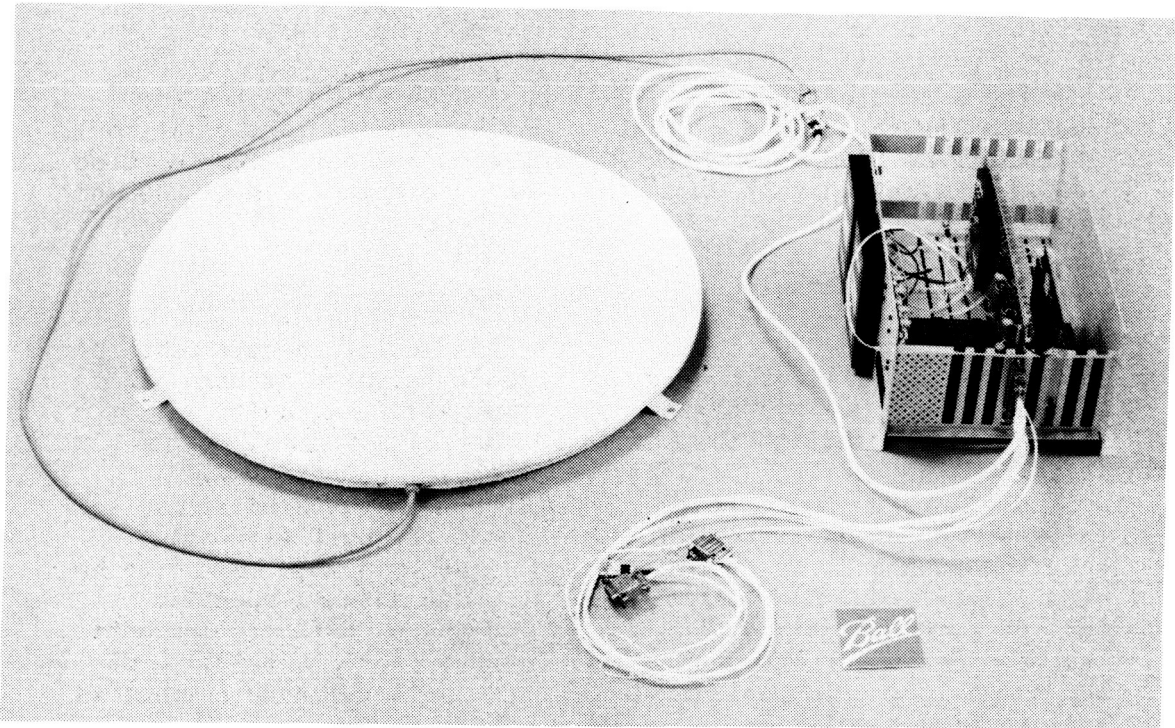


FIGURE 5: MSAT Breadboard Antenna with Pointing System

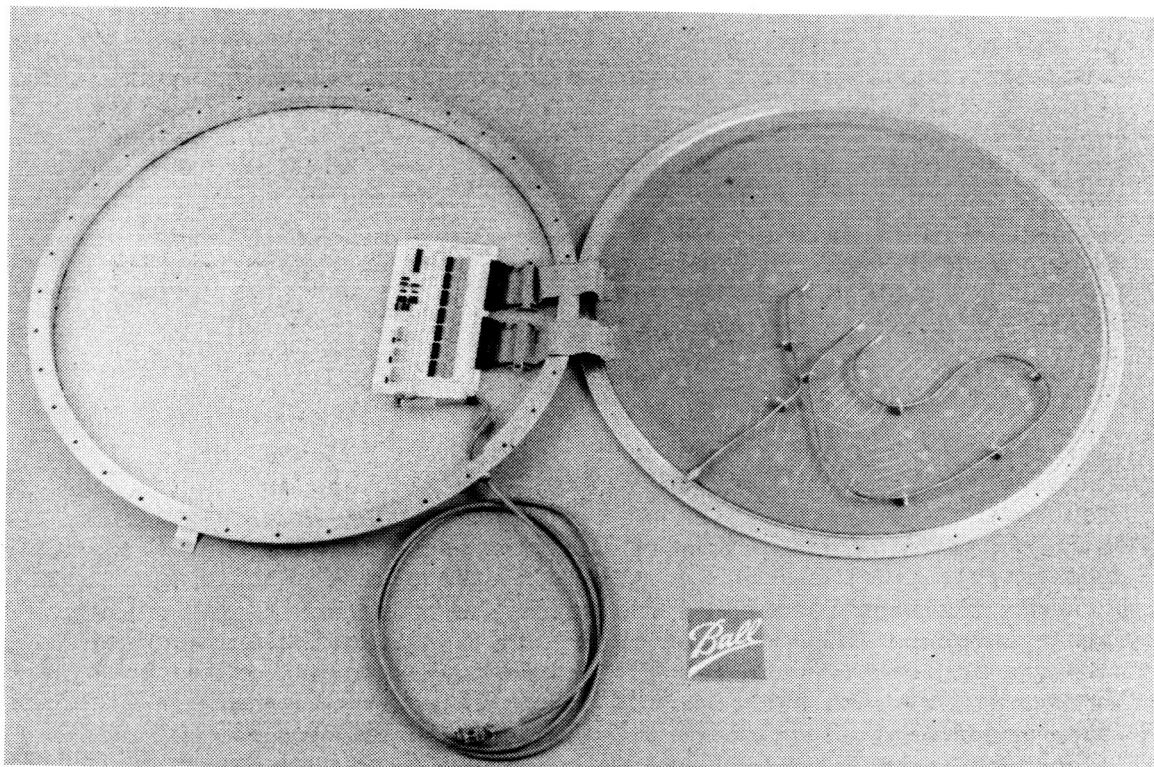


FIGURE 6: MSAT Antenna in Open Configuration for Service

MSAT-X ELECTRONICALLY STEERED PHASED ARRAY ANTENNA SYSTEM

H.H. CHUNG, W. FOY, G. SCHAFFNER, W. PAGELS, M. VAYNER, J. NELSON and S.Y. PENG

TELEDYNE RYAN ELECTRONICS

8650 Balboa Avenue
San Diego, California 92123

ABSTRACT

A low profile electronically steered phased array has been successfully developed for the Mobile Satellite Experiment Program (MSAT-X), under the contract with Jet Propulsion Laboratory (JPL). The newly invented cavity-backed printed crossed-slot was used as the radiating element. The choice of this element was based on its low elevation angle gain coverage and low profile. A nineteen-way radial type unequal power divider and eighteen three-bit diode phase shifters constitute the beamformer module which is used to scan the beams electronically. A complete hybrid mode pointing system, which uses an external rate sensor and internal error signals to optimize the angle tracking accuracy, has also been developed. The major features of the developed antenna system are broad space coverage, low profile (0.75 inch exclusive of the input RF connector and beam control DC connector), and its fast acquisition and tracking performance, even under fading conditions. Excellent intersatellite isolation (better than 26 dB) was realized which will provide good quality mobile satellite communication in the future.

INTRODUCTION

The development of low cost vehicle phased array for the MSAT-X program has been a challenging task for the antenna designer. Broad spectrum of considerations have been taken into account in the design phase so that the best antenna system was successfully developed during the contract with JPL. The design philosophy of the antenna array, beamformer and pointing system as well as the measured array performance will be discussed in the following sections.

ANTENNA ARRAY DESIGN

Among the low profile antenna candidates, the crossed-slot and patch element were considered. The cavity-backed printed stripline fed crossed-slot was selected, however, because it has (1) wider beamwidth, (2) better gain and axial ratio at low elevation angle, and (3) thinner for the same operating frequency band than that of patch antenna.

The stripline fed crossed-slot element is basically made of two separate boards. As shown in Figure 1, crossed-slot was etched on a single sided copper clad substrate and the stripline feeders were etched on another board of the same thickness. The two boards were bonded together. A set of plated through holes were required to form a cavity wall. Circular polarization was obtained by feeding the crossed-slot in phase quadrature via a integrated feed network of a 90 degrees branch line hybrid and two 180 degrees corporate circuit (Figure 2). The four point feed with symmetrical arrangement and phase rotations (0-90-180-270 degrees) is required to eliminate the higher order mode inside the cavity so that the crossed-slot can radiate efficiently.

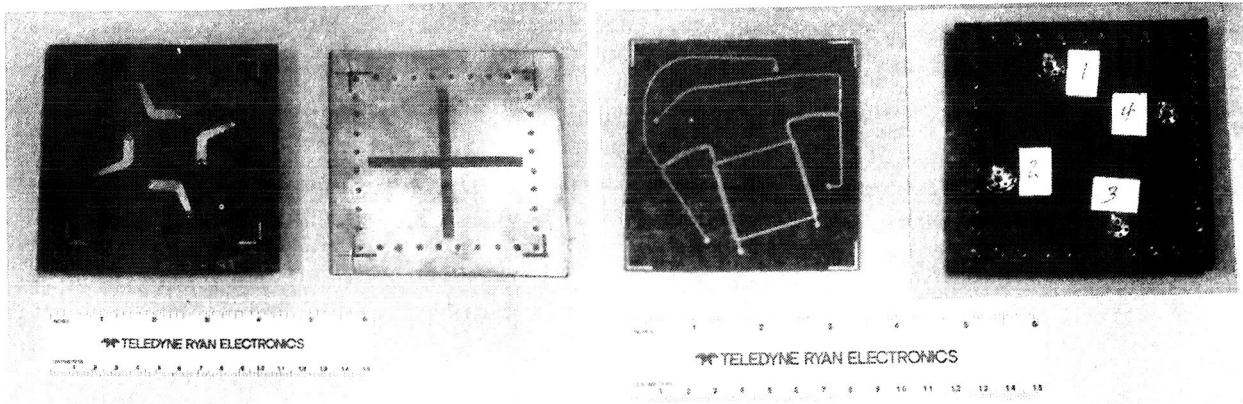


Fig. 1. Photo of the crossed-slot

Fig. 2. Photo of the hybrid feed network

The array aperture design was performed so that the required performance be achieved at the lowest cost. The major constraints on the aperture design are: (1) intersatellite isolation (20 dB), (2) array gain (10 dBic), (3) array thickness (within 1 inch), (4) manufacturing cost (\$1500.00), (5) multipath rejection capability and (6) backlobe level (12 dB).

The design philosophy is using minimum number of elements and maximum usage of the aperture as well as avoiding the grating lobes. After the detail trade off analysis, a nineteen crossed-slot element array with triangular lattice arrangement was chosen. The element spacing was 3.9 inch. Proper amplitude taper of three circular rings of relative power -6dB, -5.2 dB, and -3 dB (starting from the outside going towards the center) was used to reduce the sidelobe level so that the required 20 dB intersatellite isolation can be maintained. Array size was 22 inches which includes the mounting space. Three-bit diode phase shifter was selected to steer the antenna beam.

BEAMFORMER DESIGN

The beamformer network which consists of two major components, an unequal nineteen way power divider and a three bit phase shifter, had been successfully developed on a 20.6" diameter microstrip plane, as shown in Figure 3. The beamformer network will continue to present design challenge in the future for the low cost production with high performance and reliability.

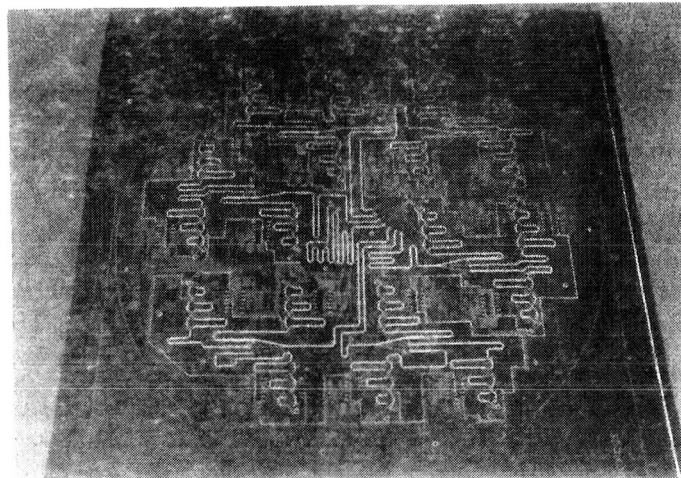


Fig. 3. Beamformer boards of the array

The unequal power divider consists of an equal seven way power divider followed by six unequal three way dividers. The divider design is based on the Wilkinson divider concept which splits the 50 ohm line into two or more quarter wave sections of the right impedance to preserve a 50 ohm impedance match. Balancing resistors bridge each arm at the ends of the matching sections. These resistors keep the match when outputs are not balanced. For unequal divisions additional quarter wave sections are required. Computer optimization using the "Touchstone" program was used to design the impedance and resistor values.

The three bit phase shifters were based on the switched line principle. This was selected to give the least phase shift error over the operating band from 1545 MHz to 1660 MHz, compared to that of the hybrid coupled phased shifter. The switched line phase shifter projects an 11 degrees error while the hybrid phase shifter projects a 19 degrees error over the same frequency band. The disadvantage of the switched line design is that twice as many diodes are required. However, the switched line configuration can be redesigned with the back to front pin diodes at common points. This leads to the possibility of using monolithic diode pairs so that the cost of antenna system will be further reduced.

POINTING SYSTEM DESIGN

A complete hybrid mode pointing system, which uses an external rate sensor and internal error signals to optimize the angle tracking accuracy over a wide of contingencies, has also been developed. Basically, the fast response operations are controlled by the angle rate sensor while the radio link corrects the rate sensor errors. Because the rate sensor bias error changes slowly, the radio link data is averaged over a 30 seconds period before correcting the rate sensor. This will filter out any attitude perturbations, shadowing or fading (multipath) effects in the radio link.

When the rate sensor is disconnected, the rate sensor correction is eliminated and the radio link loop is automatically increased. This allows somewhat less accurate but still adequate satellite tracking on pilot signal alone; however, it will no longer be able to follow vehicle turns during signal outages.

The sequential lobing dither of the radio link is held to plus and minus 1.5 degrees under normal signal strength conditions in order to have maximum intrasatellite isolation. The dither magnitude is only increased if signal level drops. This is done automatically by sensing the strength of the pilot signal. The dither frequency is a modifiable parameter which can be adjusted between 10 and 200 Hz.

The elevation angle of the antenna beam is controlled by searching for maximum signal strength. Because of the wide antenna beamwidth and the generally slow variation of satellite elevation angle, this search is done at rate of one incremental beam per second from 30 degrees through 70 degrees (from the array broadside) in increments of 5 degrees. The total number of incremental elevation beam is nine. The low search rate also separates the elevation servo information from the azimuth servo to prevent cross-coupling.

ARRAY ASSEMBLY

A total of five layers of substrate material board were used to construct the whole array which consists of antenna array module and the beamformer module as shown in Figure 4. The antenna array module consists of four boards - a top crossed-slot board, a stripline excitation feeder board, a hybrid/corporate feed network board and a bottom ground board. The top two boards (same thickness) of the crossed-slot array elements were etched on a single sided, copper clad teflon fiberglass board. The thickness of the board were 0.09 inch and 0.125 inch for the breadboard unit #1 and #2 array, respectively. The thicker board used for the unit #2 is to increase the antenna bandwidth. A set of plated through holes around the crossed-slots were required to form the cavity wall for the crossed-slot element. The bottom two boards with thickness of 0.031 inch each constitute

the integrated stripline hybrid/corporate feed network. The beamformer board and the 0.125 inch stiffner plate were bonded together using silver-bonded epoxy to form the beamformer module.



Fig. 4. A photo to show the five layers of MSAT-X array design

The antenna array module were key together with the beamformer module and then were bolted together with the back cover leaving an air gap of 0.2 inch between the beamformer circuit and the cover. Figure 5 shows a final assembled MSAT-X array. A very thin (0.002 inch) painted polyurethane type radome was employed to provide protection against the enviroment.

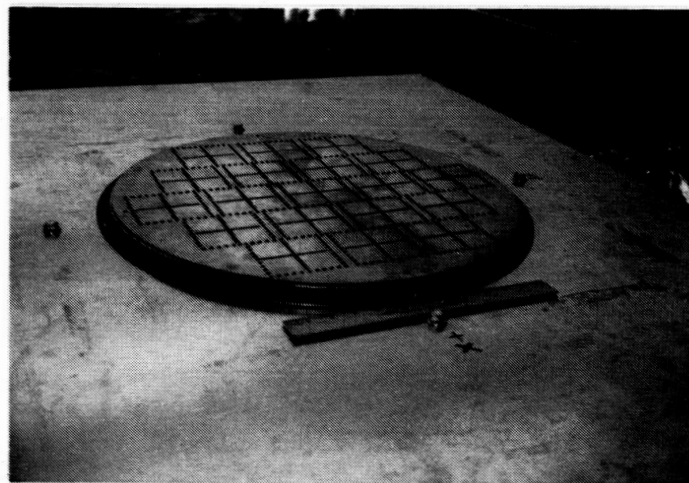


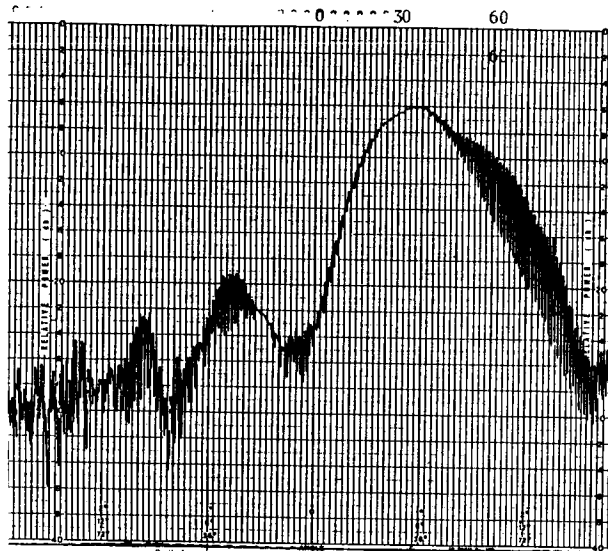
Fig. 5. Final assembled MSAT-X phased array

The total thickness of the array unit #1 and #2 were 0.68 inch and 0.75 inch, respectively. The thickness of the final production array will be reduced to 0.625 inch when the 0.125 inch stiffner plate in between the beamformer board and the antenna array board are removed.

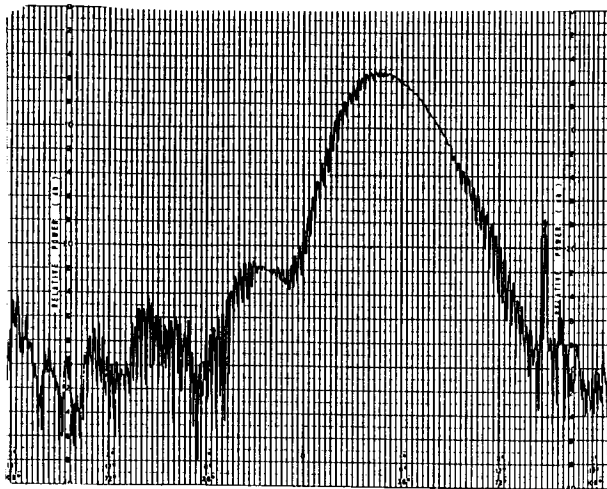
MEASURED ARRAY PERFORMANCE

Extensive measurements were performed during the contract with JPL. Typical measured array patterns are shown in Figures 6 and 7. Well behaved array patterns were observed in all the measured data. Excellent axial ratio (<5 dB) of the array pattern was achieved within 95% of the required space coverage across the operating frequency band.

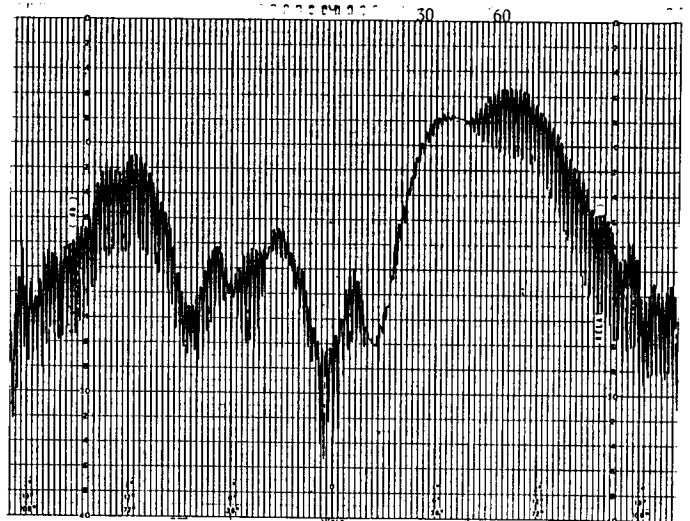
The measured array performance is summarized in Table 1. These results show that all the requirements were satisfied except the gain. However, it is believed that the 10 dBic gain at 20 degrees elevation angle will be realized in the future through the optimization of the crossed-slot excitation feeder design and the beamformer aperture distribution. Detail will be discussed in the meeting.



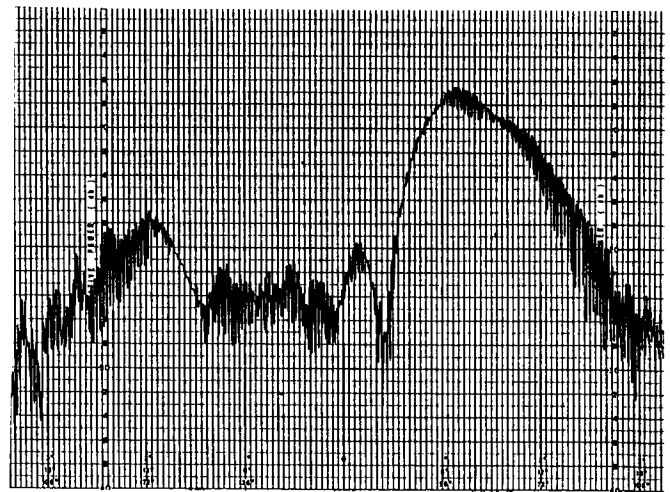
(a) 1545 MHz



(b) 1660 MHz



(a) 1545 MHz



(b) 1660 MHz

Fig. 6 Measured elevation array patterns at scan angle of 40 degrees away from array normal

Fig. 7 Measured elevation array patterns at scan angle of 60 degrees away from array normal

Table 1. Summary of Measured Array Performance

	Measured Value		Spec
	Unit #1	Unit #2	
Gain at 20° elevation angle (dBic) 1545 MHz	9.2 (average)	9.3 (average)	10
1660 MHz	7.7 (average)	8.3 (average)	10
Intersatellite Isolation (dB)	26	26	20
Backlobe (dB)	12 (95%) <12 (5%)	12 (95%) <12 (5%)	12
Multipath Rejection (dB) (pattern dropoff from 20° to 0° elevation)	>6	>6	6
Antenna Thickness (inch) (Exclusive of RF Connector)	0.68	0.75	<1

CONCLUSIONS

An L-band car-top conformal phased array has been successfully developed for the mobile satellite communications. The following conclusions can be drawn from the development work with JPL:

- (1) The printed cavity-backed stripline fed crossed-slot element is proven to be the best radiating element for the MSAT phased array.
- (2) The measured array gain at 70 degrees from the array broadside is 9.3 dBic and 8.3 dBic for the frequency 1545 MHz and 1660 MHz, respectively. 10 dBic gain across the frequency band is achievable in the future.
- (3) Excellent intersatellite isolation (26 dB) was achieved which is better than the requirement (20 dB).
- (4) The total thickness of the developed array is 0.68 inch and 0.75 inch for the unit #1 and #2, respectively.
- (5) The multipath rejection requirement was satisfied.
- (6) The backlobe level is better than 12 dB in 95% of the required space coverage. The worst backlobe is 6 dB when the array was scanned to 70 degrees from the array broadside at certain azimuth angles.

MSAT-X PHASED ARRAY ANTENNA ADAPPTIONS TO AIRBORNE APPLICATIONS**C. SPARKS, H.H. CHUNG, and S.Y. PENG, Teledyne Ryan Electronics, San Diego, California****TELEDYNE RYAN ELECTRONICS****8650 Balboa Avenue
San Diego, California 92123****ABSTRACT**

The MSAT-X Phased Array Antenna is being modified to meet future airline requirements. The proposed antenna system consists of two high gain antennas mounted on each side of a fuselage, and a low gain antenna mounted on the top of the fuselage. Each of the two high gain antennas is an electronically-steered phased array based on the design of the MSAT-X antenna, as described in a separate paper. The major difference is in the beam forming network which is connected to the array elements via coaxial cables. This approach allows the array elements fuselage conformal (0.37 inches thickness). In addition, the circuit board containing the diode phase shifters will be installed inside the aircraft to increase the MTBF and reliability, to ease of maintenance, and to ultimately reduce the cost. It is essential that the proposed antenna system be able to provide adequate communication link over the required space coverage which is 360 degrees in azimuth and from 20 degrees below the horizon to the zenith in elevation. Alternative design concepts are suggested to maximize space coverage and redundancy capabilities. Both open loop tracking system and close loop backup capabilities are discussed. Typical antenna system performance data measured are also included.

INTRODUCTION

To meet the challenging aviation satellite communication requirements, Teledyne Ryan Electronics (TRE) developed an antenna subsystem for this application, based on the MSAT-X phased array design. The major features of the developed phased array are its low profile (0.37 inch in thickness), wide space coverage (using crossed-slot element), good satellite isolation (>20 dB), built in redundancy (center element used as a low gain antenna for backup during phase shifter failure), and good pointing performance. The design concept is aimed for low cost, low drag, high reliability, ease of installation and maintenance, low technical risk, and maximum redundancy and space coverage.

SYSTEM CONFIGURATION

The original antenna subsystem configuration proposed consists of two identical high gain antennas, one low gain antenna as backup, 3 diplexers, 3 low noise amplifiers (LNA), and the associated electronics circuits and power supply. The locations proposed are the two sides of fuselage for high gain antennas and the top of fuselage for the low gain antenna as shown in Figure 1. The proposed low gain antenna is a printed crossed-slot which has low profile (0.37 inch) and wide space coverage as shown in Figure 2.

ORIGINAL PAGE IS
OF POOR QUALITY

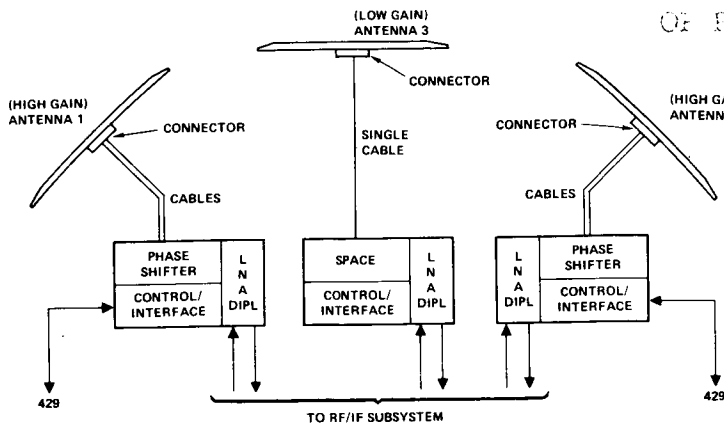


Fig. 1. Original antenna subsystem

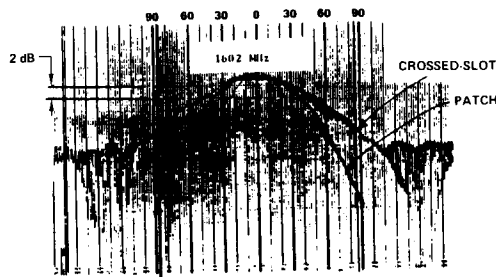


Fig. 2. Crossed-slot element radiation pattern

Note that the gain drop at 7 degrees above horizon from the peak of element pattern is about 8.5 dB. The measured peak gain is 5.5 dBic. Therefore, the gain at the 7 degrees above the horizon is -3.0 dBic which does not meet the specified gain of 0 dBic. For a patch antenna, however, the gain drop is 19 dB from the peak as shown in Figure 2. Therefore, the crossed-slot element is the best low profile element for the satellite communication. To further illustrate this fact, three conical cut pattern data for a crossed-slot element mounted on top of a Remote Pilot Vehicle (RPV) is shown in Figure 3. Note that the gain at the 0 degree azimuth angle is -3.8, -3.2, and -2.0 dBic respectively, at elevation angles of 0, 5, and 10 degrees

Since the low gain antenna cannot meet the gain requirement of 0 dBic at +7 degrees above horizon, and the redundancy is desired by airlines, an alternative system concept which consists of 3 identical high gain antennas are proposed as shown in Figure 4. The major difference from the original approach is that the new approach replaces the low gain antenna by a high gain antenna. The key advantages by doing so are to provide redundancy space coverage, to maximize the commonality of components, and to minimize the "key hole" areas. If a single top-mounted high gain antenna is desired (rather than the conformal array approach), a cap antenna using crossed-slot elements can be designed and developed to meet the need of this challenging application.

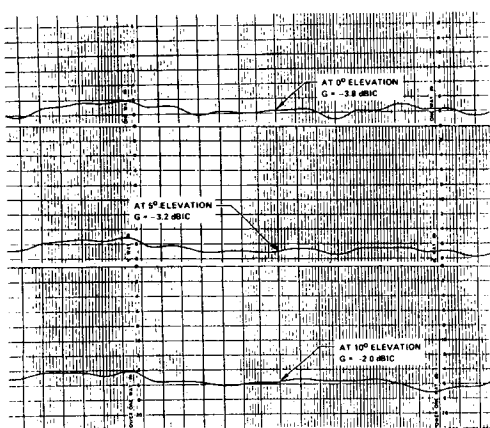


Fig. 3. Measured conical cuts of a TRE crossed-slot element at elevation angles of 0°, +5°, and +10°

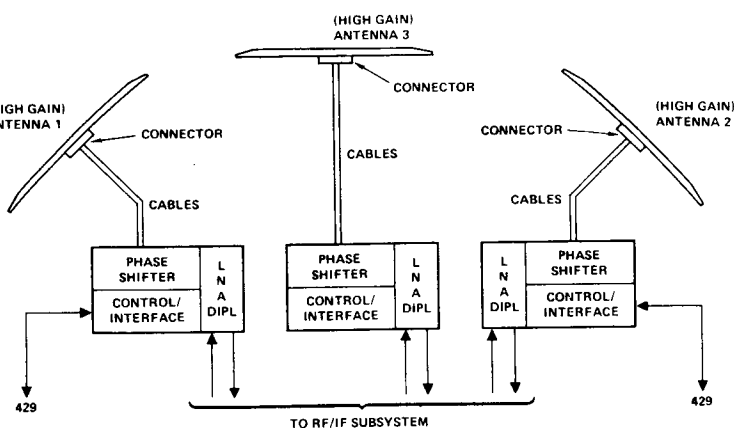


Fig. 4. Alternative antenna subsystem configuration

INSTALLATION CONCEPT

To simplify aircraft installation, the TRE's antenna subsystem has only 3 physical groups per high gain antenna: the antenna, a RF cable, and an electronic box. Figure 5 shows the proposed antenna installation concept. Note that the high gain antenna is mounted outside of the fuselage with the foot print according to the ARINC 741 characteristics which is illustrated in Figure 6. The electronics box is mounted inside the fuselage close to the high gain antenna. Figure 7 shows the proposed electronics box dimension. An 18 inch long RF cable is used for the connection between the antenna and the electronics box. One end plugs into the antenna with a special connector consisting of 19 0.141 semi-rigid cables. The other end of the RF cable plugs into a beam forming network contained inside the electronics box. Figure 8 shows a design of the 19-cable RF connector. In addition, the box also contains a diplexer, LNA, and DC power supply.

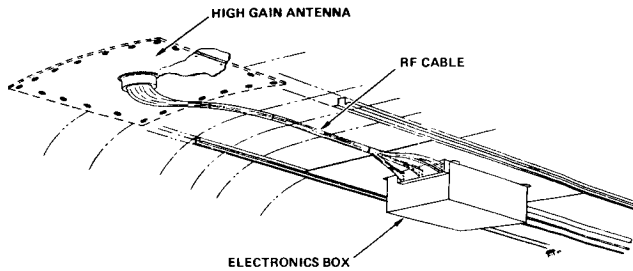


Fig. 5. Antenna installation concept

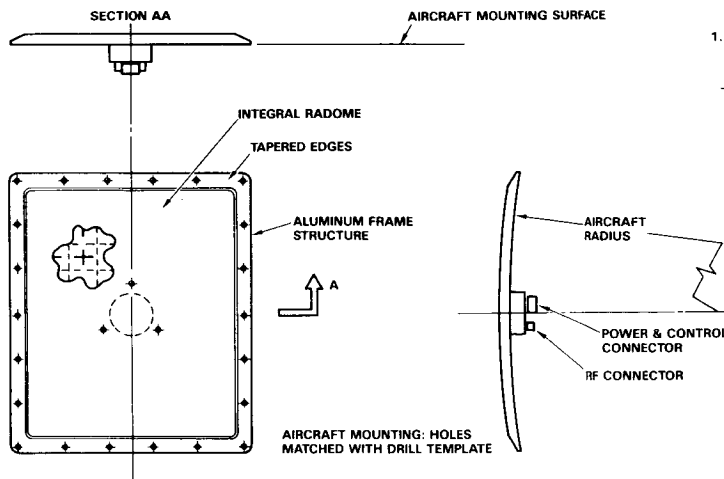


Fig. 6. High gain antenna subsystem

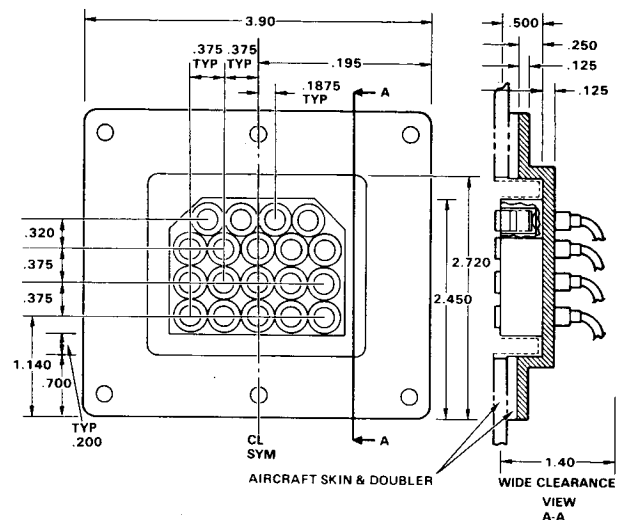
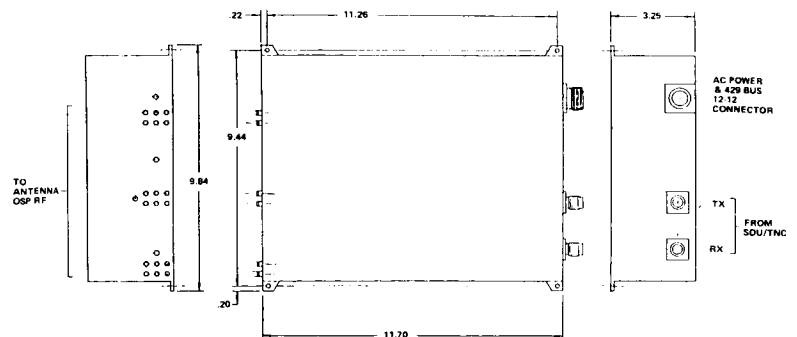


Fig. 8. A 19-cable rf connector design



- THE BOX CONTAINS:
- LNA DIPLEXER
 - BEAM FORMING NETWORK (BFN)
 - BEAM STEERING UNIT (BSU)
 - DC POWER SUPPLY

Fig. 7. Electronics box dimensions

ANTENNA SUBSYSTEM CHARACTERISTICS

As mentioned previously, the antenna subsystem has two (or three for the alternative approach) high gain antennas. Each antenna has 19 crossed-slot elements with the center one used as a reference which does not have a phase shifter. This feature provides the redundancy capability for the low gain antenna as a backup during the phase shifter failure. Table 1 summarizes the antenna subsystem characteristics for two side-mounted and one top-mounted high gain antennas. It should be emphasized that the low profile characteristics does offer the low drag property. Tables 2 and 3 show results of drag coefficient calculated by the Boeing Company for 747-400 and 767 aircraft, respectively, as a function of antenna mounting locations. Two different thickness of conformal arrays were used, such as 0.37 and 0.60 inch. Note that the 0.37 inch thick antenna has lower drag coefficient and does save money significantly in fuel burn yearly.

The array gain as a function of scan angle is given in Figure 9. Note that the gain at the 60 degrees scan angle is 12 dBic which meets the specified value. The gain drops off very fast for scan angles greater than 60 degrees. At scan angle of 90 degrees, the calculated array gain is 3 dBic. Therefore, the top-mounted high gain antenna not only provides the redundancy for the two side-mounted conformal array, but also provides better than 0 dBic (~3 dBic) antenna gain at the horizon which is required for the backup low gain antenna. In addition, the "key hole" areas are minimized, by the judicious choice of array locations. Figure 10 shows the space coverage of the two side-mounted TRE's conformal arrays which is better than other conformal arrays.

The pointing system adapted for the airborne application is based on the MSAT-X design with some modifications. The MSAT-X design uses hybrid approach which includes both the open-loop and closed-loop operation, to optimize the antenna steering toward to satellite. A rate sensor was used during the open-loop operation for the MSAT-X program which will not be adapted here. Instead, the navigation data will be provided as the input to steering the beam pointing directions. For the closed-loop operation, a sequential lobing technique was used to search track satellite locations.

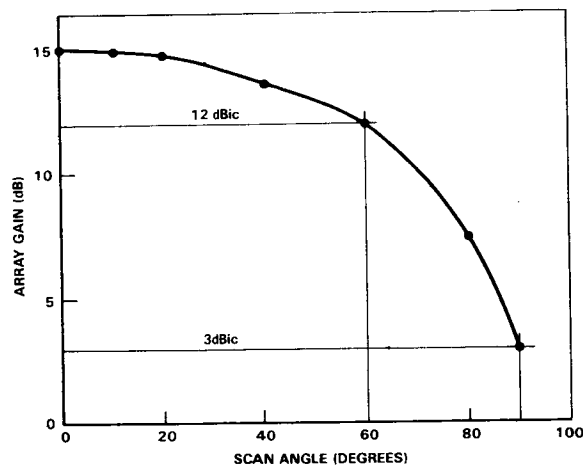


Fig. 9. Array gain as a function of scan angle away from the array normal

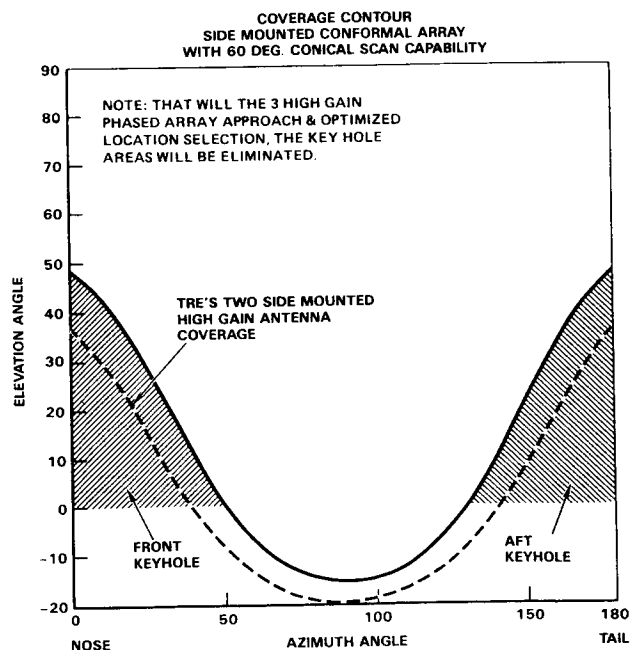


Fig. 10. Space coverage of two side-mounted conformal arrays

Table 1. Antenna subsystems characteristics	
Frequency of Operation Transmit Receive	1625.5 to 1660.5 MHz 1530.0 to 1559.0 MHz
Polarization	Right hand circular polarization (RHCP)
Gain (high gain antenna) Broadside At ± 60 scan angle	15 dBic 12 dBic
Space coverage Elevation	-20° to +90° (for two side-mounted arrays) +30° to +90° (for one top-mounted array)
Sidelobe discrimination	13 dB at 45° separation
Satellite Isolation	>20 dB
Low profile	≥ 0.5 inch in thickness above fuselage

Table 2. Satcom antenna drag estimate summary for 747-400 aircrafts (side-mounted conformal array antennas)						
Location (BST)	Drag*		CBRGW*		FCL*	
	0.37"	0.60"	0.37"	0.60"	0.37"	0.60"
450	0.025	0.045	65	115	150	270
700	0.020	0.030	50	75	120	180
825	0.025	0.030	65	75	150	180
1150	0.025	0.040	65	150	150	240
1350	0.020	0.040	50	100	120	240
1550	0.020	0.030	50	75	120	180
1750	0.015	0.025	40	65	90	150
1800	0.015	0.025	40	65	90	150
1950	0.015	0.025	40	65	90	150

Table 3. Satcom antenna drag estimate summary for 767 aircrafts (side-mounted conformal array antennas)				
Location (BST)	Drag*		FCL Burn* (GAC/Ap/Yr)	
	0.37"	0.60"	0.37"	0.60"
450	0.004	0.024	190	1020
650	0.004	0.019	150	800
730	0.003	0.018	140	760
930	0.005	0.026	200	1100
1130	0.003	0.017	130	700
1300	0.003	0.015	120	630

- * CBRGW = Constant brake release gross weight mission.
- * FCL = Fuel capacity limited mission.
- * DRAG = In percent of total airplane drag at cruise. All fuel burn penalties based upon 2000 N.U. mission. 795 flights/yr. Numbers were calculated for the 767-200. Levels for the 767-300 would be similar.

MEASURED PERFORMANCE

The measured TRE's antenna pattern performance is given in Figure 11 and 12. Figure 11 shows the measured broadside array pattern on top of a 40" x 50" groundplane. The achieved axial ratio and sidelobe level are very good for frequencies at both 1545 and 1660 Mhz. The patterns were taken using spinning linear source. Figure 12 shows the patterns scanned to 60 degrees away from the array normal. Again, the patterns and axial ratio are well behaved. The measured array gain at the 60 degrees scan angle is averaged at 10.7 dBic and 10.3 dBic, respectively, for frequencies of 1545 and 1660 MHz. The deficiency in array gain is being resolved under the present contract with JPL on the MSAT-X Mechanically Steered Array Program.

The measured pointing system performance for the MSAT-X program was very satisfactory, even under the current array gain deficiency condition. The system adapted is a hybrid mode pointing system operated under open loop and close loop conditions. The close loop operation is using a sequential lobing technique to search and track satellite signals. The open loop tracking is using an inertial sensor which was a rate sensor during tests. This hybrid system performed well during the acceptance test, under both fading and high power conditions. The measured intersatellite isolation was better than 20 dB as specified. This pointing system can easily be modified for the aviation satellite communication.

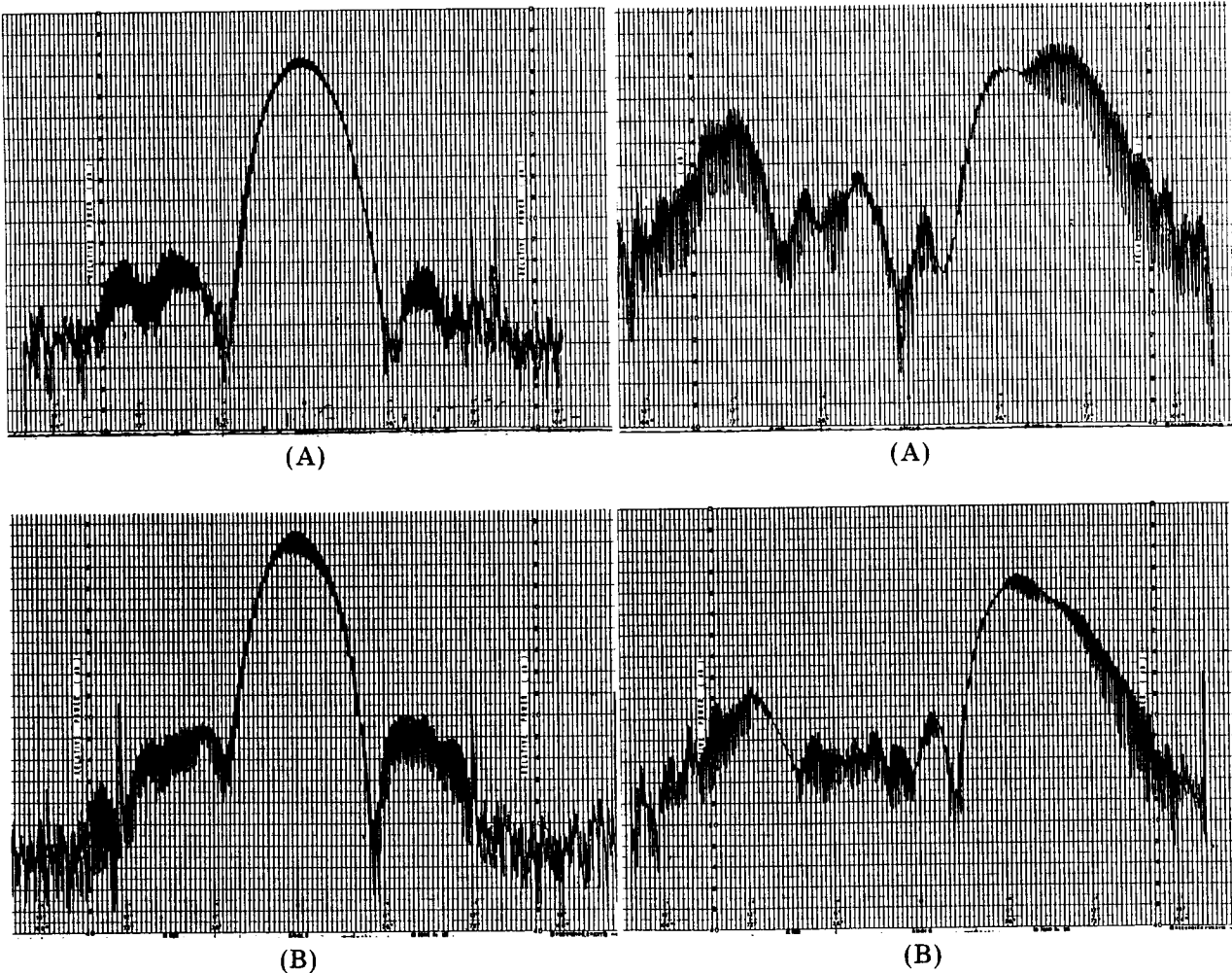


Fig. 11. Measured broadside array patterns for frequencies of 1545 and 1660 GHz

Fig. 12. Measured array patterns at scan angle of 60 degrees away from array normal for frequencies of 1545 and 1660 GHz

ADAPTIVE INTERFERENCE TECHNIQUES FOR MOBILE ANTENNAS

Prof. Lloyd J. Griffiths, University of Southern California and **Dr. E. Satorius**, Jet Propulsion Laboratory

Dept. of EE-Systems, MC 0272
University of Southern California
Los Angeles, CA 90089-0272

ABSTRACT

This paper describes the results of a study which has been performed to investigate effective, low cost adaptive signal processing techniques for suppressing mutual satellite interference that can arise in a mobile satellite (MSAT) communication system. The study has focussed on the use of adaptive sidelobe cancelling as a method to overcome undesired interference caused by a multiplicity of satellite transmissions within the field of view of the ground station. Results are presented which show that the conventional sidelobe canceller produces undesired reduction of the useful signal. This effect is due to the presence of the useful component in the reference antenna element. An alternative structure, the generalized sidelobe canceller (GSC), has been proposed which overcomes this difficulty. The GSC requires one additional multiplying unit (fixed) and one additional summing junction. It is concluded that the GSC provides an effective means for suppressing mutual satellite interference. A preliminary investigation of possible implementations of the GSC has been conducted. It was found that at most 8 bits would be required to implement the GSC processor under conditions in which the desired signal-to-interference ratio is 25 dB.

MSAT COMMUNICATION SYSTEM

For typical operational scenarios involving two or more satellites, mutual satellite interference (MSI) can degrade the performance of an MSAT communication system. In the situation where nearby satellite transmissions cannot be sufficiently isolated from each other (spatially or in frequency), some form of interference suppression must be incorporated at the various receiver/transmitter sites to mitigate the effects of MSI. Furthermore, since the relative geometry between the various transmitter and receiver terminals is constantly changing, the interference suppression techniques must be

adaptive in order to provide robust performance over a range of system geometries. The basic geometry of interest is depicted in Figure 1.

Two MSI scenarios are shown corresponding to interference received by ground stations (on receive) and by the satellites (on transmit). Satellite transponders are indicated by (S1, S2) while $S_1(t)$ and $S_2(t)$ indicate the desired signal components and $I_1(t)$ and $I_2(t)$ denote MSI components.

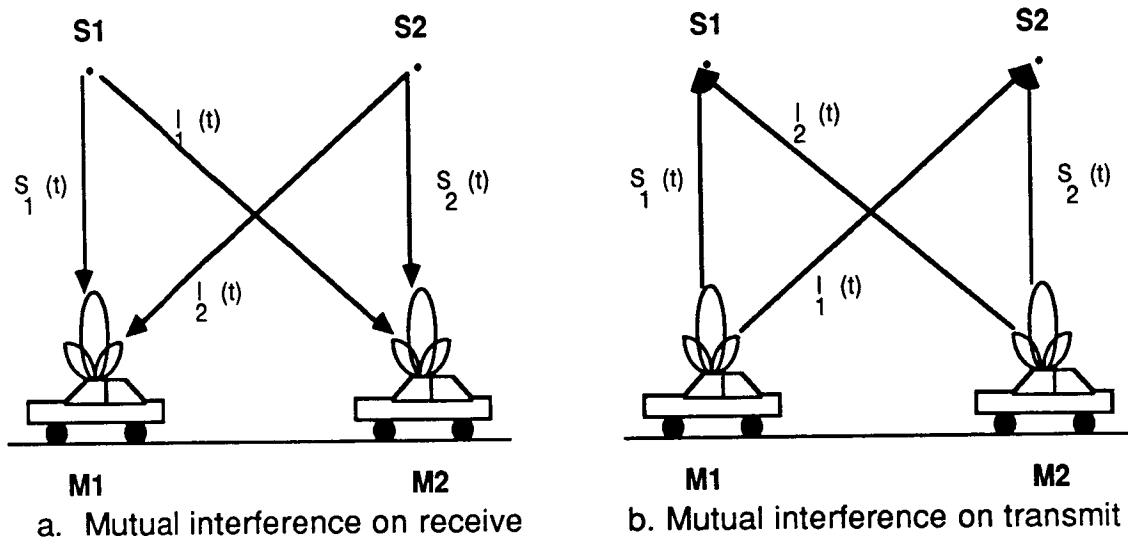


Fig.1. Mutual satellite interference between mobile users (M1, M2) and proximate satellite transponders

Observe that at the earth terminal, desired signals cannot be spatially distinguished from this interference due to the fact that both components enter through the mainlobe of the fixed-earth terminal antenna pattern.

ADAPTIVE ARRAYS

The spatial techniques studied are based on adaptive sidelobe cancelling (SLC). The array is assumed to be narrowband, which is a valid approximation for MSAT applications. The SLC approach utilizes an auxiliary antenna element, termed the reference antenna element, which is subtracted from the primary receiving antenna after appropriate weighting. The basic configuration is illustrated in Figure 2.

In this system, adaptation consists of adjusting the weight $W(n)$ such that the output power $|y|^2$ is minimized. Given that the interference component in the primary input is highly correlated with the reference input, then the minimization of output power accomplishes interference cancellation (Widrow, 1975). One simple adaptive method for minimizing $|y|^2$ is the LMS

algorithm (Widrow, 1975). This algorithm ensures that the minimum possible output power level is obtained for the overall system.

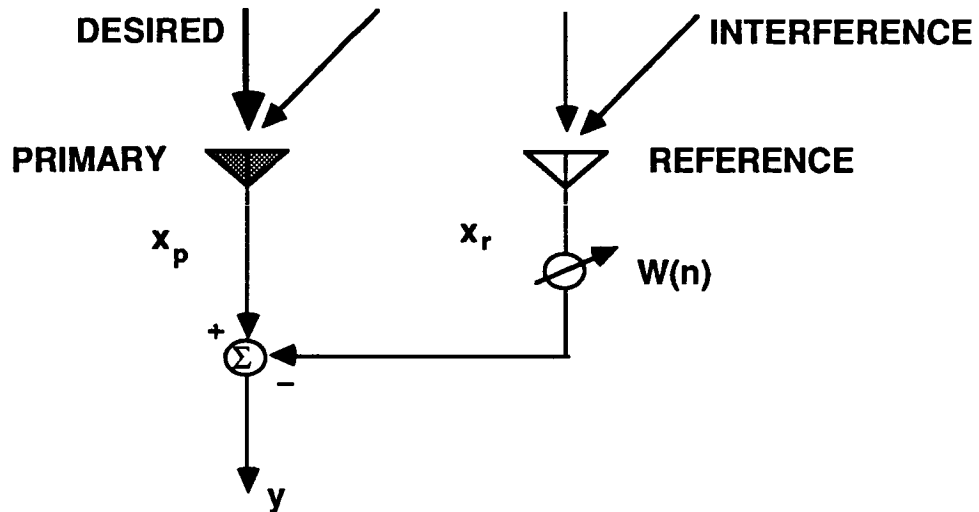


Figure 2. Basic MSAT adaptive SLC architecture.

If there is an appreciable amount of desired signal in the reference channel input, this method will lead to significant signal cancellation at the output. Effective interference cancellation is achieved only when the ratio of interference to desired signal is substantially larger in the reference antenna output than it is in the primary. Although this is the case for the nominal system, significant amounts of desired signal cancellation can nevertheless be expected to occur in MSAT geometries.

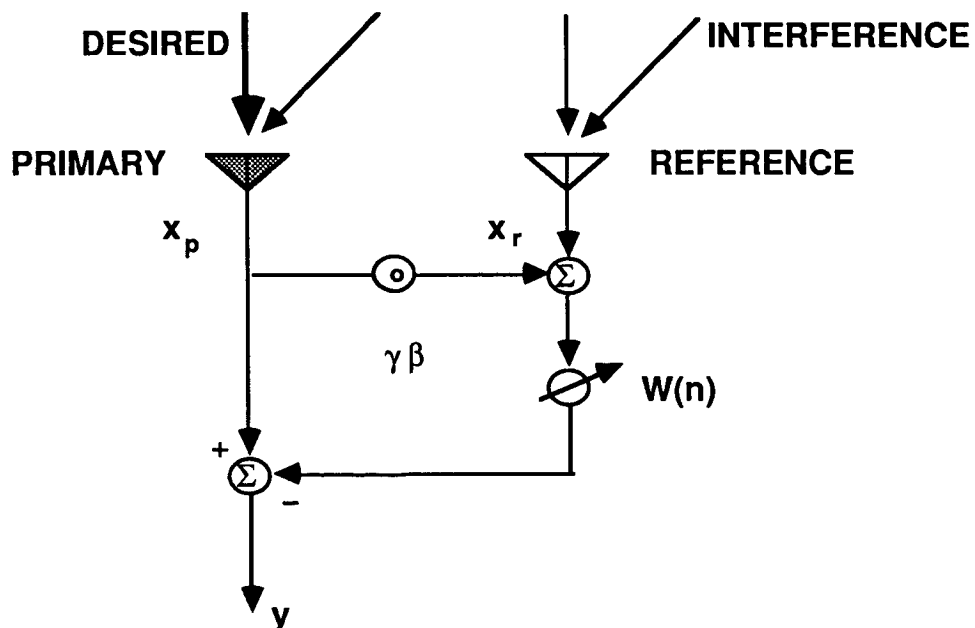


Figure 3. Generalized sidelobe canceller configuration.

The Generalized Sidelobe Canceller (GSLC) method of adaptive beamforming (Buckley, 1986) offers an approach which overcomes the signal cancellation effects observed with the basic SLC. The GSLC method utilizes the fact that *a priori* information is available regarding the anticipated gain differences between the desired signal component in the primary and in the reference beam outputs. This information would normally be available from the antenna patterns and is employed to combine the output from the two antennas *prior to the adaptive weight*, as shown in Figure 3.

The multiplier term $\gamma \beta$ between primary and reference is the gain required to equalize the difference in magnitude observed for the desired response at the primary and reference antenna outputs. The constant γ represents the polarization difference and β is the array gain term.

SIGNAL CANCELLATION EFFECTS

A numerical example was generated using a simple single interference model and the signal-to-interference power ratio (SIR) at the SLC output was computed. The example employed corresponded to a typical MSAT application in which a 19 element primary array pointed toward the desired signal was assumed. At the output terminals of this antenna, the undesired interference term is approximately 15dB below that of the desired response due to the antenna gain. A single-element reference antenna was assumed such that the gain difference β between the desired signal observed at the outputs of the primary and secondary antennas was 13dB.

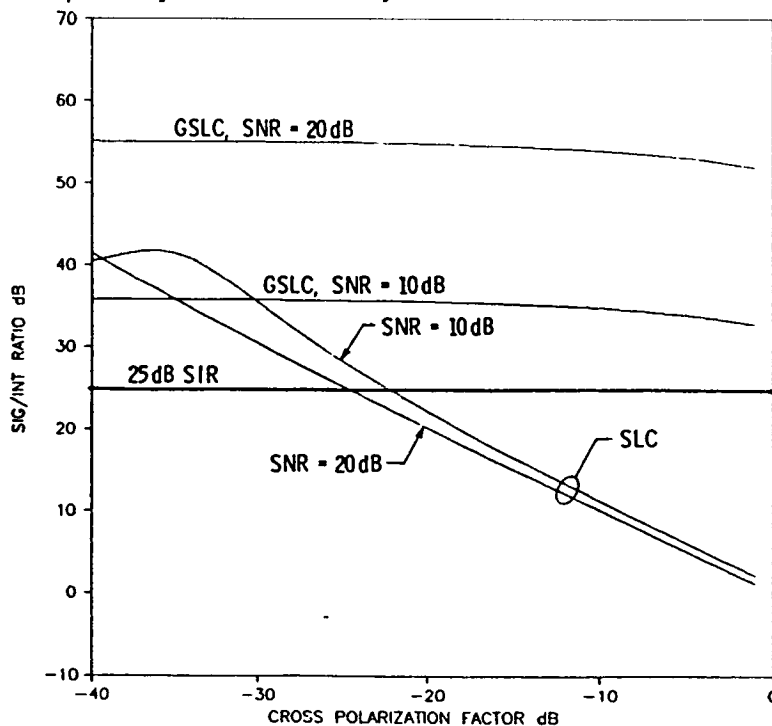


Fig. 4. Adaptive sidelobe cancelling performance curves.

Figure 4 illustrates the results as a function of the magnitude of the cross-polarization gain factor, $|\gamma|$ (with the phase of γ set at 0°), for a typical MSAT geometry. Two curves (marked SLC) are presented corresponding to two different values of signal-to-noise ratio (SNR): $\sigma_s^2 / \sigma_n^2 = 10$ dB and 20 dB. As is seen, the output SIR decreases as the cross-polarization isolation decreases due to signal cancellation. Note also that over almost the entire range of $|\gamma|$, somewhat better SLC performance is obtained at the smaller SNR values. This is a consequence of the desired signal component which is present in the reference channel. In fact, a more detailed examination of the closed form expression for SIR reveals that there exist optimal SNR values for which the output SIR is maximized.

In analogy with the SLC performance analysis calculations, the SIR at the GSLC output has been computed as a function of the magnitude of the cross-polarization factor, $|\gamma|$ (again with the phase of γ set at 0°). Two curves (marked GSLC) are presented in Figure 4 corresponding to SNR = 10 dB and 20 dB. In contrast to the SLC performance curves, the GSLC output SIR remains nearly constant as a function of the cross-polarization isolation.

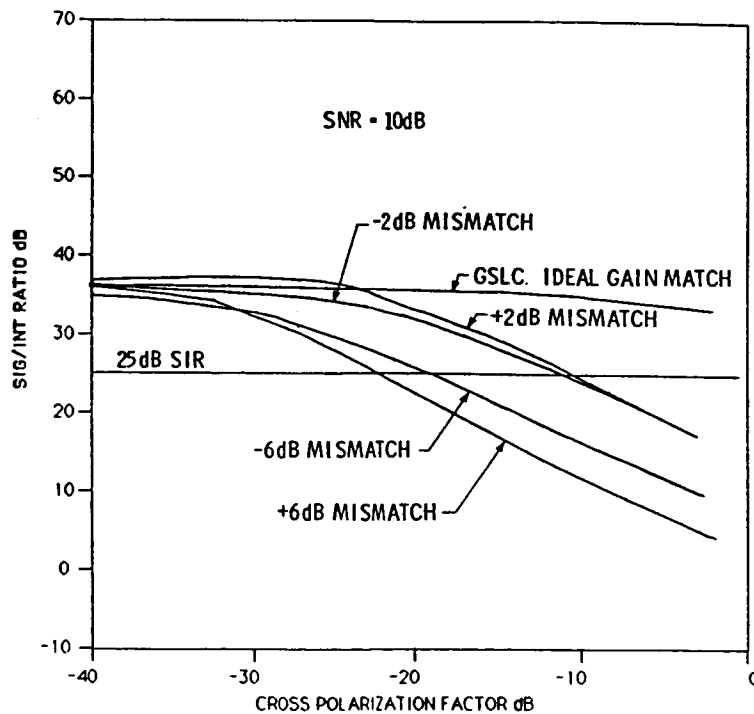


Fig. 5. Effects of gain mismatch on GSLC performance.

To further understand the performance of the simplified GSLC when the magnitude of the gain constant, $|\gamma \beta|$, is not known precisely, GSLC performance curves are presented in Figure 5 corresponding to different values of gain mismatch. As is seen, at a mismatch of ± 2 dB, 25 dB output SIR is available at the nominal 10 dB cross-polarization isolation level.

Comparing the SLC performance curves in Figure 4 with the GSLC curves in Figure 5 reveals that the GSLC operating with a ± 6 dB gain mismatch still outperforms the SLC near the nominal 10 dB cross-polarization isolation level. This demonstrates the superior performance of the GSLC in preventing signal cancellation.

DIGITAL PRECISION REQUIREMENTS

An important consideration in the design and implementation of digital adaptive sidelobe cancellers is the digital precision (bitwidth) required to represent the different variables in the weight update algorithm. The required precision is intimately related to the adaptive step size, μ , utilized in updating the adaptive weight, $W(n)$. In particular, it has been shown (Gitlin) that the required bitwidth, B , for updating the LMS algorithm must satisfy the inequality:

$$2^{-B} < 2 \text{ MIS } |y|_{\text{RMS}} / |x'|_{\text{RMS}} ,$$

where $|y|_{\text{RMS}}$ and $|x'|_{\text{RMS}}$ denote the root-mean-square (RMS) voltage levels of the GSLC output and augmented reference input, respectively, and MIS is termed the LMS algorithm misadjustment level (Widrow). For typical implementations, $|y|_{\text{RMS}}$ and $|x'|_{\text{RMS}}$ will be comparable (i.e., due to AGC limiting prior to digitization) and thus it is sufficient that 2^{-B} satisfy $2^{-B} < 2 \text{ MIS}$. Therefore, the determination of a minimum bitwidth requirement is equivalent to specifying a maximum tolerable misadjustment level, MIS. As a particularly stressing example, if the output signal-to-interference ratio is assumed to be the desired 25 dB and a fixed-weight, residual white noise level 30 dB below the desired signal in the GSLC output is assumed, then a value of $\text{MIS} = .002$ or less will ensure that the total output noise level for the adaptive system will not exceed 25 dB below the desired signal level in the adaptive GSLC output, i.e., an increase of no more than 5 dB over the ideal, fixed-weight GSLC case. This value for MIS corresponds to requiring at least $B = 8$ bits. This will most likely represent a worst-case bitwidth specification for digitally implementing the adaptive GSLC.

REFERENCES

- K. M. Buckley, L. J. Griffiths, "An adaptive generalized sidelobe canceller with derivative constraints," *IEEE Trans. Ant. Prop.*, vol. 34, pp. 311-319, March 1986.
- R. Gitlin, S. Weinstein, "On the required tap-weight precision for digitally implemented, adaptive, mean-squared equalizers," *Bell Syst. Tech. J.* vol. 58, pp. 301-321, Feb. 1979.
- B. Widrow, J. McCool, M. Ball, "The complex LMS algorithm," *Proc. IEEE*, vol. 63, pp. 719-720, April 1975.

JEFF B. BERNER, Mobile Satellite Program, Jet Propulsion Laboratory, California Institute of Technology, United States; DAVID J. BELL, Mobile Satellite Program, Jet Propulsion Laboratory, California Institute of Technology, United States.

CALIFORNIA INSTITUTE OF TECHNOLOGY
JET PROPULSION LABORATORY
4800 Oak Grove Drive 161-228
Pasadena, California 91109
United States

ABSTRACT

JPL has designed and developed a mechanically steered antenna for tracking satellites in a mobile environment. This antenna has been used to track an L-band beacon on the MARISAT satellite. A description of the antenna and the results of the satellite experiment are given.

INTRODUCTION

NASA has been developing the technology for mechanically steered vehicle antennae having 10 to 12 dBi of gain for use in L-band (1600 MHz) MSAT applications (Bell, 1986). While more expensive than omnidirectional antennae, the directional antennae offer two major advantages. First, they save spacecraft power by a possible factor of ten through higher gain and better multipath discrimination. But, more importantly, due to narrower azimuthal beams, they allow two spacecraft to provide coverage of CONUS at the same frequencies. Through proper design of the vehicle's antenna, it is possible to keep the main beam of the antenna pointed toward the desired spacecraft while radiating considerably less energy toward the second spacecraft (also operating at the same frequency).

OPERATION

Figure 1 is a block diagram of the mechanically steered antenna developed at JPL. The radiating part is a linear array of four square microstrip patches tilted with respect to the ground plane to provide elevation coverage from 20° to 60° with a minimum of 10 dBic gain. This configuration provides up to 6 dB more gain than a low gain omnidirectional antenna. The rotating antenna platform is mounted on a fixed platform that includes a stepper motor, the motor driver and the pointing system hardware. A cylindrical radome, with a diameter of 20 inches and a height of 9 inches, covers the antenna system and produces insignificant effects on the RF pattern characteristics.

The initial pointing, or acquisition of the satellite, is achieved by seeking the direction of maximum power reception from a satellite transmitted pilot signal. Subsequent tracking uses a pseudo-monopulse radar technique. The 1 X 4 antenna array is divided into two identical subarrays and signals from each subarray are passed through a hybrid coupler producing sum and difference signals. The difference channel output is modulated by a square wave and added to the sum signal via a coupler. The composite signal is routed to a receiver which decouples and detects the difference signal. The difference signal is then normalized by detected sum signal to correct for signal fading up to 250 Hz. This normalized difference signal is the antenna tracking error signal (Jamnejad, 1988).

The pointing control computer that operates the pointing control loop uses the error signal to rotate the antenna platform azimuthally with a stepper motor. A vehicle turn rate sensor is used to maintain pointing toward the satellite when the received signal level fades below a prescribed threshold. This open loop tracking mode allows the antenna to point at the satellite even if it is blocked from the antenna's view. The rate sensor also serves as an inertial reference during the initial satellite acquisition (Berner, 1987).

The rate sensor, motor controller, motor, and drive assembly are placed on the fixed base plate of the antenna system. The antenna array, the sum/difference hybrid, the coupler, and the difference signal modulator are placed on a rotating circular platform, which constitutes a "ground plane" for the array and is stacked on top of the base plate assembly. RF connection between the fixed and moving parts is made through a single channel rotary joint which forms the common central axis of the fixed lower platform and rotating upper platform of the antenna. This rotary joint is surrounded by a set of five slip rings, which provide low frequency and DC signals for the modulator. This stacked configuration is easy to breadboard and simplifies the tasks of testing and trouble shooting at this experimental stage. It also explains the 9 inch height of the assembly (Figure 2).

DEVELOPMENT STRATEGIES

Development of the 1 X 4 mechanically steered antenna was split into the parallel developments of pointing control software, signal processing hardware, platform structure, and RF elements. Interface signals were clearly defined at the outset. Efficient development was greatly facilitated by first constructing a working model of the antenna and platform with control interface signals identical to the final version. The RF portion of the antenna was modeled by a photoresistor "antenna" and circuitry that mimicked the RF sum and difference channel gain patterns. This circuitry also produced a normalized difference/sum tracking error signal modeling the output of the signal processing circuitry. A simple incandescent light near the software development station became the "satellite" test beacon. This model was demonstrated at the MSAT-X Industry Briefing (Bell, 1985). The model provided immediate feedback on software performance, speeded software development, and increased confidence and understanding of the entire pointing control loop. The success of this method was demonstrated during the final integration phase when the antenna

immediately began tracking an RF beacon in the lab after phase delay corrections were made to the RF sum and difference channel circuitry.

The mechanically steered antenna has been the result of a low budget, low manpower development effort. Off-the-shelf components were employed as much as possible to speed development. JPL plans to demonstrate a reduced 5 inch height model that will eliminate costly prototype slip rings and rate sensor electronics. In a related effort, Teledyne Ryan Electronics is currently under contract to JPL to develop a flat plate mechanically steered vehicle antenna with a height of only 1.5 inches.

SATELLITE TEST

In August of 1987, the JPL MSAT Pilot Field Experiment (PiFEX) team went to Santa Barbara, CA, to conduct satellite tracking tests on the mechanical antenna. This test is referred to as the PiFEX Satellite-1a, or S-1a, test. The antenna was mounted on the MSAT-X Mobile Laboratory/Propagation Measurement Van (PMV). The tests used an L-band beacon on the MARISAT satellite. After acquiring the beacon, the tests consisted of tracking the satellite while driving through the surrounding mountains. Over 500 MBytes of data were collected during this two week experiment.

Test Conditions

The test conditions experienced were well below ideal for the antenna. There are few satellites on the west coast with an L-band beacon. In the JPL area, the highest possible elevation angle to a satellite occurs in Santa Barbara with the MARISAT satellite and the angle is only 13°. The antenna is only designed to operate in elevation angles as low as 20°. Also, the EIRP of the beacon is 4 dB less than the nominal configuration proposed for MSAT applications. The low received signal power and the additional multipath, both due to the low elevation angle, substantially increased the noise level on the difference channel signal, which is used as the error signal in closed loop tracking. Two important tracking loop parameters were modified to fit the antenna system for operation in this reduced signal level environment. First, the tracking loop bandwidth was reduced by a factor of 8 to combat the increased noise levels. Secondly, the closed loop/open loop handover threshold was increased to improve the response to quick vehicle turns that is lost when the tracking loop bandwidth is reduced. The result was a pointing control loop that was biased to depend more heavily on the open loop mode than is necessary for the expected MSAT satellite signal levels.

In addition to the control loop changes, a low noise amplifier and bandpass filter were added to the antenna just prior to the rotary joint to increase the overall signal level and to reduce the effects of RF losses in the rotary joint and the cabling to the receiver. Plots of the sum and difference/sum signals for the satellite test are given in Figures 3 and 4.

Acquisition Tests

Acquisition testing consisted of manually moving the antenna platform off-point and issuing the start acquisition command. These tests were performed both while the PMV was stationary and mobile. Figure 5 provides a histogram of the Time to Acquire. During the mobile tests, it was possible that the satellite was blocked. If the signal was not located, the antenna platform was scanned again, until the satellite was found. The mean time to acquire was 11.97 seconds, below the requirement of 15 seconds.

Closed Loop Tracking

As was mentioned earlier, the closed loop tracking capability was limited due to the adverse test conditions. For the closed loop to be used, the road that the PMV was on had to have a clear line-of-sight to the satellite and had to have turn rates less than 10 degrees/second. Figure 6 provides a scatter plot, generated from over one hour of data, of the PMV Turn Rate versus the Degrees Off Point when tracking in closed loop. As can be seen, the pointing error remains between $\pm 2^\circ$ for turn rates in the range of ± 8 Degrees/sec. For turn rates greater than this, the antenna tracked in open loop mode. The specification that the antenna was designed to was a closed loop pointing error of $\pm 2^\circ$.

Open Loop Tracking

The purpose of the open loop tracking is to keep the antenna platform pointed at the satellite while the signal is blocked. This tracking method uses an angular turn rate sensor to provide the tracking information. The problem with using a rate sensor is that the sensor has a drift that varies with temperature and time. For the S-1a experiment, the rate sensor was temperature controlled by an oven, leaving only the drift with time. Because of the drift, the antenna pointing system was designed to operate in open loop for time periods of less than 10 seconds. The goal was to keep the pointing error between $\pm 2^\circ$ in the 10 second period. Figure 7 provides a scatter plot of the Time Spent in Open Loop versus Degrees Off Point which shows that the open loop tracking keep the error between $\pm 1.2^\circ$. Figure 8 shows a scatter plot of the open loop error versus the turn rate. Both figures were generated from 10 minutes of data. As can be seen, over a range of ± 8 degrees/sec, the antenna tracked within $\pm 1^\circ$.

Closed Loop/Open Loop Handover

When the signal fades the tracking mode switches to open loop. When the fade ends, closed loop tracking takes over again. If the transfer to open loop is too slow, closed loop tracking will continue with a difference/sum signal that is noise dominated, causing the antenna pointing error to grow. If the transfer occurs too soon, the antenna will be rapidly switching back and forth between open and closed loop. Due to the poor signal conditions, the transfer had to be quicker than it would be for the MSAT system. Figure 9 shows a one

minute history of the pointing error as the antenna switches between closed and open loop. The closed-to-open loop transfers occur at 35 seconds, 45 seconds, and 52 seconds. As can be seen, the transfer, which occurs 70 msec after the fade occurs, should have occurred sooner.

CONCLUSIONS

The JPL mechanically steered antenna has demonstrated that mechanically steered antennae can track a satellite. This low cost breadboard antenna tracked the satellite over a variety of environmental conditions and in all cases the antenna tracked the satellite within $\pm 2^\circ$.

ACKNOWLEDGMENTS

The authors would like to thank the people involved in the experiment and the data analysis that followed: Richard Emerson, Loretta Ho, Walt Mushagian, Jim Parkyn, and William Rafferty.

REFERENCES

- Bell, D., and Naderi, F. M. 1986. "Mobile Satellite Communications - Vehicle Antenna Technology Update," AIAA Space System Technology Conference, June 9-12, 1986.
- Bell, D. 1985. "Vehicle Antenna Pointing Techniques for Mobile Satellite Communications," Mobile Satellite Industry Briefing, November 13-14, 1985.
- Berner, J. B., and Winkelstein, R. 1988. "Antenna Pointing System," MSAT-X Quarterly, Number 13, January 1988.
- Jamnejad, V. 1988. "A Mechanically Steered Monopulse Tracking Antenna for PiFEx: Overview," MSAT-X Quarterly, Number 13, January 1988.

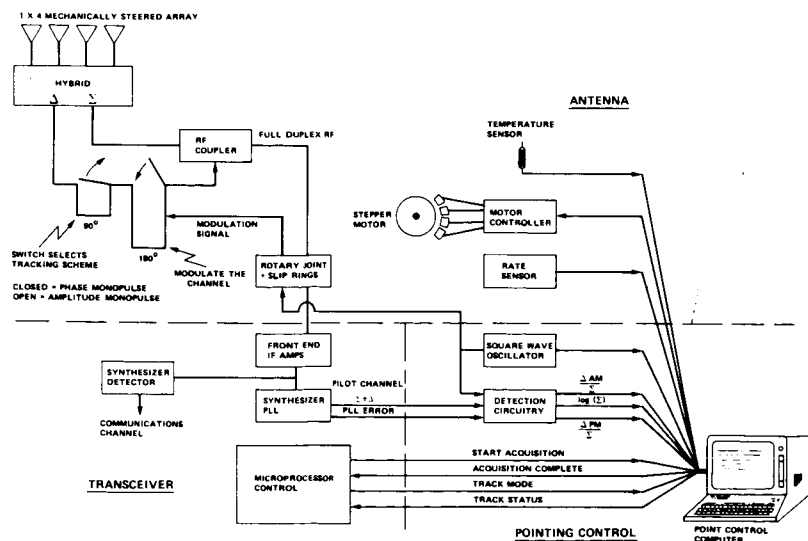


Figure 1: Antenna System Block Diagram

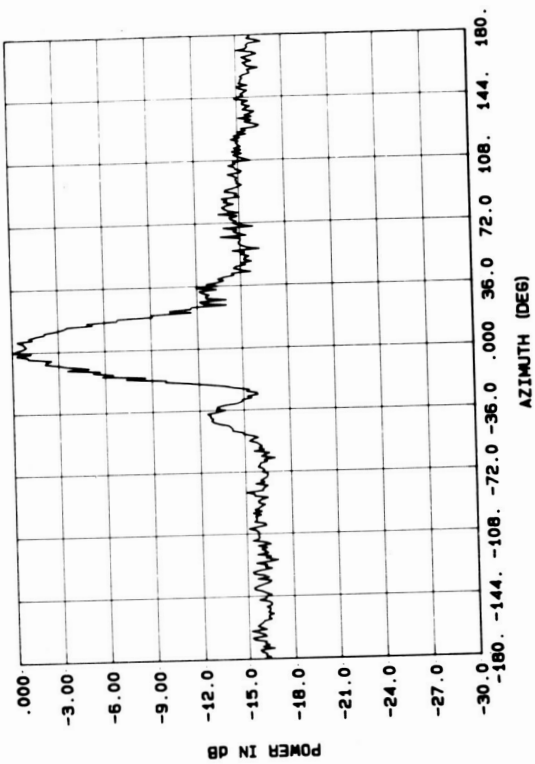


Figure 3: Received Sum Signal

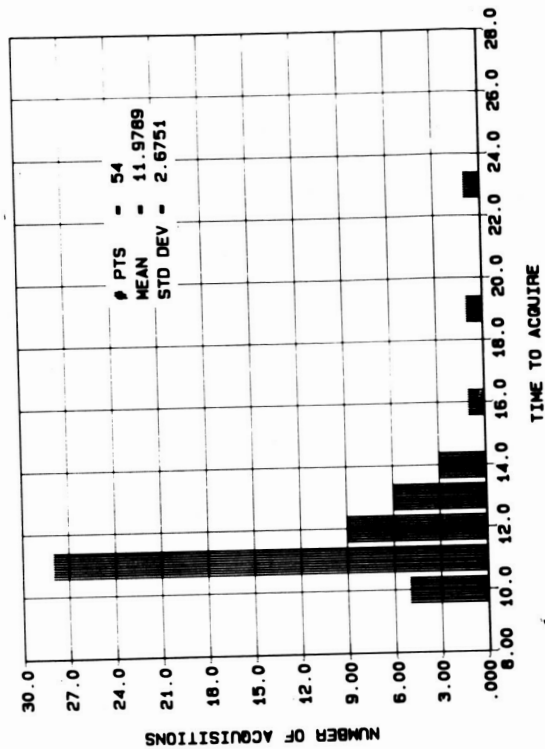


Figure 5: Acquisition Time Histogram

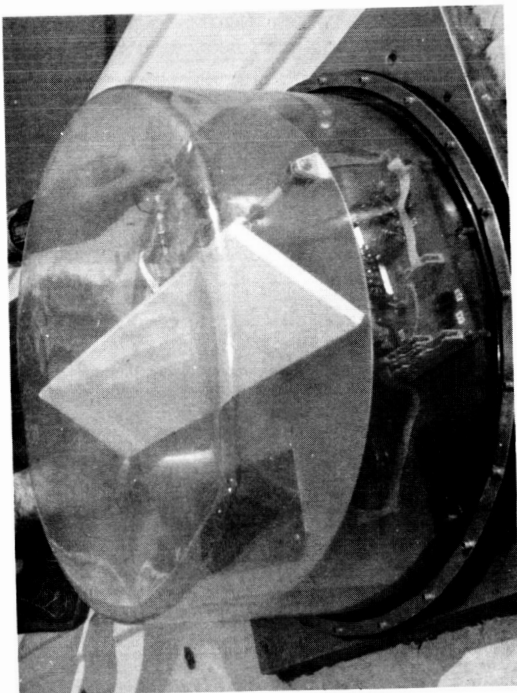


Figure 2: JPL Mechanical Antenna

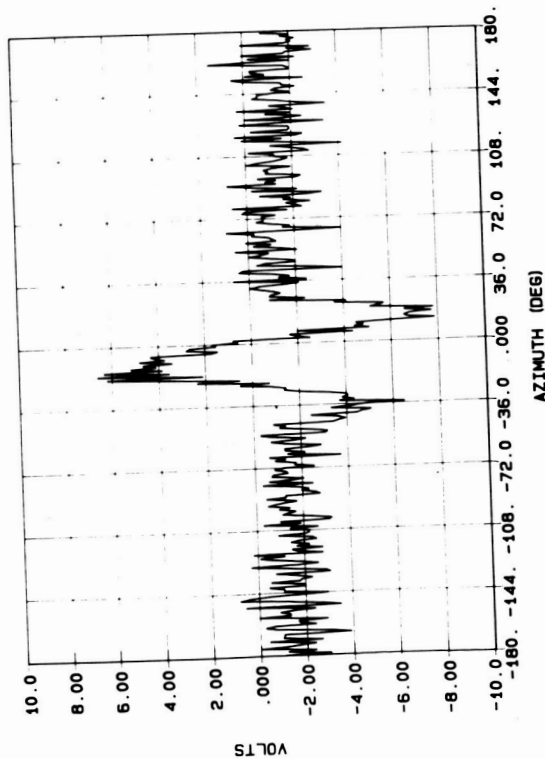


Figure 4: Difference/Sum Signal

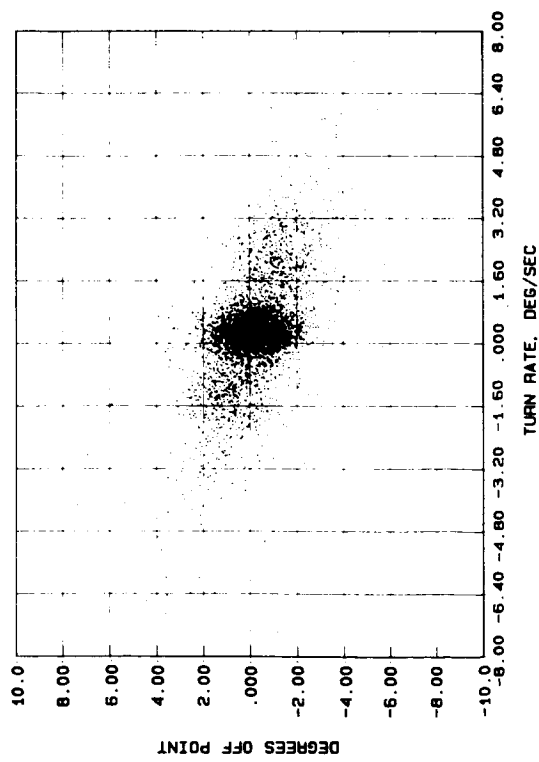


Figure 6: Closed Loop Error Versus Turn Rate

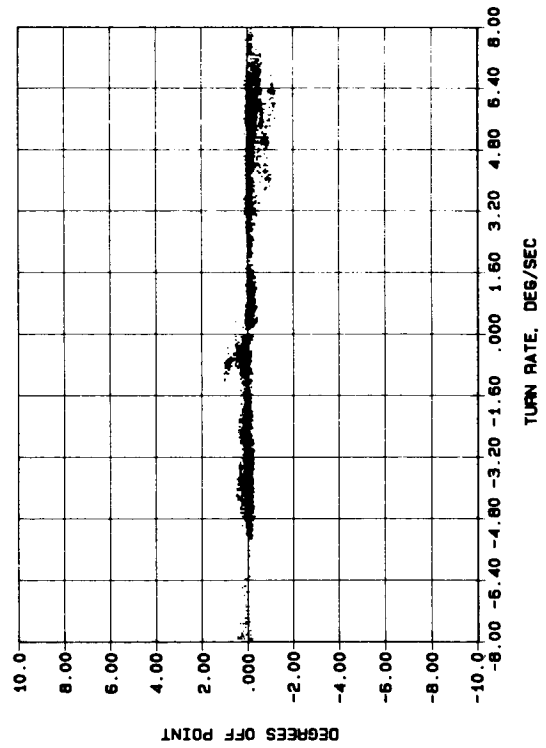


Figure 8: Open Loop Error Versus Turn Rate

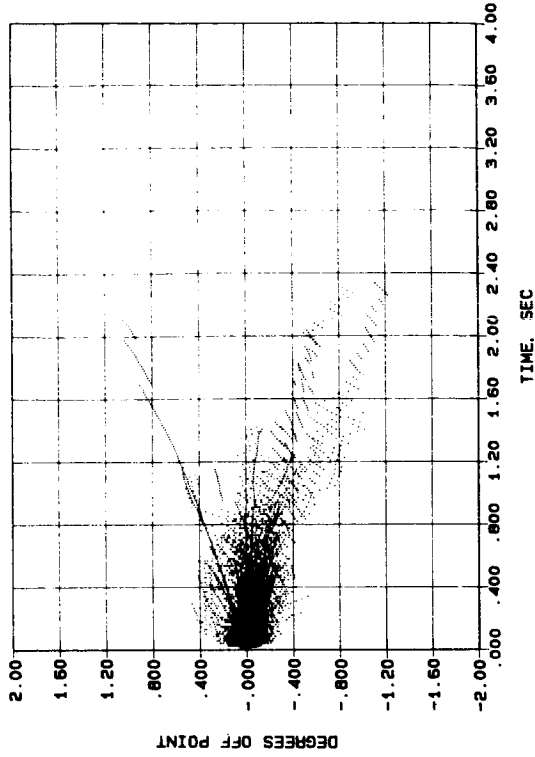


Figure 7: Open Loop Error Versus Time in Open Loop

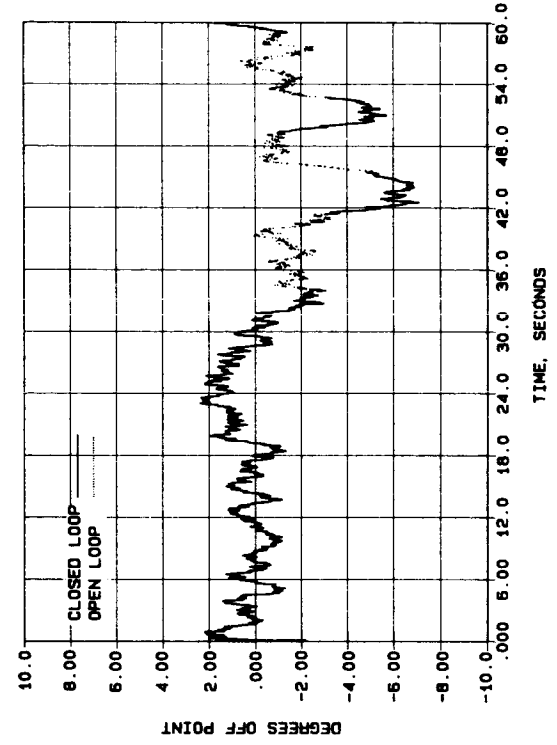


Figure 9: Pointing System Error Versus Time

SIMPLE, LOW-PROFILE, CIRCULARLY POLARIZED ARRAYS

PAUL MAYES, JAMES DREWNIAK, JAMES BOWEN AND JAMES GENTLE,
Electromagnetics Laboratory, University of Illinois, USA

ELECTROMAGNETICS LABORATORY
Electrical and Computer Engineering Department
University of Illinois
1406 West Green Street
Urbana, Illinois 61801
United States

ABSTRACT

A low-profile, circularly polarized antenna can be made using an annular sector of strip conductor parallel to a closely spaced ground plane. This antenna has a very wide impedance bandwidth and is particularly well suited for use in series-fed arrays. Control of the excitation coefficients can be accomplished by a simple variation in the geometry of each element. Interconnection of the elements has been realized both in coaxial cable and in microstrip. Axial ratios less than 1 dB in the broadside direction are easily obtainable.

INTRODUCTION

Circular polarization (CP) is required to receive signals from satellite-borne transmitters. Antennas for a mobile platform are preferably low-profile. The attainment of desired pattern shape to provide adequate gain and coverage is made possible through array techniques. Acceptance of the system is dependent upon the total cost. All of these features are well met by a new type of antenna element [Drewniak and Mayes, 1987]. In addition, this element has a wide impedance bandwidth. Since the element is constructed from strip conductor in the shape of a sector of an annulus, it is basically a curved section of strip transmission line. We shall call it the ANSERLIN (ANnular SEctor Radiating LINE) antenna.

SINGLE ANSERLIN ELEMENTS

The configuration of the conducting strip is shown in Figure 1. A triangular section on each end of the annular sector is used for connection to the center conductor of a coaxial cable. The width-to-height ratio is maintained near constant in order to provide the same impedance through the antenna from one port to the other. Since the impedance does not change appreciably at any point along the structure, a wave that is initiated at either port will traverse to the other without producing any reflections. This traveling-wave operation of ANSERLIN antennas contrasts sharply with the resonant manner in which most microstrip patch antennas work. As a result,

the impedance bandwidth of ANSERLIN elements is very much greater than that of patches. In fact, the variation of impedance is of no consideration in determining the operating bandwidth. Measured SWR less than 1.5 has been observed over bandwidths as great as 8:1. The Smith Chart of Figure 2 shows that the SWR can be held to even smaller values over a narrower band. However, the operating bandwidth is more likely to be based upon variation in power gain on boresight relative to a CP standard.

A single ANSERLIN element produces a beam of CP radiation which scans slowly with change in frequency. At the frequency where the traveling wave suffers a one degree change in phase for each degree of rotation in azimuth, the beam maximum occurs along the line perpendicular to the plane of the strip conductor. Near this frequency the radiation is very nearly CP over most of the beam; axial ratio less than 1 dB being routinely obtained near the beam maximum. A typical radiation pattern at a frequency where the above condition is very nearly realized is plotted in Figure 3. This pattern was measured in a rapidly rotating linearly polarized field to illustrate how little the polarization changes with angle. Either sense of CP can be produced depending upon the port which is excited.

Of course, achieving a single wave, traveling in the desired direction, is dependent upon maintaining the impedance match at the output port. Hence, that part of the input power that is not radiated before the wave reaches the output port must be absorbed by the matched termination. Although it is possible to increase the percentage of the input power that is radiated (by increasing the width of the strip conductor and, consequently, the height above the ground plane), even the maximum value (between 60 and 70 percent, so far) may not produce acceptable values of power gain. However, it is a relatively simple matter to combine ANSERLIN elements in a series-fed array. Then the power left at the output of the first element in the array can be delivered to the input of the next element, and so forth. In this way it is possible to radiate more than 90 percent of the incident power in an array with only a few elements.

LINEAR ARRAYS OF ANSERLIN ELEMENTS

The layout of a broadside array of six ANSERLIN elements is illustrated in Figure 4. A symmetric excitation is achieved by splitting the input power and feeding the two sides of the array at the two central elements. Further control of the excitation is provided by changing the widths of the annular sectors, using narrow strips near the input of the array and increasing the width of each succeeding element to increase the fraction of the power input to that element that is radiated. The impedance measured at the input of the power divider is plotted on the Smith Chart of Figure 5. The radiation pattern in the plane of the array measured with a spinning source antenna at 2.2 GHz is shown in Figure 6. The half-power beamwidth and sidelobe level are close to the expected values.

Fabrication of arrays of ANSERLIN elements could be facilitated, with resulting reduction in cost, by replacing the coaxial interconnections by a printed transmission medium. The upper diagram in Figure 7 shows an ANSERLIN element that is connected at both input and output ports to microstrip conductors. To maintain

the required impedance, the thinner microstrip is closer to the ground plane than the annular sector. A six-element array with hybrid interconnections is shown in the lower part of Figure 7. This is an intermediate step in the development of an array with only microstrip interconnects. Although microstrip-to-ANSERLIN transitions occur at the input and output ports of each element, the interconnection and phasing of the elements are still accomplished with coaxial lines behind the ground plane. So far, the SWR realized with the microstrip feed at each port has not been as low as the best previously obtained with coaxial feeds. The impedance measured at the input of the power divider for the array of Figure 7 is shown in Figure 8. Improved pattern performance has been achieved with the microstrip-fed elements, however, as illustrated in Figure 9. This is primarily due to a better design technique.

ARRAY WITH TILTED BEAM

The coverage area of the linear arrays of ANSERLIN elements can be changed by taking advantage of the tendency of the element patterns to scan with frequency. This effect could be used to reduce the tilt angle that would be required to cover elevation angles near the horizon. Figures 10 and 11 show radiation patterns measured for the array of Figure 4 at 2.6 GHz. Excess phase shift in the wave traveling around the element causes the beam maximum to occur off the perpendicular. The pattern in the plane of the array shows lower sidelobe level since the beam and lobe maxima are no longer located in the plane of the measurement. The pattern in the orthogonal plane displays the beam tilt, the maximum occurring almost 20 degrees away from the perpendicular to the array surface. Between 10 dB points the beam is still very nearly CP.

CONCLUSIONS

Many of the requirements for a mobile, earth-based antenna for satellite communications can be easily met with an array of ANSERLIN elements. Additional efforts in interconnection technology, pattern synthesis, and construction techniques could well provide a low-cost, high performance array that is very well suited for this service.

REFERENCES

- Drewniak, J., and P. E. Mayes 1987. Broadband, circularly polarized, radiating line antennas with an application to a series-fed array. Electromagnetics Laboratory Report No. 87-4. (Urbana, Illinois: University of Illinois).

ORIGINAL PAGE IS
OF POOR QUALITY

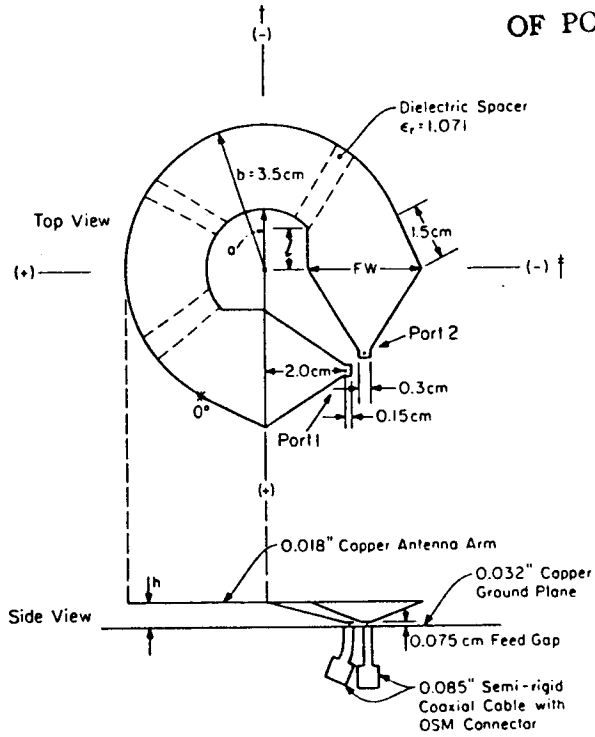


Fig. 1. An ANSERLIN element.

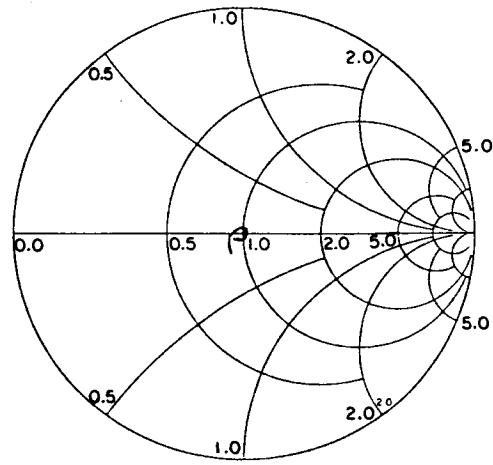


Fig. 2. Input impedance,
2-3 GHz.

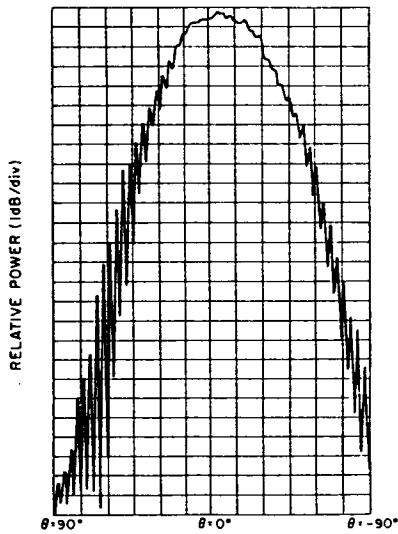


Fig. 3. Elevation-plane pattern, 2.2 GHz.

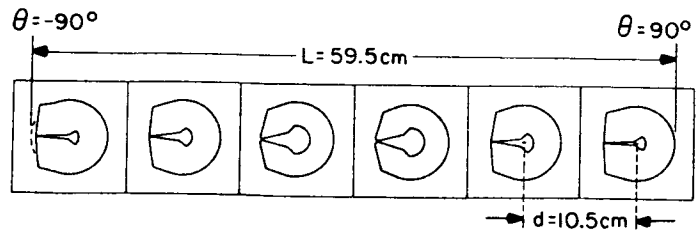


Fig. 4. Six-element array.

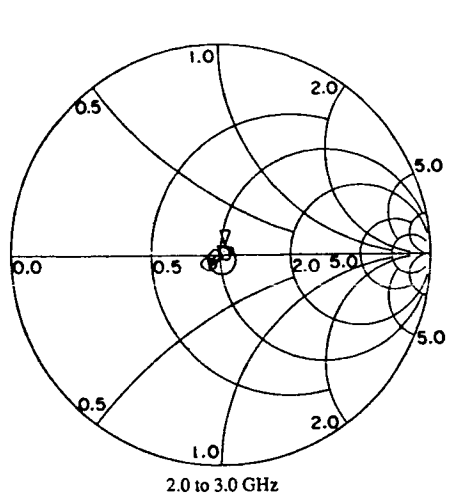


Fig. 5. Input impedance of array of Fig. 4.

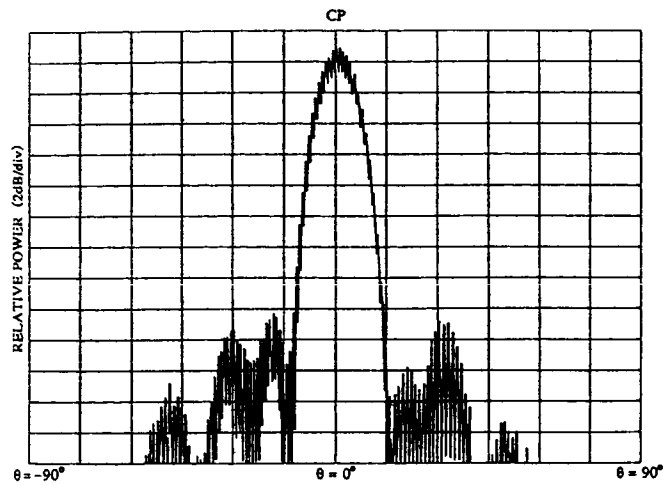


Fig. 6. Elevation-plane pattern through the plane of the array.

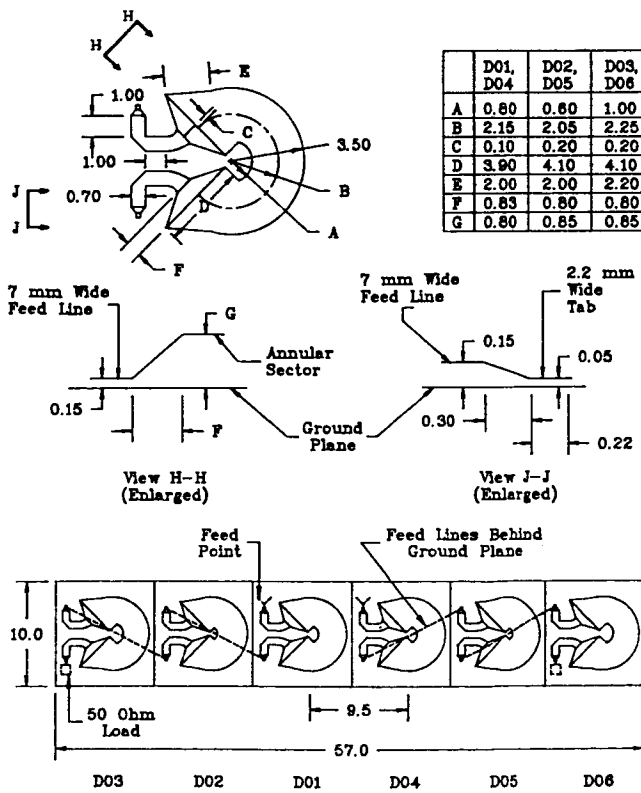


Fig. 7. Microstrip-fed ANSERLIN element and array (dimensions in cm unless stated).

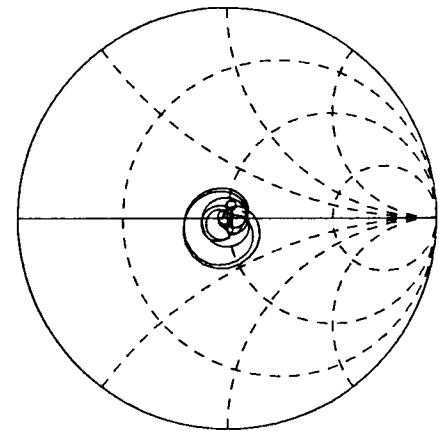


Fig. 8. Input impedance of array of microstrip-fed elements.

ORIGINAL PAGE IS
OF POOR QUALITY

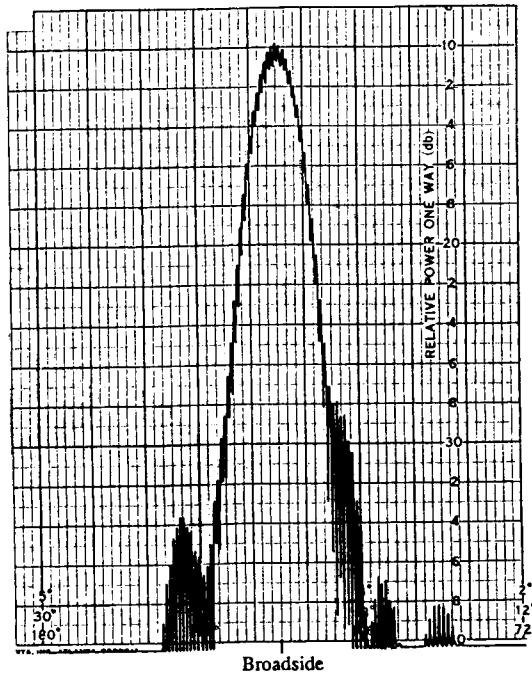


Fig. 9. Elevation-plane pattern of array of microstrip-fed elements.

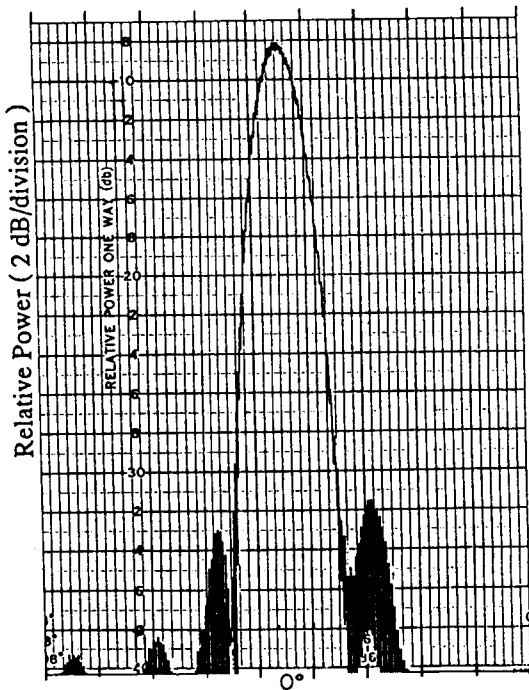


Fig. 10. Elevation-plane pattern through plane of array of Fig. 4 at 2.6 GHz.

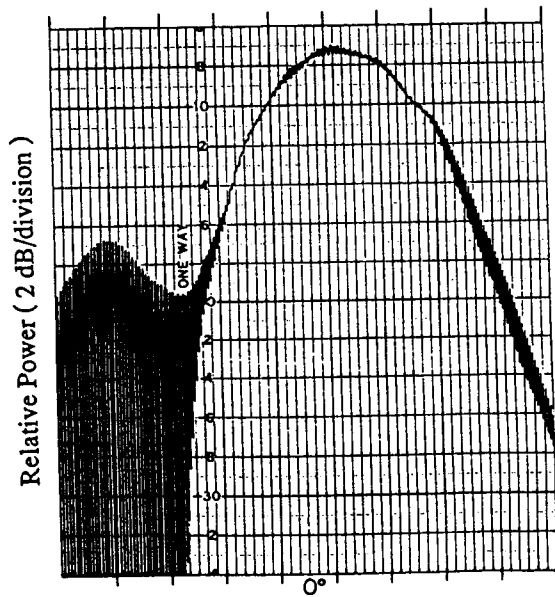


Fig. 11. Elevation-plane pattern in plane perpendicular to plane of the array of Fig. 4 at 2.6 GHz.

(20 degrees per major division)

OMNI-DIRECTIONAL L-BAND ANTENNA FOR MOBILE COMMUNICATIONS

DR. C. S. KIM, N. MOLDOVAN, and J. KIJESKY
PRODELIN CORPORATION
1700 NORTHEAST CABLE DRIVE
P. O. BOX 368
CONOVER, NORTH CAROLINA 28613
UNITED STATES

ABSTRACT

This paper discusses the principle and design of our L-band omni-directional mobile communication antenna. The antenna is a circular waveguide aperture with hybrid circuits attached for higher order mode excitation. It produces circular polarized and symmetric two split beams in elevation. The circular waveguide is fed by eight probes with a 90 degree phase shift between their inputs. Radiation pattern characteristics are controlled by adjusting the aperture diameter and mode excitation. This antenna satisfies gain requirements as well as withstanding the harsh environment.

INTRODUCTION

This paper describes the development of a circular polarized, high gain, L-band transmit antenna for mobile communications. The antenna is a circular waveguide with an integrated stripline feed circuit to produce circular polarized conical split-beam patterns into half space. Its application is for the new radiodetermination satellite service (RDSS), just approved by the FCC.

During the past few years, several antennas such as microstrip patches [1] and spiral horns [2] have been introduced for mobile communications. Both types of antennas have used hybrid circuits to produce two split broad conical beams. The ideal RF performance is to maximize the peak gain (>5 dBi) while maintaining a broad halfpower beamwidth ($>40^\circ$). The antenna presented here has radiation fields that can be controlled by adjusting aperture radius and modes of excitation (TE_{21} or TE_{31}). Radiation patterns are calculated by aperture integration. Measured radiation patterns show that good symmetry exists and that the maximum beam axis occur at plus and minus 40° . Halfpower beamwidths of approximately 40° have been achieved.

THEORETICAL BACKGROUND

The basic electromagnetic principle applied to the analysis of this antenna is Huygen's secondary source to solve integral equations for vector potentials. Radiation patterns are calculated by aperture integration over a cylindrical cavity excited by higher order modes. The radiation fields in spherical coordinates for linear polarization (E_1 & E_2) can be obtained from Silver [3]. These fields can be circularly polarized by introducing a 90° phase difference. Physically, this corresponds to phasing adjacent probes with a 90° phase difference as shown in Figure 1.

For circular polarization and desired mode excitation, probes with proper spacing are needed. These probes are located perpendicular to the side wall so that their positions are parallel with the maximum E-field vector. The fields generated from two adjacent probes are orthogonal to each other inside the circular waveguide. With this angular spacing (α) chosen, as shown in Figure 1, one probe is always situated in the null field region of the other probe, thus causing very little mutual coupling between probes [1]. In order to keep beam symmetry (Omni-Directional in azimuth) and cross polarization low, many probes should be used to suppress unwanted modes. To determine the radiation pattern for circular polarization the following equation is used:

$$E_{TE_{m1}} = \sum_{n=1}^N E_1 \sin(m\Phi) e^{j(n-1)\pi/2} \\ \pm j \sum_{n=1}^N E_2 \cos(m\Phi) e^{j(n-1)\pi/2}$$

WHERE:

- N = number of probes
- α = $360/N$ degrees
- m = $N/4$ (mode number)
- Φ = $(\phi + (n-1)\alpha)$

RADIATION PATTERN AND GAIN CALCULATION

Radiation patterns are calculated by the equation depending on the mode excitation. Gain calculation is on the basis of $G=4\pi P_k/P_t$, where P_k is the peak power at the beam peak axis and P_t is the total power radiated. Radiation patterns are shown in Figure 2 for different modes. Gain computations are also illustrated in Table 1 for both different modes and diameters.

On the basis of Table 1 and Figure 2, radiation patterns and gains are in very close relationship to each other. Usually as aperture diameter increases, higher order modes are used. Since gains of modes 2 and 3 are approximately above 5dB and beam axis is controlled between 30° and 50°, radiation pattern and gain can be optimized, depending on requirements.

TABLE 1 CALCULATED GAIN AND RADIATION PATTERN

MODE (TE)	DIAMETER (WAVELENGTH)	PEAK DIRECTION FROM BROADSIDE	GAIN (dBi)	*BEAMWIDTH
1	.6	0°	8.3	90°
	.8	0°	10.9	74°
	1.0	0°	11.8	60°
2	1.0	41°	5.73	54°
	1.1	38°	6.75	50°
	1.2	36°	7.52	46°
3	1.34	51°	3.66	49°
	1.4	50°	5.32	48°
	1.46	48°	6.0	47°
4	1.7	56°	3.25	46°
	1.8	54°	5.13	44°
	1.9	52°	5.99	42°

***BEAMWIDTH IS ONE SIDE FOR TE₂₁, TE₃₁, AND TE₄₁**

EXPERIMENTAL RESULTS

Two prototype antennas (TE₂₁, 8 probes and TE₃₁, 8 probes) were fabricated to verify their predicted performances. Each prototype consisted of a circular waveguide cavity, feed probes and off-the-shelf power dividers. In order to provide the proper phase difference between probes, coaxial delay lines were connected between the probes and power dividers.

Comparisons between calculated and measured data are shown in Figure 3 and 4. Radiation patterns with TE₂₁ and TE₃₁ have shown that a good symmetric, conical pattern exists and that both beam axis and beam widths satisfy calculated results.

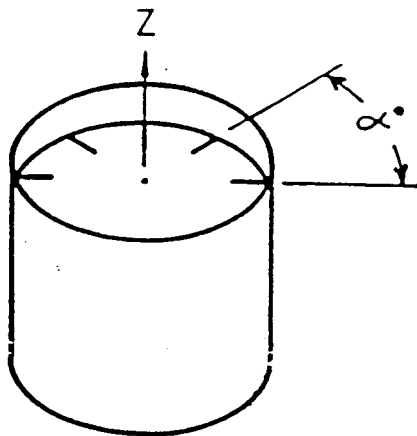


FIGURE 1

CIRCULAR WAVEGUIDE CAVITY SHOWING PROBES WITH ANGULAR SPACING α .

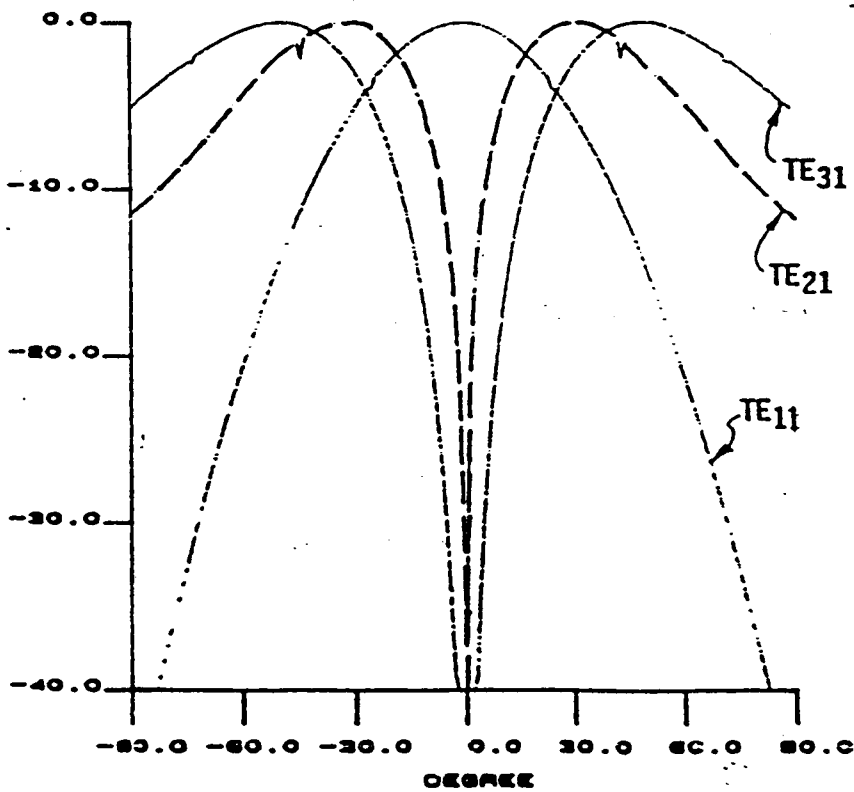


FIGURE 2

CALCULATED RADIATION PATTERNS FOR DIFFERENT MODE EXCITATIONS.

ORIGINAL PAGE IS
OF POOR QUALITY

FIGURE 3

COMPARISON BETWEEN COMPUTED AND
MEASURED PATTERNS, TE₂₁, DIA.
10.2"
F = 1.27 GHz

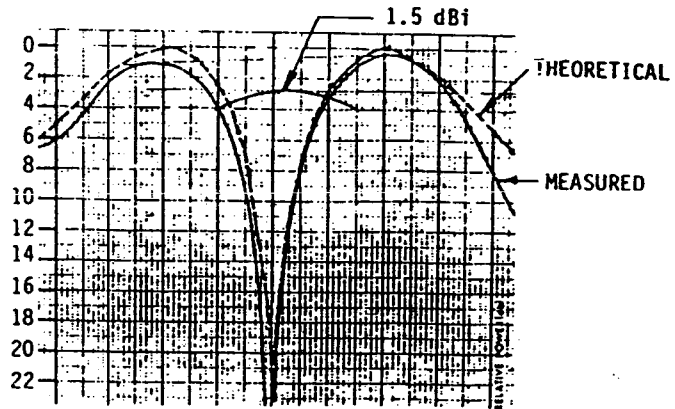


FIGURE 4

COMPARISON BETWEEN COMPUTED AND
MEASURED PATTERNS, TE₃₁, DIA.
11.5"
F = 1.62 GHz

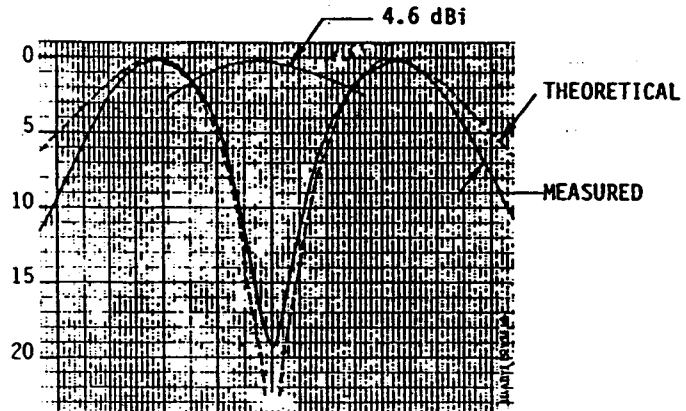
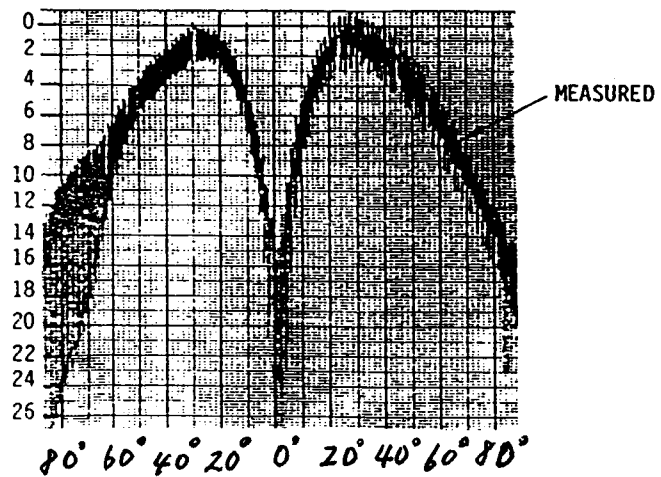


FIGURE 5

AXIAL RATIO PATTERN, TE₂₁, DIA.
10.2"
F = 1.62 GHz



The axial ratio in Figure 5 is within 2 - 3 dB near the main beam axis. The phase feeding circuitry is very sensitive to the antenna performance; small errors in phase-amplitude of the combiner and phase lines cause major changes in radiation patterns. Since edge diffraction terms are not included, errors exist between computed and measured data around 90°. Overall measured radiation patterns are in agreement with calculated values.

REFERENCES

1. J. Huang, "Circularly Polarized Conical Patterns from Circular Microstrip Antennas". IEEE Trans. on Antennas and Propagat., Vol. AP-32, No. 9, Sept. 1984, pp. 991-994.
2. R. Johnson and H. Jasik, "Antenna Engineering Handbook", McGraw-Hill Book Co., 1984 Edition, pp. 14.3 - 14.24.
3. Silver, "Microwave Antenna Theory and Design", New York, Dover 1965, pp. 334-341.

SESSION F
MODULATION AND CODING I

SESSION CHAIR: Gottfried Ungerboeck, IBM Zurich Research Laboratory
SESSION ORGANIZER: Dariush Divsalar, Jet Propulsion Laboratory

TRELLIS-CODED CPM FOR SATELLITE-BASED MOBILE COMMUNICATIONS

FARROKH ABRISHAMKAR, Technology Group, Los Angeles, CA.
EZIO BIGLIERI, Electrical Engineering Department, UCLA, Los Angeles, CA.

Technology Group, 1888 Century Park East, Suite 10, Los Angeles, CA 90067

Abstract

This paper is concerned with digital transmission for satellite-based land mobile communications. To satisfy the power and bandwidth limitations imposed on such systems, we consider a combination of trellis coding and continuous-phase modulated signals. Some schemes based on this idea are presented, and their performance analyzed by computer simulation. The results obtained show that a scheme based on differential detection and Viterbi decoding appears promising for practical applications.

1 Introduction

In satellite-based land mobile communication systems, both bandwidth and power are limited resources. In fact, they generally employ frequency-division multiple access with an assigned channel spacing, and the fraction of out-of-band power must be very small to prevent interferences to adjacent channels. On the other hand, the satellite distance from earth, its power limitation, and the need for low-cost (and hence low-gain) mobile antennas further limits the power efficiency of the system.

In an environment which is simultaneously bandwidth- and power-limited, a bandwidth- and power-efficient coding/modulation scheme must be used. Trellis coded modulation (TCM) [7] offers a viable solution, since it increases the reliability of a digital transmission system without increasing the transmitted power nor the required bandwidth. Due to the strictly bandlimited environment created by the mobile satellite channel, the signals to be used in conjunction with trellis codes must be chosen very carefully. An additional constraint comes from the requirement of constant-envelope signals to be used on satellite transponders operating in a time-division multiple access (TDMA) mode. A class of bandwidth-efficient signals that satisfies this constraint is offered by continuous-phase modulated (CPM) signals, based on phase modulation where phase continuity is introduced to reduce the bandwidth occupancy.

The synergy between TCM, which improves error probability, and CPM signals, which provide constant envelope and low spectral occupancy, is expected to provide a satisfactory solution to the problem of transmitting on mobile satellite channels.

In this paper we consider the design and the performance of three trellis-encoded CPM schemes. The detection models considered are: coherent detection, coherent detection with time diversity, and differential detection with interleaving.

The organization of the paper is the following. In Section 2 we provide a brief overview of CPM signals. A discussion of the channel impairments affecting satellite-based mobile communication systems is provided in Section 3. The modulation/detection schemes studied in this work are described in Section 4, where simulation results are also presented.

2 Continuous-phase modulated (CPM) signals

A continuous-phase modulated signal [1] is defined by

$$s(t, \mathbf{a}) = \sqrt{2\mathcal{E}_s/T_s} \cos(2\pi f_0 t + \theta(t, \mathbf{a})) \quad (1)$$

where \mathcal{E}_s is the symbol energy, T_s is the symbol time, and f_0 the carrier frequency. The transmitted information is contained in the phase

$$\theta(t, \mathbf{a}) = 2\pi h \sum_{n=-\infty}^{\infty} a_n q(t - nT_s) \quad (2)$$

with $q(t)$ the phase-shaping pulse given by $q(t) = \int_{-\infty}^t g(\tau) d\tau$, and $g(t)$ is the frequency pulse with finite duration LT_s . In (2), $\mathbf{a} = \dots, a_{-2}, a_{-1}, a_0, a_1, \dots$ denotes the symbol sequence at the output of the trellis encoder. The symbols a_n take values $\pm 1, \pm 3, \dots, \pm(M-1)$, where $M = 2^m$, m a positive integer. The parameter h is called the *modulation index*, and we shall assume $h = 2p/q$, with p, q relatively prime integers. The total number of states is qM^{L-1} . As a special case, for full-response signaling there are Mq signal paths, and q states: this reduction in the number of paths and states, and hence in the complexity of the modulator-demodulator pair, is traded for an inferior spectrum.

2.1 Detection of CPM signals

Coherent detection. Optimum (maximum-likelihood sequence) estimation of CPM signals involves maximization of the probability density function for the observed signal conditioned on the symbol sequence \mathbf{a} . Under the assumption that the only disturbance affecting the received signal is an additive white Gaussian noise process $n(t)$, i.e., that $r(t) = s(t, \mathbf{a}) + n(t)$, optimum (maximum-likelihood) detection gives a bit error probability that, for high signal-to-noise ratios, can be roughly approximated by

$$P_b(e) \approx \frac{1}{2} \operatorname{erfc} \left(\frac{d_{\text{free}}}{2\sqrt{N_0}} \right), \quad (3)$$

where

$$d_{\text{free}}^2 = \min_{\mathbf{a} \neq \mathbf{a}'} \int_{-\infty}^{\infty} [s(t, \mathbf{a}) - s(t, \mathbf{a}')]^2 dt.$$

Differential detection. The complex envelope of the received signal $\tilde{r}(t)$ is multiplied by $\tilde{r}^*(t - T_s)$ and sampled every T_s seconds. A discrete signal is obtained whose phase is $2\pi f_0 T_s + \Delta\theta_n + \eta_n$, where $\Delta\theta_n$ represents the change over one symbol interval of the signal phase, and η_n represents the change in phase due to the noise. Under the assumption that $f_0 T_s$ is an integer number, estimate of this phase provides a noisy estimate of $\Delta\theta_n$, which is used to recover the information sequence.

Discriminator detection If the observed signal $r(t)$ is passed through a limiter and a frequency discriminator, we get the derivative of the information-bearing phase.

2.2 Combining CPM with TCM

If CPM signals are combined with an external convolutional encoder, or, equivalently, they form the signal constellation to be used in a TCM scheme, a further improvement can be obtained. This new scheme is obtained by observing that at the output of the trellis encoder we get a multilevel signal, which in turn can be used as the input to the continuous-phase modulator. The design of the coding scheme and of the modulator scheme should be performed jointly, in order to maximize the Euclidean distance resulting from the combination of the two.

Two possible implementations of TCM/CPM are feasible. The first one takes advantage of both the bandwidth efficiency *and* the power efficiency of CPM codes, by using a receiver which combined the trellis structure of TCM and that of CPM. In this situation, TCM and CPM can be integrated in a single entity (see [5] and the references therein). As a result, the number of states necessary for a trellis representation of these signals is the product of the number of states needed by TCM and the number of states needed by CPM. Unfortunately, this number can grow very large, so that the complexity of the receiver becomes quickly unmanageable, and suboptimum solution must be devised. Essentially, we should trade a decrease in complexity for a decrease in power efficiency (but not in bandwidth efficiency). This is obtained by giving up maximum-likelihood decoding of the CPM signals, which are instead demodulated symbol-by-symbol through a differential demodulator, or a discriminator.

2.3 Selection of parameters

In this section we follow the notations and the numerical results contained in [6]. The selection of modulation and coding formats is based on the following data:

- \mathcal{R} , the information rate, equal to 4.8 Kbits/sec.
- B , the transmission bandwidth available, equal to 5 KHz. We assume that B includes 99.9% of the signal power.
- The error probability to be achieved is 10^{-3} .

In this case we get $\mathcal{R}/B \approx 1$ bit/sec Hz. If we consider using M -ary CPFSK with $h = 1/M$, we have $B = 2.7/T_s$, and hence $R = 2.7$ bits/channel use. This shows that octonary CPFSK may be adequate, since it gives $R = 3$. For $P(e) = 10^{-3}$ we must have, from (3), $d_{\text{free}}^2/4N_0 = 4.7$. Now, for octonary CPFSK we have $d_{\text{free}}^2/2\mathcal{E}_s = 0.2$. By denoting \mathcal{E}_b the energy per bit, $\mathcal{E}_b/N_0 = \mathcal{E}_s/RN_0 \approx 15.7$, which corresponds to 11.9 dB. Thus, coding is necessary if this signal-to-noise ratio exceeds the available value.

Consider also that the computations performed so far assume that transmission takes place over an additive white Gaussian noise channel. Some modifications have to be introduced to cope with the effects of fading: among them, we may consider introduction of time diversity and an interleaving (or interlacing) scheme.

2.4 Convolutionally encoded CPM

We consider now the design of a convolutional encoder to be put in front of the CPM encoder [4,6]. Two possible perspectives are possible to understand the interaction of CPM with the convolutional code.

On one side, we observe that the code introduces a correlation between the symbols at the input of the CPM modulator. As a result, some transitions in the CPM trellis are pruned out, thus decreasing the connectivity of the trellis. Thus, the minimum merge length is increased. Since generally larger merge lengths involve larger Euclidean distances, the error performance of the CPM system is improved.

On the other side, the system can be viewed as a trellis-encoded scheme using CPM signals in order to take advantage of their high bandwidth efficiency.

Here we consider 32-ary CPFSK, as used to transmit 3 bits per channel use in conjunction with a rate 4/5 convolutional encoder and rate-1/2 time diversity. The cutoff rate R_0 of a 32-ary CPFSK is equal to $R_0 = 3$ bits/channel use @ $\mathcal{E}_b/N_0 = 10$ dB, which shows that in principle it is possible to achieve an arbitrarily small error probability provided that $\mathcal{E}_b/N_0 > 10$ dB.

3 The channel model

Besides additive Gaussian noise, which is the standard environment for the analysis of coding schemes for the transmission of digital data or speech, there is a number of additional sources of performance degradation that must be taken into account to assess the merits of a proposed transmission scheme for mobile satellite channels. The most important among them are [2,3]:

- **Doppler shifts.** They are due to mobile vehicle motion. The information-bearing phase is shifted by an amount $2\pi f_d T_s$, where $1/T_s$ is the data symbol rate, and f_d is the Doppler frequency shift, which, for transmission at L-band, can be expected to be on the order of up to 200 Hz. At a rate of 2400 symbols per second, the corresponding phase shift is 30° .
- **Fading and shadowing.** This is the most serious source of impairment. The transmitted radio signal reaches the receiver through different paths caused by reflections from obstacles, yielding a signal whose components, having different phases and amplitudes, may either reinforce or cancel each other. Shadowing is caused by the obstruction of radio waves by buildings and hills.
- **Adjacent channel interference.** The 5-KHz mobile channel used for transmission operates in a channelized environment: in fact, it is a slot in a frequency-division multiple access systems. As a result, signals suffer from interference from signals occupying adjacent channels. Since the receiver treats the interfering signals as noise, there is an upper limit to the power level of adjacent channel interference that can be tolerated.
- **Impulsive noise.** This originates from a variety of man-made sources. This noise occurs in the form of randomly shaped pulses which may extend over several symbol intervals.
- **Channel nonlinearities.** Primarily because of the high-power amplifier in the transmitter, operated at or near saturation for better power efficiency, the channel is inherently nonlinear.
- **Finite interleaving depth.** In order to break up the error bursts caused by amplitudes fades of duration greater than symbol time, encoded symbols may be interleaved. Now, infinite interleaving provides a memoryless channel, but in practice

the interleaving frame must be limited. In fact, for speech transmission the total coding/decoding delay must be kept below 60 ms in order not to cause perceptual annoyance. If the depth of interleaving cannot be larger than the maximum fade duration anticipated, this causes a performance degradation. Similar considerations hold if interlacing is used instead of interleaving.

4 Results

4.1 Detection schemes considered

Coherent detection. For coherent detection in the presence of fading, it is necessary to assume that additive white Gaussian noise is the only disturbance affecting the received signal. In particular, the effects of fading must be removed. This can be obtained by assuming that fading sample measurements are available to the receiver.

These measurements are obtained by using a single pilot tone inserted in the middle of the bandwidth occupied by the useful signal. To do this, a notch is created in the signal spectrum by proper addition of redundant symbols to the sequence of data entering the continuous-phase modulator.

Coherent detection and time diversity. The performance of the optimum decoder of CPM over fading channels turns out to be sensitive to fading bursts. Therefore, some kind of diversity or interleaving should be used to cope with fading. However, interleaving is unfeasible with coherent detection, because it would destroy the memory intrinsic in CPM, and hence its spectral efficiency. Hence, we consider time diversity as paired with coherent detection.

In communications over fading channels, the term *diversity* refers to different observations of the same block of symbols. A simple way of achieving diversity is by repeating twice each block of m symbols. The redundancy added can be taken advantage of by using diversity selection or maximal ratio combining. If $r_1(t)$ and $r_2(t)$ denote the signals received from a block and its replica, and R_1 , R_2 denote the samples of envelope fading measured during the time intervals corresponding to $r_1(t)$, $r_2(t)$, diversity selection implies that $r_1(t)$ is accepted and processed if $R_1 > R_2$, while $r_2(t)$ is accepted and processed if $R_2 > R_1$. For maximal ratio combining, $R_1 r_1(t) + R_2 r_2(t)$ is provided to the receiver for processing. The latter operation can approximately be performed by coherently demodulating the received waveform using the pilot tone.

Symbol repetition causes a decrease in data rate, that we can avoid by doubling the number of phase levels transmitted on the channel.

Differential detection and interleaving. Assume that the complex envelope of the received signal $\tilde{r}(t)$ is delayed by T_s seconds, transformed into its conjugate $\tilde{r}^*(t - T_s)$, and multiplied by itself. Then, the real and imaginary components of the signal $\tilde{r}(t)\tilde{r}^*(t - T_s)$ are sampled every T_s seconds, deinterleaved, and then input to the trellis decoder.

4.2 Simulation results

In the first scheme we consider, trellis-encoded CPM signals are coherently detected by a maximum-likelihood sequence receiver, based on Viterbi algorithm. Simulation results are presented in Fig. 1. This refers to a 16-phase CPM with $q = 14$ and $h = 0.1429$. The

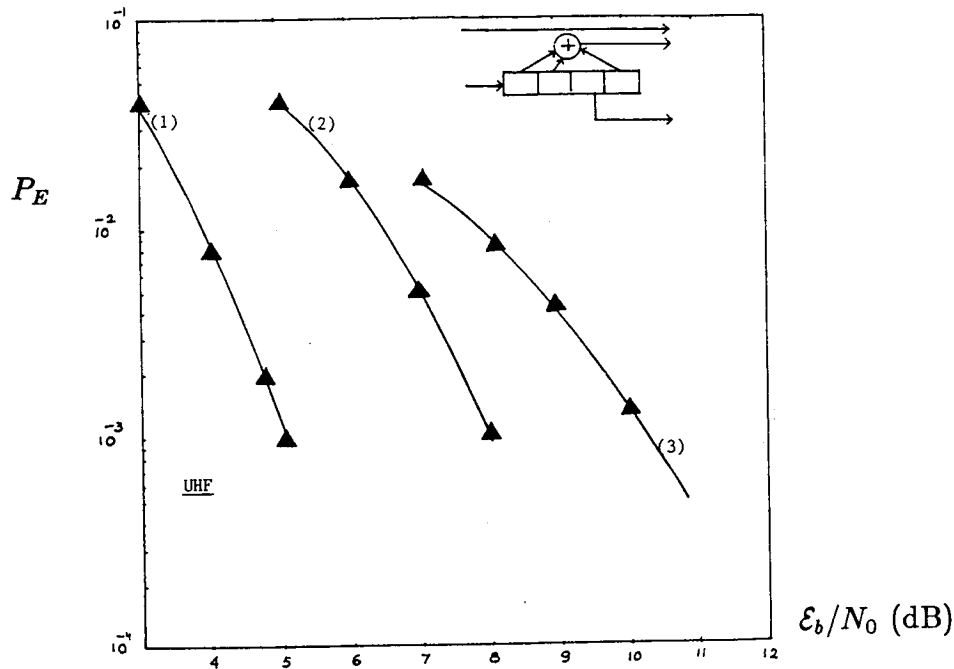


Figure 1: Simulation results. Error probability vs. E_b/N_0 . (1) Ideal coherent receiver over additive white Gaussian noise channel. (2) Ideal coherent receiver, fading channel. (3) Coherent receiver based on fading channel information obtained through a pilot tone.

Viterbi receiver has 56 states. The fading channel is simulated by using a Rice model with $K = 10$ dB. Perfect symbol synchronization is assumed.

In the second scheme we consider, diversity with maximal ratio combining is introduced to combat the effects of fading. Diversity is achieved by repeating each coded sequence twice. This implies that the number of CPM phase levels has to be increased from 16 to 32 to avoid reducing the data rate. Simulation results referring to this scheme are shown in Fig. 2. Here, $h = 0.0526$, $q = 38$, while the Viterbi detector has 76 states. The channel is the same as for the results of Fig. 1.

In our third scheme (see Fig. 3), interleaving is introduced to spread the bursts of noise due to deep fade samples. With differential detection, the interleaver can be inserted between the trellis encoder and the continuous-phase modulator. A block of I symbols is arranged in the form of an $R \times C$ matrix, $I = RC$. Then the symbols are transmitted columnwise. Deinterleaving, which consists of restoring the original order of the symbols, takes place between the differential demodulator and the Viterbi detector. Doppler frequency shift, due to a vehicle velocity v MPH, is assumed to be perfectly compensated for. Perfect symbol synchronization is also assumed.

5 Conclusions

We have considered the combination of CPM signals with trellis codes for application to digital transmission over a mobile satellite channel. Three different combination schemes have been considered, and their performance analyzed by means of computer simulation.

The results presented seem to indicate that a scheme based on differential detection, interleaving, and Viterbi decoding of the trellis code alone is promising for practical applications. In fact, differential detection is relatively easy to implement, while interleaving reduces sensitivity to channel noise bursts.

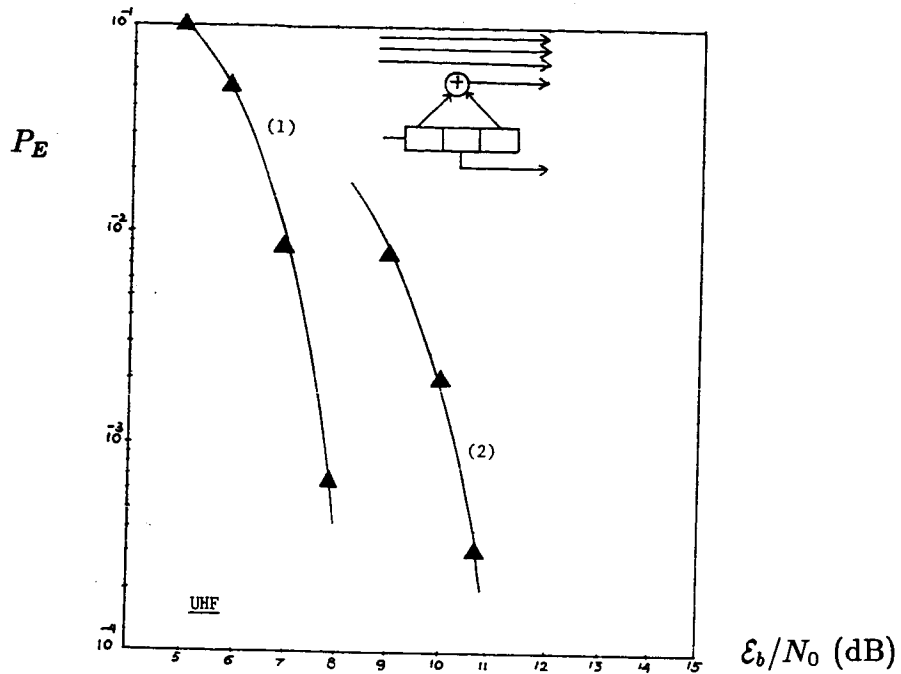


Figure 2: Simulation results. Error probability vs. \mathcal{E}_b/N_0 . (1) Ideal coherent receiver over additive white Gaussian noise channel. (2) Coherent receiver based on fading channel information obtained through a pilot tone.

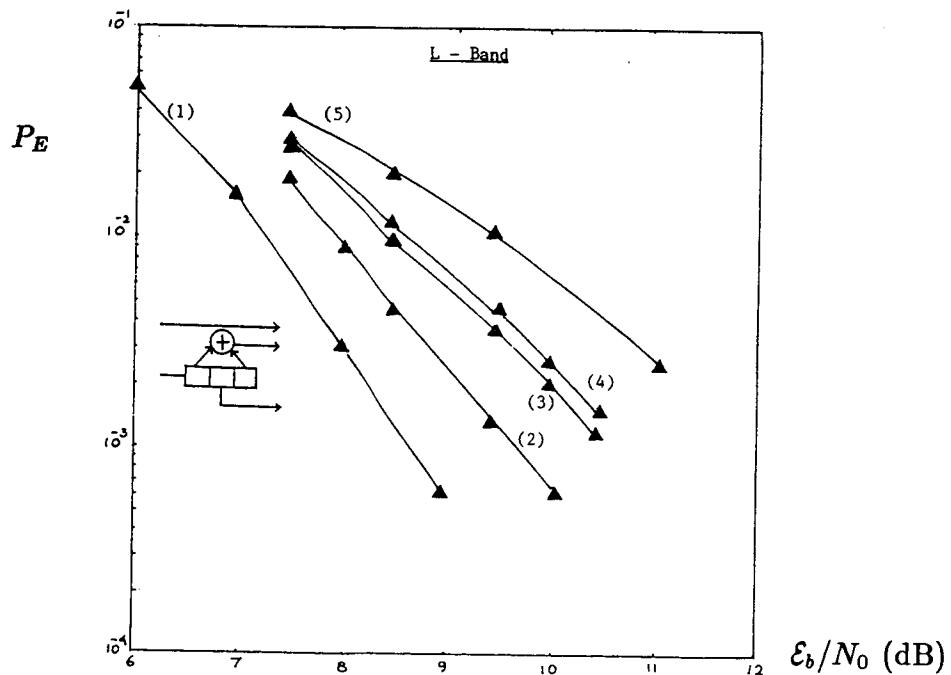


Figure 3: Simulation results. Error probability vs. \mathcal{E}_b/N_0 . (1) Ideal coherent receiver over additive white Gaussian noise channel. (2) Differentially detected CPM, with $I = 128$, $C = 16$, $v = 20$. (3) Same as in (2), with $I = 64$. (4) Same as in (3), with $v = 80$. (5) Differentially detected CPM with no interleaving.

References

- [1] J.B.Anderson, T.Aulin, and C.-E.Sundberg, *Digital Phase Modulation*. New York: Plenum Publ. Co., 1986
- [2] A.P.Clark, "Digital modems for land mobile radio," *IEE Proceedings*, Vol.132, pt. F, No. 5, pp.348-362, August 1985
- [3] D.Divsalar and M.K.Simon, "Trellis code modulation for 4800-9600 bits/s transmission over a fading mobile satellite channel," *IEEE Journal on Selected Areas in Communications*, vol.SAC-5, No.2, pp.162-175, February 1987
- [4] S.V.Pizzi and S.G.Wilson, "Convolutional coding combined with continuous phase modulation," *IEEE Trans. on Communications*, vol.COM-33, No.1, Jan. 1985, pp.20-29
- [5] B.Rimoldi, "A decomposition approach to CPM," *Submitted to IEEE Trans. on Inform. Theory*, 1987
- [6] B.Rimoldi, "Design of coded CPFSK modulation systems for bandwidth and energy efficiency," *Submitted to IEEE Trans. on Commun.*, 1987
- [7] G. Ungerboeck, "Channel coding with multilevel/phase signals," *IEEE Trans. Inform. Th.*, vol. IT-28, pp. 56-67, January 1982

INTERLEAVER DESIGN FOR TRELIS-CODED DIFFERENTIAL 8-PSK MODULATION WITH NON-COHERENT DETECTION

DR. FRANZ EDBAUER, Institute of Communication Technology, German Aerospace Research (DFVLR), Fed. Rep. of Germany.

GERMAN AEROSPACE RESEARCH (DFVLR)
Institute of Communication Technology
Oberpfaffenhofen
D-8031 Wessling
W.-Germany

ABSTRACT

Trellis-coded differential 8-DPSK with non-coherent detection is considered to be an efficient modulation scheme for satellite mobile communication. Theoretical analysis of such systems often assumes perfect, i.e., infinite interleaving. In this paper the effect of finite interleaver size on bit error rate (BER) performance of coded 8-DPSK is determined by means of computer simulations. The losses evaluated in this way include the SNR-degradation due to the timing- and frequency errors of the symbol synchronizer and the AFC (automatic frequency control) of the receiver. BER-measurements are presented using a conventional 2/3-rate convolutional 8-state trellis code for typical Rayleigh- and Rician fading channels. It is shown that for a Rician channel with Rician parameter of 7 dB, a Doppler spread of 100 Hz and a data rate of 2400 bps, an interleaver with size 16x16 symbols performs nearly as well as a very large interleaver. It is also shown that for moderately fast Rayleigh channels the BER-curves flatten out at large SNR. This is due to the fact, that the random phases of the fading channel in rare cases coincide with valid phase sequences of coded symbols, thus producing error events, even without any additive noise disturbance. For such channels an additional code design criterion would be to minimize the error floor.

INTRODUCTION

Trellis-coded modulation provides coding gain without expanding bandwidth [Ungerböck, 1982]. Most applications in the past have been concerned with coherent systems. For fading channels non-coherent modulation schemes like trellis-coded differential octal phase shift keying (coded 8-DPSK) with differentially coherent detection are probably more suitable since they do not require the derivation of a coherent reference carrier. Coded 8-DPSK has been investigated by [Simon and Divsalar 1987, McLane et al. 1987, Edbauer 1987, Makrakis et al. 1987]. Theoretical analysis of interleaved systems often assumes ideal, i.e., infinite interleaving, to make the channel to appear memoryless. In this paper the effect of finite interleaver size on BER-performance is determined by means of computer simulations for a Rayleigh and a Rician channel, which are considered to be typical of mobile satellite communications.

MODULATOR FOR CODED 8-DPSK SIGNALS

The modulator is shown in Fig. 1. The input bits are passed through a rate 2/3 trellis encoder which generates at its output coded 3-bit tuples. These are written into a block interleaver row by row. The interleaver consists of l rows and r columns and its size is denoted by $l \times r$. The 3-bit tuples are read out column by column and mapped into coded 8-PSK symbols a'_n ($|a'_n| = 1$) in the complex signal plane according to the set partitioning method [Ungerböck, 1982]. The symbols a'_n are then differentially phase encoded producing coded 8-DPSK symbols c_n .



Fig. 1. Generation of Interleaved Trellis-Coded 8-DPSK Signals

$$c_n = c_{n-1} a'_n. \quad (1)$$

These are filtered by a pulse shape filter with impulse response $h(t)$, supplying

$$x(t) = \sum_i c_i h(t - iT), \quad (2)$$

where T is the symbol period. $x(t)$ is converted to the radio frequency and transmitted.

DIGITAL RECEIVER WITH SOFT DECISION 8-PSK VITERBI DECODER FOR CODED 8-DPSK SIGNALS

A simplified block diagram of the receiver in the complex baseband is drawn in Fig. 2. Coarse AFC, AGC, filtering and interleaver synchronisation are not shown. We assume Nyquist signaling with zeros of the filter impulse response at multiples of the symbol period, satisfying Nyquist's first criterion. For the computer simulation the full Nyquist filter is placed on the transmitter side.

The receiver input signal is written in the complex baseband in the form

$$y(t) = A(t)x(t) + w(t). \quad (3)$$

$A(t)$ is a complex-valued stochastic process which describes multiplicative frequency non-selective fading. For Rayleigh- and Rician channels $A(t)$ is a complex Gaussian process. The envelope $|A(t)|$ has a Rayleigh- or Rician distribution. $w(t)$ is additive complex Gaussian noise. The input signal is sampled once per modulation interval by an A/D-converter providing the complex sample

$$y_n = A_n x_n + w_n. \quad (4)$$

x_n is the sample of $x(t)$ at time $t_n = nT - \tau$, where $n = 0, 1, 2, \dots$, and τ , with $-T/2 \leq \tau < T/2$, determines the sampling point within a symbol period. The noise samples w_n can be assumed to be complex Gaussian and uncorrelated. The average bit energy to spectral noise power density ratio is

$$\frac{E_b}{N_o} = \frac{E\{|A|^2\}}{4\sigma^2}, \quad (5)$$

where $E\{\}$ denotes expectation and σ^2 is the variance of the noise w_n in each dimension. The average signal power $E\{|A|^2\}$ can be determined by the AGC of the receiver whose time constant is large with respect to the fading period. In the following the normalization $E\{|A|^2\} = 1$ is assumed.

The receiver performs the following signal processing functions: differentially coherent 8-DPSK symbol detection, hard 8-PSK detection, automatic frequency control (AFC), symbol synchronisation (timing) and soft decision Viterbi decoding.

Differential symbol detection is performed by a one-delay symbol detector whose output is

$$z_n = y'_n y'^*_{n-1} = h(\tau) a'_n + n_n + v_n, \quad (6)$$

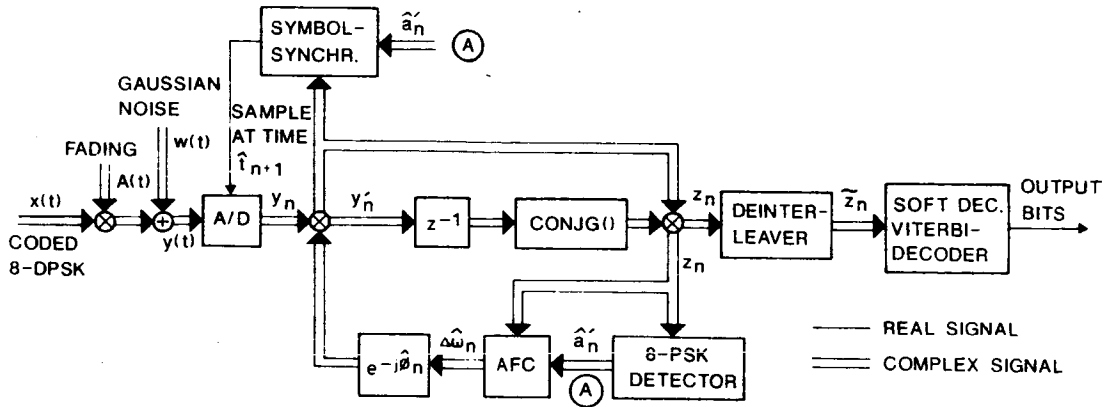


Fig. 2. Simplified Block Diagram of the Digital Receiver with Soft Decision Viterbi Decoder for Interleaved Trellis-Coded 8-DPSK Modulation

where y'_n is the back-rotated version of the received 8-DPSK symbol y_n after frequency offset compensation (see Eq. (10)), and (\cdot) denotes the conjugate complex value. n_n is additive complex noise and v_n is the intersymbol interference term which vanishes for exact timing ($\tau = 0$).

The hard 8-PSK decision \hat{a}'_n of z_n is given by that symbol \tilde{a}_n which is closest to z_n :

$$\hat{a}'_n \leftarrow \min_{\tilde{a}_n} |z_n - \tilde{a}_n|. \quad (7)$$

\hat{a}'_n is needed for decision-directed AFC and decision-directed symbol synchronisation.

An error signal for the radian frequency offset $\Delta\omega_n$ of the receiver input signal y_n is given by

$$e_{afc,n} = \text{Im}\{z_n \cdot \hat{a}'_n\}. \quad (8)$$

$\hat{\Delta\omega}_n$, being the estimate of $\Delta\omega_n$, is updated by a first order loop

$$\hat{\Delta\omega}_n = \hat{\Delta\omega}_{n-1} + \frac{e_{afc,n}}{T_{afc}}, \quad (9)$$

where T_{afc} is the AFC time constant for high SNR and small frequency errors. The frequency offset is compensated by back-rotating y_n with angle $\hat{\phi}_n$, yielding y'_n . The rotated signal then reads

$$y'_n = y_n \exp(-j\hat{\phi}_n) \quad (10)$$

with

$$\hat{\phi}_n = \hat{\phi}_{n-1} + \hat{\Delta\omega}_n \cdot T. \quad (11)$$

Symbol synchronisation for coded 8-DPSK [Edbauer, 1987] is achieved by using an approach similar to [Mueller, 1976]. It can be shown, that an error signal for the timing error $\tau = nT - t_n$, where t_n is the sampling time of the A/D-converter for symbol n , is given by

$$e_{t,n} = T \cdot \text{Re}\{y'_n y'^*_{n-1} - \hat{a}'_n |y'_{n-1}|^2\}. \quad (12)$$

Eq. (12) has the property that it is invariant against a constant phase rotation, thus enabling non-coherent operation. For a first order loop one obtains

$$\hat{t}_{n+1} = \hat{t}_n + T + \frac{4\alpha e_{t,n}}{\lambda}, \quad (13)$$

where α is the ratio of loop noise bandwidth to symbol rate, and λ is the slope of the average loop S-curve at the origin $\tau = 0$.

Decoding of the trellis code is performed by a Viterbi decoder which uses the unquantized deinterleaved symbol detector outputs \tilde{z}_n of Eq. (6) for metric computation. The Viterbi algorithm is used to determine that coded 8-PSK symbol sequence $\{\tilde{a}_n\}$ whose quadratic Euclidean distance is minimum with respect to the differentially detected noisy 8-PSK symbol sequence $\{\tilde{z}_n\}$. The metric increment over one trellis branch therefore is

$$q_n = -|\tilde{z}_n - \tilde{a}_n|^2, \quad (14)$$

where \tilde{a}_n is the coded 8-PSK symbol attributed to that branch. We note that Eq. (14) is not the optimum metric in the maximum likelihood sense, since the noise n_n of the 8-DPSK detector output (Eq. (6)) is non-Gaussian and correlated.

The digital signal processing and decoding methods, as applied here, are explained in more detail in [Edbauer, 1987].

COMPUTER SIMULATION RESULTS

Computer simulations of the proposed coded 8-DPSK system have been performed to determine the effect of finite interleaver size on BER-performance. Symbol synchronisation and AFC have been included in the simulation programs as described above. Two typical mobil satellite fading channels, a Rician and a Rayleigh channel with a Doppler spread of 100 Hz, have been chosen for the simulation. The data rate, having been used, was 2400 bps, which may allow sufficient digital speech quality for aeronautical applications. The Rician parameter K , i.e., the power ratio of the direct line of sight signal to the scattered non-coherent component, was 7 dB. The choice of channel parameters and of the data rate was mainly motivated by aeronautical channel measurements [Neul et al., 1987]. In the simulation, samples A_n (Eq. (4)) of the complex multiplicative fading were computed by digitally low-pass filtering independent Gaussian random numbers. The Doppler spread of channels, generated in this way, is twice the bandwidth of these filters. Pulse shape filtering was performed by a raised cosine Nyquist filter with roll-off of 40 % and impulse response length of 9 symbol periods. A conventional 8-state Ungerböck type convolutional code [Ungerböck 1982, Fig. 9] without feed-back was used as trellis code. Since the interleaver size should be the only varying parameter the decision delay of the Viterbi decoder was kept constant and equal to $M = 16$ symbols.

Usually the block interleaver size is chosen in that way that the time for transmission of a column - i.e. the number of rows - is of the order of expected fade durations, and that the number of columns is equal to the decoding decision delay. In the simulation even smaller interleaver sizes were selected since short delays are desirable especially for speech transmission.

The BER results for the Rician channel with the interleaver size as parameter are shown in Fig. 3. It can be seen that a small interleaver with size 16x16 is only 0.5 dB worse than the large 100x30 interleaver at all E_b/N_0 values of the figure. The smaller 8x8 interleaver would also be acceptable giving a total delay of 120 ms between transmitter and receiver for digital 2400 bps speech transmission. No further improvement was possible by using an interleaver larger than 100x30. If no interleaver were used the losses would be 12 dB and 6 dB at BER of $P_b = 10^{-4}$ and $P_b = 10^{-3}$ with respect to the largest interleaver. For comparison reasons the theoretical and the computer simulation BER-curves of uncoded 4-DPSK with differentially coherent detection are also drawn in Fig. 3.

BER-measurements for a Rayleigh channel with the same Doppler spread of 100 Hz and interleaver sizes 8x16 and 8x8 are shown to the right of Fig. 3. It is seen that the BER-curves flatten out at large E_b/N_0 . This error floor is caused by the phase variations of the fading channel which in rare cases coincide with the phases of coded symbols of an incorrect path, even without any additive noise disturbance. The error floor depends on the trellis code, the

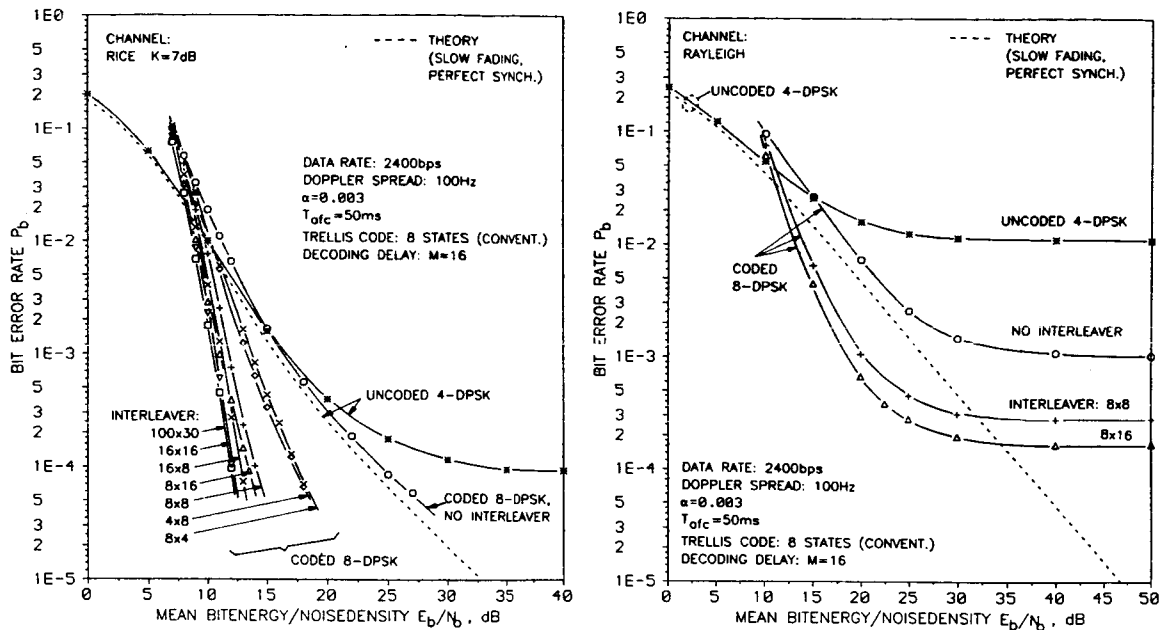


Fig. 3. Computer Simulation Results of BER-Performance of Coded 8-DPSK Modulation for Various Interleaver Sizes over a Rician and a Rayleigh Channel

interleaver size and, most significantly, on the ratio of the Doppler spread to the symbol rate. For the slower Rayleigh channel with Doppler spread of 20 Hz and similar signal processing no error floor was observed above $P_b = 10^{-5}$ [Edbauer, 1987]. It was shown by computer simulation that the effect of the AFC on the error floor is negligible. This was done by setting the AFC output to a constant which corresponded to the Doppler frequency of a vehicle moving with constant speed.

An important aspect in system design for a fading environment is the proper choice of the trellis code. [Simon and Divsalar, 1987] have analytically derived the following code design criteria for the slow fading fully interleaved Rayleigh channel with differential detection. The code should have:

- a.) large length of the shortest error event path, where equal symbols of the correct and the incorrect path do not contribute to the length,
- b.) large product of the branch distances of this path,
- c.) large minimum free Euclidean distance.

A criterion concerning the error floor does not yet exist, since this would require consideration not only of amplitude- but also of phase variations of the channel.

In view of these criteria the convolutional 8-state trellis code, used in this work, is not optimum. It was designed for the Gaussian channel [Ungerböck, 1982], mainly by considering criterion c.). The code has two minimum free distance paths of lengths 3 and 4 with distance 2.14 for the unit radius constellation. But the code also has one path with length 2 and distance 2.45, which does not meet criterion a.) very well. If an 8-state code with shortest path length of 3 would exist, some performance improvement would be possible. We therefore intend to extend this work to other codes, e.g. those proposed by [Simon and Divsalar, Globecom'87].

REFERENCES

- Ungerböck, G. 1982. "Channel Coding with Multilevel/Phase Signals". IEEE Trans. on Inf. Theory, Vol. IT-28, No. 1, Jan. 1982, pp. 55-76.
- Simon M.K., Divsalar D. 1987. The Performance of Trellis Coded Multilevel DPSK on a Fading Mobile Satellite Channel. Proc. of Internat. Conf. on Communications ICC'87, pp. 21.2.1.-21.2.7.
- McLane, P.J., Wittke, P.H., Ho, P.K., Loo, C. 1987. PSK and DPSK Trellis Codes for Fast Fading, Shadowed Mobile Satellite Communication Channels. Proc. of Internat. Conference on Communications ICC'87, pp. 21.1.1.-21.1.4.
- Edbauer, F. 1987. Coded 8-DPSK Modulation with Differentially Coherent Detection - an Efficient Modulation Scheme for Fading Channels. Conf. Record of GLOBECOM'87, Vol.3, pp. 42.2.1-42.2.4.
- Makrakis, D., Mathiopoulos, P., Feher, K. 1987. Trellis-Coded Modulation for Noncoherent Detection Schemes, Part II: Differential Detection. Proc. of The 10th Symposium on Information Theory and Its Applications SITA'87, pp. EE1-2-1 - EE1-2-5.
- Mueller K.H., Müller M. 1976. Timing Recovery in Digital Synchronous Data Receivers. IEEE Trans. on Communications, Vol. COM-24, No. 5, pp. 516-531.
- Neul, A., Hagenauer, J., Papke, W., Dolainsky, F., Edbauer, F. 1987. Aeronautical Channel Characterization Based on Measurement Flights. Conf. Record of GLOBECOM'87, Vol.3, pp. 42.3.1-42.3.6.
- Simon, M.K., Divsalar, D. 1987. Multiple Trellis Coded Modulation (MTCM) Performance on a Fading Mobile Satellite Channel. Conf. Record of GLOBECOM'87, Vol.3, pp. 43.8.1-43.8.6.

CODES FOR QPSK MODULATION WITH INVARIANCE UNDER 90° ROTATION

GOTTFRIED UNGERBOECK, IBM Research Division, Zurich Research Laboratory, Switzerland; STEVEN S. PIETROBON, South Australian Institute of Technology, Adelaide, Australia.

IBM RESEARCH LABORATORY
Säumerstrasse 4
CH-8803 Rüschlikon
Switzerland

ABSTRACT

When QPSK modulation is combined with linear rate-1/2 convolutional encoding, the resulting coded QPSK signal sequences are, at most, code invariant under 180° signal rotation. In this paper, we show that invariance under 90° rotation (and multiples thereof) is obtained by using nonlinear convolutional codes which satisfy a parity-check equation of a particular form. Tables of optimum codes in this class are presented, and the realization of encoders with 90°-differential information encoding is discussed. For the same code complexity, the new coded QPSK schemes exhibit smaller minimum distance between coded signal sequences than comparable schemes with linear encoding. However, there are also fewer nearest-neighbor sequences. As a result, the new schemes achieve almost the same real coding gains as the known schemes with linear encoding. For correct decoding, it is no longer necessary to demodulate the received coded QPSK signals with a particular carrier phase. This simplifies the receiver design, and allows fast recovery after losses of carrier-phase synchronization. The new codes should be especially useful for transmission over mobile-communication channels, where Rayleigh/Rice fading can lead to frequent losses of carrier-phase synchronization in the receiver.

INTRODUCTION

Rate-1/2 convolutional codes are frequently employed in combination with QPSK (four-phase) modulation and soft Viterbi decoding to achieve coding gains over uncoded BPSK (binary-phase) modulation at the same bandwidth efficiency of 1 bit/s/Hz. With uncoded BPSK modulation, information transparency to 180°-phase-ambiguous demodulation in the receiver is easily accomplished by differential encoding and decoding. The same holds for 90°-phase ambiguity in the case of uncoded QPSK modulation (2 bits/s/Hz). However, when QPSK signals are encoded with a linear rate-1/2 convolutional code, it is only possible to achieve code invariance under 180°-signal rotation with certain codes, whereas with other codes no such invariance exists. The lack of invariance under 90°-signal rotations requires

that QPSK signals are demodulated with correct phase before Viterbi decoding [1].¹

Transmission over phase-agile fading channels can lead to frequent losses of carrier-phase synchronization in a receiver. The time required to reestablish correct demodulation phase for decoding can cause channel outages during considerable periods of time. It is therefore desirable to find new 90°-rotation-invariant coded QPSK schemes, which allow almost instantaneous resynchronization after severe channel disturbances.

The idea of accomplishing full rotational invariance by nonlinear convolutional codes first arose in 1983 in connection with specifying an eight-state code for trellis-coded modulation with a 32-point signal constellation for use in the CCITT V.32 modem [2-5]. In this paper, the approach taken in [3,6] for constructing such codes on the basis of a nonlinear parity-check equation and achieving differential information encoding without requiring additional memory elements, is applied to QPSK modulation and extended to codes with more than eight states.

Figure 1 illustrates an encoder-modulator with natural binary mapping of code bits (y_n^1, y_n^0) into QPSK signals. This mapping induces a set-partitioning rule as introduced in [7]. Bit y_n^0 divides the QPSK signal set with minimum squared signal distance $\Delta_0^2 = 2$ into two subsets with squared signal distance $\Delta_1^2 = 4$ between the signals in these subsets. It can easily be verified that a 90° rotation of the QPSK signals corresponds to changing the code bits y_n^1 and y_n^0 into $y_n^1 = y_n^1 \oplus y_n^0$ and $y_n^0 = y_n^0 \oplus 1 = \bar{y}_n^0$, respectively, where ' \oplus ' denotes modulo-2 addition.

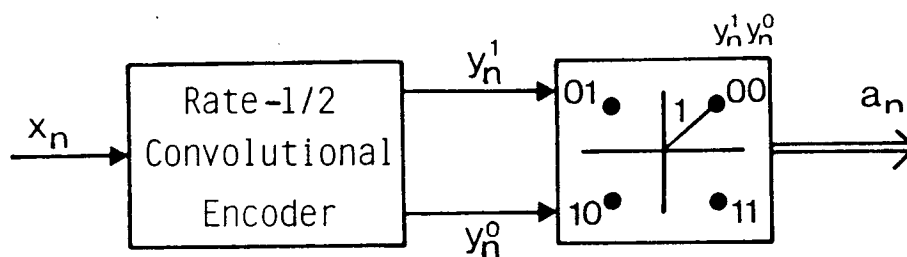


Figure 1. Encoder-modulator for rate-1/2 convolutionally encoded QPSK modulation with natural binary mapping.

An equivalent encoder-modulator for Gray-code mapping is obtained by the transformation $y_{nG}^1 = y_n^1$, $y_{nG}^0 = y_n^1 \oplus y_n^0$. With this transformation, which would normally be included in the convolutional code, Hamming distances between binary code sequences and squared signal distance between coded QPSK signal sequences become equivalent. Throughout this paper natural binary mapping is assumed. The conversion of codes to Gray-code mapping is left as an exercise to readers.

¹ The reference is general rather than specific to the topic of this paper. We are not aware of a paper available in the open literature describing the properties of QPSK modulation with linear convolutional encoding under signal rotation. Nevertheless, one can assume that the facts stated in the above paragraph are known among communication engineers working in this field.

NONLINEAR CONVOLUTIONAL CODES

In the following, binary sequences are expressed in polynomial notation with the indeterminate variable D denoting delay by one modulation interval. A convolutional code of rate $1/2$ is most compactly defined as the set of pairs of binary code sequences which satisfy a scalar polynomial parity-check equation.

From the above discussion on natural binary mapping, it follows that coded QPSK sequences are invariant under 90° rotations, if for every pair $y^1(D)$ and $y^0(D)$ which satisfies the parity-check equation of a convolutional code, also the pair $y'^1(D) = y^1(D) \oplus y^0(D)$ and $y'^0(D) = \bar{y}^0(D)$ satisfies this equation. This is not possible, if the parity-check equation is linear in the sense of modulo-2 (GF-2) arithmetic. However, invariance under 90° rotation is achieved, if the code is defined by a nonlinear parity-check equation of the form

$$(D^k + D^i)y^1(D) \oplus H^0(D)y^0(D) = [D^k y^0(D)] \& [D^i y^0(D) \oplus E(D)] ,$$

where $H^1(D) = D^k + D^i$ with $v > k > i > 0$, and $H^0(D) = D^v + D^t + \dots + D^s + 1$ with $v > t \geq s > 0$ are linear parity-check polynomials. It is important that $H^1(D)$ exhibits only two non-zero coefficients. The middle part $D^t + \dots + D^s$ in $H^0(D)$ may be absent; in this case, let $t = s = 0$. As for linear codes, the condition $v > k > i > 0$ guarantees that error events begin and end with the largest squared distance between QPSK signals, i.e., $\Delta_1^2 = 4$.

Without the nonlinear right-hand term, the parity-check equation would define a linear convolutional code with constraint length v , i.e., a code with 2^v states. The symbol ' $\&$ ' denotes a *logic-and* operation, which makes this term nonlinear. $E(D)$ is the all-one sequence $1(D)$, if the coefficient sum of $H^0(D)$ is even, and the all-zero sequence $0(D)$, if this sum is odd. Modulo-2 addition of $1(D)$ to a binary sequence inverts all elements of this sequence. The rotational-invariance property is proven by substituting $y'^1(D)$ for $y^1(D)$ and $y'^0(D)$ for $y^0(D)$ in the above parity-check equation, and using the relation $u \oplus v = u \& \bar{v} \oplus \bar{u} \& v$. Henceforth, the shorter notation $D^k y^0(D) \cdot D^i y^0(D)$ will be used for the nonlinear parity-check term.

NONLINEAR ENCODER REALIZATION

It can be shown that encoders for codes characterized by a nonlinear parity-check equation of the above form can be realized with a minimum number of $\tilde{v} = \max[v, k - i + \max(k, t) - \min(i, s)]$ binary memory elements. This means that the nonlinear code could have more than 2^v code states. In this paper we consider only codes with $\tilde{v} = v$.

As an example, we show the realization of an encoder for the code shown below in Table 1 for $v = 5$. The code is defined by the parity-check equation

$$(D^2 + D)y^1(D) \oplus (D^5 + D^3 + 1)y^0(D) = D^2 y^0(D) \cdot D y^0(D) .$$

Since the coefficient sum of $H^0(D)$ is odd, $E(D) = 0(D)$. Hence, ' \cdot ' denotes the *logic-and* operation without inversion. Figure 2(a) shows the obvious encoder realization found by expressing $y^0(D)$ explicitly in the other terms of the parity-check equation. The minimal encoder with $v = 5$ binary memory elements depicted in Figure 2(b) is then obtained by observing that the feedback part involving the ' \cdot '

operation can be left-shifted into the linear part of the encoder by two memory elements.

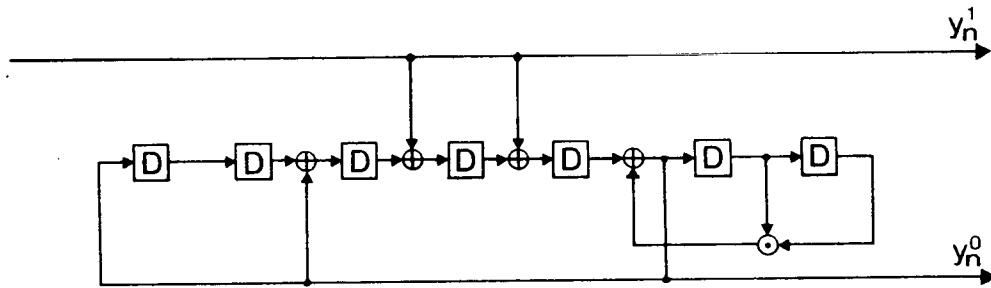
Figure 2(b) also illustrates 90°-differential encoding without additional memory elements. The operation is based on expressing the information sequence as $x(D) = D^\alpha y^0(D) \oplus D^\beta y^0(D)$ for some $\alpha \neq \beta$. A 90° rotation of the transmitted QPSK signals is equivalent to replacing $y^0(D)$ by the inverted sequence $\bar{y}^0(D)$. This inversion does not change $x(D)$. Choosing $\alpha = 0$ and $\beta = -1$, and observing the operation performed by the right-most modulo-2 adder in the minimal encoder leads to two equations

$$x(D) = y^0(D) \oplus D^{-1}y^0(D) \quad \text{and} \quad y^1(D) \oplus s^1(D) = D^{-1}y^0(D).$$

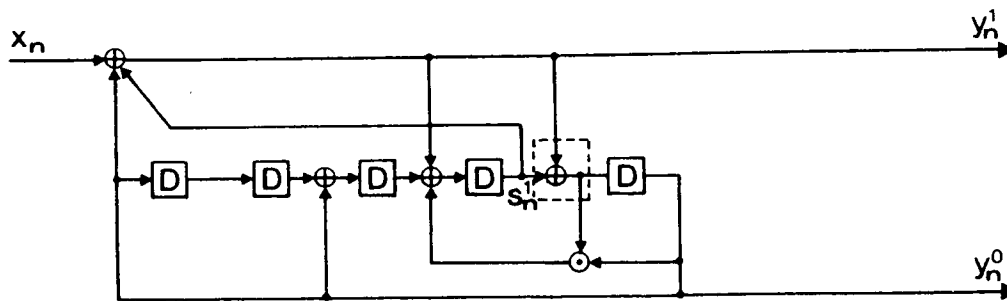
The first equation is used for differential decoding to obtain the information sequence $\hat{x}(D)$ from a received sequence $\hat{y}^0(D)$. The sum of the two equations defines the differential-encoding operation

$$y^1(D) = x(D) \oplus s^1(D) \oplus y^0(D).$$

Similar minimal encoders with 90°-differential encoding can be obtained for the other nonlinear codes presented in Table 1 below.



(a) Obvious encoder realization



(b) Minimal encoder realization with 90°-differential encoding

Figure 2. Two encoder realizations for a nonlinear 32-state code.

SEARCH FOR NONLINEAR CODES AND PERFORMANCE EVALUATION

A search for codes satisfying nonlinear parity-check equations of the form considered and permitting the construction of encoders of the form shown in Figure 2(b) was performed. The search was restricted to codes with $\tilde{v} = v$. Since the codes are nonlinear, free (= minimum) distance, d_{free} , between coded QPSK signal sequences does not necessarily occur between the signal sequence corresponding to the all-zero code sequence and a sequence diverging from and remerging with this sequence. In the code search program, an efficient dynamic-programming algorithm was used which determines d_{free} among *all* possible pairs of sequences diverging in some state and remerging later in another state.

Among codes with the same free distance for a given value of v , a code with the shortest duration of free-distance error events and the fastest minimum-distance growth between unmerged events (in this order) was selected. Then for the codes selected, the three smallest distances $d_{\text{free}} = d_1 < d_2 < d_3$ and the corresponding average multiplicities $N_{\text{free}} = N_1, N_2,$ and N_3 of error events with these distances were determined. These values were then used to compute an accurate estimate of the error-event probability by

$$P_{\text{evt}} \simeq \sum_{i=1}^3 N_i Q[d_i/(2\sigma)] ,$$

where $Q(\cdot)$ is the Gaussian error-integral function, and σ denotes the standard deviation of white Gaussian noise for one signal dimension. The value of σ follows from the definition of the signal-to-noise ratio, $\text{SNR}_{\text{dB}} = 10 \log[E_s/(2\sigma^2)]$. $E_s = 1$ represents the signal energy per QPSK signal and information bit transmitted, and $2\sigma^2 = N_0$ is the one-sided spectral noise density.

The results obtained for $\tilde{v} = v = 3, 4, 5,$ and 6 are summarized in Table 1. The coefficients of the parity-check polynomials $H^1(D)$ and $H^0(D)$ are specified in octal notation. For uncoded BPSK modulation, values $P_{\text{evt}} = 10^{-4}$ and 10^{-8} are achieved at $\text{SNR}_{\text{dB}} = 8.40$ and 11.97 , respectively.

Table 1: New rate-1/2 nonlinear codes for QPSK modulation

Invar.	$\tilde{v} = v$	$H^1(D)$	$H^0(D)$	d_{free}^2	N_{free}	d_2^2	N_2	d_3^2	N_3	$\text{SNR}_{\text{dB}}, P_{\text{evt}}$ $10^{-4}, 10^{-8}$
90°	3	006	011	10	0.50	12	1.00	14	2.00	4.33 7.83
90°	4	012	025	12	0.75	14	0.75	16	3.00	3.75 7.15
90°	5	006	051	14	1.00	16	1.75	18	3.00	3.30 6.56
90°	6	012	105	16	2.00	18	1.50	20	4.50	3.00 6.17

COMPARISON WITH LINEAR CODES

Table 2 illustrates the best linear codes and their performance. 180°-rotational invariance is achieved, if the parity-check polynomial $H^1(D)$ exhibits an even number of non-zero coefficients. For $v = 2$ and 4 , no good codes with this property exist. For the selection of the linear codes essentially the same programs were used as for the nonlinear codes. The code with $v = 6$ is equivalent to the *standard* 64-state code with Hamming distance 10 ($d_{\text{free}}^2 = 20$, when used with QPSK modulation and Gray-code mapping) often mentioned in recent literature. The values of $N_{\text{free}}, N_2,$ and N_3 are exact; they do not depend on the code sequence transmitted.

Table 2: Linear rate-1/2 codes for QPSK modulation

Invar.	ν	$H^1(D)$	$H^0(D)$	d_{free}^2	N_{free}	d_2^2	N_2	d_3^2	N_3	SNR_{dB}, P_{evt} $10^{-4}, 10^{-8}$
360°	2	002	005	10	1	12	2	14	4	4.67 8.01
180°	3	006	013	12	2	16	10	20	49	4.20 7.39
360°	4	004	023	14	3	16	3	18	3	3.73 6.84
180°	5	014	043	16	5	20	17	24	116	3.45 6.37
180°	6	042	117	20	11	24	38	28	193	2.89 5.60

A comparison of Tables 1 and 2 shows that for the same values of ν the non-linear codes achieve lower values of d_{free}^2 than the linear codes. On the other hand, the nonlinear codes exhibit smaller multiplicities of nearest-neighbor error events than the linear codes. Consequently, at moderate signal-to-noise ratios as required to achieve $P_{evt} = 10^{-4}$, the real coding gains are nearly identical. Noticeable but still small differences are found only for very low error-event probabilities.

CONCLUSION

The new rate-1/2 nonlinear convolutional codes for QPSK modulation presented in this paper allow the achievement of full 90°-rotational invariance of coded QPSK signal sequences at no significant loss in real coding gains when compared to linear codes. For mobile-communication systems operating in a fading environment with frequent periods of low signal-to-noise ratio and the possibility of losses of carrier-phase synchronization in the receiver, the invariance to 90°-ambiguous demodulation should be a significant advantage.

REFERENCES

- [1] G.C. Clark, Jr. and J.B. Cain, *Error-Correction Coding for Digital Communication*, Plenum Press, New York, 1981.
- [2] AT&T Information Systems, "A trellis coded modulation scheme that includes differential encoding for 9600 bit/sec, full-duplex, two-wire modems," CCITT SG XVII Contribution COM XVII, No. D159, Aug. 1983.
- [3] IBM Europe, "Trellis-coded modulation schemes with 8-state systematic encoder and 90° symmetry for use in data modems transmitting 3-7 bits per modulation interval," CCITT SG XVII Contribution COM XVII, No. D180, Oct. 1983.
- [4] CCITT Recommendation V.32: "A family of 2-wire, duplex modems operating at data signalling rates of up to 9600 bit/s for use on the general switched telephone network and on leased telephone-type circuits," CCITT Red Book, Volume VIII, Geneva, 1985.
- [5] L.F. Wei, "Rotationally invariant convolutional channel coding with expanded signal space - Part II: Nonlinear codes," IEEE Trans. Select. Areas Commun., vol. SAC-2, pp. 672-686, Sept. 1984.
- [6] G. Ungerboeck, "Trellis-coded modulation with redundant signal sets, Part II: State of the art," IEEE Commun. Magazine, pp. 12-21, Feb. 1987.
- [7] G. Ungerboeck, "Channel coding with multilevel/phase signals", IEEE Trans. Inform. Theory, vol. IT-28, pp. 55-67, Jan. 1982.

Trellis Coded MPSK Modulation Techniques for MSAT-X¹

Dr. Dariush Divsalar and Dr. Marvin K. Simon
Mobile Satellite Program, Jet Propulsion Laboratory
California Institute of Technology, United States of America

Jet Propulsion Laboratory
4800 Oak Grove Drive 238-420
Pasadena, California 91109
United States of America

Abstract

This paper considers various trellis coded MPSK modulation techniques for transmitting 4.8 kbps over a 5 kHz RF channel. The tradeoffs between coherent versus differentially coherent types of demodulation, and interleaving versus no interleaving will be addressed. Optimum trellis codes which have been designed for fading channels will be discussed. These coding and modulation techniques have been proposed for NASA's MSAT-X project. Simulation results are presented. The paper also discusses many issues that should be considered in designing trellis coded modulation systems for fading channels.

Introduction

Transmission of 4800 bps in a power and bandwidth limited 5 kHz land mobile satellite channel is a formidable goal especially given a required bit error rate (BER) performance of 10^{-3} at an average bit signal-to-noise ratio (SNR) of 10-11 dB to ensure good quality digital speech. Analysis of these link requirements reveals that multilevel signaling with trellis coding is essential which, of course, is functionally more complex than the simpler uncoded formats. It has been concluded that a 10 dB SNR figure is required for UHF operation. For operation in L-band, this figure has been increased to 11 dB to cope with an almost doubling in Doppler effects due to the change in carrier frequency.

The work described herein focuses on the performance of two modulation and detection techniques based on octa-phase-shift-keying (8PSK) with trellis encoding and symbol interleaving for the UHF and L-band channel models described below (also see [1,2]). The techniques are referred to as the Dual Tone Calibrated Technique (DTCT) and differentially encoded 8-PSK (8DPSK) with differential detection and Doppler correction [3]. The 8DPSK system has been shown to have the better performance of the two under the assumed operating conditions; consequently, it will be described in greater detail.

Land Mobile Satellite Fading Channel Model

One of the important considerations in the development of the modem is the effect of propagation on the modulation and coding scheme. In this section, we briefly describe the Rician fading model which is characteristic of the land mobile satellite channel. Based on

¹This work was performed at the Jet Propulsion Laboratory, California Institute of Technology, under a contract with the National Aeronautics and Space Administration.

this model, a software program was written to simulate the fading channel [4].

An RF signal at 1.5 GHz with circular polarization transmitted by a satellite to a moving vehicle in a typical land environment exhibits extreme variation in both amplitude and apparent frequency. Fading effects are due to the random distribution of the electromagnetic field in space and originate from the motion of the vehicle. Here the field is expressed by a linear superposition of plane waves of random phase with component plane waves associated with the Doppler shift. This shift is due to the vehicle motion and is a function of mobile velocity, carrier frequency, and the angle that the propagation vector makes with the velocity vector. The power spectrum of the received signal depends on the density of the arrival angles of the plane waves and the mobile antenna directivity pattern. The instantaneous frequency of the signal received at the mobile has a random variation.

We can identify three components in the received faded signal at the mobile antenna, namely, the direct line of sight (LOS) component, the specular component, and the diffuse component. These correspond to the channel model illustrated in Figure 1. The combined direct and specular components are usually referred to as the *coherent* received component and the diffuse component is referred to as the *noncoherent* received component. In this model, it is assumed that only the coherent component can be attenuated by a lognormal distributed shadowing process due to the presence of trees, poles, buildings, and vegetation in the terrain. If the received coherent component is totally blocked, then the noncoherent component dominates and the received signal envelope variation has a Rayleigh distribution.

As shown by propagation studies [5], a typical land mobile satellite channel has a strong direct component in the presence of fading; thus the resulting received signal has a Rician distribution. For the present application, the Rician fade factor, K , i.e., the ratio of the coherent signal component power to the noncoherent signal component power is assumed to be 10 dB.

The one-way Doppler frequency shift due to vehicle motion can be computed from $f_d = (v/c)f_c$ where v is the mobile velocity, c is the speed of light, and f_c is the carrier frequency. The maximum value of f_d is assumed to be 100 Hz for UHF and 200 Hz for L-band corresponding to a mobile speed of 80 mph.

A complex representation of the fading channel mathematical model used to assess the performance of trellis coded modulation (TCM) systems is illustrated in Figure 2. In the figure, $F(t)$ represents the fading process, $m(t)$ represents the lognormal shadowing process, $N(t)$ is a complex Gaussian noise process, and $\omega_d = 2\pi f_d$. Simulation of this fading channel model indicates that at a fade depth of -3 dB and a Doppler spread of 40 Hz at L-band, the average duration of a fade is 20 symbols with a standard deviation of 10 symbols. Knowledge of the fade duration statistics enables us to design the correct interleaver structure for the TCM schemes.

The 16-State Trellis Coded 8DPSK System

A 16-state trellis coded 8DPSK system has been proposed for the NASA's MSAT-X project for operation at L-band [2,3]. A block diagram of the system is illustrated in Figure 3. Input bits at 4800 bps are passed through a rate 2/3, 16-state trellis encoder [6]. This encoder has been chosen because of its low complexity and good Euclidean distance ($d_{free}^2 = 5.17$). More important, however, is the fact that this code provides a "diversity" of three which makes it particularly attractive for the fading channel application. The meaning of "diversity" as used here will be

explained shortly in the section on design criteria.

The encoder output symbols are then block interleaved to break up burst errors caused by amplitude fades of duration greater than one symbol time. The block interleaver can be regarded as a buffer with d rows representing the *depth* of interleaving and s columns represent the *span* of interleaving. Data is written into the buffer in successive rows and read out of the buffer in successive columns. At the receiver, the block deinterleaver performs the reverse operation.

The interleaving depth should be chosen on the order of the average plus three times the standard deviation of the burst fade duration at a given fade depth related to the operating point. With this definition, at a fade depth of -3 dB for example, the fade duration at 40 Hz Doppler spread (15 mph) is on the order of 50 symbols (note that the fade duration is longer at low vehicle speeds).

The interleaving span should be chosen on the order of the decoder buffer size. Due to a delay constraint imposed by the requirement to transmit speech, the size (product of the depth and the span) of the block interleaver and deinterleaver has been chosen equal to 128 8-PSK symbols. For this size, the interleaving depth was optimized by computer simulation and found to be equal to 16 symbols. Thus, the interleaving span was chosen as 8 symbols. As noted above, at low speeds, e.g., 15 mph, an interleaving depth of 50 symbols is required which is greater than the 16 symbol depth chosen for the design. Thus, the 128 symbol interleaver size is really not sufficient and one should anticipate some performance penalty because of this limitation.

The interleaved trellis-encoded symbols are next differentially encoded and pulse-shaped using root raised cosine filters with 100% excess bandwidth. This pulse shaping is used to limit adjacent channel interference to an acceptable value. The output of the pulse-shaping filters modulates quadrature RF carriers for transmission over the fading channel.

At the receiver, the faded, noise-corrupted signal is downconverted by sampling, and then passed through brick wall filters with bandwidth equal to the sum of the 8-PSK symbol rate plus the maximum Doppler shift, i.e., $2400 \text{ sps} + 200 \text{ Hz} = 2600 \text{ Hz}$. The outputs of the brick wall filters are provided to the Doppler frequency estimator and to pseudo-matched filters (consisting of a brick wall filter and a half symbol delay and add circuit). In the absence of Doppler frequency shift, these pseudo-matched filters are exactly root raised cosine filters [7]. Details of the operation and performance of the Doppler estimator can be found in [3]. An illustration of its performance (rms Doppler error versus bit SNR) over the AWGN and the fading channel is shown in Figure 4 for 8DPSK. The parameter K_{α} represents the effective number of symbols of integration [3] for the LPF in the Doppler Estimator of Figure 3. The outputs of the pseudo-matched filters are provided to a differential detector and then to a residual Doppler correction circuit. The differentially detected and Doppler corrected samples are then fed to the deinterleaver and finally to the trellis decoder. At the trellis decoder, branch metrics are computed using a correlation (Gaussian noise) metric. It can be shown that, in the absence of channel state information (CSI), this metric is approximately optimum. Each symbol time, branch metrics are provided to the Viterbi algorithm which consists of add-compare-select operations with state metric normalization to prevent buffer overflow. The size of the survivor path's buffer is chosen to be 32 symbols based on computer simulation tests. These tests have also shown that the difference in performance between a 32 symbol buffer and a 256 symbol buffer is on the order of a few tenths of a dB.

A software simulation program has been written for the system shown in Figure 3. In the simulation, floating point operation has been used and perfect timing and perfect Doppler

estimation have been assumed. Results of this simulation [3] show that with the appropriate choice of digital filter bandwidth in the Doppler estimator, there will be about 0.5 dB degradation due to the Doppler estimation error. Other simulation results for end-to-end bit error probability of the system of Figure 3 are illustrated in Figures 5 and 6.

This system has been implemented at JPL [8] using TMS32020 DSP chips. The measured bit error probabilities agree with the simulation results given here within 1 dB.

The 16-State Trellis Coded 8PSK System with Pilot-Aided Coherent Detection

This system was proposed in [1] for NASA's MSAT-X project to be used at UHF. A block diagram of the system is illustrated in Figure 7. Most components of this system are identical to those in Figure 3. The differences between the two are as follows. For coherent detection, we use two pilot tones which are inserted at the edges of the signal spectrum as shown on the figure. At the receiver, the faded, noise-corrupted signal is demodulated with pilot tones derived from the pilot tone extraction unit [9, 10] also illustrated in the figure. Unfortunately, this coherent demodulation technique introduces a 180° phase ambiguity. To resolve this ambiguity, the input bits to the trellis encoder should be differentially encoded and the output bits of the trellis decoder should be differentially decoded. Furthermore, the trellis code must be transparent to a 180° phase shift. Unfortunately, the rate 2/3, 16-state Ungerboeck code [6] does not have this transparency property.

We have designed a rate 2/3, 16-state trellis code (Figure 8) with a diversity [11] of three that is transparent to a 180° phase shift but is slightly inferior (approximately less than 0.2 dB for all error probabilities greater than 10⁻⁶) to the above Ungerboeck code. Simulation results for this new code are illustrated in Figure 9.

Design Criterion

It has been shown [11], that the appropriate criterion for designing trellis codes for the fading channel is to maximize the minimum of the squared distance

$$d^2 = \sum_{\eta} \frac{\alpha K \delta_n^2}{1 + K + \beta \delta_n^2} + \left(\frac{E_s}{4N_0} \right)^{-1} \ln \frac{1 + K + \beta \delta_n^2}{1 + K} \quad (1)$$

computed over all possible error events in the trellis diagram. Here δ_n^2 represents the squared Euclidean distance between the n th transmitted (correct) and estimated (incorrect) symbols along an error event path and η is the set of possible occurrences of such errors along that path. Also, for coherent detection with ideal channel state information (CSI)

$$\alpha = 1, \quad \beta = \frac{\bar{E}_s}{4N_0} \quad (2)$$

and for differentially coherent detection with no CSI

$$\alpha = \frac{1}{2}, \quad \beta = \frac{\bar{E}_s}{8N_0} - \frac{1 + K}{16} \quad (3)$$

where E_s/N_0 is the average received symbol SNR and K is again the Rician fade parameter.

Among the class of Ungerboeck codes [6] with low complexity, the rate 2/3, 16 state code seems to be very attractive. Indeed using our design criterion, it can be shown that the Ungerboeck code (multiplicity one) designed for the AWGN is also optimum on the fading channel and

achieves a diversity [11] of three.

Among the class of multiple trellis codes [12] investigated, the two state code with multiplicity two (see Figure 10) is very simple, effective, and optimum over Rayleigh channels. Note that this code is not optimum over the AWGN channel. The optimum code for the AWGN channel is illustrated in Figure 11 for comparison. Simulation results for these two rate 4/6 codes are illustrated in Figures 12 and 13.

References

- [1] D. Divsalar and M.K. Simon, "Trellis Coded Modulation for 4800 to 9600 bps Transmission Over a Fading Satellite Channel," JPL Pub. 86-8 (MSAT-X Report No. 129), June 1, 1986. Also see IEEE Journal on Selected Areas in Commun., Vol. SAC-5, No. 2, February 1987, pp. 162-175.
- [2] M. K. Simon, D. Divsalar, "The Performance of Trellis Coded Multilevel DPSK on a Fading Mobile Satellite Channel," JPL Pub. 87-8 (MSAT-X Report No. 144), Pasadena, CA, June 1, 1987. Also to appear in the February 1988 issue of the IEEE Transactions on Vehicular Technology.
- [3] M. K. Simon, D. Divsalar, "Doppler-Corrected Differential Detection of MPSK," accepted for publication in the IEEE Transactions on Communications.
- [4] D. Divsalar, "JPL's Mobile Communication Channel Software Simulator," Proceedings of the Propagation Workshop in Support of MSAT-X (JPL Internal Document D-2208), Jet Propulsion Laboratory, Pasadena, CA, January 30-31, 1985.
- [5] W.J. Vogel, "Land Mobile Radio Propagation Measurements at 869 and 1501 MHz," 1985 North American Radio Science Meeting, UBC, Vancouver (URSI Abstract Booklet), June 17-21, 1985, Paper N. F-2-1,, p. 348.
- [6] G. Ungerboeck, "Channel Coding with Multilevel/Phase Signals," IEEE Transactions on Information Theory, Vol. IT-28, No. 1, January 1982, pp. 55-67.
- [7] T. Jedrey, private communication.
- [8] N. Lay, T. Jedrey, D. Divsalar, C. Cheetham, D. Black, "Modem and Terminal Processor Testing on the JPL Fading Channel Simulator," MSAT-X Quarterly, No. 15, Jet Propulsion Laboratory, Pasadena, CA, April 1988.
- [9] W. Rafferty, et al., "A Proposed Design for a Land Mobile Satellite Terminal," a proposal submitted to JPL by the General Electric Co., Corp. R&D, New York, 1985.
- [10] M. K. Simon, "Dual Pilot Tone Calibration Technique (DPTCT)," IEEE Transactions on Vehicular Technology, Vol. VT-35, No. 2, May 1986, pp. 63-70.
- [11] D. Divsalar, M.K. Simon, "The Design of Trellis Codes for Fading Channels," JPL Pub. 87-39 (MSAT-X Report 147), Pasadena, CA, November 1, 1987. Also to appear (in two parts) in a future issue of the IEEE Transactions on Communications.
- [12] D. Divsalar, M. K. Simon, "Multiple Trellis Coded Modulation (MTCM)," JPL Pub. 86-44 (MSAT-X Report No. 141), Pasadena, CA, November 15, 1988. Also to appear in a future issue of the IEEE Transactions on Communications.

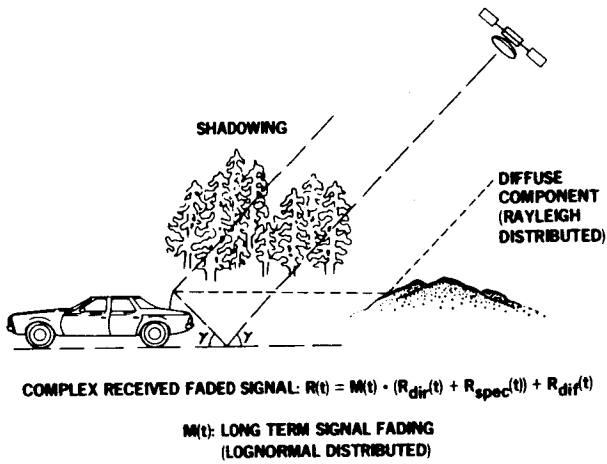


Figure 1. Land Mobile Satellite Channel Model for MSAT-X

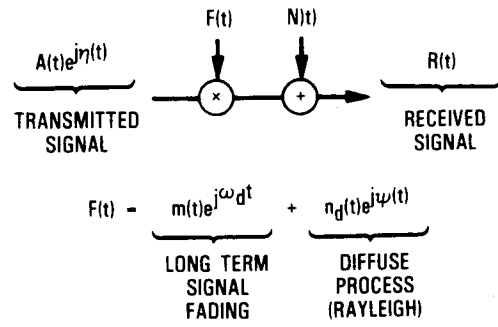


Figure 2. Complex Representation Model for Fading Channel

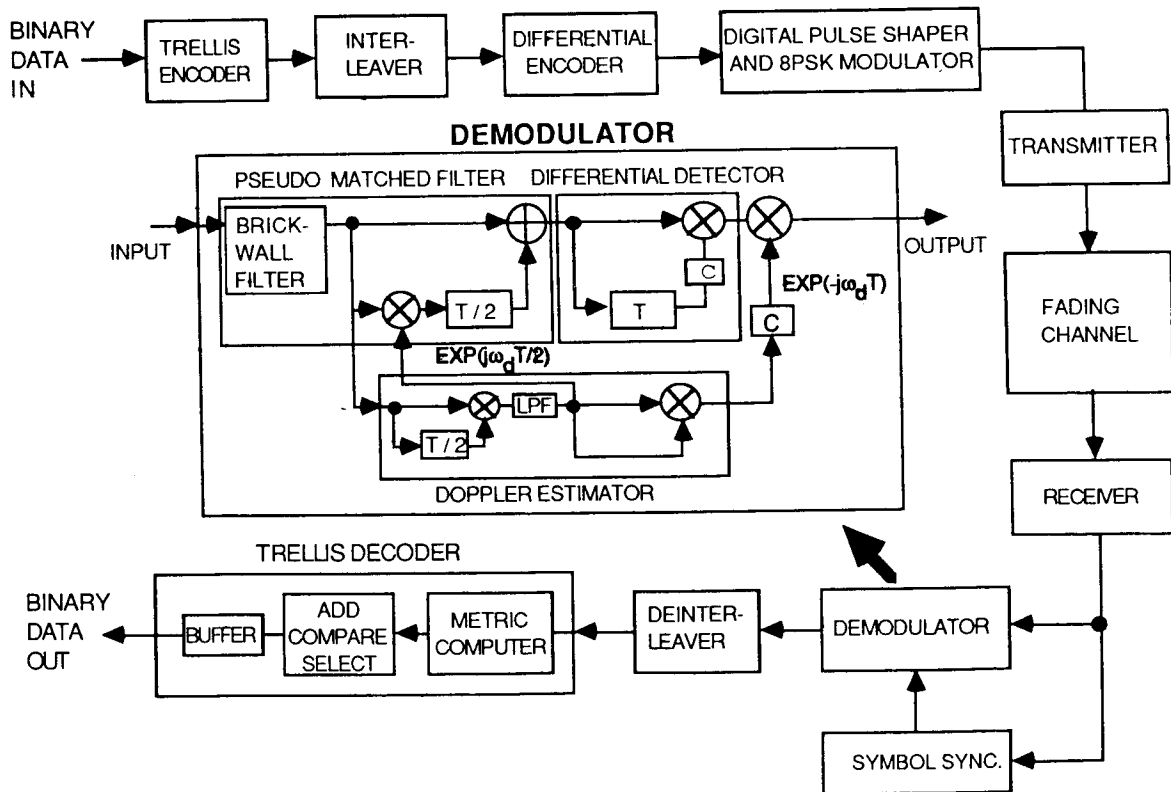


Figure 3. Block Diagram of Trellis Coded 8 DPSK System with Differential Detection and Doppler Correction

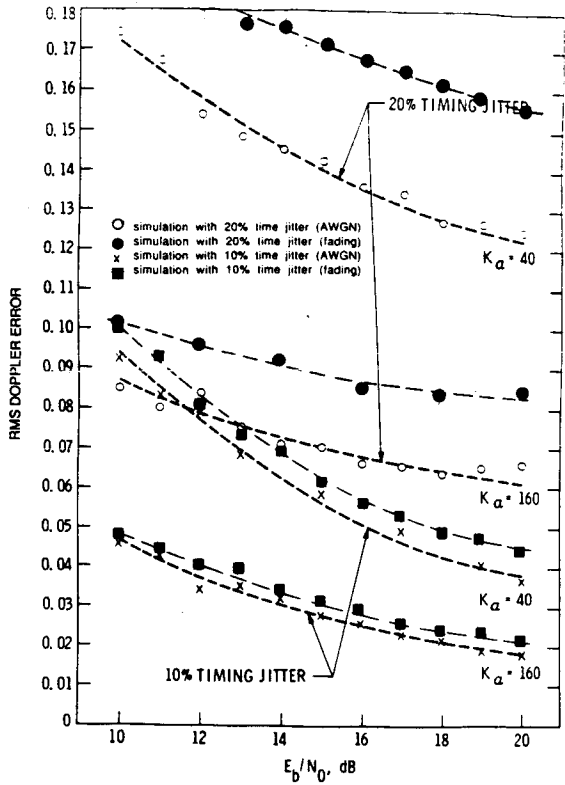


Figure 4. The RMS Doppler Error vs. the Bit Energy-To-Noise Ratio with 10% and 20% Time Jitter

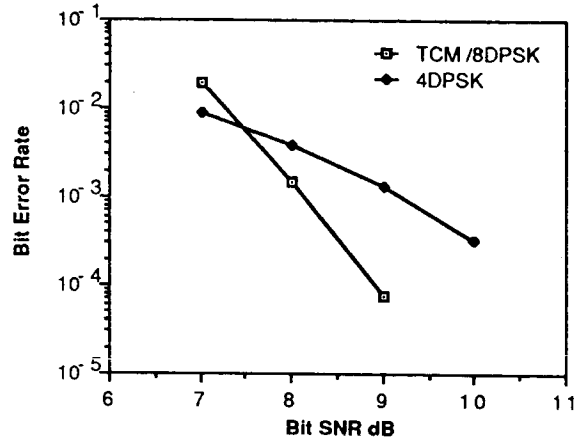


Figure 5. Simulation Results for the Bit Error Rate of Trellis Coded 8 DPSK and Uncoded 4 DPSK over AWGN Channel

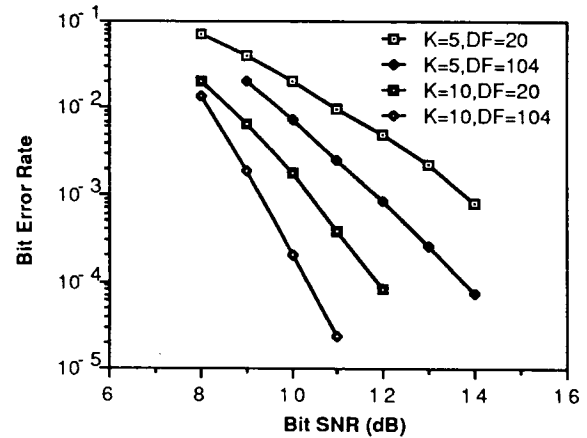


Figure 6. Simulation Results for the Bit Error Rate of Trellis Coded 8 DPSK over Rician Fading Channel with Rician Factor of 5dB, 10dB and Doppler Spread of 20Hz, 104 Hz

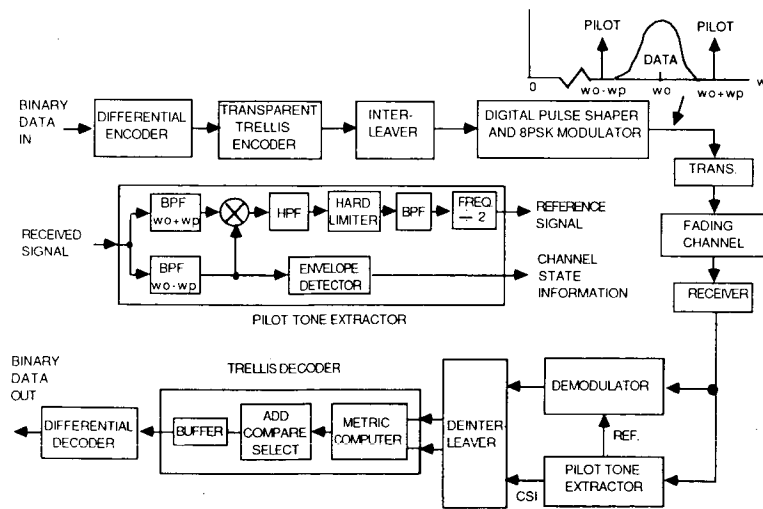


Figure 7. Block Diagram of Trellis Coded 8 PSK System with Pilot-Aided Coherent Detection

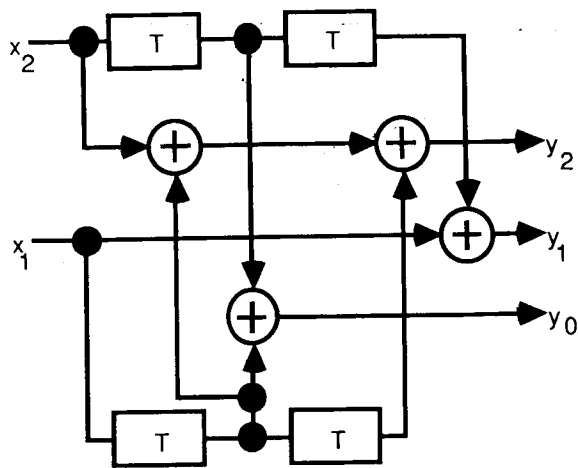


Figure 8. A New 180° Phase Invariant (Transparent) Trellis Encoder

RICIAN PARAMETER K = 10 dB PILOT BANDWIDTH = 200 Hz (UHF)
 DOPPLER SPREAD = 20 Hz (UHF) TOTAL POWER OF PILOTS/DATA POWERS = -7 dB (UHF)

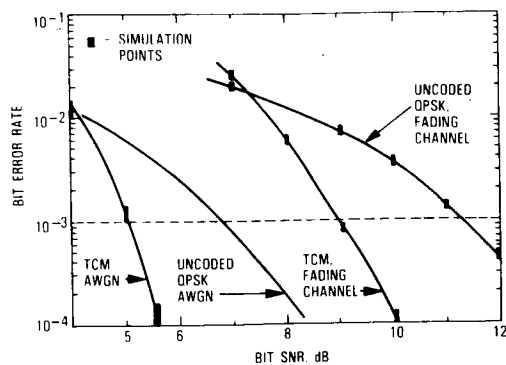


Figure 9. Simulation Results for the Bit Error Rate of Differentially Encoded, (Transparent) Trellis Coded 8 PSK with Pilot-Aided Coherent Detection

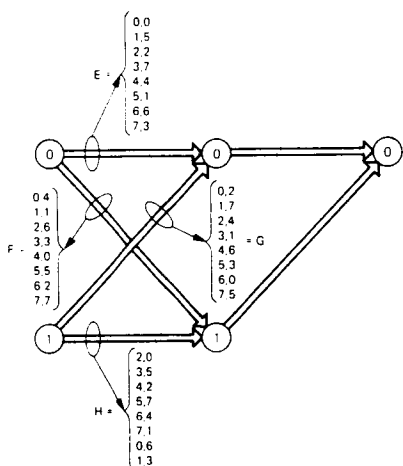


Figure 10. Trellis Diagram for Multiple (k=2), Rate 4/6 Coded 8 PSK; 2 States, Designed for Fading Channel

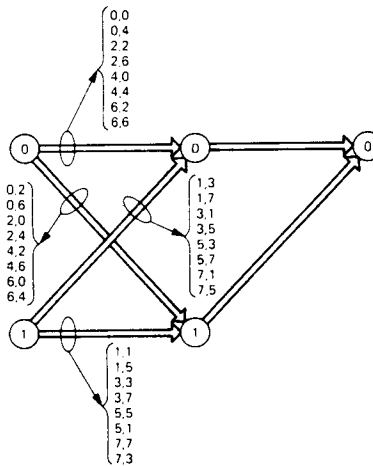


Figure 11. Trellis Diagram for Multiple (k=2), Rate 4/6 Coded 8 PSK; 2 States, Designed for a AWGN Channel

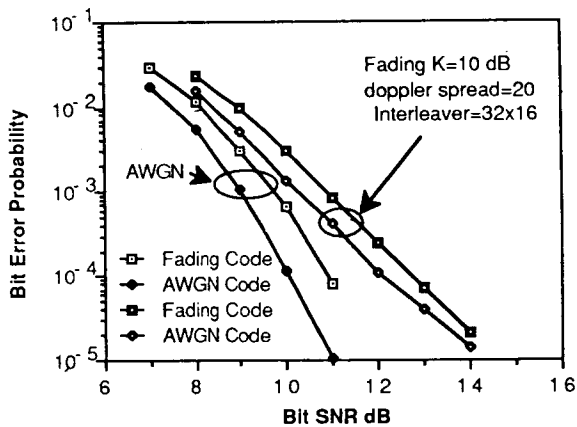


Figure 12. Simulation Results for Multiple Trellis Codes of Figures 10 and 11 with 8 DPSK over AWGN and Rician Fading (K=10dB) Channels

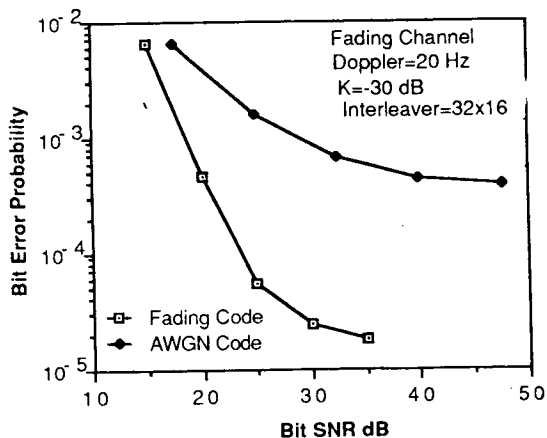


Figure 13. Simulation Results for Multiple Trellis Codes of Figures 10 and 11 with 8 DPSK over Rayleigh Fading Channel (K=30dB)

MODULATION AND CODING FOR FAST FADING MOBILE SATELLITE COMMUNICATION CHANNELS

P.J. MCLANE, P.H. WITKE, W.S. SMITH, A. LEE, Department of Electrical Engineering, Queen's University, Canada; P.K.M. HO, Simon Fraser University, Canada; C. LOO, Department of Communications, Canada.

DEPARTMENT OF ELECTRICAL ENGINEERING
Queen's University
Kingston, Ontario
K7L 3N6
Canada

ABSTRACT

The first part of this paper describes the performance of GMSK using differential detection in fast Rician fading, with a novel treatment of the inherent ISI leading to an exact solution. In the second part trellis coded DPSK with a convolutional interleaver is considered. The channel is the Rician Channel with the line-of-sight component subject to a lognormal transformation. This accounts for shadowing on the Rician Channel.

INTRODUCTION

We consider digital transmission using phase modulation over the Rician Channel. This is meant to model a mobile satellite communications link. In the first part of the paper, which is based on [Smith, 1988], GMSK is considered from an analytical point of view for the Rician case. In the second part we treat shadowing and trellis coded DPSK via Monte Carlo simulation.

GMSK IN FAST RICIAN FADING

The problem addressed here is that of obtaining an explicit analytical expression for the error performance of Gaussian baseband filtered minimum shift keying, (GMSK), using differential detection in a fast Rician fading channel with additive Gaussian noise [Smith, 1988]. This problem can be divided into two sections, namely determining the probability of error conditioned on a specific phase change over the bit period, and accounting for the intersymbol interference (ISI) inherent in GMSK modulation. The solution to the first has been reported in [Mason, 1987]. He points out that an alternate treatment is given in [Stein, 1964], which will be the approach taken here. The second step is accomplished by a new technique which allows the calculation of the expected value of a function over the probability distribution of the interference

variables. This method results in an exact explicit expression for the error probability which may be calculated to the desired degree of accuracy. The procedure is generally applicable in a wide range of digital communications problems involving ISI.

A GMSK signal is generated by passing a non-return-to-zero data stream through a Gaussian baseband filter followed by an FM modulator with modulation index 0.5. The transmitted GMSK data phase signal may be represented as

$$\theta(t) = \pi \int_{-\infty}^t \sum_{n=-\infty}^{\infty} a_n \left(\frac{1}{2T}\right) g(v - nT) dv \quad (1)$$

where $\{a_n\}_{n=-\infty}^{\infty}$ is a sequence of independent, identically distributed random variables taking on the values +1 or -1 with equal probability, T is the bit period, and g(t), the basic frequency pulse, is given in [Simon and Wang, 1984, eqn. 18]. The factor (1/2T) normalizes g(t) such that the net phase change due to one data bit, after FM modulation with index 0.5, is $\pi/2$.

The receiver consists of a standard differential detector, where the predetection bandpass filter and postdetection baseband filter are assumed to have negligible effect on the signal components. Considering a lowpass equivalent representation, the received signal at the input to the differential detector, z(t), consists of the direct component $u(t) = A \exp[j\theta(t)]$, the Rayleigh faded component $r(t) = w(t)\exp[j\theta(t)]$, and the additive Gaussian noise n(t), where A is the signal amplitude, and w(t) and n(t) are mutually independent stationary zero-mean complex Gaussian processes. The differential detector acts as a quadrature product demodulator forming the output $v(t) = (1/2)\text{Re}\{-jz(t)z^*(t - T)\}$ where * denotes conjugation, $\text{Re}\{\cdot\}$ denotes the real part of $\{\cdot\}$, and it is assumed that the carrier radian frequency $\omega = n2\pi/T$ for n an integer. This is sampled at times $t = T/2 + nT$ and the data is recovered based on the polarity of $v(T/2 + nT)$.

Consider the detection of the zeroth bit, assumed +1. Conditioned on receiving a particular phase change, $\Delta\theta = \theta(T/2) - \theta(-T/2)$, $z(T/2)$ and $z(-T/2)$ are dependent conditional complex Gaussian variables. Following the development given in [Stein, 1964], the probability of error may be expressed as

$$P(\text{error} | \Delta\theta, a_0 = 1) = 1/2 [1 - Q(\sqrt{b}, \sqrt{a}) + Q(\sqrt{a}, \sqrt{b})] - \frac{C}{2} \exp\left(-\frac{(a+b)}{2}\right) I_0(\sqrt{ab}) \quad (2)$$

$$\text{where } \begin{Bmatrix} a \\ b \end{Bmatrix} = \frac{KA}{D} [(\Lambda + K + 1) - \Lambda \rho_s \cos^2 \Delta\theta - (K + 1) \rho_n \cos \Delta\theta \mp \sqrt{D} \sin \Delta\theta]$$

$$C = (\Lambda \rho_s \sin \Delta\theta) / \sqrt{D} \quad D = (\Lambda + K + 1)^2 - (\Lambda \rho_s \cos \Delta\theta + \rho_n (K + 1))^2$$

where $\rho_s = J_0(2\pi f_D T)$, is the normalized autocorrelation function for the mobile fading spectrum with maximum Doppler frequency f_D , $\rho_n = \sin(2\pi B_{IF} T) / (2\pi B_{IF} T)$ is the normalized autocorrelation of the noise for an ideal rectangular bandpass filter with one-sided bandwidth B_{IF} ,

K is the propagation SNR, Λ is the average SNR, $Q(\alpha, \beta)$ is Marcum's Q-function and I_0 and J_0 are Bessel functions.

The foregoing analysis is conditioned on the value of the phase change over the bit interval, which depends on the infinite sequence of data bits being transmitted.

$$\begin{aligned} \Delta\theta &= \pi \sum_{k=-\infty}^{\infty} a_k \int_{-T/2}^{T/2} \left(\frac{1}{2T}\right) g(v-kT) dv \\ &= a_0 \beta_0 + \sum_{k=1}^{\infty} a_{-k} \beta_k + \sum_{k=1}^{\infty} a_k \beta_k = \beta_0 + X + Y \end{aligned} \quad (3)$$

$$\text{where } \beta_k = \beta_{-k} = \pi \int_{-T/2}^{T/2} \left(\frac{1}{2T}\right) g(v-kT) dv$$

$$X = \sum_{k=1}^{\infty} a_{-k} \beta_k \quad Y = \sum_{k=1}^{\infty} a_k \beta_k$$

In (3), a_0 the data bit being detected is assumed to be +1, and X and Y are independent random variables with identical distributions. It can be shown that the variables X and Y are singular and of the Cantor type, [Wittke et al., 1988], provided that $BT > 0.0784$. In this case, the probability distribution function of X or Y is a continuous function that takes on constant values except on a set of measure zero. The expected value of a general function conditioned on one interference variable, say X, may be evaluated as

$$E\{f(X)\} = f(R_1) - \sum_{j=1}^{\infty} \sum_{k=1}^{2^{j-1}} (2k-1)2^{-j} [f(E_{jk}) - f(S_{jk})] \quad (4)$$

$$\text{where } S_{jk} = \gamma_{j-1, k}^{-\rho_j}, \quad E_{jk} = \gamma_{j-1, k}^{+\rho_j}, \quad \rho_j = \beta_j^{-R_{j+1}}, \quad R_j = \sum_{k=j}^{\infty} \beta_k,$$

$\gamma_{j, k}$ can take on the 2^j values, $\pm \beta_1, \pm \beta_2, \dots, \pm \beta_j$ and are ordered in increasing value, and γ_{01} has been defined as zero. Conditioning on two independent identically distributed Cantor variables, as is required by this analysis, leads to the result

$$\begin{aligned} E\{f(X, Y)\} &= f(R_1, R_1) + \sum_{j=1}^{\infty} \sum_{k=1}^{2^{j-1}} \sum_{m=1}^{\infty} \sum_{n=1}^{2^{m-1}} (2k-1)2^{-j} (2n-1)2^{-m} \\ &\cdot [f(S_{mn}, S_{jk}) + f(E_{mn}, E_{jk}) - f(S_{mn}, E_{jk}) - f(E_{mn}, S_{jk})] + \end{aligned}$$

$$\sum_{j=1}^{\infty} \sum_{k=1}^{2^j-1} (2k-1) 2^{-j} [f(R_1, S_{jk}) + f(S_{jk}, R_1) - f(R_1, E_{jk}) - f(E_{jk}, R_1)] \quad (5)$$

Combining the previous two results, equations (2) and (5) gives the overall error probability. This has been plotted in Fig. 1 for varying premodulation bandwidth BT , with propagation SNR $K = 10$ dB, maximum Doppler frequency $f_D T = 0.05$, and one-sided 3 dB bandpass filter bandwidth $B_{IF} T = 1.0$. These parameters are typical of the conditions expected for the Canadian MSAT program. In evaluating the error probability, the number of terms required for 3 figure accuracy decreases with increasing premodulation filter bandwidth, BT . For example the curve for $BT=0.3$ was evaluated by truncating the series beyond $j=m=2$, and for $BT=0.5$ beyond $j=m=1$.

TCM WITH D8PSK

In this section we report on the use of interleaved, trellis coded modulation used in conjunction with D8PSK modulation. A block diagram of the system under consideration is shown in Fig. 2. Here the burst error channel is modelled as an additive white Gaussian noise channel where the gain and phase are modeled as a random process. This dynamically varying phasor represents non-static signal fading.

Most investigations [Simon and Divsalar, 1986] use the Rician model for signal fading which is composed of a constant line-of-sight (LOS) component plus a scatter component which is a complex Gaussian random process. In Canada, due to a low angle of elevation to the satellite, a shadowed Rician model has been developed [Loo, 1985]. This model has the same scatter component as the Rician, but the LOS component is subjected to a lognormal transformation. The dynamics of the fading is controlled by a third-order-Butterworth filter.

System performance is determined by digital computer simulation of the fading channel. A single sample per symbol interval is used to represent the fading process. Results using this model for 4- and 8-state trellis coded PSK and DPSK modulations were reported in [McLane et al., 1987]. It was found that for up to average shadowing conditions a fade margin of 12 dB could be maintained at a BER of 10^{-3} ; this is a relevant BER as speech transmission is regarded as the major application.

In [McLane et al., 1987] interleaved transmission was treated only from an approximate point of view. We have included the convolutional interleaver shown in Fig. 3 into our simulations. Such a convolutional interleaver is ideal for use with Ungerboeck codes as such codes use convolutional encoders as generators. Also, convolutional interleavers have lower delay than block interleavers. This is important in speech applications where the overall delay must be kept below 300 ms. As the propagation delay in MSAT is 250 ms this leaves 50 ms for Viterbi decoder plus convolutional interleaver delay. The results of our simulations are shown in Fig. 4. The case $\lambda = 6$

meets the 50 msec constraint but the $\lambda = 8$ case does not. However, we have recently found, as suggested in [McLane et al., 1987], that the Viterbi decoding delay can be reduced to make $\lambda = 8$ meet the 50 msec time delay constraint and with very little loss in BER.

CONCLUSION

Analytical techniques to determine the performance of GMSK in a fast fading Rician Channel have been presented. For TCM and DPSK modulation, system simulation has been used to determine performance when convolutional interleavers are used. We are currently applying our analytical techniques to the TCM case.

REFERENCES

- Divsalar, D. and M.K. Simon. 1986. Trellis coded modulation for 4800 to 9600 bps transmission over a fading satellite channel. JPL Publication 86-8. (Pasadena, California): also, IEEE Journal Selected Areas Comm., Vol. SAC-5, pp. 162-175, Feb. 1987.
- Loo, C. 1985. A statistical model for a land mobile satellite link. IEEE Trans. Vehicular Technology, Vol. VT-34, pp. 122-127.
- Mason, L.J. 1987. Error probability evaluation for systems employing differential detection in a Rician fast fading environment and Gaussian noise. IEEE Trans. Commun., Vol. COM-35, pp. 39-46.
- McLane, P.J., P.H. Wittke, P.K.-M. Ho and C. Loo. 1987. Performance of binary multi-h modulation for fast fading, shadowed, mobile satellite communications. IEEE Vehicular Technology Conference. (Tampa, Florida).
- Simon, M.K. and C.C. Wang. 1984. Differential detection of Gaussian MSK in a mobile radio environment. IEEE Trans. Veh. Technol., Vol. VT-33, pp. 307-320.
- Smith, W.S. 1988. Ph.D. dissertation, Queen's University, Canada.
- Stein, S. 1964. Unified analysis of certain coherent and noncoherent binary communication systems. IEEE Trans. Inform. Theory, Vol. IT-10, pp. 43-51.
- Wittke, P.H., W.S. Smith and L.L. Campbell. Infinite series of interference variables with Cantor-type distributions. Submitted to IEEE Trans. Inform. Theory.

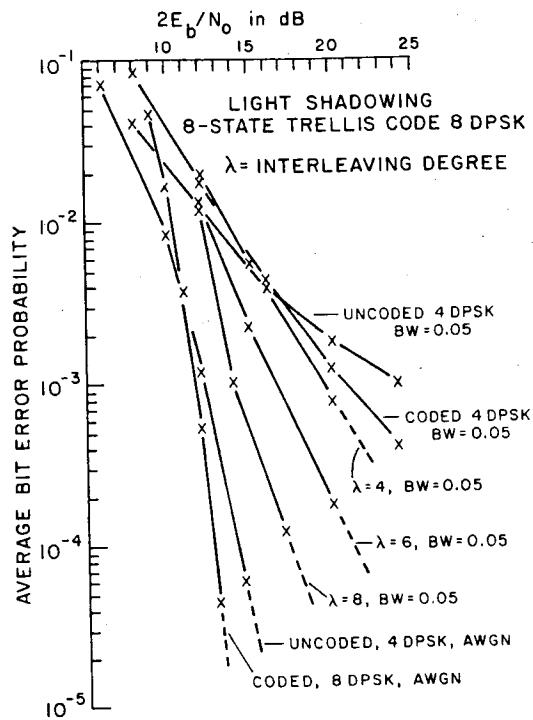
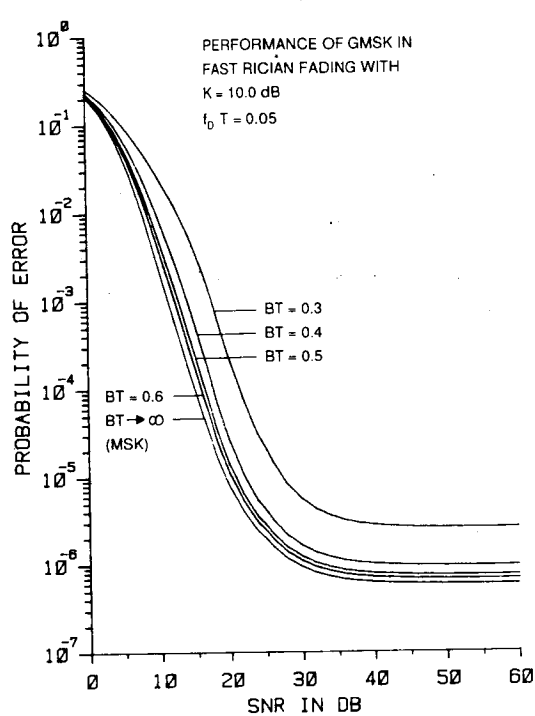


Fig. 1: GMSK Performance

Fig. 4: Coded DPSK Performance

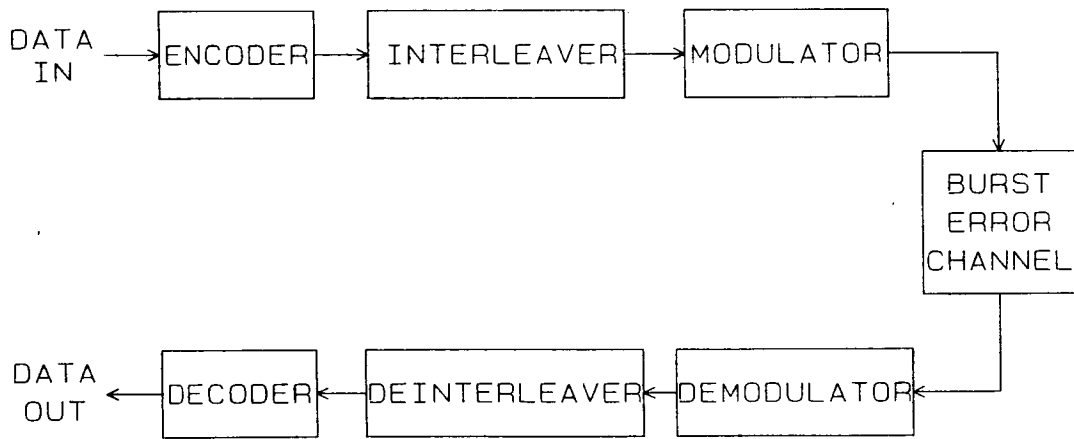


Fig. 2: Block Diagram, Interleaved and Coded DPSK

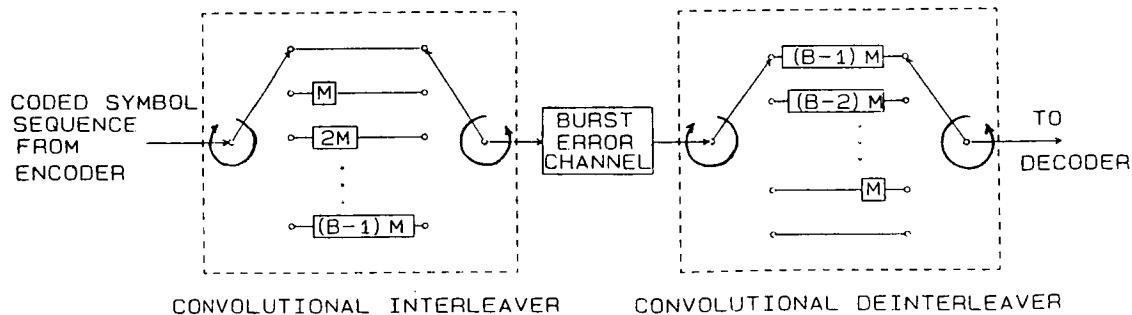


Fig. 3: Convolutional Interleaver for DPSK Trellis Codes

PERFORMANCE OF THE ICAO STANDARD "CORE SERVICE" MODULATION AND CODING TECHNIQUES

DR. JOHN LODGE, Communications Research Centre, Canada;
MICHAEL MOHER, Miller Communications Systems Ltd., Canada.

Communications Research Centre
P.O. Box 11490, Station H
Ottawa, Ontario
CANADA K2L 8S2

ABSTRACT

There is significant interest in the aviation community in establishing a satellite communications system architecture to provide comprehensive aeronautical communications services. Incorporated into the architecture is a "core service" capability, which provides only low rate data communications (e.g., 300, 600, 1200 information bps), to allow for basic air traffic services and aeronautical operational control. In November 1986, the International Civil Aviation Organization's (ICAO) Special Committee on Future Air Navigation Systems agreed upon a standard modulation technique for the core service. The new standard, designated aviation binary phase shift keying (A-BPSK), is essentially differentially-encoded symmetric binary phase shift keying with square-root 40 percent raised cosine pulse shaping. It was also agreed that the recommended coding technique is an interleaved constraint-length 7 convolutional code with rates $1/2$ or $3/4$. This paper contains material that was given in working papers to ICAO and to the Airlines Electronic Engineering Committee (AEEC). In addition, it contains more recently generated material dealing with the application of maximum likelihood principles to the problem of detection of A-BPSK modulated data, that was transmitted over a Rician fading channel.

AVIATION BINARY PHASE SHIFT KEYING

A-BPSK is a form of differentially-encoded filtered symmetric BPSK (Schwartz et al., 1966). Symmetric BPSK differs from conventional BPSK, in that every second symbol is transmitted in the quadrature channel. Note that this scheme is still binary phase shift keying in the sense that the phase, of any given transmitted symbol, can take on only one of two possible values. Therefore, symmetric BPSK exhibits the same robustness to phase noise and nondispersive fading as conventional BPSK. However, while conventional BPSK has phase transitions of π radians, symmetric BPSK has phase transitions of $\pi/2$ radians. Therefore, symmetric BPSK exhibits less spectral regrowth after filtering and hardlimiting, than does conventional BPSK.

Pulse shaping, using members of the family of square-root raised cosine filters, was studied by computer simulation. It was found that, for a wide range of roll-off factors, the resulting transmitted signal has relatively small envelope variations. The root-mean-square and extreme values of these variations were computed as a function of roll-off factor. The envelope variations are smallest in the vicinity of 40 to 50 percent. Therefore, it seems reasonable to expect that A-BPSK, which has a roll-off

factor of 40 percent, will be robust to nonlinear amplification. The power spectral density of A-BPSK, after hardlimiting, can be seen in Figure 1. While a considerable number of sidelobes have appeared, the spectrum is still much more compact than that for conventional BPSK. In fact, the spectrum is only marginally worse than that for MSK!

The performance of coherently-detected A-BPSK has been evaluated using computer simulation, for a number of different scenarios. For a variety of different fading bandwidths and K-factors, the performance of hardlimited A-BPSK is shown in Figure 2. Here, the K-factor is defined to be the ratio of the average power of the Rayleigh fading signal path to the power of the direct path. For these simulations, the symbol timing was assumed to be perfect and the carrier recovery circuit was assumed to be locked to the direct path signal. Within the accuracy of the simulations, the results in Figure 2 are practically identical to the corresponding ones that were generated for differentially-encoded coherently-detected BPSK (DECPSK).

Performance has also been evaluated for the rate 1/2 coded case. The coded performance for both static channel conditions and Rician fading conditions, with a K-factor of -7 dB, is shown in Figure 3. For these simulations, the interleaving depth is sufficiently large that there is negligible interleaving loss. The magnitude of the "soft decision" was taken to be the smallest of the two sample magnitudes affecting the given decision. Note that the presence of fading degrades the performance by less than 1 dB, over the range shown.

A PARTIALLY COHERENT APPROACH TO THE DETECTION OF A-BPSK

As was shown in the previous section, A-BPSK performs very well even when it is hardlimited. Hardlimited A-BPSK can be thought of as a type of continuous phase modulated (CPM) signal. Fortunately, attractive discrete-time receiver structures, based on maximum likelihood principles applied to Rayleigh fading channel transmission, exist for the reception of CPM signals. In this section, the application of such a receiver structure to the reception of A-BPSK is discussed.

Consider the case of Rayleigh fading transmission where the receiver down-converts the CPM signal to complex baseband, passes it through an ideal anti-aliasing filter, and then samples it. The filter bandwidth, B , is wide enough that for practical purposes all of the signal energy is passed, including the signal energy that is spread by the fading process. Furthermore, it is assumed that the filter's transfer function possesses the appropriate symmetries so that the additive Gaussian noise is still white after the sampling is performed. Once these assumptions are accepted, it is sufficient to perform all of the modelling and analysis using the discrete-time complex baseband model.

Consider the case of maximum likelihood sequence estimation, where each of M possible data sequences corresponds to transmitting a distinct constant envelope signal, with each distinct signal having a duration of N samples. Furthermore, let the amplitude of the signals be normalized so that the magnitude of each complex sample is one. Therefore, the set of possible transmitted signals can be denoted as the set of N -vectors,

$$X = \{x_1, \dots, x_M\}. \quad (1)$$

Let the corresponding signal at the output of the discrete-time channel be denoted by the N -vector y . Then the maximum likelihood detection choice is

x_k , if

$$p(y|x_k) > p(y|x_m) \quad ; m = 1, \dots, M ; m \neq k. \quad (2)$$

The detector must determine the M conditional probabilities, or M equivalent metrics. Consider the case, where the first operation performed by the detector is to compute M new vectors given by

$$y'_m = P_m y \quad ; m = 1, \dots, M, \quad (3)$$

where P_m is a diagonal matrix with ii 'th element being the i 'th element of x_k^* , and m denotes the complex conjugate. This operation can be viewed as removing the assumed modulation from the received signal, for each of the M hypotheses. It is easy to show that equations (3) represent a set of linear transformations, each with a Jacobian of magnitude one. Therefore,

$$p(y'_m|x_m) = p(y|x_m). \quad (4)$$

Let R be the Toeplitz covariance matrix with its elements being the normalized autocorrelation coefficients that correspond to the power spectral density function, $S'(f)$, of the received signal when the input to the channel is an unmodulated carrier. It can be shown that choosing the hypothesis with the maximum likelihood is equivalent to choosing the hypothesis that minimizes the quadratic metric given by,

$$J_m = y_m'^H R^{-1} y'_m \quad ; m = 1, \dots, M. \quad (5)$$

where superscript H denotes the complex conjugate transpose.

Next, a theorem will be given that forms the basis for the detection strategy. It is assumed here that $S'(f)$ is symmetrical about the origin so that the elements of R are real. Extension to the case where the elements of R are complex is straightforward but tedious.

THEOREM: Given the normalized autocorrelation coefficients $1, r_1, \dots, r_{N-1}$, let R be the positive definite Toeplitz matrix with ij 'th element $r_{|i-j|}$ ($r_0 = 1$). Then

$$R^{-1} = A^T D A, \quad (6)$$

where D is a diagonal matrix with ii 'th element $(v_{i-1})^{-1}$, and A is the forward prediction matrix given by

$$A = \begin{bmatrix} 1 & 0 & 0 & \dots & 0 \\ a_1^1 & 1 & 0 & \dots & 0 \\ a_2^2 & a_2^1 & 1 & \dots & 0 \\ \vdots & & & \ddots & \vdots \\ a_{N-1}^{N-1} & a_{N-1}^{N-2} & a_{N-1}^{N-3} & \dots & 1 \end{bmatrix}. \quad (7)$$

Here, a_j^i is the i 'th coefficient of the j 'th order linear predictor, and V_j is the corresponding normalized prediction error, with V_0 defined to be one.

From the computational point of view, well known recursive algorithms exist that allow one to compute the predictor coefficients and the expected normalized prediction errors, from either autocorrelation data or coefficients of the all-pole filter with the spectrum $S'(f)$ (Makhoul, 1975).

This theorem has an intuitively pleasing interpretation. It implies that the maximum likelihood hypothesis is the one that minimizes the sum of the weighted squared forward prediction errors, where each of these prediction error terms is weighted by the inverse of its expected value. Clearly, the prediction filters have orthogonalized the metric given in equation (5).

An interesting case is the one where $S'(f)$ can be closely approximated by an L 'th order all-pole filter, with L much smaller than N . Note that for an L 'th order model, all linear predictors of order L and greater have the same coefficients and the same expected normalized squared prediction error. Therefore, except for the first L samples, the forward error prediction filter is a time-invariant finite impulse response filter of order L . Furthermore, assuming that the modulator has a finite memory, each squared term (i.e. prior to the summation) is dependent only upon a finite number of adjacent bits. This is exactly the situation that can be efficiently handled using dynamic programming. Often, the combined memory of the modulator and channel can result in a prohibitively large number of states. In this case, a decision feedback, truncated state, or reduced state approach can be adopted.

In theory, the above receiver concept can easily be extended to include Rician fading. However, in practice, the receiver would have to accurately estimate the gain and phase of the direct path, which is undesirable. Here, a different approach is taken. The direct path, in the assumed channel model, is replaced by a slow Rayleigh fading path. The assumed $S'(f)$ for the computation of the receiver parameters is shown in Figure 4. In the simulation, the fading spectrum is Gaussian, whereas it is approximately rectangular in the assumed spectrum. Thus, there are several mismatches between the simulated channel and the assumed one, that result in a departure from true maximum likelihood detection. Further departure occurs when steps are taken to reduce the receiver complexity. The assumed composite spectrum is approximated by an eighth-order all-pole filter, with the resulting spectral characteristic shown in Figure 5. Also, the number of states was reduced to 4 by using decision-feedback detection. The resulting performance of the partially coherent receiver is illustrated Figure 6. For bit error rates less than 10^{-2} , the partially coherent receiver noticeably outperforms the ideal DECPSK receiver. However, for the higher bit error rates, typical of operation with convolutional coding, there is little difference between the performance of the two schemes. Unlike the case for DECPSK, the partially coherent receiver does not require carrier phase recovery, and requires only approximate carrier frequency estimation.

CONCLUSIONS

A-BPSK was described and simulated performance results were given that demonstrate robust performance in the presence of hardlimiting amplifiers. The performance of coherently-detected A-BPSK with rate 1/2 convolutional coding was given. The performance loss due to the Rician fading was shown to be less than 1 dB over the simulated range. A partially coherent detection scheme, that does not require carrier phase recovery, was described. This scheme exhibits similar performance to coherent detection, at high bit error rates, while it is superior at lower bit error rates.

REFERENCES

- Schwartz, M., Bennett, W.R., and Stein, S., 1966. Communications Systems and Techniques. New York: McGraw-Hill.
- Makhoul, J. 1975. Linear Prediction: A Tutorial Review. Proc. IEEE, vol. 63, pp. 561-580.

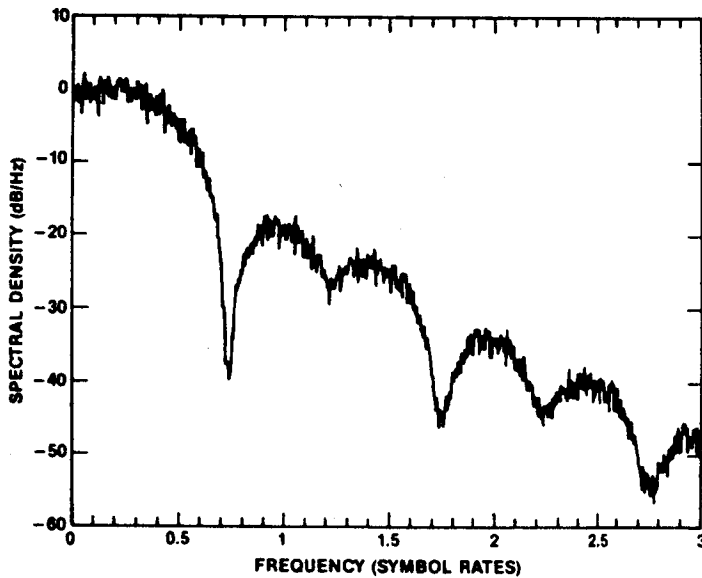


Fig. 1. The power spectral density of hardlimited A-BPSK.

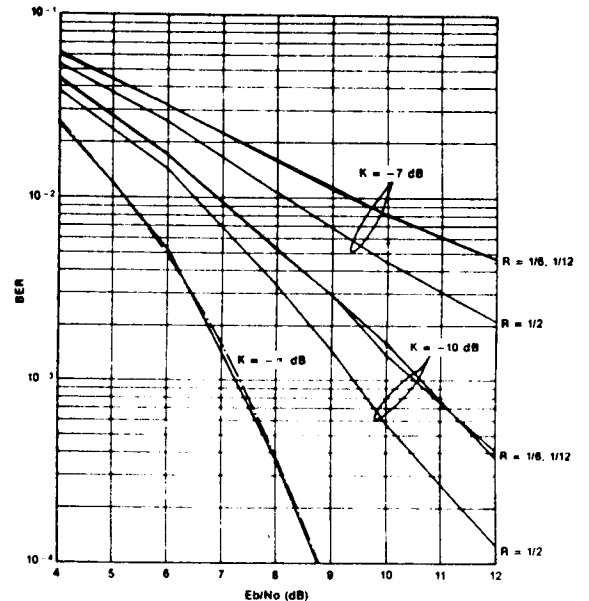


Fig. 2. The performance of hardlimited A-BPSK transmitted over a Rician fading channel. The fading rate, R , is expressed as a fraction of the bit rate.

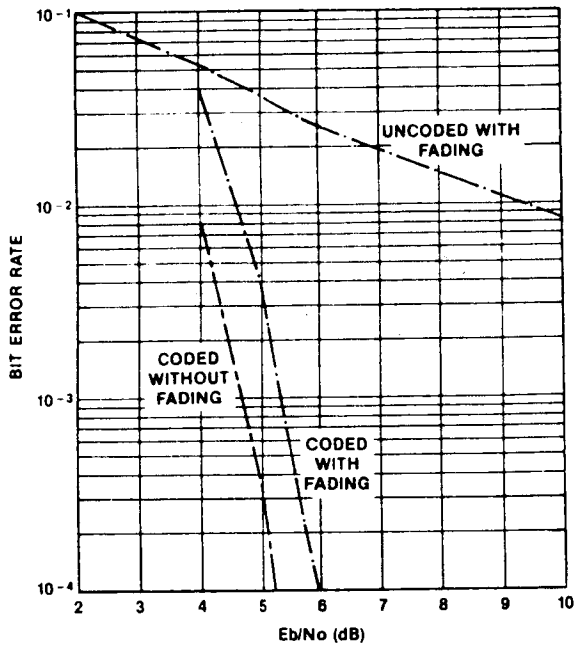


Fig. 3. The performance of A-BPSK with rate 1/2 coding, transmitted over static and Rician fading ($K = -7$ dB) channels. Here, the fading rate is 1/12 of the bit rate.

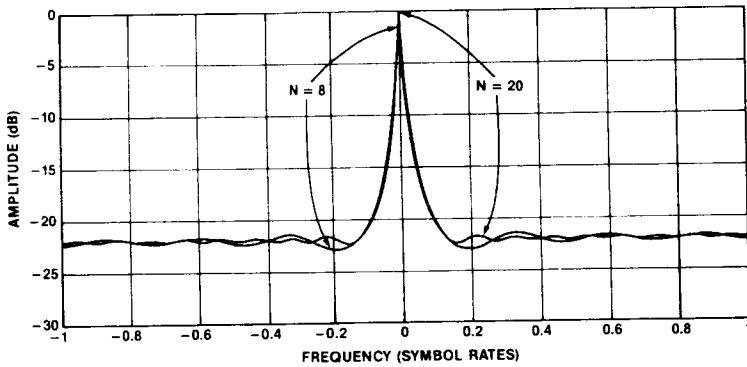


Fig. 5. The 8'th-order and 20'th-order approximations of the assumed composite spectrum.

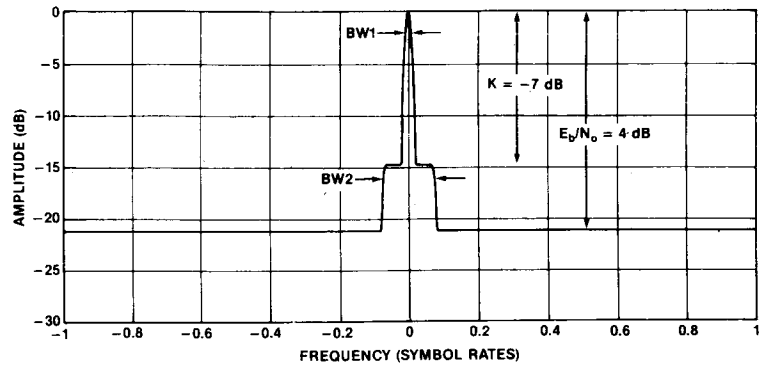


Fig. 4. The assumed composite spectrum, $S'(f)$.

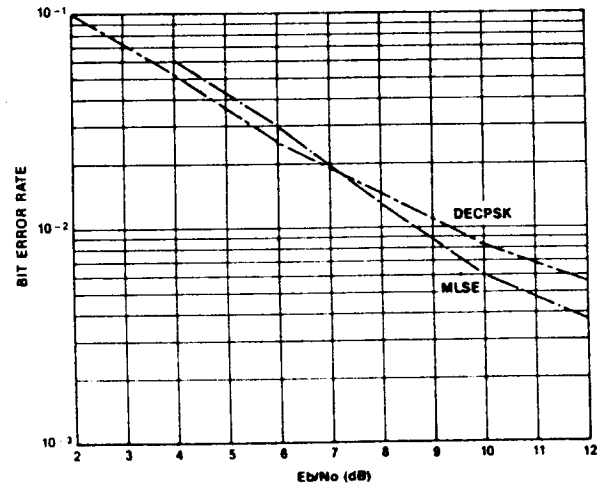


Fig. 6. A comparison of the performance of DECPSK and the partially coherent detection scheme, transmitted over a Rician fading channel ($K = -7$ dB).

COMPARISON OF CDMA AND FDMA FOR THE MOBILESTARSM SYSTEM

I.M. Jacobs, K.S.Gilhousen, L.A.Weaver, Qualcomm Inc, United States;
K. Renshaw,T. Murphy, Hughes Aircraft Company, United States.

Hughes Aircraft Company
Space and Communicatons Group
Po.Box 92919, S65/J317
Los angeles CA 90009

ABSTRACT

Spread spectrum CDMA and single channel per carrier FDMA systems are compared for spectral efficiency. CDMA is shown to have greater maximum throughput than FDMA for the MobileStarSM system which uses digital voice activated carriers and directive circularly polarized satellite antennas.

INTRODUCTION

Spread spectrum CDMA systems and single channel per carrier FDMA systems have been compared in the literature many times. When bandwidth efficiency is used as the criteria the comparison usually favors FDMA . Viterbi (1) performed such a comparison using five different rate convolutional codes. This paper extends the comparison for the MobileStarSM system.

If FDMA is used in the MobileStarSM system, the system will be designed to be bandwidth limited. In either the first or second generation of satellites, the satellite transponder bandwidth will be filled with users before all of the satellite transponder power is used. In representative system designs under consideration QPSK modulation with rate 7/8 coding is used in order to conserve bandwidth while allowing a coding gain of approximately 3.2 dB.

If CDMA is used in the MobileStarSM system, a low rate can be used. Viterbi (2) has shown that coding does not reduce the effective processing gain in a spread spectrum system. A rate 1/3 code can be used to provide a 6.2 dB coding gain without reducing the system capacity.

PREVIOUS COMPARISONS

In reference (1) the spectral efficiency for BPSK CDMA and FDMA is shown to be given by:

$$\eta = \frac{\frac{C}{N_o W_s}}{\frac{E_b}{N_o} \left(1 + \frac{C}{N_o W_s} \left(\frac{M-1}{M} \right) \right)} \approx \frac{\frac{C}{N_o W_s}}{\frac{E_b}{N_o} \left(1 + \frac{C}{N_o W_s} \right)} \quad [1]$$

Where:

- C = Total carrier power.
- W_s = Total bandwidth=CDMA chip rate
- E_b/N_o = Bit Energy/Noise spectral density required for given error rate.
- N_o = Thermal noise power spectral density.
- M = number of users in the system.

For FDMA, there is only one user per bandwidth segment, therefore for $M=1$ equation 1 becomes:

$$\eta = \frac{C}{N_0 W_s} \quad \text{for } \frac{MR_b}{W_s} < r \log_2(m)$$

And due to the bandwidth limit:

$$\eta = r \log_2(m) = \text{Max } \eta_{\text{FDMA}} \quad \text{for } \frac{MR_b}{W_s} \geq r \log_2(m) \quad [2]$$

Where:

- r = Number of information bits per baud.
- m = Signal dimension (BPSK: $m=2$; QPSK: $m=4$ etc.).
- R_b = Users information bit rate.

To relate this previous work to the MobileStarsm system, the two modulation types thought to be appropriate: FDMA QPSK with a rate 7/8 code and CDMA with a rate 1/3 code; are compared below.

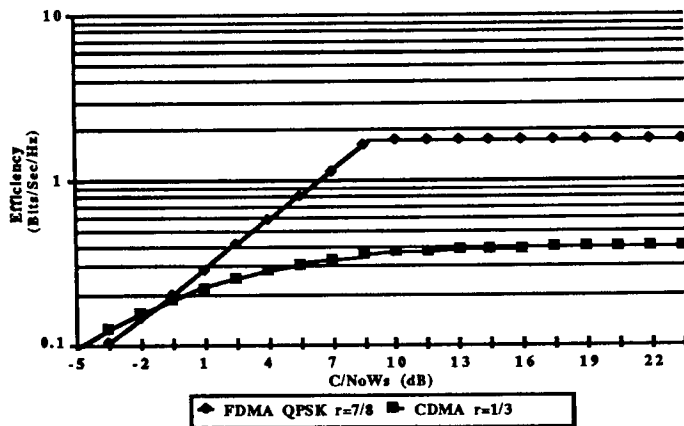


Figure 1. Comparison of efficiency (throughput in bits/sec/Hz) for FDMA QPSK rate 7/8 coded and CDMA rate 1/3.

The result shown in figure 1 is typical of that found in system studies such as (3). It was found that at large signal to noise ratios FDMA (QPSK rate 7/8) has 4.4 times greater capacity than CDMA (rate 1/3). As the signal to noise ratio gets very large the CDMA system capacity is limited by the co-channel noise or self noise. This self noise limitation can be calculated by taking the limit of equation [1] as the carrier power approaches infinity.

$$\text{Max } \eta_{\text{CDMA}} = \lim_{C \rightarrow \infty} \frac{\frac{C}{N_0 W_s}}{\frac{E_b}{N_0} \left(1 + \frac{C}{N_0 W_s} \right)} = \frac{1}{\frac{E_b}{N_0}} \quad [3]$$

The maximum efficiencies for the two modulation types can be compared using equations 1 and 2 (with $m=2$ and $E_b/N_0=4$ dB[1]).

$$\frac{\text{Max } \eta_{\text{FDMA}}}{\text{Max } \eta_{\text{CDMA}}} = \frac{[r \log_2(m)]_{\text{FDMA}}}{\left[\frac{1}{E_b/N_0}\right]_{\text{CDMA}}} = \frac{\frac{7}{8} \cdot 2}{\frac{1}{2.51}} = 4.39 \quad [4]$$

COMPARISON INCLUDING SYSTEM CONSIDERATIONS

Several factors have been identified that can alter the comparison between FDMA and CDMA. In a conference paper by Viterbi (4) and also in a system study (5) undertaken to evaluate the application of CDMA to mobile satellite communications it was found that the mobile environment has two additional factors that may reduce the self noise density and greatly alter the result of the comparison. These factors are voice activity and spatial discrimination provided by satellite steerable array antennas and multiple satellites. Similarly, antenna polarization may be exploited in order to effectively reuse the available spectrum in a CDMA system. In general, any factor which can reduce the self noise experienced by an individual channel will favorably effect the relative efficiency of CDMA.

Voice activity will greatly reduce the self noise of a CDMA system. MobileStarSM market projections indicate that 95% of the satellite channels will be used by voice services. The voice services will use voice activated carrier transmitters such that when a user is listening or has paused in the conversation, the transmitter's spread spectrum carrier is turned off and the user does not contribute self noise to the system. Conventional telephone practice (6) for satellite circuits indicates that a given user will only be talking approximately 35% of the time.

If the FDMA system is bandwidth limited, the voice activity factor does not increase capacity. A pair of circuits is allocated to a conversation for the duration of the call. When a user is listening, the circuit is still assigned to the user. The voice activity factor reduces the necessary satellite transmitter power by the activity factor and therefore increases the capacity when the satellite is operating in the power limited mode. This has the effect of shifting the FDMA line in figure 1 to the left by the voice activity factor. However, the voice activity factor does not increase the maximum number of circuits that can be assigned when the system is bandwidth limited.

Satellite antenna discrimination may be used to further reduce the system self noise observed by a particular channel. For example, a satellite with an 8 ft. x 24 ft. antenna aperture may be used to produce the type of coverage shown in figure 2. For this analysis it will be assumed that an optimal beam is formed centered on the user's longitude. If a user is transmitting a signal from a location corresponding to the center of a beam, as shown in figure 3, the satellite receives its signal at full strength, and pseudo-noise from all of the other users, such as those in other beams, are received at reduced strength. Since the pseudo-noise powers are weighted by the antenna gain, only the interferers close to the beam center contribute a large amount of co-channel noise. A sample calculation has been performed using simulated antenna patterns for the 8 ft. x 24 ft. antenna aperture. Assuming a uniform user distribution within the United States, the beam with the worst case coverage will collect only 21% of the energy of the transmitted by the entire user population. This implies that the antenna will discriminate against all but 21% of the total system self noise.

The FDMA system will also gain from the use of the above antenna. The antenna coverage can be designed to allow frequency reuse every 3°. The frequencies used in beam 1 can be reused in beam 4 and beam 7. The intersection of the coverage shown in figure 2 with and assumed uniformly distributed user population in the continental United States indicates that the full spectrum can be used twice. Hence, for FDMA the bandwidth limitation is doubled.

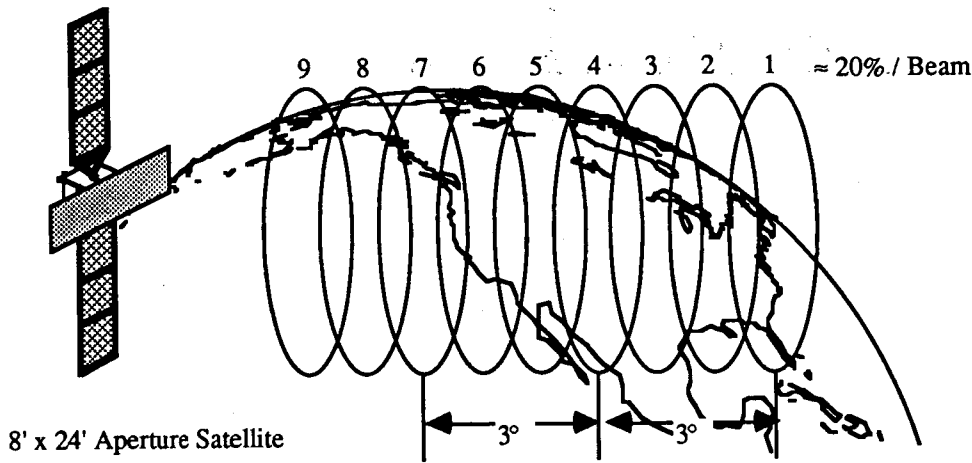


Figure 2. Assumed Antenna Coverage.

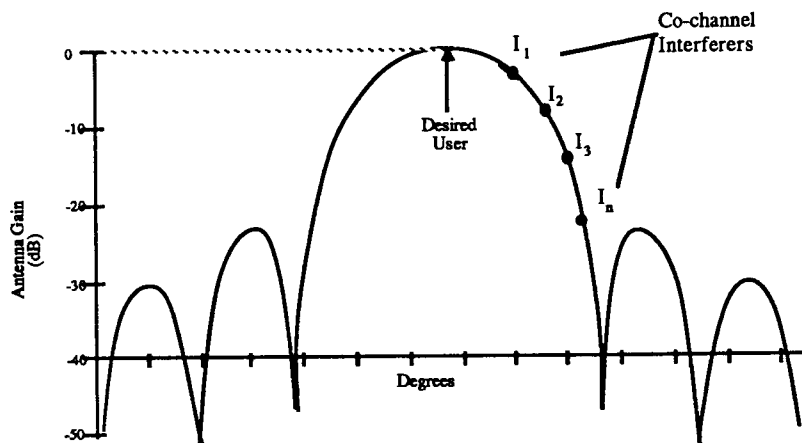


Figure 3. Co-channel (self noise) interference sources are attenuated by the antenna pattern.

In the case of CDMA the available frequency band can effectively be reused by utilizing the two opposite senses of circular polarization. The self noise is divided between the polarizations. This reuse is possible because the self noise affecting a particular channel is the sum of the self noise of the users with the same polarization plus the self noise from the users with the other polarization *attenuated by the crosspolarization ratio*. Also the self noise of the multipath-reflected signals of users operating on the opposite polarization must be considered. If a given CDMA mobile unit is operating beside a large reflective building or a truck in the next highway lane, its reflected energy will increase the interference on the opposite polarization by a factor of $1/M$. For the purpose of this comparison we shall assume that the *average* ratio of the desired polarization to the cross-polarization is 10 dB.

In an FDMA system the polarization isolation cannot be used to reuse frequencies at a given orbital slot. Reflected signals will appear at the full reflected power in the channel of the mobile unit operating on the opposite polarization sense. Under these conditions, mobile units would find themselves being jammed intermittently by users on the opposite sense polarization.

To compare FDMA and CDMA from the viewpoint of the MobileStarsm system we define the orbit slot spectral efficiency to be the *maximum throughput* (nominal data rate times the number of users) of the system as a function of the *average carrier to noise power ratio*. We use this definition because the revenue of the system is directly related to the

maximum throughput of the system. Also the cost of the satellite system is influenced by the power required. Therefore, in designing the satellite system we are interested in the average required carrier power.

An expression for the orbit slot spectral efficiency (in bits/sec/Hz) which include the effects of voice activation, antenna discrimination and polarization reuse can easily be derived. First the total noise seen by a given user can be expressed:

$$N_O' = N_O + a\rho V(M-1)E_S \quad [5]$$

Where:

a = Antenna discrimination factor.

ρ = Polarization reuse factor calculated by:

$$\rho = \frac{(1 + \text{Cross Polarization Level})}{2}$$

V = Voice activity factor

E_S = Received energy in one pseudonoise chip.

so then,

$$\frac{E_b}{N_O'} = \frac{\frac{E_b}{N_O}}{1 + a\rho V(M-1)\frac{R_b}{W_s}\frac{E_b}{N_O}} \quad [6]$$

System performance is to be measured by the orbit slot efficiency (or throughput) - MR_b/W_s , as a function of the *average* $C/N_O W_s$. The average $C/N_O W_s$ is given by:

$$\frac{C}{N_O W_s} = VM\frac{R_b}{W_s}\frac{E_b}{N_O} \quad [7]$$

From equations 6 and 7 it can be shown that the orbit slot spectral efficiency is given by:

$$\eta_{\text{slot}} = \frac{MR_b}{W_s} = \frac{\frac{C}{N_O W_s}}{\frac{E_b}{N_O}} = \frac{\frac{C}{N_O W_s}}{V\frac{E_b}{N_O}\left(1 + a\rho\frac{C}{N_O W_s}\left(\frac{M-1}{M}\right)\right)} \approx \frac{\frac{C}{N_O W_s}}{V\frac{E_b}{N_O}\left(1 + a\rho\frac{C}{N_O W_s}\right)} \quad [8]$$

The new self noise limitation can be calculated by taking the limit as before.

$$\text{Max } \eta_{\text{CDMA}} = \lim_{C \rightarrow \infty} \frac{\frac{C}{N_O W_s}}{V\frac{E_b}{N_O}\left(1 + a\rho\frac{C}{N_O W_s}\right)} = \frac{1}{V a \rho \frac{E_b}{N_O'}} \quad [9]$$

The orbit slot spectral efficiencies for the FDMA QPSK rate 7/8 coded and CDMA rate 1/3 coded cases can be compared using $a=21\%$, $\rho=0.55$ (10 dB crosspolarization) $V=35\%$, and $E_b/N_O' = 4$ dB for CDMA.

$$\frac{\text{Max } \eta_{\text{FDMA}}}{\text{Max } \eta_{\text{CDMA}}} = \frac{\left[r (\text{freq reuses}) \log_2(m) \right]_{\text{FDMA}}}{\left[\frac{1}{V a \rho (E_b/N_O')} \right]_{\text{CDMA}}} = \frac{\frac{7}{8}(2)^2}{\frac{1}{0.35(0.21)(0.55)2.51}} = 0.36 \quad [10]$$

From equation 10 it can be seen that for the assumed system parameters CDMA has 2.82 times greater maximum throughput than FDMA.

Equation 8 is plotted in figure 4. Relative to figure 1, the FDMA diagonal line is shifted to the left by the voice activity factor and the bandwidth limitation ceiling is shifted up by; 1) using QPSK and 2) the frequency reuse attributable to the satellite antenna spatial isolation illustrated in figure 2.

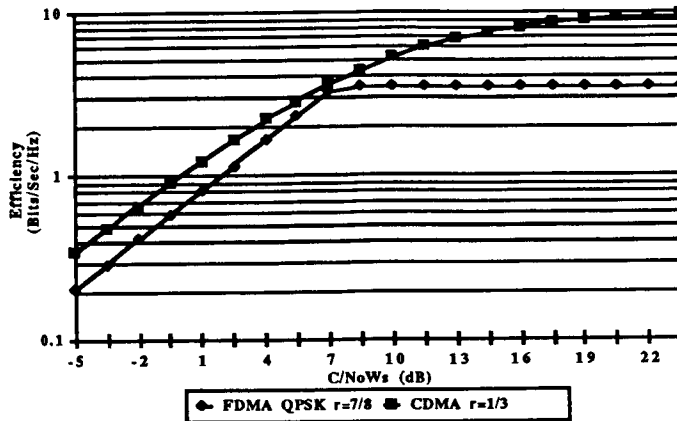


Figure 4. Comparison of orbit slot spectral efficiency (throughput) for FDMA QPSK rate 7/8 coded and CDMA rate 1/3. The effects of antenna discrimination, voice activity factor, and polarization reuse are included.

The CDMA curve is recalculated according to equation 9. It is seen that for these system specific parameters CDMA has greater orbit slot spectral efficiency than FDMA. In a MobileStarsm system context, for a given satellite power, C , and a given frequency allocation, W_s , and nominal user bit rate, R_b , the number of simultaneous users, M , is higher when using CDMA than when using FDMA.

When the demand for service grows beyond that which can be provided by a single satellite, then additional satellites must be provided. However, most mobile terminals will be equipped with very simple omni-directional antennas. Use of CDMA will allow coherent combining of signals transmitted between a terminal and both (or all) satellites in view. This coherent combining will result in an effective system capacity gain corresponding to the increased number of satellites. FDMA, on the other hand, can not provide increased capacity with additional satellites unless each mobile terminal is provided with a costly directive antenna.

References:

- 1 A.J. Viterbi, "When Not to Spread Spectrum- A Sequel", IEEE Communications Magazine, Vol. 23, No 4, (April 1985), pp.12-17
- 2 A.J. Viterbi, "Spread Spectrum Communications- Myths and Realities", IEEE Communications Society Magazine, Vol.17, No 3, (May 1979), pp.11-18
- 3 B.A. Mazur, M Mohler, "Aeronautical Mobile Satellite System Considerations: Detailed Comparison of FDMA Versus CDMA" Miller Communications Systems Ltd. report, (August 29, 1986). Presented to ICAO Special Committee on Future Air Navigation Systems Working Group, Washington D.C., September 1986.
- 4 A.J. Viterbi, Presentation at IEEE Communication Society Workshop on Communication Theory, Palm Springs. CA. April 28, 1986.
- 5 L. Weaver, "Final Report for Hughes Communications on System Studies for a CDMA Mobile Satellite System", (Oct 28, 1986), Qualcomm, Inc.
- 6 J.M Fraser, "Engineering Aspects of TASI", The Bell System Technical Journal, Vol. 38, No 2, (Mar 1959), pp.353-365

SESSION G.
MODULATION AND CODING II

SESSION CHAIR: Gottfried Ungerboeck, IBM Zurich Research Laboratory
SESSION ORGANIZER: Dariush Divsalar, Jet Propulsion Laboratory

An 8-DPSK TCM Modem for MSAT-X

THOMAS C. JEDREY, NORMAN E. LAY, DR. WILLIAM RAFFERTY, Mobile Satellite Program, Jet Propulsion Laboratory, California Institute of Technology, United States.

Jet Propulsion Laboratory
4800 Oak Grove Drive
Pasadena, California 91109
United States

ABSTRACT

This paper describes the real-time digital implementation of an 8-DPSK trellis coded modulation (TCM) modem for operation on an L-band, 5 kHz wide, land mobile satellite (LMS) channel. The modem architecture as well as some of the signal processing techniques employed in the modem to combat the LMS channel impairments are described, and the modem performance over the fading channel is presented.

INTRODUCTION

Satellite based, mobile communications have received increasing attention over the past decade. NASA, through the Jet Propulsion Laboratory, initiated a land mobile satellite experiment (MSAT-X) program [1] with the explicit goal of developing enabling concepts and technologies for a mobile satellite service. Of the many issues addressed in the program, modulation and coding were recognized as a key system consideration given the available spectrum and the satellite power limitations, and the hostile nature of the transmission channel.

Early in the program, frequency division multiplexing was selected as the preferred channel structure to maximize the number of users. The channel bandwidth was set at 5 kHz for a data transmission rate of 4800 bits per second (bps). This was considered a formidable goal especially given the required bit error rate (BER) performance of .001 at an average bit signal to noise ratio (SNR) of 11 dB for the channel model described below. Analysis of the link requirements has led to the consideration and computer simulation of many coherent and non-coherent schemes for burst operation.

The L-band LMS channel is susceptible to many propagation impairments [2]. The traditional satellite model of a line-of-sight component in the presence of AWGN must be augmented to include dynamic effects. Multipath fading and vegetative shadowing cause signal dropouts and long term envelope amplitude and phase variations. The channel model assumed in the development of this modem is the Rician fading channel with a coherent (desired) to non-coherent (scattered) power ratio of 10 dB [2]. Vegetative shadowing is also assumed to be present and to follow a log-normal distribution.

The work described in this paper focuses on the digital implementation and performance of a multipath fade tolerant, differentially coherent, 8-PSK based modem. At the receiver, differential detection using a novel matched filter arrangement, and feed forward Doppler compensation is employed to achieve many operational benefits. For this demanding L-band satellite link, the channel utilization is an efficient 1.0 bps/Hz for raw data and 1.5 bps/Hz for coded data.

MODULATOR

A block diagram of the modulator is presented in Figure 1. The modulator obtains packetized data from the terminal processor at a rate of 4800 bps. A packet consists of a packet identification word, indicating a control or data packet, and the information to be transmitted, either voice or data. In addition to this structure, the modulator prefixes a preamble and appends a postamble to the transmitted packet, both of which are used for modem specific synchronization purposes, and are not encoded as described below.

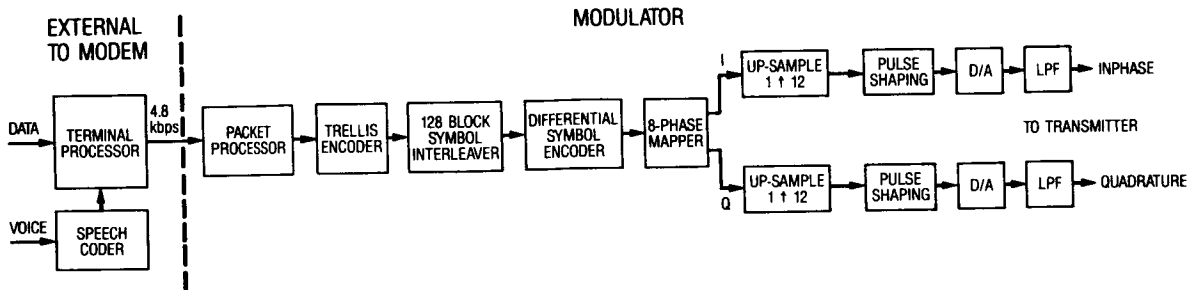


Figure 1 Modulator Block Diagram

The data to be transmitted is encoded with a rate 2/3, 16 state trellis code [3], producing a data rate of 7200 bps, or 2400 symbols per second. Following the encoder is a 128 symbol block interleaver (16x8) for burst error protection. The output of the interleaver is differentially encoded and converted to inphase (I) and quadrature (Q) components of an 8-DPSK waveform at the 2400 sample per second (sps) rate. This data is then upsampled to a rate of 28.8 kbps by zero padding and pulse shaped with a 100 percent excess bandwidth root raised cosine filter to achieve the desired spectral shape as well as satisfy certain temporal properties (two intersymbol interference (ISI) free points per symbol) necessary for Doppler estimation and matched filtering at the demodulator. The pulse shaping filters have an impulse response length equal to 6 symbol periods, with 12 samples per symbol. The resulting digital waveforms are converted to analog signals via two 12-bit D/A converters and lowpass filtered for image suppression. The baseband I and Q waveforms are then provided to the transmitter for complex modulation and transmission through the channel.

DEMODULATOR

A block diagram of the demodulator is presented in Figure 2. An important feature of the demodulator is the feed-forward nature of the processing as illustrated by the diagram. This type of architecture was chosen to combat the effects of the fading typical of the LMS channel. The architecture allows the demodulator to free wheel through deep fades and rapidly recover once the fade has ended (i.e., the signal level has returned to some nominal operational value).

The receiver presents the demodulator with the received signal at an IF frequency of 28.8 kHz. This signal is bandpass filtered for noise suppression and prechannel selection, and then sampled at four times the IF. Splitting the A/D output data into odd and even data streams, then decimating yields baseband I and Q data streams. Note that the resultant data streams are not time aligned (due to the use of a single A/D). To combat this potential source of degradation, prior to decimation the quadrature channel is interpolated to produce an estimate of the Q channel that is time aligned with the I channel. It can be shown that under ideal conditions, the interpolation reduces the relative error in the estimation of the received Q channel data at the ISI free points from approximately 4 percent to 0.1 percent.

The I and Q channels, at an aggregate data rate of 57.6 kbps are then lowpass filtered to the data bandwidth plus the maximum expected Doppler spread. These filters are implemented as 111 tap linear phase FIR filters. The samples out of the lowpass filters are then interpolated by a factor

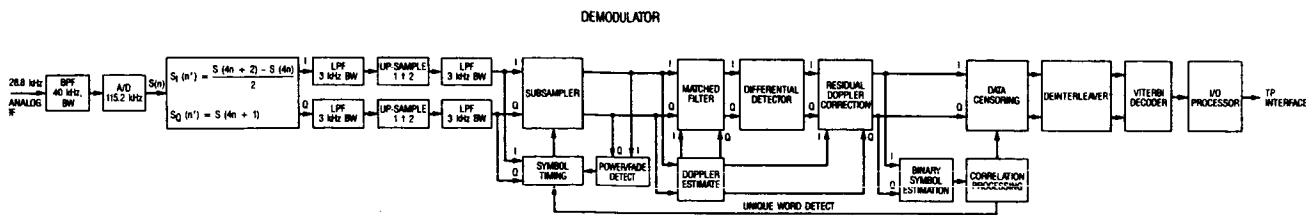


Figure 2 Demodulator Block Diagram

of two (the aggregate data rate is now 115.2 kbps) for reduction of jitter in the symbol timing recovery process, and passed on to the symbol timing and power/fade detect algorithms.

The power/fade detect algorithm corresponds to that of a modified radiometer. The I and Q channel data streams are squared and summed, lowpass filtered, and then thresholded. If the filter output exceeds the threshold, power is detected. If the filter output drops below a second threshold (once power and the start of a transmission have been detected) a fade is declared. The power/fade detect information is passed on with each symbol and used by the succeeding algorithms to reduce the effects of fades, as well as to reduce the preamble false alarm probabilities.

In the symbol timing algorithm, the received I and Q channel data is squared, summed, and bandpass filtered (centered at the symbol rate) to produce a sinusoidal timing wave of average period equal to the symbol rate [4]. This waveform is then clipped and differentiated to produce a sequence of impulses, corresponding to the zero crossings of the timing wave. The delay through the filtering is adjusted to align the positive impulses with the first ISI free symbol point per symbol period, and the negative impulses to the second. These timing impulses are used to sample the I and Q data streams at the ISI free points. It has been shown that the data dependent jitter in this timing algorithm is zero for the continuous case and approaches a constant dependent on the number of samples per symbol for the sampled data case, at these two points [5]. The impulses are also used to advance or retard a 4.8 kHz jitter clock, used to clock the Viterbi decoder output data to the terminal processor. The control mechanism for the jitter clock as well as the symbol timing algorithm is implemented as a random walk filter. In the free running or acquisition mode, the jitter clock can be advanced or retarded in steps of 1/24th of a symbol period per symbol period. In tracking mode, the jitter clock is only advanced (or retarded) after N net advances (or retards) have accumulated in an up/down counter. The acquisition mode corresponds to the preamble search (the preamble is designed to allow the symbol timing algorithm to quickly acquire correct timing) and the tracking mode corresponds to the detection of the preamble. Not only does this architecture provide a large measure of protection from fades and long runs of constant data, but it also utilizes the fade detect information to increase N during a long fade and to decrease N after the fade ends, thereby freezing the symbol timing during that period.

The subsampled data streams, sampled at the two ISI free points per symbol period are then passed on to a Doppler estimation, pseudo-matched filter, and differential detector. The Doppler estimator uses the two ISI free points per symbol period to strip the data from the received signal and derive an estimate of the Doppler [6]. This estimate is used to translate the pseudo-matched filter up to the Doppler frequency, where the matched filtering is done. This filter is termed a pseudo-matched filter due to the fact that only in combination with the ideal lowpass filters is it a true matched filter. In essence what has been implemented is a distributed form of the matched filter (primarily due to the fact that the matched filter for the 100 percent root raised cosine pulse shaping has a very simple realization). Following the matched filters, the data is differentially

detected and a residual Doppler term is removed. This architecture is described in [6] and illustrated in complex form in Figure 3. The aggregate data rate out of the residual Doppler correction is 4.8 ksp/s.

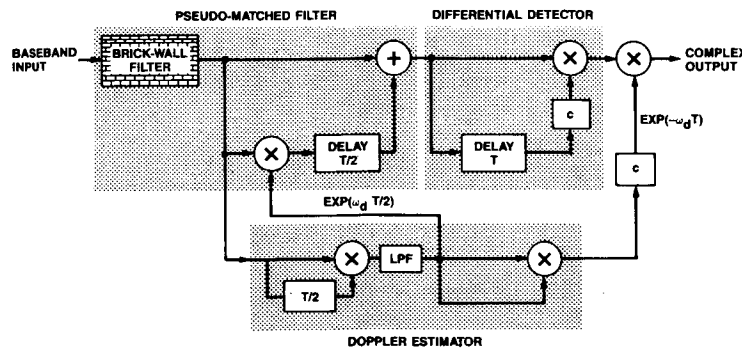


Figure 3 Complex Data Detection Block Diagram

Following the residual Doppler correction, the data is split into two paths, one for preamble/postamble detection, and the second for the actual data detection. The preamble/postamble detection algorithm is a correlator, with a detection declared in the case of the preamble if the threshold is exceeded and power is detected, and detection is declared in the case of the postamble if the threshold is exceeded within a certain time window (due to the fact that the postamble can only occur at fixed boundaries). The preamble and postamble are then censored from the received symbol stream.

The censored I and Q data streams, consisting of the received data symbols, are deinterleaved and decoded by a 16 state soft decision Viterbi decoder using the correlation metric. The decoder output is a 4800 bps data stream which is passed to the terminal processor. An indication of the data quality is also passed to the terminal processor by tagging the fade detect information to each bit as well as a 3-bit data quality estimate generated in the decoding process.

SYSTEM ARCHITECTURE

A completely programmable approach was chosen for the implementation of the digital signal processing elements of the MSAT-X modem. The flexibility afforded by a software based system allows both rapid realization and continual refinement for any variety of algorithms. In keeping with this approach, a general purpose signal processing board was developed utilizing a single DSP chip as the central element.

The core signal processor employed in the board is the Texas Instruments TMS32020. The signal processing board has a configuration of two 4K x 16 bit word spaces for program and data memory. In addition, the program memory is switchable between RAM for development purposes and EPROM for final algorithm placement. Additional circuitry supports five dedicated 16 bit parallel I/O ports (two input and three output). Three levels of hardware interrupt are accessible.

Within the modem itself, the modulator and demodulator are partitioned into two distinct systems under separate asynchronous control by an external controller. The multiprocessor design is greatly simplified by following a pipelined approach. Taken separately, the signal flow for either the modulator or demodulator can essentially be viewed as feed-forward for both control and data signals. This yields a very simple level of inter-board interfacing. Data is passed in parallel fashion sequentially from board to board on an interrupt basis. Signal processing algorithms are partitioned into a number of subprograms, each of which is executed on a single processor. The processing capability can therefore be incrementally increased by including more DSP boards and partitioning the new signal processing tasks into the additional processors.

The modulator consists of a single TMS32020 board, a clock unit (shared with the demodulator) and two D/A subsystems. The clock unit provides frequency locked clocks of 4.8 kHz and 28.8 kHz. The 4.8 kHz clock is used to transfer the data from the terminal processor to the modulator,

while the 28.8 kHz clock is used to transfer data from the TMS32020 board to the D/A subsystems. Each D/A subsystem consists of a 12 bit D/A converter and a 4 kHz lowpass filter.

The demodulator consists of an A/D subsystem, six TMS32020 boards, and two clock units. The A/D subsystem consists of a 40 kHz wide bandpass filter centered at 28.8 kHz, followed by a 12 bit A/D. The six TMS32020 boards are configured to implement the demodulator as illustrated in Figure 4. The first clock unit (common with the modulator) provides a clock at 18.432 MHz, which is divided down by the A/D subsystem to 115.2 kHz. The high clock rate allows slewing of the 115.2 kHz clock phase by the demodulator. The second clock unit is the 4.8 kHz jitter clock, used to transfer data from the demodulator to the terminal processor (this clock unit is also run from the 18.432 MHz clock unit). The clock phase of the jitter clock may be advanced/retarded by the demodulator to the data derived timing.

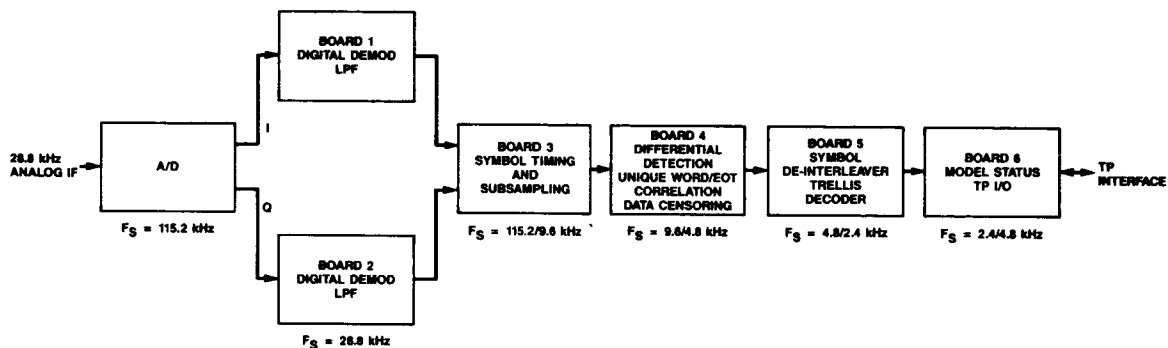


Figure 4 Demodulator Partitioning

MODEM PERFORMANCE

The modem has been tested over the land mobile satellite channel simulator described in [7]. The channel impairments simulated in these tests consist of AWGN and the Rician fading process. Symbol and bit error rates for the MSAT-X modem in the presence of AWGN are detailed in [8].

The modem performance in the presence of multipath fading with Rician K factors of 5 and 10 dB is shown in Figure 5. The signal-to-noise power calibration has a measurement error of approximately .2 dB due to the fluctuating signal level caused by the fading process. Two pairs of plots are shown in each figure comparing experimental performance to floating point simulation for Doppler spreads of 20 Hz and 104 Hz. These spread values correspond approximately to vehicle speeds of 8 mph and 44 mph at the L band link frequencies. As was expected, the modem performance is closer to the simulation results for the higher K value. However, for both values of K, the modem performs within 1 dB of the performance predicted by simulation. In these figures perfect doppler tracking and time synchronization are assumed for the simulation results.

CONCLUSIONS

The analysis of the experimental data has shown that the modem designed and constructed for MSAT-X will indeed function over the fading channel. In all cases for the conditions tested, the modem performs within 1 dB of theory/simulation. The architecture and processing algorithms in the modem allow the modem to combat the effects of deep fades and rapidly recover from them. Work is continuing on refining the modem, and in the near future a doppler estimation and correction scheme (this scheme has already been tested successfully with the demodulator in a slightly different configuration) will be implemented. Further tests will then be performed to determine its efficacy.

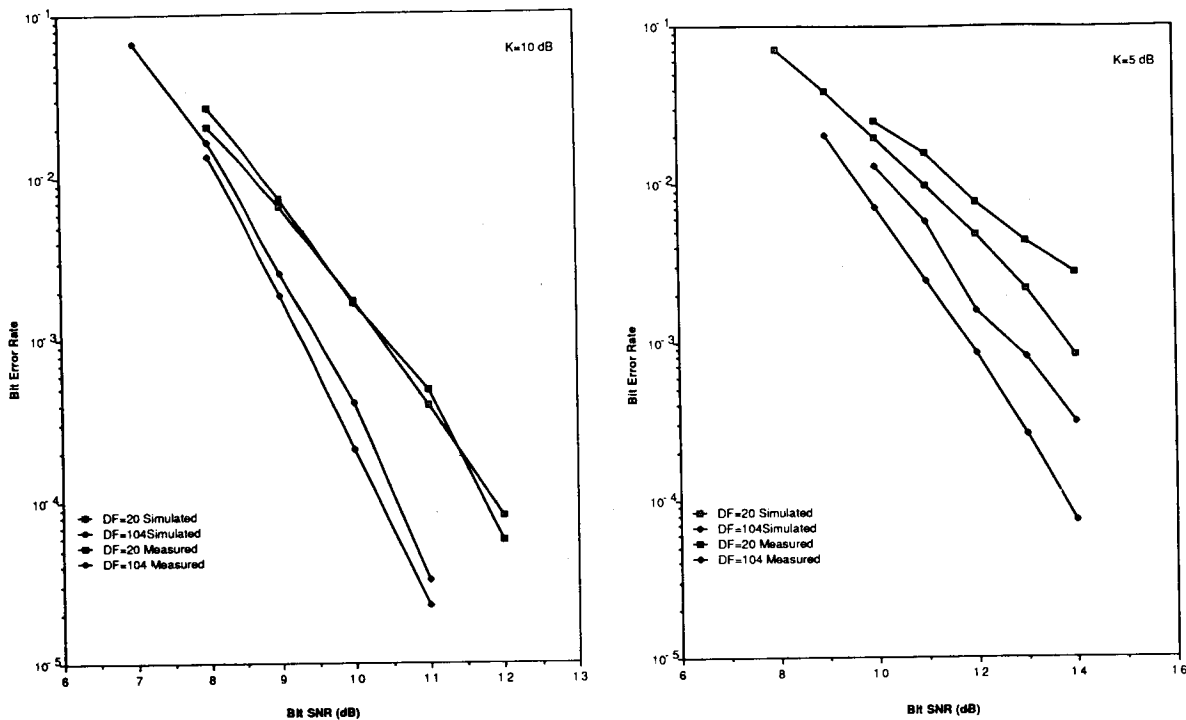


Figure 5 Trellis Coded 8-DPSK Performance in Fading Channel, $K=10,5$

REFERENCES

- [1] E. J. Dutzi, G. H. Knouse, "Mobile Satellite Communication Technology: A Summary of NASA Activities", 37th Congress of the IAF, Innsbruck, Austria, October 1986.
- [2] W. J. Vogel, E. K. Smith, "Theory and Measurements of Propagation for Satellite to Land Mobile Communication at UHF", Proc. IEEE 35th Vehicular Technology Conference, Boulder, Colorado, pp 218-223, 1985.
- [3] D. Divsalar, M. K. Simon, "Trellis Coded Modulation for 4800-9600 bps Transmission over a Fading Mobile Satellite Channel", IEEE Journal on Selected Areas in Communications, February 1987, pp. 162-175.
- [4] L. E. Franks, J. P. Bubroski, "Statistical Properties of Timing Jitter in a PAM Timing Recovery Scheme", IEEE Trans. Comm., vol. COM-22, pp. 913-920, July 1974.
- [5] T.C. Jedrey, unpublished memo.
- [6] M. K. Simon, D. Divsalar, "Doppler-Corrected Differential Detection of MPSK", submitted to IEEE Transactions on Communications.
- [7] F. Davarian, "Channel Simulation to Facilitate Mobile-Satellite Communications Research", IEEE Trans. Comm., vol. COM-35, pp. 47-56, 1987.
- [8] T. C. Jedrey, N. E. Lay, W. Rafferty, "An All Digital 8-DPSK TCM Modem for Land Mobile Satellite Communications", IEEE International Conference on Acoustics, Speech, and Signal Processing, April 11-14, 1988, New York, New York.

DEVELOPMENT OF A CODED 16-ARY CPFSK COHERENT DEMODULATOR

KEN CLARKE, Government Communications Systems Division, Harris Corporation, United States;
 ROBERT DAVIS, Advanced Technology Department, Harris Corporation, United States;
 JIM ROESCH, Government Communications Systems Division, Harris Corporation, United States.

HARRIS CORPORATION
 P.O. Box 37
 Mail Stop 3A-1912
 Melbourne, Florida 32901
 United States

ABSTRACT

Theory and hardware are described for a proof-of-concept 16-ary Continuous Phase Frequency Shift Keying (16-CPFSK) digital modem. The 16 frequencies are spaced every 1/16th baud rate for 2 bits/sec/Hz operation. Overall rate $\frac{3}{4}$ convolutional coding is incorporated. The demodulator differs significantly from typical quadrature phase detector approaches in that phase is coherently measured by processing the baseband output of a frequency discriminator. Baud rate phase samples from the baseband processor are decoded to yield the original data stream. The method of encoding onto the 16-ary phase nodes, together with convolutional coding gain, results in near QPSK performance. The modulated signal is of constant envelope; thus the power amplifier can be saturated for peak performance. The spectrum is inherently bandlimited and requires no RF filter.

MODEM OVERVIEW

We discuss a bandwidth efficient constant envelope modem: 16-ary Continuous Phase Frequency Shift Keying (16-CPFSK). Error-correction coding is applied to reduce the performance disadvantage relative to AM schemes. The modem is designed for 200 mb/s TDMA application with 100 mHz adjacent channel spacing.

Theoretical Considerations

Two novel theoretical techniques are used in this 16-CPFSK modem: I) coherent phase measurements obtained by processing an FM discriminator baseband output; II) Modulation via a closed-loop linearized VCO. Refer to Figure 1 in the following discussion.

Obtaining coherent phase from a discriminator. A discriminator outputs $\phi'(t)$, where $\phi(t)$ is the signal's phase modulation. Integration of $\phi'(t)$ recovers the desired signal, $\phi(t)$. Implementation of the integration has several practical problems: 1) Integrator output can grow without bound; 2) Initial phase, $\phi(0)$, must be determined; 3) AGC is needed on the baseband signal. Regarding problem 1), fortunately, we need only know phase Mod- 2π . Thus the growth problem is avoided by integrating Mod- 2π . How can such an integrator be implemented? It is essential only that we obtain $\phi(nT)$, phase at baud time intervals. An integrator yielding $\phi(nT)$ can be implemented as a T-interval Integrate-and-Dump (I&D) sampled by an A/D which feeds a digital accumulator that rolls over Mod- 2π . The I&D is actually a lowpass Half-Nyquist filter in this modem, but the conceptual picture remains useful.

Problem 2)--acquiring initial unknown phase, $\phi(0)$, is handled by first observing for each baud time, the phase error to the closest one of the 16-CPFSK phase nodes (Mod- 2π) equally spaced in the accumulator. This phase error is filtered by a lowpass loop filter whose output is subtracted from the

accumulator input. The initial phase error, $\phi(0)$, appears as a DC component of the error and is eliminated by the baseband loop. Frequency offset (DC offset from the discriminator) also is eliminated by this baseband loop, the equations for which are identical to those for a PLL.

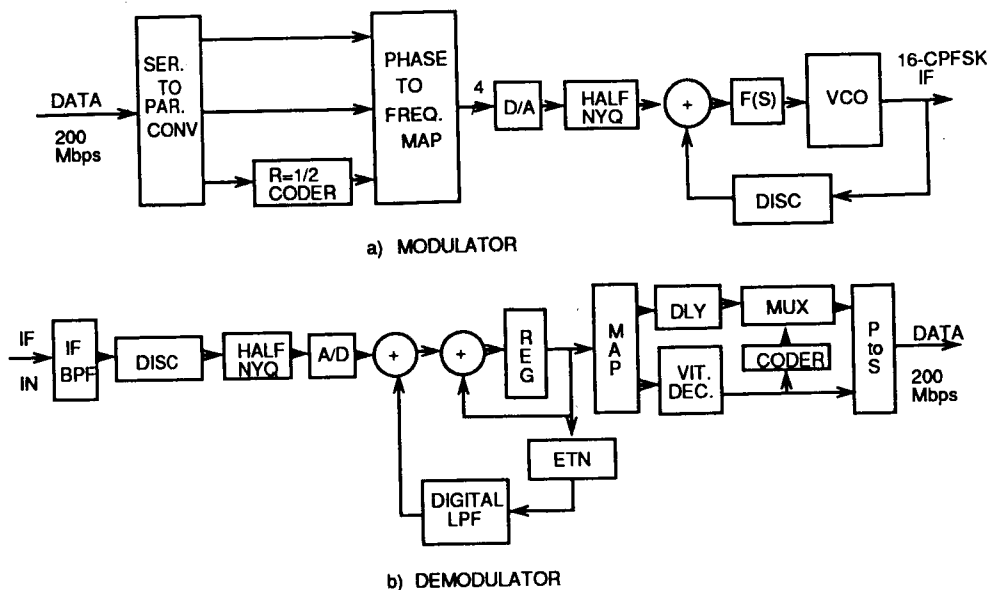


Fig. 1. Basic modem block diagram

Problem 3), AGC, is handled as shown in Figure 1. The accumulator phase error is correlated with input samples, and baseband gain is adjusted to zero the correlation.

Linearized VCO modulator. Figure 1 shows the closed-loop-linearized VCO modulator. The baseband filter output is applied through a feedback summer to the VCO. $F(s)$ is a wideband loop filter. The output of the VCO is immediately converted back to baseband by the discriminator (DISC) and subtracted from the baseband input modulating signal to generate a correction signal in the closed loop. The VCO is thus modulated with small error between the baseband modulating signal and the output of the DISC. If the modulator DISC is identical to the demod DISC, this modulator linearizes the baseband signal path through the modem's VCO/DISC combination.

Brief Description of Modem Operation.

As shown in Figure 1, incoming data is split into 3 parallel bit streams. The 2 MSBs are passed unaltered to modulator MSB positions. The LSB bit stream is coded by a rate $\frac{1}{2}$, $K=7$ convolutional encoder. The 2 resulting coded branch bits go to the 2 LSB positions of the modulator. The 4 bits produced by this encoding process specify one of 16 symbol-ending phases (Mod- 2π) from the 16-CPFSK modulator. Half-Nyquist filtering is employed at the VCO baseband on 16-ary impulses to produce the IF signal at the modulator. At the demod the IF signal is filtered and passed to the DISC. The DISC baseband signal is Half-Nyquist filtered and sampled at symbol rate by an 8-bit A/D. The Half-Nyquist filter completes shaping begun at the VCO, producing an overall Nyquist response to 16-ary impulses. The A/D samples feed the accumulator, whose output is $\phi(nT)$. These phase samples feed a Viterbi decoder for demodulation of the original 3 data streams.

Figure 2 shows the 16-CPFSK phase nodes, along with the mapping of coded 4-bit groups onto them. Any set of 4 adjacent phases contains all 4 rate $\frac{1}{2}$ code branches and has good distance structure. This fact forms the basis for our decoding strategy, to wit: retain only the 4 phase nodes nearest the received coherent phase measurement; then let the Viterbi decoder determine which of these 4 phases is most likely to have been transmitted. The 2 modulator MSBs associated with the decoder's decision are output as 2 of the decoded bits. The third bit decision is the data bit decision made by the decoder. These 3 bits form the total output data bit stream.

Figure 3 shows performance predicted for the coded 16-CPFSK modem.

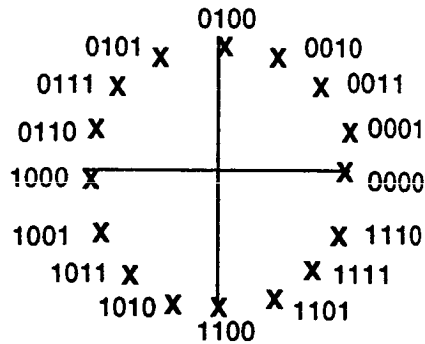


Fig. 2. 16-CPFSK phase nodes.

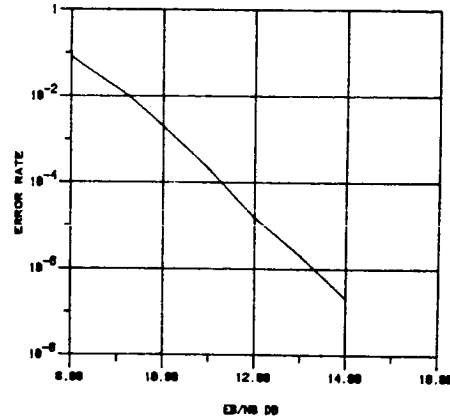


Fig. 3. Modem performance.

DIGITAL BASEBAND PROCESSING

We now discuss the Coherent Baseband Phase Detector (CBPD) hardware. Figure 4 depicts the four major functional portions of the CBPD circuitry: 1) Baseband Preprocessor, 2) Phase Accumulator/DC Restore Loop, 3) AGC Loop, and 4) Timing and Control.

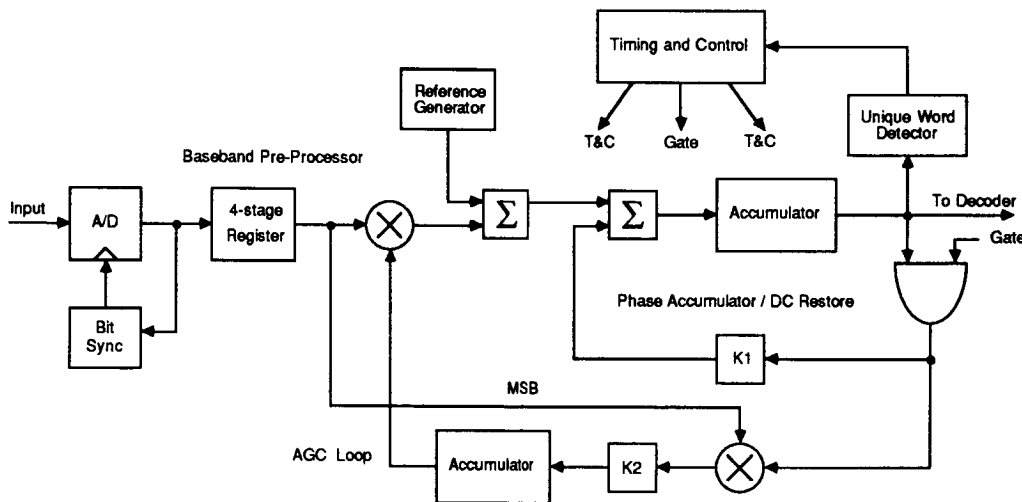


Fig. 4. Coherent Baseband Phase Detector.

Baseband Preprocessor

The filtered (Raised Cosine, 25% excess bandwidth) output of the frequency discriminator is sampled at symbol rate by an 8-bit A/D converter. The samples are sequentially stored in 4 registers to allow detection of an "all f_0 's" portion of the TDMA preamble. If detected, the remaining registers in the phase detector circuitry operate normally; otherwise, these registers are asynchronously held low. The output of the fourth register, along with a 16-bit attenuation factor, K , are input to a 16×16 ECL multiplier, which provides AGC on any gain variation at the output of the limiter/discriminator ($\pm 6.25\%$ max.). At the output of the multiplier, a binary number is added to the 12-bit two's complement product such that when an f_0 is received, zero is output to the phase accumulator circuit.

Phase Accumulator/DC Restore Loop

An error term, proportional to DC offset in the discriminator output (which results from frequency offset in the IF), is subtracted from the 12-bit number output from the baseband preprocessor. The "DC restored" value is then accumulated by a 12-bit accumulator, completing the implementation of an integrator. The output of the 12-bit accumulator represents 360° of coherent phase (Mod- 2π).

The DC restore loop is constructed in the following fashion. During the data portion of a burst (following the preamble and unique word), the transmitted phase constellation is restricted to that of 4-ary signalling (90° spacing) on every fourth transmitted symbol (called a "tracking" symbol). During the tracking symbols, the 10 LSBs, of the accumulator output, directly represent the error in hitting a phase node (error-to-node). Thus, a modulo 90° ($\pm 45^\circ$) phase detector characteristic is displayed by the 10 LSBs of accumulator output during the tracking symbol. To control DC offsets out of the discriminator, the error-to-node is multiplied by a gain factor, KL , and subtracted from the input to the coherent phase accumulator. This processing is equivalent to a 1st-order PLL correction. For a 1st order control loop with open loop gain, K , the loop noise equivalent bandwidth is given by: $B_L = K/4$ (Gardner, 1979). During the data portion of a burst, with $KL = 1/4$, and corrections being applied to the loop on every fourth symbol, $B_L = R_S/64$ MHz, where $R_S =$ the symbol rate.

Phase acquisition for independent bursts is accomplished during the all- f_0 's portion of the preamble. Initially, the phase accumulator is zeroed. After the all- f_0 's portion of the preamble has been detected by the Baseband Preprocessor, the DC restore loop is allowed to update during every symbol interval (providing maximum loop gain, and thus wide loop bandwidth). This processing acquires $\phi(0)$ and initial DC offset at the discriminator output. Since the loop corrects on every symbol, the loop gain is four times that of the "tracking" loop gain, and thus, $B_L = R_S/16$ MHz. Transport delay in the digital control loop is minimized to maintain stable closed loop response for wide loop bandwidths.

AGC Loop

An error term, proportional to gain missetting, is derived by correlating a delayed version of the discriminator sign output with the error-to-node signal. The gain error is filtered by a digital accumulator, and a detector bias (1.0) is added at the accumulator output. The resulting AGC correction factor, KA , is 1 ± 0.0625 . The input to the CBPD circuit is scaled by KA using a 16×16 ECL multiplier. Thus, fine decision-directed AGC is provided, which prevents "walkoff" of the coherent phase accumulator.

The loop bandwidth of the AGC loop is given by; $B_L = K/4$, where $K =$ Open Loop Gain. During the all- f_0 's portion of the preamble, the AGC loop updates on every symbol and the open loop gain is $R_S/16$. Like the DC Restore loop, the AGC loop updates on every fourth symbol during tracking, so that the open loop gain is $1/4$ that of acquisition. Thus, $B_L = R_S/64$ during acquisition and $B_L = R_S/256$ during tracking.

Timing and Control

The major portion of the baseband timing control circuit is the Unique Word (UW) detector. The UW consists of six unique symbols immediately following the preamble. The UW is detected when the 6 symbols fill the UW detector correlator cells, allowing one symbol error. The UW, when detected, establishes a second level time tick for burst processing (first level is symbol synchronization). The UW detector establishes the gating clock used to update the control loops on every fourth symbol during the data portion of a burst.

BASEBAND ENCODER/MODULATOR

In the baseband encoder, the data stream (at 200 Mbps) is partitioned into 3-bit symbols. The two MSBs are used directly, and the LSB is rate $1/2$, $K=7$ convolutionally encoded to produce a 4-bit symbol. This overall rate $3/4$ code, combined with the CPFSK characteristic, promotes good bandwidth efficiency.

With 3-bit symbols, the symbol rate is reduced to $1/3$ the 200 Mbps data bit rate, allowing use of off-the-shelf ECL and eliminating need for custom ICs or GaAs technology.

Figure 5 shows a block diagram of the encoder/modulator. The input data buffer translates the 200 Mbps serial data stream into a parallel 11-bit word, allowing the input data RAM to operate at 1/11th of the input bit rate. The ECL RAM input buffer is configured as a FIFO. After buffering, the data is read out of the FIFO and partitioned into three, 3-bit groups, and one 2-bit group. Each 3-bit group is operated on as previously described (2 MSBs unaltered; LSB $R=1/2$ encoded) to produce 4-bit coded symbols. The remaining 2 bits are treated as MSBs and two zero bits are appended to form the fourth 4-bit symbol. This is done as previously described to aid the demodulator in maintaining carrier lock.

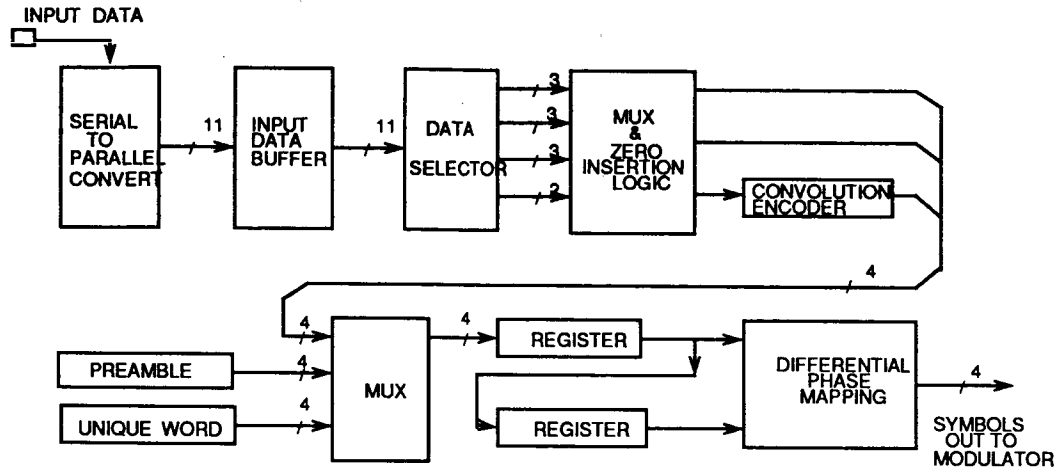


Fig. 5. Encoder block diagram.

Preamble/Unique Word

Prior to sending data, a TDMA preamble is sent. The preamble is a 32-symbol pattern alternating between the two peak frequencies of the 16-CPFSK signal, followed by 32 symbols of lowest frequency, which allows symbol synchronization and coherent phase acquisition.

A 6-symbol unique word to flag start-of-data follows the preamble. Encoded data symbols immediately follow the unique word. The preamble, unique word, and encoded data are all selected via the mux function shown in Figure 5.

Symbol Mapping

With CPFSK, transmitted frequency symbols convey "differential" phase information rather than absolute phase. For example, if the previous encoded 4-bit symbol produced a phase value of Φ_5 and the next 4-bit symbol represented phase Φ_{10} , then the modulated frequency sent out for the current symbol time is that needed to swing phase from Φ_5 to Φ_{10} . The mapping function shown in Figure 5 provides this operation. Two registers address the mapping PROM. One contains the previous 4-bit encoded symbol and the other contains the current 4-bit symbol. This provides the mapping PROM with sufficient information to determine the required frequency to transmit such that the received phase point will be that specified by the current 4-bit symbol.

Encoder Termination Sequence

At the end of the input buffered data, six zeroes are appended to the data stream sent to the convolutional encoder. This forces the encoder to start and end in state 000000 each TDMA burst. At the receiver, the Viterbi decoder function exploits this *a priori* knowledge by forcing the decoder to begin in state 000000 on every burst.

BASEBAND DEMODULATOR

Major baseband demodulator functions are highlighted in Figure 6. The 7-bit phase measurements, as received from the CBPD, are rate buffered and sent to the mapping function, which determines the 4 signal phase points closest to each demodulated value. This homes in on a quadrant of adjacent phase points retained as likely decision candidates.

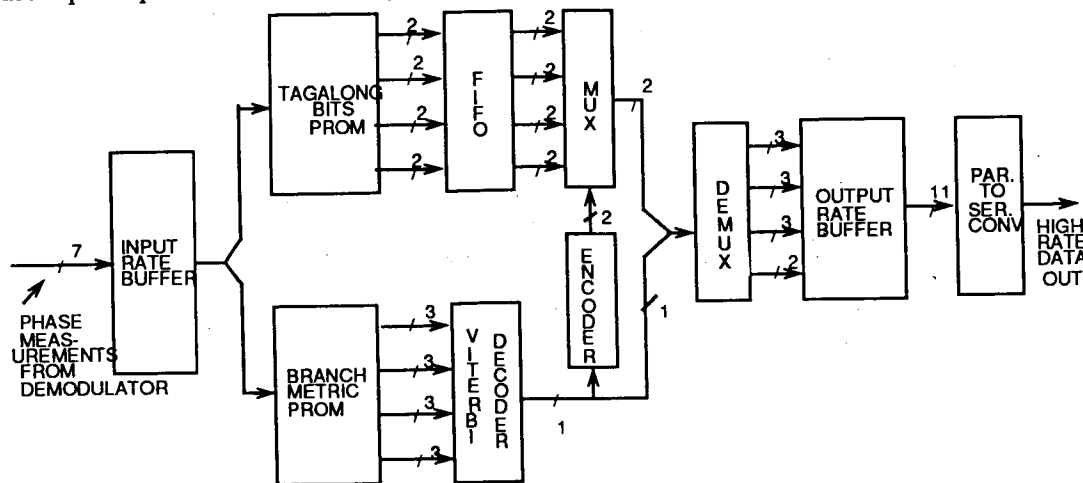


Fig. 6. Decoder block diagram.

The phase distances of these 4 candidate nodes from a given demodulated phase point serve as branch metrics to the Viterbi decoder for the four (00, 01, 10, 11) LSB $R=1/2$ code-branch bit pairs. The decoder uses these metrics directly to determine which of the four candidates was most likely transmitted.

As noted already, ANY four consecutive nodes in the signal constellation always contain the values 00, 01, 10, and 11 for the encoded LSB portion; and the two unencoded MSBs simply "tag along" with the respective encoded LSB values. These MSB tag-along bits are sent to a FIFO buffer whose length equals the throughput delay of the Viterbi decoder.

Viterbi Decoder

The four candidate branch metrics described above are fed directly into a $R=1/2$, $K=7$ Viterbi decoder to recover the coded third of the total data bit stream. The decoder output data is then re-encoded to produce an error-corrected 2-bit symbol pair (code branch). This pair selects the corresponding tag-along MSB bit pair from the tag-along FIFO. These tag-along MSB bits are regrouped with the corresponding output data bit from the Viterbi decoder to form the recovered 3-bit data group.

Final Processing

The recovered 3-bit data groups are collected. On every fourth group, only two tag-along bits are recovered (because the LSBs were forced to 00 back at the encoder to support phase tracking). In addition, the 000000 coder termination sequence is removed from the recovered data bit sequence.

The recovered data bits are then rate buffered in another FIFO whose output is then parallel-to-serial converted. This reconstructs the original data stream at the original high speed data bit rate (200 Mbps).

Parallelism in the design of the encoder/modulator and decoder/demodulator allows the use of lower speed, lower cost technology for most internal processing operations. High data rate parts are limited to the encoder/modulator input and to the decoder/demodulator output.

REFERENCES

Gardner, F.M. 1979. Phaselock Techniques. John Wiley & Sons, New York, New York.

MODEM FOR THE LAND MOBILE SATELLITE CHANNEL

STEVEN J. HENELY, United States

ROCKWELL INTERNATIONAL CORPORATION

Avionics Group

Cedar Rapids, Iowa 52498

ABSTRACT

This paper describes a modem which has been developed and implemented using a digital signal processor (DSP) for a land mobile satellite demonstration system. The requirements of this digital modem were determined by the characteristics of the land mobile satellite channel. This paper discusses the algorithms which implement the DPSK demodulator. Included is an algorithm which estimates symbol timing independent of carrier phase without the use of a square-law nonlinearity.

INTRODUCTION

The land mobile satellite demonstration system and experimental propagation results are discussed in [1] and [2]. This paper discusses the modem developed for this system. Data communications using small, low-gain antennas on the land mobile satellite channel presents new and interesting challenges to the digital modem designer. Operation with a marginal carrier-to-noise ratio requires that processing techniques achieve the highest possible efficiency. Frequency offsets due to Doppler and oscillator drift are significantly larger than the symbol rate and must be tracked to minimize detection losses. On the forward link, maintaining synchronization in the harsh shadowing and multipath fading land mobile satellite environment is critical. Consideration of all these factors is necessary in the context of the signal processor real-time throughput constraints.

The modulation selected for the land mobile satellite demonstration system is differentially coherent phase-shift keying (DPSK) at a 200-bit per second data rate with no forward error correction. DPSK modulation provides a compromise among power efficiency, tolerance to shadowing and multipath fading, fast acquisition time, and simplicity. Spectral efficiency is not a consideration for this low data rate system.

Power efficiency was a major consideration since a low-gain, omnidirectional antenna is a requirement. An omnidirectional antenna will not effectively discriminate between direct-path signal energy and reflected signal energy. With Doppler shift, these multipath signals can cause random variations in the signal amplitude and phase. The concern for the land mobile satellite channel is that the multipath fading characteristic may be too severe to allow effective maintenance of the carrier phase estimate for coherent demodulation. Since DPSK only requires an estimate of the carrier frequency, its performance is less sensitive to phase errors caused by the multipath fading environment. In addition, an automatic frequency control (AFC) loop has a wider pull-in frequency range and will achieve lock faster than a conventional Costas loop. Coherent PSK is more power efficient in a nonfading channel; however, this advantage diminishes rapidly as phase errors are introduced by multipath fading.

Optimum filtering of the received signal prior to differential detection is necessary to maximize power efficiency. In this modem design, the quantized signal is filtered by an integrate-and-dump operation after the carrier frequency ambiguity has been narrowed by an FFT-based coarse frequency algorithm. An integrate-and-dump approaches a matched filter

when the internally generated reference is in-phase with the received waveform. The integrators must be dumped at the end of each symbol interval to reduce intersymbol interference [3].

In the demodulator, a digital data transition tracking loop estimates symbol timing independent of carrier phase. The symbol timing estimator adjusts the integration window to align the integrate and dumps with received data symbol boundaries prior to AFC loop lock. Once the dump clock is synchronized, intersymbol interference is minimized and the AFC loop achieves lock. The signal loss due to small post-FFT frequency errors, when integrating over the symbol interval, is small and can be expressed by [4]:

$$\text{Signal Loss (dB)} = 20 \text{ Log } (1/T\Delta L\pi * \sin(T\Delta L\pi)) \quad (1)$$

where T = symbol period
 ΔL = frequency error

Differential detection and AFC loop updates subsequent to the integrate and dump filters are performed at the data rate. Decimation from the 6K Hz input sampling rate to the data rate is provided by the synchronized dump clock and greatly decreases the real-time processing load on the signal processor.

The purpose of this paper is to give a brief description of the digital signal processor used to implement the modem functions and to summarize the demodulator algorithms.

SIGNAL PROCESSOR

The DSP employed to implement the modem functions is a Texas Instruments TMS32020. The TMS32020, analog-to-digital converter, digital-to-analog converter, and programmable sampling clock are all implemented on a board manufactured by Atlanta Signal Processors (ASP) and contained in a Compaq PC. The ASP board also provides an interface between the TMS32020 and the Compaq via dual port RAM.

All of the algorithms which implement the modem functions are performed by one TMS32020. Implementation of these algorithms in software allows a very flexible architecture which can be optimized to changing design requirements. No high-level language was available for the TMS32020 at the project start, so all of the software modules are written in assembly language. Real-time context switching and scheduling is provided by a TMS32020 executive also developed for this modem application.

Computation on the quantized samples is based on a fixed-point, 2's complement representation. Since the TMS32020 provides a 16-bit architecture, the 12-bit samples from the analog-to-digital converter are processed in Q15 format. This means the most significant bit is a sign bit and the decimal point is to the left of the 15 least significant bits. Additional resolution is required by the FFT-based coarse frequency algorithm after squaring the FFT result to obtain the power spectral density. The power spectral density result is processed in Q31 double precision format.

DPSK MODEM

Figure 1 shows a functional block diagram of the DPSK demodulator. The DPSK differential encoding function is performed at baseband in the TMS32020; however, modulation, frequency translation, and filtering required prior to transmission are performed in hardware.

NUMERICALLY CONTROLLED OSCILLATOR

The primary computational element of the numerically controlled oscillator (NCO) is an accumulator. The size of the accumulator, the sampling rate, and the magnitude of the instantaneous phase added to the accumulator determine the rate at which the accumulator rolls over and thus the frequency output from the NCO. The least significant 6 bits of the accumulator

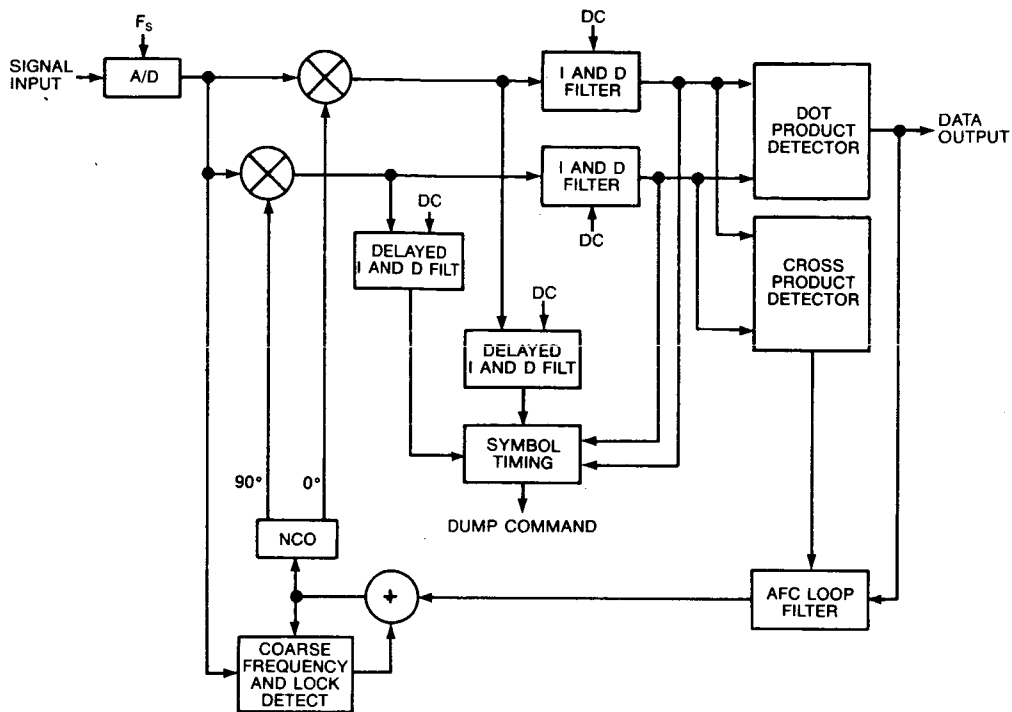


Fig. 1. Block diagram of DPSK demodulator

address fine look-up locations and the next most significant 6 bits address coarse look-up for sine and cosine. The actual quadrant of the accumulated phase is represented by the most significant 2 bits of the 14 bit accumulator.

The NCO uses the addition trigonometric identities;

$$\cos(A+B) = \cos A \cos B - \sin A \sin B \quad \text{and}$$

$$\sin(A+B) = \sin A \cos B + \cos A \sin B$$

to minimize the number of table look-up locations required to generate sine functions and cosine functions. The look-up table contains 64 locations for each of the following functions: coarse sine ($\sin A$) and cosine ($\cos A$), and fine sine ($\sin B$) and cosine ($\cos B$). The quantized look-up angles are represented in the first quadrant as:

$$A: \text{coarse} = 0 \rightarrow \pi/2$$

$$B: \text{fine} = 0 \rightarrow \pi/128$$

INTEGRATE AND DUMP FILTERS

The I and Q signals generated by multiplying the digitized signal with the NCO outputs are filtered by integrate-and-dump filters. In order to avoid intersymbol interference, the integrators (accumulators) must be reset (dumped) at the end of each symbol interval. A symbol timing algorithm samples both the I and Q channels to deliver a symbol timing error which is used to drive a first-order digital data transition tracking loop. When the error is driven to zero, the integrators are reset at the end of each symbol interval and the time-varying integrate and dump filters are synchronized to the received data symbols.

SYMBOL TIMING ALGORITHM

The symbol timing algorithm determines the reset time of the integrate-and-dump filters and thus symbol synchronization. Figure 2 shows a functional block diagram of the symbol timing algorithm. The error signal for symbol timing is based on the observation that when a non-return to zero (NRZ) data transition occurs, the integral (ignoring the effects of intersymbol interference (ISI) and channel noise) from one-half symbol before the transition to one-half symbol after the transition should be zero. This is also true for the integral of a sinusoidal signal that experiences a 180 degree phase shift.

A transition detector determines whether a transition has occurred, and, if so, calculates the direction of the transition. This information, along with delayed integrator outputs, is input to a data transition discriminator which calculates the symbol timing error [5].

$$E_n = [I_n - I_{n-1}] * (I_{n-1/2}) + [Q_n - Q_{n-1}] * (Q_{n-1/2}) \quad (2)$$

This error signal is used to drive a first-order digital data transition tracking loop. The loop filter equation can be represented as:

$$\tau_{n+1} = \tau_n + E_n \quad (3)$$

A variable loop gain allows fast symbol synchronization during acquisition while providing for a narrow loop bandwidth during tracking. This algorithm derives a symbol timing error independent of carrier phase without the use of a square-law nonlinearity.

DOT AND CROSS-PRODUCT DETECTORS

A dot-product detector estimates the value of the data bit by differential detection of the I and Q integrate and dump outputs. The dot-product detector is implemented by multiplying the I signal delayed by one symbol (one sample at the decimated rate) with the I signal. This result is added to the product of the Q signal delayed by one symbol multiplied by the Q signal. The sign of the dot-product result is the NRZ detected data bit.

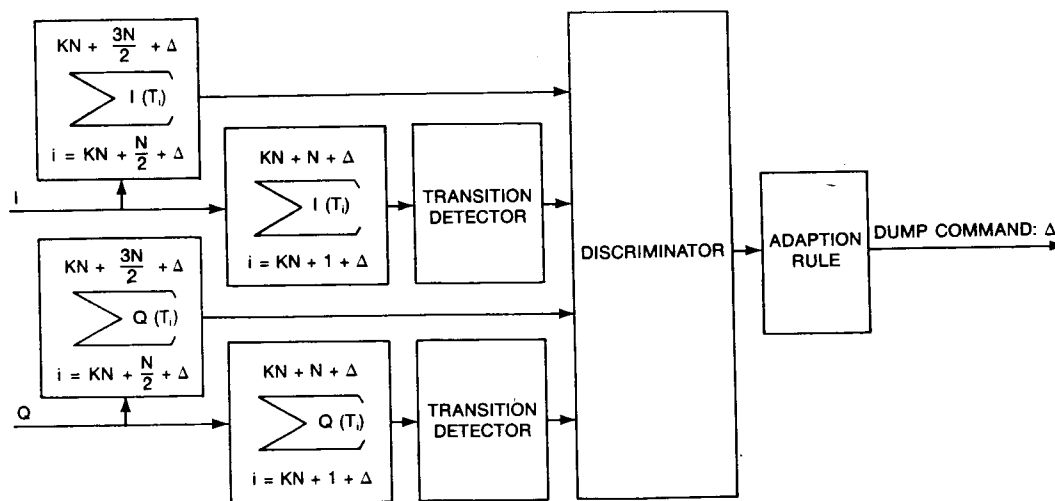


Fig. 2. Digital data transition tracking loop block diagram

A cross-product detector multiplies the I signal by the Q signal delayed by one symbol. This result is subtracted from the product of the Q signal multiplied by the I signal delayed by one symbol. The cross-product detector result is an estimate of the difference between the frequency of the received signal and the NCO output. The sign of this frequency estimate is a function of the received data phase. Dependency on the data phase is eliminated by multiplying the cross-product estimate of the NCO frequency offset by the NRZ detected data bit. The result is an error term that is proportional to the NCO frequency offset and is represented by the noise-free discriminator characteristic shown in Figure 3 [6].

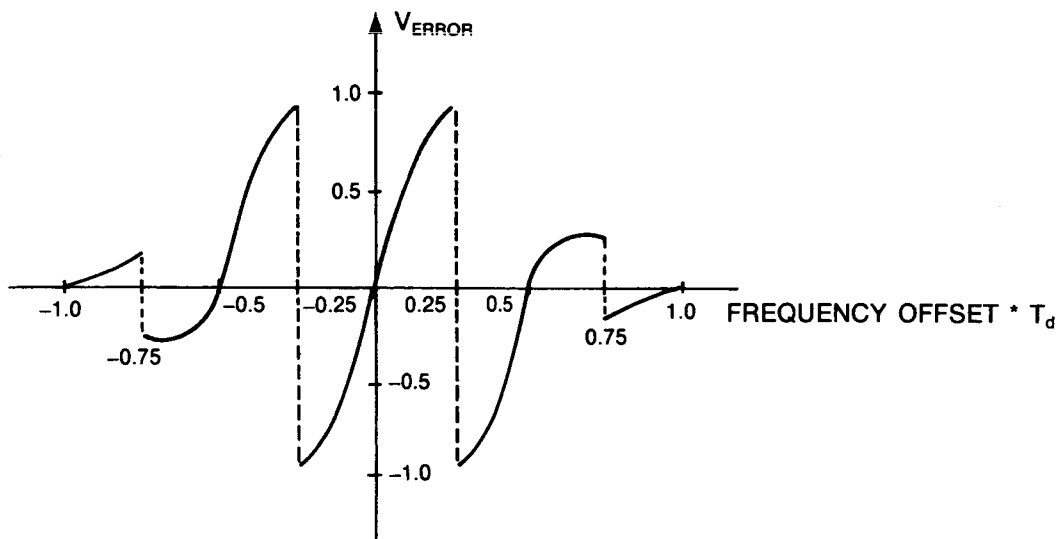


Fig. 3. Noise-free discriminator characteristic $T_d = \frac{1}{\text{data frequency}}$

AUTOMATIC FREQUENCY CONTROL LOOP FILTER

The cross-product detector error estimate is filtered by a lead-lag recursive filter and fed back to the NCO. The transfer function for the one-pole filter in the S domain is:

$$F(s) = K_L(1 + a/s) \quad (4)$$

Using the bilinear transform to convert to the z domain, the difference algorithm may be written:

$$u_n = u_{n-1} + (K_L a T_d / 2) e_{n-1} + K_L (1 + a T_d / 2) e_n \quad (5)$$

The AFC loop filter determines the dynamic performance of the AFC loop. The gain and bandwidth of the AFC loop are specified by the filter coefficients K_L and a (as in equations (4) and (5)) [7].

COARSE FREQUENCY ESTIMATE AND LOCK DETECT

The cross-product detector characteristic given in Figure 3 shows the pull-in range of the AFC loop to be less than 50 Hz with a 200-Hz data rate. An algorithm that employs an FFT estimates the frequency of the received signal at the input to the digital demodulator.

Loss of AFC loop lock is determined by comparing the coarse frequency estimate to the frequency output of the NCO. If their difference exceeds the cross-product detector pull-in range for a specified number of trials, this coarse frequency estimate is added to the AFC filter output (fine frequency) and the sum determines the NCO frequency output.

CONCLUSION

Tests of the DPSK modem are continuing as the land mobile satellite demonstration results are reviewed. Initial tests on the demodulator were performed to approximate its stability and performance. These tests indicate an implementation loss of about 1 dB with digitally generated, white Gaussian noise added to the received signal.

The symbol timing and AFC loops have shown a high resistance to the effects of shadowing and multipath fading. On a trip from Waterloo, Iowa, to Cedar Rapids, Iowa, during two-way communication via the INMARSAT satellite, the AFC loop of the land mobile satellite system remained locked despite the most harsh shadowing conditions. Although this demodulator is optimized for fast carrier acquisition, its performance appears to be very robust once synchronization is achieved.

ACKNOWLEDGEMENTS

This project was a joint effort of Rockwell International, COMSAT General, and INMARSAT. The FFT-based coarse frequency estimate algorithm was devised by D.C. Nicholas and implemented by J.F. Nields. M.D. Walby provided valuable advise during the development of the demodulator algorithms.

REFERENCES

1. G.M. Gooch, D.C. Nicholas, "Land Mobile Satellite Demonstration System," NASA, JPL Mobile Satellite Conference, Pasadena, CA, May 1988.
2. D.C. Nicholas, "Land Mobile Satellite Propagation Results," NASA, JPL Mobile Satellite Conference, Pasadena, CA, May 1988.
3. K.S. Shanmugan, *Digital and Analog Communications Systems*, John Wiley and Sons, Inc., New York, N.Y., 1979.
4. A. Hamilton, "Synchronization Preamble Study For Satellite Communications," Rockwell-Collins internal paper, September 4, 1987.
5. F.M. Gardner, "A BPSK/QPSK timing-error detector for sampled receivers," *IEEE Trans. Commun.*, Vol. Com-34, May 1986.
6. F.D. Natali, "Noise performance of a cross-product AFC with decision feedback for DPSK signals," *IEEE Trans. Commun.*, Vol. Com-34, pp. 303-307, March 1986.
7. J.F. Roesch, "An all digital demodulator using off-the-shelf VLSI technology," *Milcom Trans.*, Vol. 3, pp.46.4.1-4.6.5, October 1986.

PILOT-AIDED MODULATION FOR NARROW-BAND SATELLITE COMMUNICATIONS

DR. GARY J. SAULNIER, Electrical, Computer and Systems Engineering, Rensselaer Polytechnic Institute, United States; DR. WILLIAM RAFFERTY, Mobile Satellite Program, Jet Propulsion Laboratory, United States.

RENSSELAER POLYTECHNIC INSTITUTE
Troy, New York, 12180-3590
United States

ABSTRACT

This paper discusses a number of tone-aided modulation techniques which have been studied as part of the Mobile Satellite Experiment (MSAT-X) Program. In all instances tone(s) are inserted into data-free portions of the transmit spectrum and used by the receiver to sense the amplitude and frequency/phase distortions introduced by the channel. The receiver then uses this information in a feedforward manner to lessen the effect of the distortions on the data detection performance. Particular techniques discussed are the Tone Calibration Technique (TCT), the Dual Tone Calibrated Technique (DTCT), Transparent Tone-In-Band (TTIB) and Dual-Tone Single Sideband (DTSSB).

INTRODUCTION

The goal of the Mobile Satellite Experiment (MSAT-X) is to develop concepts and technologies which enable the creation of a mobile satellite service. To accommodate a large number of users, it has been decided that each channel will be 5 kHz wide. In addition, these channels must support a data rate of 4800 bps in order to allow telephone quality digital voice communication using vocoders of reasonable complexity. A major challenge, then, is to develop a modulation format which can provide adequate detection performance for operation of the digital voice system while maintaining adequately low signal powers. It has been determined that bit error rates under 10^{-3} at a signal-to-noise ratio of 10 dB are needed for this system.

The mobile satellite system will involve communications from moving vehicles directly to and from the satellite. Consequently, the system must contend with the presence of reflected multipath signals as well as Doppler frequency shifts. Due to the narrow bandwidth of the signals and the desired operation at L-Band, these effects can become quite severe and some type of compensation must be applied in the receiver. Highly directional antennas will help reduce some of the multipath effects but some reflected components are expected in conjunction with the desired line-of-sight component. A modem for octa-Phase Shift Keying (8-PSK) using differential detection with a Doppler correction technique has been developed as part of the MSAT-X program. This system is discussed in (Simon, 1988).

An alternate method for mitigating the effects of multipath fading and Doppler frequency shifts is the use of tone aided modulation. A number of tone aided modulation formats have been investigated in

conjunction with the MSAT-X program. The common feature of all these formats is that one or more tones are inserted into a portion of the transmit spectrum which does not contain any of the transmit data signal. These tones may reside at the edges of the data spectrum or in a frequency null that has been deliberately created within the data spectrum. In any case, the one or more tones are separated from the data signal at the receiver and used to determine the channel- and equipment-induced amplitude and phase/frequency distortions. It is assumed in this system that, due to the narrow channel bandwidth, these channel effects will be nearly uniform over the channel and, therefore, the distortion introduced in the tone(s) is the same as that introduced in the data signal.

The recovered pilot tone(s) contains the necessary information to reduce the effects of the channel distortions on the data signal. The envelope of the recovered pilot tone(s) provides information about the signal amplitude distortion. In addition, the frequency/phase modulation of the tone(s) provides an indication of the frequency and phase distortions. The basic structure of the receiver involves the recovery of amplitude and frequency/phase distortions from the pilot tone(s) and the subsequent feedforward processing of this information to compensate for the distortion effects in the data signal. Figure 1 shows the general receiver structure. The bandpass filter on the input performs the channel select function. As can be seen in the figure, the data signal is delayed in a path parallel to the pilot processor in order to maintain time alignment with the recovered distortion information obtained from the tone(s). This feedforward structure is superior to feedback techniques for this application because it allows the instantaneous "tracking" of fluctuations. In other words, the information used to correct the data signal at a particular time is obtained from the tone signal at that same time.

This paper discusses several tone-aided systems and provides information on the structure of the various receivers. Important considerations in the evaluation of the viability of a particular tone-aided format are the complexity of the modulator/demodulator structure, and the amount of extra bandwidth and power required for the insertion of the tone(s). The receiver structures presented are all bandpass (i.e. "IF") implementations, though baseband implementations are probably better suited to implementation using digital signal processors. The bandpass implementations are presented here because they more clearly illustrate the functions performed in each receiver type.

TONE CALIBRATED TECHNIQUE (TCT)

The TCT system (Davarian, 1984) employs Manchester encoding to create a null in the center of the data signal spectrum. A single pilot tone that is in phase coherence with the carrier is inserted into this null. Figure 2 shows the resulting transmit spectrum.

The TCT receiver, shown in Figure 3, consists of the pilot bandpass filter (PBPF) for the recovery of the pilot tone, the calibration system, a coherent demodulator and a Manchester decoder. The calibration system processes the pilot tone in two paths. The upper path squares the pilot tone and then lowpass filters the result to obtain the square of the pilot amplitude modulation. The lower path simply delays the pilot tone by an amount equal to the delay of the

upper path. Finally, the delayed pilot tone is divided by the square of the amplitude modulation. The net result is that, if the pilot at the input to the calibration system has amplitude modulation $A(t)$, the pilot at the output of the calibration system has amplitude modulation $1/A(t)$. The pilot processor output is fed to the data demodulator where it is used to coherently demodulate the data signal. Assuming that the data signal also has amplitude modulation $A(t)$, the amplitude modulation terms vanish in the mixing process. Finally a Manchester decoder recovers the data.

The TCT system has been analyzed and implemented for binary PSK signalling. Although BPSK does not provide the required 4800 bps throughput in the 5 kHz channel, the results indicate that the major contribution of the pilot tone is the removal of the irreducible error floor associated with coherent receivers in the presence of Rician fading (Rafferty, 1987).

Despite this important performance advantage, the drawbacks of the TCT system reduce its value for mobile satellite applications. First, the use of Manchester coding to create a null for the pilot has the undesirable by-product of doubling the signalling rate and, therefore, the transmit bandwidth. As a consequence, the number of signalling states must be doubled to maintain the same throughput as a non-tone aided PSK system, causing a loss in detection efficiency. Second, the width of the spectral null proved to be too narrow for proper operation. A sufficiently wide null must be used because the pilot tone must be recovered using a filter which will pass the faded pilot tone when subjected to the Doppler frequency shifts. Using a pilot recovery filter with a minimum bandwidth necessary to accommodate the expected Doppler spread, it was found that unacceptable amounts of data signal energy passed through the filter and appeared in the recovered pilot tone. This signal energy resulted in pilot tone amplitude and phase modulation that was not channel-induced and, as a result, degraded system performance. Later studies used high pass filters in the transmitter to increase the width of the null, resulting in the introduction of inter-symbol interference (Rafferty, 1985).

DUAL TONE CALIBRATED TECHNIQUE (DTCT)

The problems encountered with the TCT system centered upon the creation of the spectral null for the pilot tone and the related bandwidth expansion. As a solution to this problem the DTCT system (Simon, 1986), which uses two pilot tones, was derived. This system places one tone on each side of the data signal as shown in Figure 4. The two tones are used in the receiver to create a coherent reference at the carrier frequency which, as in the TCT system, is used to demodulate the data.

Figure 5 is a block diagram of an implementation of the DTCT system. The input signal is bandlimited to set the channel bandwidth. The pilot tones are recovered using two pilot bandpass filters, one at frequency $\omega_0 + \omega_p$ and a second at frequency $\omega_0 - \omega_p$. The outputs from the pilot recovery filters are mixed together to produce a tone at frequency $2\omega_0$, i.e. twice the carrier frequency of the data signal. This signal is then fed to a calibration system similar to the TCT calibration system which outputs the $2\omega_0$ signal with amplitude modulation $1/A(t)$. A tone at frequency ω_0 is produced using a frequency divider and the result is used to coherently demodulate the data signal.

The main drawbacks of the DTCT system are the extra bandwidth required for two tones, the increased processing noise in the pilot recovery system due to the use of two pilots (each recovered pilot signal contains noise) and the placement of the tones at the band edge where they are more likely to be subject to distortions. Frequency uncertainty combined with non-ideal amplitude and phase characteristics of the receiver front end filters will create some phase distortion in the pilot tones which, in turn, will affect the efficiency of the coherent demodulation process.

TRANSPARENT TONE-IN-BAND (TTIB)

The TTIB system (McGeehan, 1984) in many ways combines the best attributes of the TCT and DTCT systems. Like the TCT system, the TTIB system utilizes a single pilot tone placed at the center of the transmit signal where the distortions due to filtering are expected to be minimal. However, the spectral null for the tone is created by the somewhat unusual approach of splitting the data spectrum in a single-sideband fashion and frequency shifting the upper half upwards by ω_T and the lower half downward by the same amount. The frequency shift value, ω_T , is set to accommodate the expected Doppler spread and allow for non-zero transition bands of the sideband separation filters. Figure 6 shows the TTIB spectrum. Like the DTCT system, the data bandwidth is not expanded by the insertion of the tone, however, the TTIB data signal appears as two sections.

Figure 7 is a block diagram of a TTIB receiver. The two main functions performed by the receiver are the pilot processing, which removes the amplitude and frequency/phase distortions, and the demodulator which uses a phase-locked loop (PLL) to obtain an estimate of ω_T and, then, recombines the data sidebands.

The pilot processor splits the input signal into two paths, one path uses a notch filter to remove the pilot tone from the data sidebands and a second mixes the input signal with a subcarrier at ω_s and then uses a bandpass filter to isolate the pilot tone, now at frequency $\omega_s + \omega_T$. The pilot calibration system then inverts the amplitude modulation on the pilot. Finally, the data sidebands are mixed with the output of the pilot amplitude processor, resulting in the data sidebands on the subcarrier ω_s and some higher-order mixer products.

The output of the pilot processor is the data signal centered at frequency ω_s and containing the $2\omega_T$ spectral null. At this point, the amplitude and frequency uncertainty due to Doppler or fading has been removed through the pilot processing. The next portion of the receiver is a PLL which is a unique implementation of a Costas-type tracking loop which recombines the two sidebands by recovering the frequency shift term, ω_T . Note that the pilot processing effectively removes any significant frequency uncertainty at the input to the PLL. Consequently, a first order PLL is sufficient. Therefore the loop filter in Figure 7 is simply a gain block. The upper and lower sidebands of the pilot processor output are isolated by bandpass filters on the input to the PLL. These sidebands are then mixed to baseband using a locally generated references at $\omega_T + \omega_s$ and $\omega_T - \omega_s$, respectively. The error signal is generated by mixing these two baseband signals together. The error signal controls the voltage controlled oscillator (VCO) which generates the estimate of ω_T . Note that the PLL tracks ω_T

which is a stable frequency value and is not affected by the channel impairments.

The main disadvantages of the TTIB system are the complexity of the receiver and the non-ideal operation of the PLL which recovers ω_T . It has been found that, in processing the TTIB signal, this PLL contains a data dependent noise term in the error signal. This unwanted noise term is due to the single sideband nature of the signals and is proportional to the Hilbert Transform of the data signal (Saulnier, 1988). These data dependent terms, however, do not prevent the PLL from acquiring or maintaining lock, but may degrade its performance. Currently, experiments are being conducted to characterize the loop performance in AWGN and multipath fading. In particular the degradation in performance due to the undesired terms in the PLL error signal is being evaluated.

DUAL-TONE SINGLE SIDEBAND (DTSSB)

The DTSSB system transmits only one sideband of the data signal and uses two pilot tones, both on the same side of the data sideband, to provide frequency and amplitude compensation as well as a coherent reference for demodulation. Like the DTCT and TTIB systems, this approach does not expand the bandwidth of the data signal. Unlike the TTIB system, the DTSSB system does not require a PLL for data recovery and therefore, will not introduce the data dependent noise. However, the use of two pilots does introduce additional noise in the pilot processing and, consequently, it is not clear whether the DTSSB system provides a performance advantage over the TTIB system.

Figure 8 shows the DTSSB spectrum. One pilot tone is placed a frequency ω_T from the carrier of the single sideband. The second tone is placed ω_T from the other tone, i.e. $2\omega_T$ from the carrier. The receiver recovers both tones and uses the difference frequency to determine ω_T and, then, uses ω_T to regenerate a coherent carrier reference. The net result is that the single sideband is coherently demodulated.

Figure 9 is a block diagram of the DTSSB receiver. Two bandpass filters, one centered at frequency ω_0 and the other at $\omega_0 + \omega_T$, are used to isolate the two pilots. One pilot is processed by a calibration system to replace its envelope with its inverse, i.e. $A(t)$ is replaced by $1/A(t)$. The amplitude-processed pilot is then mixed with the other recovered pilot to produce a frequency term at frequency ω_0 . This ω_0 term is then mixed with the calibration system output to produce a tone at the data sideband carrier frequency, $\omega_0 - \omega_T$. Finally, coherent demodulation is performed to recover the data.

The main concerns with the DTSSB system are the asymmetry of the transmit signal and the distortion of the phase relationship between the pilots by the receiver front end filtering. Any error in this phase relationship will degrade the coherent demodulation process. Also, the use of two pilots introduces additional noise into the demodulation process as in the DTCT system. An advantage of the DTSSB system is the efficient use of the bandwidth by the transmission of only a single data sideband.

DISCUSSION AND CONCLUSIONS

This paper presents four pilot-aided modulation schemes and discusses some of the properties of each. The TCT system uses a very

simple receiver but suffers from the excessive bandwidth expansion caused by the use of Manchester encoding. The DTCT system uses two pilots and is more bandwidth efficient than the TCT system. The placement of the tones at the edges of the channel make this technique susceptible to degradation from non-ideal receiver filtering and, in particular, non-uniform group delay distortion. The TTIB system is more bandwidth efficient than the DTCT system because it requires only one pilot tone. The TTIB receiver, however, is much more complex than those for the other techniques due to the need for the PLL. Currently, it has not been determined if the presence of data dependent terms in the PLL error signal will seriously degrade performance. Finally, the DTSSB system provides excellent bandwidth efficiency and uses a simple receiver structure. However, the asymmetry of the signal spectrum and the additional noise due to the use of two pilots may degrade the performance of this system.

REFERENCES

- Davarian, F. 1984. High performance communication in mobile channels. IEEE 34th Vehicular Technology Conference.
- McGeehan, J., Bateman, A. 1984. Phase-locked transparent tone-in-band (TTIB): a new spectrum configuration particularly suited to the transmission of data over SSB radio network. IEEE Trans. on Comm. COM-32: 81-87.
- Rafferty, W., Anderson, J.B., Saulnier, G.J., Holm, J.R. 1987. Laboratory measurements and a theoretical analysis of the TCT fading channel radio system. IEEE Trans. on Comm. COM-35: 172-180.
- Rafferty, W., Bechtel, L.K., Lay, N.E. 1985. An additional study and implementation of tone calibrated technique of modulation. Final report on JPL Contract 957190, Jet Propulsion Laboratory, Pasadena, CA.
- Saulnier, G.J., Hladik, S., Kolb, S., Varghese, A. 1988. A study of transparent tone-in-band modulation for binary PSK signalling. (JPL internal interim report on JPL Contract 958050), Jet Propulsion Laboratory, Pasadena, CA.
- Simon, M.K. 1986. Dual pilot tone calibration technique [DTCT]. IEEE Trans. Vehicular Tech. VT-35: 63-70.
- Simon, M.K., Divsalar, D. 1988. Doppler corrected differential detection of MPSK. To be published in IEEE Trans. on Comm.

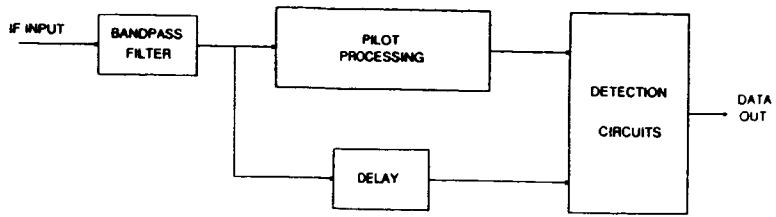


Fig. 1 General tone-aided receiver

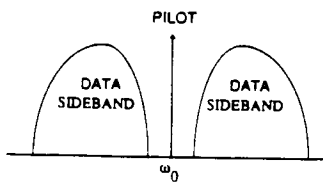


Fig. 2 TCT spectrum

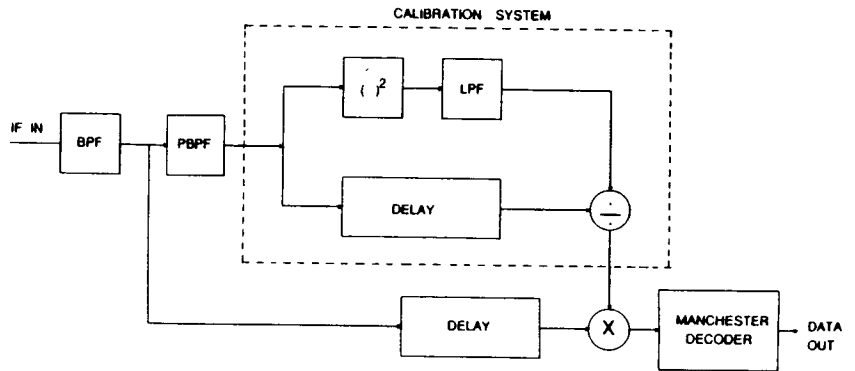


Fig. 3 TCT receiver structure

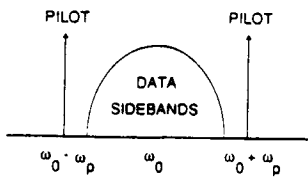


Fig. 4 DTCT spectrum

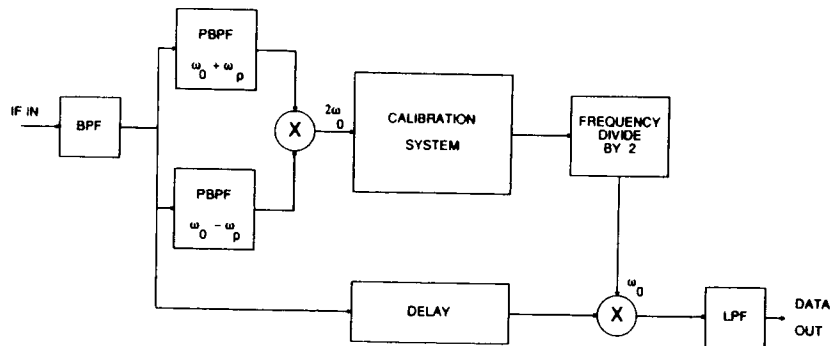


Fig. 5 DTCT receiver structure

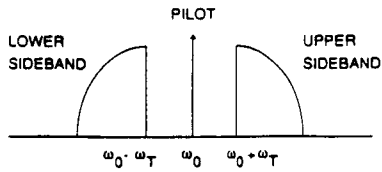


Fig. 6 TTIB spectrum

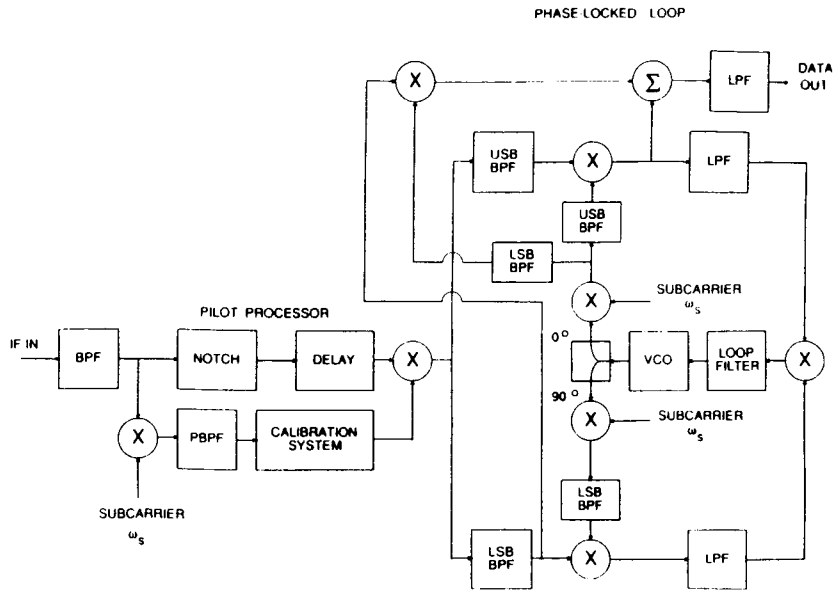


Fig. 7 TTIB receiver structure

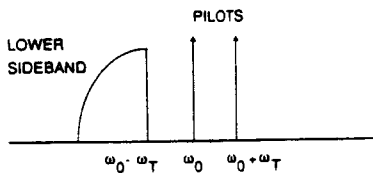


Fig. 8 DTSSB spectrum

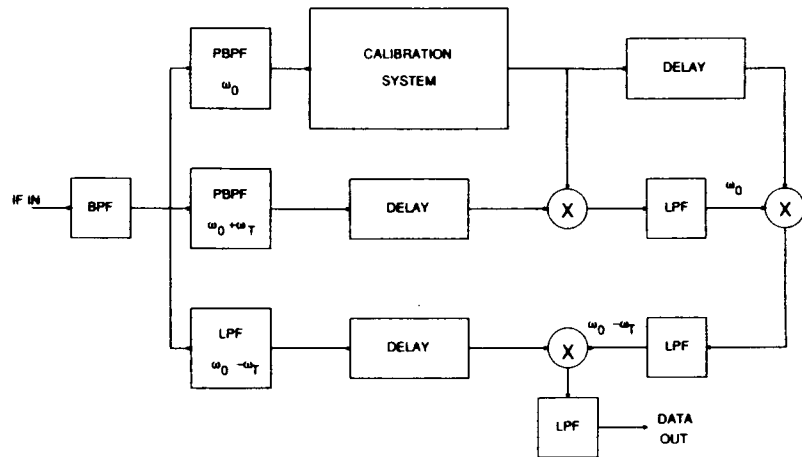


Fig. 9 DTSSB receiver structure

AN ERROR FLOOR IN TONE CALIBRATED TRANSMISSION

JAMES K. CAVERS

School of Engineering Science
SIMON FRASER UNIVERSITY,
Burnaby, B.C., V5A 1S6
Canada

ABSTRACT

Use of a low level pilot tone has been shown to eliminate the error floor in fading channels. This paper demonstrates that non-idealities in the receiver's pilot tone filter cause reappearance of the error floor. It also presents the BER in closed form, in contrast to the multidimensional numerical integration of previous work.

INTRODUCTION

Recently, a number of papers [e.g. Davarian, 1986, 1987; Simon 1986; LaRosa & Citron, 1987] have resurrected the use of a pilot tone to allow coherent reception in fading channels. The receiver extracts the pilot with a pilot bandpass filter (PBPF), and uses the result as a phase reference. The obvious costs are the non-constant envelope, the additional complexity at the receiver, and the fact that the pilot robs power from the data carrying signal. Thus we expect to see little or no improvement in the noise limited region; however, when the fade rate is high, TCT proves itself, by lowering or eliminating the error floor typical of other modulation methods.

Analyses to date have implicitly or explicitly assumed that TCT eliminates the error floor. We show here, though, that nonidealities in the PBPF lead, not just to a degraded BER, but to a nonzero error floor. Moreover, previous studies have calculated the BER by numerical integration, often in multiple dimensions. We present here a closed form solution which includes the effect of the PBPF nonidealities and a frequency offset error.

In the interest of brevity, this paper deals only with the issue of irreducible error rate, because it has not been addressed by other authors. However, the method extends in a straightforward way to include the effect of noise, and a full analysis will be published elsewhere.

SYSTEM MODEL

General Characteristics

Figure 1 is the complex envelope representation of the transmitted and received signals. The transmitted power is split between the data bearing signal and a low level pilot tone in such a manner that they do not interfere with each other. For simplicity, we will assume Manchester coding with the pilot in the center channel null, although other methods are possible; for example, the pilot could be located beside the data signal. The analysis below is restricted to two-level eyes; for convenience we assume BPSK, though the results are also valid for QPSK or OQPSK.

Data is detected with a filter matched to the transmitted pulse $p(t)$. Samples at the filter output are denoted by $u(k)$.

The PBPF, represented by the low pass equivalent filter $H_p(f)$, has unity dc gain; ideally, it is a rectangular lowpass filter with bandwidth $B_p/2$, made equal to the sum of frequency offset and Doppler.

Since the PBPF has a greater delay than the wider bandwidth matched filter, we assume that there is delay equalization in the detector branch. The PBPF output is $v(k)$. Feedforward phase correction is accomplished simply by making decisions on the basis of the phase-corrected decision variable:

$$d(kT) = \text{Re}[u(kT) v^*(kT)] \quad (1)$$

The shape and bandwidth of the PBPF have a major effect on performance. If it is too narrow, then frequency offset and Doppler spread will prevent the filter output from following the channel fluctuations, leading to degraded performance and a nonzero error floor. If it is too wide, it will admit too much channel noise and self noise from the data signal, which again leads to degraded performance. A related issue is the fact that any phase distortion in the PBPF also results in decorrelation and a non zero error floor.

We will assume that there is no additive noise in the channel; as noted earlier, our main interest here is the irreducible BER.

The Fading Channel

We assume Rice fading, in which the ratio of specular to diffuse power is K . These components of the complex gain, when each normalized to unit power, have power spectral densities $\bar{S}_{gs}(f)$ and $\bar{S}_{gd}(f)$, respectively. Although our general solution does not rest on a particular spectrum for the diffuse component, the examples will use a spectrum and autocorrelation function characteristic of isotropic scattering:

$$\bar{S}_{gd}(f) = \frac{1}{\pi} (f_D^2 - f^2)^{-1/2}; \quad \bar{R}_{gd}(\tau) = J_0(2\pi f_D \tau) \quad (2)$$

where $J_0()$ is the Bessel function of first kind and order zero and f_D is the Doppler frequency. For the specular component, we have:

$$\bar{S}_{gs}(f) = \delta(f - f_L) \quad (3)$$

where f_L is its Doppler shift. Note that $|f_L| \leq f_D$. We also allow a frequency offset error f_o between transmit and receive oscillators.

Signal Moments

The signal moments and their ratios are required for calculation of BER. Since we have assumed no noise, the variance in $u(k)$ and $v(k)$ is due to the diffuse component, and the mean is determined by the specular component. We can show that the samples at the output of the matched filter have signal to variance ratio:

$$|\mu_u|^2 / \sigma_u^2 = 2K \quad (4)$$

Similarly, at the pilot tone filter output:

$$|\mu_v|^2/\sigma_v^2 = 2K |H_p(f_o+f_L)|^2 \left[\int \bar{S}_{gd}(f-f_o) |H_p(f)|^2 df \right]^{-1} \quad (5)$$

Next, we calculate the normalized inner product of the means of $u(k)$ and $v(k)$:

$$\mu_u \mu_v^* / \sigma_u \sigma_v = 2K H_p^*(f_o+f_L) \left[\int \bar{S}_{gd}(f-f_o) |H_p(f)|^2 df \right]^{-1/2} \quad (6)$$

Finally, we calculate the correlation coefficient of $u(k)$ and $v(k)$:

$$\rho = \frac{\int \bar{S}_{gd}(f-f_o) H_p^*(f) df}{\left[\int \bar{S}_{gd}(f-f_o) |H_p(f)|^2 df \right]^{-1/2}} \quad (7)$$

DETECTION ERROR PROBABILITY

General Solution

The basic observation is that $u(k)$ and $v(k)$ are jointly Gaussian, non zero mean, complex random variables. The decision variable $d(k)$ is then of a form familiar from studies of incoherent detection; we make an error if it is negative, assuming $b(k)$ is positive. A concise derivation of the probability of this event can be found in Schwartz et al, 1966, sec8.2. Define the quantities a and b :

$$\begin{Bmatrix} a^2 \\ b^2 \end{Bmatrix} = \frac{|\mu_u|^2/\sigma_u^2 + |\mu_v|^2/\sigma_v^2 - 2\rho_i \text{Im}[\mu_u \mu_v^*] / \sigma_u \sigma_v \mp 2\sqrt{1-\rho_i^2} \text{Re}[\mu_u \mu_v^*] / \sigma_u \sigma_v}{4(1-\rho_i^2)} \quad (8)$$

and the quantity C :

$$C = \left[(1-\rho_i^2)^{1/2} + \rho_r \right] / 2(1-\rho_i^2)^{1/2} \quad (9)$$

where $\rho = \rho_r + \rho_i$. Then the probability of bit error is:

$$P_e = Q(a,b) - C I_0(ab) \exp(-(a^2+b^2)/2) \quad (10)$$

where $Q(a,b)$ is the Marcum Q-function, and $I_0()$ is the modified Bessel function of first kind and order 0. Techniques for evaluating the Q function can be found in Bird & George, 1981.

In the case of Rayleigh fading, $K = 0$, the parameters a and b are zero, and the BER simplifies to:

$$P_{eR} = 1 - C = \left[(1-\rho_i^2)^{1/2} - \rho_r \right] / 2(1-\rho_i^2)^{1/2} \quad (11)$$

Moreover, if the frequency response $H_p(f)$ is real, then $\rho_i = 0$, and:

$$P_{eR} = (1-\rho)/2 \quad (12)$$

Equations (11) and (12) illustrate the requirement for extremely high correlation between the outputs of the matched filter and the PBPf. We see that filters other than the ideal rectangular lowpass produce a correlation coefficient less than 1 in magnitude, and therefore an irreducible error rate.

APPLICATIONS

Delay Mismatch

Earlier we noted that the greater delay of the narrow PBPF meant that delay equalization is required in the matched filter branch. In an implementation based on DSP, this is unlikely to be a problem. In an analog implementation, though, it is possible to have a residual delay mismatch. We can incorporate this effect by representing an otherwise perfect PBPF as:

$$H_p(f) = \exp(-j2\pi f\tau) \quad (13)$$

where the delay mismatch τ can be positive or negative. We now have:

$$\rho = \bar{R}_{gd}(\tau) \exp(-j2\pi f_o \tau) \quad (14)$$

$$\left\{ \begin{matrix} a^2 \\ b^2 \end{matrix} \right\} = K \frac{1 + R_S \sin(2\pi(f_o + f_L)\tau) \mp \cos(2\pi(f_o + f_L)\tau) \sqrt{1 - R_S^2}}{(1 - R_S^2)}$$

$$C = 0.5 \left[\sqrt{1 - R_S^2} + R_C \right] (1 - R_S^2)^{-1/2} \quad (15)$$

where for notational convenience we have defined the quantities:

$$R_C = \bar{R}_{gd}(\tau) \cos(2\pi f_o \tau) ; \quad R_S = \bar{R}_{gd}(\tau) \sin(2\pi f_o \tau) \quad (16)$$

Once again, the case of Rayleigh fading is particularly simple. We set $K = 0$ and find, as in (11), that the error floor is:

$$P_{eR} = 0.5 \left[\sqrt{1 - R_S^2} - R_C \right] (1 - R_S^2)^{-1/2} \quad (17)$$

Figure 2 illustrates the effect of delay mismatch for $K = 10$ and for Rayleigh fading, respectively. The ratio of pilot power to data power is $r = 0.2$. We see a difference in the sensitivity to frequency errors. Rice fading is more affected by the offset frequency f_o than by the Doppler f_D . In contrast, Rayleigh fading behaviour is almost entirely determined by f_D , with little influence from f_o .

The irreducible error rate is clearly evident. Its source is the phase decorrelation introduced by the delay mismatch during intervals of rapid phase change, such as a deep fade. We can obtain a simple estimate of the error floor value in the case of Rayleigh fading, the most severe condition, by evaluating (17) for small values of $f_o \tau$ and $f_D \tau$. Using the series expansions for $\sin()$, $\cos()$, and $J_0()$, we obtain:

$$P_{eR} \approx (2\pi f_D \tau)^2 / 8 \quad (18)$$

which agrees with Figure 3. To a first approximation, the error floor depends only on Doppler, not on frequency offset. As a numerical example, if the error floor is not to exceed 10^{-3} , and $f_D = 100$ Hz,

then we must keep the delay mismatch $|\tau| \leq 0.14$ ms. Clearly, this is not a problem in digital implementations, since this maximum delay is only 1/3 bit duration in 2400 bps BPSK. Analog implementations may find it a more difficult target.

A similar approach yields a somewhat poorer approximation to the

error floor in the case of Rice fading with values of K over 5 or so. Series expansion of the transcendental functions and approximation of the integral in the $Q(a,b)$ function yields the error floor:

$$P_e \approx K (2\pi f_o \tau)^2 e^{-K} \quad (19)$$

in the special case of $f_L = 0$.

Narrow PBPF

One can readily imagine situations in which the combined frequency offset and Doppler spread carry part of the received pilot spectrum outside the window of the PBPF. Such a situation was considered by Larosa & Citron, 1987, for a dual pilot tone system, and a number of curves were obtained by numerical integration. However, the fading spectrum was taken to be rectangular. Clearly, the U-shaped spectrum (2) is more sensitive to band edge distortion because a greater fraction of its power is concentrated near $\pm f_D$.

We will model the PBPF as a rectangular LPF with unity gain for $|f| \leq B_p/2$. With amplitude distortion only, it contrasts with the delay mismatch considered earlier, which had phase distortion only.

The effect on irreducible BER can be determined by evaluating ρ , a , b , and C . We denote the normalized power of the diffuse component of the PBPF output by P_d :

$$P_d = \int \tilde{S}_{gd}(f-f_o) |H_p(f)|^2 df = \int \tilde{S}_{gd}(f-f_o) H_p^*(f) df$$

$$= \frac{1}{\pi} \arcsin(\min(1, (B_p - 2f_o)/2f_D)) + \frac{1}{2} \quad (20)$$

As for the specular component, we observe that it is present and undistorted if it lies in the PBPF passband; otherwise, it is zero. Denote by P_s the normalized power of the specular component at the PBPF output. From (3):

$$P_s = \int \tilde{S}_{gs}(f-f_o) |H_p(f)|^2 df = \begin{cases} 1, & |f_o + f_L| \leq B_p/2 \\ 0, & \text{otherwise} \end{cases} \quad (21)$$

Substitution of (20,21) into (5-9) gives:

$$\rho = \sqrt{P_d}$$

$$\left\{ \frac{a^2}{b^2} \right\} = (K/2) (1 \mp P_s/\sqrt{P_d})^2 ; \quad C = (1 + \sqrt{P_d})/2 \quad (22)$$

for substitution into the BER expression (26).

In the case of Rayleigh fading, we can substitute ρ from (22) into (12), and obtain the error floor:

$$P_{eR} = (1 - \sqrt{P_d})/2 \quad (23)$$

Since P_d should be close to 1 for a reasonable error floor, we can apply series expansions for $\arcsin()$ and square root to obtain:

$$P_{eR} \approx \frac{1}{4\pi} [2(f_D + |f_o| - B_p/2)/f_D]^{1/2} \quad (24)$$

for small excursions of $f_D + |f_o|$ beyond $B_p/2$.

As a numerical example, suppose the irreducible BER is to be held to 10^{-3} . Then from (24), $(f_D + |f_o| - B_p/2)/f_D \leq 8 \times 10^{-5}$. This is an exceedingly tight constraint; essentially it says that the slightest excursion of combined offset and Doppler frequencies beyond the PBPF window results in significant performance degradation.

Bessel PBPF

Equation (24) suggests that even moderate amounts of rolloff can do significant damage if offset and Doppler carry the "horns" of the fading spectrum into the rolloff region. Nonrectangular filters, of course, do not behave in precisely the same way, and detailed analysis requires substitution of their frequency characteristics into (5-7). We did this for a sixth order Bessel filter. Of the two integrals in (5-7), the one involving $|H_p(f)|^2$ was performed analytically; the other was evaluated numerically, after a preliminary integration by parts to remove the singularity.

The curves in Figure 3 were prepared with parameters $\alpha = f_D/R_b$ and $\beta = B_p/R_b$. Note that there is an optimum value for the pilot filter bandwidth, as we trade noise against distortion of the received pilot, and that the optimum depends on K , α , r and E_b/N_o . The values of β were near the optimum.

For $K = 10$, we see the onset of error saturation for $\alpha = 0.04$ and $\beta = 0.03$; that is, the noise bandwidth of the PBPF is only 0.375 times the Doppler bandwidth. However, even for this combination of parameters, saturation is a problem only at BERs far lower than we normally expect from mobile satellite communication. Rayleigh fading is somewhat different. For $\alpha = 0.04$, we see that the PBPF should be at least 1.25 times as wide as the Doppler bandwidth to prevent an unacceptable error floor. To put the results in context, $\alpha = 0.04$ represents 96 Hz fading at 2400 bps; that is, it is an extreme case. For more reasonable ranges, the sixth order Bessel filter appears to be adequate, and it is noise, rather than random FM, which determines system performance.

CONCLUSIONS

Nonidealities in the pilot tone filter produce an error floor which is especially marked in Rayleigh fading with large Doppler frequencies. However, for normal ranges of filter parameters, it is not likely to be a problem, and TCT's claim to suppress the error floor is justified.

REFERENCES

- Davarian, F. 1987. Mobile Digital Communications via Tone Calibration. IEEE Trans Vehicular Technology, vol VT-36, pp 55-62.
- Davarian, F. 1986. Tone Calibration Technique: a Digital Signalling Scheme for Mobile Applications. JPL 86-40 (Pasadena, California: The Jet Propulsion Laboratory).

Simon, M.K. 1986. Dual-Pilot Tone Calibration Technique. IEEE Trans Vehicular Technology, vol VT-35, pp 63-70.

LaRosa C.P. & Citron T.K. 1987. Performance Analysis of the Dual-Pilot Tone Calibration Technique. Intl. Conf. Communications, Seattle.

Schwartz M., Bennett W.R., Stein S. 1966. Communication Systems and Techniques, McGraw-Hill.

Bird J.S. & George D.A. 1981. The Use of the Fourier-Bessel Series in Calculating Error Probabilities for Digital Communication Systems. IEEE Trans Communications, vol COM-29, pp 1357-1365.

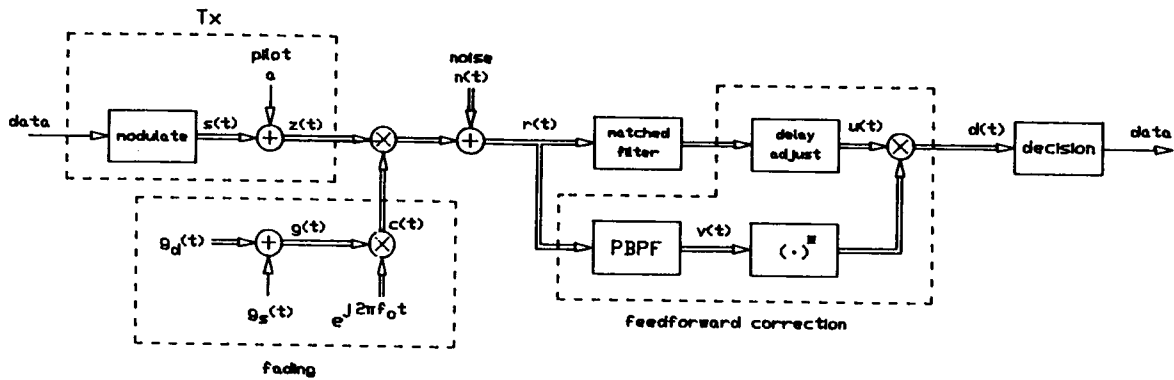


Fig. 1. Complex Baseband Model of TCT System

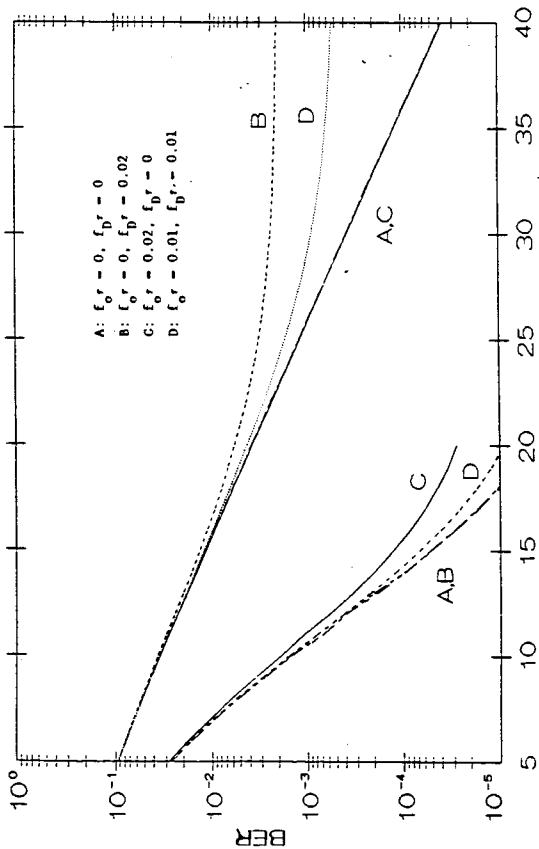


Fig. 2. Delay Mismatch, Rice (K=10) and Rayleigh Fading

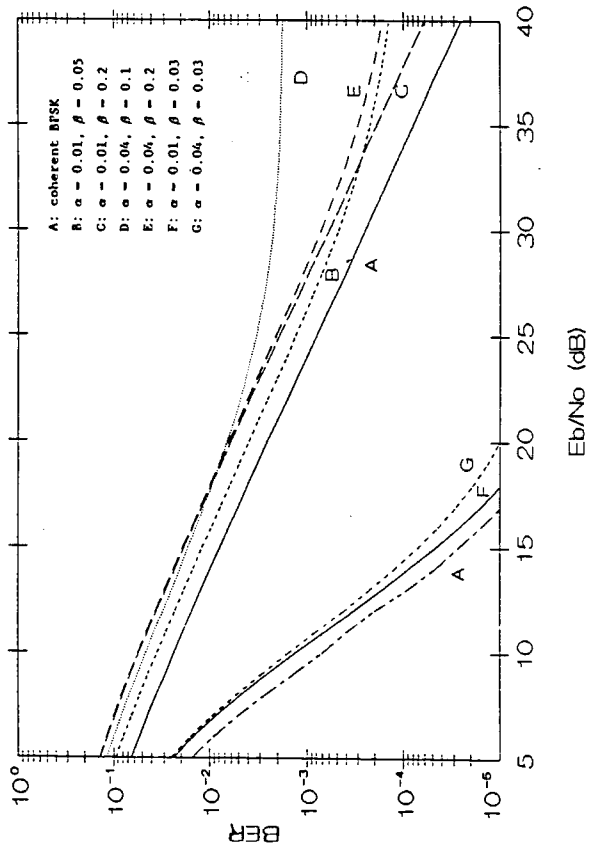


Fig. 3. Bessel PBPF, Rice (K=10) and Rayleigh Fading

EXTENDING THE IMPULSE RESPONSE IN ORDER TO REDUCE ERRORS
DUE TO IMPULSE NOISE AND SIGNAL FADING

JOSEPH A. WEBB, ANDREW J. ROLLS, AND H.R. SIRISENA, Department of
Electrical and Electronic Engineering, University of Canterbury,
Christchurch New Zealand.

Department of Electrical and Electronic Engineering,
University of Canterbury,
Christchurch,
New Zealand.

ABSTRACT

A FINITE IMPULSE RESPONSE (FIR) DIGITAL SMEARING FILTER WAS DESIGNED TO PRODUCE MAXIMUM INTERSYMBOL INTERFERENCE AND MAXIMUM EXTENSION OF THE IMPULSE RESPONSE OF THE SIGNAL IN A NOISELESS BINARY CHANNEL. A MATCHED FIR DESMEARING FILTER AT THE RECEIVER THEN REDUCED THE INTERSYMBOL INTERFERENCE TO ZERO. SIGNAL FADES WERE SIMULATED BY MEANS OF 100% SIGNAL BLOCKAGE IN THE CHANNEL. SMEARING AND DESMEARING FILTERS OF LENGTH 256, 512, AND 1024 WERE USED FOR THESE SIMULATIONS. RESULTS INDICATE THAT IMPULSE RESPONSE EXTENSION BY MEANS OF BIT SMEARING APPEARS TO BE A USEFUL TECHNIQUE FOR CORRECTING ERRORS DUE TO IMPULSE NOISE OR SIGNAL FADING IN A BINARY CHANNEL.

DISCUSSION:

Smearing and desmearing filters have not received much attention in the literature. Whether this is due to simple oversight is not at all clear, but our own analysis of these filters indicates that their advantages are such that they deserve further investigation. They appear to have characteristics which are ideally suited to counter both impulse noise and sudden signal fades.

The earliest paper which we found on smearing and desmearing filters was that by Wainwright in 1961 [1]. This paper and that of subsequent authors such as Engel [2], Richter et al [3], and Beenker et al [4], discuss using smearing filters to reduce the effects of impulse noise in a data transmission system. Filter lengths were relatively short, and except for Beenker, matched filters were used at the transmit and receive terminals. Beenker showed acceptable results without precisely matched filters.

In our work, we found it difficult to define a simple model for impulse noise which was generally accepted as an objective model. Instead, we decided to demonstrate the effects of smearing filters on sudden signal fades. Although complex models of signal fading

PRECEDING PAGE BLANK NOT FILMED

are available, for purposes of simplicity, we decided to assume a 100% fade, knowing that lesser fades would always show improvements over our very simple model.

Figure 1 is a block diagram of our model of a smearing filter in operation. Figure 2 is the frequency response curve for our model, a baseband data transmission system with frequency response from dc to 4 khz. Sampling rate for all of the data given in this paper is 10 khz.

The zero phase impulse response for the filter shown in Figure 2 is given in Figure 3, with inset showing greater detail of the center region of the response. This impulse response is for a filter of length 1024.

The smearing filter phase response, based on the same filter of length 1024, is shown in Figure 4. This phase response is the integral of a linear time delay from dc to midband, followed by a linear return to zero delay. Although this is a different phase response from that used by previous authors, we found that it produced very good results in terms of low passband ripple and low stopband sidelobe levels. The impulse response for this smearing filter is shown in Figure 5.

To simulate a 100% signal fade, the time signal in the channel was simply made zero at somewhere near midpoint in the data stream, for a variable period.

To provide a plot of bit errors, the output of the smearing filter was detected, then correlated with the original data stream. The result, which we call a "scatter diagram", shows a line at 1.0 for all normal noiseless data. Detected data bits which fall below zero in this scatter diagram are detected as errors.

Figure 6 is a typical scatter diagram for a zero phase filter of length 1024. The 100% signal fade in this case is 112 bits in length. Total errors are 49, from an expected 56 for a binary signalling system. (We found less than expected errors for the zero phase filter in all of our measurements).

Figure 7 is a typical scatter diagram for the comparable smearing filter, for a 100% signal fade of 112 bits in length. Total errors in this case was 7. Filter length again was 1024.

Figure 8 is a plot of fade duration versus average number of errors, for 100% signal fade of various lengths, for filters of length 256, 512, and 1024. The zero phase filter characteristic is also plotted, showing an improvement over expected errors in all cases.

Figure 9 shows the same data plotted in terms of percentage improvement ratio (probability of correcting an error), versus duration of fade, for the same filters, including the zero phase filter (length 1024).

In conclusion, although we have not yet tried these smearing filters on a complex model of a data signalling system, the simulations to date indicate good reason for optimistic expectations of the smearing filter as a counter to signal fades.

Because of the similarities, as far as the filter is concerned, between disruption due to sudden signal fades and disruption due to impulse noise, it seems reasonable to conclude that this filter may also have application as a counter to impulse noise.

REFERENCES

- Wainwright, R.A. On the Potential Advantages of a Smearing-Desmearing Filter Technique in Overcoming Impulse-Noise Problems in Data Systems, IRE Transactions on Communication Systems, pp. 362-366, December 1961.
- Engel, J.S. Digital Transmission in the Presence of Impulse Noise, Bell System Technical Journal, pp 1699-1743, October 1965.
- Richter, W.J., and Smits, T.I. Signal Design and Error Rate of an Impulse Noise Channel, IEEE Transactions on Communications Technology, Vol. COM-19, No. 4, pp 446-458, August 1971.
- Beenker, G.F., Claasen, T.A. and Gerwen, P.J. Design of Smearing Filters for Data Transmission Systems, IEEE Transactions on Communications, Vol. COM-33, No. 9, pp 955-963, September 1985.

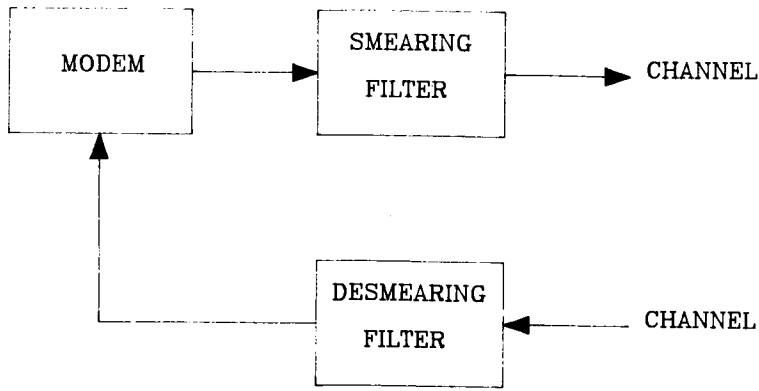


Figure 1. Block diagram showing smearing and desmearing filters in relation to a data modem.

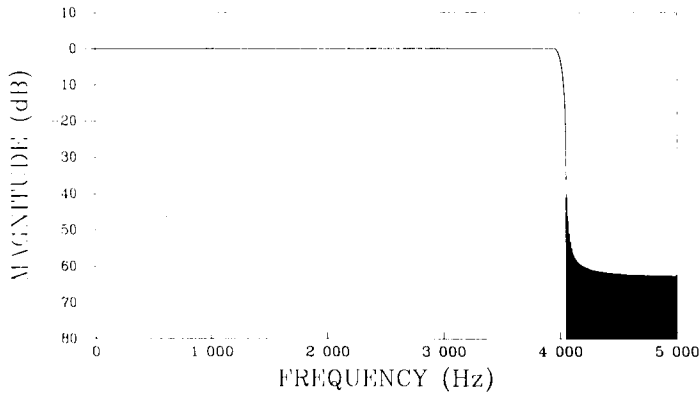


Figure 2. Frequency response of the smearing and desmearing filters.

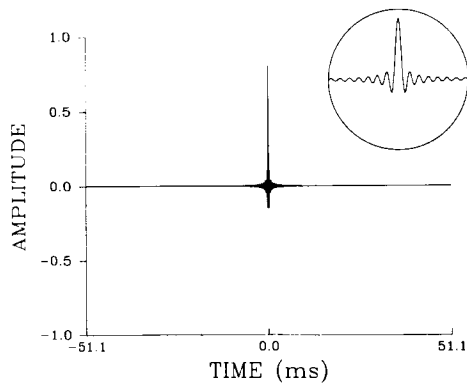


Figure 3. Zero phase impulse response of a filter of length 1024 with the frequency response of Figure 2.

ORIGINAL PAGE IS
OF POOR QUALITY

ORIGINAL PAGE IS
OF POOR QUALITY

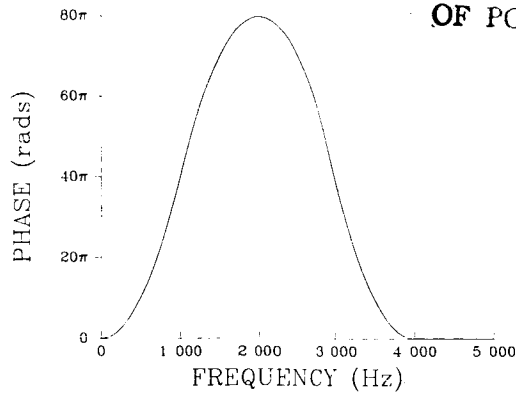


Figure 4. Cumulative phase delay of the smearing filter of length 1024.

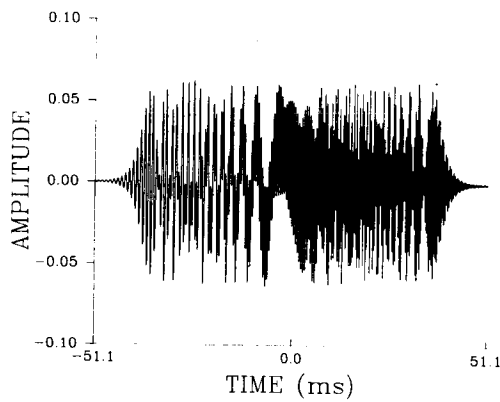


Figure 5. Impulse response of the smearing filter with phase delay as in Figure 4.

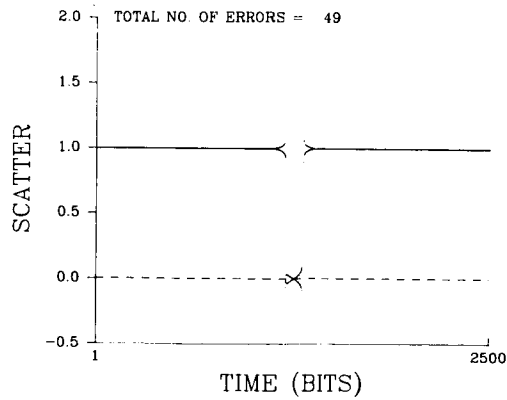


Figure 6. Scatter diagram for a zero phase filter with a 100% signal fade of length 112 bits.

ORIGINAL PAGE IS
OF POOR QUALITY

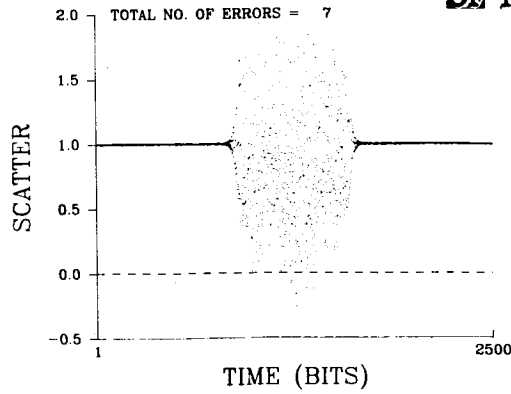


Figure 7. Scatter diagram for a 1024 length smearing filter with a 100% signal fade of length 112 bits.

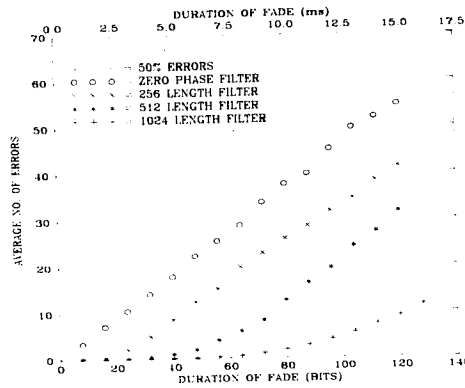


Figure 8. Average errors versus 100% fade length.

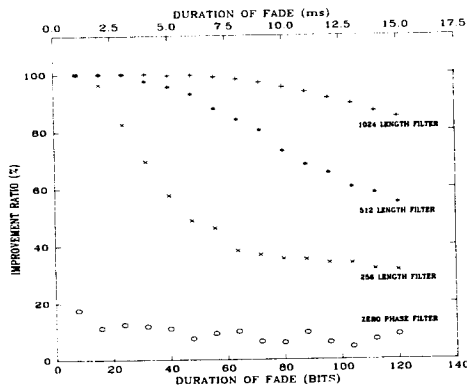


Figure 9. Average improvement ratio versus fade length.

ACSB - A MINIMUM PERFORMANCE ASSESSMENT

LLOYD THOMAS JONES, Institute for Telecommunication Sciences, National Telecommunications and Information Administration, United States; WILLIAM A. KISSICK, Electromagnetic Fields Division, National Bureau of Standards, United States.

Institute for Telecommunication Sciences
National Telecommunications and Information Administration
U.S. Department of Commerce
325 Broadway ITS.N1
Boulder, CO 80303-3328
United States

The work presented in this paper was supported by the National Institute of Justice of the U.S. Department of Justice as part of their Technology Assessment Program.

ABSTRACT

Amplitude companded sideband (ACSB) is a new modulation technique that uses a much smaller channel width than does conventional frequency modulation (FM). Among the requirements of a mobile communications system is adequate speech intelligibility. This paper explores this aspect of "minimum required performance." First, the basic principles of ACSB are described, with emphasis on those features that affect speech quality. Second, the appropriate performance measures for ACSB are reviewed. Third, a subjective voice quality scoring method is used to determine the values of the performance measures that equate to the minimum level of intelligibility. It is assumed that the intelligibility of an FM system operating at 12 dB SINAD represents that minimum. It was determined that ACSB operating at 12 dB SINAD with an audio-to-pilot ratio of 10 dB provides approximately the same intelligibility as FM operating at 12 dB SINAD.

INTRODUCTION

The underlying impetus for this work is the growing crowding of the frequency spectrum for mobile radio users. Since the use of less bandwidth per channel is an apparently obvious way to reduce crowding, there has been increased interest in recent years in "narrowband technologies." The advantages of narrowband techniques are of considerable importance in the Mobile Satellite Service (MSS) as well as the land mobile services, since maximum utilization must be made of a limited spectrum allocation. Both analog and digital techniques

have been explored for possible use in MSS applications. ACSB is an analog technique that requires only a fraction of the channel width required by frequency modulation (FM). While a narrow channel width may contribute to spectrum efficiency, a wide channel width may contribute to voice quality. The goal, therefore, has been to find a modulation scheme that increases spectrum efficiency and retains the voice-quality level that mobile radio users require.

The purpose of the work reported herein is to identify the appropriate performance measures for ACSB, and to determine the values of such measures that represent the minimum level of acceptable performance. Many aspects of performance were considered. These include spectrum efficiency, propagation range, application flexibility, noise susceptibility, and voice quality. In this paper some of these are discussed, but the focus is on voice quality. The minimum level of acceptable voice-quality performance for ACSB is chosen to be the same as the minimum level of acceptable performance for FM, and the quantifiable aspect of voice quality used to represent this performance is chosen to be intelligibility as represented by the articulation score (AS).

In what follows, a brief technological description of ACSB is given and the applicable voice quality measures are described. Last, the measurements made to determine the values of the chosen performance measures are described.

HISTORY OF ACSB

Early research and development of ACSB was sponsored by the Federal Communications Commission. Much of this early work was done by Bruce Lusignan and others at the Communication Satellite Planning Center at Stanford University. Based on this work, the FCC issued a Notice of Inquiry (NOI) to solicit comments regarding the introduction of narrowband technology into the land mobile bands (FCC, 1980). The responses ranged from strong support for ACSB to claims that the Stanford study was incomplete. Other comments indicated that more investigation was necessary and that the spectrum efficiency was not well defined. In spite of the controversy, it was clear that narrowband technology was a better answer to the need for more land mobile channels than to allocate more spectrum. Following this NOI, the FCC allowed developmental licensing of ACSB stations in the 150 MHz land mobile band.

A Notice of Proposed Rulemaking (NPRM) released later proposed 5-kHz channel assignments in the 150 MHz land mobile band. This NPRM resulted in the adoption of 5 kHz channels with an offset of 2.5 kHz, and amendments were made to Part 90 of the FCC Rules and Regulations (FCC, 1985a). This action authorized permanent licensing (as opposed to developmental licensing) of private land mobile stations using narrowband technology.

FUNCTIONAL DESCRIPTION OF ACSB

ACSB is a form of single-sideband suppressed carrier (SSBSC) modulation. The main advantages of SSBSC are its efficient use of the

frequency spectrum and superior signal-to-noise characteristics compared to conventional double sideband amplitude modulation (AM). Since SSBSC uses only one of the two sidebands generated in AM, the bandwidth required is only the bandwidth of the voice frequencies. Since no carrier is generated in SSBSC, the transmitter has no power output until it is modulated. Also, all power is concentrated in the sideband, where the information is contained. This factor, combined with the narrower bandwidth, leads to superior signal-to-noise characteristics (for the same transmitter power) for the demodulated signal of SSBSC as compared to AM.

While the absence of the carrier contributes to the superior signal-to-noise characteristics, it is a major drawback of SSBSC. Since no carrier is received, one must be reinserted by the receiver in order to demodulate the signal, and if the reinserted carrier is not precisely on frequency, the result will be serious distortion of the demodulated signal. The voice frequencies will be offset in frequency by the amount of the error in the frequency of the carrier that is reinserted. Since ACSB transmits a pilot tone as a frequency reference, this problem is eliminated.

The ACSB equipment currently manufactured in the United States uses a tone-above-band pilot at 3100 Hz. Figure 1a illustrates an idealized frequency spectrum of an ACSB transmitter in the currently accepted format. Figure 1b illustrates the frequency spectrum of the same transmitter, but with a 1-kHz tone audio input.

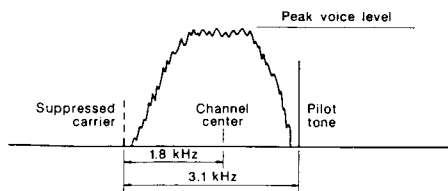


Figure 1a.

Idealized emission spectrum of an ACSB signal illustrating the envelope of voice modulation. The nominal range of the voice band is from 300 to 3,000 Hz.

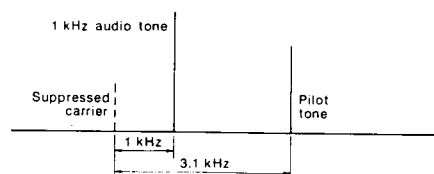


Figure 1b.

Idealized emission spectrum of an ACSB signal modulated with a 1-kHz tone.

Besides providing an accurate frequency reference for the receiver, the pilot tone also may provide:

1. automatic gain control at rf and/or IF,
2. squelch,
3. selective signaling, and
4. expander gain control (feed forward gain control).

ACSB uses syllabic companding in addition to the pilot tone. The term "compand" is a combination of two other words: compress and

expand. A compandor is a device that performs companding functions. It should be noted that the term "compandored" is often used and that it means the same thing as companded. The term companded is used throughout this report. Compression (and pre-emphasis) occurs in the audio circuits of the transmitter and expansion (and de-emphasis) occurs in the audio circuits of the receiver. The term "syllabic companding" implies that the compression and expansion response times are consistent with the syllabic rates in speech. The system currently employed by manufacturers of ACSB land mobile equipment in the United States uses two stages of 2-to-1 compression in the transmitter and two stages of 2-to-1 expansion in the receiver. Figure 2 illustrates this companding with the introduction of noise in the transmission path. The dynamic range of the illustrated signal

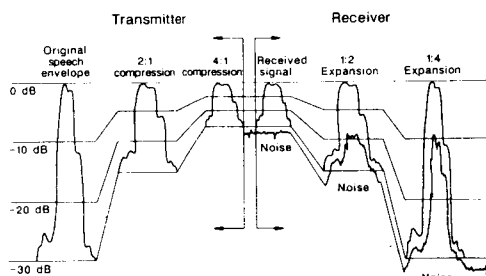


Figure 2. Effect of ACSB Expansion.

(consider it to be a syllable) is 30 dB at the input to the first compressor. The dynamic range of the signal leaving the first compressor is 15 dB. Next, the signal enters the second compressor; the signal leaving the second compressor has a dynamic range of only 7.5 dB--1/4 of that entering the first compressor. The effect of reducing the dynamic range of the signal is to increase significantly the median level.

The received signal-to-noise ratio is improved by the use of compression, and the dynamic range of the audio signal is restored by expansion. Expansion does not improve the signal-to-noise ratio because the instantaneous expander gain must be applied to both the signal and the noise at the same time.

Figures 3 and 4 are simplified block diagrams of an ACSB transmitter and receiver, respectively. The block diagram for the transmitter shows the locations of the two compressors and the injection of the pilot tone before the second compressor. The receiver block diagram shows the locations of the two expanders and the processing of the pilot tone to provide frequency lock, automatic gain control, and expander gain control.

Using a computer model based on these block diagrams, some simple results may be obtained. Figure 5 shows a comparison of the emitted rf power contained in the information sidebands for ACSB and SSBSC. This shows the effect companding has on the output power. Figure 6 shows the relative amounts of rf power contained in the information sideband and the pilot for ACSB.

PERFORMANCE CRITERIA

The ultimate goal in setting specifications for equipment is to determine if the equipment performs as expected by the user. Determining precisely what is expected is not possible for each piece of equipment and every user. Therefore, the specifications are usually given in terms of parameters that are user-oriented either by design

ORIGINAL PAGE IS
OF POOR QUALITY

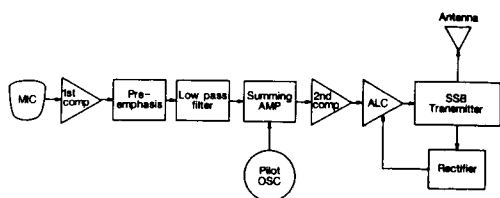


Figure 3.
Simplified ACSB transmitter block
diagram.

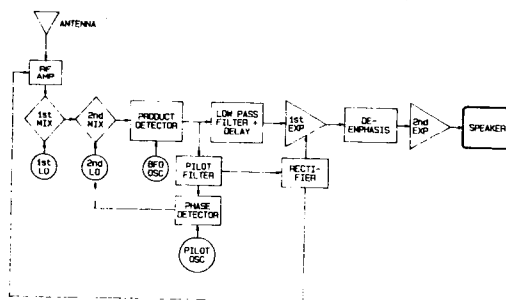


Figure 4.
Simplified ACSB receiver block
diagram.

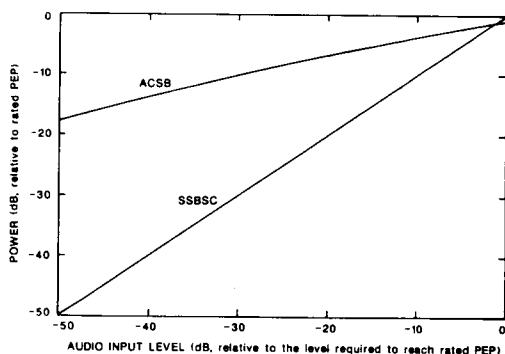


Figure 5.
The rf power contained in the
information sidebands of ACSB and
SSBSC vs. audio input level.

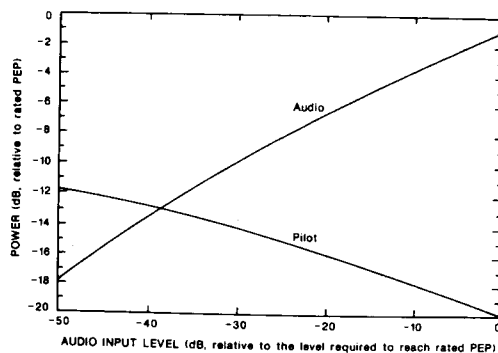


Figure 6.
The rf power contained in the
audio component and the pilot vs.
audio input level.

or by becoming accepted due to a long period of use. In this study, the use of the subjective intelligibility testing procedure using phonetically balanced word lists and trained listener panels is chosen as the user-oriented measure (ANSI, 1960).

The subjective tests are usually too expensive to be used for routine specification testing, so an objective measure that can be related to the subjective tests is required. Here, SINAD is proposed because it includes interference and distortion.

SINAD--the objective measure to be used in these tests--is the acronym for

$$\text{SINAD} = 10 \log \frac{s + n + d}{n + d} \text{ dB}$$

where s = signal
n = noise
d = distortion

The relationships between the subjective and objective measures for both ACSB and FM are shown in the illustration of Figure 7. A thorough review of all the subjective and objective measures is not possible in this paper so the discussion is limited to the chosen subjective and objective measures.

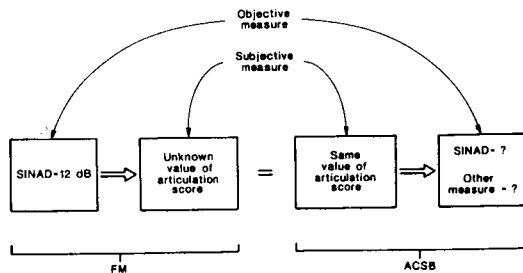


Figure 7.
Relationships between the known and unknown measures for FM and ACSB showing the role of subjective articulation scoring.

It is easy to design a subjective measure for the purpose of specifying the performance of a voice channel. However, the paucity of good designs that include detailed protocol for the testing presents a tremendous obstacle to the understanding and acceptance of voice-performance measures. For our purposes, a subjective measure must be selected that can be related to some objective measure since using subjective measures for acceptance testing has proved to be expensive.

Subjective testing is reviewed in Nesenbergs et al. (1981). The types of tests that have been used are too numerous to be covered here. The two types of testing that have gained credibility are first, the intelligibility tests, and a distant second, the diagnostic tests such as the diagnostic rhyme test (House, 1965).

Since the goal is to determine the acceptability of equipment performance but not the reason that the performance is acceptable or unacceptable, and because of the high costs, the diagnostic tests were eliminated from further consideration. Even though some of the diagnostic tests measure characteristics other than intelligibility, there is little evidence that these measures are useful for predicting user acceptability for systems that use analog modulation. Thus, the relatively simple intelligibility testing using the phonetically balanced (PB) word lists and trained listener panels was used.

The phonetically balanced word lists are divided into word groups of 50 words. These word groups are recorded using several male and female talkers so that one 50-word group represents a cross section of the talkers. The talkers are carefully chosen, usually from radio broadcasters and the recordings are done under studio conditions with the recording level on the tape carefully controlled.

The articulation scoring is done by the U.S. Army Electronic Proving Ground, Ft. Huachuca, AZ. The procedure uses 50-word phonetically balanced word groups, selected and trained listener panels, and computerized analysis of responses. The results are generally accepted as accurate and repeatable and thus suitable for comparison to objective measures (Nesenbergs et al. 1981). Because of the structured nature of the test, and the psychological nature of speech perception, the results may not be conveniently applicable to a user perception of "real life" requirements. However, the testing and

interpretation have displayed a longevity indicating a degree of usefulness that is not easily measured.

In most cases, the signal is a 1-kHz tone which is used as input to the baseband of the transmitter. If the methods of making the measurements are specified, SINAD represents a measurement which is repeatable.

A rather interesting finding is indicated in Figures 8 and 9. Figure 8 shows that at a given audio component signal strength the SINAD of unit A is dependent on the audio-to-pilot ratio. However, in Figure 9 it is seen that for a given audio component signal strength the SINAD of unit B is relatively independent of the audio-to-pilot ratio. This difference in performance apparently results from the use of a more narrow pilot filter in unit B.

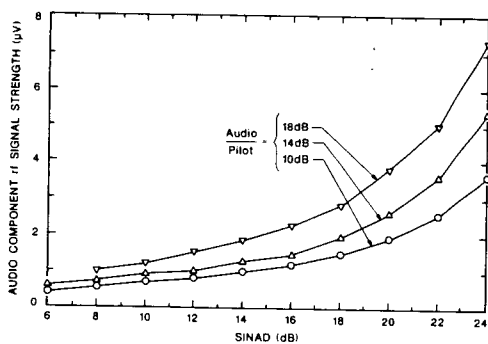


Figure 8.

Measured SINAD vs. audio component rf signal strength for unit A.

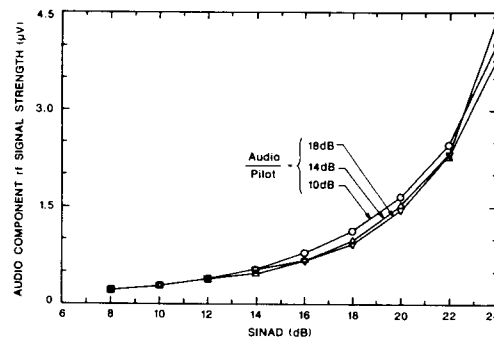


Figure 9.

Measured SINAD vs. audio component rf signal strength for unit B.

CONCLUSIONS

From Figure 8 we see that for some ACSB receivers, SINAD is significantly dependent on the audio-to-pilot ratio. Therefore, the SINAD sensitivity for ACSB radios should be specified at a particular audio-to-pilot ratio. The articulation scores versus SINAD (audio-to-pilot ratio of 10 dB) for the two ACSB radios are plotted on Figure 10. The results for the FM radios are plotted on Figure 10. At 12 dB SINAD the articulation scores for the two FM radios are very nearly the same, and if these are averaged, the result is 88.6%. The articulation scores for the two ACSB radios are not the same, but if they are averaged the result, 88.5%, is very close to the average for the two FM radios. The analysis easily leads to the following conclusion: ACSB operating at 12 dB SINAD with an audio-to-pilot ratio of 10 dB provides very nearly the same intelligibility as FM operating at 12 dB SINAD.

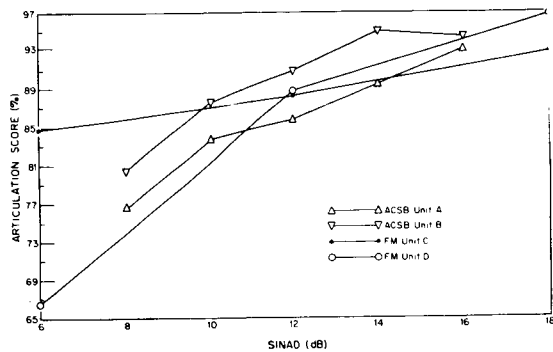


Figure 10.
 Articulation score vs. SINAD for
 ACSB operating at 10 dB audio-to-
 pilot ratio compared to FM.

REFERENCES

- ANSI 1960. Method for measuring monosyllabic word intelligibility, American National Standards Institute, 10 East 40th Street, New York, NY.
- FCC 1980. Notice of Inquiry, PR Docket 80-440, Adopted August 1, 1980, Released September 9, 1980.
- FCC 1985a. Report and Order, PR Docket 84-279, Adopted March 1, 1985, Released March 29, 1985.
- House, A. S., C. Williams, M. H. L. Hecker, and K. D. Kryter, 1965. Psychoacoustic speech tests: a modified rhyme test, ESD-TDR-63-403, Hanscom Field, Bedford, MA.
- Nesenbergs, M., W. J. Hartman, and R. F. Linfield, 1981. Performance parameters for digital and analog services modes, NTIA Report 81-57.

A Study on the Co- and Adjacent Channel Protection Requirements for Mobile
Satellite ACSSB Modulation

JOHN T. SYDOR, Mobile Satellite Program, Communications Canada

COMMUNICATIONS RESEARCH CENTRE
3701 Carling Avenue
PO Box 11490, Station 'H'
Ottawa, Ontario, Canada K2H 8S2

ABSTRACT

Samples of speech modulated by NBFM (cellular) and ACSSB radios were subjected to simulated co- and adjacent channel interference environments typical of proposed FDMA mobile satellite systems. These samples were then listened to by a group of evaluators whose subjective responses to the samples were used to produce a series of graphs showing the relationship between subjective acceptability, C/No, C/I, and frequency offset. The results show that in a mobile satellite environment, ACSSB deteriorates more slowly than NBFM. The co- and adjacent channel protection ratios for both modulation techniques were roughly the same, even though the mechanism for signal deterioration is different.

INTRODUCTION

Previous studies conducted by the Communications Research Centre (CRC) have shown that ACSSB is a robust modulation technique capable of providing high quality voice communications in low C/No mobile satellite propagation environments (Ref. 1). The next logical step was to examine ACSSB performance under conditions of co- and adjacent channel interference. Understanding how ACSSB behaves under such conditions would provide mobile satellite engineers with design parameters and give insight into questions regarding frequency reuse, channel spacing, satellite antenna design, and ultimately, user loading levels on ACSSB/FDMA mobile satellite systems.

TEST SET UP AND SUBJECTIVE TESTING METHODOLOGY

The purpose of the experimental set up shown in Figure 1 was to model the return link of a mobile satellite system. The set up was intended to simulate a link where two terminals transmit over independently varying propagation paths and interfere with one another at a common base station on a co- and adjacent channel basis. Desired and interfering signals were controlled in both amplitude (± 1 dB) and frequency (± 1 Hz), and transmitted over separate propagation paths prior to their summation, demodulation, and taping for subjective evaluation. Propagation path conditions for both the desired and interfering signals were controlled by two independent simulators which could statistically emulate Rician propagation (Fig.2) and noise characteristic of mobile satellite environments. System linearity was such that the worst case two tone third order

intermodulation products were -31 dBc or better for any test condition.

Speech samples for subjective evaluation were created by recording Harvard sentence pairs that had been passed through the experimental set up and corrupted with known amounts of thermal noise and co- and adjacent channel interference. The recorded samples were randomized and played to a total of 68 subjects who listened to the samples over standard telephone handsets. Subjects were asked to rate individual samples of speech as bad, poor, fair, good, or excellent. The five opinion categories were assigned numerical values from 1 (bad) to 5 (excellent). Responses to a particular sample of speech (and test interference test condition) were averaged over the population of subjects, thereby generating a Mean Opinion Score (MOS) for that condition. This subjective test procedure was based on the Absolute Category Rating (ACR) method defined in Annex A of Ref. 2.

SIGNAL CALIBRATION

The ACSSB modems used for this study were developed in-house at CRC. The DSP modulation algorithms for these modems have been optimized for satellite propagation conditions. The modems use the general concepts of transparent tone-in-band and feed forward signal regeneration for SSB speech modulation (Refs. 3,4). Figure 4 shows the baseband ACSSB spectrum.

The NBFM modems used for these tests came as part of two Motorola DynaTac™ 2000 cellular telephones. These are commercially available radio transceivers with performance optimized for 800 MHz terrestrial cellular operation. It was decided to use these transceivers because they represent an acceptable standard of performance by virtue of their widespread use. A test-tone to noise test was conducted on these radios and performance, as a function of C/No, is shown in Figure 3. The audio frequency responses of the ACSSB and NBFM terminals were approximately equal. The -6 dB bandwidth of the NBFM was 300 to 3100 Hz. The ACSSB -6 dB bandwidth was approximately 300 to 3000 Hz.

Throughout the experiment there was an effort to ensure that signal modulation levels were kept constant and within realistic limits. With the NBFM modulator the amplitude of the input speech was set so that peak deviation would not exceed 12 kHz. Nominally, the average deviation was 4-6 kHz. The power of the NBFM signal was easy to monitor and control because of its constant envelope characteristic.

The ACSSB spectrum has an envelope that varies in proportion to the input speech. Measurement of average carrier power requires a technique which samples and averages the carrier envelope power over a period of time during which speech is continuous. To do this, a sampling system was devised which used a spectrum analyzer to view the ACSSB spectrum through a 10 kHz resolution bandwidth filter. The detected spectrum was rectified and passed through a video filter having a width of 30 to 300 Hz. The resultant output was the ACSSB envelope which varied at the syllabic rate (this output is called the short term mean power of the speech signal, Ref. 5). The envelope was sampled at 1000 Hz by a digital voltmeter and the resultant samples were stored on disk for analysis.

The sampled data was analyzed by a computer program which calculated the difference in mean power between an ACSSB signal containing speech and pilot tones and an ACSSB signal containing only pilot tones. The pilot tone ACSSB signal had a constant envelope, and its absolute power was easily measured using conventional power measurement techniques. With the absolute measurement and the relative difference in the mean power of the

two ACSSB signals, it was possible to calculate the absolute, short term mean power of the ACSSB speech signal.

With the CRC ACSSB modems the mean power of an ACSSB signal containing speech and pilot tones was approximately 3 dB above the power of an ACSSB signal containing only pilot tones. It should be noted that within this study, ACSSB carrier power is defined as the mean power of the signal containing continuous speech. For the propagation environments, all carrier powers are specified at unfaded levels.

TEST RESULTS AND ANALYSIS

Figure 5 compares the performance of ACSSB and NBFM in a static environment. As can be seen, the best ACSSB performance is achieved at a C/No between 50 and 55 dB-Hz. Above 55 dB-Hz the ACSSB performance will not improve because digital signal processing noise of the modem dominates the thermal noise of the channel. This limitation is a constraint due to equipment. More recent implementations of ACSSB have exceeded this limit. Below 50 dB-Hz, ACSSB static performance degrades slowly to a MOS of 3 at 45 dB-Hz.

NBFM deteriorates only slightly under Rician propagation providing the C/No is high (compare Figs. 5 and 7). However, if the signal level is lowered from 65 to 58 or 51 dB-Hz, the effects of propagation become quickly apparent. The rapid deterioration of NBFM is attributed to the threshold effect common to this modulation. NBFM signals undergoing Rician propagation are driven below threshold, causing a rapid drop in the baseband S/N. For the cellular transceivers, a 2 dB variation of the C/No at approximately 60 dB-Hz will result in a 2-3 dB degradation of output S/N. At 53 dB-Hz, such a variation will result in a 6 dB degradation (see Fig.3).

ACSSB deteriorates in a slower, more linear fashion and does not exhibit a threshold like NBFM. As C/No is reduced, the subjective acceptability of ACSSB in a Rician environment drops slowly and shows less of a dependence on signal strength than NBFM. This is seen in the variation in MOS of Rician ACSSB between 51 and 45 dB-Hz.

With ACSSB the most significant source of deterioration is due to the propagation channel. Comparing static ACSSB to Rician ACSSB at 51 dB-Hz, there is almost a one opinion category drop (i.e. from "good" MOS of 4.0 to "fair" of 3.0). This drop can be attributed to several factors, one of these being the decrease in mean signal power which drops by 2.5 dB in the Rician environment from its static unfaded value. A second source of degradation that is evident in a Rician environment (and is non-existent in the static case) are the instances where the received signal has deep fading (Fig.2). Deep fades are compensated by the ACSSB demodulator but their duration is such that there is a noticeable effect on perceived quality.

With both ACSSB and NBFM, the effects of co-channel interference become noticeable at a C/I of approximately 15 dB (see Figs. 6 and 7). The general mechanism of deterioration is due to the energy of the interference adding to the thermal noise of the channel. With ACSSB this is more pronounced if the interfering signal falls directly on top of the desired signal, corrupting the pilot tones carrying the companding information. Even at the relatively low C/I levels of 20 dB one can see a difference in MOS when the interfering signal falls directly on top of the desired signal and when it is offset by several hundred Hertz (see Fig.9 with $\Delta F=0$ Hz).

Figures 8 and 9 show the effect adjacent channel interference has on the NBFM and ACSSB demodulators. Both figures show that the desired signals' performance deteriorates as a function of interferer power and frequency.

It is interesting to note that the response of ACSSB to adjacent channel interference is non-symmetric. This is due to the power of an ACSSB signal being unevenly distributed around the pilot tones (see Fig. 4). An ACSSB interferer overlapping the desired signal on the positive frequency side will result in the relatively high power low frequency components of the interfering signal overlapping the low power high frequency components of the desired signal. Conversely, when the interferer approaches from the negative frequency side, the low power high frequency components interfere with the desired signals' high power low frequency components. The result of this is that the perceived S/N will be lower in the former case. This is borne out by the results shown in Figure 9: for the same magnitude of frequency offset, mean opinion scores are slightly better on the negative frequency offset side.

CONCLUSIONS

The purpose of this study was to determine protection ratios for ACSSB modulation operating under co- and adjacent interference conditions in a Rician propagation environment. For the purpose of this study, protection ratio is defined as the C/I at which the quality of the desired signal deteriorates by 0.5 MOS units from the condition where no interferer is present. Using this definition, the protection ratio for co-channel interference in a Rician environment for ACSSB is approximately 11 to 13 dB. Cellular NBFM requirements under identical conditions is about the same. The estimated adjacent channel protection ratio for ACSSB in a Rician environment is -12 to -15 dB for interferers one channel spacing higher in frequency than the desired signal and -15 dB for interferers one spacing lower. For cellular NBFM the ratio is -12 to -15 dB.

ACKNOWLEDGEMENTS

I would like to thank my colleagues at CRC for their help in undertaking this experiment and the participants from the Department of Communications and Telesat Canada who volunteered their services as evaluators. Special thanks to Barbara-Anne Chalmers at DOC/CRC for helping pull this work together.

REFERENCES

1. Morris, S.C., December 1985, A subjective evaluation of the voice quality of MSAT modulation schemes, Bell Northern Research Report OCTR 85-0006
2. CCITT Supplement No.14-Subjective Performance assessment of digital processes using the modulated noise reference unit (MNRU), CCITT Red Book, Vol. 5, Malaga, 1984
3. McGeehan, J.P. and Bateman A.J., 1983, Theoretical and experimental investigation of feedforward signal regeneration (FFSR) as a means of combatting multipath propagation effects in pilot based SSB mobile radio systems, 1983 IEEE Transactions on Vehicular Technology, vol. VT-32, February 1983, Pages 106-120
4. Lodge, J. and Boudreau, D. 1986. The implementation and performance of narrow band modulation techniques for mobile satellite applications, IEEE International Conference on Communications, Toronto 1986, Conference Record, Volume 3, Pages 44.6.1-44.6.7.
5. Richards D.L., May, 1964, Statistical properties of speech signals, Proceedings of the IEE, Vol. III, No. 5, Pages 941-949

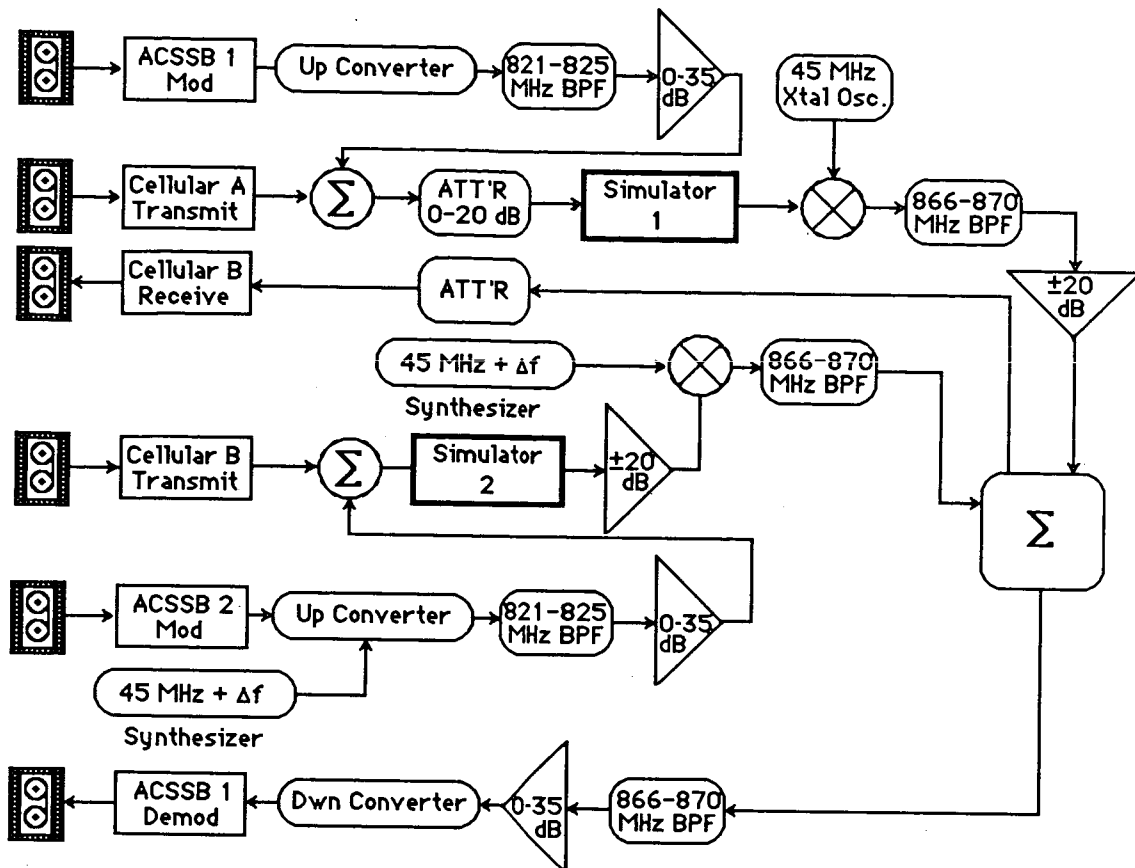


Fig 1. Test set up.

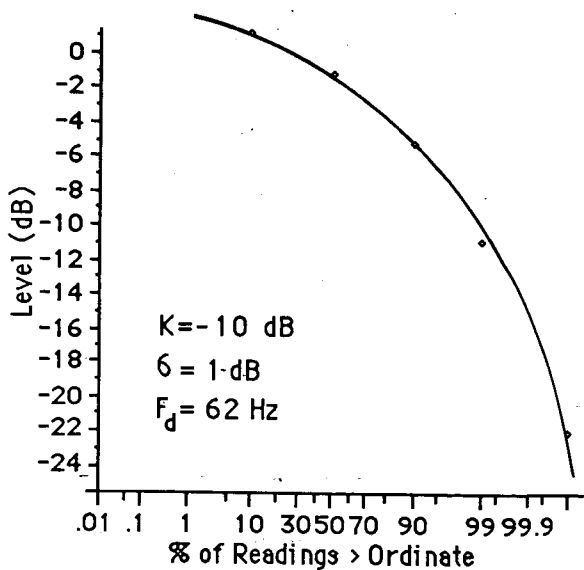


Fig.2 Cumulative Distribution Function for Rician Fading

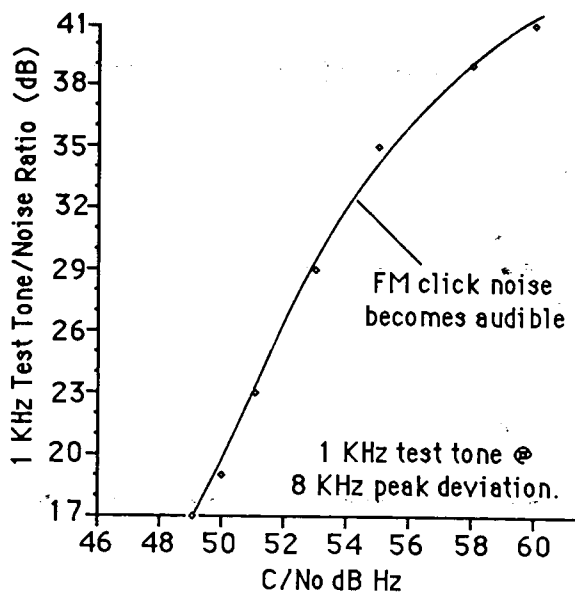


Fig. 3 Test Tone to Noise Ratio vs. C/No Performance for the Cellular FM Transceivers

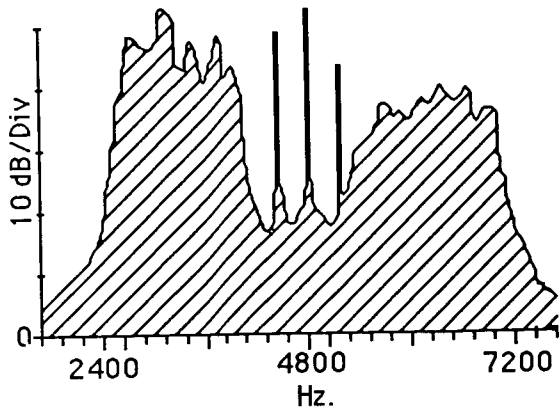


Fig. 4 Base Band ACSSB Spectrum

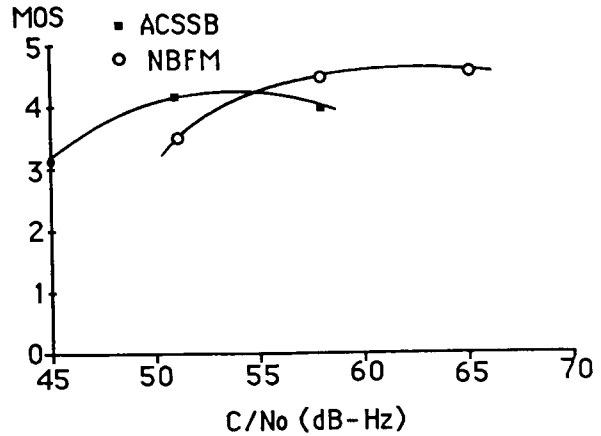


Fig. 5 ACSSB and NBFM Performance Static Environment No Interference $C/I = \infty$

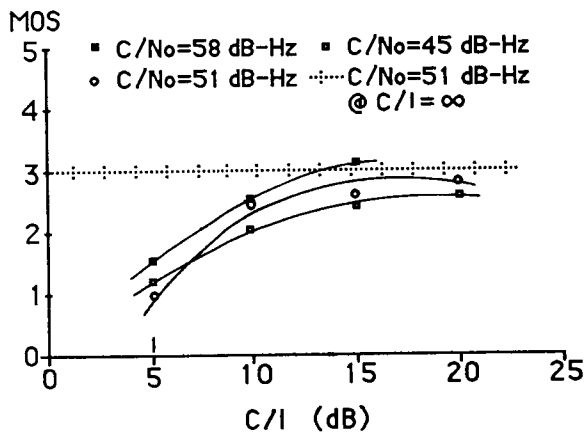


Fig. 6 ACSSB Co-Channel Performance Rician Propagation Environment

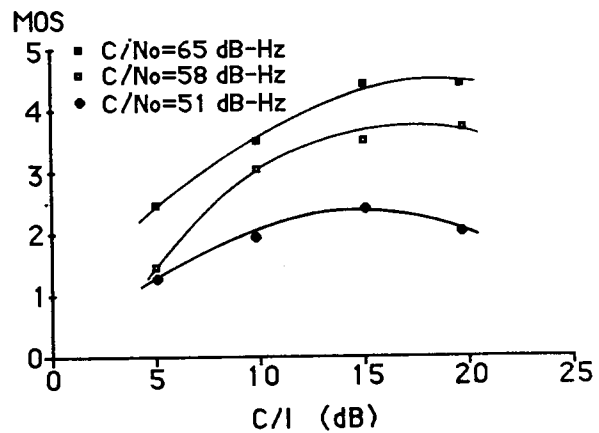


Fig. 7 NBFM Co-Channel Performance Rician Propagation Environment

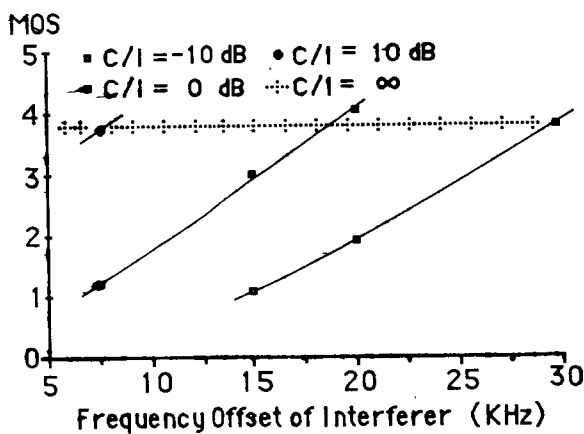


Fig. 8 NBFM Adjacent Channel Performance Rician Propagation Environment with $C/No = 58$ dB-Hz

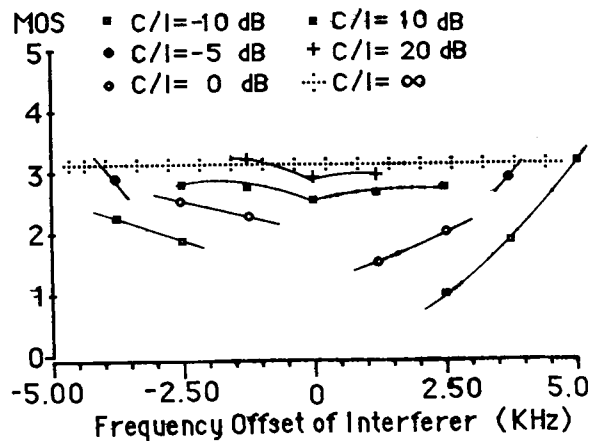


Fig. 9 ACSSB Adjacent Channel Performance Rician Propagation Environment with $C/No = 51$ dB-Hz

SESSION H
NETWORKING

SESSION CHAIR: Harry Tan, University of California, Irvine
SESSION ORGANIZER: Tsun-Yee Yan, Jet Propulsion Laboratory

A FRAMEWORK FOR IMPLEMENTING DATA SERVICES IN MULTI-SERVICE MOBILE SATELLITE SYSTEMS

MOHAMMED O. ALI, MPR Limited, Canada; DR. VICTOR C.M. LEUNG, The Chinese University of Hong Kong, Hong Kong; ANDREW I. SPOLSKY, MPR Limited, Canada.

MICROTEL PACIFIC RESEARCH LIMITED

8999 Nelson Way
Burnaby, B.C. V5A 4B5
Canada

ABSTRACT

Mobile satellite systems being planned for introduction in the early 1990's are expected to be invariably of the multi-service type. Mobile Telephone Service (MTS), Mobile Radio Service (MRS), and Mobile Data Service (MDS) are the major classifications used to categorize the many user applications to be supported. The MTS and MRS services encompass circuit-switched voice communication applications, and may be efficiently implemented using a centralized Demand-Assigned Multiple Access (DAMA) scheme. Applications under the MDS category are, on the other hand, message-oriented and expected to vary widely in characteristics; from simplex mode short messaging applications to long duration, full-duplex interactive data communication and large file transfer applications. For some applications under this service category, the conventional circuit-based DAMA scheme may prove highly inefficient due to the long time required to set up and establish communication links relative to the actual message transmission time. It is proposed that by defining a set of basic bearer services to be supported in MDS and optimizing their transmission and access schemes independent of the MTS and MRS services, the MDS applications can be more efficiently integrated into the multi-service design of mobile satellite systems.

INTRODUCTION

Mobile satellite systems (MSS) being planned for introduction early in the next decade are expected to support wide-area MTS, MRS, and MDS services. MTS and MRS will support voice communication applications, with subscribers in the MTS service allowed direct access to and from the public switched telephone network (PSTN) in much the same way as possible with terrestrial-based cellular mobile services. Gateway Stations are the ground segment network elements which will

interface MTS service subscribers to the PSTN.

MRS, on the other hand, will be tailored to private networks of closed user groups and will not provide direct access to the PSTN. A typical private MRS network will consist of a number of mobile user terminals and a single-channel Base Station through which communication links will be established. The Base Station will normally interface to the private organization's dispatch console or a PBX, as required in the individual application.

Plans for first generation MSS systems suggest that the MTS and MRS services will be provided through circuit-switched voice connections, under the control of a centralized DAMA system. Because of the high unevenness in the sources of traffic in a typical MRS network (i.e. several mobile terminals accessing a limited capacity Base Station), a large number of requests from mobile terminals will encounter blockage due to the Base Station being busy on another call. For this reason, the DAMA scheme for MRS service should ideally be capable of handling call attempts from mobile terminals on a blocked-calls-queued basis. The queuing in this case will be for establishing order in the processing of multiple requests to the same destination rather than as a means of handling lack of channels in the system.

MDS is intended to provide data communication capabilities between a customer's facility and mobile or portable terminals belonging to the same private network. A variety of data communication applications have been proposed for first generation MSS systems including, but not limited to: interactive digital messaging (including vehicle dispatch), paging, vehicle location, data acquisition and control, data collection, data broadcast, and bulk data transfer (data, image, text). Data Hubs are the network elements which have been designated to support applications under the MDS category. Typically, these facilities will be shared among many private data networks, with data links being established between the Hub station and individual organizations. Where required, access to public data networks (e.g. Datapac, Dataroute) will be provided through these stations.

Mobile and portable terminals will be developed to support applications under the three service categories. Although terminals for the MTS and MRS services are expected to be capable of in-band data transmission on a circuit-switched basis, applications falling under the MDS category are planned to be supported through data-only terminals with capability for operating on packet-switched connections. Different types of MDS terminals may be required to economically accommodate the anticipated wide range of data communication applications.

ALTERNATIVES FOR IMPLEMENTING THE MDS SERVICE

Unlike the MTS and MRS services, the networking plan and control facilities for supporting applications under the MDS service have, for the most part, not been clearly defined. Some proposals have been put forward to try to establish the manner in which these applications will be accommodated in the multi-service architecture of first generation MSS systems. A number of existing proposals appear to favour an

integrated approach to implementing the three services. The most popular ones are discussed below.

Use of a Common DAMA Scheme for Voice and Data Services

One alternative proposed for accommodating the MDS service is to use the control facilities of the MTS and MRS services to support the planned data communication applications. Under this option, MDS calls are handled in a similar fashion as voice calls, where a communication channel is assigned for each request and considered in use until relinquished by the parties on the channel.

Regardless of the criteria used to relinquish communication channels, there are some basic disadvantages to using DAMA-assigned channels for packet-based messaging. If connections are setup and torn down on a per-message basis, the overhead requirements will significantly lower the data handling capacity of the system. If, instead, connections are maintained on a per-session basis, too much idle time will result between successive transmissions. Furthermore, in systems where data services are provided through circuit-switched connections, service billing is generally based on the total channel holding time rather than on the volume of data transferred. This can be very expensive for some data users.

Use of Common Facilities for Voice and Data Calls

A variation of the above method is where data and voice calls are interspersed on the same set of available communication channels. Under this approach, data calls are assigned to idle communication channels on a single-transmission-per-request basis with preassigned transmission start and end times (i.e. using closed-end channels). Voice calls are assigned idle communication channels on an open-ended basis. A data call request which is received when all communication channels are in use carrying a mixture of open-ended and closed-end calls is queued up for a closed-end channel with the shortest delay, and assigned a transmission start time to permit completion of the data call.

Although this integrated approach has the potential to increase the overall communication channel utilization efficiency, complex timing manipulations will be required to handle applications where multi-packet transmissions from the same terminal are necessary or when packet errors occur. Further, if at any point in time the network experiences a high volume of voice traffic, data users will be blanked out or at least severely delayed. Likewise, a peak of high data traffic in the network could cause excessive delays for voice requests. For these reasons, the technique of integrating voice and data traffic in the manner described above may not suffice as a general purpose data communication algorithm to support the proposed MDS applications.

Use of Dedicated Facilities for MDS Applications

A more efficient way of accomodating MDS applications may be through use of dedicated facilities. In one such investigation, an adaptive DAMA scheme for integrated circuit- and packet-oriented services was proposed [Yan, 1986]. Under this

plan, the set of channels in the network is maintained in a pool which is functionally partitioned into sets of request, open-end, and closed-end channels. Voice and data call requests from mobile terminals are sent over the request channels, and the open-end and closed-end channels are assigned on demand to process circuit-oriented and packet-oriented calls, respectively. The partitioning of the available set of system channels is dynamically adjusted by the NCC to minimize the blocking probability of the voice traffic and the total average delay of the data traffic.

With most data messages in the MDS service expected to be short (in the order of 1 kbits), the inherent overhead associated with a DAMA scheme such as proposed will make the technique less efficient in the majority of applications. As well, as with any closed-end allocation scheme, there is the problem of handling errors. Closed-end assignments for data messaging work well only in an error-free channel. In a severe propagation environment such as to be expected in MSS [Lutz, 1986], some ARQ protocols will have to be employed. Messages will either have to be transmitted many times until received error-free, or a new reservation request be issued before each retransmission of an unreceived message. In one case message transmission times will have a large variance and call end times will be difficult to estimate, and in the other, additional channel set-ups and hence overheads will be involved, lowering the capacity of the data channel.

A DECENTRALIZED APPROACH TO PROVIDING THE MDS SERVICE

The majority of proposed MSS implementation schemes appear to try to optimize, on an integrated-services basis and simultaneously, the two sets of resource management problems; i.e. (i) partitioning of bandwidth for the different services, which must be changeable but does not require a high degree of dynamism; and (ii) real-time allocation of resources to users. An examination of the proposed applications indicates that integration of the three services under a common control scheme will at best result in inefficient utilization of channel resources and possibly increased customer dissatisfaction due to potentially long delays in accessing the network.

We therefore propose that the resource management problems be uncoupled such that bandwidth partitioning remains centrally controlled by the network management function at the NCC, but the real-time allocation of channel time in the MDS service is decentralized and managed by the Data Hubs. Further, considering that the many MDS applications could be more adequately and efficiently addressed through further categorization according to traffic characteristics, a set of bearer services is proposed to perform the transportation of data packets between mobile terminals and the Data Hubs. Channel access modes for each bearer service are then proposed to address the individual traffic characteristics and unique requirements of the services.

Proposed Bearer Services

We propose classifying MDS applications under three categories of bearer services:

- full-duplex (FDX) data service,
- inbound simplex (ISX) data service, and
- outbound simplex (OSX) data service.

The FDX service will encompass all two-way data communication applications, including interactive digital messaging, bulk data transmission, data acquisition and control, and vehicle dispatch. The ISX service will cover one-way data transmission applications such as vehicle tracking and location determination, and data collection from remote platforms. The OSX data service will cover point-to-multipoint data applications such as wide area paging and data broadcasting. Future applications can be classified as appropriate under the three bearer services.

Characterization of the Outbound Links

Because of the differences in characteristics among the bearer services, it is anticipated that optimum packet size requirements for the three services will differ. As such, for efficient utilization of the channels and in attempt to minimize the processing complexity at the terminal end, it is recommended that separate outbound channels be provided for the FDX and the OSX data services. These channels will operate in TDM mode, carrying control and synchronization information, and user traffic from the Data Hub. The outbound channel for the OSX data service may also be used to carry acknowledgement messages for the ISX service, if required.

Inbound Link for the Simplex Data Service

Data transmissions from terminals in the ISX service are expected to be of the single-packet type, although the required packet size is yet to be determined. As well, it is expected that traffic from any one data source will be low in volume and periodic in occurrence. Depending on the optimum packet length for applications under this bearer service, TDMA with very long frames may be used for the inbound link, or polling via an outbound channel. This channel may also be used to carry acknowledgement messages for the OSX data service, if required.

Inbound Link for the Full-Duplex Data Service

The FDX service is expected to handle potentially large volumes of data entering the system at infrequent and unscheduled times. For such applications, resource sharing approaches that use fixed allocation of capacity tend to be wasteful and inefficient. It is proposed that for better utilization of the channel resources, the inbound channel for the FDX service be operated with a reservation type multiple access scheme (e.g. reservation ALOHA, Demand-Assigned TDMA) controlled from the Data Hub.

Some duplex data applications may only require the transmission of single packet messages from the terminal end. For these, a contention type multiple access scheme (e.g. slotted ALOHA) may be used to avoid the overhead associated with reservation type schemes.

Network Registration Requirement for MDS Service Terminals

It should be noted that the proposed decoupling of resource management functions in the MDS service is in no way intended to isolate data service terminals from any control by the NCC. On initial power up, all MDS terminals will be required to log-in through the network signalling channel terminating at the NCC, just like the MTS and MRS service terminals. Upon recognizing a data terminal and verifying its validity, the NCC will direct the logged-in terminal to the appropriate data channel terminating at the Data Hub serving the user group. Only then will the terminal be allowed to use the network facilities for data transfers.

SUMMARY AND RECOMMENDATIONS

Applications that are planned to be supported under the MDS service category are many and widely varied in characteristics. An examination of implementation schemes proposed for integrating this service into the multi-service design of MSS systems indicates that no single scheme could adequately and efficiently perform as a general purpose algorithm to serve all applications. By uncoupling the satellite resource management problems and grouping the proposed data applications into three sets of bearer services, a more efficient approach to implementing the MDS service was described. It is recommended that the network-wide transponder bandwidth management function be left centralized at the NCC, but that the real-time allocation of channel time for MDS applications be decentralized and controlled from the Data Hubs.

Under this decentralized implementation proposal, it is further recommended that the FDX data service be provided using a reservation type multiple access scheme (e.g. DA-TDMA) for handling multi-packet messages, and a contention type access scheme (e.g. Slotted ALOHA) for applications using single-packet message transmissions from user terminals. The ISX data service, with single-packet, fairly periodic messaging requirements, may be efficiently accommodated using TDMA or polling, depending on the optimum packet length for this bearer service.

Application studies are currently under way to address the next level of design; i.e. examining specific MDS applications and how they would fit into the proposed bearer services. This will lead into the determination of optimum packet sizes, error control requirements, and expected traffic handling capacities of each service.

REFERENCES

- T.- Y. Yan 1986. Network Design Considerations of A Satellite-based Mobile Communications System. A Collection of Technical Papers: AIAA 11th Communication Satellite Systems Conference. AIAA CP 862, pp. 405-410.
- E. Lutz, et al. Land Mobile Satellite Communication Channel Model, Modulation and Error Control. Proceedings of ICDS-7, pp. 537-541.

L-BAND AND SHF MULTIPLE ACCESS SCHEMES FOR THE MSAT SYSTEM

MICHAEL RAZI, ALIREZA SHOAMANESH, BAHMAN AZARBAR
Telesat Canada, Canada

TELESAT CANADA
333 River Road
Ottawa, Ontario, Canada
K1L 8B9

ABSTRACT

The first generation of the Canadian Mobile Satellite (MSAT) system, planned to be operational in the early 1990s, will provide voice and data services to land, aeronautical, and maritime mobile terminals within the Canadian land mass and its territorial waters. The system will be managed by a centralized Demand Assignment Multiple Access (DAMA) control system. Users will request a communication channel by communicating with the DAMA Control System (DCS) via the appropriate signalling channels.

Several access techniques for both L-band and SHF signalling channels have been investigated. For the L-band, Slotted Aloha (SA) and Reservation Aloha (RA), combined with a token scheme, are discussed here. The results of Telesat studies to date indicate that SA, when combined with token scheme, provides the most efficient access and resource management tool in a mobile propagation environment.

For SHF signalling channels, slim-TDMA and SA have been considered as the most suitable candidate schemes. In view of the operational environment of the SHF links, provision of a very short channel access delay and a relatively high packet success rate are highly desirable. Studies carried out generally favour slim-TDMA as the most suitable approach for SHF signalling channels.

1.0 INTRODUCTION

Communication Services within urban centres and surrounding areas are readily available using terrestrial and fixed satellite systems. Recently, the demand for reliable nationwide mobile communications in rural areas has significantly increased. This paper briefly introduces Telesat's baseline networking concept and control architecture as foreseen for provision of Mobile Satellite (MSAT) services. The emphasis is placed on the various multiple access schemes contemplated for interconnecting the network elements as are presently defined. These schemes are tailored to satisfy the projected Canadian needs, while being in harmony with the present state of the relevant technology.

2.0 BACKGROUND

MSAT is intended to provide cost effective, spectrally efficient services for voice and data communications across Canada. There will be a large number of mobile users, each characterized by bursty traffic and a low activity factor; therefore, the system's available spectrum will best be utilized by a Demand Assignment Multiple Access (DAMA) control system.

The DAMA Control System (DCS) will be responsible for network supervision and providing interconnection among various network elements such as mobile terminals, base stations, and gateways. It will also be communicating with the network management system, responsible for long-term resource planning, overall supervision and maintenance of the system.

The major categories of service that have been identified to date as potential applications for MSAT upon its introduction are: a) Mobile Radio Service (MRS) targetting mobile communities of various sizes consisting of one or more base stations (dispatch centres) and a number of MRS terminals; b) Mobile Telephone Service (MTS) destined for mobile users requiring Public Switched Telephone Network (PSTN) interconnectivity, via gateway stations; c) MSAT Data Services (MDS) for users with one-way or two-way data transmission requirements; and d) MSAT Aeronautical and Marine Services.

To provide these services, two distinct types of channels are required within the pool of MSAT channels:

- Communication channels used by all the users to transmit and receive voice or data, and
- Signalling channels used by all the users as well as the DCS to transmit and receive call requests/responses, commands, etc.

The signalling among the DCS, gateways, and base stations will be over the SHF-SHF links (or in some cases they may interface using terrestrial links). For mobile terminals, signalling will be via L-band-SHF links to the DCS.

It should be noted that packet switched data communications would be provided by data hubs using slim-TDMA channels. These channels will be assigned dynamically to data hubs from the pool of MSAT channels; however, circuit switched data communications would be treated the same as the voice channels. The study of packet switched data services will not be addressed here.

3.0 ACCESS SCHEMES

Different access techniques for both L-band and SHF signalling channels have been investigated. The request and assignment channels will form the major interface between the user and the MSAT DCS. As a result, it will be critical that their operation satisfies the criteria imposed by both the user and the system requirements. In comparing various access schemes, the degree with which the following design objectives are met by each approach should be carefully quantified:

- Minimizing the number of signalling channels;

- Minimizing the call set-up/take-down delay;
- Ensuring stability of the channels; and
- Minimizing mobile terminal complexity.

Furthermore, there are two more important resource management issues to be assessed before defining selection criteria.

First, it is highly desirable to assign a communication channel when the called party goes off hook, as opposed to assigning a channel upon a call request and waiting for the called party's response. Such a deferred communications channel assignment approach will result in significant savings in the scarce satellite power and bandwidth.

Second, the size of the packets on the signalling channels has a direct relationship with the number of signalling channels required to support the traffic generated by the MSAT users. A packet consists of information bits, overhead bits, and guard time. Presently, a packet size of 150 bits[1] appears to be sufficient for MSAT system.

3.1 L-Band Signalling Channels

For the L-band signalling channels, Slotted Aloha (SA) and Reservation Aloha (RA), combined with a token scheme, have been investigated and their performances are described here. The L-band signalling channels are divided into three categories:

- Request channels will be used by mobile terminals to communicate with the DCS, and will be in SA or RA mode.
- Token channels will be used by mobile terminals to transmit on-hook, off-hook, and acknowledgments to messages received from the DCS.
- Assignment channels will be used by the DCS to respond to mobile requests and issue commands to mobiles.

The signalling channels will be operating at 2400 bps using Differential Minimum Shift Keying (DMSK) modulation.

The channels in SA mode will be used solely for transmission of call request, log-on, log-off, and ranging messages. The log-on/log-off message transmissions are expected to occur during the non-busy-hour period. The 2400 bps channel is divided into 16 slots of 150-bits long for these messages.

The RA scheme is based on a random access scheme (SA) to reserve a particular slot for transmitting a call request packet. The Reservation Request Channel (RRC) is divided into two different types of slots: First, large slots (150 bits) used for transmission of call request, log-on, log-off, and ranging messages; second, mini-slots (15 bits) used to transmit a four-bit token in SA mode to reserve one of the large slots for transmitting call request and log-off messages. Every large slot is followed by a group of ten mini-slots.

The downlink part of RRC is used to transmit the reservation response messages from the DCS to the mobiles.

For the token scheme, the 2400 bps channel is also divided into 15-bit slots. During the call set-up procedure (after reception of call request) the DCS will designate one slot to the L-band called-party. This slot will be used by the mobile to transmit four-bit tokens signifying on-hook, off-hook, and acknowledgement to messages received from the DCS.

3.2 Link Availability of L-Band Signalling Channels

The performance of signalling channels will be significantly dependant on the propagation effects, which in turn depends on the elevation angle to the satellite as well as the amount and type of blockage and shadowing predominate in the service area. The baseline system design assumes that mobiles would be limited to a service area defined by a minimum elevation angle of 20° to the satellite. It is to be noted that a very large proportion of the potential mobile users in Canada fall within this limit. Application of measured fade statistics for areas in which woodlands constitute up to 35% of the land area[2] indicated that a 99% availability for the signalling channels is attainable. The probability of packet loss on forward and reverse links for mobiles is calculated to be limited to 11% and 11.6%, respectively. The probability of token misdetection on the reverse link is expected to be 0.3%[1].

3.3 Comparison of Access Schemes

For brevity, the channel performance and delay analysis for both access schemes would not be presented here in detail. Interested readers may refer to Reference 1 for a detailed performance analysis of these schemes. Figures 1 and 2 show channel performance versus delay curves for both SA and RA schemes combined with a token scheme. In Figure 1, the percentage of packets transmitted successfully after m transmissions on the request channel is plotted against the call set-up delay. Note that call set-up delay accounts for the time from transmission of first indication of call request from mobile until successful reception of ringback message (acknowledgement) by the mobile from the DCS. Table 1 further compares the performance of the two schemes:

Table 1 Comparison of SA and RA

	Slotted aloha		Reservation aloha	
	Success rate	Delay (sec)	Success rate	Delay (sec)
First try	69.3	0.92	76.3	1.96
Second try	17.6	1.99	1.0	2.72
Third try	7.5	3.06	14.5	3.97
Fourth try	3.25	4.13	5.4	5.89
Total	98.95%		97.2%	

In Figure 2, the channel throughput (in terms of number of packets) is plotted against the average delay on the channel. As shown, the delay experienced by RA is usually twice as much as that of SA, since the process involves transmission of two messages from the mobile to the DCS (one token, one message).

It is interesting to note that increasing the number of signalling channels in SA scheme improves the performance of the network, while its effect on RA is insignificant. SA is more adaptable to environments with various propagation characteristics,

while RA is more susceptible to high packet error rates on the link. In addition, RA uses one more L-band downlink channel than SA for transmitting the reservation response messages. One of the advantages of RA scheme is its capability of handling up to seven calls/sec/channel compared to SA handling only four calls/sec/channel, ensuring channel stability as shown in Figure 2.

The above study clearly shows that, under the assumptions used, SA outperforms the RA access scheme.

3.4 SHF Signalling Channels

The baseline traffic model developed for the first generation MSAT indicates that the Canadian mobile satellite network will consist of about 150 base stations and four gateways, each generating varying amounts of SHF traffic[3]. It is assumed that every station would transmit a message every 2.3 seconds[3]. With the main objective to minimize the channel access delay, the following access schemes have been considered:

- Random access, and
- Fixed assignment.

The only candidate considered for random access is SA due to its higher performance compared to pure Aloha and its faster response with respect to RA. Typically, the channel throughput for an SA channel would be approximately 15% for a reasonable degree of packet collisions and packet delay. As a result, the number of required channels would be 30 channels. One of the major drawbacks of this access scheme is that collision of messages such as off-hook, on-hook, and acknowledgments could result in long call processing delays and chaos in signalling channels.

For fixed assignments, an FDMA system with dedicated channels, or a TDMA system with permanently assigned time slots, have been investigated. Due to the requirement for transmitting on average one message every 2.3 seconds, an FDMA system would not be practical. Even though there would be no channel access delay for this scheme, the channel throughput would be very low (in the order of $1/(16 \times 2.3) = 2.7\%$ assuming a 2400 bps data rate and 150-bit packets).

In the case of a TDMA system with 2.3 second long frames, and every station being assigned to a particular time slot in a channel, the channel utilization will be very high, requiring only five signalling channels. However, in such a system, the average channel access delay will be excessively high (about 1.15 seconds long). For the purpose of analysis, an average channel access time of 300 ms is assumed to be reasonable. To accommodate such channel access delays, the frame size could be reduced to 600 ms resulting in approximately sixteen signalling channels. Note that channel utilization will be 24.5% assuming a 2400 bps data rate. The channel efficiency would be increased to 26% if the transmission rate is increased to 4800 bps. The number of required channels in this case will be half of the previous case, so the SHF spectrum requirement will remain the same.

The assignment channels are similar to broadcast channels. The DCS would be the only transmitter on these channels. The SHF stations will monitor them continuously while they are logged on to the system.

Telesat's studies indicate that the TDMA access scheme with a 600 ms frame size can satisfy the Canadian system and user requirements. The channel performance will be the highest and the average channel access time will be 300 ms. It should be pointed out that the data transmission rate would not influence the signalling channels' performance significantly; however, the packet transmission time and packet processing delay will be reduced.

Note that base stations and gateway stations will share the signalling channels. A dynamic signalling channel assignment scheme should be implemented to provide flexibility in the system operation.

The most important phenomenon affecting the SHF link performances is the attenuation of the signal by rain in the earth-to-space paths. Telesat's studies indicate that a one-way propagation availability better than 99.99% of time can be achieved for most Canadian users. This availability could be further improved if uplink power control is used at the central control station site.

4.0 CALL SET-UP PROCEDURE

Figure 3 provides a time diagram describing how the various access schemes would be used in setting up/taking down a call. As shown, a base station initiates a call by transmitting a call request to the DCS. The mobile party would be informed via L-band assignment channels. The ringing message would be acknowledged by an Ack token on the token channel. A second token would indicate an off-hook. At this point in time, a voice channel would be assigned to both parties.

For call take-down, one of the parties goes on-hook which causes transmission of a tone over the voice channel to the other party. The terminal then informs the DCS. In the case of mobile users, a token would be sent over the a token channel. The DCS sends call termination messages to both parties and reclaims the voice channel.

5.0 CONCLUSION

Candidate multiple access schemes for L-band and SHF signalling channels in the Canadian MSAT system have been described here. It was shown that the most appropriate channel access scheme for the mobile terminals would be SA combined with a token scheme using L-band channels. Furthermore, slim-TDMA with short frames was shown to be the superior approach for the SHF signalling channels.

REFERENCES

- [1] "MSAT DAMA System Study", Telesat Canada, prepared for Department of Communications, Ottawa, Canada, July 1986.
- [2] Butterworth, J. "Propagation Measurements for Land-Mobile Satellite Systems at 1542 MHz", Department of Communications Report, Ottawa, Canada, August 1984.
- [3] "MSAT System and Service Definition", Telesat Canada, prepared for Department of Communications, Ottawa, Canada, October 1987.

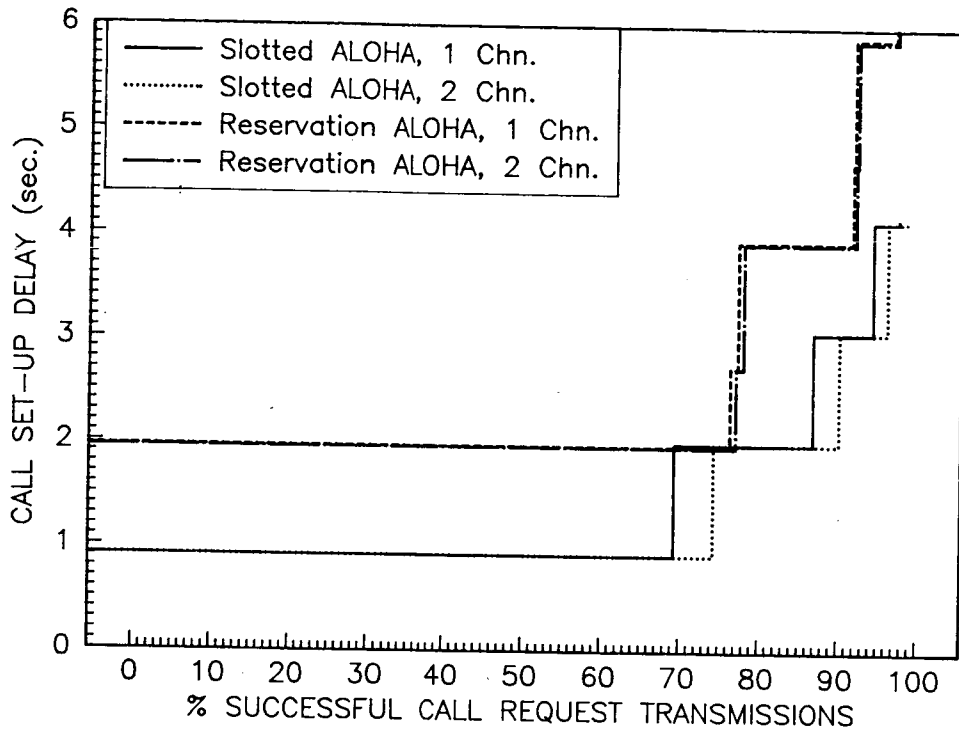


Fig 1. Comparison of slotted aloha and reservation aloha access schemes based on call set-up delay

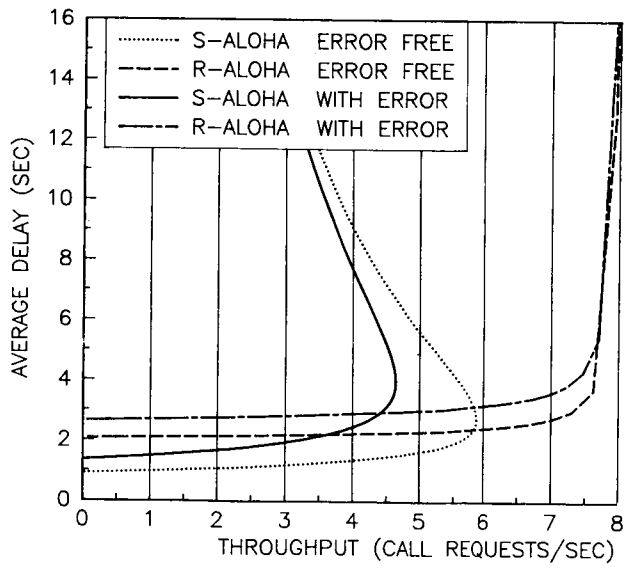


Fig. 2. Total capacity of slotted aloha and reservation aloha schemes versus average delay

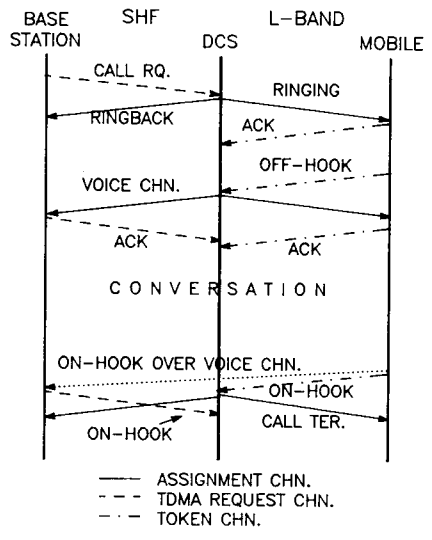


Fig 3. Call set-up/take-down procedure for an MRS call

**REARRANGEMENT PROCEDURES IN REGENERATIVE MULTIBEAM MOBILE
COMMUNICATIONS SATELLITES WITH FREQUENCY REUSE**

GIANNI COLOMBO, Special Networks Section, CSELT, Italy; FRANCO SETTIMO, Special Networks Section, CSELT, Italy; ANTONIO VERNUCCI, Networks and Services Group, Telespazio, Italy

CSELT
Centro Studi e Laboratori Telecomunicazioni
Via G. Reiss Romoli, 274
I10148 Torino
ITALY

ABSTRACT

After a short overview on the European tendencies about a Land Mobile Satellite Service, this paper describes an advanced system architecture, based upon multiple spot-beams and On-Board Processing, capable of providing message and voice services over a wide European coverage, including some North-Africa and Middle-East countries. A remarkable problem associated to spot-beam configurations is the requirement for flexibility in the capacity offer to the various coverage areas. This means incorporating procedures for changing the on-board modulator-to-spot associations, respecting the constraints imposed by frequency reuse. After discussing the requirements of the rearrangement procedure, an on-purpose algorithm is presented. This paper is derived from work performed on contract to ESA, the European Space Agency.

1. INTRODUCTION

A Land-Mobile Satellite System (LMSS) in Europe can complement the Pan-European terrestrial cellular network (usually referred to as "GSM" network), covering the regions not served by it. An important market is represented by transportation companies, which already expressed the need of communicating with lorries travelling in Europe and neighbouring countries. The integration is doubtful in the short and medium run, because of the very different technical solutions among which the use of different frequency bands (around 900 MHz for GSM and around 1.5 GHz for the LMSS) is not a minor item.

Two basic solutions are currently investigated: the Standard-C (designed in the INMARSAT context) and the PRODAT, developed by ESA. A major objective is to supply the voice service in the second or third-generation LMSS. Several studies have been conducted by ESA to determine the required technologies for the advanced configurations of a LMSS capable of satisfying medium traffic demands (about 3000 erlang).

A study by TELESPIAZIO with ANT, CSELT and DORNIER Systems as sub-contractors [ESA 1983] led to the following main conclusions:

- 19 spot beams for mobile station coverage, with 37 dB antenna gain are enough for Europe and neighbouring countries

- On-Board Processing (OBP) is needed for providing routing functions, Demand Assignment (DA) and reconfiguration capability
- frequency reuse is a must, since the frequency band for LMSS is limited to 23 MHz (WARC '87) against a requirement of 28.8 MHz (7.5 kHz with QPSK modulation for each 9.6 kbps voice channel).

2. AN ADVANCED ARCHITECTURE FOR A EUROPEAN LMSS

The system topology is based upon several (10 to a maximum of 100) Fixed Stations (FS) containing gateway functions with the terrestrial network and a multitude of Mobile Stations (MS) [Kriedte et alii, 1985]. Two links can be distinguished, a Forward Link (FL) for FS-to-MS communications and a Return Link (RL) in the opposite way: each comprises an Up (U) and Down (D) section so that four links (FUL, FDL, RUL and RDL) can be identified.

A single-frame high bit-rate TDMA scheme (frame length=1 ms) has been selected for the FUL (dimensioned for about 3600 channels at 9.6 kbps), so that each FS capacity requirement is fulfilled with the lowest granularity, although in a fixed way; a single FSs coverage, furthermore, simplifies system architecture and payload design.

In the FDL, a multiple carrier-per-spot solution, at relatively low bit-rate, seemed the most appropriate, in regard of MS complexity and operability. The payload, thus, performs several functions for interfacing the different FUL and FDL schemes including: burst-mode demodulation, frame storing, routing on individual channel basis, speed conversion, on-board modulators-to-spot patching. The FL repeater block diagram is shown in Fig. 1.

After demodulation, a baseband processor routes the individual FUL channels into several low-rate TDM streams (480), each multiplexing 8 channels; this is a trade-off result among number of on-board modulators, bit rate and resolution in channel assignment to spot beams. A switching matrix feeds the TDMS to a phased-array antenna (a conventional multibeam antenna would not allow the same flexibility in RF power allocation). Its switching configuration can be occasionally rearranged to cope with traffic variations.

The same carrier frequency is used for different modulators, patched to different spot-beams. Frequency reuse schemes based upon 3, 4 and 7 sub-bands were evaluated, by considering both the impact on the antenna sidelobes performance requirements and the actual bandwidth saving, in a non uniform traffic environment. The 4-subband solution was chosen, with a bandwidth occupancy of 17 MHz.

About the RL, the regenerative solution was preferred, since it allows to perform on-board some peculiar functions of the Network Coordination Station (NCS), required to manage the network. This would yield the advantages [Colombo et alii, 1985] of reduction of the call set-up delay, simpler network control and saving of NCS/satellite communication links.

The MSs access follows a Single-Channel-Per-Carrier (SCPC) scheme, with the aim to minimize MS complexity and RF power requirements. On-board "multicarrier demodulators" were proposed and studied in detail, embedded in a payload configuration (Fig. 2) which yields a rearrangement capability specular to that of the FL. The OBP converts the FDMA structure of the RUL channel into a single TDM structure in the RDL, such as to optimize the FS equipment and the utilization of RF power.

The system performance is improved by DA techniques so that resources are shared by different traffic sources; Occasional Basis DA (OBDA) and Call Basis DA are alternatively present at various system levels. In particular, OBDA has been provided for associating the modulators (and the multicarrier demodulators) to the various spot beams; this is by far the most critical point for transmission resources efficiency and OBDA can powerfully cope with: forecasting errors on dimensioning data, traffic pattern variations on seasonal basis, peak hour variations due to time shift and different living habits.

3. RECONFIGURATION REQUIREMENTS

Fig. 3 summarizes the steps leading to the re-assignment of the modulators to the spots. This is the most important item, which heavily affects on-board complexity and coordination protocols in the network. The crucial point is the rearrangement procedure but a few comments are spent about the other traffic assignment features:

- The traffic demand is estimated by the NCS so as to follow the influence of mobile movement and peak hour variations on the resource needs. This part belongs to the classical estimation theory; it is only pointed out that the NCS knows how many mobiles are active in each spot.
- Once some predefined traffic thresholds are crossed, a decision is taken about the optimal partition of the modulator set among all the spots on the base of the estimated local traffic. Two algorithms have been studied with the objective of achieving a nearly uniform loss probability among the spots.
- On the base of the obtained modulator-to-spot partition, the consequent band portions are assigned to each spot according to the constraints imposed by the chosen frequency reuse strategy. Fig. 3 shows that, in general, the new partition may not be compatible with the available band and the minimum reuse distance; if this happens, a backward step is possibly needed for re-assessing the partition with higher values of loss probability.
- The frequency plan updating can result by management actions consequent to forecasting errors and traffic pattern variations.

As soon as the updated frequency plan is chosen, the passage from the present to the new plan via a rearrangement procedure starts. This is a separation instant between the previous phases (not interacting with the system state) and the step by step procedure leading to the final configuration.

4. THE REARRANGEMENT PROCEDURE

Before describing the procedure, some assumptions are remarked:

- each modulator works on a fixed bandwidth: frequency-agile modulators are a less restrictive particular case;
- only the FL is described; for the specular arrangement of the RL, "modulator" must be changed into "multicarrier demodulator".

Even if the procedure is quite general, it is described in the case of single reuse (double use). Fig. 4 clarifies the adopted notations: natural numbers are chosen for labeling the elementary frequency ranges (carriers) composing the available bandwidth. The modulators working on the same carrier are identified with its label.

Explicitly, the rearrangement consists in updating a frequency plan over S spots by passing from an initial modulator-to-spot configuration A_1, A_2, \dots, A_S to a final one B_1, B_2, \dots, B_S , obeying to new traffic needs. According to Fig. 4 notations, A_i and B_i ; $i=1,2,\dots,S$ are subsets, non necessarily disjoint, of the set of carrier labels:

$$A_i = \{n_1(i), n_2(i), \dots, n_{m(i)}(i)\}; \quad B_i = \{k_1(i), k_2(i), \dots, k_{r(i)}(i)\}; \quad i=1,2,\dots,S$$

being $m(i)$ and $r(i)$ the initial and final dimensioning of the i -th spot respectively (number of associated modulators). It is assumed that the updated configuration is compatible with the on-board switching capability and the frequency reuse constraints.

Service quality considerations require that no calls in progress are suppressed: the modulators to be moved are partially emptied by the natural end of conversations and by rejection rules for the incoming calls exceeding the final dimensioning. Secondly, even in the "transient" rearrangement phase, a minimum capacity N_i is always guaranteed to the i -th spot:

$$N_i \leq \min \{m(i); r(i)\}; \quad i=1,2,\dots,S \quad (1)$$

where the sign of equality represents a reasonable condition for N_i . The procedure has an asynchronous step-by-step behaviour, with each step j characterized by the accomplishment of two basic operations:

$S(j)(n)$: the couple of modulators working on the n -th carrier are switched on the spots they are assigned to in the final plan;
 $R(j)(n)$: Release of the modulators working on the n -th carrier; it is made possible by the occurred switching and has a random duration, owing to the residual conversation times.

During step j , $S(j)(n)$ follows the previous releases and creates further release possibilities compatible with (1). Initially, only a release phase is, in general, possible in those spots whose capacity decreases. During the process evolution, a state can be encountered for which the release of a modulator does not produce a switching possibility; in this case, the residual calls are moved to an extra modulator, temporarily used for carrying voice traffic. The extra modulators work on a bandwidth portion shared by the entire set of spots.

For a general step j , let:

$$A_i^{(j)}, \quad B_i^{(j)}; \quad i=1,2,\dots,S$$

be the sets of modulators still belonging to the initial plan and already switched according to the final plan, respectively. Let $E_i(j)$ denote the number of modulators that can be released in step j , respecting (1). The procedure is initialized (step 0) by considering as already assigned to the final plan the modulators which need no re-switching. Step 0 is then characterized by:

$$A_i^{(0)} \equiv \{k: k \in A_i, k \notin A_i \cap B_i\}; \quad B_i^{(0)} \equiv A_i \cap B_i; \quad E_i^{(0)} = m(i) - N_i \quad i=1,2,\dots,S$$

Step j ($j \geq 1$) is now described with a brief comment on the involved algebraic operations:

a - The set $I^{(j)}$ of the spots where at least one modulator can be

released is found:

$$I^{(j)} \equiv \{i: E_i^{(j-1)} > 0\}$$

- b - Within $I^{(j)}$, the set of modulators $M_i^{(j)}$ belonging to each i -th spot which can be moved according to the final plan is found:

$$M_i^{(j)} \equiv \bigcup_{\substack{k \in I^{(j)} \\ k \neq i}} [A_i^{(j-1)} \cap A_k^{(j-1)}]; \quad i \in I^{(j)}$$

In fact, the switching possibility is conditioned on the availability of both homologous modulators.

- c - The overall set of the switchable modulators:

$$M^{(j)} \equiv \bigcup_{i \in I^{(j)}} M_i^{(j)}$$

is obtained and an element of $M^{(j)}$, say n_j , is chosen such that at least another couple of modulators can be switched within step $j+1$. In other words, n_j must produce, after switching, the possibility of releasing another couple of homologous modulators. If this is not possible, n_j is chosen randomly within $M^{(j)}$ and an extra modulator is properly associated in the following step ($M^{(j+1)} \neq \emptyset$).

- d - The Release phase starts and, at the end of the residual conversations, the related Switching is performed:

$$R^{(j)}(n_j) \rightarrow S^{(j)}(n_j)$$

- e - The new sets $A_q^{(j)}$, $A_r^{(j)}$ and $B_u^{(j)}$, $B_v^{(j)}$ are calculated by moving n_j ; q, r obviously represent the couple of spots releasing the modulators n_j ; u, v the couple of spots receiving them. In analogy $E_q^{(j)}$, $E_r^{(j)}$, $E_u^{(j)}$, $E_v^{(j)}$ are re-defined.

- f - The procedure enters the $(j+1)$ -th step unless the condition $A_i^{(j)} \equiv \emptyset \quad \forall i$ is reached which means that the final plan is accomplished.

For brevity, some particular cases are omitted. A general study on the required amount of spare modulators does not exist, but the procedure has been applied to examples with quite dissimilar (old and new) frequency plans and one spare modulator, at most, has been required.

5. CONCLUSIONS

A satellite system for advanced LM services has been described together with the need of incorporating facilities for following the average offered traffic, especially on the mobiles side, where the rather limited capacity does not allow a high trunk group efficiency. To this purpose, a procedure has been conceived and its qualifying points illustrated; a further investigation should be devoted to generalize some heuristic point and to evaluate the procedure efficiency in terms of accomplishment delay.

REFERENCES

- ESA 1983. Study of systems and repeaters for future narrowband communications satellites. ESTEC Contract 5484 83/NL/GM/(SC)
- G. Colombo, W. Heine, K. Jesche, W. Schreitmuller, F. Settimo 1985. System architecture and management of advanced regional satellites for land mobile applications. Globecom '85, New Orleans, USA
- W. Kriedte, A. Vernucci 1985. Advanced regional mobile satellite system for the nineties. Globecom '85, New Orleans, USA

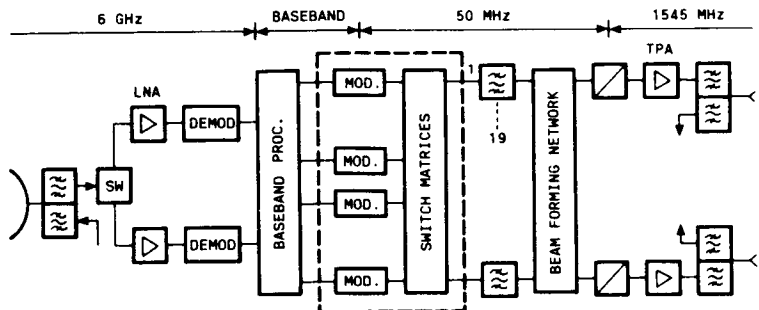


Fig. 1 - Repeater block diagram Forward-link

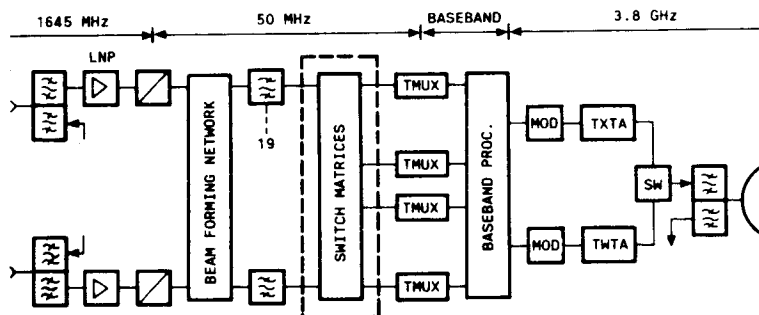


Fig. 2 - Repeater block diagram Return-link

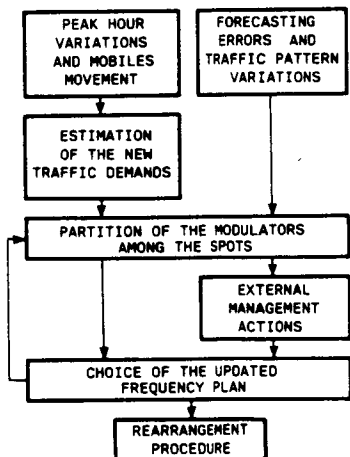


Fig. 3 - Flow diagram of rearrangement operations

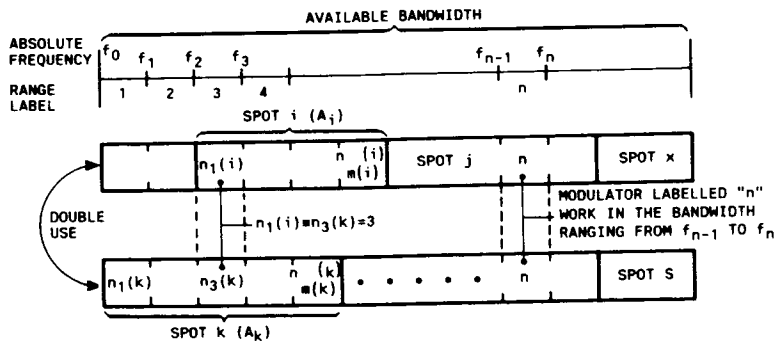


Fig. 4 - Frequency plan with double frequency use

DESIGN MOBILE SATELLITE SYSTEM ARCHITECTURE AS AN INTEGRAL PART OF THE CELLULAR ACCESS DIGITAL NETWORK

E. S. K. CHIEN, J. A. MARINHO, and J. E. RUSSELL SR., Cellular Telecommunications Laboratory, AT&T Bell Laboratories, United States

AT&T BELL LABORATORIES
Whippany Road
Whippany, New Jersey 07981
United States

ABSTRACT

The Cellular Access Digital Network (CADN) is the access vehicle through which cellular technology is brought into the mainstream of the evolving integrated telecommunications network. Beyond the integrated end-to-end digital access and per call network services provisioning of the Integrated Services Digital Network (ISDN), the CADN engenders the added capability of mobility freedom via wireless access. One key element of the CADN network architecture is the standard user to network interface that is independent of RF transmission technology.

Since the Mobile Satellite System (MSS) is envisioned to not only complement but also enhance the capabilities of the terrestrial cellular telecommunications network, compatibility and interoperability between terrestrial cellular and mobile satellite systems are vitally important to provide an integrated moving telecommunications network of the future. From a network standpoint, there exist very strong commonalities between the terrestrial cellular system and the mobile satellite system. Therefore, the MSS architecture should be designed as an integral part of the CADN. This paper describes the concept of the CADN, the functional architecture of the MSS, and the user-network interface signaling protocols.

1. EVOLUTION OF CELLULAR TECHNOLOGY

Historically, the development of cellular technology dates back to the early 1940's when AT&T Bell Laboratories' engineers explored various means to increase the availability of radio telephone service in vehicles in metropolitan areas [MacDonald, 1979]. As a result of these studies, the fundamental elements of cellular technology emerged as: (a) frequency reuse in small geographic areas (i.e. cells) to increase the capacity of a limited frequency spectrum to serve many users, and (b) automatic switching of channels when an active user crosses a cell boundary (i.e. hand-off). The first United States commercial cellular system began operations in Chicago in October 1983. Since then, the market for cellular service has grown steadily at a pace far exceeding the expectations of the industry.

Coincidental with the growth of the cellular market, there has been a change in technology usage. The original purpose of cellular technology was to provide voice telephone service to automobiles in metropolitan areas. However, in the past few years, there has been increasing use of briefcase-mounted and hand-held cellular telephones. Furthermore, the high quality of

cellular radio channels has encouraged cellular service subscribers to use the channels for other telecommunications applications such as the transmission of voiceband data. Quality and convenience are the reasons why cellular systems are being introduced to smaller and smaller cities where the need for frequency reuse is less imperative compared to congested metropolitan areas.

Therefore, it is clear that market forces are moving cellular service from a means of voice communication in vehicles to a general means of communication for people and machines on the move, or at locations where wired telecommunications services are not practical or readily available. This application evolution requires the definition of a new cellular network architecture that supports an integrated *moving* access as a complement to the traditional *fixed* access telecommunications network. This architecture, which is referred to as the Cellular Access Digital Network (CADN) [Chien, 1987a,b], provides a generalized moving access via the CADN Digital Subscriber Channel.

2. CELLULAR ACCESS DIGITAL NETWORK

Modern telecommunications networks are migrating toward an infrastructure where various network resources can be used as an integrated entity to convey all types of information among people and machines. For fixed networks, the Integrated Services Digital Network (ISDN) has defined a means by which such integrated network resources are accessible via a single standard user-network interface. Through this interface, the network can provide the user integrated end-to-end digital access and per call network service provisioning. In a complementary and parallel fashion, the CADN provides the integrated service access capability similar to ISDN in conjunction with user mobility. As a moving access network, the CADN merges the wireless transmission and user location capability of cellular systems with the resources of fixed telecommunications networks.

The control architecture and internal communications structure of the CADN is designed to (a) provide compatibility and interoperability with the ISDN and (b) provide sufficient flexibility to accommodate a broad and evolving range of RF environments. Figure 1 identifies three environments, which in ascending order of traffic density but in descending order of rigor concerning their communications channels, are (a) moving terminals in remote areas communicating with a mobile communications satellite, (b) moving terminals in rural, suburban, or urban areas served by terrestrial base stations (or "cell sites"), and (c) moving terminals within or near buildings served by indoor wireless communications systems. To provide the best possible service in a given environment, a specific combination of RF transmission techniques, speech code, modulation format, channel code, and multiple access method will have to be carefully selected to achieve an effective balance among the goals of quality, cost, and capacity for that particular environment. Nevertheless, moving access users should be able to enjoy consistent service access and capabilities across the various environments (e.g. mobile satellite, terrestrial, and indoor wireless systems), as well as the compatibility and interoperability between the *fixed* ISDN and the *moving* CADN network. To accomplish this service transparency, the concept of a CADN Digital Subscriber Channel has been proposed (see Figure 1). Section 4 of this paper will describe in detail the standards proposed for this CADN Digital Subscriber Channel in the Mobile Satellite System (MSS) environment.

3. MSS AS AN INTEGRAL PART OF THE CADN

Because of the wide coverage attainable by a satellite-based base station, the Mobile Satellite System can easily provide cellular services to remote or thinly populated areas where terrestrial cellular systems are not economically feasible [Bell, 1985]. Thus the MSS plays a very important role in making cellular service a *ubiquitous* service so that moving access users can obtain telecommunications services regardless of where they are. However, this will be possible only if consistent service capabilities and service access are provided to moving access

users through a standardized user-network interface. Therefore, it is imperative that the architecture of the MSS be designed as an integral part of the CADN. In the following sections of this paper, the MSS will be treated as a specific implementation of the CADN, and the term MSS will be used synonymously with the term CADN.

3.1 MSS Functional Architecture

As shown in Figure 2, functionally the MSS consists of a switching system, a base station, network terminations, and user equipment.

3.1.1 Network Termination As noted in the preceding sections, the most important aspect of the CADN architecture is the user-network interface. This interface must be designed so as to enable the user terminal to be transparent to the specific RF transmission technology of the MSS.

The network termination provides the *physical* appearance of a wireless access channel for the MSS user. Working as a complementary pair with the satellite RF channel equipment, the MSS network termination equipment (MNTE) controls all of the cellular RF channel functions. Examples of these functions are access to common control channels, assignment of traffic channels, and control of transmitter power. In addition to providing RF transport for its own signaling and control messages, the MNTE provides RF transport for user information and signaling through information (I) channels and control (C) channels.

3.1.2 MSS User Terminal An MSS user terminal is very similar to an ISDN terminal in providing access to voice and data services with signaling and control capability. However, it differs from the ISDN terminal in that it will not have access to a fixed "2B+D", 144 kb/s capability due to the limited availability of RF spectrum. Instead, it will provide a CADN basic access via a "2I+C" format. In most environments, the rates of the I and C channels will be significantly lower than the corresponding B and D channels of ISDN. For example, the voice will be processed from 64 kb/s down to, say, 4 kb/s before interfacing with the network termination equipment. In addition, depending on user service requirements, the network will provide just enough RF resource for either 2I+C, I+C, or a mere C channel for each connection.

3.1.3 MSS Switching System Like the Mobile Telephone Switching Office (MTSO), the MSS switching system will coordinate the connections of MSS users to the landline network, terrestrial cellular network, or other MSS users. It will also control cellular functions such as paging, handoff, and RF channel assignment. In addition, it will provide ISDN-like integrated voice, data, and signaling service capabilities. Since the MSS switching system will interconnect with other CADN networks as well as with public and private networks, it should support international signaling standards such as ISDN, Signaling System 7 (SS7), and the Mobile Application Part [CCITT, 1988].

One implementation of the MSS switching system consists of a Network Management Center (NMC) and a Gateway Switch [Bell, 1985], where the former is mainly responsible for the control functions while the latter is responsible for cross connection and interface to other networks. The significant deviation of this implementation from terrestrial cellular systems is that all links between the MSS switching system and the base station are based on radio links.

3.1.4 MSS Base Station In addition to terminating RF channel links and performing cellular functions under the control of the MSS switching system, the MSS base station performs several autonomous functions. For example, it determines the user movement direction in preparation for a handoff.

One implementation of the MSS base station consists of a mobile satellite and a Telemetry, Tracking and Control (TT&C) station [Bell, 1985]. The significant deviation of this implementation from the terrestrial cellular system is that the MSS has only one base station with cells created via multiple spot beams.

4. MSS DIGITAL SUBSCRIBER CHANNEL STANDARDS

The key aspect of the CADN Digital Subscriber Channel is the separation of RF channel technology and subscriber access. RF channel technology reflects technology dependent multiple access schemes, modulation and encoding methods, and bandwidth allocations. For the MSS, such functions can be aggregated into functional modules that comprise the MSS network termination equipment (MNTE). In a similar fashion, subscriber access is comprised of functions that are intrinsic to moving access networks regardless of which specific RF channel technology is used. Having specified a functional separation between network channel specific and user terminal specific functions, a reference point by which to identify the MSS user-network interface is created (see Figure 2). It is at this reference point that the *Cellular ISDN standards* can be defined. This point not only supports the same level of services and capabilities associated with the fixed ISDN within the limitation of the RF channel, but also accommodates the user location schemes associated with the moving access point in the MSS. Similarly, the RF channel specific functions that are defined by *Cellular Digital RF standards* accommodate the resource allocation and control schemes associated various RF channel technologies (e.g. TDMA, FDMA, etc.). The combined functionality of both standards is the basis for MSS Digital Subscriber Channel Standards.

4.1 Cellular ISDN Standards

The Cellular ISDN standards define an ISDN-like basic access structure via a virtual connection that supports a "2I+C" capability. The Cellular ISDN information (I) and control (C) channels are analogous to the ISDN bearer (B) and data (D) channels. The unique terminology for Cellular ISDN (i.e. I and C) emphasizes the fact that the MSS environment will not support the defined ISDN bit rates due to the scarcity of radio frequency spectrum. To maximize spectrum usage in the MSS as well as other CADN environments, channel flexibility is provided for by defining I and C channels as multiples of unit (U) channels at the rate of 1 kb/s. In this way, the access rate and channel usage can vary according to environmental constraints and per-call user service needs. Similar to the ISDN protocol model, the Cellular ISDN protocol model is also based on the Open System Interconnection (OSI) reference model [Jenkins, 1984]. The Cellular ISDN protocol architecture is comprised of three layers which are 1. the Virtual Physical Layer, 2. the Data Link Layer, and 3. the Message Layer (see Figure 3).

4.1.1 Layer 3 The Cellular ISDN Message Layer provides the requisite functionality for coordination of all call processing and data transport activities. In the same fashion that ISDN supports user packet data transport on the D channel, the Cellular ISDN supports user packet data transport on the C channel.

4.1.2 Layer 2 The Data Link Layer provides the logical connection by which Cellular ISDN messages are exchanged across the CADN user-network reference point. The logical connection conforms to the set of procedures defined by Link Access Procedures on the Cellular ISDN Control channel (LAPC). Functionally, LAPC supports the exchange of Layer 3 call control and user information in data link frames, acknowledged exchange of information based on logical data link connections, logical channel initialization and termination, logical error checking and recovery, and channel supervision concerning Layer 1.

4.1.3 Layer 1 Layer 1 of the Cellular ISDN protocol provides the means by which "peer" Data Link Entities can exchange Cellular ISDN frames across the MSS user-network reference point. Functionally, it provides a virtual physical connection that specifies the characteristics of I and C channels. Channel variability is supported by the specification of I and C channels as multiples of the U channel rate (i.e. 1 kb/s). An I channel comprised of 16 U channels is specified as I(16) and supports a 16 kb/s rate. Similarly, a C channel comprised of 2 U channels is specified as C(2) and supports a 2 kb/s rate. In this fashion the rates of I and C channels can vary in accordance with environmental constraints and call-by-call user service needs. In addition to the "2I+C", other basic access configurations of "I+C" and "C" are also

defined for Cellular ISDN.

4.2 Cellular Digital RF Standards

Functionally, the MSS network termination provides wireless physical transport for the Cellular ISDN I and C channels. It performs standard functions such as carrier frequency synthesis, and modulation and demodulation. In addition, it provides the capability to control and manage the RF channel that is unique to the cellular system. The Cellular Digital RF standards, as in the case of Cellular ISDN, are also structured in a layered fashion. Since the MSS RF channel technology will evolve with time, Cellular Digital RF standards provide the flexibility to support such RF technology advancements.

In accordance with the OSI reference model, the Cellular Digital RF standards are comprised of three layers which are 1. the RF Physical Layer, 2. the RF Data Link Layer, and 3. the RF Channel Management Message Layer (refer to Figure 4). Unlike the ISDN, however, prior to the establishment of a dedicated point-to-point resource, call control signaling must first request the resource via the Common Access and Control (CAC) channel. This channel is a shared resource among all users in a given cell. Once the dedicated resource is allocated, the terminal then relies upon the User Specific Control (USC) channel for message transport, and the associated I channels for user traffic transport. The combined functionality of both CAC and USC channels is the transport vehicle for the Cellular ISDN C channel.

4.2.1 Layer 3 The Cellular Digital RF Channel Management Message Layer provides the requisite functionality for coordination of all RF channel related activities, such as: channel address assignment (e.g. frequency, time slot), bandwidth allocation, power level control, forward error correction, etc., so as to make the MSS RF environment transparent to the MSS user-network interface.

4.2.2 Layer 2 The RF Data Link Layer provides the logical connection by which Cellular Digital RF Channel Management messages are exchanged across the MSS digital RF channel. The logical connection is governed by a set of procedures as defined by the Link Access Procedures on the Radio Control channel (LAPRC). Functionally, LAPRC supports the exchange of Layer 3 RF Channel Management messages in data link frames, acknowledged exchange of information based on data link connections, channel initialization and termination, error checking and recovery, and channel supervision concerning the RF media.

4.2.3 Layer 1 The Physical Layer of the Cellular Digital RF standards provides the interface to the MSS RF environment for transport of Cellular ISDN I and C channel information. This layer provides for the variability in RF environments identified in Figure 1. For the MSS environment, Layer 1 provides for the capability to conform to satellite transmission directionality and power constraints. In addition, it also provides for overcoming channel impairments due to sunspots and thick clouds, as well as multipath effects.

5. MSS SERVICE CAPABILITIES

With digital RF transmission and low bit rate speech processing schemes, the MSS can protect voice service from any "casual" listener. With the Cellular ISDN standards, the MSS can provide a fuller set of data services to the user, ranging from circuit-switched data service to packet-switched data service. They can be used for applications such as data base inquiry/response, location update, vehicular alarm reporting, electronic mail/message, navigation, etc. The cellular ISDN C channel not only provides the service capability for user packet data transport but also provides the signaling capability for end-to-end connection and service control.

With the MSS Digital Subscriber Channel standards, the call control messages are separated from the RF channel control messages (see Figure 5), which facilitates the application of advanced digital encryption schemes to the user traffic without causing difficulties in cellular channel management.

Because the MSS can provide ISDN-like simultaneous voice, data and signaling capabilities, it could even become a viable candidate for providing fixed telecommunications services to residents in remote and rural areas.

6. DISCUSSIONS

This paper has described the Mobile Satellite System architecture as an integral part of the Cellular Access Digital Network (CADN). The most significant breakthrough of the new architecture and associated channel structure is the separation of RF channel technology and user access based upon the CADN Digital Subscriber Channel concept. This paper has also described the MSS Digital Subscriber Channel Standards which consists of Cellular ISDN standards and Cellular Digital RF standards. The Cellular Digital RF standards can easily accommodate RF technology advancements envisioned for the MSS environment as well as other RF technologies required by other applications such as terrestrial cellular systems and indoor wireless systems. The Cellular ISDN standards can support a user-network interface that remains unchanged across the various RF environments and provide ISDN-like services. With the MSS Digital Subscriber Channel standards, the MSS not only can provide advanced telecommunications services to the MSS users in a consistent manner but will also facilitate the interworking between the MSS and other CADN environments. Through such interworking and compatibility, the MSS and other CADN systems together form a ubiquitous moving access network to provide telecommunications services to people and machines on the move.

REFERENCES

- Bell, D. J. and Townes, S. A. 1985. MSAT-X System Definition and Functional Requirements. Revision 2.
- CCITT 1988. CCITT Study Group XI, Working Party 1, Question 14. *Recommendation Q.1051 - Mobile Application Part*. In 1988 CCITT Recommendation Book (to be published).
- Chien, E. S. K., Goodman, D. J. and Russell, J. E. Sr. 1987a. Cellular Access Digital Network. *International Conference On Digital Land Mobile Radio Communications - Proceedings*. Venice, pp. 84-93.
- Chien, E. S. K., Goodman, D. J. and Russell, J. E. Sr. 1987b. Cellular Access Digital Network (CADN): Wireless Access to Networks of the Future. *IEEE Communications Magazine*, vol. 25, no. 6, pp. 22-31.
- Jenkins, P. A. and Knightson, K. G. 1984. Open Systems Interconnection - the reference model. *British Telecom Tech. Jour.*, vol. 2, no. 4, pp. 18-25.
- MacDonald, V. H. 1979. The Cellular Concept. *The Bell System Technical Journal*, vol. 58, no. 1, pp. 15-42.

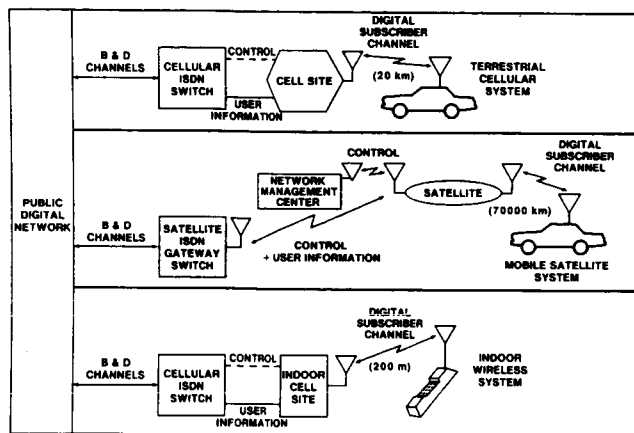


Figure 1. CADN Environments

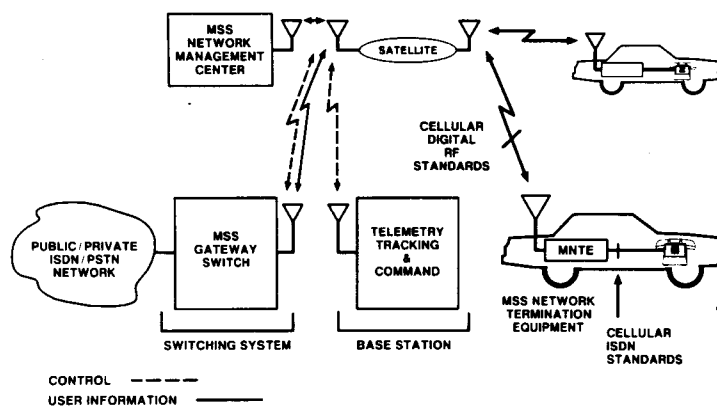


Figure 2. MSS Functional Architecture

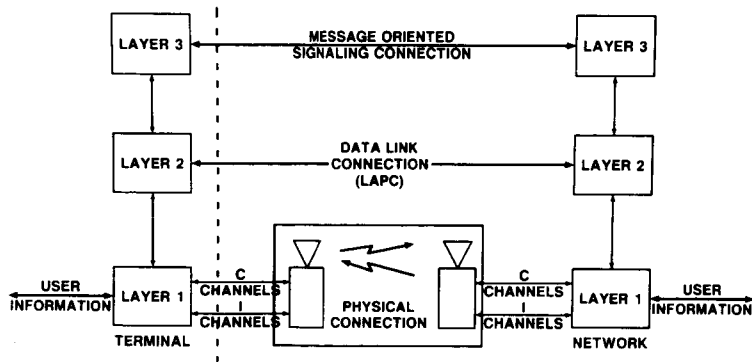


Figure 3. Cellular ISDN Protocol Architecture

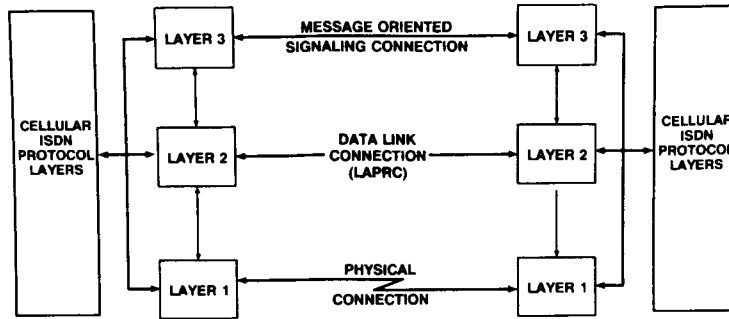
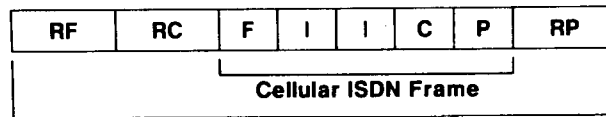


Figure 4. Cellular Digital RF Protocol Architecture



- Radio Channel Frame**
- RF** Radio Framing Bits
 - RC** Radio Control Signalling Bits
 - F** CISDN Framing Bits
 - I** CISDN Information Channel Bits
 - C** CISDN Control Channel Bits
 - P** CISDN Parity Bits
 - RP** Radio Channel Error Correction Coding Bits

Figure 5. Digital Subscriber Channel Format

AN ACCESS ALTERNATIVE
FOR
MOBILE SATELLITE NETWORKS

W.W. WU
INTELSAT

ABSTRACT

Conceptually, this paper discusses strategies of digital satellite communication networks for a very large number of low density traffic stations. These stations can be either aeronautical, land mobile, or maritime. The techniques can be applied to international, domestic, regional, as well as special purpose satellite networks. The applications can be commercial, scientific, military, emergency, navigational or educational. The key strategy is the use of a non-orthogonal access method, which tolerates overlapping signals. With n being either time or frequency partitions, and with a single overlapping signal allowed, a low cost mobile satellite system can be designed with $n^2(n^2+n+1)$ number of terminals.

1. INTRODUCTION

As new demands and requirements of satellite communications change, the network strategy and the technological utilization need to change accordingly. Mobile satellite communication, either aeronautical, land or maritime, has created both technical and nontechnical challenges. Among the technical challenges likely to be encountered would be a network consisting of a very large number of small earth stations, where there is signal degradation due to deflection, reflection, shadowing, doppler shift, and other interference effects, as a consequence of receivers in motion and operation in various channel environments.

As an example of the number of stations in a mobile satellite network there are about 25,000 vessels above 1600 gross tonnage registered in the three oceanic regions, and there are around 330,000 general aviation

aircrafts worldwide. By the year 2000 there are likely to be more than 12,000 commercial passenger-carrying airliners in operation [1]. For land mobile satellite communication, the number of users can be easily extended to six figures. On the other hand, because of the need for mobility, the size of user stations are getting smaller, which results in weaker signal reception and is increasingly prone to interference difficulties.

At present, all satellite networks, employing either mobile or fixed earth stations, operate on the principle of a controlling, or a number of controlling, stations. The network architecture is determined primarily by the satellite access method used by the earth stations in the network. Since multiple access technique affects a satellite network more than any other network element, in this paper we therefore discuss multiple access strategies particularly from a mobile satellite network viewpoint. In Section 2, some background information on multiple access techniques is briefly described. In Section 3, the fundamental characteristics of random multiple access is outlined. In Section 4, the error probability expression is derived. The application of random multiple access to mobile satellite communication is discussed in the concluding remarks in Section 5.

2. BASIC ACCESS SCHEMES

Based on the resources of frequency, time, and space (or location), some of the basic access techniques for satellite communication are shown in Figure 1. From this it can be observed that most multiple access techniques can be derived from the division of combinations of the basic resources. Basic orthogonal access methods utilizing separate time and frequency division have been designed, implemented, and become operational on satellite networks. However, due to either frequency instability or time jittering, finer frequency or time division allocation alone becomes a practical difficulty for a network with a very large number of stations, and other access means must be sought.

As shown in Figure 1, when TDMA is combined with SDMA we have satellite-switched TDMA. When FDMA is combined with TDMA we have a time-frequency (TF) access scheme, which includes frequency hopping (FH) and time hopping (TH). When a spreading effect is applied to

time we have time spreading (T-SPD); when it is applied to frequency we have frequency spreading (F-SPD) or a spread spectrum (SS) arrangement. From a mechanization standpoint, FH can produce F-SPD, as TH can produce T-SPD.

As indicated in Figure 1, we classify ALOHA multiple access systems as time division systems. ALOHA or ALOHA-derived systems are different from conventional TDMA systems in that ALOHA is not periodic in time and most message slots are not fixed in length. In ALOHA systems, although one can transmit messages randomly, the system cannot guarantee their reception randomly because of possible message collisions from other accessing stations. For this reason, we do not consider ALOHA-type access schemes to be truly random. The discussion of other access schemes such as satellite polling is omitted here and they can be found in [2]. In the next section, we discuss a different type of random multiple access, unrelated to ALOHA, for mobile satellite applications.

3. RANDOM MULTIPLE ACCESS

Starting with the use of the TF matrix for station access, depending on the division of time and frequency, with different detection and implementation process, variations of TF systems may be designed. Basically, a TF system makes use of the elements or cells of the time and frequency two-dimensional matrix resulting in the use of both time and frequency divisions. A specific type of access method, which utilizes the TF matrix and with deterministic signatures of prescribed characteristics, has been referred to as random multiple access (RMA). The definition, configuration, and the tradeoffs of such an access scheme are described in [2], and the signature generation algorithm for the purpose of random multiple accessing is illustrated in [3].

Depending on the practical constraints as to whether time or frequency can be more finely divided, n can be either the number of time or the number of frequency divisions. If n is the number of time divisions as shown in Figure 2, then it has been worked out by Wu [1], that:

The number of frequency divisions $f = n^2$
 The number of symbols in the TF matrix = n^3
 The number of stations in the network = $n^2(n^2+n+1)$.

In the derivation and proof of the above results, the assumptions were that n is a power of a prime (i.e., $n = p^m$), and single element overlap in the TF matrix is tolerated. In the case that time can be more finely divided as shown in Figure 3, then n becomes the number of frequency divisions, and n^2 the number of time divisions. The number of entries or symbols in the TF matrix and the number of earth stations in the network remain the same under the same condition of single element overlapping. The number of divisions n needed with respect to the number of stations in a network is shown in Table 1, with n up to 31 for near one million stations.

4. PERFORMANCE WITH ONBOARD QUEUE

In RMA, a collection of s signatures (addresses, or sequences) is assigned to each of the stations in the network. Each signature assembles E number of time-frequency elements out of a possible total number $T \times F$, where T and F are the number of time and frequency division elements in a given frame. The receiver must determine which one of the s signatures was transmitted, based on the received E elements. Let us assume that the collection of E elements is randomly chosen, and the probability of the event for a particular E element to occur is $P(E) = E/TF$. The probability for this event not to occur is $P(\bar{E}) = 1 - P(E)$. For k users in the network not to have any one of the particular E elements, the probability is

$$P_k(\bar{E}) = [1 - P(E)]^k = \left[1 - \frac{E}{TF} \right]^k \quad (1)$$

But for false detection to occur, all E elements must match, and this can occur with the probability

$$\begin{aligned} F_k(E) &= (1 - P_k(\bar{E}))^E \\ &= \left\{ 1 - \left[1 - \frac{E}{TF} \right]^k \right\}^E \end{aligned} \quad (2)$$

which can happen for any one of the E element collections. Since there are s number of collections (signatures), we then have for each user

$$F(k, E, s) = s F_k(E). \quad (3)$$

Now assume that a mobile satellite with an onboard queue, and a network in which all users are statistically independent, each user i with Poisson arrival rate λ_i and departure rate μ_i . If the users can only be increased or decreased one at a time (a realistic assumption), then the network can be modelled as a Markovian birth-death process. In this case, the probability of a station accessing in Δt is $\lambda_n \Delta t$, and that of a station dropping out is $\mu_n \Delta t$. The steady state probability of n accessing stations remaining in operation at time t is

$$P_n = P_o \prod_{i=1}^n \frac{\lambda_{i-1}}{\mu_i} \quad (4)$$

For a maximum number of K stations we have

$$\begin{aligned} \sum_{n=0}^K P_n &= P_o \sum_{n=0}^K \prod_{i=1}^n \frac{\lambda_{i-1}}{\mu_i} \\ &= P_o \left[1 + \sum_{n=1}^K \prod_{i=1}^n \frac{\lambda_{i-1}}{\mu_i} \right] = 1 \end{aligned} \quad (5)$$

or

$$P_o = \frac{1}{1 + \sum_{n=1}^K \prod_{i=1}^n \frac{\lambda_{i-1}}{\mu_i}} \quad (6)$$

The series in the denominator of (6) converges when $(\lambda_{i-1}/\mu_i) < 1$ for all i . Combining the results of (4), (6), (1), and (3), we have the false detection error probability,

$$\begin{aligned}
F(k, E, s, K) &= \sum_{k=0}^K P_k \cdot F(k, E, s) \\
&= \frac{s \left\{ 1 - \left[1 - \frac{E}{TF} \right]^k \right\}^E \prod_{i=1}^k \frac{\lambda_{i-1}}{\mu_i}}{1 + \sum_{k=1}^K \prod_{i=1}^k \frac{\lambda_{i-1}}{\mu_i}} \quad (7)
\end{aligned}$$

where K is the maximum number of stations designed for the system, and k is the number of simultaneous stations accessing the satellite channel during the time of detection.

Equation (7) can be simplified for identical user parameters, i.e., $\lambda_i = \lambda$, $\mu_i = \mu$ for all i . A sample evaluation of (7) is shown in Table 2 which assumes $\lambda_{i-1} = \lambda$, $\mu_i = \mu$ for all i and $K = 1,000$; k varies from 10 to 60. For K equal to 60, E changes from 3 to 16, and ρ equal to 0.9, the false detection error probability $F(k, E, s, K)$ is shown in Figure 4.

5. CONCLUDING REMARKS

Without referring to a specific application of aeronautical, land mobile, or maritime, this paper conceptually discusses the use of a random multiple access method with prescribed deterministic signatures for mobile satellite networks. In the special case of single element overlap being allowed, over a million station network can be designed for the signature length $n = 32$.

A possible RMA for mobile satellite network arrangement is shown in Figure 5, where RMA generation and detection functions may be combined into a coded phase modem. Such a modem is extensively discussed in the session on Modulation and Coding in this conference and elsewhere. On the other hand, for minimization of complexity or low cost reasons, digital frequency modulation or frequency shift keying scheme can also be used.

A new investigation on RMA is presently under way jointly by the University of Technology, Sydney and the Overseas Telecommunications Commission of Australia [4, 5].

REFERENCES

- [1] A. Ghais, G. Berzins, and D. Wright, "INMARSAT and the Future of Mobile Satellite Services," IEEE Journal on Selected Area in Communications, Volume SAC-5, No. 4, May 1987.
- [2] W.W. Wu, Elements of Digital Satellite Communication, Volume I - System Alternatives, Analyses and Optimization, Computer Science Press, 1984, Chapter 3.
- [3] W.W. Wu, Elements of Digital Satellite Communication, Volume II - Channel Coding and Integrated Service Digital Satellite Networks, Computer Science Press, 1985, Chapter 3.
- [4] M. Yates and T. Stevenson, Private Communications, 12 February 1988.
- [5] G. Brann, G. Richardson, T. Percival, M. Friedgut, and E. Bachmann, Private Communication, 12 February 1988.

Table 1
Parameters for RMA sequences up to length 31.

n	p^m	Number of Symbols n^3	Number of Stations $n^2(n^2 + n + 1)$
1	1 ¹	1	3
2	2 ¹	8	28
3	3 ¹	27	117
4	2 ²	64	336
5	5 ¹	125	775
7	7 ¹	343	2793
8	2 ³	512	4672
9	3 ²	729	7371
11	11 ¹	1331	16093
13	13 ¹	2197	30927
16	2 ⁴	4096	69888
17	17 ¹	4913	88723
19	19 ¹	6859	137541
23	23 ¹	12167	292537
27	3 ³	19683	551853
29	29 ¹	24389	732511
31	31 ¹	29791	954273

Table 2

Calculations of false detection error probability in random multiple access.

K(Max. Stations) = 1000			
E	ρ	k	$\bar{F}(k, E, s, K)$
3	.1	10	1.60333491E-05
4	.1	10	5.12182990E-07
8	.1	10	1.65816949E-15
16	.1	10	2.05177104E-38
3	.2	10	1.60493668E-05
4	.2	10	5.12694672E-07
8	.2	10	1.65982604E-15
16	.2	10	2.05382081E-38
3	.5	10	1.60493878E-05
4	.5	10	5.12695343E-07
8	.5	10	1.65982821E-15
16	.5	10	2.05382349E-38
3	1.0	10	1.60493811E-05
4	1.0	10	5.12695129E-07
8	1.0	10	1.65982752E-15
16	1.0	10	2.05382264E-38
3	.1	40	4.00833630E-06
4	.1	40	1.28045777E-07
8	.1	40	4.14542372E-16
16	.1	40	5.12942975E-39
3	.2	40	4.01234463E-06
4	.2	40	1.28173822E-07
8	.2	40	4.14956914E-16
16	.2	40	5.13455918E-39
3	.5	40	4.01234312E-06
4	.5	40	1.28173774E-07
8	.5	40	4.14956757E-16
16	.5	40	5.13455724E-39
3	1.0	40	4.01234312E-06
4	1.0	40	1.28173774E-07
8	1.0	40	4.14956757E-16
16	1.0	40	5.13455724E-39
3	.1	60	2.67222463E-06
4	.1	60	8.53638462E-08
8	.1	60	2.76361563E-16
16	.1	60	3.41961936E-39
3	.2	60	2.67489686E-06
4	.2	60	8.54492100E-08
8	.2	60	2.76637925E-16
16	.2	60	3.42303898E-39
3	.5	60	2.67489688E-06
4	.5	60	8.54492107E-08

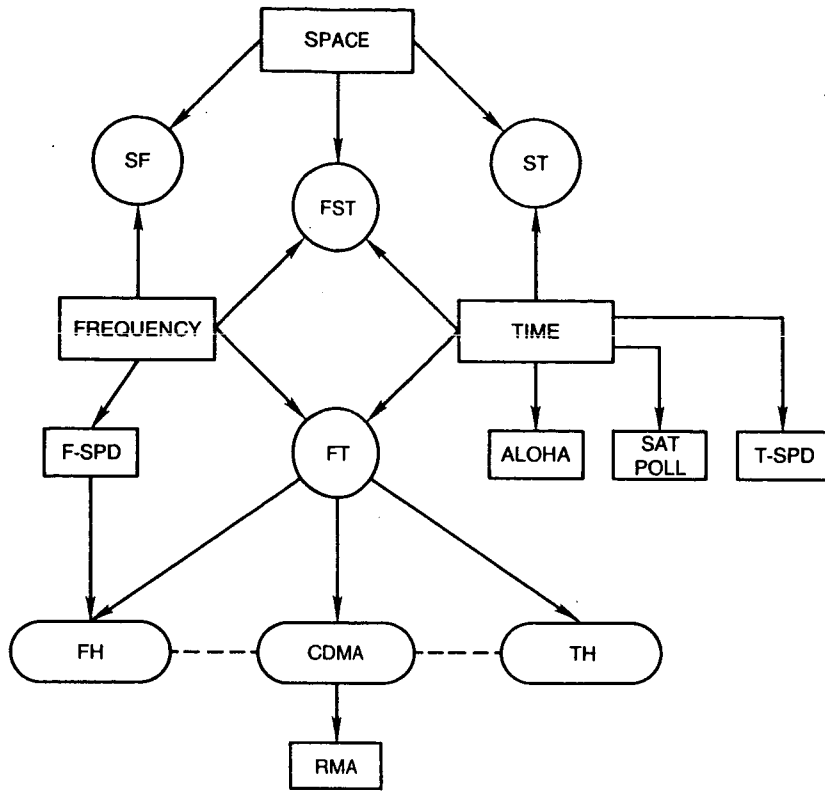


Figure 1
MULTIPLE ACCESS METHODS

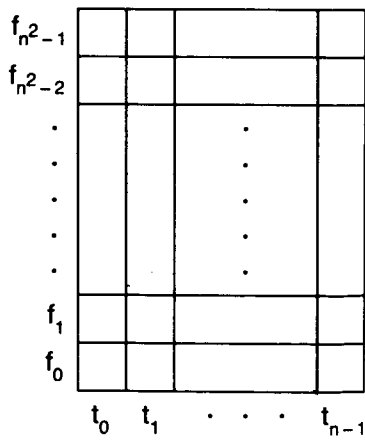


Figure 2
TF MATRIX WITH $f = n^2$

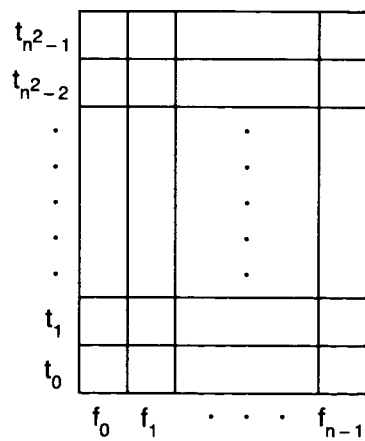


Figure 3
TF MATRIX WITH $t = n^2$

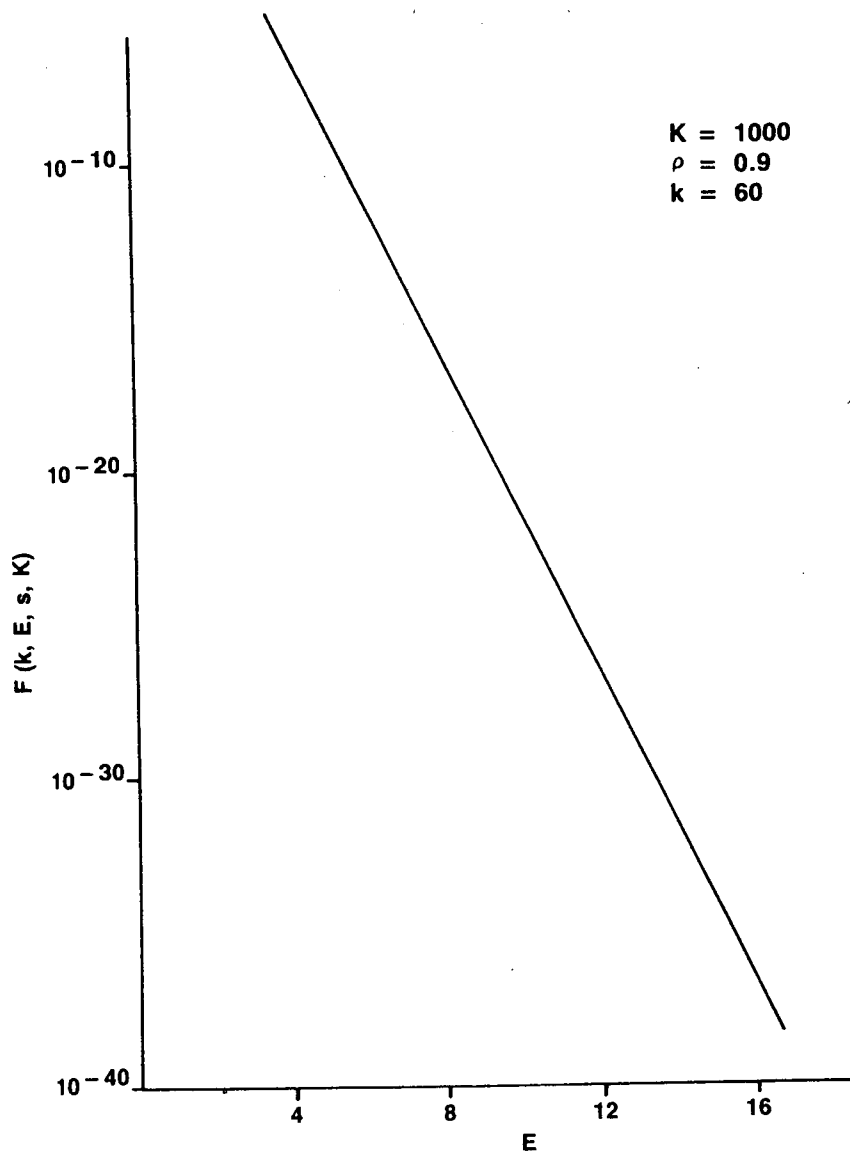


Figure 4
FALSE DETECTION ERROR PROBABILITY OF
RANDOM MULTIPLE ACCESS SYSTEMS



Figure 5
MOBILE SATELLITE APPLICATIONS WITH RANDOM MULTIPLE ACCESS

AN OPERATIONAL OPEN-END FILE TRANSFER PROTOCOL FOR MOBILE SATELLITE COMMUNICATIONS

Charles Wang, Unjeng Cheng and Tsun-Yee Yan
Jet Propulsion Laboratory
California Institute of Technology
4800 Oak Grove Drive
Pasadena, CA 91109

ABSTRACT

This paper describes an operational open-end file transfer protocol which includes the connecting procedure, data transfer, and relinquishment procedure for mobile satellite communications. The protocol makes use of the frame level and packet level formats of the X.25 standard for the data link layer and network layer, respectively. The structure of a testbed for experimental simulation of this protocol over a mobile fading channel is also introduced.

1. INTRODUCTION

The concept of mobile communications through a geosynchronous satellite has been studied extensively in recent years [1,2]. Currently, the Mobile Satellite Experiment (MSAT-X) project at the Jet Propulsion Laboratory (JPL) is aimed at validating the ground segment technologies for future generations of the Land-Mobile Satellite System (LMSS) [3,4]. Such a satellite-based mobile communications network can provide open-end and closed-end services to mobile subscribers throughout a vast geographical area. In [5], a generic concept of open-end and closed-end services has been presented.

In data communications, a set of rules, called a protocol, must be followed to set up and take down a logical link and ensure reliable transmissions between the sender and the receiver. To decouple the interactions between various functions of a protocol, most network protocols are organized as a series of layers. Each layer only interfaces with the layers one level above and below it. The purpose of this hierarchy is to shield each layer from the details of how other layers are actually implemented. Hence, the implementation of each layer can be modified and changed without affecting the implementation of other layers. The International Standards Organization (ISO) has developed an Open Systems Interconnection (OSI) Reference Model to standardize the protocol development. This reference model includes 7 layers, namely, from the lowest to the highest, physical layer, data link layer, network layer, transport layer, session layer, presentation layer, and application layer [6].

Developing a protocol for a mobile communications network is a challenging problem. Various protocols such as BISYNC, SDLC, ADCCP, HDLC, DDCMP, X.21, X.25, X.28, etc., have been developed for different applications. X.25 is the protocol which has been widely used to interface Data Terminal Equipment (DTE) with the packet switched data network. Specifically it comprises the lowest three layers of the ISO-OSI reference model. In this paper, we make use of the data link layer and network layer formats of X.25 for implement-

ing the open-end file transfer service for mobile satellite communications. This allows an existing commercial DTE to access the mobile satellite network with minor modifications.

In this paper, Section 2 describes the conceptual open-end file transfer for mobile satellite communications. In Sections 3 and 4, we illustrate how X.25 format can be used for the network layer and data link layer, respectively. Finally, Section 5 presents the structure of a testbed for experimental simulation of this protocol in a mobile fading environment.

2. FILE TRANSFER FOR OPEN-END CONNECTIONS

In a mobile communications network, the service of transferring long data files is often necessary. Since the duration of a data file may not be known in advance, the network must maintain the allocation of the resource to the file transfer until termination. As stated in [5], a subscriber must send a connection request for transmission through a request channel to the Network Management Center (NMC) whenever it wishes to initiate an open-end connection. After sending out a request, the subscriber waits for an assignment packet, which also serves as an acknowledgment to the request, from the NMC. If the subscriber does not receive the assignment packet within a preset timeout period, it retransmits the request after a backoff delay.

Upon receiving a successful open-end connection request, the NMC checks whether the destination party is busy or whether all open-end channels are occupied. In either case, the NMC sends a busy status to the requester. Otherwise, the NMC attempts to notify the destination party. If this is successful, the NMC sends an assignment packet to the requester. If this assignment packet is received correctly, the requester tunes to the assigned open-end channel and starts transmitting the file. At the end of file transfer, the requester sends a relinquishment message to NMC for taking down the channel.

3. CONNECTING AND RELINQUISHMENT PROCEDURES USING X.25 PACKET LEVEL PROTOCOL

The connecting and relinquishment procedures described above can be implemented using the packet level logical interface of X.25 [6,7]. Figure 1 summarizes the control packets of X.25 used in our scenario. The procedures to establish and terminate an open-end connection are described in Figures 2 and 3, respectively. The frame structures of various control packets are illustrated in Figures 4(a) through 4(d). Note that the CALL-REQUEST and INCOMING-CALL packets must contain the addresses of the calling DTE and the called DTE. Furthermore, for INCOMING-CALL and CALL-CONNECTED packets, the channel # field is used to identify the assigned data-transmission channel.

To establish a file transfer session, the calling DTE sends a CALL-REQUEST packet to the NMC through a request channel. It then waits for a CALL-CONNECTED packet from the NMC. If the calling DTE does not receive the CALL-CONNECTED packet within T_{CR} seconds from the NMC, it will retransmit the same CALL-REQUEST packet.

After receiving the CALL-REQUEST packet successfully from the calling DTE, NMC sends an INCOMING-CALL packet to the called DTE if the called DTE is not busy and an open-end channel is available (referred to as the line-not-busy case, see Figure 2(a)); otherwise, it sends a CLEAR-INDICATION packet back to the calling DTE (referred to as the line-busy case, see Figure 2(b)). Note that the CLEAR-INDICATION packet is also

used in the call-clearing procedure (see the following discussion). The INCOMING-CALL packet contains the identity of the assigned data-transmission channel and the scheduled transmission-start-time. The assigned channel is allocated by NMC at the moment that the INCOMING-CALL packet is issued. After receiving the INCOMING-CALL packet successfully, the called DTE responds with a CALL-ACCEPTED packet to NMC through the assigned data-transmission channel. Since the CALL-ACCEPTED packet is sent through the allocated channel, the address of the called DTE is not required. The CALL-ACCEPTED packet can be viewed as an acknowledgement to the INCOMING-CALL packet. In case the CALL-ACCEPTED packet is not received within a time-out period (T_{IC} seconds), NMC will retransmit the same INCOMING-CALL packet. Since the channel error rate is high in the mobile environments, the same INCOMING-CALL packet may be transmitted to the called DTE more than once. Hence the scheduled transmission-start-time on each retransmitted INCOMING-CALL packet may be different to account for the time delay caused by retransmissions. Furthermore, the time-out period for retransmitting the INCOMING-CALL packets must be long enough to ensure that the CALL-ACCEPTED packet received by NMC acknowledges the most recent INCOMING-CALL packet.

After successfully receiving the CALL-ACCEPTED packet from the called DTE, NMC sends a CALL-CONNECTED packet to the calling DTE. In case the CALL-CONNECTED packet is lost or not received correctly, the calling DTE will retransmit the CALL-REQUEST packet after a time-out period T_{CR} . The CALL-CONNECTED packet contains the identity of the assigned data-transmission channel and the transmission-start-time. After the calling DTE successfully receives the CALL-CONNECTED packet, the file transfer session will begin at the scheduled transmission-start-time.

During data transmission phase, NMC monitors the allocated channel for a CLEAR-REQUEST packet. The relinquishment procedure will be initiated by the calling DTE to send a CLEAR-REQUEST packet to NMC through the data-transmission channel. As shown in Figure 3, the relinquishment procedure is the dual of the line-not-busy case of the connecting procedure with the CALL-REQUEST, INCOMING-CALL, CALL-ACCEPTED and CALL-CONNECTED packets being replaced by the CLEAR-REQUEST, CLEAR-INDICATION, DTE-CLEAR-CONFIRMATION, and DCE-CLEAR-CONFIRMATION packets, respectively. Since NMC knows who are using the allocated channels, the terminal identity is not necessary in the CLEAR-REQUEST and DTE-CLEAR-CONFIRMATION packets.

4. DATA LINK CONTROL USING X.25 LINK LEVEL PROTOCOL

In the mobile environment, to ensure reliable communications between the sender and the receiver, an automatic retransmission protocol must be utilized. The data link level protocol, i.e. Link Access Protocol, Balanced (LAP-B), of X.25 provides an efficient retransmission scheme that can be used for the data link control in open-end file transfers.

Figure 5 shows the standard X.25 frame structure. In X.25, a flag pattern, 01111110, is used to indicate the beginning and the end of a frame. If this flag pattern is corrupted by the channel noise or fading, the entire content of the frame will be considered lost. Thus, in our applications, a new flag pattern is designed to cope with the high bit error rate in the mobile environment. The address field (ADDR) identifies the terminal to which the frame is sent. The control field (CTRL) is used for sequence numbers, acknowledgments, and other purposes, as discussed below. The data field (DATA) contains the data which is in

the packet format from the network layer. In X.25, the DATA field may be arbitrarily long; however, our previous study showed that the DATA field length should be kept below 512 bits in order to achieve an acceptable packet error rate in the mobile fading environments [8]. The FCS field is a minor variation of the well-known cyclic redundancy code (CRC) which allows lost flag bytes to be detected.

There are three kinds of frames: Information (I), Supervisory (S), and Unnumbered (U), specified by the CTRL field. Figure 6 shows various formats of these frame types. The Information (I) frames encapsulate the data packets of the file and the control packets for the connecting and relinquishment procedures. The sequence numbers, N(S) and N(R), use 3 bits for which up to 7 unacknowledged frames may be outstanding at any instant. N(S) is the sequence number of the currently transmitted frame. N(R) is the expected sequence number of the next received frame.

In the Supervisory frames, Receiver-Ready (RR), Receiver-Not-Ready (RNR), and Reject (REJ) frames represent various kinds of acknowledgments. RR is an acknowledgment frame used to indicate the next expected frame. RNR acknowledges all frames up to but not including N(R). Although it looks like RR, it tells the sender to stop sending. This is to indicate certain temporary problems with the receiver, such as out of buffer space. When the problem is cured, the receiver sends RR, REJ or other control frames. REJ is a negative acknowledgment frame to the N(R) frame. The sender then must re-send all outstanding frames starting at N(R) in the current sliding window. This constitutes the Go-Back-N retransmission scheme. The X.25 does not provide a selective-repeat retransmission scheme. However, another similar data link protocol, High-Level Data Link Control (HDLC), does provide the selective repeat scheme by adopting an additional control field format, selective reject (SREJ). In that case, SREJ is also a negative acknowledgment frame to the N(R) frame. Nevertheless, it only asks for retransmission of the N(R) frame in sender's current sliding widow.

The unnumbered formats, SABM, UA, FRMR, and DISC, are used to report the status of the terminal or some odd situations of the transmission. They are not of the most importance as far as the normal file transfer is concerned and are not discussed here (see [9] for details).

5. A TEST-BED SIMULATOR FOR THE PROTOCOL

A test-bed which can experimentally simulate the proposed open-end file transfer protocol is developed. Figure 7 illustrates the configuration of this test-bed simulator. It consists of three major components, two programmable protocol analyzers and an IBM PC AT equipped with a 68020 co-processor board. The protocol analyzers perform the data link layer and network layer protocols and are used to emulate the network elements such as the calling party, the called party, and the NMC. The co-processor board inside the IBM PC AT performs the physical layer protocol which includes modulation/coding, demodulation/decoding, and mobile fading channel. Inside the IBM PC AT, there are two IBM synchronous data link control (SDLC) communication adapters which are connected to the protocol analyzers via RS232-C cables. This setup allows us to intercept all data communicating between two protocol analyzers.

Theoretically, three protocol analyzers should be used to represent three distinct network elements. However, in our scenario, all three elements do not communicate with each other simultaneously. For example, at the phase of making connection (call-setup) and

relinquishment (call-clearing), either the calling party or the called party needs to communicate with the NMC, whereas, at the data transmission phase, only the calling party and the called party are active. Therefore, only two protocol analyzers are necessary to perform the protocol simulation. Figure 8 shows a command flow diagram among two protocol analyzers (emulating three entities) and the IBM PC AT.

Using this test-bed, we can simulate various scenarios in the mobile fading environment. Protocol parameters can be adjusted to optimize the system performance. It has been shown that this protocol is efficient to combat the disturbances, such as packet error, packet loss, and packet insertion, during connecting, data transmission, and relinquishment phases.

REFERENCES

1. G.H. Knouse and P.A. Castruccio, "The Concept of an Integrated Terrestrial/Land Mobile Satellite System," *IEEE Trans. on Veh. Tech.*, Vol. VT-30, August 1981. pp.97-101.
2. R.E. Anderson, R.L.Frey, and J.R.Lewis, "Technical Feasibility of Satellite-Aided Land Mobile Radio," *Proc. Inter. Conf. on Comm.*, June 1982. pp.7H2.1-7H2.5.
3. F. Naderi, G.H. Knouse, and W.J. Weber, "NASA's Mobile Satellite Communications Program; Ground and Space Segment Technologies," *Proc. International Astronautics Federation Congress, Laussane, Switzerland, October, 1984.*
4. W.J. Weber and F. Naderi, "NASA Mobile Satellite Experiment (MSAT-X)" *Proc. National Electronic Conf.*, Vol. 37, Chicago, Illinois, June 1983. pp.328-330.
5. V.O.K. Li and T.-Y. Yan, "An Integrated Voice and Data Multiple Access Scheme for a Land Mobile Satellite System," *Proc. of the IEEE, Special Issue on Satellite Communication Networks*, Nov. 1984.
6. W. Stallings, *Handbook of Computer Communications Standards, Volume 1, A Stallings/MacMillan Book*, 1987.
7. A.S. Tanenbaum, *Computer Networks*, Prentice Hall, Inc., 1981.
8. C.C. Wang and T.-Y. Yan, "Performance Analysis of An Optimal File Transfer Protocol for Integrated Mobile Satellite Services", *Proceeding of GLOBECOM'87, Tokyo, Japan, December, 1987.*
9. R.J. Deasington, *X.25 Explained: Protocols for Packet Switching Networks, Second Edition*, Halsted Press, 1986.

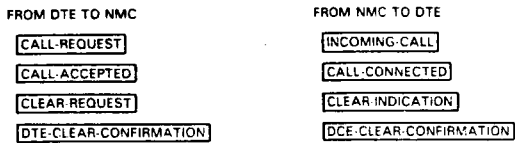


Figure 1. X.25 Control Packet Types for Connecting and Relinquishment Procedures

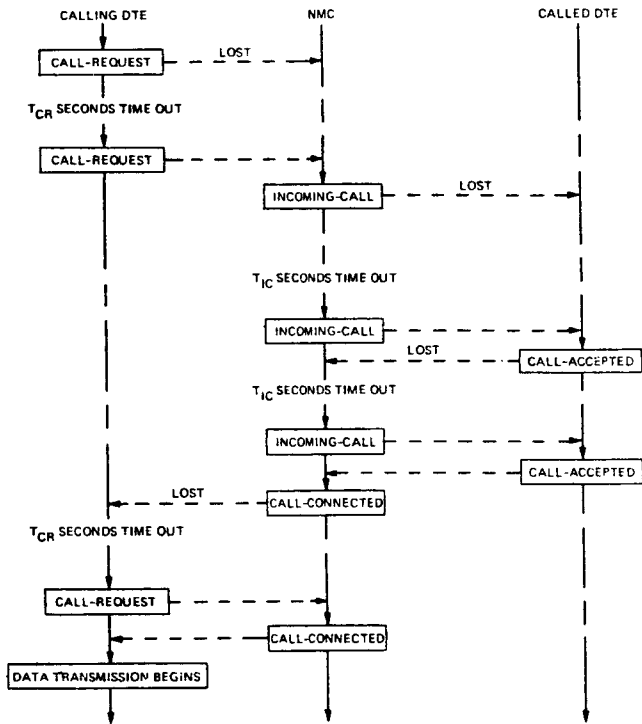


Figure 2(a). Establishing an Open-End File Transfer Session: Line-Not-Busy Case

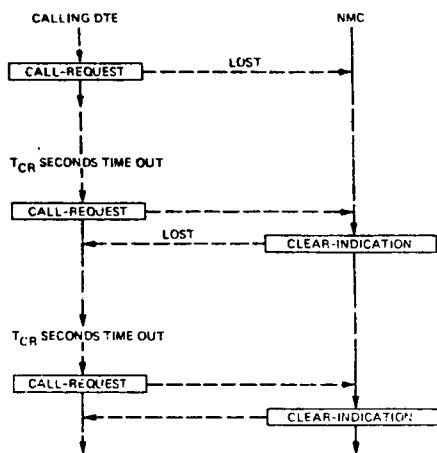


Figure 2(b). Establishing an Open-End File Transfer Session: Line-Busy Case

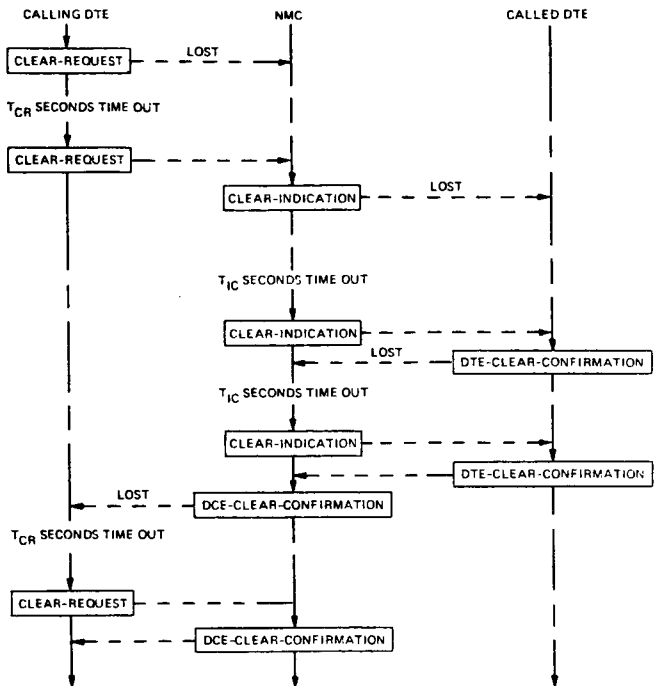


Figure 3. Relinquishing an Open-End File Transfer Session

BITS	8	7	6	5	4	3	2	1
OCTETS 1	0	0	0	1	GROUP #			
2	CHANNEL #							
3	0	0	0	0	1	0	1	1
4	CALLING ADDRESS LENGTH					CALLED ADDRESS LENGTH		
5	UP TO 14 OCTETS ADDRESSES							
n ₁	0	0	FACILITY FIELD LENGTH					
n ₂	OPTIONAL FACILITY FIELDS UP TO 16 OCTETS							

Figure 4(a). CALL-REQUEST and INCOMING-CALL Packet Format

BITS	8	7	6	5	4	3	2	1
OCTETS 1	0	0	0	1	GROUP #			
2	CHANNEL #							
3	0	0	0	0	1	1	1	1

Figure 4(b). CALL-ACCEPTED and CALL-CONNECTED Packet Format

BITS	8	7	6	5	4	3	2	1
OCTETS 1	0	0	0	1	GROUP #			
2	CHANNEL #							
3	0	0	0	1	0	0	1	1

Figure 4(c). CLEAR-REQUEST and CLEAR-INDICATION Packet Format

BITS	8	7	6	5	4	3	2	1
OCTETS 1	0	0	0	1	GROUP #			
2	CHANNEL #							
3	0	0	0	0	0	1	1	1

Figure 4(d). DCE-CLEAR-CONFIRMATION and DTE-CLEAR-CONFIRMATION Packet Format

FLAG	ADDR	CTRL	DATA	FCS	FLAG
------	------	------	------	-----	------

FLAG : 01111110
 ADDR : '00000011' COMMANDS FROM DCE TO DTE
 AND RESPONSES FROM DTE TO DCE
 '00000001' COMMANDS FROM DTE TO DCE
 AND RESPONSES FROM DCE TO DTE
 CTRL : INFORMATION
 SUPERVISORY
 UNNUMBERED
 DATA : FROM NETWORK LAYER
 FCS : FRAME CHECK SEQUENCE (2 BYTES)

Figure 5. Structure of X.25 Data Link Layer Frame

FORMAT	COMMANDS	BITS:	8	7	6	5	4	3	2	1
I	I			N(R)		P		N(S)		0
S	RR			N(R)		PF	0	0	0	1
S	RNR			N(R)		PF	0	1	0	1
S	REJ			N(R)		PF	1	0	0	1
*S	SREJ			N(R)		PF	1	1	0	1
U	SABM		0	0	1	P	1	1	1	1
U	UA		0	1	1	F	0	0	1	1
U	FRMR		1	0	0	F	0	1	1	1
U	DISC		0	1	0	P	0	0	1	1

* FOR HDLC ONLY

Figure 6. Control Field Format for Various X.25 Frames

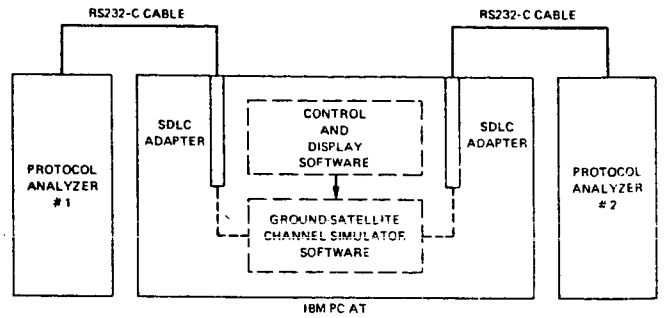


Figure 7. Hardware Configuration of a Test-Bed Simulator for Open-End File Transfer

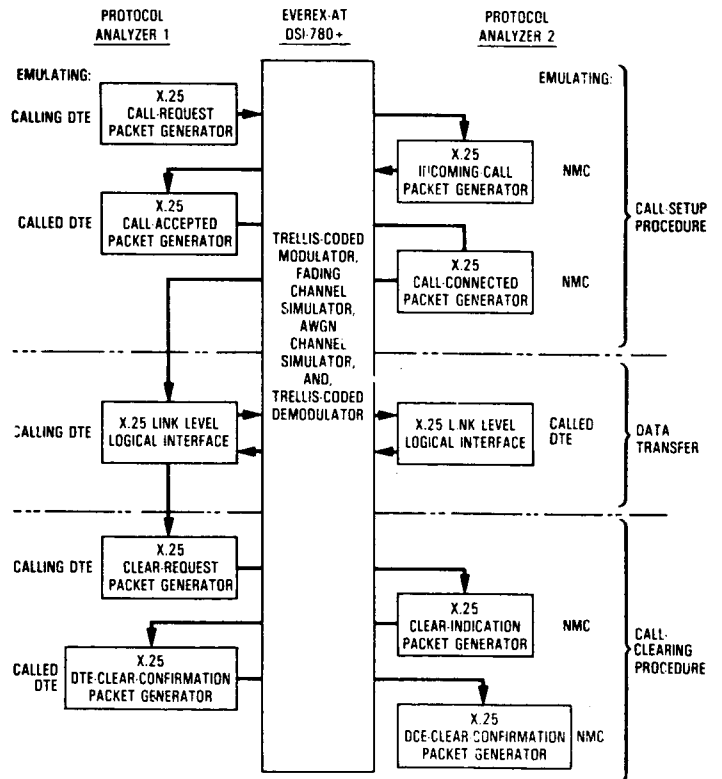


Figure 8. Control Flow Diagram of the Test-Bed Simulation

INTEGRATED VOICE/DATA PROTOCOLS FOR SATELLITE CHANNELS

CHENG-SHONG WU; VICTOR O.K. LI

UNIVERSITY OF SOUTHERN CALIFORNIA
Department of Electrical Engineering-System
Los Angeles, CA 90089-0272
United States.

ABSTRACT

In this paper, several integrated voice/data protocols for satellite channels are studied. The system consists of two types of traffic; voice calls which are blocked-calls-cleared and the data packets which may be stored when no channel is available. The voice calls are operated under a demand assignment protocol. We introduce three different data protocols for data packets. Under RAD, the ALOHA random access scheme is used. Due to the nature of random access, the channel utilization is low. Under DAD, a demand assignment protocol is used to improve channel utilization. Since a satellite channel has long propagation delay, DAD may perform worse than RAD. We combine the two protocols to obtain a new protocol called HD. The proposed protocols are fully distributed and no central controller is required. Numerical results show that HD enjoys a lower delay than DAD and provides a much higher channel capacity the RAD. We also compare the effect of fixed and movable boundaries in partitioning the total frequency band to voice and data users.

1 INTRODUCTION

In this paper, we propose distributed multiple access protocols for satellite channels. In [3,4], integrated voice and data multiple access protocols are studied. In [3] a central controller implements reservation-based protocols for voice calls and data packets in a land-mobile satellite network. Coviello and Vena [2] described the Slotted Envelope Network scheme for multiplexing voice and data traffic on a communication link using TDMA such that the number of slots reserved for voice

calls in each TDMA frame varies from frame to frame. Similar concepts, called movable boundary schemes, are studied in [5,6].

For data service in satellite channels, the well-known ALOHA scheme is simple but suffers from low channel capacity. Demand assignment protocols, on the other hand, provide higher channel capacity but require channel access control. In addition, the delay of demand assignment scheme is larger than the ALOHA scheme when the offered traffic is light.

In this paper, a multiple-channel satellite providing both voice and data service is considered. For data packets, three different protocols are proposed. Under RAD, the ALOHA random access scheme is used. Under DAD, a demand assignment protocol is used to improve channel utilization. Since a satellite channel has long propagation delay, DAD may perform worse than RAD. We combine the two protocols to obtain a new protocol called HD. In fact, HD behaves like RAD when the offered traffic is low and like DAD when the traffic is high.

We also study a movable boundary scheme in which the data packets can use the idle voice channels. Note that all of the protocols proposed are fully distributed, that is, no central controller is necessary.

2 PROTOCOL DESCRIPTION

There are two types of traffic: voice calls and data packets. Voice calls will be blocked-calls-cleared, while data packets which arrive when all channels are busy may be stored. The system consists of a large number of voice and/or data users and a satellite which serves as a relay. The total bandwidth of the satellite is divided into multiple channels. There are R reservation channels and M message channels. The word "message" here refers to either voice call or data packet. All channels are slotted and the length of a slot time is equal to the transmission time of a data packet. A time slot in a reservation channel is further divided into n minislots and the length of each minislot is equal to the transmission of a request packet. Thus there are a total of $N = nR$ minislots per slot time in which to make reservations. Among the N minislots, the first M_v of them, called voice request minislots, are for voice requests and the others, called data request minislots, are for data requests. Here M_v is the maximum number of voice calls allowed in the system at the same time. M_v is a system design parameter.

2.1 Voice Protocol

All potential voice users monitor the reservation channels at all times and voice calls are operated on a demand assigned basis. When a voice user attempts to communicate with another, he will first send a request on a voice request channel and then begin his voice call on a message channel if the request is successful. More specifically, suppose user i has a voice call to user j . First user i checks all of the voice request minislots. If all of them are busy, then no channel is available at this time and the voice call will be blocked; otherwise, user j picks at random one

of the idle voice request minislots, say the k th voice request minislot, within the next slot and sends a request packet. The request packet contains the I.D. of the destination node. It also sends a jamming signal on the k th voice request minislot of the S following slots, where S is the round-trip propagation of the satellite channel measured in slots. This ensures that both node i and node j will learn whether the request signal is successful or not. If this request packet is successful, that is, the packet does not suffer a collision, node j will tune his receiver to the k th message channel and node i will start his transmission on this channel when he hears his request packet. If the request packet is not successful, node i will wait a random time and try again. Note that while node i is transmitting, he will keep on sending jamming signal in the corresponding voice request minislot to prevent potential interference from other users.

2.2 Data Protocols

Three different protocols are developed for data transmissions. Suppose that there are m message channels available for data.

2.2.1 Random Access Data (RAD) Protocol

The data packets are transmitted under a multi-channel slotted-ALOHA scheme and no reservation channel is required. If node i wants to send a packet to node j , then node i will send the data packet on the j_m th, $j_m = j \bmod m$, channel. In other words, multiple nodes may be receiving packets on the same channel, although not at the same time. Since there may be many channels available, it is not practical for a receiver to listen to all channels and wait for incoming packets. In this protocol, node j will only listen to the j_m th channel.

2.2.2 Demand Assignment Data (DAD) Protocol

The maximum throughput of m -channel slotted-ALOHA is $0.368m$. Here we propose a demand assignment protocol to improve it. Suppose node i wants to send a packet to node j . Node i will send a request packet on the reservation channels. In particular, node i chooses one of the reservation minislots at random, and sends a request packet containing the destination I.D. If the request is successful, node i puts this request on his request queue and waits for the scheduled time to transmit the packet. In this protocol, all users continuously monitor the reservation channels and track the successful reservation requests in the system. Upon hear a successful request, it puts the request in its request queue. Due to the broadcast nature of satellite channels, all nodes will receive the same request information and, thus, the request queue for every user is identical. According to the request queue, all packets with successful request are transmitted on a first come first served basis. At the beginning of a time slot, the user who has a request queued at the k th, $k \leq m$ position of the request queue will transmit the packet on the k th data channel. Up to m packets can be transmitted in a slot time and the corresponding requests

of the transmitted packets in the request queue will be deleted at the end of the slot. Since the receiver (node j) also has the transmission schedule, he can tune his receiver to the proper channel to receive the packet from node i . Note that a user needs only keep information on the length of the queue, the position of his own request, and the requests in which the corresponding data packets are destined to him. Thus we have a fully distributed scheduling scheme which does not require much bookkeeping.

2.2.3 Hybrid Random Access and Demand Assignment Access Data (HD) Protocol

The delay under DAD is larger than that under RAD when the offered traffic is light, especially on a long propagation delay channel such as satellite channels. However, we can combine these two protocols and get a hybrid protocol which behaves like a random access scheme when the traffic is light and like a reservation scheme when the traffic is heavy.

Again every user keep on monitoring the reservation channels so that everyone knows the system request queue at any time. Suppose node i has a packet to node j at slot β , it will send a request on the data request minislot. Whether this request is successful or not is unknown until one round-trip delay later, i.e., the scheduled time for this packet is at least S slots from now. Since all nodes have the system schedule information at slot β , node i knows whether there will be some idle channels at the next slot or not. If there are some, say k , idle channels, node i can send the packet, called an R-packet, on the j_k th channel at the next slot; otherwise, the operation of the protocol is exactly the same as DAD. Note that node I still needs to make a reservation for this packet, since the R-type packet may result in a collision.

2.3 Integrated Voice and Data Protocols

We can mix the voice protocol with any one of the three data protocols mentioned above to provide an integrated voice and data service. The M message channels are divided into two groups. One group, containing M_v channels, is allocated for voice calls; the other group, containing $M_d = M - M_v$ channels, is for data packets.

2.3.1 Fixed Boundary Strategy

In this strategy, the data packets are not allowed to use the M_v voice channels even if some of them are idle.

2.3.2 Movable Boundary Strategy

The difference between the fixed and movable boundary strategies is that in the latter the data packets may occupy any of the voice channels not currently in use. An arriving voice call, however, has higher priority to receive service in the

voice channels. Since the voice calls have higher priority, the operation of the voice users is the same as the voice protocol mentioned above. However, the operation of the data user needs some minor modifications. In this strategy, a data user must check the status of the voice request minislots in every slot. Since an active voice call will keep on sending jamming signal on the corresponding voice request minislot, the data user can find out how many and which voice channels are idle by checking the voice request minislot. If there are v voice channels free, then the data users will operate as if there are $M_d + v$ data channels at the next slot.

3 PERFORMANCE ANALYSIS

We now analyse the performance of the multipleaccess schemes proposed in the previous section.

3.1 Model Assumptions

The following assumptions will be made in the analysis:

1. The users collectively generate Poisson data packet traffic at rate λ_d packets/second and Poisson voice traffic at rate λ_v calls/second.
2. The data packets are of fixed length. The voice call duration is exponentially distributed with mean $1/\mu_v$ seconds.
3. Channels are slotted. Let T denote the slot length which equals the transmission time of a packet and S be the round-trip delay of the channel measured in slots.
4. The retransmission delay for a request or a random access data packet is uniformly distributed between 0 and K slots.

3.2 Voice Blocking Probability

The average voice duration $1/\mu_v$ is expected to be much longer than the slot time T and for a reasonable blocking probability, $\lambda_v T$ should be much less than one. The probability of collision of voice requests is negligible. In addition, since the channel is slotted, a voice call of length X sec. will occupy $\lceil \frac{X}{T} \rceil$ slots = $\lceil \frac{X}{T} \rceil T$ sec. We shall approximate this by X sec. The error introduced is negligible. The voice channels can be modeled as an M/G/s/s s-server loss system. The blocking probability for an s-channel system is given by the Erlang B formula,

$$P_B = \frac{\left(\frac{\lambda_v}{t_v}\right)^s / s!}{\sum_{k=0}^s \left(\frac{\lambda_v}{t_v}\right)^k / k!} \quad (1)$$

where $1/t_v$ is mean call duration time $1/\mu_v$ plus the round-trip delay time ST . Furthermore, for typical voice calls, the call duration is much larger than the round-trip

delay. We can further simplify the system to an M/M/s/s queue and the probability that a system with s channels has n active voice calls is given by

$$\pi_v(n) = \frac{\left(\frac{\lambda_v}{\mu_v}\right)^n / n!}{\sum_{k=0}^s \left(\frac{\lambda_v}{\mu_v}\right)^k / k!} \quad (2)$$

3.3 Data Channel Analysis

3.3.1 Random Access Data (RAD) Protocol

Define p_{suc_data} to be the probability that a data packet will be successful on a data channel RAD. Clearly $p_{suc_data} = \lambda_d T / m \times e^{-\lambda_d T / m}$ for an m data channel system. The throughput of such a system η_{RAD} is $p_{suc_data} m = \lambda_d T e^{-\lambda_d T / m}$. The average delay under RAD can be obtained from

$$D_{RAD}(m) = (1.5 + S + (e^{\lambda_d T / m} - 1)(1 + S + \frac{K-1}{2}))T \quad (3)$$

where $e^{\lambda_d T / m} - 1$ is the average number of retransmissions required for the data packet.

3.3.2 Demand Assignment Data (DAD) Protocol

The analysis of the reservation channels, which operates under random access, is similar to that of the data channel under RAD. Define p_{suc_req} to be the probability that a request packet will succeed in a reservation minislot. Then, $p_{suc_req} = \lambda_d T / l \times e^{-\lambda_d T / l}$ and the throughput of the reservation channel η_{rs} is $l \times p_{suc_req}$ per slot, where l is the number of data request minislots per slot. The delay of a successful request is $t_{rs} = (1 + S + (e^{\lambda_d T / l} - 1)(1 + S + \frac{K-1}{2}))T$. The maximum throughput of the reservation channel is $0.368l$ requests/slot. If there are m data channels, then $l = 3m$ is enough to achieve the maximum utilization of the data channels.

In the analysis of the data channels, we use p_i to denote the probability that i requests succeed in a slot and define π_i to be the probability of having a total of i successful requests enqueued in the system at the beginning of a slot, then

$$p_i = \binom{l}{i} p_{suc_req}^i (1 - p_{suc_req})^{l-i} \quad (4)$$

and from [1] we get

$$\Pi(z) = \frac{P(z)[\Pi_m(z)z^m - \Pi_m(z)]}{z^m - P(z)} \quad (5)$$

where $\Pi(z) = \sum_{i=0}^{\infty} \pi_i z^i$, $\Pi_m(z) = \sum_{i=0}^{m-1} \pi_i z^i$ and $P(z) = \sum_{i=0}^{\infty} p_i z^i$. Note that $\Pi'(1)$ is the average queue length.

The total packet delay D_{DAD} consists of three parts: the request packet delay t_{rs} , the queueing delay t_q and the propagation delay S . The queueing delay, given

by Little's formula, is $\Pi'(1)/\eta_{rs}$. Now the total packet delay under DAD is

$$D_{DAD} = t_{rs} + t_q + (S + 0.5)T \quad (6)$$

$$= \left\{ 1.5 + 2S + \frac{\Pi'(1)}{\lambda_d T e^{-\lambda_d T/l}} (e^{\lambda_d T/l} - 1) \left(1 + S + \frac{K-1}{2} \right) \right\} T \quad (7)$$

3.3.3 Hybrid Data (HD) Protocol

Under HD, the time slots which are not scheduled for packets can be used to transmit packets in a random access manner. The random access type transmission can be used only when the system state, defined as the number of requests enqueued in the system at the beginning of a slot, is less than the total number of data channels. A packet transmitted in the random manner is called an R-packet. Let $\lambda_d^R T$ be the average number of successful R-packets per slot. Then,

$$\lambda_d^R T = \sum_{i=0}^{m-1} \pi_i \lambda_d T e^{-\frac{\lambda_d T}{m-i}} \quad (8)$$

Note that R-packets will be transmitted again during their normal scheduled time. This is necessary since the packets transmitted under random access may collide. The delay of successful R-packets if successfully transmitted under random access is $D^R = (S + 1.5)T$ and the delay of R-packets if transmitted at the scheduled time is D^{DR} which is greater than $(2S + 1.5)T$. Let us denote the average delay of packets other than R-packets by D^N . We get

$$D^N = \frac{D_{DAD} \times \lambda_d - D^{DR} \times \lambda_d^R T}{\lambda_d - \lambda_d^R} \quad (9)$$

$$\leq \frac{D_{DAD} \times \lambda_d - (2S + 1.5)\lambda_d^R T}{\lambda_d - \lambda_d^R} \quad (10)$$

Now we can get the upper bound of the average delay under HD with m data channels:

$$D_{HD}(m) = \frac{\lambda_d^R}{\lambda_d} D^R + \frac{\lambda_d - \lambda_d^R}{\lambda_d} D^N \quad (11)$$

$$\leq D_{DAD}(m) - ST \frac{\lambda_d^R}{\lambda_d} \quad (12)$$

3.4 Analysis of Integrated Protocols

Since the voice calls have higher priority in their own channels, the blocking probability of voice call is not affected by data packets and can be obtained from section 3.2 directly. The following analyzes the delay of data packets in the integrated protocols.

3.4.1 Fixed Boundary Intergrated Protocols

Under the fixed boundary strategy, the data packets are not allowed to use the voice channel. The transmissions of voice calls and data packets do not affect each other. Thus, the performance analyses are the same as in sections 3.3.1, 3.3.2, and 3.3.3.

3.4.2 Movable Boundary Integrated Protocol

The data packets can use the idle voice channels under this strategy. The typical call duration is about 100 seconds and the typical slot time is in the order of 10^{-2} seconds or smaller. To simplify the caculations, we can assume the data queues reach their stationary state when v , $0 \leq v \leq M_v$ voice calls are active. Then the average packet delay is

$$Delay = \sum_{k=0}^{M_v} \pi_v(k) D_{data}(M - M_v) \quad (13)$$

D_{data} is obtained from either (3), (7) or (12), depending on which data protocol is used.

4 NUMERICAL RESULTS

Figure 3 shows the delay-throughput relationship for the three data protocols under the fixed and the movable boundary strategies. We consider a system with $M = 10$, $M_v = M_d = 5$, $S = 20$, and a voice call arrival rate and service rate corresponding to a blocking probability of 0.02 for five voice channels. As expected, the delay of each protocol increases as the throughput increases, approaching infinity at the maximum throughput. Under RAD, the maximum throughput is $0.368 \times M_v$, while the maximum throughput under DAD and HD is M_v . For light traffic, the delay under RAD is smaller than that under DAD. The hybrid protocol HD has the best delay characteristics for medium to heavy traffic and is only slightly inferior to RAD at light traffic. We conclude that most of the improvement for HD is due to R-packets. When the traffic is high the scheduled packets dominate the system and the improvement is small. We also find that the movable boundary strategy is superior to the fixed strategy, but the improvement is very small under DAD.

5 CONCLUSIONS

We have proposed several distributed protocols for integrated voice/data service in satellite channels. We find that random access performs best under light traffic, while a hybrid random access-demand assignment protocol performs best for medium to heavy traffic. In addition, a movable boundary strategy performs better than a fixed boundary strategy.

References

- [1] J. F. Chang and Li-Yi Lu. High capacity low delay packet switching via a processing satellite. In *IEEE INFOCOM*, pages 1E.5.1–1E.5.5, 1982.
- [2] G. I. Coviello and P. A. Vena. Integration of circuit/packet switching by SENT (slotted envelope network) concept. In *Proc. Nat. Telecommunications Conf.*, pages 42.12–42.17, Dec. 1975.
- [3] Victor O. K. Li and Tsun-Yee Yan. An integrated voice and data multiple-access scheme for a land-mobile satellite system. *Proc. of the IEEE*, 72:1611–1619, Nov. 1984.
- [4] T. Suda, H. Miyahara, and T. Hasegawa. Performance evaluation of an integrated access scheme in satellite communication channel. *IEEE J. Selected Areas in Communications*, SAC-1:153–164, Jan. 1983.
- [5] C. J. Weinstein, M. L. Nappass, and M. J. Fischer. Data traffic performance of an integrated circuit- and packet-switched multiplexing structure. *IEEE Trans. Commun*, COM-28:873–878, June 1980.
- [6] G. F. Williams and A. Leon-Garcia. Performance analysis of integrated voice and data hybrid-switched link. *IEEE Trans. Commun*, COM-32:695–706, June 1984.

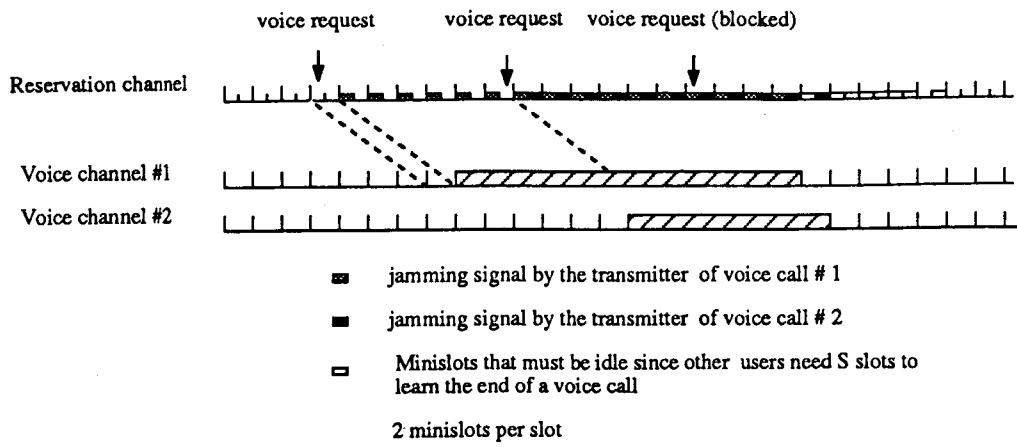


Figure 1. Time diagram for voice calls

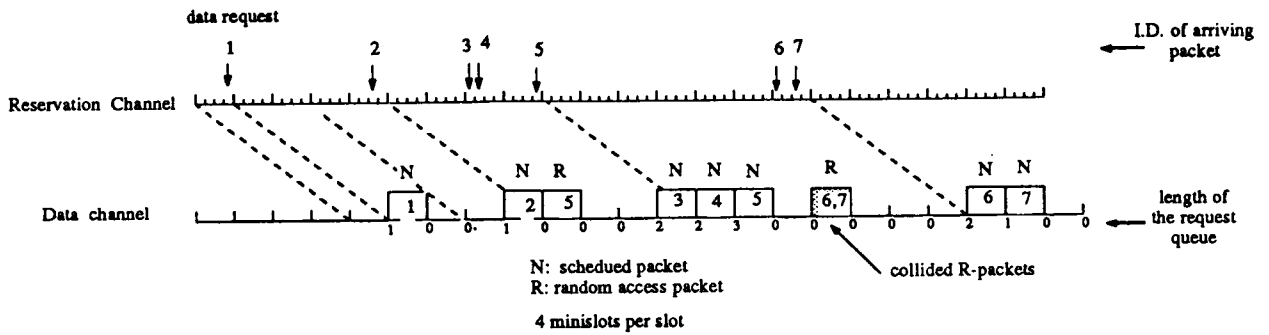


Figure 2. Time diagram for the hybrid data protocol

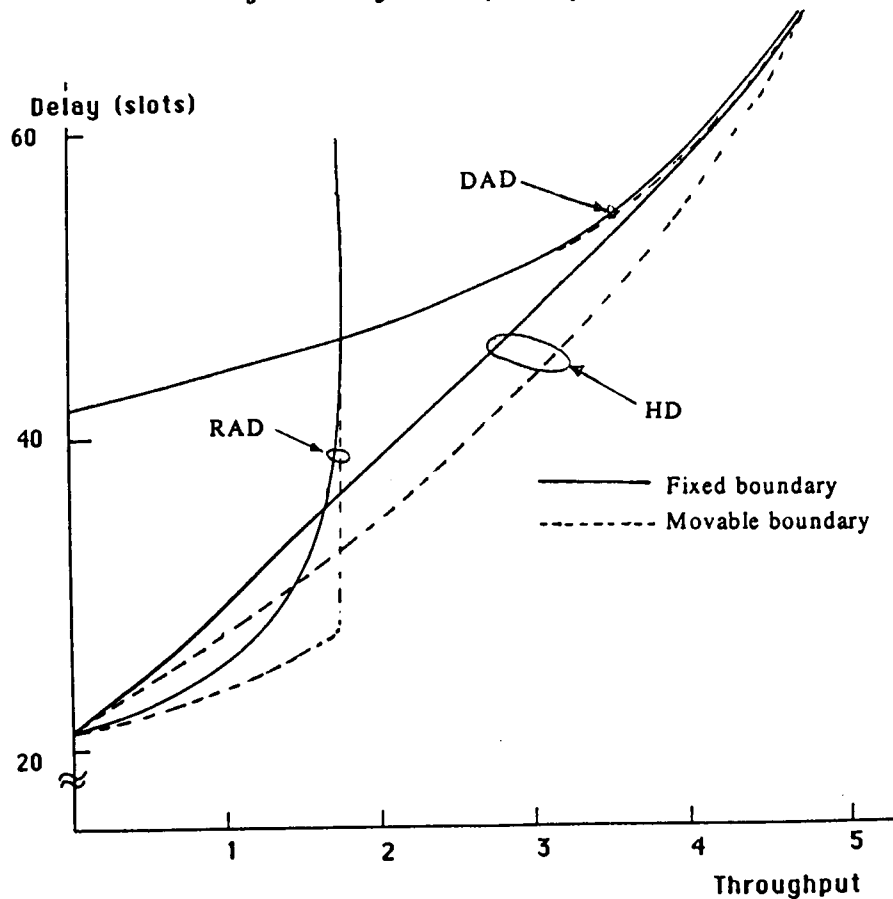


Figure 3. Performance comparisons of the three data protocols under the fixed and movable boundary strategies.

EVALUATION OF CDMA SYSTEM CAPACITY FOR MOBILE SATELLITE SYSTEM APPLICATIONS

MR. PATRICK O. SMITH, Communications Systems Engineer, TECHNO-SCIENCES, Inc., United States; DR. EVAGGELOS A. GERANIOTIS, Department of Electrical Engineering, University of Maryland, United States.

TECHNO-SCIENCES, Inc.
7833 Walker Drive, Suite 620
Greenbelt, MD 20770
United States

ABSTRACT

We discuss a specific Direct-Sequence/Pseudo-Noise (DS/PN) Code-Division Multiple-Access (CDMA) mobile satellite system (MSAT) architecture. We evaluate the performance of this system in terms of the maximum number of active MSAT subscribers that can be supported at a given uncoded bit-error probability. Our evaluation decouples the analysis of the multiple-access capability (i.e., the number of instantaneous user signals) from the analysis of the multiple-access multiplier effect allowed by the use of CDMA with burst-modem operation. We combine the results of these two analyses and present numerical results for scenarios of interest to the mobile satellite system community.

I. INTRODUCTION

The use of Direct-Sequence/Pseudo-Noise (DS/PN) Code-Division Multiple Access (CDMA) has significant technical advantages for mobile satellite system (MSAT) applications relative to the use of Demand-Assignment /Frequency-Division Multiple Access (DA/FDMA). CDMA offers an improved method of exploiting the statistical characteristics of user behavior. In this paper, we refer to this effect as the multiple-access multiplier effect. In addition, the use of DS/PN CDMA can mitigate the effects of multipath channel characteristics and provide interference rejection of intentional or unintentional interference sources.

In this paper, we outline a specific DS/PN CDMA MSAT communications system and provide a preliminary performance evaluation of the number of active users that can be supported at a given uncoded bit-error probability. The analysis of the multiple-access capability (i.e., the maximum number of instantaneous users for a given bit-error probability) is decoupled from the analysis of the multiple-access multiplier effect. The two analyses are combined to obtain preliminary estimates of the system capacity. More complete descriptions, analyses, and results can be found in [TECHNO-SCIENCES, 1988].

II. COMMUNICATIONS SYSTEM DESCRIPTION

A. MSAT System Overview

The MSAT system is intended to provide low data rate (i.e., less than 9.6 kbps) communications to a large number of geographically-dispersed low-duty-cycle mobile users. The MSAT system consists of a Network Management Center (NMC), multiple

hub/gateway stations, a single geosynchronous communications satellite, and the mobile users. The NMC grants access to the system, provides demand-assignment of available resources, and maintains appropriate network status and billing information. Hub/gateway stations provide connectivity to and from the Public Switched Telephone Network (PSTN). Base stations are similar to hub/gateway stations but are used by a specific subset of mobile users only.

B. Satellite Architecture / System Connectivity

Figure 1, Satellite Architecture / System Connectivity, shows the functional satellite architecture and system connectivity for the CDMA MSAT communications system analyzed in this paper. As shown, the satellite provides for "bent-pipe" frequency translation of mobile transmissions at L-Band to Ku-Band for reception at the NMC or hub/gateway stations. Similarly, Ku-band transmissions from the NMC or hub/gateway stations are frequency translated to L-Band for reception by the mobile receivers.

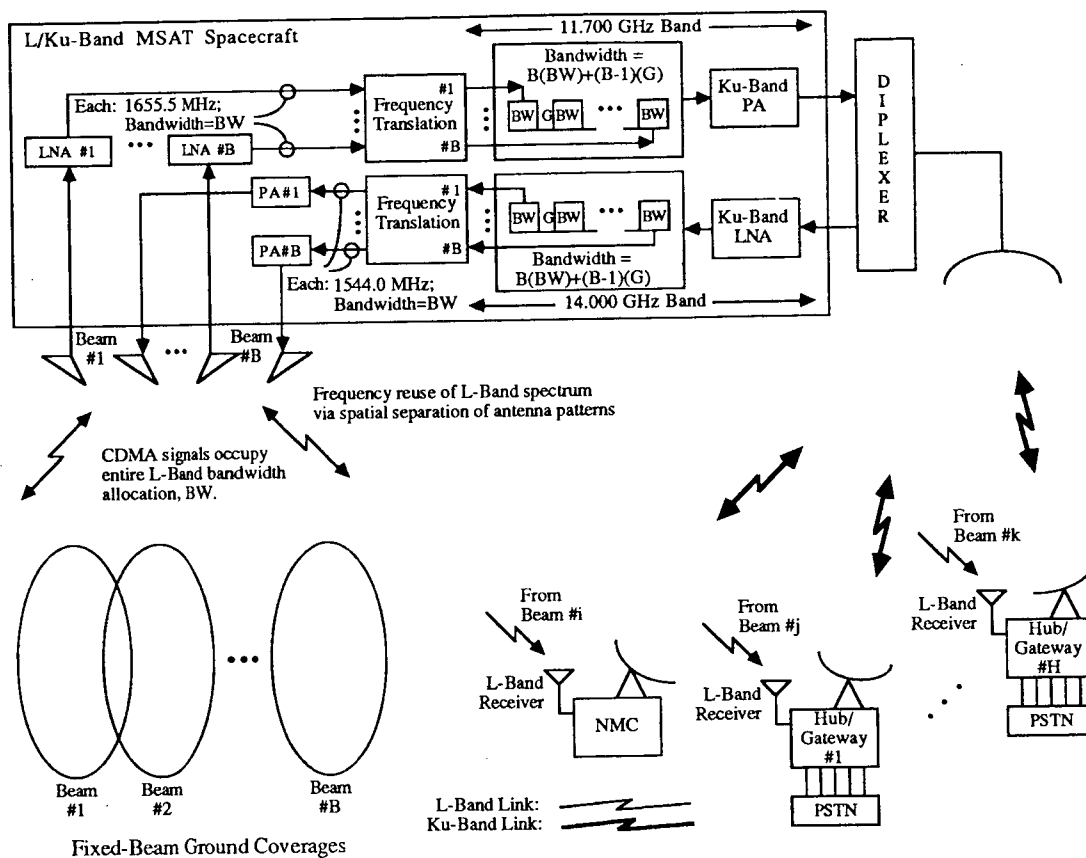


Figure 1. Satellite Architecture / System Connectivity

Frequency reuse of the L-Band spectrum is provided by spatial separation of B L-Band coverage beams. Figure 1 shows the use of fixed L-Band coverage beams. Each fixed L-Band coverage beam maps to a unique, nonoverlapping portion of Ku-Band spectrum. Thus, B-times frequency reuse of the L-Band spectrum corresponds to B-times frequency expansion of the Ku-Band spectrum.

An alternative to the use of fixed coverage beams is the use of electronically-steerable coverage beams. In this case, each of the B L-Band coverage beams would now span the entire coverage region. Signals received by each L-Band coverage beam are again downlinked at Ku-Band using a unique portion of Ku-Band spectrum. However,

in this case each NMC and/or hub/gateway station must appropriately align the relative phases of the B received beams to focus the effective antenna gain pattern at an optimal location. The effective antenna gain pattern can be focussed anywhere within the entire coverage region. Antenna patterns can be formed on a mobile-by-mobile basis by the use of independently operating beam-steering equipments. Explicit use of the CDMA signal characteristics of each mobile allow for the beam-steering capability without the need for geographical knowledge of the mobile location [Davisson and Flikkema].

C. DS/PN Codes and Phase Relationships

A broadcasted short DS/PN code provides system synchronization among all elements. This synchronization allows the use of a single DS/PN long code to provide simultaneous access of the channel by numerous users. Each user is allocated a unique phase epoch of the long code relative to system time at the NMC. The phase epochs are chosen and maintained so that overlap of different phase epochs cannot occur at any receiver. Figure 2, CDMA DS/PN Network Design, shows the DS/PN phase relationships for signals transmitted by the NMC.

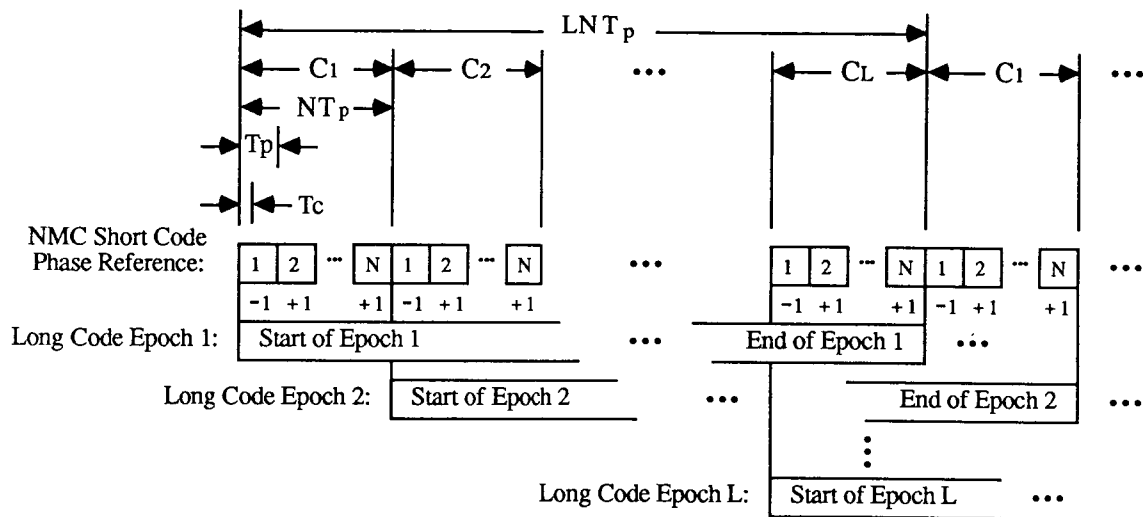


Figure 2. CDMA DS/PN Network Design

1. Short Codes. The NMC short code length, T_p , must be long enough to mitigate a given multipath delay spread and to provide favorable spectral content but short enough to allow reasonable DS/PN epoch acquisition times for mobiles entering or reentering the system. The mobile transmitters will use short codes of similar length to provide a random-access capability for circuit allocation requests. Several mobile transmitter short codes with good cross correlation properties can be used.

2. Long Code. Time shifted versions of a single long code are used to create a circuit allocation capability. Long code epochs are separated by N repetitions of the NMC short code epoch, where the first repetition of the NMC short code in each long code epoch is a complemented version of the NMC short code.

D. Mobile Transceiver Requirements

The use of an omni-azimuth mobile antenna pattern and DS/PN signal processing techniques provides for low-cost mobile transceivers in large quantities. The NMC short code must be acquired and continually tracked to provide an accurate time and frequency reference. Variable power control is required to optimize system capacity and minimize

shadowing effects for a given bit-error probability and availability. Burst-modem transmission and reception is required to achieve the resource-sharing multiplier effect allowed by CDMA. Burst operation simplicity and performance is considerably enhanced by the use of the NMC short code as a reference for the mobile.

III. EVALUATION OF SYSTEM CAPACITY

A. Single-Beam Analysis Considerations and Simplifying Assumptions

Our preliminary performance results are based on a number of simplifying assumptions, some of which are now stated. The results of this paper are valid for the fixed-beam MSAT spacecraft described in Section II B. We have assumed the simplified generic beam scenario as shown in Figure 3, which shows an arbitrary beam having two adjacent, partially overlapping beams. As shown there are two distinct coverage regions within the generic beam, namely, a center of beam region and an edge of beam region. The number of users in any given area is assumed to be proportional to the area. Now, the total number of active users that can be supported by the CDMA MSAT system will depend on the actual geographical location of the users and will be upper-bounded by Bk and lower-bounded by k for a given user location scenario. Here, B is the number of spacecraft transmit/receive L-Band beams required to span the entire coverage region and k is the number of active users supported by the generic beam.

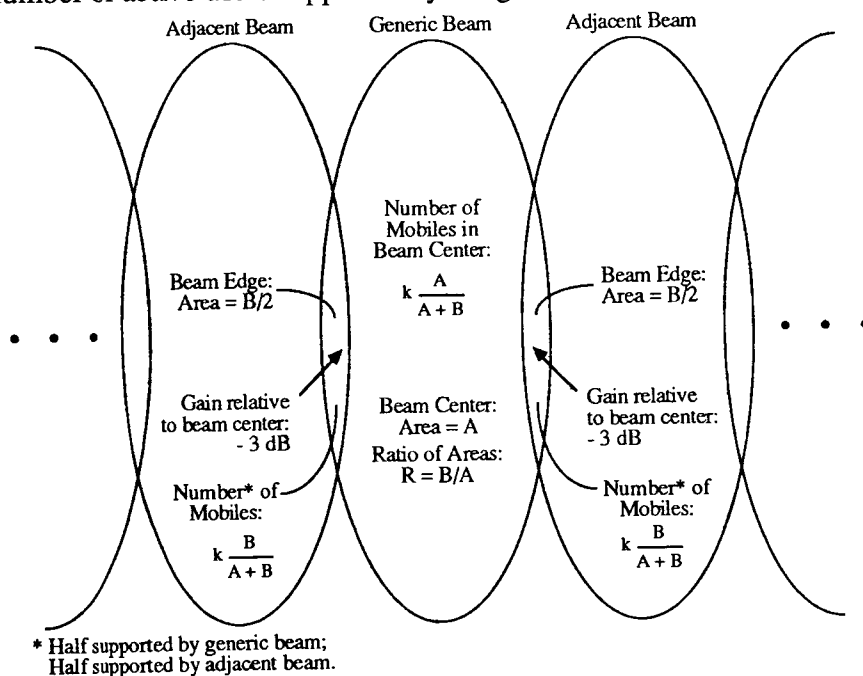


Figure 3. Simplified (Two Region) Beam-Coverage Scenario

We have assumed uncoded BPSK chip and data modulation over a Rician, frequency-selective channel with coherent demodulation. We have not restricted the available mobile terminal EIRP or spacecraft EIRP. In addition, we have assumed a simple power allocation scheme, which is based solely on user location relative to the two coverage regions of Figure 3, viz., mobiles in the edge of the beam area are allocated twice the power of mobiles in the center of the beam area.

For the hub-to-mobile direction we assume that the DS/CDMA signals are combined using pairs of orthogonal carriers with randomized chip delays. In the mobile-to-hub direction, it is not feasible for pairs of mobile transmitters to maintain orthogonal carriers.

B. Bit-Error Probability vs. Number of Instantaneous Subscribers (Hub-to-Mobile)

The reader is referred to the references for a more complete presentation of the subsequent results. Based on the previously stated assumptions and simplifications, the bit-error probability at time t , $\text{BEP}_{\text{center}}(k,t)$, at a mobile receiver in the center of a generic beam supporting k instantaneous users is given by:

$$\text{BEP}_{\text{center}}(k,t) = Q \left\{ \left[\left[2\alpha(t) \frac{E_b}{N_0} \right]^{-1} + \frac{\gamma^2}{3\eta} + \left(\frac{1 + \gamma^2}{3\eta} \right) \left(\frac{1 + 4R}{1 + 2R} \right) k \right]^{-1/2} \right\} \quad (1a)$$

which approximates to:

$$\text{BEP}_{\text{center}}(k,t) \approx Q \left\{ \left[\frac{\gamma^2}{3\eta} + \left(\frac{1 + \gamma^2}{3\eta} \right) \left(\frac{1 + 4R}{1 + 2R} \right) k \right]^{-1/2} \right\} \quad \text{for } 2\alpha(t) \frac{E_b}{N_0} \gg 1 \quad (1b)$$

where the notation is defined as follows:

- γ^2 = the power ratio of the reflected path to direct path of the Rician channel
- R = the ratio of the edge of beam area to the center of beam area
- η = the ratio of the data-bit modulation period to the chip modulation period
- $\alpha(t)$ = direct signal attenuation factor at time t

$$Q(x) = \frac{1}{\sqrt{2\pi}} \int_x^{\infty} e^{-u^2/2} du$$

The relation for the bit-error probability, $\text{BEP}_{\text{edge}}(k,t)$, of a mobile receiver at the edge of a generic beam supporting k instantaneous users is identical to (1a) and (1b) except the factor $(1 + 4R)$ is replaced with $(1 + 6R)$. Thus, a more refined power allocation algorithm is desirable.

C. Multiple-Access Multiplier Factor

The question to be answered is the following. Given that a generic beam can support a total of k active users, how many users should be granted the resources of a circuit allocation? One rule would be to allocate the number, N , of users such that with a probability of say 0.95 the number of instantaneous users does not exceed the maximum that can be supported at a given bit-error probability. Here we describe a simple first-order statistical analysis to answer this question. For simplicity, we will assume the all-voice-traffic scenario with burst-modem operation, i.e., a mobile or hub DS/PN modulated signal is transmitted only during segments of conversation.

Let $\{X_i, Y_i\}$, $i = 1, 2, \dots, \infty$, represent the on/off process of a voice-activated modem, where X_i and Y_i represent the transmitter-on and transmitter-off durations, respectively, for the i th cycle of the process. The process $\{X_i, Y_i\}$, $i = 1, 2, \dots, \infty$, consists of a sequence of independent, identically distributed (i.i.d.) random variables. At a randomly selected time, the probability that the transmitter is on is $E\{X\}/[E\{X\} + E\{Y\}]$ [Karlin and Taylor, 1975]. If there are N active, simplex voice transmitters in the hub-to-mobile direction and each voice transmitter has a similar but independent i.i.d. process, then at stationarity the number of signals present at a randomly selected time instant is binomially distributed with parameters N and $E\{X\}/[E\{X\} + E\{Y\}]$.

Thus, for a given allocation of users, N , the distribution of the number of instantaneous users accessing the channel is given in terms of the average values of the transmitter-on and transmitter-off durations of the users. This simple first-order model can be generalized to any collection of transmitter processes that can be reasonably modelled as mutually independent i.i.d. processes.

D. Numerical Results

Figure 4, $BEP_{center}(k,t)$ vs. k , shows that a generic beam can support several hundred instantaneous users at an uncoded bit-error probability of 10^{-3} for $\eta = 3333$, 1666, and 833. These values of η correspond to an 8 MHz chip rate with a user data rate of 2.4, 4.8, and 9.6 kbps, respectively. Other parameters of Figure 4 are $\gamma^2 = 0.1$, $R = 1/4$, and $2\alpha(t)\frac{E_b}{N_0} \gg 1$. As shown in Table 1, Multiple-Access Multiplier Values, most of the achievable multiplier effect is obtained for values of k_{max} exceeding 50. Thus, the overall system capacity can be estimated at about 2.5B times k_{max} assuming the all-voice traffic scenario and a voice transmitter activity ratio of one third. The asymptotic multiplier effect is equal to $[E\{X\} + E\{Y\}]/E\{X\}$ for other data sources. In any case, the system capacity is roughly given by MBk_{max} for a given scenario.

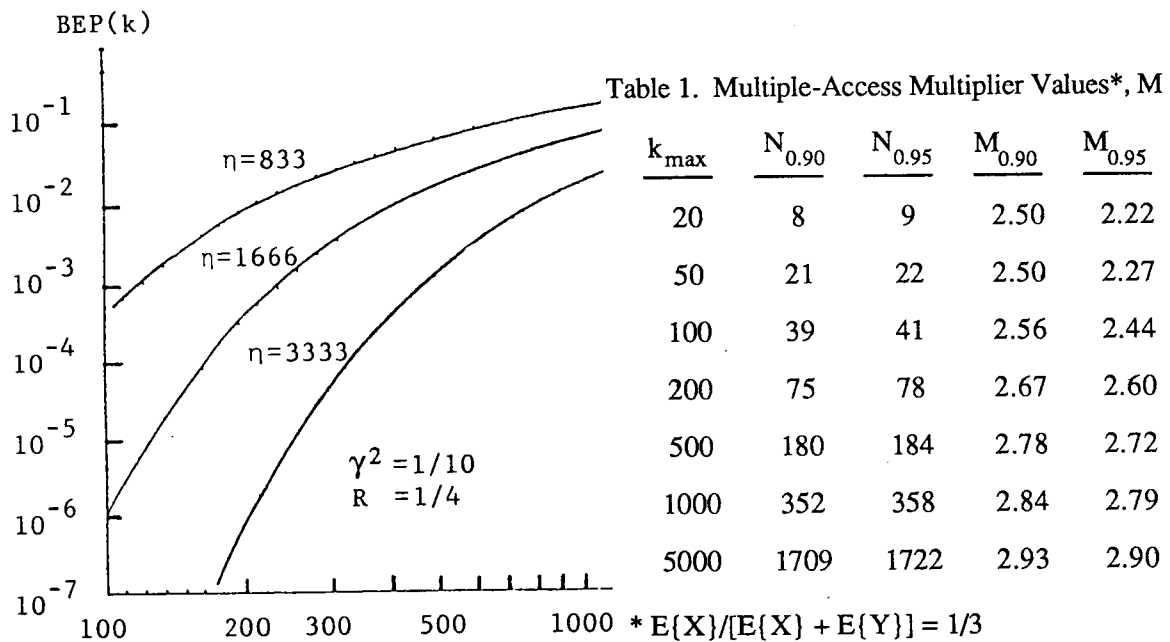


Figure 4. $BEP(k)$ vs. k

REFERENCES:

- Davisson, L. and Flikkema, P. Accepted for publication. "Fast Single-Element PN Acquisition for the TDRSS MA System," IEEE Trans. on Commun.
- Geraniotis, E. 1984. "Performance of Broadcast Direct-Sequence Spread-Spectrum Communications," in Proc. Conf. Inform. Sci. Syst., Princeton Univ., 1984.
- Karlin, S. and Taylor, H. 1975. A First Course in Stochastic Processes, Second Edition, Academic Press, 1975, pp. 201 and 202.
- TECHNO-SCIENCES, 1988. "Evaluation of CDMA System Capacity: SBIR Phase I Technical Report," to be submitted to NASA JPL.

SESSION I
SPACECRAFT TECHNOLOGY

SESSION CHAIR: Yahya Rahmat-Samii, Jet Propulsion Laboratory
SESSION ORGANIZER: Yahya Rahmat-Samii, Jet Propulsion Laboratory

CONSIDERATIONS FOR SPACECRAFT DESIGN FOR M-SAT

KUNVANA HING, System Engineering; HARRY J. MOODY, Advanced Systems,
Spar Aerospace Limited, Canada

SPAR AEROSPACE LIMITED
21025 Trans Canada Highway
Ste-Anne-de-Bellevue, Quebec H9X 3R2

ABSTRACT

The paper describes the system design considerations and design activities performed at Spar Aerospace in the last eighteen months in support of the development of a Canadian Mobile Communication satellite (M-SAT).

Recent evolving international agreements and events of importance to M-SAT are the emergence of the U.S. Operator and the Mobile WARC 1987. Their impacts on the system requirements and system design are discussed.

Solutions to these new requirements are implemented into the 9 Beam baseline design. The system design and the parallel technology development enable Spar Aerospace to be ready to support a commercial flight program.

INTRODUCTION

Canada has been pursuing for some years the study of systems and technology for a Canadian Mobile Satellite System (M-SAT). Agreements between the Department of Regional Industrial Expansion and Spar Aerospace has provided funding for the development of the M-SAT space segment, work which is reported in this paper.

Since July 1986, a number of events in the United States and in Canada^a have quickened the pace of commercial M-SAT development. Recently evolving international agreements and events have added other considerations to the system design. Of particular importance has been the emergence of the U.S. Operator and the desire of the U.S. and Canadian Operators to provide interoperable systems. The Mobile WARC conference in 1987 has established the L-band as the frequency band for mobile satellite service and has added some complexity to the L-band power and frequency flexibility requirements.

This paper will describe the current work at Spar Aerospace on the development of an all L-band system where the above requirements have been considered.

^a Kidd, 1987

PRECEDING PAGE BLANK NOT FILMED

SYSTEM REQUIREMENTS

Basic System Design Requirements and Guidelines

The system design based on Canadian requirements of the L-band M-SAT space segment are to provide full Canadian coverage, full CONUS/Alaska backup coverage and to provide sufficient capability to support 60,000 Canadian Users with a ten year lifetime.

The system design resulting from these requirements is to stay within the following guidelines:

- 1) The spacecraft should be designed such that it can be launched by an Ariane IV vehicle as part of a dual launch. However, the spacecraft should be configured to take advantage of evolving expendable launch vehicle systems.
- 2) The payload mass should be maintained below 350 kg (770 lbs) without margin and the payload DC power should be maintained below 2500 Watts without margin.
- 3) The payload should be configured for a typical three axis body stabilized spacecraft.
- 4) The overall system should be designed for a mix of service: 40% transportable and 60% ground mobile, with 12 dBi and 9 dBi respective mobile antenna gain.

This is to constrain the final design of the payload while maintaining the desired performance. Spacecraft with the above weight and power capabilities are now being built for the latest generation of domestic communication satellites.

Impacts of Mobile WARC 1987

Prior to Mobile WARC 1987, the system design and the technology development have been based on a 9 MHz continuous spectrum in accordance with the Federal Communication Commission (FCC)^b frequency allocation. However, a two segment L-band allocation for LMSS spanning 29 MHz has been established by Mobile WARC 1987.

There is some indication that the M-SAT operators might want to provide service in four bands, namely, MMSS, AMSS and the two segments of spectrum allocated to LMSS by Mobile WARC 1987^c, for the first generation system.

This new requirement along with the need for flexibility for evolving user demands and distribution lead to the following update of the pre WARC design:

b Brassard, 1988

c WARC MOB-87

Impacts of Mobile WARC 1987 (cont'd)

- 1) Minimization of back-haul spectrum and optimization of L-band spectrum efficiency/flexibility.
- 2) Interaction (trade-offs) between back-haul power and L-band spectrum efficiency/flexibility.
- 3) Local Oscillator frequency generation and IF plan to take into account the much larger number of sub-bands required.
- 4) Intermodulation analysis taking into account the discontinuous nature of signal spectrum in the new frequency plan.
- 5) A wider instantaneous bandwidth (i.e. 29 vs 9 MHz) is required for the L-band high power amplifier.
- 6) Passive Inter Modulation (PIM) performance of L-band antenna components taking into account the reduction of PIM order from 15th to 7th.
- 7) L-band input/output filter performance taking into account the wider operating bandwidth and the narrower separation between transmit and receive bands.

Impacts of the Interoperable North American System

The emergence of the U.S. Operator has brought up the following additional considerations to the M-SAT space segment design:

- 1) The system design should involve both a Canadian and U.S. spacecraft with a primary mode of servicing their respective territories. Prior to launch of the second spacecraft, or in the case of one of the spacecraft failing, either spacecraft should be capable of providing both a Canadian and a U.S. service up to the capacity of a single spacecraft.
- 2) The concept should allow the two spacecraft to occupy orbital slots separated by up to 20 degrees of longitude.
- 3) The spacecraft hardware for both the Canadian and the U.S. spacecraft should be functionally identical.

The first and third considerations have no technical impact on the system design. The mass, power, coverage and frequency reuse provided in the basic design requirements are sufficient to cover these new items.

The second consideration requires some adjustment to the 9 Beam L-band antenna coverage pattern.

SYSTEM DESIGN

Concept Trade-off

Two candidate system concepts for the M-SAT space segment have been considered: the conventional spot beam approach (with varying amounts of overlap) and the scanning system employing the Frequency Addressable Beam (FAB) technique. Prior to Mobile WARC 1987, a complete trade-off study had been made between the 9 Beam concept and the FAB concept. The following parameters have been studied:

- 1) DC Power
- 2) Spacecraft mass
- 3) System capacity
- 4) System reliability
- 5) System flexibility including
 - Operation with two co-located satellites
 - System growth potential
- 6) Technical risk including
 - PIM
 - Deployments

The study result has shown that neither of the two schemes offers overriding advantages. However, after Mobile WARC 1987 and the decision to provide full 29 MHz service, the 9 Beam concept appears to be a better candidate due to its PIM performance (separate versus common transmit/receive antenna in view of the lower order PIM). All efforts have been shifted to cover various design aspects of the 9 Beam concept.

CONCLUSION

A 9 Beam system meeting all the basic design requirements and guidelines, had been defined prior to Mobile WARC 1987^d. Solutions to the considerations discussed earlier, are being implemented to the baseline design to make it compliant to the requirements as currently understood. Spar Aerospace is considering applying for a patent on the design concept to provide power flexibility.

A parallel technology development of payload units, in support of the system concept, is well advanced at Spar Aerospace^e.

Possible modifications of the requirements such as the addition of Mexican coverage can easily be implemented in the updated baseline design.

The system design activities and the parallel technology development enable Spar Aerospace to be ready to support a commercial flight program.

REFERENCES

- Kidd, A.M., Karlsson, I., Whittaker, N., 1987. M-SAT System and Payload Development. The Canadian Satellite User Conference, pp. 394-399.
- Brassard, G., 1988. L-Band linear high power amplifier using Class C transistors. R.F. Expo '88.
Final Acts of WARC MOB-87
- Cox, R.P., Zacharatos, J., Williamson, B., Morgan, C., Cox, J.R.G., 1988. System Trade Off for a North American Mobile Satellite. AIAA 12th ICSSC.
- Karlsson, I., Patenaude, Y., Stipelman, L., 1988. Antenna System for M-SAT Mission. JPL Mobile Satellite Conference.

d Cox, 1988

e Karlsson, 1988

ANTENNA SYSTEM FOR M-SAT MISSION

INGMAR KARLSSON, YVES PATENAUDE and LEORA STIPELMAN, Antenna Development Engineering, Spar Aerospace Limited, Canada

SPAR AEROSPACE LIMITED
21025 Trans Canada Highway
Ste-Anne-de-Bellevue, Quebec H9X 3R2

ABSTRACT

Spar has evaluated and compared several antenna concepts for the North American Mobile Satellite.

The paper describes some of the requirements and design considerations for the antennas and demonstrates the performance of antenna concepts that can meet them.

Multiple beam reflector antennas are found to give best performance and much of the design effort has gone into the design of the primary feed radiators and beam forming networks to achieve efficient beams with good overlap and flexibility. Helices and cup dipole radiators have been breadboarded as feed element candidates and measured results are presented.

The studies and breadboard activities have made Spar ready to proceed with a flight program.

INTRODUCTION

Since the late 1970's Spar Aerospace Limited has studied and evaluated different concepts and payload designs for a Canadian Mobile Communication Satellite (M-SAT). These studies have been funded by the Canadian Department of Communication and have been aimed towards the design of a demonstration model. Growing commercial interest in both the USA and Canada has changed the program into an industry led commercial program. From being a UHF band system the concept evolved into a combined L and UHF band system in 1986. The WARC conference in 1987 established the L-band as the frequency band for mobile satellite service and M-SAT is now an L-band only system.

Spar has had a leading role in defining system requirements and proposing suitable designs. Reference 1 describes the baseline system requirements. It is assumed that two identical spacecrafts, one US and one Canadian, each operated independently, would enable a commercial system to be implemented by the early 1990's. This first generation system would allow mutual backup in the event of a spacecraft failure.

This paper describes some of the antenna configurations and hardware that have been and are considered for the M-SAT space segment.

PRECEDING PAGE BLANK NOT FILMED

ANTENNA REQUIREMENTS AND CONSIDERATIONS

The space segment of a mobile satellite communication system must provide high power densities (EIRP) on the ground to allow mobiles with small, low gain, antennas to communicate. The limited spectra allocated for mobile services requires maximum possible frequency reuse. The user distribution is uncertain and will vary during the satellite lifetime. There is thus a need to have flexibility in spectrum and power allocations over the coverage region.

High gain spot beam antennas are well suited to meet these requirements. Electrically the challenge is to design a multiple beam antenna system with good beam overlap, low sidelobes and high efficiency, that also allows for flexibility. Mechanically the challenge is to provide large antenna apertures meeting the mass and volume constraints of the spacecraft. Mesh reflector suppliers have achieved good performance with breadboarded reflectors and associated deployment hardware.

Spar has systematically studied and evaluated suitable antenna candidates, several of which are described in the next section. All reflector concepts assume offset reflector with 5m projected aperture.

ANTENNA CONFIGURATIONS

9-Beam 15 Shared Feed Element Reflector Antenna Concept

Nine beams are generated by a 15 element feed cluster. The beams share feed elements to get good overlap and antenna efficiency. Typically 4 feeds with uniform excitation are used for each beam. The feed cluster layout is shown together with the resulting coverage in Figure 1.

The minimum coverage directivity is 33.0 dBi based on calculations assuming cup dipole primary radiators. Frequencies can be reused every third beam with 22 dB isolation.

Low level beam forming and distributed amplifiers are used to facilitate the excitation. Power flexibility can be achieved by combining varying numbers of power modules or by varying the collector voltage of a fixed size amplifier. However, this flexibility results in lower power efficiency and has implications on weight and complexity.

9-Beam 11 Shared Feed Element Reflector Antenna Concept

The region of interest can be covered by the same number of beams with fewer feed elements with just a slight reduction in coverage gain. The feed cluster layout is shown in Figure 2 with the corresponding coverage. Typically 4 feed elements are used for each beam. Two beams are generated by the same 4 feeds using reciprocal non uniform excitation in the North-South direction i.e., for the US and Canada beams. The beams share feed elements in the East-West direction in order to achieve good beam overlap. The resulting coverage directivity is 32.5 dBi except for small areas in the South of the USA. Frequencies can be reused every third beam with 20 dB isolation.

A low level beam forming system similar to the one described in the previous section can also be used here.

This antenna concept is the main candidate for M-Sat.

9-Beam Independent Feed Element Reflector Antenna Concept

This concept utilizes one feed element per beam so that no beam forming is required. The feed element must be physically small to achieve the desired beam separation. Small feed elements result in low efficiency because of high spillover losses. Spar has investigated the use of cup dipole radiators and helix radiators for this concept. Despite the high aperture efficiency of the cup dipole the minimum coverage directivity is only 30.5 dBi. The helix radiator has an effective aperture that is larger than its physical area and can thus be placed closer together to achieve better beam overlap. Closely spaced helices have strong interaction (mutual coupling) and their radiation patterns are greatly affected. However, the performance can benefit from mutual coupling effects as the active patterns can be shaped to have very flat top and steep fall-offs. Figure 3 shows a layout of the helix cluster and the achieved coverage contours. Frequencies can be reused every third beam with 18 dB isolation. The coverage is calculated using measured primary patterns of helices located in their representative feed cluster environment.

The coverage directivity is 32 dBi except for a small corner in the south of the USA. This is 1.5 dB better than what can be achieved with cup dipole radiators, but still 0.5 dB lower than for the main candidate system. However, excitation errors of the shared feeds reduces the gain difference to about 0.3 dB.

The independent feed per beam concept significantly reduces the complexity and weight of the transponder and feed assembly. No beam forming networks are required and the number of radiators, filters and amplifiers is reduced. This concept is considered as a good candidate for a low cost system.

Direct Radiating Array Antenna Concept

The advantage of a direct radiating array with scanning beams is the increased flexibility. The beams can be scanned to increase the gain in specific areas either due to changed traffic requirements or a change in orbital location. Beams can also be repointed to compensate for failure of an amplifier or of a complete beam.

One of the antenna candidates studied is a 5.1 x 4.5 m hexagonal direct radiating array. The radiating elements used are high efficiency short backfire radiators. A total of 127 elements are arranged in 23 groups, each powered by a separate amplifier. The groups are formed such that the amplifiers are loaded with equal power. The power is distributed within each group using a low loss TEM line network. With this design concept the target area is covered by 9 scannable beams each with its variable low level beam forming network.

The grouping of the elements and the associated non ideal phase excitation makes the outermost beams less efficient resulting in a minimum coverage directivity of 32.3 dBi.

The main drawback of using a hexagonal direct radiating array is the complex deployment scheme required and the weight of the antenna. The mass and complexity also make it impossible to have separate transmit and receive antennas which increases the risk of distortions caused by passive intermodulation. A hexagonal direct radiating array is thus not seen as an attractive option for M-SAT. However, a rectangular array as described in reference 2 can be implemented and offers good flexibility.

Imaging Reflector Antennas Concept

Single and dual reflector imaging antennas with electronic beam scanning have also been investigated.

The single reflector imaging system is realized using a reflector and a relatively small feed array. The feed array is located between the reflector and the focal point. This way, the field distribution of the feed array is approximately recreated over the reflector aperture and a scan of the feed array results in a proportional scan of the antenna.

A dual reflector imaging system comprises a main reflector, a sub-reflector, and a feed array. The sub-reflector is located in the near field of the feed array and the reflectors are arranged confocally such that a magnified image of the array is formed over the main reflector aperture (3). Compared to a direct radiating array the number of radiators is smaller which leads to a simplification of the beam forming network and a substantial reduction of the mass of the array itself. A large array can hardly be folded while a large deployable reflector can be stowed in a relatively small volume compatible with launcher envelopes. It is also feasible to have separate transmit and receive antennas.

Both systems were optimized using a 5 m diameter main reflector. The dual reflector imaging system resulted in a minimum coverage directivity of 31.6 dBi compared to 31.2 dBi for the single imaging system. The sidelobe performance of the imaging systems is poor, reducing the possibility of frequency reuse. Imaging antenna systems are thus not considered a very attractive option.

RADIATOR DEVELOPMENT

Cup Dipole Radiator

A cross dipole with unequal arm lengths fed by a split-coax balun and placed inside a circular or a square cup provides a simple and efficient circularly polarized radiator for narrowband applications. The cup dipole radiator is thus a very good candidate for the M-SAT primary feed radiators. Table 1 presents measured data for three different cups over the M-SAT transmit frequency band 1530 - 1559 MHz.

Helix Radiator

Helices have been investigated as feed elements, especially for the independent beam configuration. In particular, the effects of mutual coupling between helices in an array have been studied.

The helix test model uses an 8 turn copper plated steel spring conductor which is supported by a high density polystyrene cross support. The helix circumference is 1.1λ . Four tapered turns are used to improve the axial ratio performance. The helix is placed in a circular cup whose diameter and depth are experimentally determined to optimize mutual coupling effects. The measured axial ratio on-axis is better than 0.2 dB for the isolated helix and better than 1 dB for a helix in a cluster. Figure 4 compares the radiation patterns of an isolated helix, and the same helix in a 6-element cluster. The active pattern has lower peak gain but has a flat top which makes it efficient as a primary radiator for a reflector. The test results together with the secondary pattern calculations demonstrate that helices can be used efficiently as independent feed elements for multiple beam antennas.

CONCLUSION

Desirable features of antenna systems for Mobile Communication Systems have been defined and a number of suitable antenna designs have been described.

The performances of the candidate concepts have been systematically evaluated by Spar and some of the major considerations are given in this paper. The 9 beam shared feed horn reflector concept with 11 feed elements is presently considered to be the best approach. This system offers efficient beams with good overlap, sidelobes that allow frequency reuse, good power flexibility and separate transmit and receive antennas. Design and evaluation of concepts are continuing as the system requirements are becoming more well defined.

Some hardware has been developed to support the conceptual designs. Test results from cup dipole and helix radiators are presented here. Both radiators show more than adequate performance for M-SAT requirements.

Spar is also co-operating with mesh reflector suppliers and has performed tests of a 5 m mesh reflector together with Aerospatiale. Similar tests will be performed with MBB during 1988.

REFERENCES

- [1] Hing, K. et al. Considerations for spacecraft design for M-Sat. paper to be presented at The Mobile Satellite Conference JPL 1988
- [2] Rosen, H. Frequency Addressable beams for Satellite Communications. Telcom 87 Geneva
- [3] Dragone, C. Gang, M.J. Imaging reflector arrangements to form a scanning beam using a small array. The Bell System Technical Journal. Vol. 58, No. 2, February 1979.

Table 1. Cup Dipole Performance

	EFFICIENCY %	AXIAL RATIO [dB]			RETURN LOSS [dB]		
		1530	1545	1559 MHz	1530	1545	1559 MHz
Circular cup $\theta = 1.3\lambda$	99	1.8	0.8	1.2	-27	-29	-31
Circular cup $\theta = 0.65\lambda$	97	0.4	0.3	0.3	-16	-20	-21
Square cup $d = 0.65\lambda$	97	0.5	0.4	0.2	-17	-25	-24

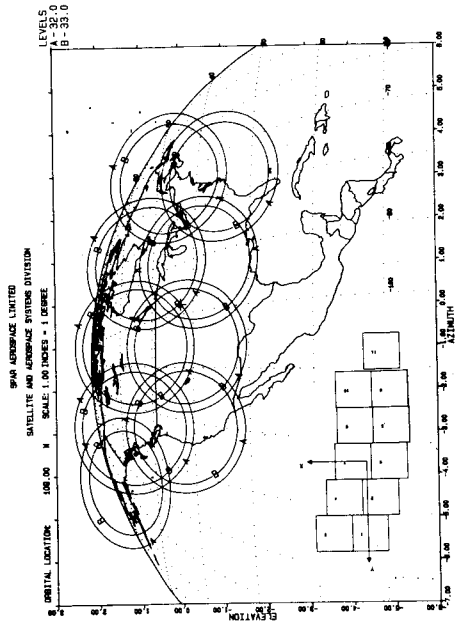


Figure 2 Coverage with 11 Shared Feed Elements

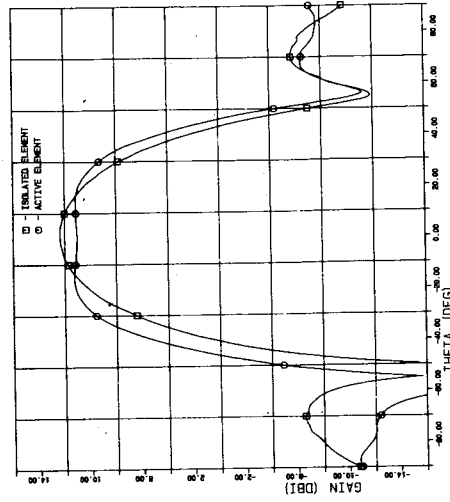


Figure 4 Helix Radiation Patterns

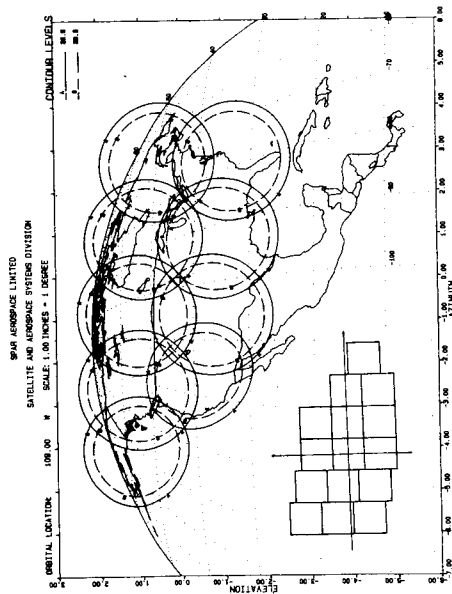


Figure 1 Coverage with 15 Shared Feed Elements

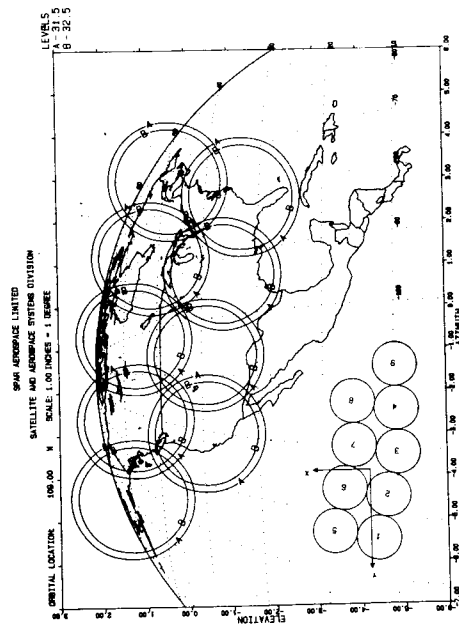


Figure 3 Coverage with 9 Independent Helix Feed Elements

ANTENNA TECHNOLOGY FOR ADVANCED MOBILE COMMUNICATION SYSTEMS

DR. EMMANUEL RAMMOS, DR. ANTOINE ROEDERER, MR. ROGER ROGARD,
European Space Agency, ESTEC, Noordwijk, The Netherlands

EUROPEAN SPACE AGENCY
Postbox 299, 2200 AG Noordwijk
The Netherlands

ABSTRACT

The onboard antenna front end is the key subsystem conditioning configuration and performance of mobile communication satellites. The objectives of this paper are to demonstrate this key role and to review L-band satellite antenna technology for earth coverage and regional applications.

Multibeam arrays, are first discussed, then unfurlable and inflatable reflector antennas are described.

These technologies are now qualified in Europe for future mobile systems, for which the optimum choice of antenna technology has been found to be the key to efficient use of spectrum and power resources.

INTRODUCTION

Although studies on mobile communication satellites were initiated in the late sixties, it is only recently that, thanks to the creation of INMARSAT, the availability of satellites in orbit has allowed to test and evaluate new system concepts. The limitations of global beam earth coverage have also been evidenced and this has led to the understanding that multibeam (array) systems were the only solution to cope with increased traffic and smaller terminals. Multibeam arrays represent a quantum jump with respect to single global beam payloads as MARISAT and MARECS. The antenna optimisation so strongly influence the overall system concept and performance that system design for multibeam payloads must involve in depth antenna engineering from the onset. This is illustrated in the next sections where the interaction between antenna and system designs is highlighted.

ANTENNA RELATED SYSTEM REQUIREMENTS

In view of the limited frequency bandwidth available and of the increase in traffic, frequency re-use and therefore multibeam operation are mandatory to progress. In addition, traffic distribution is far from being uniform. Some areas, such as the North Atlantic region, carry such a large percentage of the traffic, that dedicated multibeam systems for these areas could be considered, the remaining ones being covered by simpler systems. In addition, introduction of electronically - steerable beams could be an efficient means to cope with traffic

fluctuations and/or to reduce the amount of redundant beam forming hardware.

Optimum choice of beam number, shape and lattice also has a large impact on overall system performance, and several iterations are required before detailed payload specifications can be firmed up. For instance, whereas linear arrays can be used in regional applications (Canada, Conus, Europe) with performance advantages and hardware simplification, a global beam requirement for earth coverage seriously constraints the antenna configuration and spotbeam shapes.

Another example of the dependance of system design on antenna optimisation is the spreading of intermodulation products in multibeam arrays (and not multibeam focussing reflector antennas) which strongly affects the required system linearity and its efficiency. Similarly, the required signal dynamic range has a large effect on system performance. This figure not only depends on the mix of terminals in the system, but also on spacecraft and mobile antenna specifications.

Frequency re-use requirements have a direct impact on satellite antenna size and illumination. They affect differently the forward and return links and beam decoupling factor specification is very complex and system dependent. Typical values are 20 dB on the forward link and 25 dB on the return link, in a one satellite system. They are increased in a multisatellite environment with small terminals.

For historical reasons (MARISAT using helices), single circular polarisation has been considered until now. The use of two circular polarisations might be envisaged, since it can provide, at the cost of no or little added complexity, much needed isolation between transmit and receive and/or between adjacent coverage areas. As will be shown in the next section, the required flexibility both in antenna design and technology, is indeed available to cope with the next generations of mobile communication satellites.

ARRAY ANTENNA TECHNOLOGIES

A typical block diagram of a multibeam array front end is shown in fig. 1. Each element chain includes a radiator, a diplexer, transmit and receive amplifiers and frequency converters. The beam forming matrices create a different phase (and possibly amplitude) front for each beam and operate at IF (100 to 200 MHz). A few agile beams can be included for redundancy and/or to increase flexibility in traffic allocation to different areas. Each beam port is connected to the channel to beam switching matrix which allows to vary the number of channels available to beams. Note that the power in each beam originates from all the element amplifiers.

The advantages of active arrays over focussing reflector antennas are the increased flexibility in channel to beam allocation, the lossless generation of overlapping beams, and the relatively graceful degradation of performances with element chain failures.

Different array configurations are envisaged for multibeam earth coverage with a global beam requirement and for regional applications. Fig. 2 shows a possible configuration used to generate the beams of fig. 3 in the "ARAMIS" system, and a global shaped beam. The array is arranged in 21 non identical subarrays of microstrip patches. Arrays of short backfire elements or of short horns are also considered. Fig. 4 shows a foldable array, oriented E-W, proposed to generate the beams

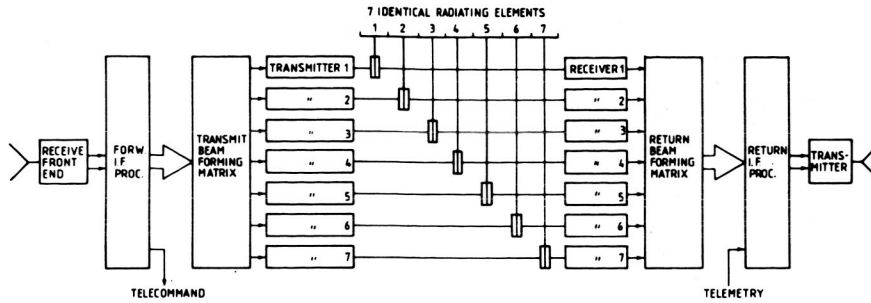


Fig. 1 Multibeam array payload block diagram

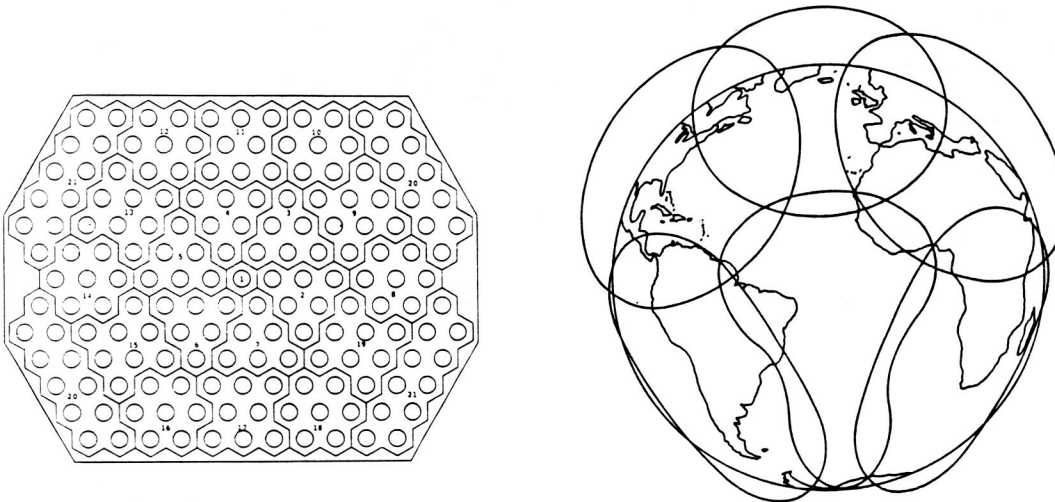


Fig.2 Array for global earth coverage Fig.3 Multibeam earth coverage

of fig. 5. Subarrays are oriented N-S and low sidelobes are achieved by a gap and a power taper at the outer elements. Larger arrays are considered to generate more beams [1]. Elements are microstrip patches.

Short backfires have been developed [2] as elements for non foldable arrays. An engineering model is illustrated in fig. 6.

Short horns, with typical diameter and length of 0.9 and 0.8 wavelength respectively, have been shown [3] to provide around 9 dB of gain when fed by a strip line incorporated in the radiator. They are a potential candidate for applications where subarraying is required, as in the array of fig. 2. Grouped in subarrays of 4 (Fig. 7), their performances are comparable to those of short backfires. An advantage of the short horns is their low sensitivity to dimensional changes in view of their broadband performance. To limit the array thickness an integrated support structure is included.

Broadbanded microstrip patches have been developed [4]. A technology model with 19 patches is shown in figure 8. The patches have two point excitation and a center post. Broadbanding is achieved by proper choice of ground plane separation and by a special matching circuit. A gain of 8 dB per patch is achieved with cross polarisation isolation better than 20 dB. The design incorporates a NOMEX core bonded to a Kevlar front skin and a copper clad carbon fiber rear skin

ORIGINAL PAGE IS
OF POOR QUALITY

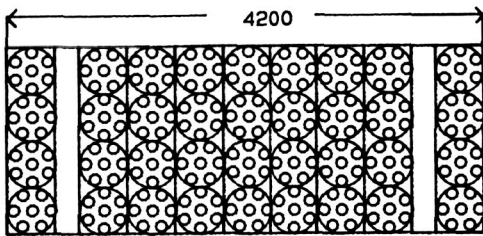


Fig.4 Foldable four beam array

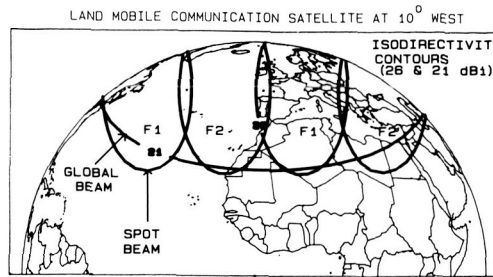


Fig.5 Four beam regional coverage

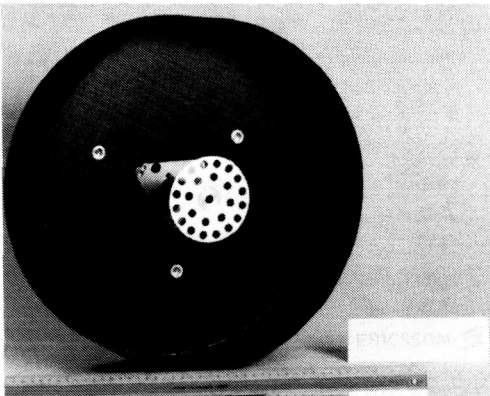


Fig.6 Short backfire element

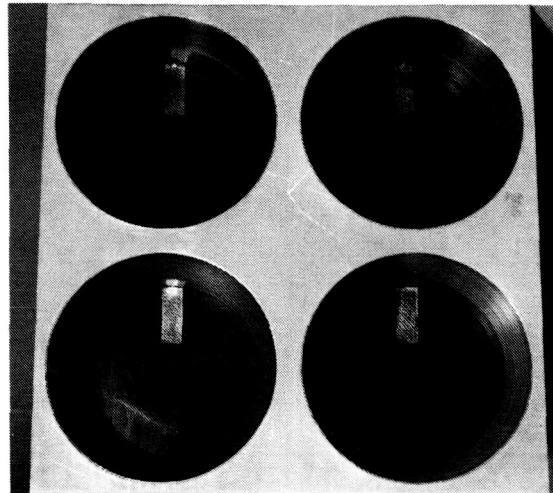


Fig.7 Short horn elements

using film adhesive. The same copper layer is used as ground plane for the patches and as upper groundplane for the triplate power divider. The array of figure 8 has been tested for multipaction and for passive intermodulation product (PIMP) generation.

All other RF components in the front end are space qualified.

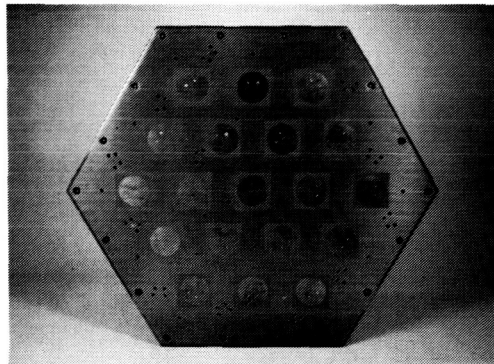


Fig.8 Microstrip patch array

REFLECTOR ANTENNA TECHNOLOGIES

To achieve re-use of the frequency with many narrow beams (fig. 9) antenna apertures with dimensions exceeding 10 meters are needed and foldable planar arrays become impractical. Large focussing reflectors, fed by overlapping beam feed clusters (fig. 10) can be used. Then power to beam allocation flexibility is limited by that of the amplifier associated to each beam. To eliminate this limitation, an imaging system (fig. 10) where a small array is magnified by a system of two reflectors can be envisaged. Intermediate configurations with more or less feed array defocussing can also be considered. In

ORIGINAL PAGE IS
OF POOR QUALITY

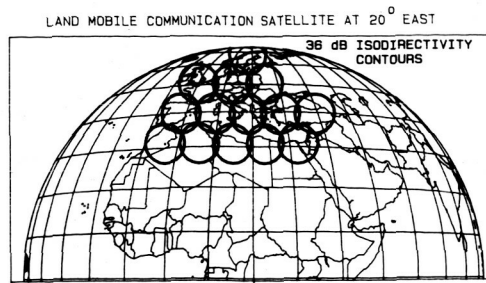


Fig.9 Multibeam coverage

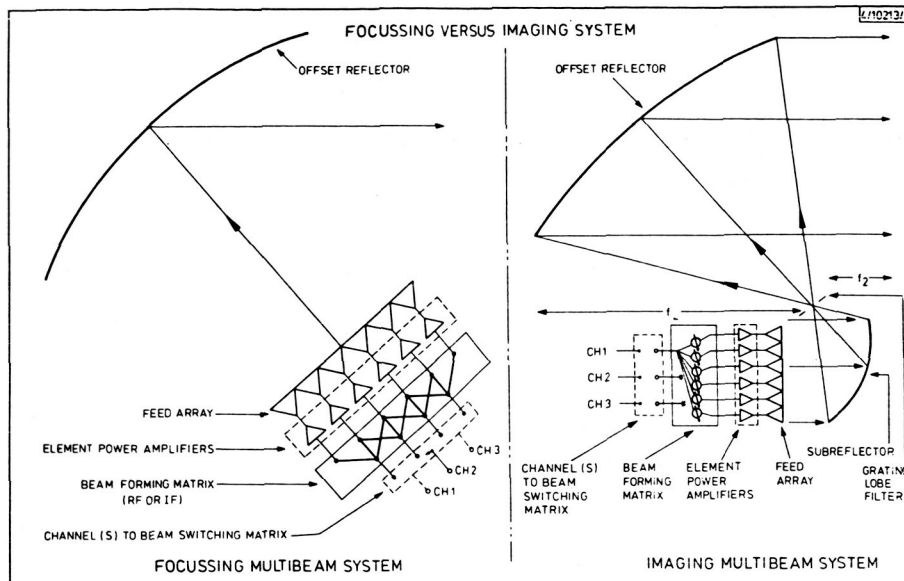


Fig.10 Focussing and imaging multibeam front-ends

all cases a large reflector and numerous feed elements are required. The array element technologies described earlier are also applicable to feeds. Three types of large reflectors are presently available in Europe.

One is a mesh umbrella with radial foldable ribs, under development with ESA funding at MBB (D). A 6 meter engineering model (Fig. 11) is presently under test. The originality of this design is the use of intermediate ribs made of graphite epoxy ribbons and integrated in the mesh between each of the supporting ribs. This provides improved surface control without use of a secondary tensioning system.

Another development, supported by CNES, is ongoing at Aerospa-tiale (F). It uses a truss structure with spring loaded joints. A functional and an electrical model have been successfully tested and this technology should also be available for flight in the early nineties (Fig. 12).

A different concept is under development under ESA funding at Contraves (CH). The reflecting surface is supported by a torus, inflated in space and rigidized under solar radiation. A photograph of a 3 m model is shown in fig. 13.

It has been demonstrated on several models that tolerances for L-band operation can easily be met. A 10 meter engineering model is presently being manufactured in flight technology.

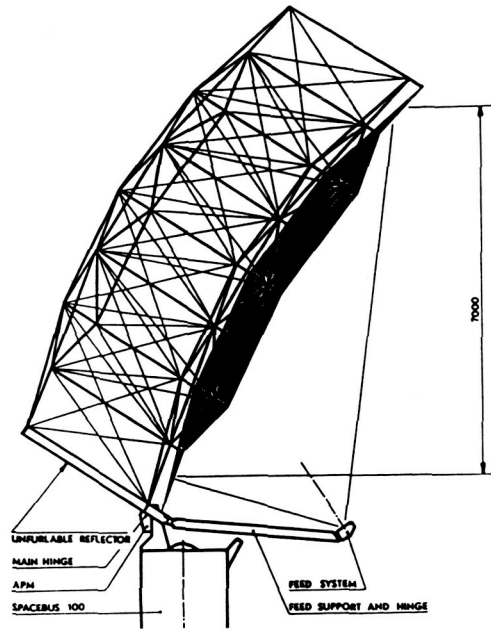
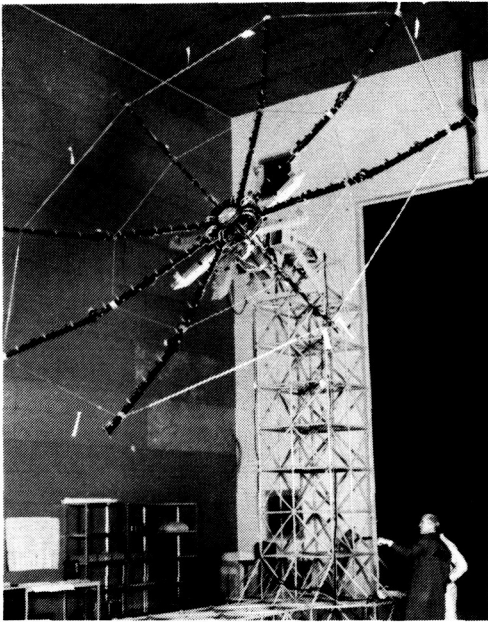


Fig.11 Mesh Umbrella (MBB) Fig.12 Mesh truss reflector (Aerospatiale)

CONCLUSIONS

The key technology for the next generation of mobile communication satellites : multibeam active arrays is ready in Europe for flight in the early nineties. Large foldable arrays and array fed reflectors for future regional applications are at a very advanced stage of development for apertures up to 6 meters. A serious additional effort will be required for larger apertures, in particular in the area of test techniques and facilities.

REFERENCES

- [1] Roederer, A. 1985. "A foldable multibeam array for satellite communications" ISAP '85, Kyoto Japan, pp. 385-388
- [2] Ericsson Radio Systems, 1987. "L-Band short backfire design..", June 1987, ESTEC Contract No. 5455/83, Final Report
- [3] Rammos, E. 1988. "The short tetra-horn : an efficient radiator for limited scan arrays", to be published
- [4] GEC-Marconi, 1988. "Development of a microstrip patch antenna..", ESTEC Contract No. 6180/85, Final Report

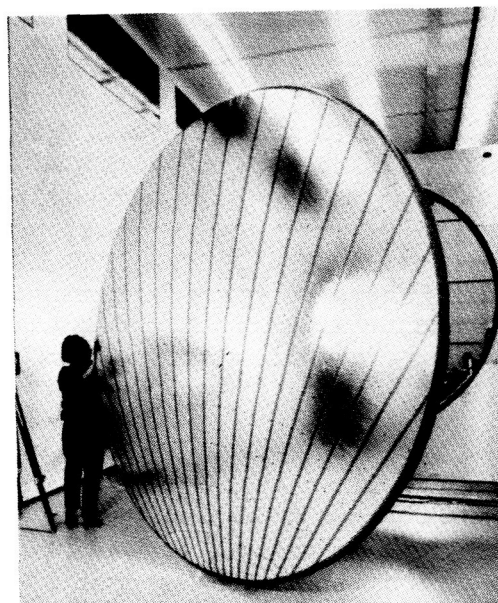


Fig.13 Inflatable reflector (Contraves)

FREQUENCY ADDRESSABLE BEAMS FOR LAND MOBILE COMMUNICATIONS

J.D. THOMPSON, Hughes Aircraft Company, United States; G.G. DuBELLAY, Hughes Aircraft Company, United States.

HUGHES AIRCRAFT COMPANY
Space and Communications Group
P.O. Box 92919
Low Angeles, CA 90009

ABSTRACT

Satellites used for mobile communications need to serve large numbers of small, low cost terminals. The most important parameters affecting the capacity of such systems are the satellite EIRP and G/T and available bandwidth. Satellites using frequency addressed beams provide high EIRP and G/T with high-gain antenna beams that also permit frequency reuse over the composite coverage area. Frequency addressing is easy to implement and compatible with low cost terminals and offers higher capacity than alternative approaches.

INTRODUCTION

Communication satellites have served a variety of communications needs over the past two decades. During this time, satellite systems have become more tailored to the specific needs of the community being served. Although satellites are currently used to provide mobile communications, significant performance improvements are available with satellite designs which are better suited to the requirements of the mobile communications communities.

MOBILE COMMUNICATIONS CHARACTERISTICS

An efficient system architecture for land mobile communications by satellite must be responsive to the characteristics of the mobile communications environment. In general, mobile systems are characterized by a large mobile user population communicating to fixed points through a satellite and base stations (see Figure 1). The satellites for this service operate in two frequency bands: the allocations for satellite communication to and from the mobile users are at L-band,

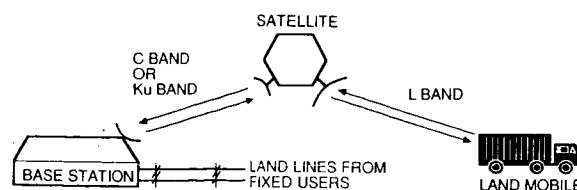


Fig. 1. Mobile satellite system

with the down- and uplink bands separated by approximately 100 MHz; the satellite-to-base station links are at C-band for the maritime mobile service, while use of Ku-band has been suggested for land mobile base station service. Furthermore, the traffic is of a point-to-point nature, and there is a scarcity of bandwidth to support the anticipated large community of mobile users, with the various services each allocated only a small portion of the frequency spectrum.

Mobile systems are further characterized by a geographically dispersed user population, each of whom has a low percentage use of the system. Hence, the economic viability of such systems requires a large subscriber base of users. The economics of the system also require low cost mobile terminals, not only since the number of users is large, but also to encourage further population growth.

Another characteristic of mobile systems is that any given signal is of a point-to-point nature (user to/from base station). Accordingly, there is little or no need for a broadcast capability to address all parties simultaneously. System characteristics are summarized in Table 1.

The characteristics described above clearly influence other aspects of such a system. Since the mobile user stations are limited in power and gain, it is of great advantage to achieve high gains for the spacecraft L-band antenna. And since traffic is of a point-to-point nature, the limited bandwidth allocation can be circumvented by frequency reuse in different geographic service regions.

A system design that most easily meets these requirements is one that uses multiple uplink and downlink high-gain beams over the coverage region of interest. The high gain supports the EIRP and G/T requirements, while the multiplicity of beams permits frequency reuse, thus increasing the available bandwidth.

Table 1. Mobile communications characteristics

Mobile users	Spacecraft
<ul style="list-style-type: none"> • Large population • Geographically dispersed • Low duty cycle per user • Low cost terminal • Low gain antenna 	<ul style="list-style-type: none"> • L-band links with users • C- or Ku-band links with base stations
	Traffic (point-to-point)
Base Station	Bandwidth (limited allocations)
<ul style="list-style-type: none"> • Few in number • Intermediary role 	

FIXED MULTIPLE BEAM SYSTEM

The EIRP advantage offered by multiple-beam systems is illustrated in Figure 2. A single beam over the entire coverage area is depicted in Figure 2a, while two-beam coverage of the same area is shown in Figure 2b. The single-beam coverage provides some reference EIRP over the full coverage region and over the full allocated bandwidth.



Fig. 2. Beam arrangements

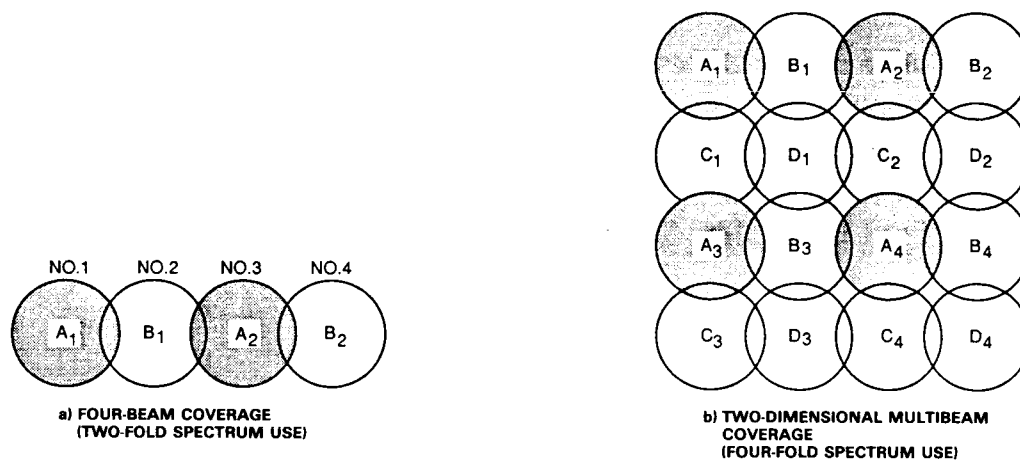


Fig. 3. Beam arrangements with frequency reuse

For the two-beam system, the bandwidth is divided into two equal portions, A and B, and each portion is assigned to one of the two beams. Each beam covers half of the total coverage area and, thus, has 3 dB higher gain than a total coverage area beam. Normally in such systems, the bandwidth is divided into portions by filters, and the two filter outputs are routed to separate power amplifiers which, in turn, drive the separate transmit beams. The relevant figure of merit for this situation is EIRP/unit bandwidth. When the total transmit power is held constant with respect to the single-beam system, the two-beam system provides a 3 dB EIRP increase over the single-beam system. The G/T is also increased by the same factor.

In general, the total coverage can be divided into N beams, with a corresponding division of the bandwidth into N portions, to provide an EIRP increase (in dB) of $10 \log (N)$. The G/T performance is also increased by the same factor of N. Ultimately, the value of N is limited by the aperture size required to form a beam of $1/N$ th coverage size, as well as by the filters required to divide the bandwidth into N portions. High Q filters at L-band tend to be bulky. Alternatively, surface acoustic wave (SAW) filters can be used at some appropriate intermediate frequency (IF). In either approach, some portion of the allocated spectrum is lost to guardbands between the usable portions of the bandwidth.

The frequency reuse advantage offered by a one-dimensional multiple beam system is illustrated in Figure 3. In particular, Figure 3a shows a four-beam system. The frequency band is split into two subbands, A and B. The spatial isolation provided by beam 2 allows band A to be used in beams 1 and 3, while the spatial isolation provided by

beam 3 allows band B to be used in beams 2 and 4. Thus, the one-dimensional four-beam system provides two uses of the frequency spectrum and the EIRP/unit bandwidth improvement is 3 dB.

The bandwidth increase associated with spatially isolated beams at L-band must be accompanied with additional bandwidth at C- or Ku-band for the links with the base stations.

The multibeam principle can be extended from a one-dimensional arrangement of multiple beams to a two-dimensional arrangement, as shown in Figure 3b. In this case, 16 beams are used to achieve four-fold use of the spectrum, with each quadrant of the coverage constituting a spectral use. Within each quadrant, the four beams are each associated with one of four portions of the quadrant, the four beams are each associated with one of four portions of the spectrum (A, B, C, and D). This arrangement permits spatial isolation of beams in both the azimuth and elevation planes. The 16-beam system offers a 6 dB bandwidth advantage and a 6 dB EIRP/unit bandwidth advantage over a single-beam system.

In general, for an N beam system with K spectral uses, the EIRP/unit bandwidth advantage is N/K , where

$1 \leq K \leq N/2$ for one-dimensional beam arrangements

$1 \leq K \leq N/4$ for two dimensional beam arrangements

The corresponding improvement in G/T for an N beam system with K spectral uses is simply equal to N, since it is not related to spacecraft power and grows as the number of beams is increased.

MULTIPLE BEAMS WITH DIRECT RADIATING ARRAYS

Using a direct radiating array antenna has distinct advantages over the reflector and feeds implementation for the mobile traffic application. For each beam the signals go through a beam forming network (BFN) that establishes the proper phase relationship at the inputs to the array elements. The multibeam composite BFN consists of an individual BFN for each beam, along with a hybrid summing network for each element. Since the composite BFN can have substantial loss, individual power amplifiers are used after the BFN. Each amplifier drives an azimuth array element, thus forming an active array. A similar arrangement of low-noise receivers is used before the receive BFN.

This configuration implies that all signals pass through all amplifiers. If a particular zone is lightly loaded, power can be re-allocated to other zones by means of base station uplink power control or by servicing more users in the other zones. This ability to re-allocate power dynamically provides additional system flexibility.

In an active array, it is desirable that all amplifiers operate at the same output backoff to achieve the best compromise between amplifier efficiency and linearity. When frequency reuse is not required and sidelobe performance is of no consequence, the active array amplifiers are equal in size and produce a uniform aperture distribution across the array. When frequency reuse is required, the sidelobe levels must be controlled, and a tapered aperture distribution must be used. To avoid the design and production costs of many amplifiers of different power levels, the unequal powers required for the array distribution are obtained by using hybrid-coupled dual

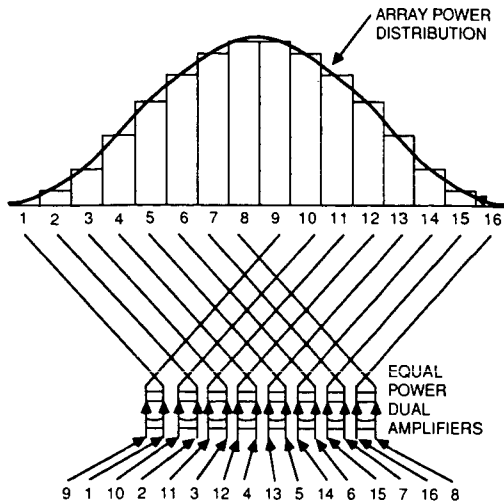


Fig. 4. Equal power amplifiers in unequal power array

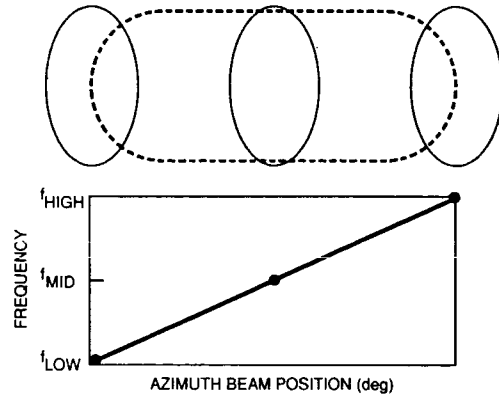


Fig. 5. Frequency address beam arrangements

amplifiers, as shown in Figure 4. In this arrangement, high and low power elements are paired in a systematic manner such that all pairs require the same total power. All amplifiers are then equal in power rating and operate at the same power level despite the unequal powers at their input and output hybrid ports.

The active array described in Figure 4 has the advantage of low risk from passive intermodulation products (PIMs), since the power is generated by a large number of amplifier pairs with each pair driving two or more array elements.

FREQUENCY ADDRESS MULTIPLE BEAM SYSTEMS

The frequency address system also uses a multitude of smaller beams to provide coverage over a large area. Like the fixed-beam system, this approach provides increased EIRP and G/T and allows multiple reuse of the frequency spectrum. However, the frequency address system enjoys certain other advantages which will soon become apparent.

In its simplest form, a frequency address system consists of a one-dimensional series of high-gain beams whose position within the coverage region is proportional to frequency. Such a beam arrangement is shown in Figure 5. High-gain beams at the left, middle, and right azimuth position of the coverage area correspond to frequencies at the low, middle, and high end of the allocated frequency spectrum. Since the beam position is a continuous function of frequency, there is actually a continuum of beam positions across the coverage region. This is an important distinction with respect to fixed multiple beam systems, where beam positions are restricted to discrete locations. The frequency address system enjoys the advantage of being able to place a beam peak at or very close to the user location in azimuth by proper frequency selection. At the azimuth beam peak, there is still gain variation in the elevation direction dependent upon the user location. When using uplink power control at the base station to radiate equal EIRPs to all users, the EIRP value is only about 0.7 dB below the peak, a significant advantage over the fixed beam approach.

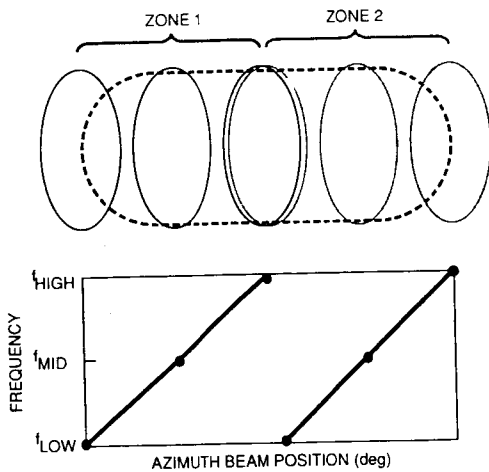


Fig. 6. Frequency address with spectral reuse

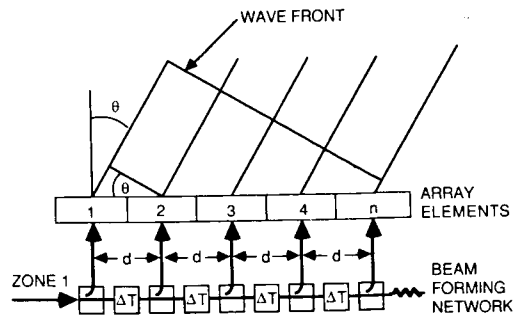


Fig. 7. Frequency address implementation

The frequency address architecture also readily lends itself to frequency reuse, as shown in Figure 6. The total coverage region is divided into two zones, with the frequency address feature being replicated in each zone. Any beam in Zone 1 and its counterpart in Zone 2 are separated in angle by a zone width. In this gap, beams operate at other frequencies. This angular separation allows spatially isolated beams to reuse the frequency address beam should be no larger than approximately half a zonewidth in azimuth.

A frequency address beam system is most easily realized by using an array antenna where the interelement phase shift is frequency dependent. This arrangement causes the beam direction to vary as a function of signal frequency.

The frequency dependent phase shifts for the antenna elements are generated in a beam forming network (BFN). This network consists of an alternating series of couplers and time-delay elements where each coupler is associated with an array element (see Figure 7).

The array interelement time delay (ΔT) yields a beam squint angle given by $\theta = \lambda/d (\Delta f) (\Delta T)$. Thus, the beam position angle, θ , is linearly related to the frequency of the signal.

For applications with relatively large bandwidths, the time delays can be realized in transmission line. For narrowband allocations, like those for mobile service, the time delays are best realized as resonant networks. Figure 8 shows a BFN made up of hybrid

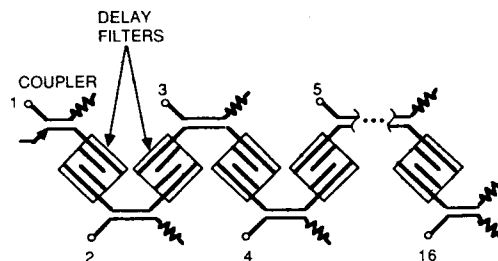


Fig. 8. Beam forming network

couplers and two-pole interdigital filters as delay elements. This network is realizable in TEM line to form a lightweight and compact BFN.

Multiple zones are used when reuse of the frequency spectrum is desired. In this case, the zones are normally adjacent and approximately equal in size. Multiple zones can also be used for multiple services, with each service segregated by frequency in the L-band spectrum. In this case, the zones need not be similar in size, and no constraints exist regarding zone overlap. It should be noted that the composite BFN for frequency addressable beams is simpler than for fixed beams because the number of zones is generally half the number of fixed beams required for the same frequency reuse.

Additional advantages are inherent to a frequency address system using an active array. First, all signals for all zones pass through all amplifiers with a prescribed set of relative phases. In each amplifier, intermodulation (IM) products are generated, and a large percentage of these, generated from signals in different zones, have distorted aperture phase distributions. As a result, some geographic IM dispersion takes place. A two-equal zone case provides about 2 dB reduction in IM levels over the regions of interest. Second, because of the hybrid-coupled amplifier arrangement, IM products generated within the amplifier pairs are geographically dispersed. The carrier-to-intermodulation ratio (C/IM) over the coverage region is improved by about 2 dB. This improvement is additive to the IM improvement from multizone operation of an active array.

In summary, the frequency address concept offers four key advantages over the fixed multiple-beam approach: increased EIRP and G/T; simpler implementation with fewer filters and less complex BFNs; increased flexibility through re-allocation of power between beams; and enhanced linearity performance through IM dispersal.

FREQUENCY ADDRESS FOR LAND MOBILE SERVICES

The benefits of the frequency addressable beam concept become even more evident when applied to an actual application such as land mobile service. The satellite for this system is designed to provide high-gain beams over the United States and Canada. In addition, it is desirable to reuse the L-band frequency spectrum, and a threefold spectral use was chosen in conjunction with an antenna aperture size of practical dimensions.

As shown in Figure 9, each zone is 3° wide in the azimuth direction and corresponds to one complete spectral use. At the intersection of two adjacent zones, the high frequency end of one zone coincides with the low frequency end of the other zone.

Since the zones are each 3° wide, frequency reuse occurs at 3° intervals. The interference between spatially isolated beams is kept within an acceptable level by selecting a tapered aperture distribution with low sidelobes. In particular, the cosine squared power distribution shown in Figure 4 is used, resulting in sidelobes at least 23 dB below the beam peak. Furthermore, the half-power beamwidth is selected to be 57% of the zone width, a factor which causes the half-power point of the pattern in one zone to coincide with the first null of the pattern of the same frequency signal in the adjacent zone. This arrangement, shown in Figure 10, results in a carrier-to-

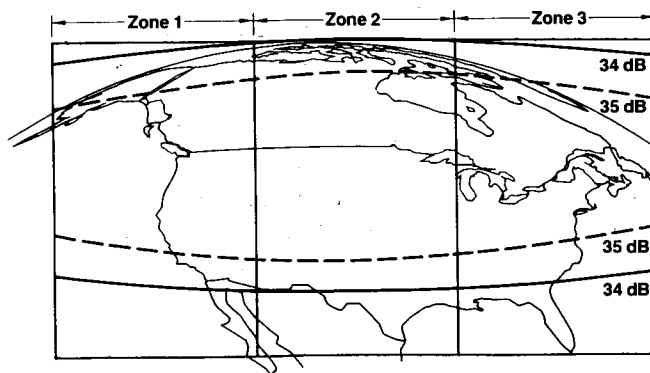


Fig. 9. Antenna gain over coverage area

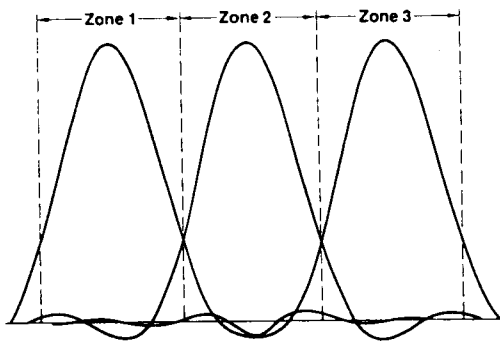


Fig. 10. Zonal frequency reuse

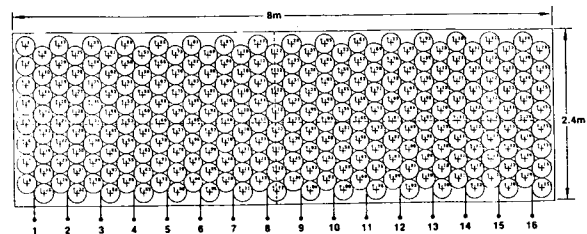


Fig. 11. Array antenna

interference ration (C/I) of 23 dB between adjacent zones. The effective achievable antenna gain over the coverage area resulting from the frequency address concept is shown in Figure 9. Note that a major portion of the service area is covered by the 35 dB gain contour.

These frequency address beams are generated by an antenna array 8 meters wide by 2.4 meters high. The array consists of a close packed arrangement of circularly polarized cup dipoles, as shown in Figure 11. The array has 32 columns. However, columns may be driven in pairs, so that only 16 drive points are required. Since the array is used for both transmit and receive beams, a diplexer is required at each drive point.

The threefold use of the frequency spectrum with a single array requires the use of a three-zone BFN, as shown in Figure 12. The corresponding outputs of the individual zone BFNs are combined in summing networks consisting of hybrid couplers to form single outputs for each antenna drive point.

As noted earlier, the risk of PIMs is much reduced compared to an offset fed dish antenna. The maximum RF power handled by any one diplexer is 12.5% of the total, while the maximum power in any one cup-dipole is 1.5% of the total radiated power. Since the direct radiating array has low coupling to the other spacecraft surfaces, there is little risk of PIMs there, either.

Additional flexibility in the allocation of frequencies can be obtained, with a modest increase in hardware complexity, by interweaving additional zones with the existing three, as shown in Figure 13.

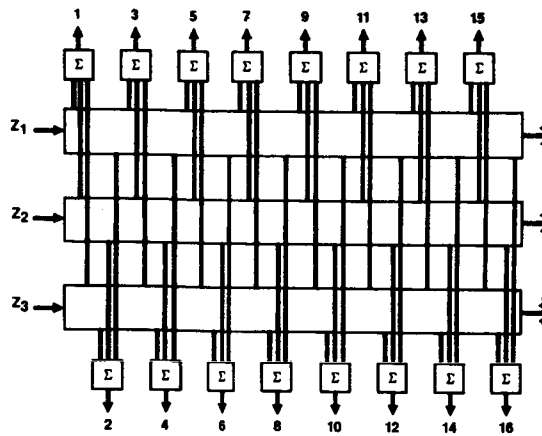


Fig. 12. Three-zone beam forming network

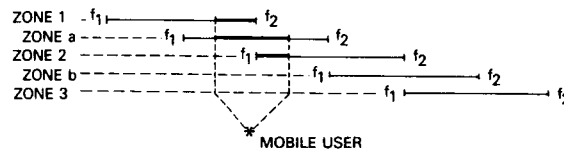


Fig. 13. Overlapping zones

This does not change the amount of frequency reuse because of the spatial separation requirement between users of the same frequency. But virtually the whole frequency band is within reach of any one user rather than only half for the nonoverlapping-three-zones case.

The C/IM improvement due to frequency addressing, in conjunction with the active array and the use of hybrid coupled amplifiers, was evaluated through computer simulation. For the three-zone case it amounts to 5.1 dB. This improvement can be used to provide a higher C/IM value or can be used to operate the transmitters more efficiently at a reduced output backoff.

The frequency address system is realizable in a straightforward configuration. The three-zone system with three uses of the L-band spectrum requires a comparable amount of spectrum at Ku-band for links to the base stations. This is easily achieved by using three separate channels at Ku-band. These channels are converted to the assigned spectrum at L-band by use of three different local oscillator frequencies in the up- and downconverters. These repeater elements as well as the L-band elements previously discussed are shown in Figure 14.

The satellite configuration is shown in Figure 15 for both the stowed and deployed states. The outer portions of the L-band array are hinged so that it can be stowed compactly for launch. Small Ku-band arrays are provided about the L-band array for the links to the base station.

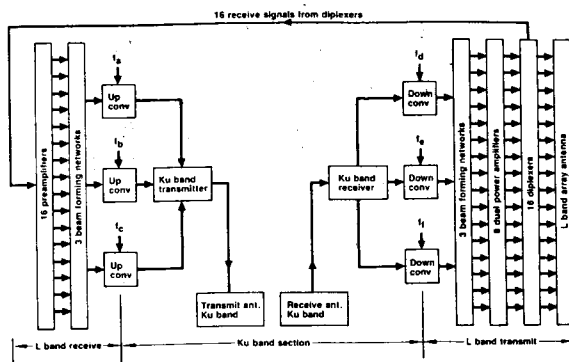


Fig. 14. Mobile satellite block diagram

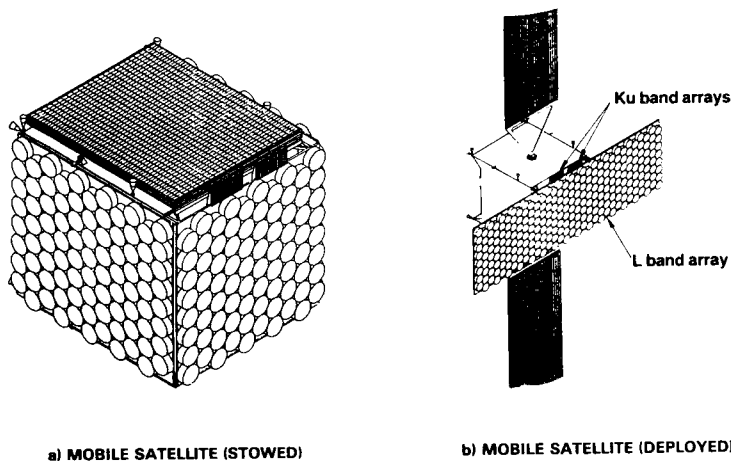


Fig. 15. Mobile satellite configuration

CONCLUSIONS

Frequency addressing provides the ability to achieve high satellite EIRP and G/T performance and permits reuse of the frequency spectrum to generate increased operating bandwidth. Its implementation is simpler than that of other multiple beam approaches and it offers improved linearity performance through IM dispersion, as well as improved flexibility in allocation of power among the beams. Furthermore, it has been shown that frequency addressing is well suited to the land mobile requirements for North America and that it can be implemented on a satellite in a straightforward manner.

LARGE ANTENNA EXPERIMENTS ABOARD THE SPACE SHUTTLE
-- APPLICATION OF NONUNIFORM SAMPLING TECHNIQUES

Dr. Y. RAHMAT-SAMII, Senior Research Scientist

Jet Propulsion Laboratory
California Institute of Technology
Pasadena, CA 91109

ABSTRACT

Future satellite communication and scientific spacecraft will utilize antennas with dimensions as large as 20 meters. In order to commercially use these large, low sidelobe and multiple beam antennas, a high level of confidence must be established as to their performance in the 0-g and space environment. Furthermore, it will be desirable to demonstrate the applicability of surface compensation techniques for slowly varying surface distortions which could result from thermal effects. In this paper, an overview of recent advances in performing rf measurements on large antennas is presented with emphasis given to the application of a space based far-field range utilizing the Space Shuttle and the concept of a newly developed nonuniform sampling technique.

1. INTRODUCTION

It is very likely that antennas in the range of 20 meters or larger will be an integral part of future satellite communication and scientific spacecraft payloads. For example, Fig. 1 depicts the conceptual evolution of the Land Mobile Satellite System which is anticipated to evolve from utilizing approximately 6-9 meter reflectors to 55 meter reflectors in the era spanning the late 1980's to early 2000. In order to commercially use these large, low sidelobe and multiple-beam antennas, a high level of confidence must be established as to their performance in the 0-g and space environment. Certain ground (1-g) testing can be performed to validate the workability of different segments of such large structures; however, it will be a formidable task to characterize the performance of the entire structure on the ground. For this reason, a conceptual study has been initiated with the intention to describe an experiment aboard the Space Shuttle to demonstrate the deployment reliability of the antenna

structure, to measure thermal and dynamic structural characteristics, and to verify performance specification under all expected conditions. In particular, special consideration is being given to the rf far-field pattern measurements which should provide the ultimate characterization for the antenna performance (Fig. 2).

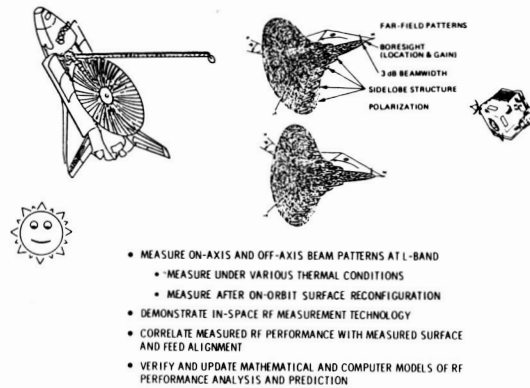
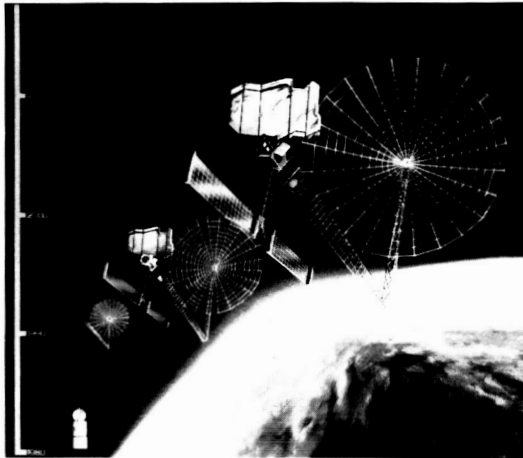


FIG. 1. Evolution of the proposed Land Mobile Satellite System (LMSS). FIG. 2. Spaced-based rf experiment objectives aboard the Space Shuttle.

Several potential scenarios have been considered and the relative merits of each of them are shown in a qualitative manner in Fig. 3. Among all these possibilities the application of the scenario shown in the last row appeared most feasible. The rf experiment is anticipated to be performed on a 20-meter offset reflector at L-band using the Remote Mini-Flyer, a NASA-developed reusable and retrievable spacecraft (a modified Spartan), as the carrier for an rf beacon. This beacon is used to illuminate the antenna in a similar fashion as one does in the ground-based far-field ranges using transmit illuminators. An artist's rendition of this space-based experiment is depicted in Fig. 4.

2. RF MEASUREMENT CONSIDERATIONS

In order to reduce the cost of the experiment, it has been anticipated that no gimbal mechanism will be used to accurately control the position of the antenna with respect to the illuminator. Instead, the relative motion of the Shuttle and free-flier in a controlled manner will be utilized to provide the angular range of interest. Depending on what the exact covered u-v space will be, several scenarios could be considered. The schematics of two possible measurement scenarios are shown in Figs. 5 and 6.

Since without any gimbal system it will be impractical to measure antenna patterns in specified ϕ cuts, one may

have to perform the measurement in a specified $u-v$ angular range in a time period in which the antenna structure is not changed appreciably from an rf viewpoint. Fig. 5 shows the possibility of measuring very dense but nonuniformly measured data points from which the needed ϕ -cuts or contour patterns can be constructed. If it is proven that the possibility of measuring a very dense set of data may not be realistic, an alternate scheme should be available. This alternate scheme is depicted in Fig. 6, which assumes that the measured amplitude and phase are obtained at relatively sparse and nonuniformly distributed $u-v$ points. The question is, then, whether or not one can construct the ϕ -cuts from a set of nonuniformly distributed measured data points.

TECHNIQUES	CONFIGURATION	COMPLEXITY	USEFULNESS	COST
NEAR FIELD TECHNIQUES				
COMPACT RANGES				
BEACON ON THE GROUND				
RECEIVING ANTENNAS ON THE GROUND				
RADIO STAR SOURCES				
GEO SATELLITE SOURCES				
FREE-FLYER AS A BEACON				

FIG. 3. A qualitative comparison of different measurement techniques aboard the Space Shuttle.



FIG. 4. An artist's rendition of the proposed large antenna Shuttle experiment.

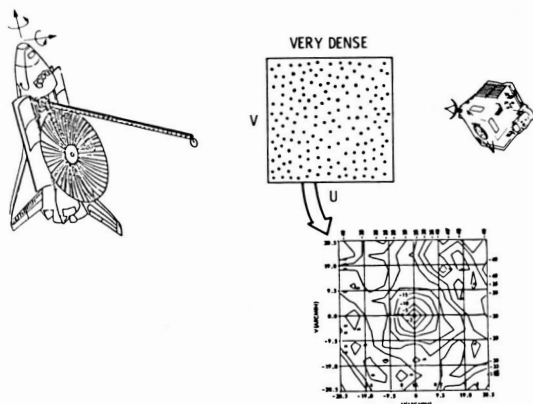


FIG. 5. Schematic of nonuniform and very densely measured sampled points.

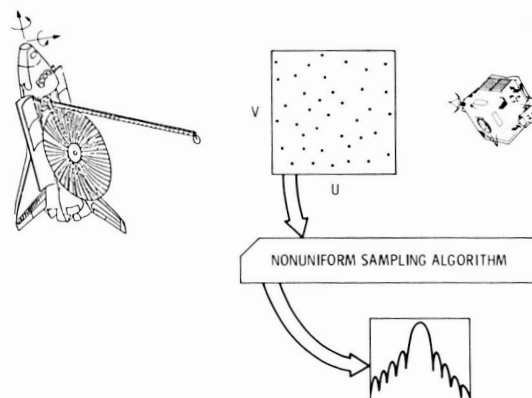


FIG. 6. Schematic of nonuniform and relatively sparsely measured sampled points.

Recently, Rahmat-Samii and Cheung [1] have demonstrated that a two-dimensional nonuniform sampling technique which utilizes irregularly spaced samples (amplitude and phase)

can be used to generate the far-field patterns. The mathematical developments of this two-dimensional nonuniform sampling technique have been detailed in [1]. Additionally, a powerful simulation algorithm has then been developed to test the applicability of this sampling technique for a variety of reflector measurement configurations [1]. For example, Figs. 7 and 8 show the simulated nonuniform sample points and the reconstructed far-field patterns in specified ϕ -cuts for a 20 meter offset reflector antenna with a defocused feed operating at L-band [1]. In Fig. 8, the solid curves are reconstructed co-polar and cross-polar patterns using the nonuniform sampling technique. It is noted that even though no sample points are captured in these cuts, the reconstructed patterns agree well with the ideal patterns in the angular range where the nonuniform sample points have been generated, i.e., ± 3.2 degrees. Many tolerance studies have also been performed to demonstrate the required measurement accuracies in applying the nonuniform sampling technique [1].

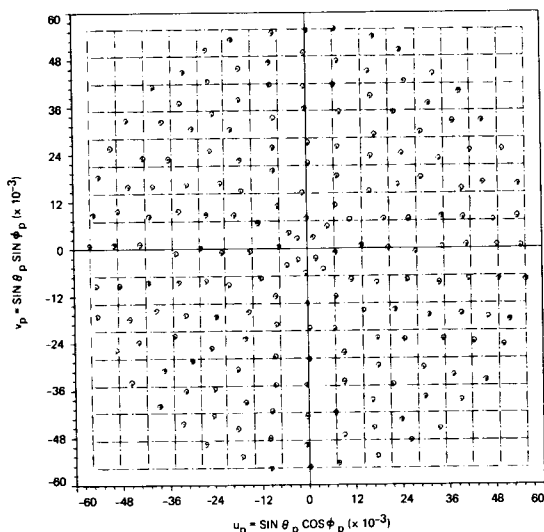


FIG. 7. One hundred ninety two nonuniform sampled point distribution in (u,v) coordinates which covers an angular region of $\theta = \pm 3.2$ degrees.

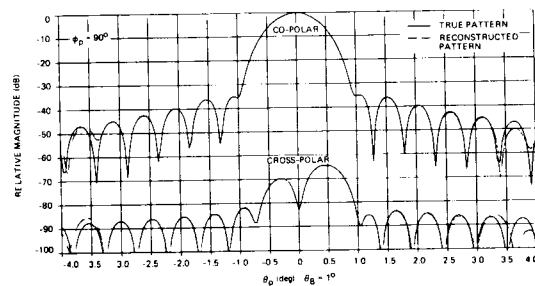


FIG. 8. Reconstructed far-field patterns from 192 sampled points using nonuniform sampling technique.

To validate the accuracy of the nonuniform sampling technique for antenna pattern construction, several measurements have been performed as reported in [2]. In one of the measurements JPL's 1200-ft far-field range was used, where a 1.47-m circularly polarized Viking reflector antenna [3] (Fig. 9) was measured at X-band (8.415 GHz) using a corrugated horn as the illuminating antenna. The far-field amplitude and phase were measured in the directions shown in Fig. 10 which consisted of 585 nonuniformly distributed sampled points in (u,v) coordinates.

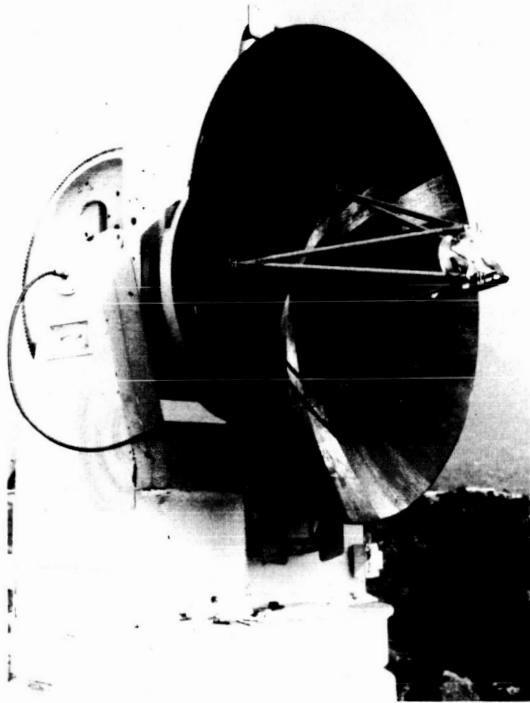


FIG. 9. The 1.47-m circularly polarized Viking reflector antenna operating at X-band (8.415 GHz).

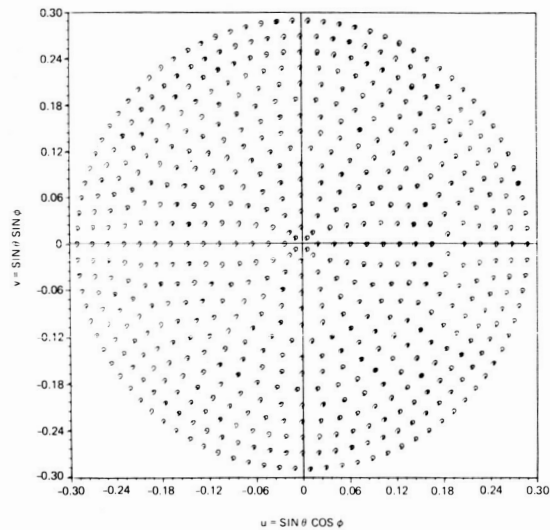


FIG. 10. Five hundred eighty five measured data point distribution in (u,v) coordinates which covers an angular region of $\theta = \pm 16.8$ degrees.

The total system errors for amplitude measurement have been estimated to be less than 0.2 dB at -40 dB level relative to the boresight power level and the phase measurement error has been within ± 5 degrees. The pointing accuracy has been estimated to be better than ± 0.1 degrees. The co-polar far-field patterns for $\phi = 90$ degrees are depicted in Fig. 11. The solid curves are the standard azimuth cuts and the dashed curves are the reconstructed patterns using the nonuniform sampling technique. These patterns are constructed by utilizing the window concept as discussed in [1,2]. Note that asymmetric patterns have resulted even though a symmetric reflector was used. This is due to the feed and strut blockage effects. In the angular range of ± 16.8 degrees where the measured data are available, the comparison between the solid and dashed curves demonstrates close agreement. Note that even though no sampled point has been used at the boresight, the peak of the beam has been reconstructed very well.

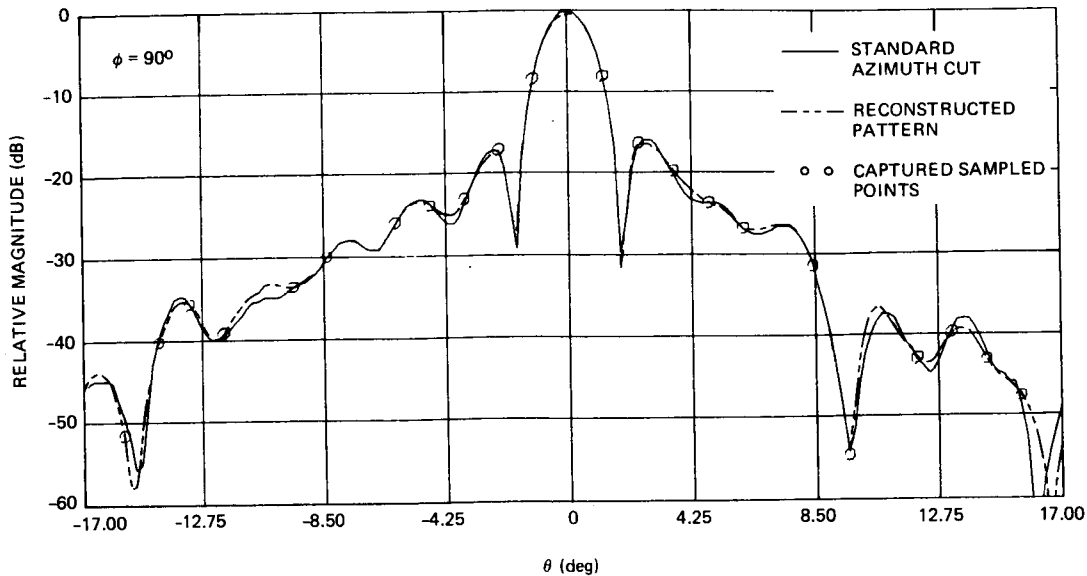


FIG. 11. Reconstructed far-field patterns of the Viking reflector at X-band using nonuniformly distributed measured data.

ACKNOWLEDGEMENTS

The research described in this paper was carried out at the Jet Propulsion Laboratory, California Institute of Technology, under contract with the National Aeronautics and Space Administration. The Author would like to thank R. Cheung for his assistance during the development and testing of the two-dimensional nonuniform sampling algorithm.

REFERENCES

1. Rahmat-Samii Y. and R. Cheung, "Nonuniform sampling techniques for antenna applications," IEEE Trans. Antennas Propagat., vol. 35, pp. 268-279, 1987.
2. Cheung R. and Y. Rahmat-Samii, "Experimental verification of nonuniform sampling technique for antenna far-field construction," Electromagnetics, vol. 6, no. 4, pp.277-300, 1986.
3. Rahmat-Samii Y. and M. Gatti, "Far-field patterns of spaceborne antennas from plane-polar near-field measurements," IEEE Trans. Antennas Propagat., vol. 33, pp. 638-648, 1985.

15-METER ANTENNA PERFORMANCE OPTIMIZATION USING AN INTERDISCIPLINARY APPROACH

WILLIAM L. GRANTHAM, NASA Langley Research Center, United States;
LYLE C. SCHROEDER, NASA Langley Research Center, United States;
MARION C. BAILEY, NASA Langley Research Center, United States;
THOMAS G. CAMPBELL, NASA Langley Research Center, United States

LANGLEY RESEARCH CENTER
Mail Stop 490
Hampton, VA 23665-5225
UNITED STATES

ABSTRACT

A 15-meter diameter deployable antenna has been built and is being used as an experimental test system with which to develop interdisciplinary controls, structures, and electromagnetics technology for large space antennas. The program objective is to study interdisciplinary issues important in optimizing large space antenna performance for a variety of potential users.

The 15-meter antenna utilizes a hoop column structural concept with a gold-plated molybdenum mesh reflector. One feature of the design is the use of adjustable control cables to improve the paraboloid reflector shape. Manual adjustment of the cords after initial deployment improved surface smoothness relative to the build accuracy from 0.140 inches RMS to 0.070 inches.

Experiments have been completed in which preliminary structural dynamics tests and near-field electromagnetic tests were made. The antenna is now being modified for further testing. Modifications include addition of a precise motorized control cord adjustment system to make the reflector surface smoother and an adaptive feed for electronic compensation of reflector surface distortions. Although the previous test results show good agreement between calculated and measured values, additional work is needed to study modelling limits for each discipline, evaluate the potential of adaptive feed compensation, and study closed-loop control performance in a dynamic environment.

INTRODUCTION

The development of large, self-deployable antennas has been a major technology thrust for NASA during the past two decades. The need for

larger aperture antennas evolved from the requirements of increased gain and resolution to improve remote sensing, space based radar, satellite communications, and space science missions. The hoop column antenna is one space-frame concept being studied at LaRC to satisfy this technology need.

In order to include experimental testing as part of the technology development program, a 15-meter diameter hoop column antenna (Fig. 1) has been built and initial structural and electromagnetic tests completed. Structural tests were conducted at the Harris corporation where the antenna was built and at Langley Research Center. Electromagnetic tests were conducted in the Near-Field Test Laboratory (NFTL) at Martin Marietta Aerospace (MMA) in 1985. Details of these results and antenna design specifics are given in several references (Hoover, 1986; Anon., 1986; Campbell, 1988; Belvin, 1987).

The antenna structure is stiffened by cables from the column ends to the hoop (Fig. 1). Both the hoop and the column are composed of laminated graphite epoxy material. The lower chords are made of graphite, while the upper chords are quartz for good RF transparency. Control cords (96) on the backside of the reflector provide limited shape control of the RF reflective mesh surface. The shape of the reflecting surface is such that each reflector quadrant is a separate paraboloid segment with the associated vertex and focal point offset about 20 inches from the axis of the column.

After completion of the initial electromagnetic and structural dynamic tests, a 4-year technology development effort was initiated involving Controls, Structures, and Electromagnetics Interaction (CSEI) for large space structures. This paper describes the CSEI program and some preliminary results of related analytical work.

The CSEI program objectives are to examine interdisciplinary issues important in optimizing Large Space Antenna (LSA) performance for a variety of potential users. New antenna features are being added (Fig. 2) which include motorized cord control for more accurate and rapid remote surface actuation to improve the RF performance. Cords were adjusted manually in the 1985 near-field tests. Other new features planned are the adaptive feed and the real-time antenna figure sensor for open and closed-loop control tests of the flexible structure.

PERFORMANCE IMPROVEMENT

RF performance can be optimized not only by making the reflector surface smoother (Ruze, 1966), but by electronic compensation using an adaptive feed array. The principle of this concept is shown in figure 3. If a physical distortion occurs in the reflector, as shown in the figure, a proportional phase distortion will occur in the aperture plane degrading the far-field pattern shape and boresite gain. Partial compensation for the distorted phase front can be realized using a feed array with adjustable phase and amplitude distribution. This type of performance correction should be possible for both rapid and slowly changing antenna shape in the CSEI program.

Computer simulations representing a multi-element feed array with the 15-meter reflector and the actual 61 mils RMS surface distortions show both boresite gain and sidelobe level improvement at C-band (figs. 4,5). Figure 4 also shows how smooth the surface must be in order to have a performance improvement equivalent to the adaptive feed. Radiation pattern improvement near the main beam is indicated in figure 5 compared to the one feed element case. As can be seen, the main beam shape is essentially restored to the perfectly smooth case when the 37-element feed is used to compensate for the surface distortion. Other studies are underway to evaluate the adaptive feed compensation at higher frequencies and rougher surfaces as might occur in space.

CONCLUDING REMARKS

Fabrication and assembly of the surface adjustment system is near completion and tests are expected to begin early in the spring of 1988. The first set of tests will examine three primary areas of interest: limit of surface smoothness that can be accomplished using the precision control motors, deployment repeatability for multiple deployments, and dynamic surface vibration control using measured cord tension as input to the motorized cord controller.

Following these experiments, electromagnetic tests will be conducted in the MMA near-field facility and will involve adaptive feed tests and later include closed-loop control dynamic testing for real-time surface control. These tests will address conditions that could exist in space due to slew-and-track and slew-and-point antenna maneuvers.

REFERENCES

- Hoover, John 1986. Kefauver, Neill; Cencich, Tom; and Osborn, Jim. Near-Field Testing of the 15-Meter Model of the Hoop Column Antenna. NASA CR-178059 (vo. I), CR-178060 (vol. II), CR-178061 (vol. III). March 1986.
- Anon. 1986. Development of the 15 Meter Diameter Hoop Column Antenna. NASA CR-4038. December 1986.
- Campbell, T. G. 1988. Bailey, M. C.; Belvin, W. K. The Development of the 15-Meter Hoop Column Deployable Antenna System With Final Structural and Electromagnetic Performance Results. ACTA Astronautica, Vol. 17, No. 1, pp. 69-77.
- Belvin, W. K. 1987. Edighoffer, H. E.; Herstrom, C. L. Quasi-Static Shape Control of a 15-Meter Hoop Column Antenna. AIAA/ASME/ASCE/AHD 28th Structures, Structural Dynamics and Materials Conference. Monterey, CA. April 6-8, 1987.
- Ruze, John 1966. Antenna Tolerance Theory - A Review. Proceedings of IEEE, Vol. 54, No. 4, pp. 633-640. April 1966.
- Bailey, M. C. 1986. Multiple-Aperture Mesh Reflector Antenna Radiation Pattern Characteristics. 1986 International IEEE AP-S Symposium Digest. Philadelphia, PA. June 9-13, 1986.



Fig. 1. 15-meter antenna in Martin Marietta Near Field Facility

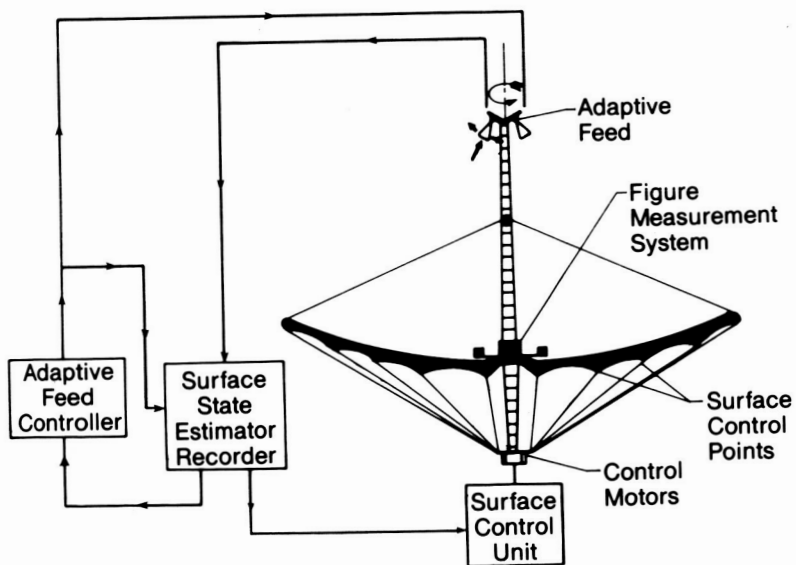


Fig. 2. 15-meter antenna geometry for the interdisciplinary research program

ORIGINAL PAGE IS
OF POOR QUALITY

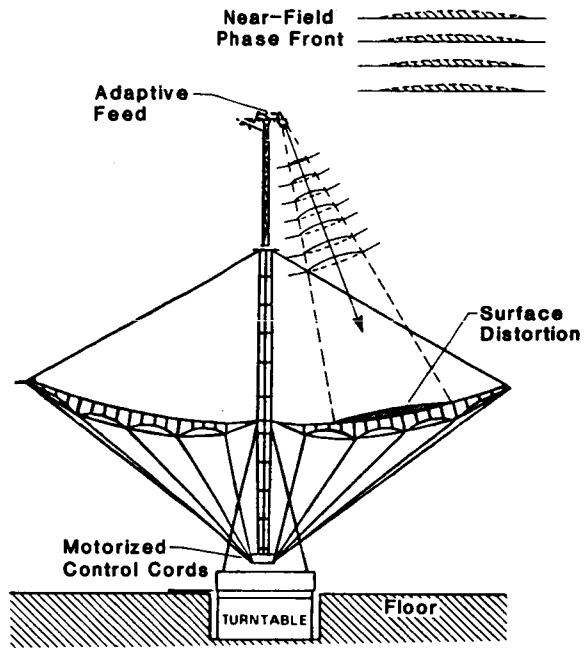


Fig. 3. Adaptive feed compensation

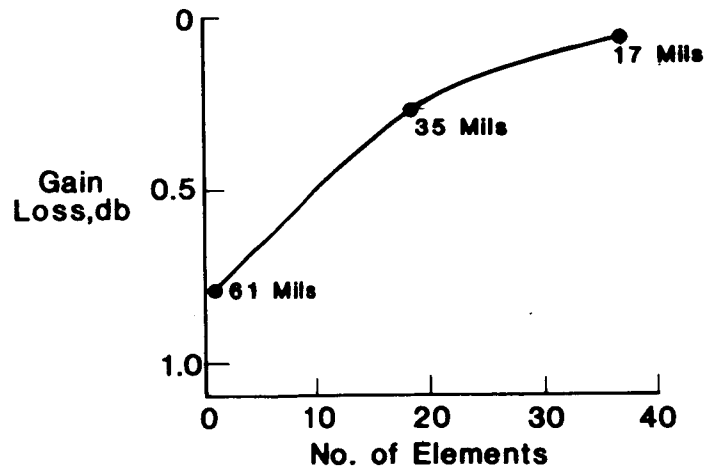


Fig. 4. Boresite gain improvement (C-band)

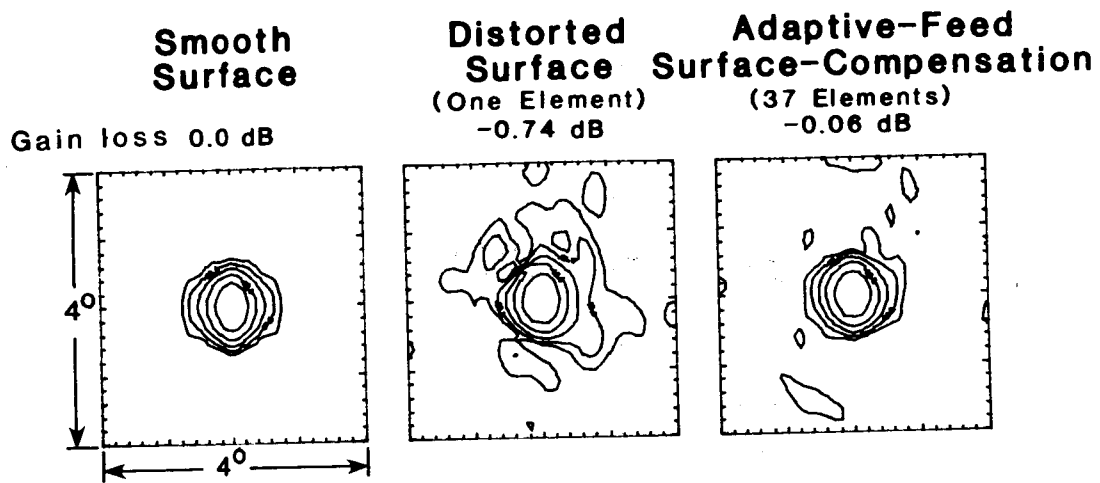


Fig. 5. Radiation patterns (C-band)

A MICROSTRIP ARRAY FEED FOR MSAT SPACECRAFT REFLECTOR ANTENNA

DR. JOHN HUANG, Mobile Satellite Program, Jet Propulsion Laboratory,
United States.

JET PROPULSION LABORATORY
4800 Oak Grove Drive, 161-213
Pasadena, California 91109
United States

ABSTRACT

An L-band circularly polarized microstrip array antenna with relatively wide bandwidth has been developed. The array has seven subarrays which form a single cluster as part of a large overlapping cluster reflector feed array. Each of the seven subarrays consists of four uniquely arranged linearly polarized microstrip elements. A 7.5% impedance (VSWR <1.5) as well as axial ratio (<1 dB) bandwidths have been achieved by employing a relatively thick honeycomb substrate with special impedance matching feed probes.

INTRODUCTION

Very large multiple-beam satellite reflector antennas in the 20 to 55 meter range have been planned for the future U.S. Land Mobile Satellite Systems (LMSS)^[1]. From 40 to 90 contiguous beams covering Continental United States (CONUS) are to be generated from overlapping cluster feed arrays^[2] with diameters of up to 6 meters. A structure of this size should have the capability of being folded and stowed in the satellite launching vehicle. Consequently, the feed array should be low in profile and light in weight. An earlier experimental feed array to demonstrate the feasibility of generating contiguous beams by using the overlapping cluster feed concept was successfully developed and tested^[3]. In that feed array, relatively narrowband microstrip patches were used in order to reduce the complexity of the experiment.

This paper describes the development of a new array which has a relatively broadband performance sufficient to cover the bandwidth requirements of the Land Mobile Satellite System. To meet the light weight requirement of the system and to cover both downlink frequencies (1545 to 1559 MHz) and uplink frequencies (1646 to 1660 MHz), the microstrip antenna with a half-inch thick honeycomb-supported substrate has been selected. Since a half-inch (0.07 wavelength) substrate is relatively thick for microstrip radiators, four feed probes are required^[4] per single element to suppress the undesired higher order modes and thus to generate acceptable circular polarization (c.p.) across the total bandwidth. For a large array, such a single-patch four-probe feed system would increase the complexity of an already complex feed beam-forming network, and will make it heavier and more prone to RF losses.

In a previous paper^[5] the theoretical background was presented for obtaining a circularly polarized array from single-probe fed linearly polarized patch elements. The c.p. is achieved by having a basic 2×2 subarray with specific orientation and phase arrangement for the feed elements. As shown in Figure 1, the feed elements' angular orientation as well as phase are arranged in the 0° , 90° , 180° , 270° fashion. With such a system, not only is the feed complexity reduced, but also the bandwidth performance is improved. To demonstrate the concept, a single cluster array composed of seven subarrays with 28 single-feed linearly polarized patches has been constructed and tested.

HARDWARE DESCRIPTION AND RESULTS

The overlapping cluster array concept can be demonstrated by 2 clusters of arrays as shown in Figure 2. The two large circles represent the arrays to generate two contiguous beams, and each small circle is a sub-array consisting of four microstrip patches. The array that has been constructed and tested is one of the large circles and has a total of 28 microstrip patches. Dimensions of this array are illustrated in Figure 3. The relatively sparse element spacing is a result of the overlapping cluster arrangement for optimum reflector illumination with a minimum number of elements in the array. The array has an amplitude taper so that the reflector is illuminated with proper edge taper required for achieving low sidelobe levels. Each of the 7 subarrays are fed by a stripline 4-way hybrid power divider so that 0° , 90° , 180° , 270° feeding phases for the elements can be realized.

The fabricated array is illustrated in Figure 4 where the placement of the feed probes in the 4 patches of each subarray is similar to that shown in Figure 1. Since the honey-comb supported microstrip substrate is relatively thick, it generates a large amount of surface waves which cause significant mutual coupling between subarrays. These surface waves and the consequent mutual coupling effect cause asymmetry in the field components and degrade the c.p. performance. Introduction of metallic baffles between the subarrays can block out most of the surface waves and thus reduce the mutual coupling between subarrays. It is found that one-inch tall metallic baffles are required between all the subarrays to bring the on-axis axial ratio from 3 dB to less than 1 dB. Within each subarray, however, due to the 0° , 90° , 180° , 270° element orientation and phase arrangement, most of the unwanted field components caused by surface waves are cancelled and field symmetry is preserved.

In feeding a microstrip antenna with a thick substrate, generally a large inductance occurs around the feed probe. Normally, an impedance matching circuit can be etched prior to each feed probe for tuning out the probe inductance. This, however, introduces complexity and additional loss to the hybrid circuit. Furthermore, there may not be enough real estate available on the hybrid circuit board layer to accommodate the matching circuits and, consequently, an additional layer of circuit board may be needed. To reduce this complexity, a tear-drop shaped probe has been used to effectively tune out the inductance and provide 7.5% bandwidth. The tear-drop shape introduces

an appropriate amount of capacitance to cancel the undesired inductance and provide a gradual change of the field from the coaxial line into the thick microstrip antenna substrate.

The measured radiation patterns of the array shown in Figures 3 and 4 are illustrated in Figure 5. These patterns are produced by a spinning-linear-dipole technique to demonstrate the c.p. quality of the array. Figure 5(a) is the pattern measured at 1545 MHz for $\phi = 45^\circ$ plane cut, while Figure 5(b) is measured at 1660 MHz. Patterns measured at other plane cuts will be presented in the conference. The worst axial ratio on the main beam peak is less than 0.8 dB for both frequencies. The main beam of the array is rather symmetrical, and its 10 dB beamwidths for $\phi = 0^\circ$, 45° , and 90° planes are nearly equal. The main beam below 10 dB and the sidelobes, however, are different for various cuts. The design goal was to achieve circular symmetry of the main beam down to 15 dB from the peak. A reflector with edge taper of this level will produce better than 30 dB sidelobe levels. Because of the inherent circular asymmetry of the 7-subarray feed, perfect symmetry for the feed pattern in all the cuts is hardly feasible.

The relatively high feed array sidelobe levels are a consequence of the relatively large separation of the subarrays (1.5 and 1.3 wavelengths in 0° and 90° plane) imposed by the overlapping cluster requirement of the contiguous multibeam system^[2]. These high sidelobes will result in large spill-over past the reflector edge and hence lower reflector efficiency when compared with a gain optimized reflector. A complete three dimensional pattern integration shows that the relatively high sidelobes encountered here will only contribute to less than 0.3 dB of gain loss.

CONCLUSION

A circularly polarized feed array for a spacecraft reflector antenna has been constructed by using linearly polarized microstrip elements. The array achieved an axial ratio better than 0.8 dB at the pattern peak and better than 3 dB down to 20 degrees from the peak, across a 7.5% frequency bandwidth. A tear-drop shaped feed probe is used to achieve wideband input impedance matching for the relatively thick microstrip substrate. Due to the success of this experimental study, a circularly polarized microstrip array can have a simplified feed mechanism, reduced RF loss in the feed circuit, and improved radiation performance over a wide frequency bandwidth. It is expected that 10 to 15 percent bandwidth can be achieved by using the same technique if the substrate thickness is further increased.

REFERENCES

- [1] F. Naderi, G. H. Knouse, and W. J. Weber, "NASA's Mobile Satellite Communications Program; Ground and Space Segment Technologies," 35th International Aeronautics Federation Congress, Lausanne, Switzerland, October 10, 1984.

- [2] V. Jamnejad, "Multibeam Feed System Design Considerations for Single Aperture Large Space Antennas," NASA Conference on Large Space Antenna Technology, December 1984.
- [3] K. Woo, "Multiple Beam Antenna Feed Development," 1986 AP-S International Symposium Digest, pp 409-412, June 1986.
- [4] J. Huang, "Circularly Polarized Conical Patterns from Circular Microstrip Antennas," IEEE Transactions on Antennas and Propagation, Vol. AP-32, No. 9, pp 991-994, September 1984.
- [5] J. Huang, "A Technique for an Array to Generate Circular Polarization with Linearly Polarized Elements," IEEE Transactions on Antennas and Propagation, Vol. AP-34, No. 9, pp 1113-1124, September 1986.

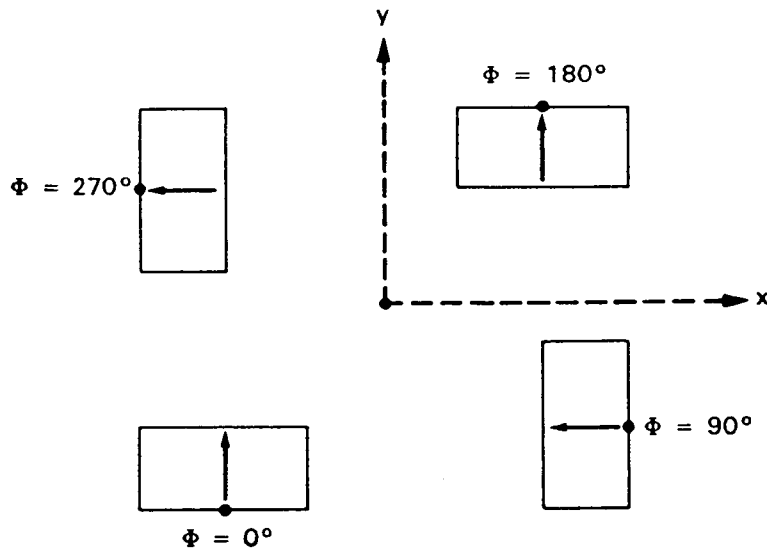


Figure 1. Square grid 2 x 2 subarray of 4 identical linearly polarized microstrip elements that together generate C.P. The heavy dot on each patch indicates the feed location and ϕ indicates the feed phase. Arrows are E-field polarization directions.

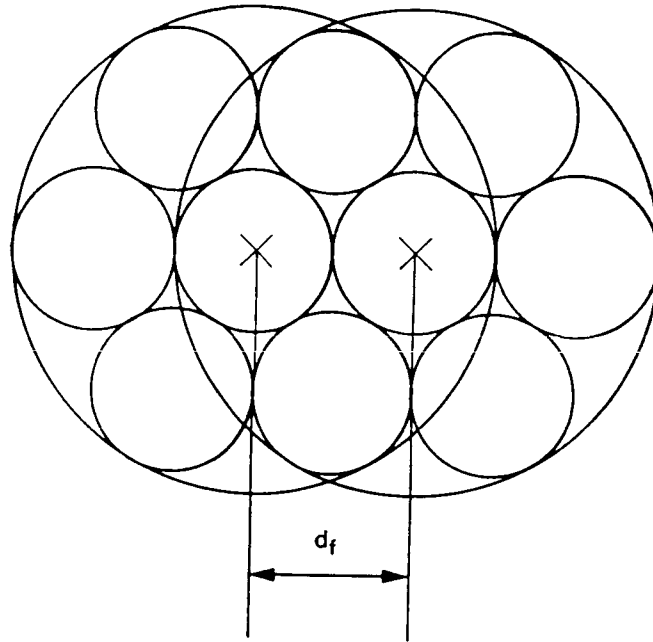


Figure 2. Two overlapping 7-subarray cluster feeds. d_f is separation distance between any two adjacent subarrays and between two cluster feeds.

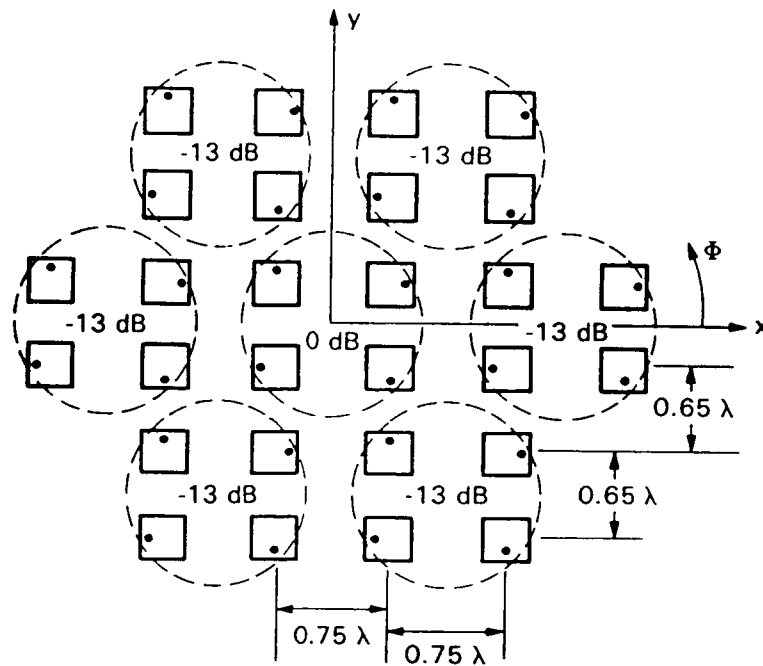


Figure 3. 7-subarray single cluster feed with 28 microstrip patches.

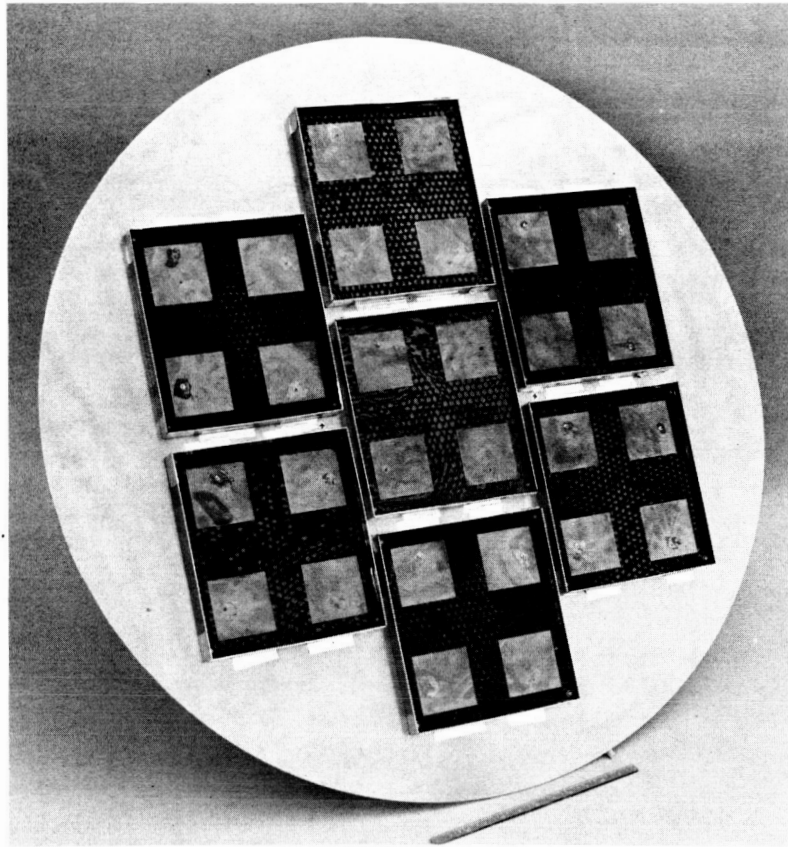


Figure 4. Constructed 7-subarray single cluster feed with 28 microstrip patches. Each subarray is enclosed by 1.0-inch tall aluminum baffles.

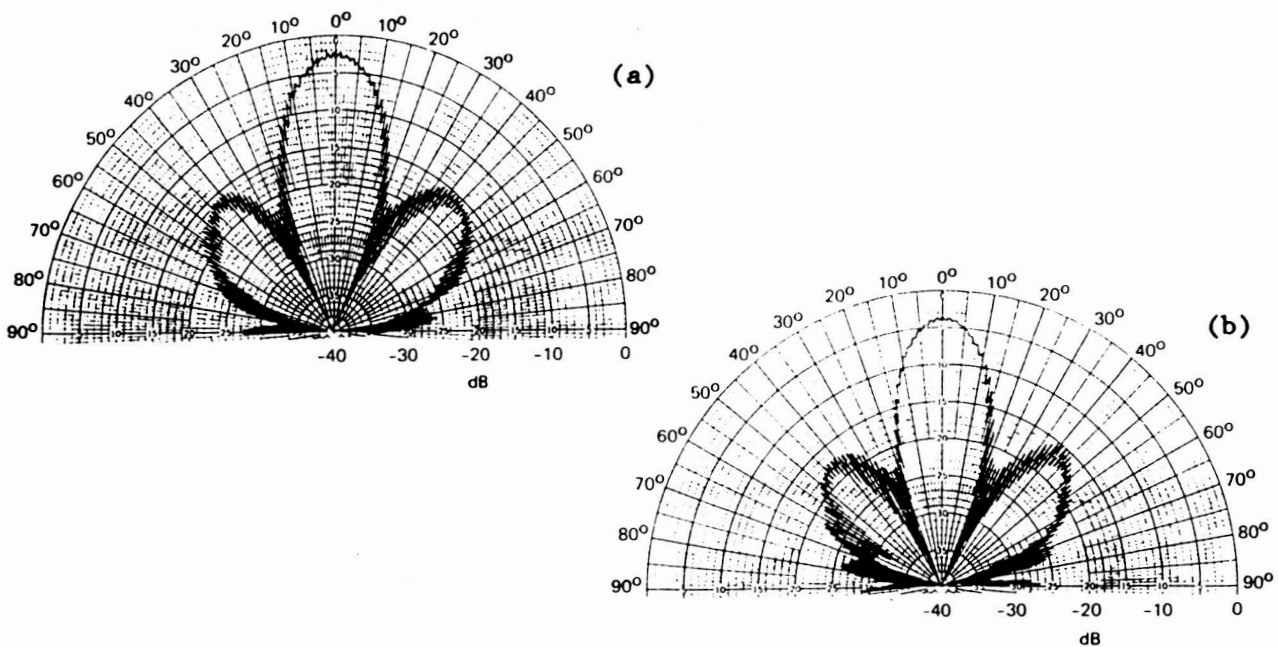


Figure 5. Measured array patterns at $\phi = 45^\circ$ plane cut for:
(a) frequency = 1.54 GHz and (b) frequency = 1.66 GHz.

TECHNOLOGIES FOR ANTENNA SHAPE AND VIBRATION CONTROL

Edward Mettler,* Robert Scheid,* Daniel Eldred*

This paper describes the application of advanced control methods and techniques to the second- and third-generation mobile satellite (MSAT) configurations having wrap-rib offset feed construction. The technologies are generically applicable to other designs such as hoop-column and other elastically deformable non-rigid structures. The focus of the discussion is on reflector shape determination and control, dynamics identification, and pointing jitter suppression.

INTRODUCTION

The static shape determination and control of the MSAT reflector as an on-orbit capability is required to provide knowledge of the shape to an accuracy of 0.3 mm, and to then control the deformations to an accuracy of 1.0 mm using rib-root actuators. The shape determination methodology involves the combination of structure deformation modeling with electro-optic sensing to estimate overall distortion. Shape control to achieve the desired radio frequency (RF) pattern quality incorporates the shape determination inputs and synthesizes the predicted control function to correct for elastic deformations that are quasi-static in nature.

The antenna dynamic control objectives include active correction of both feed and reflector boom structural dynamic motions so as to provide reflector hub-to-feed line-of-sight stability of $\leq 0.07^\circ$ (BW/10) for a 20-meter dish at 1.61 GHz. To support this control precision, a dynamics characterization of the overall structure system, based on in-situ measurements and system identification processing methods, is integrated into the control system design.

Representative control hardware is identified in Figure 1, which refers to the JPL Antenna Technology Shuttle Experiment definition effort in 1986. That study provided examples of control methods that have a general utility for MSAT-X spacecraft concepts of the 20- to 64-meter diameter reflector class. The following sections provide an overview of selected techniques for static and dynamic antenna control.

*Member of Technical Staff, Jet Propulsion Laboratory, California Institute of Technology, Pasadena, California 91109.

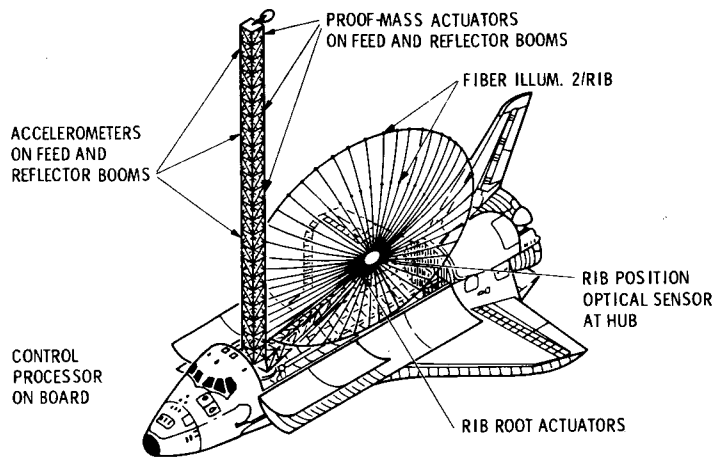


Fig. 1. Antenna Control Hardware

STATIC SHAPE DETERMINATION AND CONTROL

Many important applications in the shape control of large flexible space structures can be analyzed as static distributed systems. In this context one can include applications where the time-varying effects of the model are changing slowly with respect to the scale on which control operations must be carried out. These quasi-static disturbances may include gravity gradient, aerodynamic, and thermal effects, and the control system may be designed to carry out a local temporal averaging of the resulting quasi-static effects.

The introduction of statistical model errors allows the treatment of effects that have been ignored in the modeling or that occur on too fine a scale to be adequately modeled. As a result, the observational data can be statistically referenced to a plant, and the shape estimates can be addressed in the framework that includes modeling errors and observational errors. This makes it possible to use a variety of models and sensing/actuation systems. These may range from coarse geometric models that characterize overall features to fine-scale structural models that can resolve local features. The fine-scale models we consider are represented by stiffness matrices or elliptic partial differential equations.

Our particular interest concerns the proposed large space antennas where requirements in communications and radiometry call for antenna diameters in the tens of meters and a global root mean square (RMS) surface error of $\lambda/60$, and require on-line shape determination/control after deployment and periodically during operations.

Algorithm Descriptions

In this section, the static shape determination and control algorithms are summarized. This approach, depicted in Figure 2, is an integrated methodology that combines the techniques of modeling, optical sensing, and estimation for static control of distributed systems that are characterized by infinite-dimensional state and parameters spaces. A more complete discussion is given in [1].

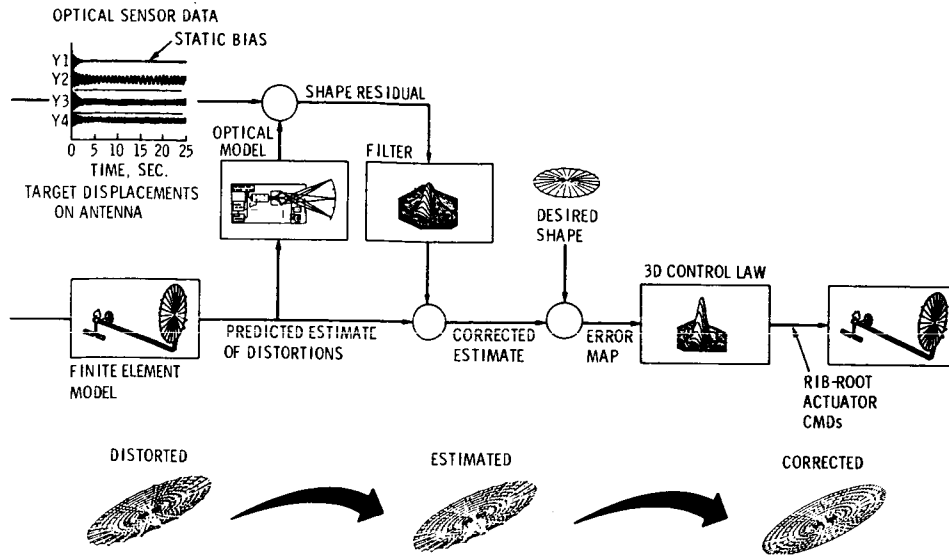


Fig. 2. Integrated On-Orbit Shape Determination and Control

Modeling. Let the state variable be given by u . The models considered have the general form

$$A(\theta)u(\theta) = B(\theta)\omega + C(\theta)f \quad (1)$$

$$Y(\theta) = H(\theta)u(\theta) + F(\theta)\eta. \quad (2)$$

Here A is an operator that represents the system model. Detailed resolutions are obtained by taking A to be a stiffness matrix. This can be idealized by assuming A to be a self-adjoint elliptic differential operator defined over some spatial domain and to be invertible with inverse ϕ . H is an operator that characterizes the state-to-observation map, and C is an operator that models the relevant deterministic forces including controls. It is assumed that the observation space has dimension N_s , which corresponds to a finite-dimensional sensing scheme, and that the control space has dimension N_a , which corresponds to a finite-dimensional actuation system. The appropriately dimensioned operators $B(\theta)$ and $F(\theta)$ model the statistical influence of the process error ω and the measurement error η_s , which are treated as normalized spatial white noise. The limiting cases $B \rightarrow 0$ and $F \rightarrow 0$ represent the assumptions of perfect modeling and perfect measurements, respectively. The integrated form of the observation equation is given by

$$Y(\theta) = H(\theta)\phi(\theta)C(\theta)f + H(\theta)\phi(\theta)B(\theta)\omega + F(\theta)\eta. \quad (3)$$

Estimation. The preceding assumptions lead to a framework for the analysis of minimum variance estimators of the state. Here the expected observation m is characterized by

$$m = H\phi C f \quad E[y] = m \quad E[(y-m)(y-m)^*] = R_\omega + R_\eta \quad (4)$$

and uv^* denotes the outer product, and u^*v denotes the inner product. The process, measurement, and estimator covariances R_ω , R_η and P are given by

$$R_{\omega} = \Phi B B^* \Phi^* \quad R_{\eta} = F F^* \quad P = R_{\omega} - R_{\omega} H^* (R_{\eta} + H R_{\omega} H^*)^{-1} H R_{\omega}. \quad (5)$$

The resulting formulas are analogous to what is typically derived for finite-dimensional systems. The estimate u_{est} has the form

$$u_{est} = C f + G(y-m) \quad g = R H^* (R_{\eta} + H R_{\omega} H^*)^{-1}. \quad (6)$$

Control. After the estimation problem has been solved, it is then possible to consider the associated control problem

$$\min_{f_c} \|u_o - \Phi C f_c\|^2 + \|f_c\|^2 \quad u_o = u_d - u_{est}. \quad (7)$$

Here u_o is the correction from the accepted shape estimate u_{est} to the desired shape u_d . And f_c is the control force that is constrained to be in a set which corresponds to the limits of the actuation system. The solution of this problem is given by

$$f_c = (I + C^* \Phi^* \Phi C)^{-1} C^* \Phi^* u_o. \quad (8)$$

DYNAMICS IDENTIFICATION AND CONTROL

Identification

In order to support the dynamic control methodology, an accurate structural model is required. Accordingly, a multifaceted approach to identification and control is developed as shown in Figure 3. The structural survey response to thruster firing is analyzed first using Fourier methods to establish the integrity of the system and the existence of the major bending groups, and to establish bounds on their frequencies and damping ratios. These results are used to develop an input sequence for high-precision parametric identification, which maximizes the model information returned by the sensors. For excitation, proof-mass actuators (PMAs) are used. Sensing consists of accelerometers distributed about the antenna and support structures in sufficient numbers to provide adequate observability of the major dynamic modes (Figure 1). Processing methods, including recursive least squares, maximum likelihood estimation, prediction error, and other methods in the time domain are used to derive final parameter values.

Jitter Control

The objective of hub-to-feed line-of-sight jitter control is to correct for static and dynamic motions that adversely affect RF pattern precision. Static errors (those that occur very slowly) are caused by mechanical bias errors and thermal loading. Dynamic motion is primarily caused by spacecraft thruster firing and/or control moment gyro (CMG) induced vibration. For vibration suppression, three methodologies are considered (Figure 4). The simplest strategy is to use proportional rate plus position feedback in the PMAs (Figure 4a). This results in moderate performance but the robust behavior of the control system. For increased performance and higher bandwidth vibration suppression, the linear quadratic Gaussian (LQG) methodology is used to suppress jitter in

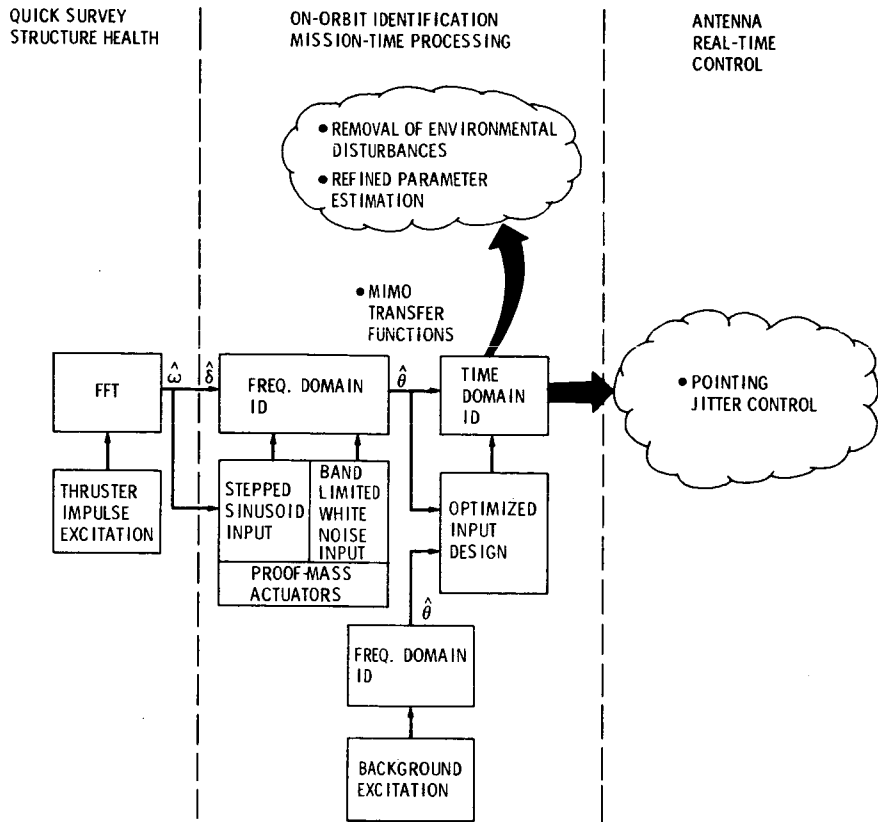


Fig. 3. Dynamics Identification Strategy

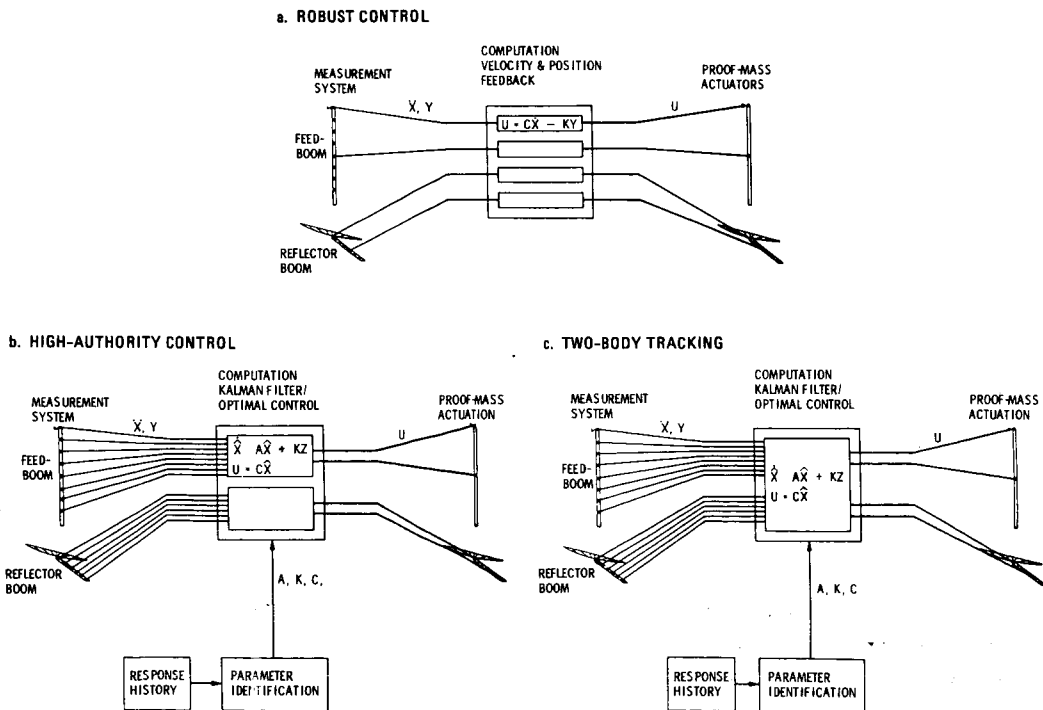


Fig. 4. Antenna Vibration and Pointing Jitter Control

each of the major structural components independently (Figure 4b), while for highest precision the RF performance measure is maximized directly as the control objective, again using LQG methodology (Figure 4c). Simulation studies demonstrate that pointing jitter can be dramatically suppressed by employing these control strategies.

CONCLUSIONS

This paper has highlighted the significant role to be performed by using integrated sensing, control, and actuation technologies for the MSAT space segment. Advanced methodologies in on-orbit system identification, shape estimation, and distributed control are ready to be applied to the next generation of systems.²⁻⁶ These key control technologies are seen to be basic to the attainment and on-orbit maintenance of the high-precision mobile satellite communications that is the goal of the MSAT-X initiative.

ACKNOWLEDGEMENT

The research described in this paper was performed by the Jet Propulsion Laboratory, California Institute of Technology, under contract with the National Aeronautics and Space Administration.

REFERENCES

1. R. Scheid, G. Rodriguez, "An Integrated Approach to Modeling, Identification, Estimation and Control for Static Distributed Systems," Fourth IFAC Symposium on Control of Distributed Parameter Systems, Los Angeles, California, June 1987.
2. D.S. Bayard, F.Y. Hadaegh, and D.R. Meldrum, "Optimal Experiment Design for On-Orbit Identification of Flexible Body Parameters in Large Space Structures," Fourth IFAC Symposium on Control of Distributed Parameter Systems, Los Angeles, California, June 1986.
3. E. Mettler and M.H. Milman, "System Identification and Modeling for Control of Flexible Structures," First NASA/DOD CSI Technology Conference, Norfolk, Virginia, November 1986.
4. D.S. Bayard, F.Y. Hadaegh, D.R. Meldrum, and E. Mettler, "On-Orbit Flexible Body Parameter Identification for Space Station," Vibration Damping 1986 Workshop II, Las Vegas, Nevada, March 5, 1986.
5. R.L. Kosut, "On-Line Identification and Control Tuning of Large Space Structures," Proc. Fifth Yale Conference on Adaptive Systems Theory, Yale University, May 1987.
6. D. Eldred and H. Vivian, "A Facility for Control Structure Interaction Technology Validation," Second NASA/DOD CSI Technology Conference, Colorado Springs, Colorado, November 17-19, 1987.

SESSION J
SPEECH COMPRESSION

SESSION CHAIR: N.S. Jayant, AT&T Bell Laboratories
SESSION ORGANIZER: Thomas Jedrey, Jet Propulsion Laboratory

SPEECH CODING AT 4800 BPS FOR MOBILE SATELLITE COMMUNICATIONS†

Allen Gersho, Wai-Yip Chan, Grant Davidson‡, Juin-Hwey Chen‡, and Mei Yong

Communications Research Laboratory
Department of Electrical & Computer Engineering
University of California, Santa Barbara, CA 93106

ABSTRACT

At UCSB, a speech compression project has recently been completed for the NASA Mobile Satellite Experiment (MSAT-X) to develop a speech coding algorithm suitable for operation in a mobile satellite environment aimed at providing telephone quality natural speech at 4.8 kbps. The work has resulted in two alternative techniques which achieve reasonably good communications quality at 4.8 kbps while tolerating vehicle noise and rather severe channel impairments. The algorithms are embodied in a compact self-contained prototype consisting of 2 AT&T 32-bit floating-point DSP32 digital signal processors (DSP). A Motorola 68HC11 microcomputer chip serves as the board controller and interface handler. On a wirewrapped card, the prototype's circuit footprint amounts to only 200 sq cm, and consumes about 9 watts of power.

1. Introduction

At the University of California at Santa Barbara (UCSB), we have completed a three year project for the NASA Mobile Satellite Experiment (MSAT-X) managed by the Jet Propulsion Laboratory (JPL). The objective of the project is the exploration of novel speech compression algorithms, culminating in a prototype voice codec that delivers "near-toll" quality speech at a data rate of 4800 bps and is suitable for use in MSAT-X field trials. An additional goal is to exhibit the potential for low fabrication cost, and low space and power consumption. Resulting from this work are two coding algorithms, VAPC (Vector Adaptive Predictive Coding) [1] and PVXC (Pulse Vector Excitation Coding) [2], with complexity in terms of simulation Flops count of 3.5 and 1.5 MFlops respectively, where one Flops stands for one floating-point multiply-and-add per second and a hardware prototype that implements both algorithms. At this stage, the prototypes (Fig. 1) are slated to enter field trials in the summer of 1988. We believe that, coupled with up-to-date product engineering, the prototype can be readily transformed into a cost effective voice coding component for mobile satellite terminals.

2. System Overview

2.1. Algorithm Review

The theme of our algorithm development was the extensive use of vector quantization (VQ), a powerful generic technique for efficient coding of sets of parameters that characterize attributes of a speech sound. With VQ, a relatively short binary word is often sufficient for accurately specifying the amplitude of a large number of parameter values or waveform samples needed for reproducing speech sounds at the receiver. The two algorithms we have developed evolved from two different approaches. VAPC stems from a vector quantized and

† This work was performed for the Jet Propulsion Laboratory, California Institute of Technology, sponsored by the National Aeronautics and Space Administration.

‡ G. Davidson is currently with Dolby Laboratories. J.-H. Chen is currently with Codex Corporation.

frame-adaptive extension of DPCM and PVXC from excitation coding techniques, such as Multipulse LPC and Code Excited Linear Prediction (CELP). In VAPC, a frame of speech samples is analyzed to determine the pitch, pitch predictor, LPC predictor, and gain. The speech frame is partitioned into vectors, from each of which the pitch prediction is removed. Then a frame-specific *zero-state-response* (ZSR) codebook is synthesized from a chain consisting of a gain-normalized residual codebook, the quantized gain and LPC predictor, plus a perceptual weighting filter derived from the quantized predictor. By searching for the best matching codevectors in the ZSR codebook, the prediction residual of the frame is efficiently vector-quantized. At the decoder, coding noise in the resynthesized speech is suppressed by an adaptive postfilter that includes compensation for spectral tilt.

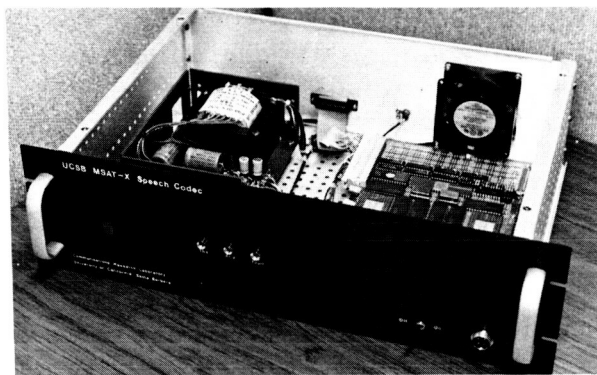


Figure 1. Codec Prototype

The analysis-by-synthesis model of PVXC consists of a codebook of excitations, a gain scaling operation, pitch and short-term LPC inverse filters, and a perceptual weighting filter, in that order. Quantized prediction parameters are employed in both synthesis filters, whereas unquantized LPC coefficients are used to obtain the parameters of the perceptual weighting filter. Per-frame short-term LPC analysis is performed prior to pitch extraction and long-term prediction coefficient computation. The excitation codebook driving the synthesis chain contains sparse pulse-excitation vectors, for each of which a quantity related to the energy of its synthetic speech vector is precomputed in every frame period. A separate gain parameter is associated with each best-matching (in the synthetic speech space) excitation vector selected from the codebook. In the decoder, a postfilter adapted by the received short-term LPC parameters enhances the decoded speech.

Both algorithms encode telephony bandwidth speech sampled at 8 KHz. Speech is analyzed without frame overlap at 20 ms and 22.5 ms intervals, respectively for PVXC and VAPC; the corresponding data frame sizes are 96 and 108 bits. Both algorithms employ VQ to code the residual or excitation signals. The vector dimension for VAPC is 20 samples, or 2.5 ms, and is 40 samples or 5 ms for PVXC. The LPC quantization schemes for both coders are quite similar, although the quantization tables and bit allocations differ. Ten LPC prediction coefficients are converted to Line Spectral Pair (LSP) parameters, processed by Switched-Adaptive Interframe Vector Prediction (SIVP) [2], and then scalar quantized. VQ is also applied to quantizing the 3rd order pitch predictor in each algorithm. The remaining parameters are scalar quantized: pitch; and gains, one for each frame in VAPC and each vector in PVXC. The VQ codebooks are trained from a multiple-speaker speech database. Unstructured, the codebooks can be partitioned among parallel processing element to achieve higher throughput. Decoder processing is relatively non-intensive, with VQ table lookups replacing the intensive VQ searches in the encoder, and includes such communication tasks as frame

alignment and error control.

2.2. Channel and Operation Conditions

In the mobile environment, we are confronted with rather severe conditions at the acoustic frontend and in the transmission channel. The background noise in a roaming mobile could be very loud, nonstationary, and have periodic components. Simulation and implementation-based tests have confirmed that, in the presence of additive noise, the two schemes have the robustness of higher bit-rate waveform coders[3] but not the serious degradations characteristic of low-rate vocoders. JPL simulation studies found an average bit-error rate of 10^{-3} in the MSAT-X channel and, in spite of the countering effect of extensive interleaving in the modem, the errors are predominately bursty due to fading. In listening tests using error patterns derived from an MSAT-X channel simulator, significantly audible clicks were noticed only occasionally in the absence of error protection. Maintenance of frame synchronization is however critical to the overall voice quality, so part of the 4800 bps capacity must be devoted to framing. A one way end-to-end coding delay objective of 50 ms. for the codec (for an error-free, zero-delay channel) is a small fraction of the overall transmission delay of the MSAT-X channel which can include two satellite-hops of delay and other delays in the modem and the network center. Due to additional buffering for channel errors and data management, the delay in our current implementation is slightly higher, approximately 60 ms. Coding delay is minimized by transmitting coder data as close as possible to the order in which they are generated.

In a complete MSAT-X Voice/Data Terminal, the speech codec is located between a handset and the JPL *Terminal Processor* (TP) driving the modem looking into the network. The only dialing function that the codec is responsible for is hook switch monitoring; an "off-hook" signal activates the coder. Voice data is transferred synchronously at 4800 bps to the TP; the data clock originates from the same source as the local sampling clock. From the TP, the codec receives Receive voice data (clocked independently of the Transmit stream), reception condition information, and all the Transmit and Receive clocks. Frame timing, though transparent to the transport network, is indicated to the TP so that it can enforce frame alignment.

2.3. Framing and Error Control

The low channel bandwidth limits the number of bits available for link maintenance. We have therefore chosen to realize only 4 overhead bits/frame (or 200 bps), one framing bit and 3 error control bits. The number of framing bits needed per frame is determined by the required reframing time, which is usually desired to be inversely related to the fading dropout rate of the channel. For random bit patterns and an error-free channel, the mean reframing times using 1 framing bit is about 200 ms, assuming a false locking probability of 10^{-3} . To prevent false locking onto imitative patterns in the data stream, and to simplify the frame-tracking firmware, we have opted to use the simple periodic framing pattern 1010... In acquisition mode, a frame-size register that keeps track of the surviving framing-bit candidates is logical-ANDed with the exclusive-OR of consecutive frame-size blocks of Receive data; this is equivalent to correlation matching with 1 correlation memory bit per data bit. Since loss of frame synchronization occurs rarely, and since the preponderant burst errors tend to garble some sync bits whenever they occur, out-of-frame condition is not declared unless either a predetermined number of pattern violations in a window of frames occurs, or the modem has been asserting channel fade condition for more than a specific timeout period. During fades, the frame clock is flywheeled.

During frame synchronized epoches, some form of error control is desirable. With only 3 bits allocated for this purpose, we could only cater to the most critical need: detection of

burst error. By using each bit to check the parity of every other 3 bits in a frame, the probability of missing a block error is reduced to one-eighth. Though this is hardly a small number, our coders are quite resilient to hits even with no error control. When the parity bits do not check, a previous frame is repeated if the number of consecutive prior repetitions is below a threshold; otherwise silence is filled in. An ongoing effort in our laboratory is studying an efficient countermeasure for VQ based coders against channel errors, that reduces the degradation in speech quality without sacrificing channel bits: a generalized Gray coding technique for assigning binary indices to codevectors and codebook design accounting for channel errors[3, 4].

3. Hardware

3.1. The Signal Processor

We elected to use the commercially available AT&T-DSP32 DSP [5] primarily because of its 32-bit floating point arithmetic. This feature eliminates the need for scaling and double precision arithmetic and substantially reduces the software development time. The C-like constructs of the DSP32 assembly language also facilitated programming immensely, though this was somewhat offset by semantic constraints imposed by non-transparent pipeline latency effects. It is difficult for the DSP32 to serve additionally as a codec controller because the chip is limited in I/O support and booting from slower EPROMs is complicated by the lack of wait state generation. The instruction cycle time of the DSP32 chips used in our codec is 160 ns (6.25 MFlops).

3.2. Circuit Board

To ease development effort and to facilitate experimentation with high performance versions, our initial prototype was designed for 3 DSPs [6]. Recent studies have shown that the codec can be adapted to handle bit rates ranging as high as 16 kbps and performance improves smoothly with the bit rate. In the sequel, we will describe only the final version of our prototype, which has only two DSPs and has enough processing power to handle all bit rates of interest.

Although a single DSP possesses almost enough power to handle both encoding and decoding in real time at 4800 bps, to minimize coding delay and to facilitate the handling of the 2 asynchronous voice streams, it is desirable to run the coder and decoder on separate processors. The board was designed with sufficient built-in flexibility for servicing the voice and TP interfaces. Only the RAM chips and master clock oscillator need to be changed to accommodate faster processor chips.

Each DSP (Fig. 2) can access 8K words (32K bytes) of dedicated external RAM, plus 1K words of on-chip refreshed RAM. The DSPs' serial ports are connected to an AT&T high precision codec/filter chip and their parallel ports to the 68HC11 controller. Data transfer between DSP memories and I/O ports is via DMA. The encoder/decoder DSP receives/transmits 15-bit PCM samples from/to the codec chip. The codec chip is not unlike ordinary mu-law codec chips except that the dynamic range and SNR have been improved to 80 dB and 60 dB respectively. The chip is driven by a 2.048 MHz clock provided by the modem's modulator and this clock also is the source of the 4.8 kHz Transmit data clock. The 2.048 MHz clock is divided down to 8 kHz for A/D and D/A sampling and for codec-chip/DSP data transfer. Because the Transmit and Receive data clocks are asynchronous, the decoder has to compensate for clock frequency offset between the remote and local clocks by monitoring its incoming data buffer and D/A speech buffer for sample dropping or insertion; the absolute stability of the oscillator limits this drift to less than 1 Hz. This simple scheme allows the use of a single codec/filter

chip to perform the A/D and D/A conversion. The analog side of the codec/filter chip is connected to simple analog circuitry for side-tone and signaling tone insertion and for interfacing to a Shure handset which has low sensitivity to breath noise.

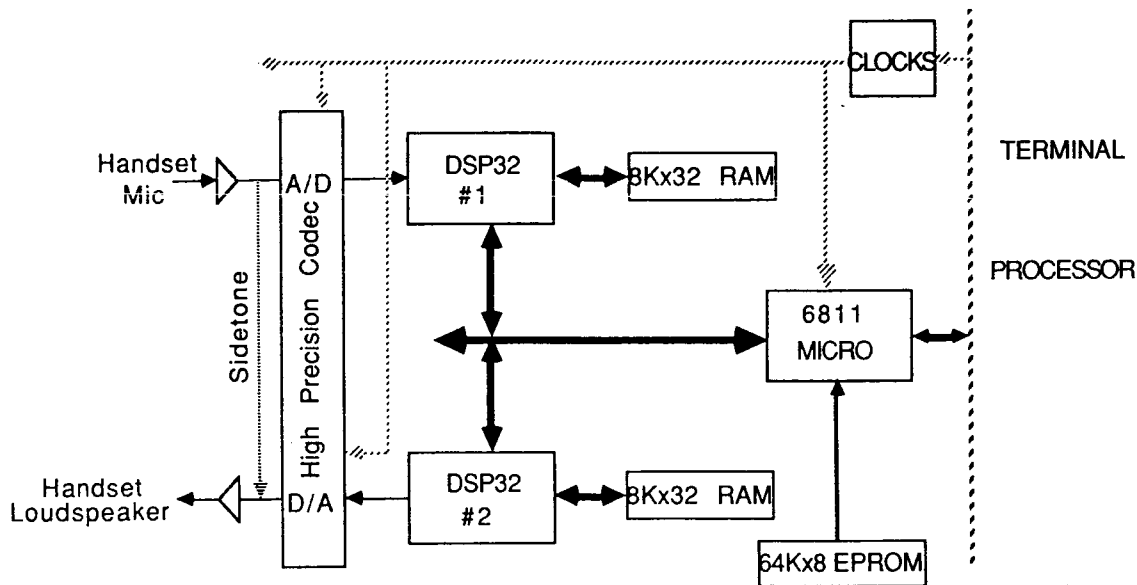


Figure 2. Prototype Board Block Diagram

The parallel ports of the DSPs are connected to an 8-bit bus mastered by a Motorola 68HC11 microcomputer chip, basically a 0.5 Mips engine. On power up, the micro copies DSP code from a 64Kx8 EPROM into the RAMs of the DSPs. Rudimentary system integrity is verified through check-summing the EPROM and comparing downloaded programs with EPROM content. With the aid of several glue chips, including PALs, the micro orchestrates the operation of the entire codec: full-duplex data transfer management across the TP Interface and the DSP/controller interfaces as well as hook monitoring. The controller can handle a real-time load up to at least 16 kbps. The health of the DSPs is monitored during run time by enabling interrupts caused by the detection of instruction parity error and data address alignment error.

The prototype codec circuitry consumes about 200 cm^2 of space and 9 watts of power on a wirewrap card. A single-DSP implementation on a printed circuit board would shrink the space and power consumption by 40%. Manufacturing cost for such a card would only be a few hundred dollars. Owing to the high precision codec and premium quality handset, the speech quality in PCM-loopback configuration is considerably better than typical digital sets.

4. Firmware

When a breakdown of the time and storage utilization of the encoder processor was examined, it became apparent that VQ precomputation and codebook searching are the dominant activities, consuming more than 60% of DSP execution time and 50% of storage space. In contrast, LPC analysis, a significant task for DSPs not so long ago, consumes only a few percent of processor time. Even SIVP quantization of the spectral envelopes requires twice as much time as LPC analysis. The dominant data structure in VAPC is its residual codebook, which holds 128 vectors, each consisting of 20 mu-law coded samples. The PVXC codebook is considerably simpler since the 256 40-dimensional vectors have only on the average 4 pulses per vector; each pulse is coded by a mu-law amplitude and a position byte.

The final processor flop counts are 3.3 times and 1.8 times the algorithmic (implementation independent) flop counts of PVXC and VAPC, respectively; these numbers give a measure of matching between the algorithms and the DSP architecture.

5. Conclusion

The real-time prototype was a necessity for verifying and fine-tuning algorithm performance in the laboratory as well as providing a resource for MSAT-X field trials. It enabled observation of such performance characteristics as degree of speaker dependence, effects of acoustical noise and background speakers, and channel originated degradations. We have, for instance, noticed a mild degree of quality variation across speakers and genders. We have also verified that extraneous signals do not cause the speech coding to breakdown as is typical of low rate vocoders.

We have described a real-time realization of two 4800 bps voice coding algorithms that exhibits cost-effective product prospect. The voice quality is quite good for the 4.8 kbps bit rate, though more effort is needed to assess the level of user acceptance amidst the selected pool of potential MSAT users. In the immediate future, we will be able to acquire performance data under realistic transmission scenarios.

Though developed for MSAT-X, the algorithms are suitable for other 4.8 kbs applications where "communication quality" is acceptable. Furthermore, substantially improved quality is attainable as the bit rate is increased and we see a strong potential for application of both algorithms for other telecommunications applications at bit-rates of 8, 9.6, and 16 kbps.

In summary, the prototype offers a reasonably satisfactory, natural voice quality and demonstrates that a compact low cost implementation of the codec is feasible with current technology.

ACKNOWLEDGMENT

UCSB graduate students who have contributed at various stages to this work are Mark Grosen, Vijaykumar Narayanan, Shihua Wang, Jae-Hsin Yao, Mei Yong, and Kenneth Zeger. We also direct our gratitude to NASA and JPL for their sponsorship of this project. We acknowledge the substantial support and cooperation of many JPL engineers and managers, and in particular, Steve Townes (currently with MITRE), William Rafferty, and Thomas Jedrey, who have served as technical liaisons with UCSB.

References

1. J.H. Chen and A. Gersho, "Real-Time Vector APC Speech Coding at 4800 bps with Adaptive Postfiltering," *Proc. ICASSP*, p. 51.3, April 1987.
2. G. Davidson, M. Yong, and A. Gersho, "Real-Time Vector Excitation Coding of Speech at 4800 bps," *Proc. ICASSP*, p. 51.4, April 1987.
3. J.H. Chen, G. Davidson, A. Gersho, and K. Zeger, "Speech Coding for the Mobile Satellite Experiment," *Proc. ICC*, June 1987.
4. K.A. Zeger and A. Gersho, "Zero Redundancy Channel Coding in Vector Quantisation," *Electronics Letter*, p. 654, May 7, 1987.
5. "WE DSP32 Digital Signal Processor Information Manual," *ATT*, June 1986.
6. W.Y. Chan, G. Davidson, J.H. Chen, and A. Gersho, "A Prototype 4800 bps Voice Terminal for the Mobile Satellite Experiment," *Proc. GLOBECOM*, Nov. 1987.

A 4.8 KBPS CODE EXCITED LINEAR PREDICTIVE CODER

THOMAS E. TREMAIN, JOSEPH P. CAMPBELL, JR., VANOY C. WELCH

U.S. Department of Defense, R5
Fort Meade, Maryland, U.S.A. 20755-6000

Abstract

In 1984, the Department of Defense established a program under the direction of the National Security Agency (NSA) to develop a secure voice system (STU-III) capable of providing end-to-end secure voice communications to all segments of the Federal Government, Federal Government contractors, and citizens of the United States. Based on the work performed by the Digital Voice Processor Consortium, NSA determined that the terminal for the new system should be built around the DoD Standard LPC-10 voice processor algorithm.

While the performance of the present STU-III as a processor of speech is considered to be good, its response to nonspeech sounds, such as whistles, coughs and impulse-like noises, may not be completely acceptable. Speech in noisy environments also causes problems with the LPC-10 voice algorithm. In addition, there is always a demand for something better. We hope to complement LPC-10's 2.4 kbps voice performance with a very high quality speech coder operating at a higher data rate. This new coder is one of a number of candidate algorithms being considered for an upgraded version of the STU-III in late 1989. In this paper, we address the problems of designing a code excited linear predictive (CELP) coder to provide very high quality speech at a 4.8 kbps data rate that can be implemented on today's hardware.

1 INTRODUCTION

Speech coding algorithms that achieve high quality speech at high data rates are well known (i.e., 64 kbps PCM, 32 kbps ADPCM and 16 kbps APC). However, high quality speech coding at lower data rates has been achieved only very recently. Codebook excited linear prediction (CELP) was introduced by B.S. Atal and M.A. Schroeder at the 1984 International Communications Conference [1]. The introduction of CELP sparked one of the speech coding community's greatest research efforts to achieve high quality speech at 4.8 kbps within reasonable computational complexity.

In this paper, we present a detailed description of our CELP coder, various tradeoffs to obtain a 4.8 kbps data rate, and computational complexity reduction methods to allow practical implementation of our coder using a pair of new generation digital signal processor (DSP) chips.

2 CELP DESCRIPTION

Our CELP decoder is shown in Figure 1. The parameters required for this model are the codebook index and gain, the pitch index and gain, and the short-term predictor parameters. To further

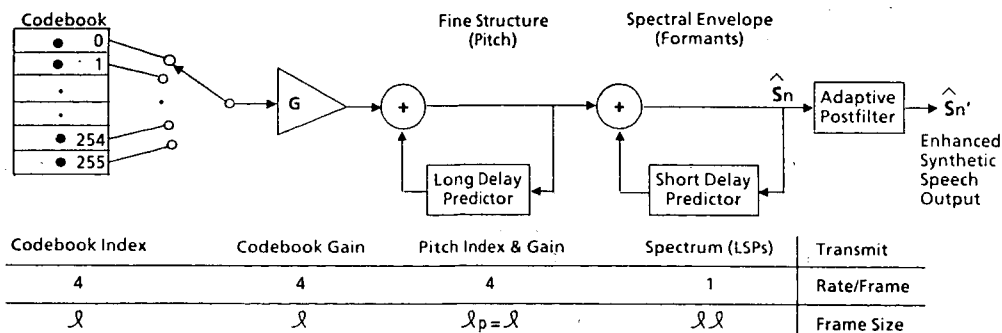


Figure 1: CELP decoder.

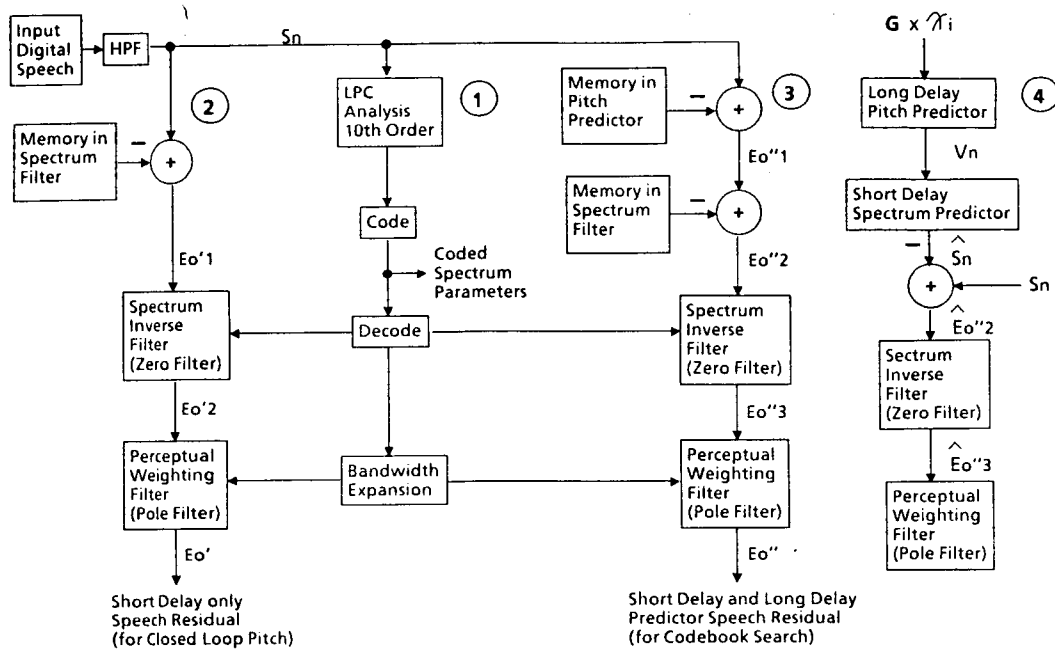


Figure 2: CELP encoder.

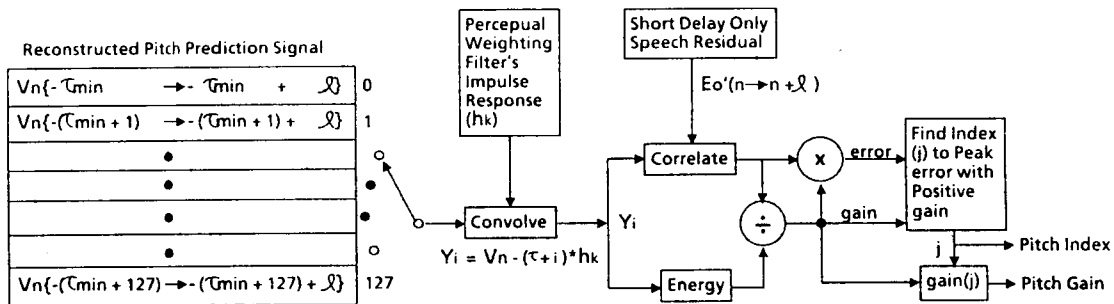


Figure 3: Closed loop pitch calculation.

reduce the quantizing noise at the expense of negligible computation, we added a postfilter based on the pole-zero filter described in reference [2] with adaptive spectral tilt compensation.

As labeled in Figure 2, the CELP encoder consists of four parts: 1) The short-term predictor (spectrum) parameters are calculated in an open loop format; 2) The pitch index and gain are calculated on a spectrum-only residual signal in a closed loop format on a subframe basis relative to the spectrum parameters; 3) The codebook index and gain are calculated on a spectrum and pitch residual signal in a closed loop format on a subframe basis relative to the spectrum parameters; 4) The decoder is run in the transmitter to update all the filter states, which are then used to calculate the next frame of speech in the closed loop format.

Figure 3 shows the closed loop pitch calculation using the filtering approach. The reconstructed pitch prediction signal, V_n , is convolved with the perceptual weighting filter's impulse response. The convolution is calculated for each of the 128 pitch lags, which vary from a minimum (τ_{min}) of 16 to a maximum of 143. For this convolution, there is only one impulse response in the convolution interval. Each pitch lag's convolution is then correlated with the short-delay (spectrum only) predictor's speech residual. The optimum pitch lag for a 1-tap predictor maximizes the error function and has positive gain. Since the pitch predictor is calculated over 128 lags, a brute force calculation requires 33 million instructions (multiplies and adds) per second (33 MIPS). However, as shown in Section 4, the number of instructions can be significantly reduced.

The codebook search using the filtering approach is given in Figure 4. The codebook is convolved

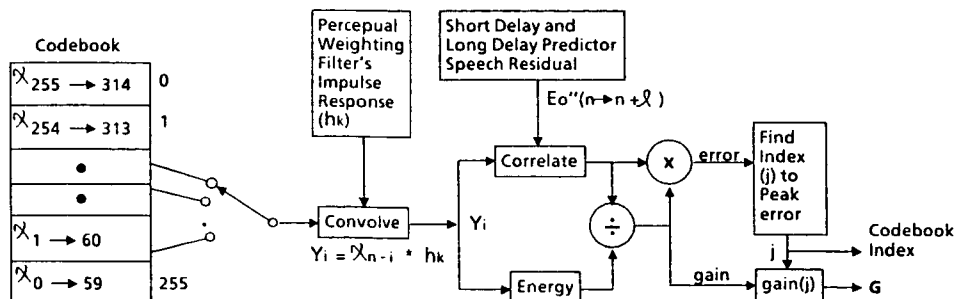


Figure 4: Codebook search.

Table 1: Options studied for a 4.8 kbps CELP coder.

Option	1	2	3	4	5	6
Spectrum Frame	20 msec	20 msec	22.5 msec	25 msec	25 msec	30 msec
Samples @8 kHz	160	160	180	200	200	240
Bits @4.8 kbps	96	96	108	120	120	144
Spectrum (LSPs)	36	36	36	36	36	36
Pitch Index	$2 * 7 = 14$	$2 * 7 = 14$	$2 * 7 = 14$	$4 * 7 = 28$	$2 * 7 = 14$	$4 * 7 = 28$
Pitch Gain	$2 * 3 = 6$	$2 * 3 = 6$	$2 * 4 = 8$	$4 * 4 = 16$	$2 * 4 = 8$	$4 * 5 = 20$
Codebook Index	$2 * 14 = 28$	$4 * 5 = 20$	$4 * 6 = 24$	$4 * 5 = 20$	$4 * 8 = 32$	$4 * 8 = 32$
Codebook Gain	$2 * 6 = 12$	$4 * 5 = 20$	$4 * 6 = 24$	$4 * 5 = 20$	$4 * 6 = 24$	$4 * 6 = 24$
Bits Used	96	96	106	120	114	140

with the perceptual weighting filter's impulse response. The convolution is calculated for each of the 256 codewords. For this convolution, there can be several impulse responses in the convolution interval as determined by the pitch index. Each codeword convolution is then correlated with the speech residual from the short-delay (spectrum) predictor and long-delay (pitch) predictor. The optimum codeword maximizes the error function for the codebook. For a 256 codeword codebook, a brute force calculation requires 66 MIPS. However, as shown in Section 4, the number of instructions can be significantly reduced.

3 CODING AND COMPLEXITY ESTIMATES

Option 1 in Table 1 is a coding scheme presented by Bell Labs in reference [3]. This approach was not studied because it is too computationally complex. As shown in Table 2, it requires more than 5 billion multiplies and adds per second (5 GIPS) using brute force calculations. Options 2 and 3 are more practical from the implementation point of view; however, the output speech is very rough because of the small codebook size and the pitch is not updated at the same rate as the codebook. Option 4 provides better speech quality than 2 or 3 because the pitch is updated at the same rate as the codebook. However, the speech is still rough because of the small codebook. Option 5 has an acceptable size codebook, but the speech is rough because the pitch and codebook are updated at different rates.

We selected Option 6 because it provides the best speech quality of the options listed in Table 1 and it is practical to implement. Tables 2 and 3 show that the codebook and pitch calculations with brute force calculations require about 100 MIPS. Table 4 shows most of CELP's remaining calculations, which add up to only 1.27 MIPS.

Table 2: Computational Complexity Comparisons for Codebook Calculations.

<i>Option</i>	<i>1</i>	<i>2</i>	<i>3</i>	<i>4</i>	<i>5</i>	<i>6</i>
Convolution	3240	820	1035	1275	1275	1830
Size	*16,384	*32	*64	*32	*256	*256
Instructions	53,084,160	26,240	66,240	40,800	326,400	468,480
Correlation	32,768	64	128	64	512	512
Frame	*80	*40	*45	*50	*50	*60
Instructions	2,621,440	2560	5760	3200	25,600	30,720
Total Inst.	55,705,600	28,800	72,000	44,000	352,000	499,200
Rate	*100	*200	*177,777	*160	*160	*133.33
Total IPS	5,570,560,000	5,760,000	12,800,000	7,040,000	56,320,000	66,560,000

Table 3: Computational Complexity Comparisons for Closed Loop Pitch Calculations.

<i>Option</i>	<i>1</i>	<i>2</i>	<i>3</i>	<i>4</i>	<i>5</i>	<i>6</i>
Convolution	3240	3240	4095	1275	5050	1830
Pitch Lags	*128	*128	*128	*128	*128	*128
Instructions	414,720	414,720	524,160	163,200	646,400	234,240
Correlation	256	256	256	256	256	256
Pitch Frame	*80	*80	*90	*50	*100	*60
Instructions	20,480	20,480	23,040	12,800	25,600	15,360
Total Inst.	435,200	435,200	547,200	176,000	672,000	249,600
Pitch Rate	*100	*100	*88.88	*160	*80	*133.33
Total IPS	43,520,000	43,520,000	48,640,000	28,160,000	53,760,000	33,280,000

Table 4: Remaining calculations in CELP coder

<i>Operation</i>	<i>IPS/call</i>	<i>Times Called</i>	<i>Total IPS</i>
Zero Filter	88,000	3	264,000
Pole Filter	80,000	4	320,000
Pole Weighting Filter	81,333	5	406,667
Pitch Filter	8,000	3	24,000
Matrix Load & Invert	92,667	1	92,667
Adaptive Postfilter	162,667	1	162,667
Total IPS			1,270,000

Table 5: End-Correction Computational Complexity Reduction.

Operation	Closed Loop Pitch			Codebook		
	Brute Force	End-Correct	End-Correct 30 Impulse	Brute Force	End-Correct	End-Correct w/75% zeros
Convolve	1830	1830	1830	1830	1830	1830
	*128	+127*60	+127*30	*256	+255*60	+255*15
Instructions	234,240	9,450	5,640	468,480	17,130	5,655
Correlate	256	256	256	512	512	512
	*60	*60	*60	*60	*60	*60
Instructions	15,360	15,360	15,360	30,720	30,720	30,720
Total Inst.	249,600	24,810	21,000	499,200	47,850	36,375
Rate	*133.33	*133.33	*133.33	*133.33	*133.33	*133.33
Total IPS	33,280,000	3,308,000	2,800,000	66,560,000	6,380,000	4,850,000

4 COMPUTATION REDUCTION STUDIES

End-correction, shown in equations 1 - 3, can be applied to the closed loop pitch convolution calculation. The results are identical to the brute force convolution. As shown in Table 5, the computation is reduced by an order of magnitude from 33 to 3 MIPS. Also, a slight further reduction can be obtained by reducing the weighted impulse response from 60 to 30 samples.

$$y_{0,0} = 0 \quad (1)$$

$$y_{i,0} = \sum_{j=0}^{i-1} x_{offset+j} \cdot h_{i-j} \quad \text{where } 1 \leq i \leq \ell \quad (2)$$

$$y_{i,k} = y_{i-1,k-1} + x_{offset-k} \cdot h_i \quad \text{where } 1 \leq i \leq \ell \text{ and } 1 \leq k \leq \text{lags} \quad (3)$$

In Atal and Schroeder's original design [1], their codebook was generated from a zero-mean unit-variance white Gaussian sequence where each codeword consisted of an independent segment of this sequence. End-correction can also be applied to the codebook convolution calculation if a special form of codebook with overlapping codewords is used. In our case, each codeword contains one new sample and all but one sample of the previous codeword. When using overlapped versus independent codebooks, the difference in synthesized speech is virtually unnoticeable and the reduction in segmental signal-to-noise ratio is less than a fraction of a decibel for a 256 codeword codebook. As shown in Table 5, end-correction reduces the computation by an order of magnitude from 66 to 6 MIPS for a 256 codeword codebook. Also, a slight further reduction can be obtained by taking advantage of any zero samples in the codebook (which we center clip 75% of the samples to reduce high frequency noise).

5 IMPLEMENTATION

Implementation of our CELP coder on a pair of new generation DSP chips is very practical. The end-correction techniques we have described, when applied to the pitch and codebook calculations, yield a 10 MIPS CELP algorithm. When implementing speech coders of this type on DSP chips, typically, only one-third to one-half of the DSP chip's peak computational power can be used because of breaks in the multiply-accumulate pipeline, random logic, and control overhead. By analyzing our CELP coder's computationally intensive algorithm segments, we determined that it can be implemented on various new generation DSP chips or other processor chips (i.e., AT&T's Graph Search Machine). For example, our CELP algorithm can be implemented on a pair of AT&T's 12.5 MIPS DSP32C DSP chips or on a pair of TI's 16.6 MIPS TMS320C30 DSP chips. If slightly optimistic processor

utilization efficiency can be attained, our CELP algorithm may even fit on a pair of TI's 10 MIPS TMS320C25 DSP chips!

6 CONCLUSIONS

In this paper, we described the practical implementation of a CELP coder, we examined different bit allocations that can be used to implement a 4.8 kbps coder, and we determined the computational complexity of the coder for each bit allocation. The CELP coder we describe produces high quality speech and is practical to implement on a pair of new generation DSP chips.

The end-correction techniques applied to the codebook search and closed loop pitch calculations have each been shown to reduce the computational requirements by an order of magnitude without causing a loss in the quality of the output speech signal. We also found that the best speech quality was obtained with the parameters referred to as Option 6 in Section 3.

Our CELP coder has no problems with background noise (in fact, it is faithfully reproduced) and even works well with multiple speakers. *Informal* listening tests indicate that our CELP's speech intelligibility and quality are comparable with 16 kbps APC and 32 kbps CVSD!

We formally measure speech intelligibility and quality using Dynastat's diagnostic rhyme test (DRT) and diagnostic acceptability measure (DAM), respectively. We will report our CELP's DRT and DAM scores in the future. (As reference points, 32 kbps CVSD has a DRT score of 93.2 and a DAM score of 63 while 2.4 kbps LPC-10 has a DRT score of 90 and a DAM score of 53.)

Our future work will focus on error protection techniques and determining a 4.8 kbps standard to allow interoperability between current and future CELP coders. We expect future CELP coders to offer even better performance by exploiting the next generation's more powerful hardware.

7 ACKNOWLEDGMENTS

We are grateful to the following for their contributions: Tom Barnwell, Shawn and Elizabeth Campbell, Allen Gersho, George Kang, Dan Lin and Bell Communications Research. We thank our in-house support, especially Dave Kemp, and our in-house tools development team. We wish to give special recognition to the AT&T Bell Laboratories Acoustics Research Department, especially Bishnu Atal and Peter Kroon, for their outstanding contributions.

References

- [1] Atal, B.S. and M.R. Schroeder, "Stochastic Coding of Speech at Very Low Bit Rates," Proc. of International Communications Conference, 1984, pp. 1610-1613.
- [2] Chen, J.H. and A. Gersho, "Real-Time Vector APC Speech Coding at 4800 bps with Adaptive Postfiltering," Proc. of Int. Conf. Acoust., Speech, and Signal Process., 1987, pp. 2185-2188.
- [3] Kroon, P. and B.S. Atal, "Quantization Procedures for the Excitation in CELP Coders," Proc. of Int. Conf. Acoust., Speech, and Signal Process., 1987, pp. 1649-1652.

REAL-TIME SPEECH ENCODING BASED ON CODE-EXCITED LINEAR PREDICTION (CELP)

WILFRID P. LEBLANC, Carleton University, Canada;
S.A.MAHMOUD, Carleton University, Canada.

CARLETON UNIVERSITY
Department of Systems and Computer Engineering
Ottawa, Ontario
Canada
K1S 5B6
Tel: 1-613-564-6655, 1-613-564-2793

ABSTRACT

This paper reports on the work proceeding with regards to the development of a real-time voice codec for the terrestrial and satellite mobile radio environments. The codec is based on a complexity reduced version of CELP. The codebook search complexity has been reduced to only 0.5 MFLOPS (million floating point operations per second) while maintaining excellent speech quality. Novel methods to quantize the residual and the long and short term model filters are presented.

INTRODUCTION

Since the introduction of CELP [Schroeder 1985], there has been considerable interest in techniques to reduce its complexity, and efficient techniques to encode the long and short term model filters. In Schroeder's and Atal's classic paper, the residual was quantized at only 2 kbps, with no quantization of the remaining parameters (gain, long and short term predictor). It was believed that a high quality voice codec, based on CELP, could be realized at an aggregate rate of 4.8 kbps.

However, the computational complexity of CELP is unwieldy, which hinders the real-time implementation of such a technique. Various authors [Davidson 1986, Trancoso 1986, Chen 1987] have addressed the complexity issue and have arrived at marginally acceptable systems.

In this paper, we propose a new structure—referred to as KELP—which has a greatly reduced complexity. We also discuss novel techniques to encode the long and short term predictor parameters.

The original CELP algorithm is shown in Fig. 1, The filter $A(z)$ is referred to as the short term inverse filter and is given by [Markel 1976]

$$A(z) = 1 - \sum_{k=1}^p a_k z^{-k}$$

where p is the predictor order and the a_k 's are the predictor parameters. The long term inverse filter $B(z)$, is given by

$$B(z) = 1 - \sum_{k=-q}^q b_k z^{-(M+k)}$$

where the b_k are the long term predictor parameters and M is the pitch period. The order is large but many of the coefficients are zero. The noise weighting filter $W(z)$ is just

$$W(z) = \frac{A(z)}{A(z/\gamma)}$$

where $\gamma \approx 0.73$.

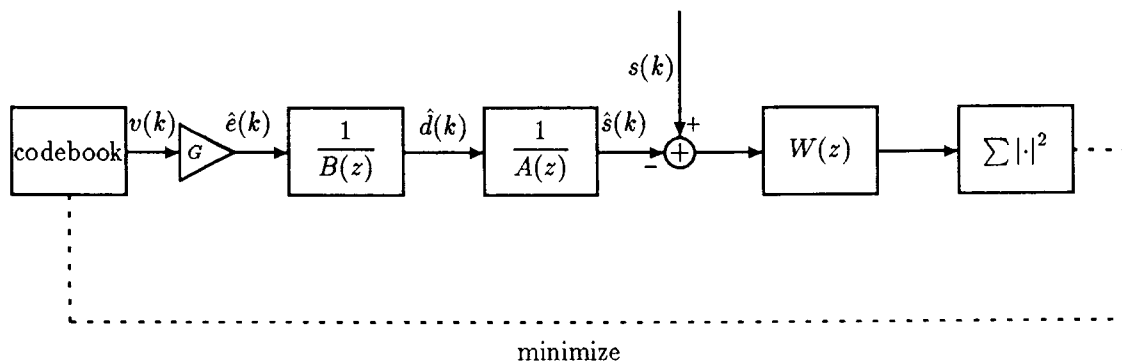


Fig. 1. The Original CELP Search Algorithm

The search complexity for the optimal excitation from the L level, K dimensional codebook is just

$$\begin{aligned} C &= LK(3p + 2q + 2)f_s/K \text{ FLOPS} \\ &\approx 300 \text{ MFLOPS} \end{aligned}$$

for $L = 2^{10}$, $K = 40$, $p = 10$, $q = 1$, and a sampling frequency (f_s) of 8 kHz.

REDUCED COMPLEXITY CELP (KELP)

In this section we introduce a technique to greatly reduce the computational complexity of the CELP algorithm while maintaining excellent speech quality.

As the first step, we move the location of $W(z)$ and separate the zero state and zero input responses of the long and weighted short term model filter ($A(z/\gamma)$). If the pitch period is greater than the vector dimension ($M > K + q$), the zero state response of $B(z)$ is unity. Thus, we may redraw the structure as shown in Fig. 2. Note that the ordering of G and $A(z/\gamma)$ is not important since we are dealing with the zero state response only.

We note that the structures of Fig. 1 and Fig. 2 are not amenable to fast search non-exhaustive algorithms. By moving the location of the codebook, and quantizing $x(k)$, a non-exhaustive (tree search) is possible. In addition, if the denominator of $W(z)$ is fixed, (as in [Kroon 1986]), no degradation would result. With a variable denominator filter, degradation will result. However, $A(z/\gamma)$ is relatively flat and contains no pitch information. Thus, quantizing $x(k)$ should be very efficient. Forcing the codebook elements to the unit circle implies that minimizing the mean squared error is equivalent to maximizing the correlation

$$G = \sum_{k=0}^{K-1} x(k)\hat{x}(k)$$

over the whole codebook. The modified search procedure is shown in Fig. 3. With the search structured in this manner, we may use a non-exhaustive tree search for the optimum excitation.

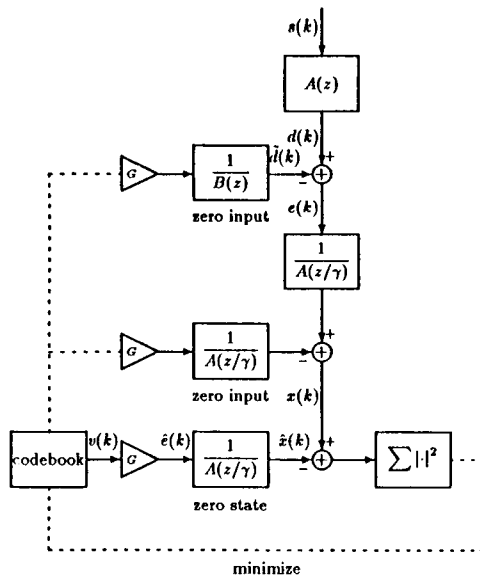


Fig. 2. CELP, Modified Search

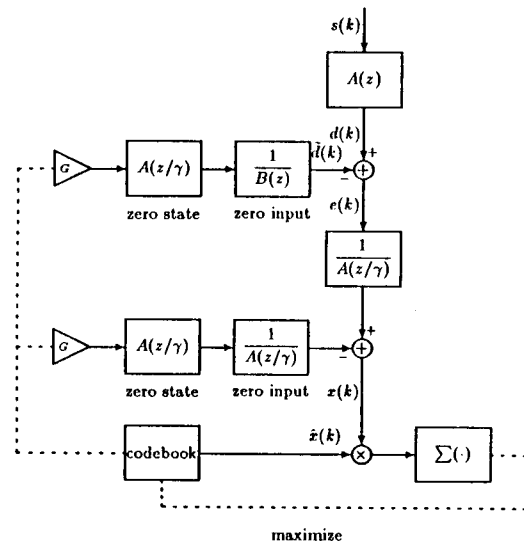


Fig. 3. KELP

The search complexity for this structure is greatly reduced. For a full search code the complexity (for the above parameters) is 8 MFLOPS. By using a binary tree search, or a 32-32 tree search [Makhoul 1985], we obtain complexities of 160 KFLOPS, and 500 KFLOPS respectively. A 32-32 tree search is a good tradeoff between computational complexity and memory requirements.

Typically the pitch predictor is optimized to minimize the open loop residual energy. However, the input to the pitch predictor contains an appreciable amount of quantization noise. By redefining the noise weighting filter we can circumvent

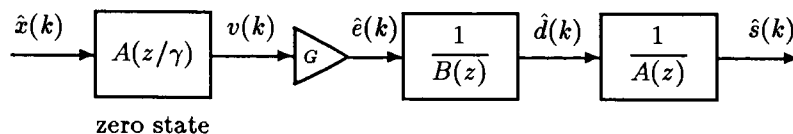


Fig. 5. The KELP Synthesis Structure

is quantized. Intermediate frames are found by linear interpolation between two adjacent frames.

The short term predictor is quantized based on the Line-Spectrum-Pairs [Kabal 1986]. Each pair is quantized in a two dimensional vector quantizer. The mean squared error was minimized during the design of the vector quantizers. Thirty-two bits were allocated for quantizing the short term predictor, with a {6,7,7,6,6} bit assignment. It was found that this assignment lead to a good perceptual quality. Furthermore, channel errors can be easily handled since the short term filter is quantized on a block by block basis with no inherent memory.

With 32 bits allocated to the short term model filter we require a bit rate of 1.6 kbps.

QUANTIZATION OF THE LONG TERM PREDICTOR

The long term predictor is optimized based on minimizing the open loop residual. It is updated every 10 msec.

The pitch predictor is chosen from a large codebook (128 levels) to minimize the open loop residual error. The codebook is designed using the Inverse Filter Matching Principle. The average residual error was minimized in the codebook design process. Thus the distortion measure is a simple matrix multiply, and the centroid calculation consists of averaging the covariance matrices in each cell [LeBlanc 1988]. The codebook elements were stabilized as discussed in [Ramachandran, 1987].

The pitch period is quantized to seven bits and is in the range (20,147). Thus, 1.4 kbps is allocated to quantizing the long term model filter.

GAIN QUANTIZATION

The gain is quantized on a log-mse scale to five bits. A Lloyd-Max scalar quantizer was used. The gain is updated every 5 msec. This leads to a rate of 1 kbps for the gain.

The resultant codec based on KELP (Fig. 4) has excellent speech quality. The total bit rate using the aforementioned quantization procedures is 6 kbps. By exploiting the intraframe memory of the various parameters, improved performance could be realized at a corresponding increase in complexity. Note, however,

that the introduction of memory would lead to a degradation in the presence of channel errors.

CONCLUSION

This paper introduced a novel method to greatly reduce the complexity of the CELP algorithm while maintaining excellent speech quality. The structure was modified into a form amenable to fast search non-exhaustive algorithms. The computational complexity has been reduced to 0.5 MFLOPS with only a very slight increase in memory requirements.

BIBLIOGRAPHY

- J.D. Markel and A.H. Gray Jr., Linear Prediction of Speech, Springer-Verlag, New York, New York, 1976.
- J. Makhoul, S. Roucos, and H. Gish, "Vector Quantization in Speech Coding," Proceedings of the IEEE, Vol. 73, No. 11, November 1985.
- M.R. Schroeder and B.S. Atal, "Code-Excited Linear Prediction (CELP): High Quality Speech at Very Low Bit Rates," IEEE International Conference on Acoustics Speech and Signal Processing, Tampa Florida, March 1985.
- I.M. Trancoso and B.S. Atal, "Efficient Procedures for Finding the Optimum Innovation in Stochastic Coders," IEEE International Conference on Acoustics Speech and Signal Processing, Tokyo Japan, 1986.
- G. Davidson and A. Gersho, "Complexity Reduction Methods for Vector Excitation Coding," IEEE International Conference on Acoustics Speech and Signal Processing, Tokyo Japan, 1986.
- P. Kroon, R.J. Sluyter, and E.F. Deprettere, "A Low Complexity Regular Pulse Coding Scheme With a Reduced Transmission Delay," IEEE International Conference on Acoustics Speech and Signal Processing, Tokyo Japan, 1986.
- J. Chen, G. Davidson, and K. Zeger, "Speech Coding for the Mobile Satellite Experiment", IEEE International Conference On Communications, Seattle, Washington, 1987.
- P. Kabal and R. Ramachandran, "The Computation of Line Spectral Frequencies Using Chebyshev Polynomials", IEEE Transactions On Acoustics Speech and Signal Processing, Vol. ASSP-34, No. 6, December 1986.
- R. Ramachandran and P. Kabal, "Stability and Performance Analysis of Pitch Filters in Speech Coders", IEEE Transactions On Acoustics Speech and Signal Processing, Vol. ASSP-35, No. 7, July 1987.
- W. LeBlanc, An Advanced Speech Coder Based on a Rate-Distortion Theory Framework, Masters Thesis, To be published, Carleton University, Ottawa, Canada, 1988.

SINUSOIDAL TRANSFORM CODING
FROM 2400 to 9600 BPS

ROBERT J. McAULAY, Massachusetts Institute of
Technology, Lincoln Laboratory, Speech Systems Technology,
USA; THOMAS F. QUATIERI, Massachusetts Institute of
Technology, Lincoln Laboratory, Speech Systems Technology,
USA.

LINCOLN LABORATORY
Massachusetts Institute of Technology
244 Wood Street
Lexington, Massachusetts 02173-0073
United States

ABSTRACT

It has been shown that an analysis/synthesis system based on a sinusoidal representation of speech leads to synthetic speech that is essentially perceptually indistinguishable from the original [McAulay/Quatieri 1986]. Strategies for coding the amplitudes, frequencies and phases of the sine waves have been developed that have led to a multirate coder operating at rates from 2400 to 9600 bps. [McAulay/Quatieri 1987,1988]. The encoded speech is highly intelligible at all rates with a uniformly improving quality as the data rate is increased. A real-time fixed-point implementation has been developed using two ADSP2100 DSP chips. In this paper the methods used for coding and quantizing the sine-wave parameters for operation at the various frame rates are described.

INTRODUCTION

An analysis/synthesis system has been developed based on a sinusoidal representation of speech. The system leads to synthetic speech that is essentially perceptually indistinguishable from the original [McAulay/Quatieri 1986], offering the potential for a high-quality speech coding system. Since the parameters of the sinusoidal model are the amplitudes, frequencies and phases of the underlying sine waves, and since for a typical low-pitched speaker there can be as many as 80 sine waves in a 4 khz speech bandwidth, it is not possible to code all of the parameters directly.

In this paper the algorithms for encoding the amplitudes, frequencies and phases will be described that allow the Sinusoidal Transform Coder (STC) to operate at rates down to 2400 bps. The notable features of the resulting class of

coders are the intelligibility and naturalness of the synthetic speech, the preservation of speaker-dependent qualities so that talkers were easily recognizable, and the robustness against background acoustic noise and channel errors.

ESTIMATION OF THE PARAMETERS OF THE UNDERLYING SINE WAVES

The method for identifying the amplitude, frequencies and phases of the underlying sine waves is to first locate the peaks of the high-resolution spectrum of a frame of input speech. The latter is computed using the short-time Fourier transform applied to a speech buffer that is $2\frac{1}{2}$ times the average pitch period. The latter constraint is essential for correctly resolving all of the sinusoidal components. Setting the window therefore requires the computation of an average pitch period, and while any good pitch extractor could be used for this purpose, the STC system uses a new pitch estimation technique that has been derived by applying statistical decision theoretic methods to the sinusoidal model. The basic principle is to determine the fundamental frequency of a harmonic set of sine waves that provides a best fit to the measured set of sine waves. Therefore, as shown in Figure 1, the first step in the STC analysis system is to perform a high-resolution spectral analysis over the 0-1000 Hz frequency region to a speech buffer that is $2\frac{1}{2}$ times the lowest anticipated pitch period (25 ms). In the current implementation, a 512-point FFT is used over the entire speech bandwidth (0-4000 Hz), but computational efficiencies could be obtained by low-pass filtering, downsampling and the using a 128-point FFT over the 1000 Hz baseband region. In addition to the pitch, a voicing measure is determined and for those estimates corresponding to strongly voiced speech a short-term average pitch is computed, which is used to set the analysis window for the second analysis stage.

SINUSOIDAL ANALYSIS AND FINE-GRAINED PITCH ESTIMATION

The second analysis stage consists of another 512-point FFT over the entire 4000 Hz speech bandwidth. The magnitude of the resulting short-time Fourier transform (STFT) is examined for peaks, and now the amplitudes, frequencies and phases corresponding to the peaks are used to define the underlying speech model. The amplitudes and frequencies over the 0-1000 Hz region are supplied to the fine-grained pitch extractor which estimates the pitch using the same principles as that in the first analysis stage. Since the notion of "pitch" has no meaning in the case of unvoiced speech, it is better to think of the procedure as one of fitting a harmonic set of sine waves to the measured set of sine waves. It is a remarkable property of the STC system that this technique is capable of replicating both the voiced and unvoiced sounds as long as means are provided for properly accounting for the associated sine-wave phases. In fact it turns out that in the STC system all of the voicing information is embedded in the sine-wave phases. Preserving that information at low data rates requires suitable phase models that are tied to the voicing measure, a measure which is determined implicitly by the fine-grained pitch estimator.

AMPLITUDE AND PHASE CODING

Once the pitch has been estimated and coded (6-7 bits for pitch, 2-3 bits for voicing depending on the rate) it is used to determine a quasi-harmonic set of frequency bins which are applied to the original sine-wave set to assign one sine-wave per bin. A piece-wise linear envelope is fitted to the resulting set of amplitudes and frequencies and a piece-wise constant envelope is fitted to the resulting set of phases. If these envelopes are sampled at the harmonics of the coded pitch then very high quality, highly intelligible synthetic speech can be generated. The goal is to try to code these harmonic samples as efficiently as possible.

The first step in coding the amplitudes is to use the coded pitch to determine the number of sine-wave amplitudes that need be coded, which in turn determines the number of bits per amplitude. For a high-pitched speaker (170 Hz), all of the sine-wave amplitudes can be coded provided differential encoding is applied to the logarithmic values of the amplitudes of the neighbouring sine waves. The exact number of bits per differential is determined by the number of bits available at a given rate and the number of sine waves to be coded at that pitch. For low-pitched speakers it is not possible to encode all of the amplitudes, since for example a 50 Hz pitch corresponds to 80 sine waves which at even 1 bit per differential would require 4000 bps. which precludes operation at rates below 4800 bps. In the case of low-pitched speakers, therefore, only a certain number of the baseband sine waves are coded but then the frequency spacing between amplitude samples is increased logarithmically to exploit the critical band properties of the ear. The overall spectral level is preserved by coding the log-amplitude of the fundamental using 5 bits to cover a 90 dB dynamic range [McAulay/Quatieri, 1987]. The coding method is therefore similar to a channel vocoder [Holmes, 1980], for which the channel locations are pitch adaptive.

For rates above 4800 bps assigning more bits to the amplitudes does not lead to significantly better quality. At these rates it is better to begin to code the phases of the baseband sine waves. This is done using straightforward PCM encoding techniques with 5 bits assigned to each phase. As the rate is increased more of the baseband phases are coded to use up the remainder of the coding budget.

REGENERATION OF SINE-WAVE PARAMETERS AT THE RECEIVER

At the synthesizer (see block diagram in Figure 2), the first step is to decode the pitch and determine the bit allocation and coding tables that were used at the transmitter. If the logarithmic channel spacings were used, then an amplitude envelope is recreated which is sampled at the harmonics of the coded pitch to recover the sine-wave amplitudes. The phases are decoded and assigned to the appropriate number of baseband sine waves. For the sine waves for which no phases were coded, an artificial phase is regenerated by first phase-locking all of the sine waves to the phase of the fundamental, and then adding a random phase having a standard deviation that is determined by a nonlinear mapping of the the voicing measure.

At this stage a set of amplitudes, frequencies and phases have been regenerated at the coding frame rate, which typically is 50 Hz. for most applications.

COMPUTATIONALLY EFFICIENT SINE-WAVE SYNTHESIS

In the basic sinusoidal analysis/synthesis system speech reconstruction is done by matching the sine-wave parameters obtained on successive frames and applying linear interpolation to the amplitudes and cubic phase interpolation to account for the interaction of the phases and frequencies. While this model leads to high-quality synthetic speech, it is computationally expensive since it requires that every sine-wave be regenerated on a per sample basis. Studies have shown that this process itself could require as many as 3 ADSP2100 chips for 4000 Hz bandwidth speech. In order to achieve computational efficiency, the sine waves are most easily recreated using the inverse FFT overlap-add technique. Since the low-rate coders operate at a 50 Hz frame rate, the overlapping triangular windows are 40 ms wide and this leads to a roughness in the synthesized speech. This is due to the fact that the sine-wave parameters, which correspond to the vocal tract articulators, do not remain stationary for such a long interval of time. In fact in the development of the sine-wave model [McAulay/Quatieri 1986], it was found that the overlap-add method worked quite well provided the frame-rate was of the order of 100 Hz. In order to exploit the FFT method therefore, it is necessary to use the sine-wave parameters received every 20 ms to generate an interpolated set of parameters every 10 ms. This can be done by using the fact that the birth/death frequency matcher has established contiguous sets of sine-wave parameters at the 50 Hz rate. The amplitudes and frequencies can then be interpolated linearly, and the phases are then interpolated using a rule that requires that the mid-point phase lead to a sine wave that is a best fit to the trailing edge of the preceding sine wave and to the leading edge of the succeeding sine wave. With this new set of sine-wave parameters, the inverse FFT overlap-add method can then be applied at an effective 100 Hz frame rate, and as a consequence the roughness is eliminated, [McAulay/Quatieri 1988].

One of the fundamental objections to the STC system has been the fact that for speech in a very noisy background, the harmonic frequency coding has led to a synthetic background noise that has had a tonal quality. Although the coded noisy speech has been very intelligible, it has reduced the quality of the system since most listeners find the tonality of the synthetic noise to be very objectionable. To eliminate this effect, the receiver uses the voicing measure to update an average spectrum for the background noise during strongly unvoiced frames. This spectrum is then used to first suppress the harmonic representation of the noise [McAulay/Malpass 1980], and replace it with a wideband noise having the same spectral shape but with completely random amplitudes and phases, thereby totally eliminating the tonality. Moreover, since the randomization is done to the FFT coefficients before the inversion, there is little increase in computational complexity.

CONCLUSIONS AND DISCUSSION

The sinusoidal model has proven to be an effective parametric technique for the analysis and synthesis of speech. It has been used for modifying the time-scale and pitch-scale of speech [Quatieri/McAulay 1986] and for the enhancement of speech in AM radio broadcasting [Quatieri/McAulay 1988]. This paper has summarized the attempt to use the sinusoidal model for low-rate speech coding. The effort has led to a multi-rate speech coder that can operate effectively from 2400 to 9600 bps producing very intelligible speech with a quality that improves more or less uniformly as the data rate is increased. The coder is very robust in acoustic background noise and with 5 bits assigned for modest bit error detection and correction it can operate effectively over a channel with at least 1% bit errors. Furthermore, as a result of timing studies of the real-time fixed-point realization, computational choke-points have been located and the algorithm modified so that now the entire STC system has been realized using 2 ADSP2100 chips. The current effort is now focussed on developing more efficient coding strategies for improving the quality at 2400 bps and for operating the coder at even lower rates, perhaps down to 1200 bps.

ACKNOWLEDGEMENT

The authors would like to thank Marilyn Malpass of Lincoln Laboratory for her work on the architecture studies for the ADSP2100 implementation of the STC system as this led to the identification of the computational choke-points. In addition all of the error protection work was her own. They would also like to acknowledge the interesting discussions with Dr. Michael Sabin of CYLINK, who has independently developed an implementation using two of the TMS320C25 DSP chips.

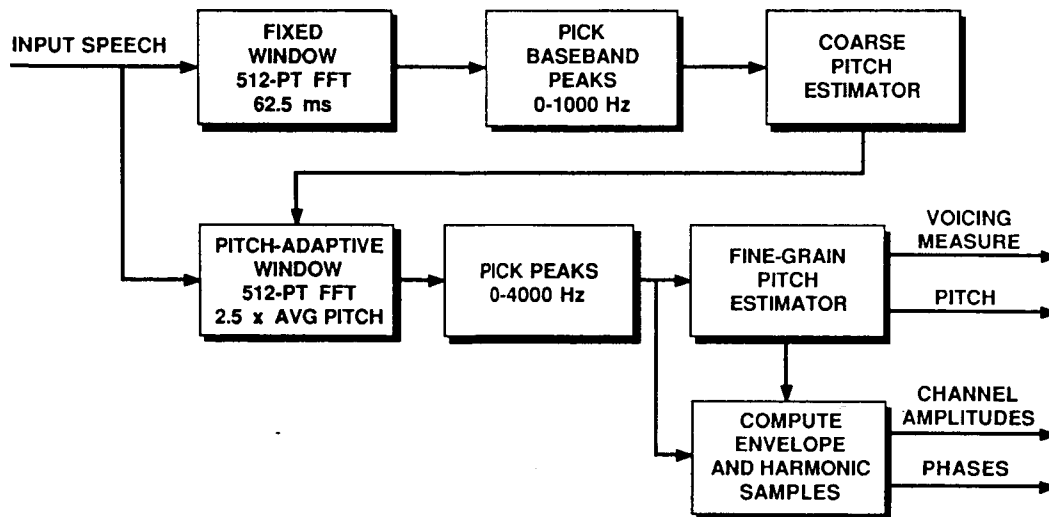


Fig. 1. STC Analysis.

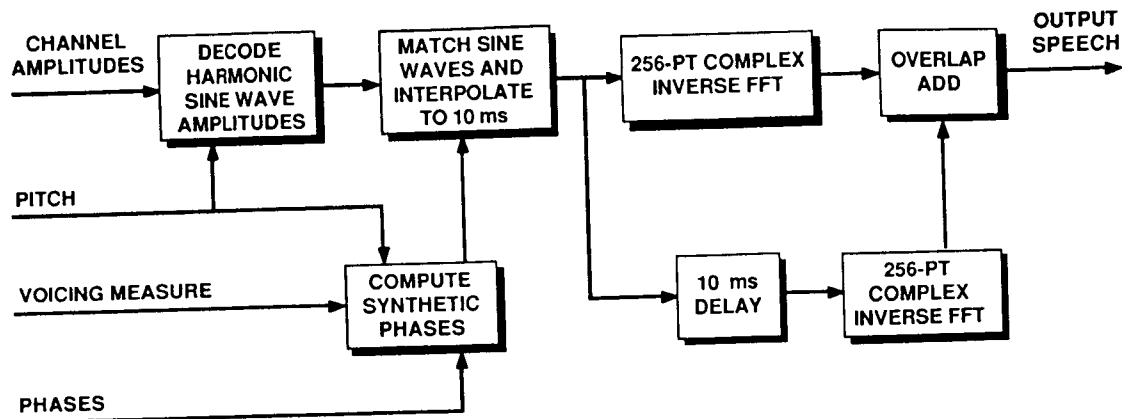


Fig. 2. STC Synthesis.

REFERENCES

- McAulay, R.J., Quatieri, T.F. 1988.
 Computationally efficient sine-wave synthesis and its application to sinusoidal transform coding. International Conference on Acoustics, Speech and Signal Processing, ICASSP '88, New York.
- Quatieri, T.F. and McAulay, R.J. 1988.
 Sinewave-based phase dispersion for audio preprocessing. International Conference on Acoustics, Speech and Signal Processing, ICASSP '88, New York, N.Y.
- McAulay, R.J., Quatieri, T.F. 1987.
 Multirate sinusoidal transform coding at rates from 2.4 Kbps. International Conference on Acoustics, Speech and Signal Processing, ICASSP '87, Dallas, TX.
- McAulay, R.J., Quatieri, T.F. 1986.
 Phase modelling and its application to sinusoidal transform coding. International Conference on Acoustics, Speech and Signal Processing, ICASSP '86, Tokyo, Japan.
- McAulay, R.J., Quatieri, T.F. 1986.
 Speech analysis/synthesis based on a sinusoidal representation. IEEE Trans. Acoustics, Speech and Signal Processing, ASSP-34, No. 4, pp. 744-754.
- Quatieri, T.F. and McAulay, R.J. 1986.
 Speech transformations based on a sinusoidal representation. IEEE Trans. Acoustics, Speech and Signal Processing, ASSP-34, No. 6, pp. 1449-1464.
- McAulay R.J. and Malpass, M.L. 1980.
 Speech enhancement using a soft-decision noise suppression filter. IEEE Trans. Acoustics, Speech and Signal Processing, ASSP-28, No. 2, pp. 137-145.
- Holmes, J.N. 1980. The JSRU channel vocoder. In IEEE Proceedings Vol. 127, Pt. F, No. 1, pp. 53-60.

The DESIGN and PERFORMANCE of a REAL-TIME SELF EXCITED VOCODER¹

Richard C. Rose, T. P. Barnwell III, S. McGrath

Georgia Institute of Technology
School of Electrical Engineering
Digital Signal Processing Laboratory
Atlanta, Georgia 30332
United States

Abstract

This paper is concerned with a generic class of predictive speech coders that includes the newly proposed The Self Excited Vocoder (SEV) [5] and the well known Code Excited Linear Predictive Coder (CELPC) [6]. All members of this class form an excitation sequence for a linear predictive model filter using the same general model for the excitation signal. The general excitation model is based on a block coding technique where each sequence is drawn from an ensemble of sequences. This paper reports on two developments related to this general model. The first development is a new type of excitation ensemble that can in general be populated by many different types of sequences. The second development is a means of populating this new type of ensemble based on a vector quantizer design procedure using a new distortion measure.

1 Introduction

A general model for the excitation signal in linear predictive speech coders was originally presented in [5]. Formal subjective tests, summarized in [4], characterized the performance of selected coders in this general class of predictive speech coders. A Self Excited Vocoder has been implemented in real time on a single circuit board using the AT&T DSP32 floating point digital signal processing devices [1]. This implementation will serve as a prototype vocoder in the NASA sponsored Mobile Satellite Communications Project.

This paper presents a new approach to the excitation modeling problem in self excited and code excited vocoders. The paper begins by reviewing the general model for the excitation signal in this class of predictive speech coders, and introduces a new type of excitation ensemble. Then a new procedure for populating the excitation ensemble using a procedure based on an iterative vector quantizer design algorithm is discussed. Finally, the last section, a new distance measure for the vector quantization procedure is introduced.

2 A New Class of Excitation Ensembles

The general model for the excitation signal in this class of coders is described by the block diagram in Figure 1a. The excitation signal, $e[n]$, is a linear combination of component excitation sequences, $e_k[n]$, where the k th sequence is chosen from the associated excitation ensemble, \mathcal{F}_k . An excitation ensemble is simply a collection of discrete functions, $f_\gamma[n]$, indexed in sample space by γ and indexed in time by n . The optimum ensemble index,

¹This work was supported by the Jet Propulsion Laboratory under contract number 957074

γ_k , and gain, β_k , associated with the k th excitation sequence are found by exhaustively searching through the excitation ensemble, \mathcal{F}_k , for that ensemble function that minimizes a weighted mean squared error [5].

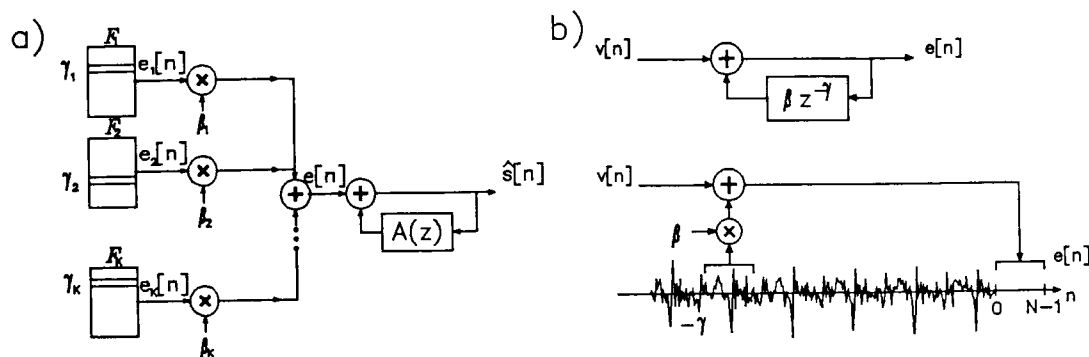


Figure 1: a) Model of the excitation signal for a generic class of predictive speech coders. b) Ensemble search interpretation of a single tap long-term predictor.

Examples of some existing predictive coders can be identified if the excitation ensemble is constrained to contain a particular class of sequences. For example, the well known CELPC chooses an optimum excitation sequence from a stochastic ensemble, where each ensemble sequence is populated by Gaussian random varieties [6]. Figure 1b shows how a simple long-term predictor can be interpreted as a time-varying excitation ensemble. In this case, the ensemble is the memory of a long-term predictor, whose predictor delay can vary over the expected range of a pitch period in speech. Each ensemble sequence is formed by sliding an N point rectangular window along the memory of the long-term predictor. The optimum ensemble sequence corresponds to an N point sequence beginning at sample $-\gamma$ in the memory of the long-term predictor. This type of ensemble, referred to here as the "self excitation" ensemble, forms the basis for the SEV. After a brief period of initialization, the SEV derives its excitation signal, $e[n] = \beta e[n - \gamma]$, solely from this type of ensemble.

The flexibility of the most general model of the excitation signal is derived from the fact that it poses no structure on the functions contained in the excitation ensemble. From the model definition, there is no fundamental requirement that an excitation ensemble be homogeneous. Thus, a single excitation ensemble can contain more than one class of sequences. For example, an ensemble can be formed by combining a set of time-varying sequences chosen from the memory of a long-term predictor with a set of fixed Gaussian random sequences. Figure 2a illustrates an interpretation of a simple coder whose excitation is derived from this type of ensemble. While the figure suggests that a hard classification procedure is taking place, this is actually not the case. The ensemble search procedure chooses a single sequence from the entire ensemble, so the determination of which class of sequences is used is made by choosing the single sequence which results in the least measured distortion. This type of excitation ensemble will be referred to as a nonhomogeneous ensemble, and can, in general, contain many different classes of sequences. The particular ensemble illustrated by the block diagram in Figure 2a is described by the excitation signal, $e[n] = \beta z_\gamma[n]$, where

$$z_\gamma[n] = \begin{cases} v_\gamma[n] & 1 \leq \gamma \leq C \\ e[n - \gamma] & C < \gamma \leq F \end{cases}, \quad (1)$$

and the fixed sequences, $v_\gamma[n]$, may be populated in many different ways.

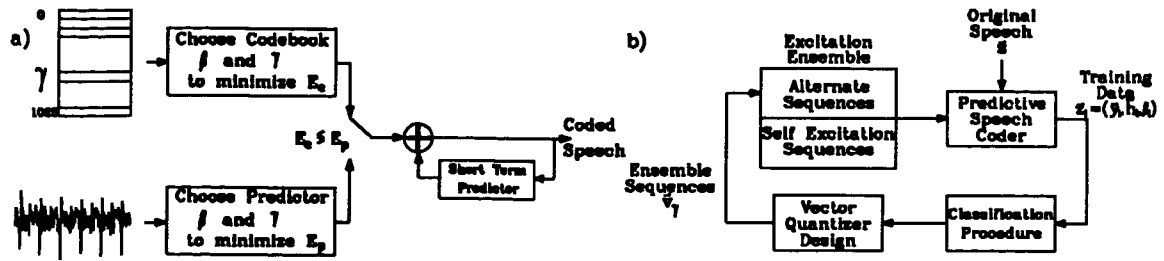


Figure 2: a) An interpretation of a simple nonhomogeneous predictive speech coder. b) Block diagram illustrating a procedure for determining the fixed ensemble sequences in a nonhomogeneous excitation ensemble.

3 Populating Nonhomogeneous Ensembles

This section describes a technique for determining the fixed sequences, $v_\gamma[n]$, in Equation 1 using the vector quantizer design procedure of Linde et al [2]. Following the reasoning of Davidson et al, the distance measure used for the vector quantization procedure can be the same weighted mean squared distance used for coding the excitation signal in this class of coders [7]. The following discussion describes the vector quantizer design procedure as it applies to populating the fixed sequences of the nonhomogeneous excitation ensemble.

The generalized Lloyd algorithm, originally introduced in [2], is an iterative algorithm for designing an optimum vector quantizer by a method of successive approximation. The vector quantizer design procedure determines the sequences, $v_\gamma[n]$, $\gamma = 1, \dots, C$, of Equation 1 from the training vectors, \bar{z}_i , $i = 1, \dots, n$, derived from the original speech. At each iteration of the algorithm the training vectors are partitioned into clusters, and cluster centroids are computed based on the partitioning of the data. The splitting algorithm of Linde et al is used here to provide the initial cluster centroids. The cluster centroids that exist upon termination of the algorithm form the resulting excitation ensemble.

Figure 3 is a block diagram illustrating the computation of the distortion, $d(\bar{v}_\gamma, \bar{z}_i)$, that is used for the vector quantizer data set partitioning and clustering procedures. For each excitation analysis frame, i , the coder represents the residual vector, \bar{r}_i , with an ensemble vector, \bar{v}_γ . The coder also computes the short-term predictor, $A_i(z)$, and the excitation gain, β_i . The Atal LPC based weighting filter, $W_i(z)$ [6], is used to compute the weighted Euclidean distance. The distance between training vector, \bar{z}_i , and ensemble vector, \bar{v}_γ can be expressed as

$$d(\bar{z}_i, \bar{v}_\gamma) = \sum_{n=0}^{N+L-2} \left(y_i[n] - \beta_i \sum_{l=0}^{N-1} v_\gamma[n] h_i[n-l] \right)^2, \quad (2)$$

where $h_i[n]$ is a finite length impulse response approximation to the cascaded synthesis and error weighting filters in Figure 3. The length of this impulse response is approximated as L samples ($L \approx 10$). The distance calculation in Equation 2 suggests the form of the training data required for each excitation frame. To compute this distance for the i th excitation frame, the weighted speech \bar{y}_i , the impulse response \bar{h}_i , and the ensemble gain β_i must all be derived from the input speech. The form of each training vector is then given as $\bar{z}_i = (\bar{y}_i, \bar{h}_i, \beta_i)$. Therefore, the training data is derived from the original speech using the

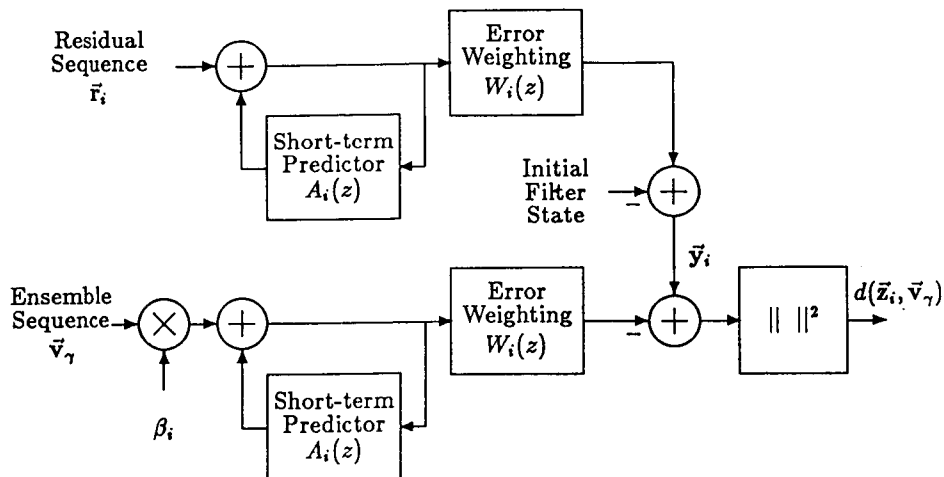


Figure 3: Block diagram illustrating the distortion measure computation for Equation 2.

predictive speech coder itself. The specification of an initial excitation ensemble for this coder is necessary for the generation of the training data.

In this research, a nonhomogeneous ensemble was generally divided into *self excitation sequences* and *alternate sequences*. The procedure for populating the alternate sequences of the nonhomogeneous ensemble shown in Figure 2a is illustrated by the block diagram shown in Figure 2b. The procedure begins by generating the training data, \bar{z}_i , using an predetermined set of signals for the alternate sequences. In this research, the alternate sequences are populated by independent Gaussian random varieties. Once the training data has been generated, a classification procedure is used to select a subset of the training data to be used as input to the vector quantizer design procedure. This classification procedure simply chooses those training vectors where the predictive speech coder provides a poor representation of the original speech. Finally, the vector quantizer design procedure produces sequences that are used to populate the alternate sequences in the nonhomogeneous ensemble. This procedure is described in the next section.

4 A New Vector Quantizer Distortion Measure

This section describes a new distance measure for use in the iterative excitation vector quantization procedure. The new distance measure follows immediately from Equation 2, and results in circularly defined excitation ensemble sequences. The discussion is broken into three parts. First, the centroid calculation following from the weighted Euclidean distance measure of Equation 2 is described. Second, the short-comings of this distance measure when applied to vector quantization of the excitation signal are discussed. Finally, the new distance measure is introduced.

Determining the centroid for a given cluster of training vectors corresponds to finding that sequence, \bar{v}_γ , that minimizes an average distortion for the distance measure in Equation 2. This average distortion represents an average over all of the training vectors belonging to the cluster. Minimizing the average error for a cluster containing M training vectors with respect to $v_\gamma[k]$, $k = 0, \dots, N - 1$, yields the matrix equation

$$\sum_{i=1}^M \bar{q}_i = \sum_{i=1}^M \mathbf{R}_i \bar{v}_\gamma. \quad (3)$$

The vector \bar{q}_i is an N length vector where the k th element corresponds to the crosscorre-

lation between the weighted speech and the impulse response for excitation frame i ,

$$q_i[k] = \beta_i \sum_{n=0}^{N+L-2} y_i[n] h_i[n-k], \quad k = 0, \dots, N-1. \quad (4)$$

The matrix \mathbf{R}_i is an $N \times N$ toeplitz matrix where the element in the l th row and k th column is given by the impulse response for excitation frame i ,

$$R_i[l, k] = \beta_i^2 \sum_{l=0}^{N-1} h_i[n-l] h_i[n-k]. \quad (5)$$

The matrix order, N , corresponds to the length of the excitation analysis frame, which is typically about twenty samples. Hence, computing the cluster centroid is not a computationally expensive procedure, requiring only the solution of a twentieth order Toeplitz matrix equation.

A major shortcoming of the above algorithm concerns the weighted Euclidean distance given in Equation 2. By this measure, the distance between two training vectors, where both vectors represent very similar excitation signals, may actually be very large. This is due to the fact that the excitation analysis window is placed asynchronously with respect to any significant events that may occur in the excitation signal. About 24,000 training vectors derived from isolated words uttered by a single speaker were used as training data for this algorithm. Ensemble sequences derived from this algorithm were used to code a short utterance from the same speaker. There was a significant improvement in segmental signal-to-noise ratio using this new ensemble over that of a Gaussian ensemble. However, the improvement in subjective performance was not significant when judged by the authors in informal listening tests. A modification to this procedure is proposed here that reduces the dependency of the training vectors on the position of the associated excitation analysis frame. The modification to the design procedure results in a redefinition of the distance measure and centroid calculation of the vector training algorithm.

The modification is based on simple permutations of the weighted speech that is used to form the training vector \bar{z}_i . The vector valued permutation π_k is a k sample circular right shift,

$$\pi_k(\bar{y}) = (y[N-k], y[N-k+1], \dots, y[0], y[1], \dots, y[N-k-1]). \quad (6)$$

By applying one of the permutations, $\{\bar{\pi}_k : k = 0, \dots, N-1\}$, to the training data, similar events occurring in different excitation frames may be aligned in time.

The distance measure and centroid calculation can be modified to exploit this behavior. First, the k th permutation of the i th training vector is defined as $\bar{\pi}_k^i(\bar{z}_i) = (\bar{\pi}_k^i(\bar{y}_i), \bar{\mathbf{h}}_i, \beta_i)$. The weighted Euclidean distance of Equation 2 is restated as

$$d(\bar{z}_i, \bar{\mathbf{v}}_\gamma) = \min_{\bar{\pi}_k^i : k=0, \dots, N-1} d(\bar{\pi}_k^i(\bar{z}_i), \bar{\mathbf{v}}_\gamma). \quad (7)$$

The distance between a training vector and a cluster centroid is therefore defined as the minimum weighted Euclidean distance across all possible permutations of the input data. Having found the optimum partition by minimizing the average distortion, the centroid vector, \mathbf{v}_γ , for centroid, γ , can be determined by solving the matrix equation,

$$\sum_{i=1}^M \bar{\pi}_k^i(\bar{\mathbf{q}}_i) = \sum_{i=1}^M \mathbf{R}_i \bar{\mathbf{v}}_\gamma. \quad (8)$$

In this equation, $\bar{\pi}_k^i$ is the optimum permutation for training vector i , and M is the total number of training vectors in the cluster.

5 Conclusions

This paper has introduced the nonhomogeneous excitation ensemble as a new type of ensemble used in a generic class of predictive speech coders. An iterative vector quantization procedure using a newly defined distance measure has been discussed as a means for populating the sequences for a specific nonhomogeneous ensemble. In this new procedure, the optimum choice of ensemble sequence is less dependent on the alignment of the excitation analysis frame with the original speech waveform. The procedure involves applying a set of circular permutations to the training data in order to time align similar events in different training vectors. The ensemble search procedure for this newly defined ensemble involves an exhaustive search, computing the weighted mean squared coding error for each circular permutation of each N point ensemble sequence. This is essentially equivalent to increasing the number of sequences in the ensemble from F sequences to FN sequences. However, the number of operations required to search this ensemble can be considerably reduced by using the recursive ensemble search procedure introduced in [3].

References

- [1] T. P. Barnwell III, R. C. Rose, and S. McGrath. A real-time implementation of a 4800 bps. self excited vocoder using the AT & T WE-DSP32 signal processing microprocessor. *Proc. Speech Technology Conf.*, Apr. 1987.
- [2] Y. Linde, A. Buzo, and R. M. Gray. An algorithm for vector quantizer design. *IEEE Trans. Commun.*, COM-28:84-95, Jan. 1980.
- [3] R. C. Rose and T. P. Barnwell III. The design and performance of an effective class of predictive speech coders. *Submitted for Review IEEE Trans. Acoust., Speech, Signal Processing*, June 1987.
- [4] R. C. Rose and T. P. Barnwell III. Quality comparison of low complexity 4800 bps. self excited and code excited vocoders. *Proc. Inter. Conf. on Acoustics, Speech, and Signal Proc.*, April 1987.
- [5] R. C. Rose and T. P. Barnwell III. The self excited vocoder—an alternate approach to toll quality at 4800 bps. *Proc. Inter. Conf. on Acoustics, Speech, and Signal Proc.*, 453-456, April 1986.
- [6] M. R. Schroeder and B. S. Atal. Code excited linear prediction: high quality speech at very low bit rates. *Proc. Inter. Conf. on Acoustics, Speech, and Signal Proc.*, 937-940, April 1985.
- [7] G. Davidson M. Yong and A. Gersho. Real-time vector excitation coding of speech at 4800 bps. *Proc. Inter. Conf. Acoust., Speech, Sig. Processing*, 51.4.1-51.4.4, 1987.

ROBUST VECTOR QUANTIZATION FOR NOISY CHANNELS

J.R.B. DE MARCA, Pontificia Universidade Catolica do Rio de Janeiro, Brazil, N. FARVARDIN, University of Maryland, USA, N.S. JAYANT, AT&T Bell Labs, USA, Y. SHOHAM, AT&T Bell Labs, USA;

AT&T Bell Laboratories
600 Mountain Ave.
Murray Hill, New Jersey United States

Abstract

The paper briefly discusses techniques for making vector quantizers more tolerant to transmission errors. Two algorithms are presented for obtaining an efficient binary word assignment to the vector quantizer codewords without increasing the transmission rate. It is shown that about 4.5 dB gain over random assignment can be achieved with these algorithms. It is also proposed to reduce the effects of error propagation in vector-predictive quantizers by appropriately constraining the response of the predictive loop. The constrained system is shown to have about 4 dB of SNR gain over an unconstrained system in a noisy channel, with a small loss of clean-channel performance.

1. Introduction

Vector quantization (VQ) is used for data compression and digital transmission in two basic forms: memoryless VQ and memory-based, vector-predictive quantizers (VPQ) [1,2]. Significant advantage over scalar quantization can be achieved with both systems. However, the effects of *noisy* channels on the VQ and VPQ performance are not yet fully understood. In this paper, we briefly describe two techniques for making VQ and VPQ more robust to transmission errors. The first technique is to use an efficient binary index assignment which can be considered to be zero-bit channel coding. Two algorithms will be described for obtaining an efficient index assignment. The first one is *deterministic* in nature [3] and the second one is a *stochastic* algorithm which is based on the concept of *simulated annealing* [4,5]. Other approaches to this problem can be found in [6,7]. The second technique applies to VPQ and is used to reduce the channel error propagation effect by controlling the response of the vector-predictive loop. This is done by appropriately modifying the root locations of the predictive loop. The robustness to channel errors is obtained without a significant loss in the VPQ performance.

2. The Index Assignment Problem

A vector quantizer of dimension M maps a vector-source symbol \mathbf{x} to a codevector \mathbf{c}_i in a codebook $C = \{\mathbf{c}_0, \mathbf{c}_1, \dots, \mathbf{c}_{N-1}\}$ of size N by minimizing a given distortion measure $d(\mathbf{x}, \mathbf{c}_i)$ with respect to i . The size N determines the rate of the quantizer $B = \log_2 N$ in bits/vector. The indices of the codevectors are transmitted over a digital channel in a form of binary words of length B by using a predetermined binary assignment function $b(i)$.

Transmission bit errors alter the received indices and erroneous codevectors are sometimes retrieved from the codebook at the receiver side. Let i and j be the correct and erroneous indices, respectively. The channel causes an additional *channel distortion* $d(\mathbf{c}_j, \mathbf{c}_i)$ on top of the *quantization distortion* $d(\mathbf{x}, \mathbf{c}_i)$. Let $p(i)$ be the a-priori codevector probability and $p(j | i)$ be the transitional probability of receiving \mathbf{c}_j given that \mathbf{c}_i was transmitted. The transitional probability clearly depends on the mapping $b(i)$ used by the quantizer. The average channel distortion is given by

$$D_c = E\{d(\mathbf{c}_i, \mathbf{c}_j)\} = \sum_{i=1}^N \sum_{j=1}^N p(i) p(j | i) d(\mathbf{c}_i, \mathbf{c}_j) \quad (1)$$

It can be shown that for the squared-error distortion measure $d(\mathbf{x}, \mathbf{c}_i) = \|\mathbf{x} - \mathbf{c}_i\|^2$ used in this study and for an *optimal* (clean-channel) codebook C , the overall average distortion is $D = E\{d(\mathbf{x}, \mathbf{c}_j)\} = D_q + D_c$ where $D_q = E\{d(\mathbf{x}, \mathbf{c}_i)\}$ is the average quantization distortion.

Since there are many (but finite number of) ways of assigning binary words to codevectors, a fundamental question arises as to what is the best assignment $b(i)$ in the sense of minimum overall distortion D or, equivalently, minimum channel distortion D_c . Two algorithms are suggested below for finding such an index assignment function.

3. Deterministic Algorithm for Binary Index Assignment

This algorithm is based on modeling the noisy channel as a memoryless binary symmetric channel with a negligible probability of having more than one bit error in a word. For this model the transitional probabilities are given by

$$p(j | i) = \begin{cases} p_e & \text{if } H(b(i), b(j)) = 1 \\ 0 & \text{if } H(b(i), b(j)) > 1 \\ 1 - p_e B & \text{if } \mathbf{c}_i = \mathbf{c}_j \end{cases} \quad (2)$$

where p_e is the channel bit error probability and $H(\dots)$ is the Hamming distance between two binary words. Assume that \mathbf{c}_i was transmitted and let $S(i)$ be the set of B nearest codevectors to \mathbf{c}_i in the sense of the distortion $d(\mathbf{c}_j, \mathbf{c}_i)$. The distortion induced by the channel is the least if the B binary words $\{b(j) : \mathbf{c}_j \in S(i)\}$ satisfy $H(b(j), b(i)) = 1$. In general it is impossible to satisfy this condition for all the codevectors in C . Therefore, the assignment $b(i)$ has to be determined according to some measure of priority. This measure depends on a-priori probability $p(i)$ and the *conditional distortion* (given \mathbf{c}_i) $\sum_{j \neq i} p(j | i) d(\mathbf{c}_j, \mathbf{c}_i)$ which, due to (2),

is proportional to the sum

$$\alpha(\mathbf{c}_i) = \sum_{j | \mathbf{c}_j \in S(i)} d(\mathbf{c}_j, \mathbf{c}_i) \quad (3)$$

The following empirical function sets a priority order among the codevectors:

$$F(\mathbf{c}_i) = \frac{p(i)}{\alpha^\beta(\mathbf{c}_i)} \quad (4)$$

The parameter β determines the relative importance of the conditional distortion and the a-priori probability. $\beta=0.3$ was found experimentally to be a good choice for this parameter.

The binary words are assigned to the codevectors in a decreasing order of $F(\mathbf{c}_i)$. For each \mathbf{c}_i , the algorithm attempts to assign binary words to all members of $S(i)$ not previously assigned binary words. First, an initial assignment $\{b(i), i=0, \dots, N-1\}$ is found for the largest $F(\mathbf{c}_i)$. Then, the algorithm attempts to improve it by interchanging the binary assignments of

all the pairs (i, j) , one pair at a time. However, only successful interchanges which reduce the distortion, are accepted. This index perturbation has been found to significantly improve the initial assignment.

The efficiency of the algorithm was tested by comparing the resulting average distortion to that obtained by a random index assignment. The average gain of the proposed algorithm over random assignment was about 2.7 dB and 4.7 dB in terms of signal-to-noise ratio, for code lengths of $B=3$ and $B=6$, respectively. This indicates a trend of higher efficiency for longer codes which is particularly important for high-dimensional, low-rate coding systems. More details on these experimental results can be found in [3].

4. Stochastic Algorithm Based on Simulated Annealing

Simulated Annealing has successfully been applied to complex combinatorial optimization problems with many local optima. The process mimics an objective function associated with a combinatorial optimization problem as the *energy* associated with a physical system, and by slowly reducing an appropriately defined *effective temperature* of the system, seeks the minimum energy state. Here, the objective function to be minimized with respect to the mapping $b(i)$ is the channel distortion D_c , which depends on $b(i)$ through the transitional probabilities. The mapping vector $b = \{b(i), i=0, \dots, N-1\}$ defines the *state* of the system and the channel error D_c defines the *energy* of the system.

The simulated annealing algorithm works as follows. The effective temperature T is set to an initial high value $T = T_0$ and an initial state b is chosen randomly. Then, a new state b' is obtained by interchanging the assignments of a randomly chosen pair of indices and the change in the distortion (energy) $\Delta D_c = D'_c - D_c$ is calculated. D'_c is the energy associated with the state b' . If $\Delta D_c < 0$, b is replaced by b' . Otherwise, b is replaced by b' with probability $\exp\{-\frac{\Delta D_c}{T}\}$. If the number of energy drops exceeds a prescribed number or if too many unsuccessful interchanges (not resulting in energy drops) occur, then, the temperature is lowered. Otherwise, the interchanging continues as above. If the temperature T goes below some prescribed freezing temperature T_f or if it appears that a stable state is reached, the algorithm stops with the final assignment b .

Note that the algorithm allows for "bad" perturbations to occur with some probability in order to climb out from local minima. This probability, however, diminishes as the temperature goes down. It has been shown that with a suitable perturbation scheme and with a sufficiently slow cooling schedule, the algorithm converges with probability one to the globally optimal binary assignment.

The algorithm was tested with a first-order autoregressive Gaussian source to verify its efficiency. 6-dimensional 1 bit/sample optimal vector quantizers were designed for a memoryless Gaussian source with a correlation factor $\rho = 0.0$ and for a heavily correlated Gaussian source with $\rho = 0.9$. To simplify the numerical computations, a single-error-per-word channel was assumed, as for the deterministic algorithm (Sec. 3.), with the transitional probabilities given in (2). In this case, the *normalized* channel distortion is given by

$$\frac{D_c}{p_e} = \frac{1}{M} \sum_{i=0}^{N-1} p(i) \sum_{j: H(b(c_j), b(c_i))=1} d(c_i, c_j), \quad (5)$$

The algorithm was run with an initial (melting) temperature $T_0 = 10.0$ and a final (freezing) temperature $T_f = 2.5 \times 10^{-4}$. The *cooling schedule* was as follows. The temperature was reduced by a factor $\alpha = 0.97$ after *five* drops (not necessarily in a row) in the average distortion

or after more than 200 perturbations. The algorithm terminated when the temperature dropped below T_f or if 50,000 consecutive perturbations did not result in a drop in the average distortion. The above choices of parameters were obtained experimentally and yielded satisfactory results. Plots A and B of Figures 1 illustrate the evolution of the simulated annealing algorithm for the memoryless and the correlated Gaussian source, respectively, for the dimension $M = 6$. The normalized channel error is plotted as a function of the effective temperature. The figure shows that the algorithm reduced the channel error by about 4.5 dB and 2.0 dB for the memoryless and correlated sources, respectively, compared to random-assignment performance.

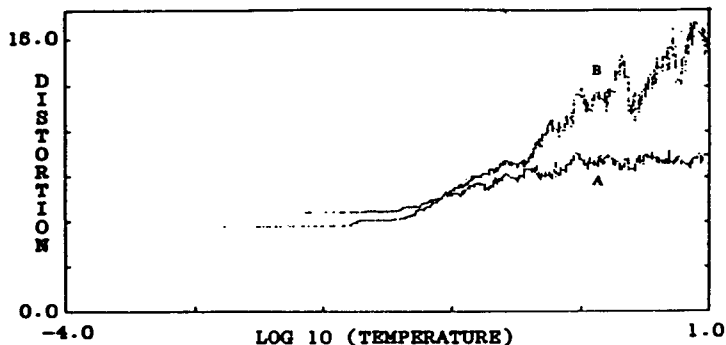


Figure 1. Average channel distortion as a function of the temperature during a run of the Simulated Annealing algorithm. A. Memoryless source ($\rho=0.0$). B. Correlated source ($\rho=0.9$).

5. Error Propagation Control in VPQ

In this section we deal with a different type of problem which arises in noisy channels, namely, the problem of error propagation in memory-based coding systems. Specifically, we present a simple technique for reducing such an effect in Vector Predictive Quantizers (VPQ). VPQ is basically an adaptive DPCM type of coding system extended to the vector space [2]. In the VPQ system studied here, an M -dimensional (column) input vector \mathbf{x}_n at a time instant n is quantized in two steps. First, the current vector is predicted from the p immediate past quantized vectors using the M -by- p matrix $\hat{Q}_n = [\hat{\mathbf{x}}_{n-1}, \hat{\mathbf{x}}_{n-2}, \dots, \hat{\mathbf{x}}_{n-p}]$. The prediction at time n is given by $\tilde{\mathbf{x}}_n = \hat{Q}_n \mathbf{y}$ where \mathbf{y} is a p -dimensional vector of prediction coefficients selected from a *predictor codebook* so as to minimize the distortion $d(\mathbf{x}_n, \tilde{\mathbf{x}}_n) = \|\mathbf{x}_n - \tilde{\mathbf{x}}_n\|^2$. In the second step, the residual vector $\mathbf{r}_n = \mathbf{x}_n - \hat{Q}_n \mathbf{y}$ is vector-quantized using a second codebook called the *residual codebook*. The quantized error vector $\hat{\mathbf{r}}_n$ minimizes the norm $\|\mathbf{r}_n - \hat{\mathbf{r}}_n\|$. The final quantized output is given by $\hat{\mathbf{x}}_n = \tilde{\mathbf{x}}_n + \hat{\mathbf{r}}_n$. The overall coding rate in number of bits per vector is $B = \log_2 (N_c N_r)$ where N_c and N_r are the predictor and residual codebook sizes, respectively.

This VPQ system is characterized by a time-variant IIR linear system (feedback loop)

$$L_n(z) = \frac{1}{1 - \sum_{i=1}^p y_{n,i} z^{-i}} \quad (6)$$

where $y_{n,i}$ is the i^{th} component of \mathbf{y} selected at time n so as to minimize the prediction error. Minimizing the prediction error sometimes yields marginally stable or even unstable system. Thus, $L_n(z)$ may have an extremely long impulse response which tends to spread channel errors

over many time frames.

One method for restricting the impulse response duration of the predictive loop is to move the filter poles away from the unit circle. First an unconstrained predictor codebook is designed so as to maximize the prediction gain. Then, the codebook is modified in order to constrain the system impulse response. Let $h(n)$ be an impulse response corresponding to some codevector in the predictor codebook. We denote the effective duration of $h(n)$ by L_e . This quantity is defined by

$$L_e = \max(L) \quad : \quad \frac{\sum_{n=0}^L h^2(n)}{\sum_{n=L+1}^{\infty} h^2(n)} \leq T_e \quad (7)$$

where T_e is an effective threshold that is equal to the power ratio of the leading part (0 to L_e) to the tailing part (L_e+1 to ∞) of $h(n)$. The predictor codebook is modified such that the effective lengths of all of its entries are bounded by a predetermined effective length corresponding to a predetermined effective threshold. The modification is achieved by moving the roots of the predictors radially towards the origin, that is, by modifying the predictor coefficients as follows:

$$y'_i = \gamma^i y_i \quad ; \quad 0 < \gamma < 1 \quad (8)$$

The modification expressed in (8) is repeated with some predetermined γ and threshold T_e until (7) is satisfied for a desired length L_e .

This technique was incorporated in vector-predictive quantization of the LPC spectral vectors derived from a speech database at a rate of one per 20 msec. A 20-bit VPQ was designed, with a 6-bit predictor codebook and with a 14-bit residual codebook (which was split into two 7-bit codebooks). The predictor codebook was modified to constrain the loop response by using $\gamma=0.98$, $T_e=0.01$ and $L_e=10$. Figure 2. shows the response of the time-variant loop L_n to a sequence of pulses spaced 100 time units (frames) apart. Plots A and B show the response of an unconstrained and a constrained loops, respectively, for a VPQ prediction order $p=8$. While the unconstrained responses may extend over more than 100 frames, the effective length of the constrained responses is around 10 frames.

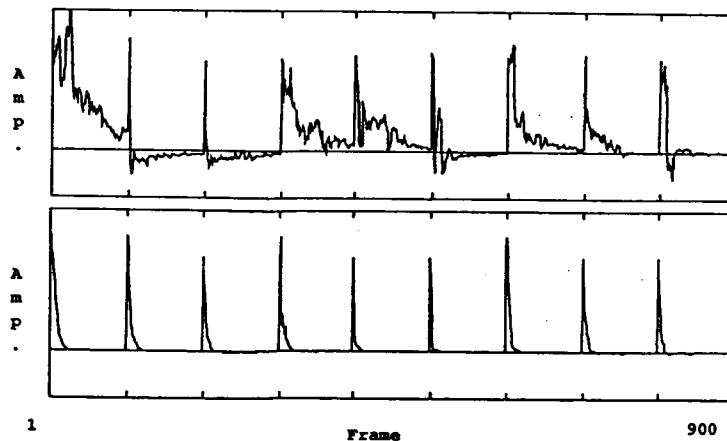


Figure 2. Impulse responses of the time-variant Predictive loop
A. Unconstrained loop. B. Constrained loop.

The VPQ was exposed to channel errors with various bit error rates (BER) and its performance was measured in terms of spectral SNR. The performance figures, summarized in Table 1., show that the constrained VPQ is much more robust to channel errors than the unconstrained quantizer, with a very small degradation of clean-channel performance.

BER	Unconstrained VPQ	Constrained VPQ
0.000	15.44	15.33
0.001	13.94	14.63
0.010	7.57	11.44

Table 1. Spectral SNR (dB) of unconstrained and constrained VPQ's in presence of channel errors.

6. Conclusions

The paper briefly discussed a few techniques for making vector quantizers more tolerant to transmission errors. Two algorithms were presented for an efficient binary word assignment. It was shown that a gain of about 4.5 dB over random assignment could be achieved with those algorithms. A method for constraining the error propagation in predictive VQ was presented. The constrained VPQ was shown to be more robust to channel errors, with a small loss of clean-channel performance.

REFERENCES

1. R. M. Gray, "Vector Quantization," *IEEE Acoust., Speech, Signal Processing Magazine*, Vol. 1, pp. 4-29, April 1984.
2. Y. Shoham, "Vector Predictive Quantization of the Spectral Parameters for Low Rate Speech Coding," *IEEE Proc. ICASSP-87*, Vol. 3, pp. 51.2.1-4, Apr. 1987.
3. J. R. B. DeMarca and N. S. Jayant, "An Algorithm for Assigning Binary Indices to the Codevectors of A Multidimensional Quantizer," *Proc. IEEE Int. Comm. Conf.*, Seattle, WA, pp. 1128-1132, June 1987.
4. S. Kirkpatrick, C. D. Gelatt and M. P. Vecchi, "Optimization by Simulated Annealing," *Science*, Vol. 220, pp. 671-680, May 1983.
5. B. Hajek, "A tutorial Survey of Theory and Application of Simulated Annealing," *Proc. 24th Conf. Dec. & Cont.*, FL, Dec. 85, pp. 755-760.
6. J.-H. Chen, G. Davidson, A. Gersho and K. Zeger, "Speech Coding for the Mobile Satellite Experiment," *Proc. IEEE Int. Comm. Conf.*, Seattle, WA, pp. 756-763, June 1987.
7. K. A. Zeger and A. Gersho, "Zero Redundancy Channel Coding in Vector Quantization," *IEE Electronics Letters*, Vol. 23, pp. 654-655, June 1987.

DEVELOPMENT OF AN 8000 BPS VOICE CODEC FOR AvSat

JOSEPH F. CLARK, AvSat Program, Aeronautical Radio, Inc., United States

AERONAUTICAL RADIO, INC.
2551 Riva Road
Annapolis, Maryland 21401
United States

ABSTRACT

Air-mobile speech communication applications share robustness and noise immunity requirements with other mobile applications. The quality requirements are stringent, especially in the cockpit where air safety is involved. Based on these considerations, a decision was made to test an intermediate data rate such as 8.0 and 9.6 kb/s as proven technologies.

A number of vocoders and codec technologies were investigated at rates ranging from 2.4 kb/s up to and including 9.6 kb/s. The "proven" vocoders operating at 2.4 and 4.8 kb/s lacked the noise immunity or the robustness to operate reliably in a cabin noise environment. One very attractive alternative approach was Spectrally Encoded Residual Excited LPC (SE-RELP) which is used in a multi-rate voice processor (MRP) developed at the Naval Research Lab (NRL). The MRP uses SE-RELP at rates of 9.6 and 16 kb/s. The 9.6 kb/s rate can be lowered to 8.0 kb/s without loss of information by modifying the frame. An 8.0 kb/s vocoder was developed using SE-RELP as a demonstrator and testbed. This demonstrator is implemented in real-time using two Compaq II portable computers, each equipped with an ARIEL DSP-16 Data Acquisition Processor.

INTRODUCTION

The Airlines Electronic Engineering Committee (AEEC) has undertaken development of a "characteristic" for satellite communications equipment — in effect a guideline for equipment and airframe manufacturers, aviation users, and service providers. Designated Project 741, it is being developed in parallel with a wide variety of intense activities in the mobile satellite communications area.

The primary schedule constraint for the AEEC has been introduction of a new generation of aircraft to be delivered "satcom ready" starting in 1989. As a consequence, the AEEC formulated a three-phase schedule for Project 741. By late 1986, the Satellite Subcommittee of the AEEC formed a working group to recommend a voice coding standard. Although there has been a hiatus in the activity of that working group, its

efforts both in fulfilling its mission and in assuring that all aspects of the voice communication system be considered together are continuing.

This paper reports on the specific effort to develop a voice coding standard using the transmission rate of 8.0 kilobits per second (kb/s) and focuses on the similar performance, as shown in testing, of the 8.0 kb/s and 9.6 kb/s codecs available today.

ADAPTING TO THE USER COMMUNITY

The aviation community is loosely divided between "general aviation" and commercial passenger aviation. The aircraft used vary in size from the very large to the very small. The length of flights varies from less than one hour to more than eight hours. Although data communications increasingly is the mechanism for reporting aircraft status and for routine operational exchanges, one common denominator is a requirement for cockpit voice — a communication path for the flight crew to talk with ground crews.

While the primary volume application of voice appears to be passenger telephony, the cockpit voice quality requirements may be the primary determinant of the overall requirements because of the ties to safety.

While only experimental equipment has been installed to date, it is clear that aviation will use both high-gain and low-gain antennas. The service providers will be using a mix of global beams and spot beams from the satellite. As a result, three classes of service can be provided: low-rate data; medium-rate data and low-rate voice; and the nominal, which is medium-rate data and "near-toll-quality" voice.

We suggest that a single algorithm for both low-rate and medium-rate voice would be the preferred solution. This approach was developed by the Naval Research Laboratory (NRL)¹ and is in operation today. The method for providing voice communication through a low-rate data service is to buffer short messages coded at the nominal voice rate, and transmit them as extended messages at the actual channel data rate.

PERFORMANCE REQUIREMENTS

So far, no one has defined well enough the measurable parameters for repeatable measurements of "near toll quality." However, the achievable performance of codecs is well known. Figure 1 depicts the achievable performance of a wide variety of codecs as determined in tests. But in order to specify a required performance, it is necessary to determine minimum acceptable performance in terms of parameters that can be measured in a consistent way. Unfortunately, voice quality is by its very nature subjective. It can only be quantified as a statistic derived from inherently variable data.

The performance requirements endorsed by the AEEC Voice Working Group² are simple:

- Subjective evaluation measured by Mean Opinion Score - midway between Fair and Good (3.25 on a scale of 1-5).
- Intelligibility measured by Rhyme Test - 87 or better.
- Conversational evaluation - 75 or better.
- Delay measured with codecs back to back - no more than 65 milliseconds.

- Performance measured with a channel bit error rate (BER) of 1 in 1000 bits.

In addition, the group recognized that the operational environment would include low-rate data transmissions, rather severe outages and interfaces with established terrestrial telephone networks. It was decided that data should be routed around the codecs. Not only does the requirement for coding data as well as voice put significant demands on the coding algorithm, it implies significant additional acceptance testing.

The new CCITT coding standard for digital transmission of wideband audio signals, G.722, provides a similar bypass mechanism for user data. The separation of voice and data allows a better system design³.

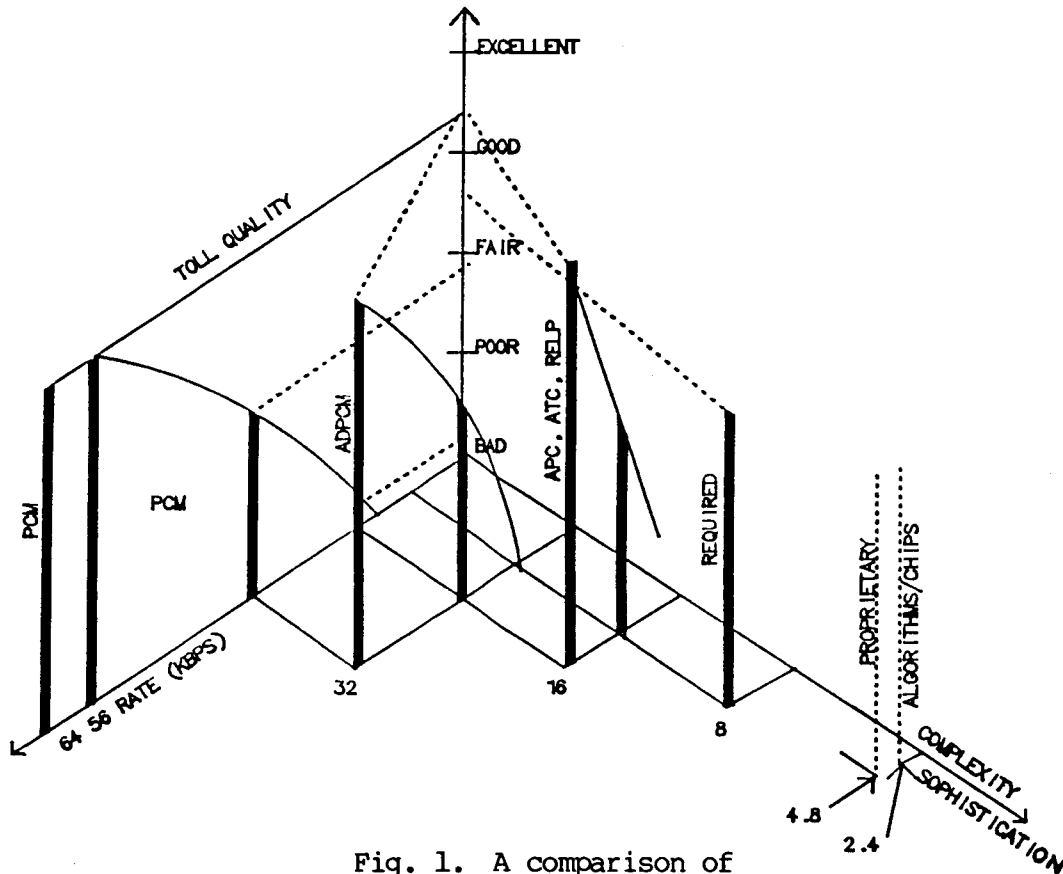


Fig. 1. A comparison of speech transmission

APPROACHES

A CCITT standard ADPCM would simplify the task, but there is more complexity in the transmission channel. Limitations of the medium, and power and bandwidth constraints drive the choice of rates to the lowest possible. On the other hand, the realizable quality at a given rate drives the choice upwards. The result then, is a compromise on an intermediate rate that approximates the desired performance without devouring all available capacity.

The rate issue has resolved to a choice between 8.0 kb/s and 9.6 kb/s. The 8.0 kb/s rate is based on compatibility with expected subchannelling of the ISDN basic 64 kb/s communication rate. Intuitively, there should not be much difference in performance at these rates relative to, say, performance at 16 kb/s or at 4.8 kb/s. This intuition is supported by the evaluations received so far. (See Figures 2 and 3.)

Furthermore, performance differences seem to be related more to implementation than to algorithm. This result is quite reasonable since most of the algorithms are variations on the idea of using residual excitation with a linear prediction filter.

The conclusion then is that the AEEC's voice working group could not recommend a specific algorithm, or even a data rate. Only implementations of voice systems can be evaluated and recommended.

From an overall systems point of view, there is a significant difference between these rates. Choosing 9.6 kb/s without gaining a significant performance advantage is wasteful. In the best of proposed implementations, 9.6 kb/s uses \$1.20 worth of resources for every \$1.00 used by 8.0 kb/s. For SCPC voice channels as proposed in Project Paper 741, the 9.6 kb/s implementation requires almost twice as much bandwidth as the 8.0 kb/s implementation. (See Table 1.)

Table 1. Voice Channel Frame Parameters*

Voice Rate (bits)	FEC Rate	Channel Rate (bit/s)	Channel Spacing KHz	Bits in Frame		
				Voice/25 (v)	Data/96 (SU) (n)	Dummy (d2)
9600**	0.50	21000	17.5	192	3	84
8000**	0.75	12600	10.0	160	6	8

*Extracted from Project Paper 741, Part 2.

**Preferred Voice Channels

The AEEC voice working group with the assistance of the Boeing Airplane Corporation developed a standard test tape. This tape was distributed to approximately twenty-five organizations which had expressed an interest either in developing codecs for the aviation industry or in evaluating voice codecs. The tapes were fed in and out of candidate codecs, and the resulting tapes analyzed in listening tests conducted by Dynastat.

ONE 8.0 KB/S SOLUTION

There were two major concerns in dealing with established manufacturers of voice codecs. First, a satisfactory licensing agreement for the algorithm and implementation must be available to all avionics manufacturers. Second, manufacturers might continue to focus on products designed only for their terrestrial markets, i.e., codecs designed

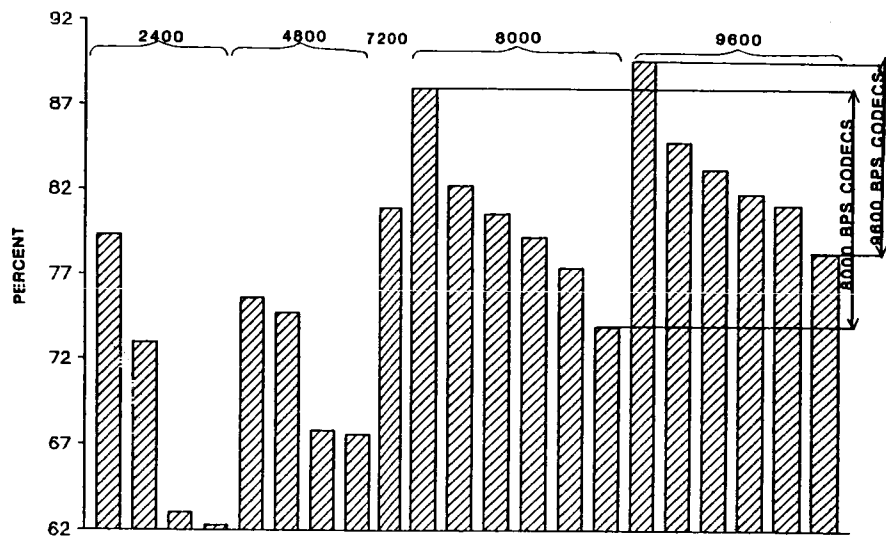


Fig. 2. Intelligibility: Cockpit Noise Environment

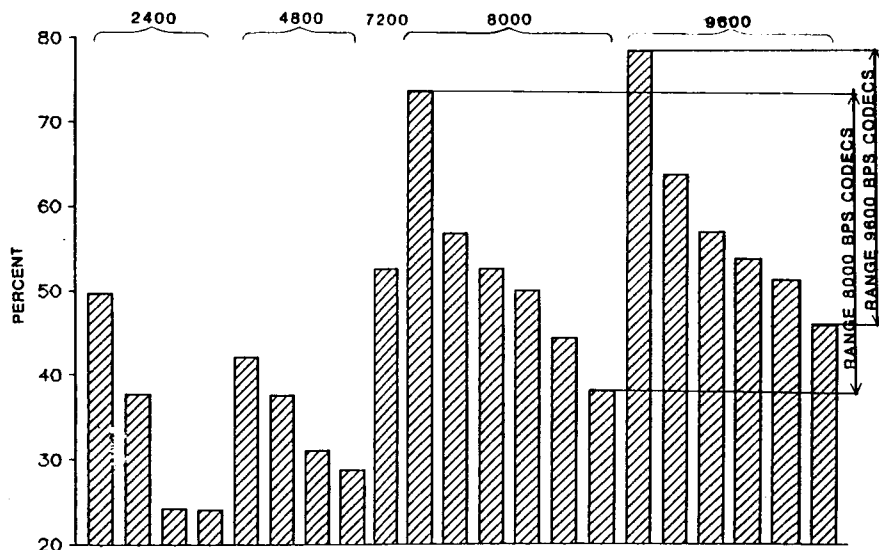


Fig. 3. Probability of User Acceptance Based on Cockpit Noise Environment

for 2.4 kb/s, 4.8 kb/s, and 9.6 kb/s even though 8.0 kb/s is a demonstrably better choice for the emerging aviation industry characteristic.

In view of these concerns, ARINC contracted with Techno-Sciences, Incorporated (TSI) of Greenbelt, Maryland, to develop an 8.0 kb/s voice codec from information published in the public domain. The premise was: if a credible voice codec could be developed by one or two key people working with limited time and budget, then avionics manufacturers could derive non-proprietary sources for voice codecs, and on a realistic schedule with confidence.

TSI, with ARINC assistance, developed a pair of 8 kb/s voice codecs operating in real time. The codecs are connected through the serial (RS232) ports of two Compaq Portable II computers. Speech is sampled 8000 times a second and blocked into groups of 180 samples. Ten reflection and filter coefficients are calculated using autocorrelation. The quantized reflection coefficients are used to form the filter which then is used to generate the prediction residual.

A 96-component spectral representation of the prediction residual is computed using the Winograd algorithm. These components are quantized and coded into a 180-bit block with the reflection coefficients. A new block is generated and transmitted 44.4444 times per second. The key factors in the codec performance are the reflection coefficient calculation and the number of transmitted spectral components. The current codec transmits 126 spectral components, the same number transmitted in the NRL 9.6 kb/s rate codec.

After 6 months of development, a codec emerged that is credible but admittedly is incomplete and needs improvement. Several areas of the basic LPC algorithms have been tagged for further work in a second phase of the project. In the second phase of the codec development, vector coding of the spectral components will be introduced. There is good confidence in the expected results.

CONCLUSION

The AEEC Voice Working Group, with cooperation of the Boeing Airplane Company, the Federal Aviation Administration, the Rome Air Development Center and others, has developed a set of standards for voice codecs in the air mobile environment, collected a representative set of samples for a variety of codecs using a uniform test tape, and received an unbiased formal evaluation of the sample tapes. The results of the evaluation indicate that at least 7.2 kb/s speech coding will be required to reliably meet requirements in the aviation satellite environment. These results (see Figures 2 and 3) also indicate that performance at 8.0 kb/s is in the same range as performance at 9.6 kb/s — making 8.0 kb/s the better overall choice for a power and bandwidth-limited satellite environment to be globally interconnected with ISO-conforming networks.

REFERENCES

1. Kang, G. S. and Fransen, L. J., Second Report of the Multirate Processor for Digital Voice Communications, NRL Report 8614, September 30, 1982.
2. AEEC Letter 87-014/SAT-33, p. 11, Aeronautical Radio, Inc., 2551 Riva Road, Annapolis, MD 21401, February 13, 1987.
3. Mermelstein, Paul, G.722, a New CCITT Coding Standard for Digital Transmission of Wideband Audio Signals, IEEE Communications Magazine, Vol. 26, No.1, January 1988.
4. AEEC 700 Quick Check #50, November 4, 1987.
5. Techno-Sciences, Inc., Report No. 870909, 8 kbps Speech Demo Project, prepared for Aeronautical Radio, Inc., September 9, 1987.

ANALYSIS AND IMPROVEMENT OF THE VECTOR QUANTIZATION IN SELP

W. B. KLEIJN, D. J. KRASINSKI, and R. H. KETCHUM

AT&T BELL LABORATORIES

200 Park Plaza

Naperville, IL 60510, USA

ABSTRACT

The SELP algorithm is described as a speech coding method employing a two-stage vector quantization. The first stage uses an adaptive codebook which efficiently encodes the periodicity of voiced speech, and the second stage uses a stochastic codebook to encode the remainder of the excitation signal. The adaptive codebook performs well when the pitch period of the speech signal is larger than the frame size. An extension is introduced, which increases its performance for the case that the frame size is longer than the pitch period. The performance of the stochastic stage, which improves with frame length, is shown to be best in those sections of the speech signal where a high level of short-term correlation is present. It can be concluded that the SELP algorithm performs best during voiced speech where the pitch period is longer than the frame length.

1. INTRODUCTION

The Stochastically Excited Linear Prediction (SELP) algorithm for speech coding, originally proposed by Atal and Schroeder [1], is a method of vector quantizing the sampled speech signal on a frame-by-frame basis. The algorithm vector quantizes a signal which, ideally, contains no short-term correlation. When the quantized signal is filtered through an appropriate linear filter (determined with LPC methods) to provide the correct short-term correlation, synthetic speech results. The signal can be synthesized at the receive end of the speech coder by transmitting both an index to the particular excitation vector selected from the codebook and a description of the filter.

The effect of the present frame excitation on the synthetic speech in the present frame can be expressed as a convolution of the excitation with the filter impulse response. This convolution can be implemented as a matrix multiplication of the excitation vector with a lower-triangular Toeplitz matrix \mathbf{H} containing the filter impulse response along the first column. The synthetic speech signal \mathbf{y} produced by a candidate excitation vector \mathbf{r} is now:

$$\mathbf{y} = \mu \mathbf{H} \mathbf{r} + \mathbf{z}, \quad (1)$$

where μ is a scaling factor, and \mathbf{z} represents the zero-input response of the filter describing the present frame response to the preceding excitation.

Ideally the excitation vector \mathbf{r} results in a synthetic speech signal identical to the original speech. It is this ideal "target" excitation vector, \mathbf{t} , which is vector quantized in the SELP algorithm. The squared error between the original speech signal and the synthetic speech signal can be used as the quantization error criterion. Expressed in terms of excitation vectors, it becomes:

$$\epsilon = (t - \mu r)^T H^T H (t - \mu r). \quad (2)$$

The error criterion described represents the squared error of the synthetic speech signal. It does not consider that uniform matching of the speech signal over its entire spectrum does not minimize the perceived noise level. The error signal is less perceptible in those sections of the spectrum which contain relatively high energy (the formants). Thus, it is advantageous to move more of the error signal under the formants, while reducing the error signal in other regions [2]. This can be accomplished by moving the poles of the filter inward by a factor γ , which is chosen in the range between 0.7 and 0.9. An added advantage of this "noise-weighting" procedure is that it dampens the impulse response significantly, so that it can be truncated at a relatively short length. From here on we assume that the matrix H includes noise weighting.

The development of fast algorithms benefits from increased symmetry. By truncating the impulse response after R samples, and considering this entire response length for each sample of the excitation vector in the error criterion, a more symmetric spectral-weighting matrix $H^T H$ can be created [3]. This modified error criterion compares the response of the excitation vector to that of the target excitation vector in the present as well as subsequent frames. The resulting $H^T H$ matrix is still $N \times N$ but is now a Toeplitz band matrix. A fast algorithm which takes advantage of this symmetry is described in [3].

Two codebooks are used in our SELP implementation. The first codebook is adaptive, adjusting to the periodicity of the speech signal. The method is similar to procedures described in [4] and [5]. The adaptive codebook is constructed by buffering the synthetic excitation. If M samples of past excitation are stored, and the frame length is N samples, then the adaptive codebook contains $M - N + 1$ distinct candidate vectors. Neighboring candidate vectors differ by a shift of one sample.

Because of the linearity of the filtering procedure, the excitation vector selected from the adaptive codebook can be subtracted from the target excitation vector t to obtain a new target vector for the second vector quantization procedure. Since the LPC filter models the short-term correlation, and the adaptive codebook the long-term correlation of the speech signal, the new target vector has a noisy character. The stochastic codebook consists of a set of vectors containing normally distributed samples. It is often center clipped to increase computational speed [3], [6], [7].

During the vector quantization procedures of both the adaptive and stochastic codebooks all candidate vectors are scaled by optimal scaling factors. This allows for the large dynamic range present in speech. It is easily shown from equation (2) that the optimal scaling factor μ for a candidate vector r takes the value $r^T H^T H t / r^T H^T H r$. The scaling factors also must be transmitted to the synthesizer.

2. ANALYSIS AND IMPROVEMENT OF SELP

2.1 The Adaptive Codebook

The adaptive codebook procedure performs best in voiced sections of speech. The codebook vector selected usually contains a section of synthetic excitation that had been applied one or more integer number of pitch periods prior to the present frame. Figs. 1a and 1c illustrate the probability density function for the delay (in samples) between the selected candidate vector and the present vector for speech from a female and a male speaker, respectively. The probability density function for each speaker was approximated

from an analysis of 10000 frames of 8 kHz sampled speech using a SELP coder with two codebooks of 256 vectors and a frame length of 40 samples. The pitch period of the speakers is clearly displayed in these distributions. For the male speaker a delay of one pitch period is most prevalent, but two and three pitch delays contribute significantly also. For the female speaker, a delay of one pitch period cannot be chosen, because the frame length is longer than the pitch period. Instead, delays of two through five integer pitch periods are prevalent.

The subjective performance of the SELP coder is better for the speech signal with a pitch period longer than the frame length. However, we have found that, at fixed codebook size, the segmental signal to noise ratio decreases smoothly as a function of increasing frame length. Thus, the modeling accuracy is not affected significantly by the frame length being longer or shorter than the pitch period. However, only if the frame length is shorter than the pitch period will noise resulting from inaccurate modeling be repeated at the same rate as the pitch pulses. This leads to desirable harmonics in spectral regions which are numerically unimportant in the evaluation of the error criterion. The harmonics at the high end of the spectrum, which contains less energy, are often created from noise signals. This effect is eliminated when the pitch period is shorter than the frame length.

Since (at constant codebook size) the bit rate of the SELP coder is inversely related to frame length, it is desirable to minimize the negative impact of increased frame length. This can be accomplished with an extension of the adaptive codebook which results in enhanced periodicity [3]. In the conventional method, the candidate vector containing the most recent synthetic excitation starts exactly N samples before the present frame. A candidate vector starting at a more recent sample is incomplete. However, if the existing portion of such a vector is presented in the first part of the present frame, it will create a periodicity. If the vector starts p samples previous to the present frame, then the periodicity will be p samples. This periodicity can be maintained by repeating the existing portion of the vector again, starting p samples into the present frame. Thus, the adaptive codebook can be extended with "virtual" vectors with a period equal to the length of the existing portion.

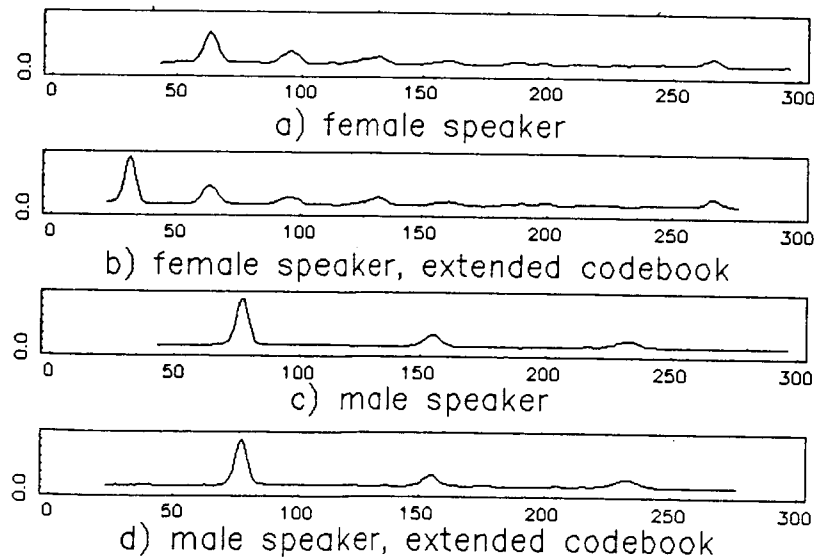


Fig. 1. Probability Density of Delay

At an equal number of candidate entries, the extended adaptive codebook results in an improved subjective performance when the frame length is longer than a single pitch period. Fig. 1b displays the probability density function for the delay of the selected vectors for the extended codebook case. The candidate vectors chosen most often are those with a delay of one pitch period, which were completed in the manner described above. This means that in a large number of frames, the newly created periodic entries in the codebook provided the best match to the target excitation vector t . In Fig. 2 spectra generated with and without the extension are shown. The virtual candidates create a periodicity, resulting in enhanced harmonicity of the spectrum, especially between 1200 and 3000 Hz. It is this enhanced periodicity which improves the subjective speech quality. However, the associated segmental signal to noise ratio increased only about 0.1 dB. The improvement of the subjective speech quality for the female speaker is in contrast to the results for the male speaker (Fig. 1d), for whom the revised codebook with the modified range of available delays has no noticeable effect on overall performance.

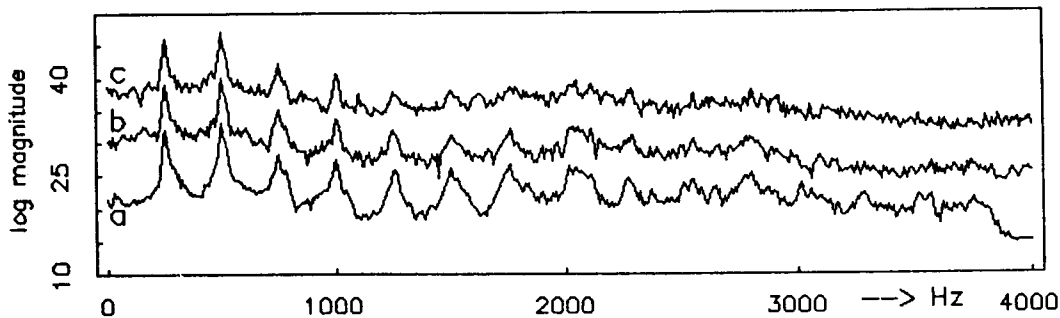


Fig. 2. Spectral Characteristics
a: original, b: extended codebook, c: conventional codebook

2.2 The Stochastic Codebook.

The performance of the stochastic codebook can be evaluated by assuming that the part of the excitation signal which remains after the first vector quantization stage contains normally distributed random samples. Its error criterion is simplified when expressed in the eigenspace of the $\mathbf{H}^T\mathbf{H}$ matrix. The diagonal transform of the spectral weighting matrix is $\Lambda = \mathbf{U}\mathbf{H}^T\mathbf{H}\mathbf{U}^T$, where \mathbf{U} is a unitary matrix. The transforms of the excitation vectors are $\tau = \mathbf{U}t$ and $\rho = \mathbf{U}r$ respectively. Since the vectors t and r were assumed to be sequences of normally distributed independent samples, and since $\mathbf{H}^T\mathbf{H}$ is positive definite, τ and ρ are also normally distributed independent sequences. Equation (2) can now be written as:

$$\epsilon = (\tau - \mu\rho)^T \Lambda (\tau - \mu\rho). \quad (3)$$

The behavior of the error criterion ϵ is a function of the framelength N , the eigenvalues described by Λ , and codebook size.

When trying to match noise signals, the matrix $\mathbf{H}^T\mathbf{H}$ tends to be close to the identity matrix. Fig. 3 shows the dependence of the minimized error criterion ϵ , normalized to a per sample basis, on the frame length for a weighting matrix whose eigenvalues are all equal. Six error curves are shown for codebooks of various sizes. In addition, the error as a function of frame size under the constraint of constant bit rate for the codebook index is

shown. From the latter curves it appears that the coding efficiency is identical at all frame lengths. This is not the case, however, since additional bits must be spent on the encoding of the scaling factor used in the quantization procedure. Since this overhead becomes smaller with increasing frame length, the encoding becomes more efficient at larger frame lengths.

A high level of short-term correlation results in a large range for the magnitudes of the eigenvalues of the spectral weighting matrix. Then, only a small fraction of the components of the target vector τ (those associated with large eigenvalues) are of importance in the evaluation of the error criterion. It is illuminating to consider the extreme instance where only one eigenvalue is nonzero. In this case only a single component of the target vector τ must be matched. Using an optimal scaling factor, any vector not orthogonal to this component will result in zero error. However, the quantization of this scaling factor will introduce error in an actual coder.

Using these two extreme cases as guideline, it is seen that the stochastic quantization procedure can be expected to perform best in voiced speech, which has pronounced formants. Thus, the stochastic codebook search will perform best in the same voiced regions where the adaptive codebook search performs best. These results are consistent with intuition; the speech coders perform best where the signal has the most structure (low entropy, low information content), and worst where the signal has the least structure (high entropy, high information content). These results lead to segmental signal to noise ratios which are high during speech and low during background noise.

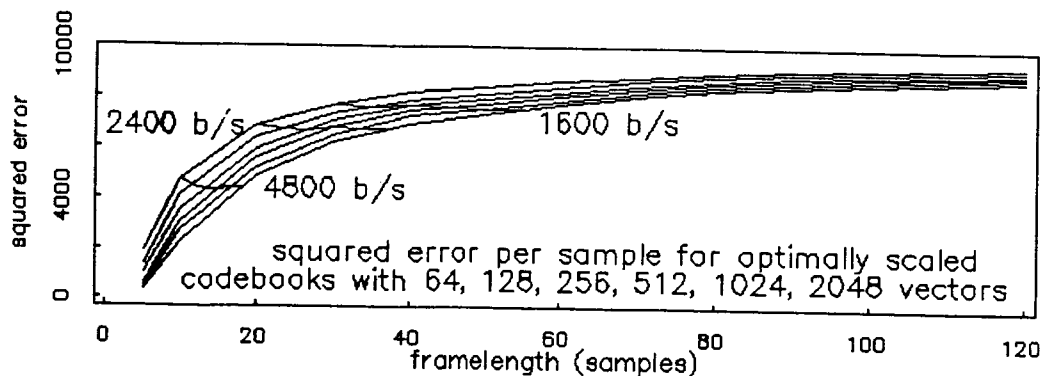


Fig. 3. Squared Error for Noise Signal

3. CONCLUSION

The encoding of the periodicity of the excitation signal of SELP coders deteriorates when the frame length exceeds the length of a pitch period. This effect can be diminished by extending the adaptive codebook with vectors of progressively shorter periodicity. The performance of the stochastic codebook improves when the frame length is increased. Both the adaptive and stochastic codebook quantization procedure perform best during voiced speech where both short-term and long-term correlation are highest.

It is natural that the adaptive codebook quantization is performed before the stochastic quantization, with the latter acting as a correction to an already good excitation sequence. Because of the recursive character of the adaptive codebook, it is logical to apply the stochastic codebook correction before entering the excitation into the adaptive codebook.

This means that the stochastic codebook frame length must fit an integer number of times in the frame length used for the adaptive codebook. This and the fact that the stochastic codebook performs better with increasing length means that the frame length of the stochastic codebook is best chosen to be equal to that of the adaptive codebook.

REFERENCES

- [1] Atal B.S. and M.R. Schroeder, "Stochastic Coding of Speech at Very Low Bit Rates", *Proc. of ICC*, Amsterdam, 1610-1613, 1984.
- [2] Atal, B.S. and M.R. Schroeder, "Predictive Coding of Speech Signals and Subjective Error Criteria" *IEEE Trans. Speech Signal Proc. Vol. ASSP-27, no 3*, 247-254, 1979.
- [3] Kleijn, W.B., D.J. Krasinski, and R.H. Ketchum, "Improved Speech Quality and Efficient Vector Quantization in SELP" *Proc. Int. Conf. Acoust., Speech and Sign. Process.*, New York, 1988.
- [4] Singhal S. and B.S. Atal, "Improving Performance of Multi-Pulse LPC Coders at Low Bit Rates", *Proc. Int. Conf. Acoust., Speech and Sign. Process.*, San Diego, 1.3.1-1.3.4, 1984.
- [5] Rose, R.C. and T.P. Barnwell, "Quality Comparison of Low Complexity 4800bps Self Excited and Code Excited Vocoders", *Proc. Int. Conf. Acoust., Speech and Sign. Process.*, Dallas, 1637-1640, 1987.
- [6] Lin, D., "New approaches to Stochastic Coding of Speech Sources at Very Low Bit Rates", in *Signal Processing III: Theories and Applications*, I.T. Young et al. eds., Elsevier, 445-447, 1986.
- [7] Davidson, G. and A. Gersho, "Complexity Reduction Methods for Vector Excitation Coding", *Proc. Int. Conf. Acoust., Speech and Sign. Process.*, Tokyo, 3055-3058, 1986.

SESSION K
GOVERNMENT AGENCY

SESSION CHAIR: George Knouse, NASA Headquarters
SESSION ORGANIZER: Valerie Gray, Jet Propulsion Laboratory

MOBILE SATELLITE COMMUNICATIONS IN THE FOREST SERVICE

JOHN R. WARREN, Advanced Electronics Group, United States Forest Service,
Department of Agriculture, United States.

UNITED STATES FOREST SERVICE
Boise Interagency Fire Center
3905 Vista Avenue
Boise, Idaho 83705

ABSTRACT

The USDA Forest Service manages 191 million acres of public-owned land in the 156 National Forests of the nation. Much of this land is in remote locations with poor or no commercial communication services. Normally, communications from Ranger stations are handled by the telephone companies. For working communications, a Forest usually has base stations and repeaters which cover a large part of the area. Mobile radios are used in land vehicles as well as aircraft and can usually maintain contact directly or via a repeater. Handheld radios are also used. There are usually some places within a Forest that do not have adequate coverage due to line-of-sight or other reasons. These areas are generally known by the foresters and radio technicians and allowances made for that when working or traveling in those areas. However, when wildfire or other emergencies occur, communications are vital because wildfires can require hundreds of firefighters and cover thousands of acres. During these emergency operations the existing communications are not adequate and complete radio systems are moved into the area for the conduct of fire communications. Incident Command Posts (ICP's) and Fire Camps are set up in remote locations and there is constant need for communications in the fire area and to agency headquarters and dispatch offices. Mobile satellite communications would be an ideal supplement to the Forest Service's current communications system in aiding forest fire control activities.

FIRE COMMUNICATIONS

The Department of Agriculture (Forest Service) and the Department of Interior spend an average of \$220,000,000 annually in the suppression of wildland fires. The number of personnel of a large fire may vary from 300 to over 2000. Due to the hazards and logistical complexities associated

with large wildland fire management, it is essential that adequate communications are available. Fire Camps and ICP's are often located in remote areas. It is necessary to provide eating, sleeping, and sanitation arrangements, as well as transportation of people, equipment, and supplies often during rapidly changing situations.

Communications at the fire scene are accomplished with VHF/UHF radio systems which include base stations, portable repeaters, mobiles, and hand-held radios. These are set up quickly and operated efficiently by skilled communications technicians. Communications means to agency headquarters and dispatch centers vary widely, depending on the locations and what means can be made available. Often there are no telephone lines available to the ICP. Portable repeaters may permit some radio communications after they can be installed and activated if they can be tied in with the outside locations. However, sometimes this may not be timely or even possible because of line-of-sight, distance, repeater location accessibility and other reasons. During the past few years satellite communications from some of these remote locations have been used successfully. Very Small Aperture Terminals (VSAT's) which are transportable are available and can be used.

The Forest Service is starting to use computers and digital data transmission systems at the ICP locations to facilitate resource ordering, reporting, recordkeeping, timekeeping, resource status, situation status, data base access, etc. Traditionally, all communications were conducted by voice. Computers and data systems are now used routinely throughout the Forest Service. The use of data transmissions within the ICP and to the externally located agency offices can expedite messages, avoid misunderstandings or incorrect copying of orders, and improve the effectiveness and efficiency of the operations. Interagency studies are being completed and field testing planned to determine the extent to which data transmission should be accomplished.

Mobile satellite communications would provide a means for providing communications during the early stages of the operations and even while the fire staff personnel are enroute to the scene. Any of the currently available communications means requires time to set-up, check, and become operational. Mobile satellite communications would be ideal during that interim time. They would also be an ideal supplement to existing "cached" communications systems for those extra-ordinary years when the number and extent of wildfires simply overwhelm the normally available systems. The mobile-sat equipment could also be used in normal years for smaller fires or in areas where setting up the more complex systems might not be appropriate. Mobile-sat equipment should also be useful during the final phase-down operations. This would permit the larger systems to be removed and transported to other locations without isolating the remaining mop-up crews.

AIRBORNE COMMUNICATIONS

The Forest Service also uses airborne infrared systems to locate and "map" wildfires and also to detect newly started lightning or other fires. When those fires can be geo-referenced on board the aircraft, the fire

perimeter and hot spot locations could be transmitted to the ground in latitude and longitude coordinates. This could be done without a mobile satellite system but that requires the aircraft to establish a line-of-sight RF link with the ground receiving site and retain it until all the data are transmitted. In the typical rugged terrain that can be a time-consuming task that subtracts from the available airborne time, requires the aircraft to deviate from the best route to the next destination, may interfere with other airborne operations, and uses a frequency which may be in short supply. The use of a mobile satellite link on the aircraft would permit transmission of the fire data from virtually any location while the plane is proceeding to the next destination.

ROUTINE COMMUNICATIONS

Finally, for normal routine operations there are some areas which are not covered by the Forests' VHF radio system but where personnel must conduct activities from time to time. The mobile satellite system would be ideally suited to provide communications for those areas. That could also perhaps eliminate the expense and upkeep of selected repeater sites on a planned basis where sites are maintained primarily for occasional coverage of areas to determine if the use of mobile satellite communications would be less expensive than existing Forest radio communications. It is likely that when the capability is available and used there will be a number of other applications that will be identified.

MOBILE SATELLITE SERVICE IN THE UNITED STATES

DR. CARSON E. AGNEW, Hughes Communications Mobile Satellite Services, Inc., United States; JAI BHAGAT, MCCA Space Technologies Corporation, United States; EDWIN A. HOPPER, McCaw Space Technologies, Inc., United States; JOHN D. KIESLING, Mobile Satellite Corporation, United States; MICHAEL L. EXNER, Skylink Corporation, United States; LAWRENCE MELILLO, North American Mobile Satellite, Inc., United States; GARY K. NOREEN, Transit Communications, Inc., United States; BILLY J. PARROTT, Satellite Mobile Telephone Co., United States.

TRANSIT COMMUNICATIONS, INC.
P.O. Box 90425
Pasadena, California 91109-0425
United States

ABSTRACT

Mobile Satellite Service (MSS) has been under development in the United States for more than two decades. The service will soon be provided on a commercial basis by a consortium of eight U.S. companies called the American Mobile Satellite Consortium (AMSC). AMSC will build a three-satellite MSS system that will offer superior performance, reliability and cost effectiveness for organizations requiring mobile communications across the U.S. The development and operation of MSS in North America is being coordinated with Telesat Canada and Mexico. AMSC expects NASA to provide launch services in exchange for capacity on the first AMSC satellite for MSAT-X activities and for government demonstrations.

INTRODUCTION

Mobile Satellite Service (MSS) will provide reliable mobile and thin-route communications throughout the United States. MSS is uniquely suited to organizations with geographically dispersed operations and with requirements for ubiquitous communications. MSS will be provided in this country by the American Mobile Satellite Consortium (AMSC, 1988).

The AMSC MSS system has substantial advantages over alternative systems for wide area mobile communications and position location. The system uses an SCPC architecture that is flexible and that can address broad markets, resulting in economies of scale. The system is well suited to fleet management applications, particularly where flexibility and reliability are critical. It is also well suited to the support of public safety, aviation safety, and resource exploration and development applications.

The Federal Communications Commission has determined that MSS will be provided in the United States by AMSC, which includes all eight qualified U.S. MSS applicants (see Table 1). Each of the members of AMSC has placed \$5 million in a joint escrow account. This \$40 million joint account may be used for initial capitalization of the consortium. AMSC filed a Joint Amendment to the applications of its eight members on February 1, 1988 that describes its MSS system. The AMSC MSS system is also described in a companion paper in this volume.

Table 1. American Mobile Satellite Consortium Participants

Hughes Communications Mobile Satellite Services, Inc. P.O. Box 92424 Los Angeles, California 90009 Phone: (213)607-4000	North American Mobile Satellite, Inc. 733 Third Avenue New York, New York 10017 Phone: (212)355-3440
MCCA Space Technologies Corporation 1500 Capital Towers Jackson, Mississippi 39201 Phone: (601)969-1500	Satellite Mobile Telephone Co. 57 East 11th Street New York, New York 10003 Phone: (212)460-5022
McCaw Space Technologies, Inc. 409 S.W. 9th Avenue Portland, Oregon 97205-3208 Phone: (503)243-3333	Skylink Corporation 1800 30th Street Boulder, Colorado 80301 Phone: (303)442-8866
Mobile Satellite Corporation 65 Valley Stream Parkway, Suite 110 Malvern, Pennsylvania 19355 Phone: (215) 640-9660	Transit Communications, Inc. P.O. Box 90425 Pasadena, California 91109-0425 Phone: (818) 577-8720

Telesat Canada, the designated Canadian MSS operator, and AMSC plan to develop, produce and operate closely coordinated satellite and ground systems. Joint implementation of the space segment eliminates the need for separate in-orbit spare satellites, since the Telesat and AMSC systems can back up each other. Further savings will be achieved in the ground segment by producing similar Network Operations and TT&C centers to operate the Telesat and AMSC mobile satellite systems. These ground facilities will then provide mutual backup.

The mutual backup of both the space and ground segments between Telesat and AMSC assures high system reliability. Communications between a fleet controller and mobiles can be relayed directly through the satellite, circumventing terrestrial links entirely and ensuring continuity of communications during disasters.

In studies and experiments over the past two decades, NASA has demonstrated all technical concepts necessary for mobile communications by satellite (ATS 1971-1982). AMSC looks forward to close cooperation with NASA as it implements its system. NASA has offered to provide launch services to AMSC in return for use of some of the capacity of the first generation mobile satellite system (NASA, 1985). NASA would use this capacity to perform technology experiments and to enable government agencies to assess the usefulness of MSS to their operations. Government applications include public safety, aviation safety, communications for wide and remote area coverage (police and border control), monitoring of hazardous material transport, and others. Two years after launch, NASA will return this capacity to AMSC. NASA includes a reservation for the AMSC launch in its current ELV manifest.

AMSC SERVICES

AMSC will provide a comprehensive "generic" mobile satellite service, providing economical services to land, maritime and aeronautical users. Through the use of a common space segment to provide all three classes of service, economies of scale are achieved that have prevented implementation of land or aeronautical mobile satellite services in the past.

AMSC will provide four basic services through its mobile satellite system:

- Mobile Telephone (interconnected with the public switched telephone network)
- Mobile Radio (dispatch), including voice and data services
- Aeronautical Service
- Transportable Telephone Service

Taken together, the potential market for these mobile satellite services is quite large. Market studies indicate that there is sufficient potential demand for these four basic services, beyond that which terrestrial systems could reasonably or economically satisfy, to fill the capacity of the AMSC mobile satellite system several times over (AMSC, 1988).

AMSC anticipates supporting other, ancillary services as well. These potential services include point-to-multipoint data distribution, paging, remote data collection, position location and new mobile services using alphanumeric terminals.

Land Mobile

The primary class of mobile satellite service for which AMSC perceives an unfilled need is communications for land vehicles over long ranges or in lightly populated areas. Land mobile satellite service applications for which substantial demand has been established include (AMSC, 1988):

- Rural Mobile Telephone and Radio
- Rail Mobile Telephone
- Interstate Trucking
- Mobile Paging/Dispatch
- Commercial Forest Services
- Emergency Services
- Government Services, including:
 - Public Safety (law enforcement, fire fighting, disaster management, search & rescue, and rural health)
 - Forest Service
 - Customs and Immigration

Aviation

The aviation community, through the Federal Aviation Administration (FAA) and the Canadian Department of Transportation (DOT), is now assessing its long range needs for aeronautical services (FAA, 1985). Those requirements include operational and passenger communications. Approximately 10% of the United States major air carrier fleet now provides terrestrial based passenger telephone service.

Satellites offer the only economically viable technology to serve certain aviation market requirements. The most important of the aeronautical services to be supplied by AMSC are those related to the safety and regularity of flight, the AMSS(R) services. While these services are of paramount importance, they do not require the full capacity of the system and cannot economically support a satellite system on their own. By supporting land, maritime and aeronautical mobile satellite services, a mobile satellite operator can build a system providing the lowest cost service to all users.

Maritime Services

Although inland and coastal marine vessels now enjoy a variety of communications options, many marine communications requirements remain inadequately addressed. For example, commercial operators of vessels operating over long routes through inland and

coastal waterways face substantially the same fleet management requirements and problems faced by interstate trucking. Indeed, the same safety and competitive pressures are at work in the marine freight transportation industry which drive the need for wide area private networks.

Transportable Services

Other services which the AMSC system can ably provide are characterized by a need for wide area coverage and long range or remote operation without the requirement that they operate from moving vehicles. These may be termed "transportable" because they typically involve transporting a portable terminal to the site where it will be used.

Rural telephone service, for those who can obtain it, has traditionally been expensive despite the telephone companies' high degree of subsidization by revenue generated from urban residential and business users. The high price is due to low subscriber densities (less than five subscribers per square mile). In addition, the very long local loops which are required to provide this service can have a significant impact on cost.

Despite these high costs in the past, the cross-subsidization of rural local loops restricted technological innovation. Now, deregulation of the telecommunications industry and other regulatory developments are reducing or eliminating the revenue sources that provided past subsidies. MSS will supplement existing and developing terrestrial technologies in the provision of ubiquitous rural telephone service.

In addition to rural voice telephone service, the gathering of data for production control, monitoring, and planning purposes at oil and gas wells, on natural gas and other pipelines, and electric utility remote transmission and distribution facilities can often only be effectively supported through a satellite service. The AMSC system will be especially attractive for these data transmission requirements because it can economically support low capacity transportable terminals.

Other activities with similar requirements include aeronautical navigation aid monitoring, flood control, and water management at dams, remote weather and forest fire observation stations, seismic monitoring, and remote security systems.

ALTERNATIVE SYSTEMS

Terrestrial Systems

The predominant methods of land mobile communications currently include cellular radio telephone service, Specialized Mobile Radio (SMR), and private networks. While each of these services, within their current geographical areas, provide users with a reasonable level of service, there are limitations of each upon which MSS can improve.

The economic feasibility of all terrestrial based mobile systems is sensitive to subscriber density. At lower densities, MSS will be more economical than terrestrial services. MSS also offers improved service in areas difficult to serve because of rough terrain. Moreover, MSS offers private network users distinct advantages when large areas of coverage are required. For example, the AMSC MSS system is independent of any ground network, and is thus not susceptible to terrestrial disasters.

Satellite Systems

Two satellite systems have been proposed as early alternatives to MSS: the Omnet "Omnetracs" system (Omnet, 1987) and the Geostar Radiodetermination Satellite Service (RDSS) system (Geostar, 1985).

Only the AMSC mobile satellite system can provide voice services. AMSC will also provide data and positioning services much more effectively than any alternative.

Satellite-based systems, if properly designed, are not susceptible to disruptions in the terrestrial network caused by local disasters. This makes them particularly attractive for applications which require high reliability and which must count on immediate access in emergencies. Of the satellite systems now under development, only the AMSC system can circumvent the terrestrial network through the use of base stations at private control centers. Also, only AMSC will have backup capacity available on both the ground and in space. Thus, only the AMSC MSS system is satisfactory for applications in which full redundancy and independence of terrestrial links is critical.

Also, the AMSC system will cost substantially less for subscribers than the Omnitrac and Geostar systems. Omnitrac requires complex, expensive K_u band terminals and uses K_u band transponder capacity inefficiently. RDSS is inherently more expensive to provide than MSS because of the need for extra satellites for triangulation measurements, the need for separate transmit and receive antennas on mobiles and the inability to aggregate services through a common satellite (precluding economies of scale).

Table 2 compares mobile communications and position location alternatives.

Table 2. Mobile Communications and Position Location Comparison

System	MSS	Cellular	SMR	Private	Omnitrac ¹	RDSS ²
Coverage	North America	Local	Local	Local	U.S.	U.S.
Voice	Yes	Yes	Yes	Yes	No	No
Base Stations	Yes	No	No	Yes	No	No
Redundant Ground Segment	Yes	No	No	No	No	No
Mobile Antennas	1	1	1	1	1	2
Position Location	Yes ³	No	No	No	No ⁴	Yes

¹ Omninet has not been authorized to provide service.

² RDSS has been authorized to provide only position messaging and ancillary messaging. It is not authorized to provide communications services.

³ MSS can determine position through use of satellite ranging or integrated MSS/GPS transceivers.

⁴ Omnitrac uses Loran-C receivers for position location.

ACKNOWLEDGEMENTS

Richard Cooperman of Mobile Satellite Corporation, Dr. Teresa Ferguson of Hughes Communications, Inc. and Glenn E. Noreen of Transit Communications, Inc. made significant contributions to this paper.

REFERENCES

- AMSC, 1988. Joint Amendment of the American Mobile Satellite Consortium, filed at the Federal Communications Commission, February 1, 1988.
- ATS, 1971-1982. Numerous MSS experiments were conducted with NASA's ATS-1 through -6 satellites. See General Electric Company (1971) *Final Report on Phases 1 and 2 VHF Ranging and Position Fixing using ATS Satellites*, prepared by General Electric Company Corporate Research and Development, Schenectady, New York for Goddard Space Flight Center, Greenbelt, Maryland, May 1, 1971, Con-

tract No. NAS5-11634, NASA-CR-125538; Boeing Aircraft Company (1973), *ATS-5 Multipath/Ranging/Digital Data L-Band Experimental Program - Program Summary*, prepared by Boeing Commercial Airplane Company for the Federal Aviation Administration, April 1973, Report No. FAA-RD-73-57, AD-783 581; General Electric Company (1972) *Final Report on Phase 3 ATS Ranging and Position Fixing Experiment*, prepared by General Electric Company Corporate Research and Development for Goddard Space Flight Center, December 1, 1972, Contract No. NAS5-11634, NASA-CR-132755; General Electric Company (1977) *Application of Satellite Communication and Position Fixing Techniques to Land Mobile Systems*, prepared by General Electric Company Corporate Research and Development for Drug Enforcement Administration and Immigration and Naturalization Service, US Department of Justice, Washington, DC, April 1977, Contract DEA-76-20, PB 267 019, SRD-77-001; Protopapa, Sejfi (1977) *Air Traffic Control Experimentation and Evaluation with the NASA ATS-6 Satellite, Volume I: Executive Summary*, Prepared by the Transportation Systems Center for the Federal Aviation Administration, Report No. FAA-RD-75-173.I, AD A046509; Anderson, R.E., et al., *Land Mobile Communications and Position Fixing Using Satellites*. IEEE Transactions on Vehicular Technology. VT-28, No. 3, pp. 153-170, August 1979; Anderson, Roy E., et. al. (1980), *Position Surveillance using One Active Ranging Satellite and Time-of-Arrival of a Signal from an Independent Satellite*, prepared by G.E. Corporate R&D for Goddard Space Flight Center, NASA-CR-166647, N81-20147, January 1980; Anderson, Roy E., et. al. (1980) *Satellite-Aided Mobile Communications Limited Operational Test in the Trucking Industry*, prepared by G.E. Corporate R&D for Goddard Space Flight Center under Contract No. NAS5-24365, NASA-CR-166658, N81-20337, July 1980; Anderson, R.E., et. al., *Position Surveillance Using One Active Satellite and Time-of-Arrival of a Signal from an Independent Satellite*, *Navigation*, Vol. 27, No. 4, pp. 305-317, Winter, 1980-1981; Burge, Cecil D. and Frank K. Nagurney, *Experimental Evaluation of Satellite Communications for Emergency Medical Services: Demand, Cost, and Benefits*, Final Report under Contract NAS13-95, University of Southern Mississippi, Hattiesburg, Mississippi, May 1981; and Anderson, Roy E., et. al., (1982) *Communications Equipment for Alphanumeric Communication via ATS-3 Satellite*, prepared by G.E. Corporate R&D for Ames Research Center under Contract No. NAS2-10764, June 1982.

FAA, 1985. Assessment of Satellite Concepts and Aviation Spectrum Requirements, February, Federal Aviation Administration, 1985.

Geostar, 1985. Geostar Satellite System Compendium of Application and Technical Information, submitted to the FCC on April 5, 1985.

NASA, 1985. *Opportunity Notice for a Mobile Satellite Agreement*, Office of Space Science & Applications, NASA Headquarters, February 25, 1985.

Omninet, 1987. Application of Omninet Corporation for Blanket Authority to Construct and Operate a Private Network of Transmit/Receive Earth Stations and a Hub Station at Los Angeles, California, submitted to the FCC on December 16, 1987.

1. Report No. 88-9		2. Government Accession No.		3. Recipient's Catalog No.	
4. Title and Subtitle Proceedings of the Mobile Satellite Conference May 3-5, 1988				5. Report Date May 1988	
				6. Performing Organization Code	
7. Author(s)				8. Performing Organization Report No.	
9. Performing Organization Name and Address JET PROPULSION LABORATORY California Institute of Technology 4800 Oak Grove Drive Pasadena, California 91109				10. Work Unit No.	
				11. Contract or Grant No. NAS7-918	
				13. Type of Report and Period Covered External Report JPL Publication	
12. Sponsoring Agency Name and Address NATIONAL AERONAUTICS AND SPACE ADMINISTRATION Washington, D.C. 20546				14. Sponsoring Agency Code RE4 BP-650-60-15-01-00	
15. Supplementary Notes					
16. Abstract A satellite-based mobile communications system provides voice and data communications to mobile users over a vast geographic area. Currently, many emerging international Mobile Satellite Systems (MSSs), including the U.S., Canadian, Australian, European and INMARSAT systems, have been proposed to supply such mobile services for land, maritime and aeronautical applications. The technical and service characteristics of these, and other, international systems are presented within these proceedings and form an in-depth view of the current MSS status at the system and subsystem levels. Major emphasis is placed on developments, current and future, in the following critical MSS technology areas: vehicle antennas, networking, modulation and coding, speech compression, channel characterization, space segment technology and MSS experiments. Also, the mobile satellite communications needs of government agencies are addressed, as is the MSS potential to fill them. Over 70 papers, covering 10 technical areas and the government agency MSS application, are published within these proceedings. The breadth and diversity of these papers are a clear indication of the maturity of MSS system concepts and the supporting technology.					
17. Key Words (Selected by Author(s)) Communications			18. Distribution Statement Unclassified; unlimited		
19. Security Classif. (of this report) Unclassified		20. Security Classif. (of this page) Unclassified		21. No. of Pages	22. Price